

**SYNTHETIC STUDIES ON PROTEIN KINASE D, BOTULINUM NEUROTOXIN A1
LIGHT CHAIN, AND NUCLEAR ANDROGEN RECEPTOR MODULATORS, AND
EFFORTS TOWARDS THE TOTAL SYNTHESIS OF 9-DESMETHYLPLEUROTIN**

by

James Kenneth Johnson

B.A., Boston University, 2011

Submitted to the Graduate Faculty of

The Kenneth P. Dietrich School of Arts and Sciences in partial fulfillment

of the requirements for the degree of

Doctor of Philosophy

University of Pittsburgh

2017

UNIVERSITY OF PITTSBURGH
THE KENNETH P. DIETRICH SCHOOL OF ARTS AND SCIENCES

This dissertation was presented

by

James Kenneth Johnson

It was defended on

April 28th, 2017

and approved by

Dennis P. Curran, Distinguished Service Professor of Chemistry and Bayer Professor,
Department of Chemistry

W. Seth Horne, Associate Professor, Department of Chemistry

Zhou Wang, Professor and Director of Urological Research, Department of Urology

Dissertation Advisor: Peter Wipf, Distinguished University Professor, Department of
Chemistry

Copyright © by James Kenneth Johnson

2017

SYNTHETIC STUDIES ON PROTEIN KINASE D, BOTULINUM NEUROTOXIN A1 LIGHT CHAIN, AND NUCLEAR ANDROGEN RECEPTOR MODULATORS, AND EFFORTS TOWARDS THE TOTAL SYNTHESIS OF 9-DESMETHYLPLEUROTIN

James Kenneth Johnson, PhD

University of Pittsburgh, 2017

The first chapter outlines the synthesis of pyrazolo[3,4-d]pyrimidines as inhibitors of Protein Kinase D, a potential target for cancer therapy. The second chapter describes the synthesis of novel inhibitors of Botulinum Neurotoxin A1. First, the synthesis of a constrained analog that contains a dibenzo[*b,g*][1,5]thiazocine is discussed. Second, we explore the use of a Staudinger *aza*-Wittig reaction to produce 1,2,4-triazines and report the progress towards an inhibitor of BoNT/A with increased metabolic stability.

The third chapter describes the development of antagonists of the androgen receptor, a potential target for the treatment of castration-resistant prostate cancer. A small library of analogs was synthesized to assess a structure-activity relationship of a hit compound. The new lead compound was tested *in vivo* and further optimized to improve its metabolic stability. This chapter also describes the synthesis of small molecule affinity labeled conjugates to identify the mechanism of action of the antagonists. The final chapter of this dissertation describes the progress towards the total synthesis of 9-desmethylpleurotin.

TABLE OF CONTENTS

LIST OF ABBREVIATIONS	XX
ACKNOWLEDGEMENTS	XXIV
1.0 SYNTHESIS OF SMALL MOLECULE INHIBITORS OF PROTEIN KINASE D....	1
1.1 INTRODUCTION	1
1.1.1 Small Molecule Inhibitors of PKD	4
1.1.2 Small Molecule Inhibitors of PKD: Previous Work in the Wipf Group.....	9
1.2 RESULTS AND DISCUSSION.....	10
1.2.1 Synthesis of Pyrazolo[3,4-d]pyrimidine-Based Analogs.....	11
1.2.2 Biological Activity of PP1 Analogs	13
1.3 CONCLUSIONS.....	14
2.0 SYNTHESIS OF BOTULINUM NEUROTOXIN A METALLOPROTEASE INHIBITORS	16
2.1 INTRODUCTION	16
2.1.1 Peptide Based Inhibitors of BoNT's	20
2.1.2 Small Molecule Inhibitors of BoNT's.....	22
2.1.3 Structure-Activity Relationship of NSC 240898: Previous Work in the Wipf Group.....	25
2.2 RESULTS AND DISCUSSION.....	27

2.2.1	Synthesis of 3-(4,5-Dihydro-1 <i>H</i> -imidazol-2-yl)-9-(6-(4,5-dihydro-1 <i>H</i> -imidazol-2-yl)-1 <i>H</i> -indol-2-yl)-6,7-dihydro-5 <i>H</i> -dibenzo[<i>b,g</i>][1,5]thiazocine	28
2.2.2	Biological Activity of Thiazocine Analogs	34
2.2.3	Synthesis of 1,2,5,6-Tetrahydro-1,2,4-triazines	35
2.2.3.1	Screening and Optimization of 1,2,4-Triazines.....	38
2.2.3.2	Efforts Towards the Synthesis of 6-(1,2,5,6-Tetrahydro-1,2,4-triazin-3-yl)-2-(4-(4-(1,2,5,6-tetrahydro-1,2,4-triazin-3-yl)phenoxy)phenyl)-1 <i>H</i> -indole	40
2.3	CONCLUSIONS.....	43
3.0	SYNTHESIS OF ANTAGONISTS OF THE NUCLEAR ANDROGEN RECEPTOR FOR THE TREATMENT OF CASTRATION-RESISTANT PROSTATE CANCER.....	45
3.1	INTRODUCTION	45
3.1.1	Treatments of PCa and CRPC.....	50
3.1.2	High Throughput Screen and Structure Activity Relationship: Previous Work in the Wipf Group	55
3.2	RESULTS AND DISCUSSION.....	61
3.2.1	Biological Data.....	64
3.2.2	Improving the Metabolic Stability of JJ450	70
3.2.3	Biological Data of JJ450 Analogs: Cell Data and Metabolism	72
3.2.4	Synthesis of Chemical Probes to Elucidate the Mechanism of Action	81
3.2.5	Biological Activity of Analogs for Affinity Labeling.....	91
3.3	CONCLUSIONS.....	92

4.0 EFFORTS TOWARDS THE TOTAL SYNTHESIS OF 9-DESMETHYLPLEUROTIN	95
4.1 INTRODUCTION.....	95
4.1.1 Previous Syntheses: Hart.....	98
4.1.2 Synthesis of a Pleurotin Analog: Kraus	104
4.1.3 Previous Synthetic Work: Wipf Group	105
4.2 RESULTS AND DISCUSSION.....	112
4.2.1 Retrosynthetic analysis	112
4.2.2 Approach 1: Synthesis of γ-Butyrolactone 4.97	113
4.2.3 Approach 1: Investigation of the Key Dötz Benzannulation and IMDA Sequence Using Lactone 4.97	115
4.2.4 Approach 2: Synthesis of γ-Butyrolactone 4.110.	116
4.2.5 Approach 2: Investigation of the Key Dötz Benzannulation and IMDA Sequence Using Nitrile 4.119.....	119
4.2.6 End Game: Progress Toward the C10 Inversion Sequence and Preliminary Investigation Into the Reductive Etherification to Deliver the Hexacyclic Core of 9-Desmethylpleurotin	122
4.2.7 Future Directions	124
4.3 CONCLUSIONS.....	125
5.0 EXPERIMENTAL PART.....	126
5.1 GENERAL EXPERIMENTAL.....	126
5.2 CHAPTER 1 EXPERIMENTAL PART.....	128
5.3 CHAPTER 2 EXPERIMENTAL PART	152

5.3.1	Synthesis of Thiazocine Inhibitor 2.15	152
5.3.2	Synthesis of 1,2,4-Triazines	167
5.3.3	Synthesis of Triazine Analogs 2.51a-c	172
5.3.4	Synthesis of 6-(1,2,5,6-Tetrahydro-1,2,4-triazin-3-yl)-2-(4-(4-(1,2,5,6-tetrahydro-1,2,4-triazin-3-yl)phenoxy)phenyl)-1H-indole.....	182
5.4	CHAPTER 3 EXPERIMENTAL PART	190
5.4.1	Synthesis of JJ450 Analogs.....	199
5.4.2	Synthesis of Analogs for Affinity Labeling	260
5.5	CHAPTER 4 EXPERIMENTAL PART	285
5.5.1	First Approach	285
5.5.2	Second Approach	290
APPENDIX A	307
APPENDIX B	314
APPENDIX C	317
APPENDIX D	334
BIBLIOGRAPHY	443

LIST OF TABLES

Table 1.1. <i>In vitro</i> radiometric kinase inhibition assay for PP1 analogs against PKD1.	14
Table 2.1. Structure-activity relationship of NSC 240898.	27
Table 2.2. Biological activity of NSC 240898 analogs.	34
Table 2.3. Screening of conditions for SAW cyclization.	39
Table 3.1. Structural modifications in zones 1 and 2.	59
Table 3.2. Modifications to amide of zone 3.	60
Table 3.3. Structural modifications in zones 4 and 5.	61
Table 3.4. Biological activity of <i>cis</i> -cyclopropane analogs.	66
Table 3.5. PK data for JJ450	67
Table 3.6. Liver microsome data for JJ450 and enzalutamide.	67
Table 3.7. Biological activity and liver microsome data for 4-fluoro substituted analogs.	73
Table 3.8. Biological activity and liver microsome data for 4-trifluoromethyl substituted analogs.	75
Table 3.9. Biological activity and liver microsome data for 3-trifluoromethyl substituted analogs.	76
Table 3.10. Biological activity and liver microsome data for 4-pentafluorosulfanyl substituted analog.	77

Table 3.11. Biological activity and liver microsome data for 3-pentafluorosulfanyl substituted analogs.	78
Table 3.12. Biological activity and liver microsome data for heteroaryl substituted analogs.....	79
Table 3.13. Biological activity of affinity precursors.	91
Table 5.1. DSC data for hydrazines 2.47b and 2.47c	189
Table 5.2. Screening conditions for lactone formation.	293
Table A.1. Crystal data and structure refinement for (1 <i>R</i> ,2 <i>S</i>)- JJ450	308
Table A.2. Atomic coordinates and equivalent isotropic atomic displacement parameters (\AA^2) for (1 <i>R</i> ,2 <i>S</i>)- JJ450	309
Table A.3. Bond lengths (\AA) for (1 <i>R</i> ,2 <i>S</i>)- JJ450	310
Table A.4. Bond angles ($^\circ$) for (1 <i>R</i> ,2 <i>S</i>)- JJ450	310
Table A.5. Anisotropic atomic displacement parameters (\AA^2) for (1 <i>R</i> ,2 <i>S</i>)- JJ450	312
Table A.6. Hydrogen atomic coordinates and isotropic atomic displacement parameters (\AA^2) for (1 <i>R</i> ,2 <i>S</i>)- JJ450	312

LIST OF FIGURES

Figure 1.1. The PKD family.	1
Figure 1.2. Early PKD modulators.	6
Figure 1.3. Recent inhibitors of PKD.	9
Figure 1.4. PKD inhibitors developed in the Wipf Group.	10
Figure 1.5. Zones of structural modification around PP1 core.	11
Figure 2.1. Structure of BoNTA (PDB: 3BTA) rendered in PyMol, HC _C (Blue), HC _N (Pink), LC (green), catalytic Zn (grey).	17
Figure 2.2. Mechanism of BoNT intoxication.	19
Figure 2.3. Structures of peptide-like inhibitors of BoNT/A.	22
Figure 2.4. Hydroxamic acid and covalent inhibitors of BoNT.	23
Figure 2.5. Other small molecule non-peptidic inhibitors of BoNT.	25
Figure 2.6. Zones for structural modifications of NSC 240898.	25
Figure 2.7. Structures of 2.10 , lactam, and thiolactam analogs.	28
Figure 2.8. Bond angle of diaryl (thio)ether linkage.	29
Figure 2.9. Effect of oxidation on pK _a of imidazolines vs 1,2,4-triazines.	35
Figure 2.10. Structure of noelaquinone.	36
Figure 3.1. AR gene and functional domains.	46

Figure 3.2. Signaling pathways of AR.....	47
Figure 3.3. 1 st generation antiandrogens.....	52
Figure 3.4. 2 nd generation treatments of CRPC.....	53
Figure 3.5. Recent inhibitors of the AR.....	55
Figure 3.6. Hits identified from HTS.....	57
Figure 3.7. Zone of structural modification.....	57
Figure 3.8. Proposed fluorine substitution for increased metabolic stability.....	62
Figure 3.9. Resolution of racemic JJ450 and crystal structure of (1 <i>R</i> ,2 <i>S</i>)- JJ450	64
Figure 3.10. Effect of JJ450 on LNCaP, 22Rv1, and VCaP s.c. tumor xenografts in nude SCID mice.....	69
Figure 3.11. Proposed zones of structural modification.....	70
Figure 3.12. Zones of structural modification on JJ450	80
Figure 3.13. Comparison of the IR spectra of the unconjugated blank bead to the conjugated bead.....	85
Figure 3.14. Proposed flexible linker modifications to 3.25	85
Figure 3.15. Proposed structural modifications to improve chemical stability.....	87
Figure 3.16. Proposed amide bead precursor 3.49	89
Figure 3.17. Proposed cyclopropane analog 3.58	90
Figure 3.18. Affinity purification of AR from C4-2 whole cell lysate using immobilized 3.34 ..	92
Figure 3.19. Structural improvements leading to compound 3.211	93
Figure 4.1. Structure of pleurotin.....	96
Figure 4.2. Perhydroindan scaffold 4.12 and pleurotin.....	99
Figure 4.3. Proposed model system of pleurotin, 9-desmethylpleurotin.....	112

Figure 4.4. Diels-Alder transition state models.	121
Figure 5.1. DSC thermogram for 2.47b	189
Figure 5.2. SFC chromatograms for JJ450 and separated enantiomers.	198
Figure 5.3. SFC chromatograms for 3.21c and separated enantiomers.	209
Figure 5.4. SFC chromatograms for 3.23 and separated enantiomers.	213
Figure 5.5. SFC chromatograms for 3.21f and separated enantiomers.	217
Figure 5.6. SFC chromatograms for 3.21g and separated enantiomers.	221
Figure 5.7. SFC chromatograms for 3.21h and separated enantiomers.	225
Figure 5.8. SFC chromatograms for 3.21k and separated enantiomers.	234
Figure 5.9. SFC chromatograms for 3.21l and separated enantiomers.	238
Figure 5.10. SFC chromatograms for 3.21n and separated enantiomers.	245
Figure 5.11. SFC chromatograms for 3.21o and separated enantiomers.	249
Figure A.1. X-ray crystal structure of (1 <i>R</i> ,2 <i>S</i>)- JJ450	307
Figure B.1. CD spectra for enantiomers of JJ450	314
Figure B.2. CD spectra for enantiomers of 3.23	315
Figure B.3. CD spectra for enantiomers of 3.21c	315
Figure B.4. CD spectra for enantiomers of 3.21f	315
Figure B.5. CD spectra for enantiomers of 3.21h	316
Figure B.6. CD spectra for enantiomers of 3.21k	316
Figure B.7. CD spectra for enantiomers of 3.21n	316
Figure C.1. EC ₅₀ curves for 3.13a	317
Figure C.2. EC ₅₀ curves for 3.13b	318
Figure C.3. EC ₅₀ curves for 3.21a	318

Figure C.4. EC ₅₀ curves for (1 <i>S</i> ,2 <i>R</i>)- 3.21a	318
Figure C.5. EC ₅₀ curves for (1 <i>R</i> ,2 <i>S</i>)- 3.21a	319
Figure C.6. EC ₅₀ curves for 3.21b	319
Figure C.7. EC ₅₀ curves for 3.21c	319
Figure C.8. EC ₅₀ curves for (1 <i>S</i> ,2 <i>R</i>)- 3.21c	320
Figure C.9. EC ₅₀ curves for (1 <i>R</i> ,2 <i>S</i>)- 3.21c	320
Figure C.10. EC ₅₀ curves for 3.21d	320
Figure C.11. EC ₅₀ curves for (1 <i>S</i> ,2 <i>R</i>)- 3.21d	321
Figure C.12. EC ₅₀ curves for (1 <i>R</i> ,2 <i>S</i>)- 3.21d	321
Figure C.13. EC ₅₀ curves for 3.21e	321
Figure C.14. EC ₅₀ curves for (1 <i>S</i> ,2 <i>R</i>)- 3.21e	322
Figure C.15. EC ₅₀ curves for (1 <i>R</i> ,2 <i>S</i>)- 3.21e	322
Figure C.16. EC ₅₀ curves for 3.21f	322
Figure C.17. EC ₅₀ curve for (1 <i>S</i> ,2 <i>R</i>)- 3.21f	323
Figure C.18. EC ₅₀ curve for (1 <i>R</i> ,2 <i>S</i>)- 3.21f	323
Figure C.19. EC ₅₀ curves for 3.21g	323
Figure C.20. EC ₅₀ curves for (1 <i>S</i> ,2 <i>R</i>)- 3.21g	324
Figure C.21. EC ₅₀ curves for (1 <i>R</i> ,2 <i>S</i>)- 3.21g	324
Figure C.22. EC ₅₀ curves for 3.21h	324
Figure C.23. EC ₅₀ curves for (1 <i>S</i> ,2 <i>R</i>)- 3.21h	325
Figure C.24. EC ₅₀ curves for (1 <i>R</i> ,2 <i>S</i>)- 3.21h	325
Figure C.25. EC ₅₀ curves for 3.21i	325
Figure C.26. EC ₅₀ curves for 3.21j	326

Figure C.27. EC ₅₀ curves for 3.21k	326
Figure C.28. EC ₅₀ curves for (1 <i>S</i> ,2 <i>R</i>)- 3.21k	326
Figure C.29. EC ₅₀ curves for (1 <i>R</i> ,2 <i>S</i>)- 3.21k	327
Figure C.30. EC ₅₀ curves for 3.21l	327
Figure C.31. EC ₅₀ curves for (1 <i>S</i> ,2 <i>R</i>)- 3.21l	327
Figure C.32. EC ₅₀ curves for (1 <i>R</i> ,2 <i>S</i>)- 3.21l	328
Figure C.33. EC ₅₀ curves for 3.21m	328
Figure C.34. EC ₅₀ curves for 3.21n	328
Figure C.35 EC ₅₀ curves for (1 <i>S</i> ,2 <i>R</i>)- 3.21n	329
Figure C.36. EC ₅₀ curves for (1 <i>R</i> ,2 <i>S</i>)- 3.21n	329
Figure C.37. EC ₅₀ curves for 3.21o	329
Figure C.38. EC ₅₀ curves for (1 <i>S</i> ,2 <i>R</i>)- 3.21o	330
Figure C.39. EC ₅₀ curves for (1 <i>R</i> ,2 <i>S</i>)- 3.21o	330
Figure C.40. EC ₅₀ curves for 3.21p	330
Figure C.41. EC ₅₀ curves for 3.21q	331
Figure C.42. EC ₅₀ curves for 3.21r	331
Figure C.43. EC ₅₀ curves for 3.23	331
Figure C.44. EC ₅₀ curves for (1 <i>S</i> ,2 <i>R</i>)- 3.23	332
Figure C.45. EC ₅₀ curves for (1 <i>R</i> ,2 <i>S</i>)- 3.23	332
Figure C.46. EC ₅₀ curves for 3.24	332
Figure C.47. EC ₅₀ curves for 3.25	333
Figure C.48. EC ₅₀ curves for 3.55	333
Figure C.49. EC ₅₀ curves for 3.58	333

LIST OF SCHEMES

Scheme 1.1. Retrosynthetic approach to PP1 analogs.....	12
Scheme 1.2. Synthesis of PP1 analogs.....	13
Scheme 2.1. Mechanism of SNAP-25 hydrolysis.....	19
Scheme 2.2. Retrosynthetic approach to common intermediate lactam 2.17	29
Scheme 2.3. Synthesis of thiazocinone 2.17	30
Scheme 2.4. Attempted synthesis of thiolactam 2.25	31
Scheme 2.5. Synthetic approach to <i>N</i> -nosyl thiazocine 2.28	32
Scheme 2.6. Synthesis of coupling product 2.32	33
Scheme 2.7. Completion of the synthesis of 2.15•TFA	34
Scheme 2.8. Linear synthesis of 1,2,4-triazines.....	36
Scheme 2.9. Debenzylation of triazine 2.40a	36
Scheme 2.10. Synthesis of hydrazones 2.46a and 2.46b	37
Scheme 2.11. Synthetic route to 1,2,4-triazines.....	37
Scheme 2.12. Synthesis of 3,4-dimethoxybenzyl protected hydrazine 2.47c	38
Scheme 2.13. Deprotection of PMB and 3,4-dimethoxybenzyl protecting groups.....	40
Scheme 2.14. Retrosynthetic approach to 2.54	41
Scheme 2.15. Synthesis of diacid 2.56	41
Scheme 2.16. Synthesis of protected bis-1,2,4-triazines 2.62a-2.62c	43

Scheme 3.1. Synthesis of cyclopropane analogs 3.13a and 3.13b .	62
Scheme 3.2. Synthesis of JJ450 .	64
Scheme 3.3. Proposed metabolic oxidation and hotspots on JJ450 .	69
Scheme 3.4. Synthetic route to analogs of JJ450 .	71
Scheme 3.5. Synthesis of deuterocyclopropane 3.23 .	72
Scheme 3.6. Revised sites of metabolism on JJ450 .	80
Scheme 3.7. Bead conjugation of alcohol-containing molecules.	81
Scheme 3.8. Initial proposed analog 3.25 for affinity labeling.	82
Scheme 3.9. Retrosynthetic approach to analog 3.25 .	82
Scheme 3.10. Synthesis of styrene 3.28 .	83
Scheme 3.11. Synthesis of 3.25 .	84
Scheme 3.12. Conjugation of 3.25 to agarose beads.	84
Scheme 3.13. Synthesis of acrylate linker 3.39 .	86
Scheme 3.14. Synthesis of 3.36 .	87
Scheme 3.15. Synthetic approach to ether intermediate 3.47 .	88
Scheme 3.16. Synthesis of amine linker 3.53 .	89
Scheme 3.17. Synthesis and conjugation of analog 3.55 .	90
Scheme 3.18. Synthesis of cyclopropane analog affinity labeling precursor 3.58 .	91
Scheme 4.1. Proposed bioreductive alkylation mechanism of pleurotin.	98
Scheme 4.2. Hart's initial radical cyclization discovery.	99
Scheme 4.3. Synthesis of radical cyclization precursor 4.21 .	100
Scheme 4.4. Hart's radical cyclization.	100
Scheme 4.5. Synthesis of ketone 4.35 .	101

Scheme 4.6. Synthesis of pentacyclic core 4.42	102
Scheme 4.7. Completion of the synthesis of pleurotin.	103
Scheme 4.8. Synthesis of pleurotin analog 4.53	105
Scheme 4.9. Initial retrosynthetic approach to pleurotin.	106
Scheme 4.10. Early synthetic studies towards pleurotin.....	107
Scheme 4.11. Synthetic approach to side chain inversion.	108
Scheme 4.12. Attempts to invert C10 stereochemistry.....	108
Scheme 4.13. Attempted alkene isomerization.....	109
Scheme 4.14. 2 nd generation retrosynthetic approach to pleurotin.	110
Scheme 4.15. Synthesis of naphthalene 4.78	110
Scheme 4.16. Synthesis of enyne fragment 4.86	111
Scheme 4.17. Synthesis of alcohol 4.91	111
Scheme 4.18. Attempts at installation of the side chain at C10.....	112
Scheme 4.19. Retrosynthetic approach to 9-desmethylpleurotin.....	113
Scheme 4.20. Initial synthetic route to alkyne 4.97	114
Scheme 4.21. Synthesis of alkyne 4.97	115
Scheme 4.22. Synthesis of diene 4.107	116
Scheme 4.23. 2 nd Generation retrosynthesis of 9-desmethylpleurotin.....	117
Scheme 4.24. Proposed synthesis of cyano-substituted lactone.	117
Scheme 4.25. Synthesis of lactone 4.110	118
Scheme 4.26. Synthesis of alkyne 4.119	119
Scheme 4.27. Dötz and IMDA reaction sequence.....	120
Scheme 4.28. Synthesis of lactone 4.131	122

Scheme 4.29. Proposed inversion of side chain configuration.	122
Scheme 4.30. Progress towards the inversion of the C10 configuration.	123
Scheme 4.31. Reduction of allylic alcohol 4.139 and reductive etherification to 4.142	124
Scheme 4.32. Proposed endgame for the synthesis of 9-desmethylpleurotin.	124
Scheme 4.33. Proposed synthesis of pleurotin by late stage methylation.	125

LIST OF ABBREVIATIONS

Ac.....	acetyl
AIBN.....	azobisisobutyronitrile
Am.....	amidine
AR.....	androgen receptor
Bn.....	benzyl
Boc.....	<i>tert</i> -butyloxycarbonyl
BoNT.....	botulinum neurotoxin
<i>n</i> -BuLi.....	<i>n</i> -butyllithium
CAN.....	ceric ammonium nitrate
cat.....	catalytic
COSY.....	correlation spectroscopy
CRPC.....	castration-resistant prostate cancer
DBU.....	1,8-diazabicyclo[5.4.0]undec-7-ene
DCE.....	dichloroethane
DIBAL-H.....	diisobutylaluminium hydride
DIPEA.....	<i>N,N</i> -diisopropylethylamine
DMAP.....	4-dimethylaminopyridine
DMA.....	<i>N,N</i> -dimethylacetamide

DMF*N,N*-dimethylformamide
DMSOdimethylsulfoxide
DEPCdiethyl cyanophosphonate
DMPDess-Martin periodinane
DPPAdiphenylphosphoryl azide
EDCI1-ethyl-3(3-dimethylaminopropyl)carbodiimide
EC₅₀.....effective concentration of 50% of maximal response
eeenantiomeric excess
ESI.....electrospray ionization
EtOAcethyl acetate
equiv.....equivalent(s)
erenantiomeric ratio
GFPgreen fluorescent protein
GI₅₀.....growth inhibition of 50%
h.....hour(s)
HATU2-(7-aza-1*H*-benzotriazole-1-yl)-1,1,3,3-tetramethyluronium
hexafluorophosphate
HOAt.....1-hydroxy-7-azabenzotriazole
HPLChigh performance liquid chromatography
HRMShigh-resolution mass spectroscopy
HSPheat shock protein
HTDhigh throughput docking
HTS.....high throughput screen

Im2-imidazoline
IMDAintramolecular Diels-Alder
ICP-OESinductively coupled plasma optical emission spectroscopy
IR.....infrared spectroscopy
K_i.....inhibitor binding affinity
LAHlithium aluminum hydride
LCMS.....liquid chromatography mass spectroscopy
LClight chain
LDAlithium diisopropylamide
LD₅₀.....lethal dose at 50% survival
MBTS.....2-mercaptobenzothiazole disulfide
Mn(dpm)₃manganese (III) tris dipivaloylmethane
MMPPmanganese monoperphthalate
MTBEmethyl *tert*-butyl ether
MWmicrowave irradiation
NMRnuclear magnetic resonance
Ns (nosyl).....4-nitrobenzenesulfonyl
PBU₃*tri-n*-butylphosphine
PDTproduct
PCa.....prostate cancer
P-gp.....p-glycoprotein
PIFAphenyliodine bis(trifluoroacetate)
PKpharmacokinetic

PKDprotein kinase D
PMB*p*-methoxybenzyl
PMe₃.....trimethylphosphine
PMePh₂methyl diphenylphosphine
PPh₃.....triphenylphosphine
Pypyridine
PyBroPbromotripyrrolidiniophosphonium hexafluorophosphate
rtroom temperature
scsubcutaneous
SCIDsevere combined immunodeficiency
SFCsupercritical fluid chromatography
SM.....starting material
STABsodium triacetoxyborohydride
T3P1-propanephosphonic anhydride
TBDPS*tert*-butyldiphenylsilyl
TBHP*tert*-butyl hydroperoxide
Tf.....trifluoromethanesulfonyl
TFA.....trifluoroacetic acid
TFAAtrifluoroacetic anhydride
THFtetrahydrofuran
TLCthin layer chromatography
TMDStetramethyldisiloxane

ACKNOWLEDGEMENTS

First, I would like to thank Professor Peter Wipf for the opportunity to work in his laboratory along with providing me with his infinite guidance and support. I would also like to thank him for the incredible training that I have received during my doctoral studies. I am thankful of Professors Dennis Curran, W. Seth Horne, Zhou Wang, and Kazunori Koide for serving on my committees.

I would like to thank all of the members of the Wipf group, both past and present, for their support and interesting conversations over the years. In particular, I would like to thank Kara Rosenker and Joshua Sacher for their continuing support and advice.

I would like to thank my family for their love and support over the years. Finally, I would like to thank Steph McCabe for being wonderful in every possible way.

1.0 SYNTHESIS OF SMALL MOLECULE INHIBITORS OF PROTEIN KINASE D

1.1 INTRODUCTION

Since the early 2000s, protein kinase D (PKD) has been a target for cancer therapy¹⁻¹⁰ due to its association with a number of tumors, including prostate,^{2,10-15} breast,¹⁶⁻¹⁹ pancreatic,^{9,20-25} lymphoma,²⁶⁻²⁸ and colon²⁹⁻³⁰ cancer. PKD forms a subgroup of the Ca²⁺/calmodulin-dependent kinase (CAMK) family and consists of three isoforms, 1, 2, and 3 (Figure 1.1). Initially, PKD1 and PKD3 were thought to be a subclass of PKC and were named as PKC μ ,³¹ and ν ,³² respectively. The three isoforms each have specialized roles in signaling pathways, which stem from their varying expression in different tissues.^{30,33}

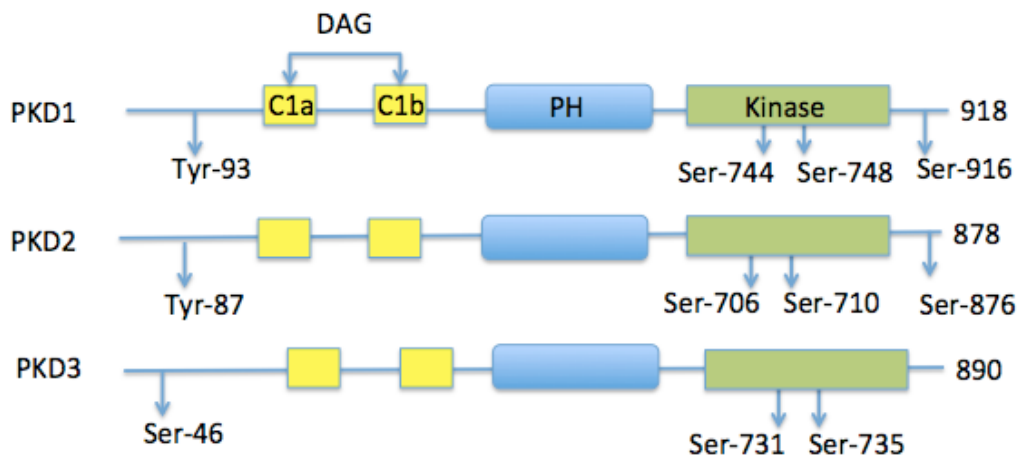


Figure 1.1. The PKD family.

Structurally, the three PKD isoforms show greater than 70% similarity (Figure 1.1). The cysteine rich domains (CRD) C1a and C1b, and the catalytic domain show high homology for

PKD1–3. The order of the domains is also conserved for the three isoforms and contains the CRD, a Pleckstrin Homology (PH) domain, and the catalytic kinase domain. The CRD are cysteine-rich zinc fingers that bind DAG (diacylglycerol) and PMA (phorbol ester).³⁴ The PH domain is involved in the autoinhibition of PKD.³⁵⁻³⁶ Upon activation by PKC, PKD1 is phosphorylated at Ser 744, 748, and 916.³⁷ Once PKD is phosphorylated, it can maintain its activity through auto-phosphorylation in the presence of an agonist.^{22,36-37}

PKD has been shown to play important roles in a number of cellular pathways including cell migration and invasion through protein exocytosis from the trans Golgi network (TGN), activation of the Ras-Raf-MEK-ERK pathway, inhibition of the JNK pathway, response to oxidative stress via NF- κ B activation,^{33,38-39} and nuclear export of histone deacetylases (HDAC's).^{37,40-44} In hypoxic tumors, PKD2 overexpression is important for tumor vascularization through stabilization of hypoxia inducible factor 1 α (HIF1 α), and subsequent NF- κ B activation. Heat shock protein 90 (HSP90) plays an important role in regulating the stability of PKD2 and could be used for synergistic therapy to treat hypoxic tumors.⁴⁵⁻⁴⁶

PKD activation begins with extracellular signaling via G-protein coupled receptors (GPCR) or a receptor tyrosine kinase (RTK). This signaling activates phospholipase C, which hydrolyzes PI4,5P₂ (phosphatidylinositol-4,5-bisphosphate) into the corresponding DAG and IP3 (inositol-1,4,5-triphosphate). DAG can bind to the CRD of nPKC, which in turn phosphorylates PKD, or directly binds to the CRD of PKD.^{36,42,47-48} Once PKD has been phosphorylated, it circulates through the cytosol where it can phosphorylate Ras and Rab interactor 1 (RIN1).⁴⁹ The phosphorylated RIN1 releases Ras, which triggers the extracellular signal-regulated kinase (ERK) pathway involved in cell proliferation.⁴⁹⁻⁵⁰ Overexpression of PKD is involved in the

upregulation of ERK and has been shown to be present in a number cell types including prostate cancer cells,⁵¹ mouse embryonic fibroblasts (Swiss 3T3),⁵²⁻⁵³ and endothelial cells.⁵⁴

PKD can also downregulate the c-Jun *N*-terminal kinase (JNK) pathways through phosphorylation of c-Jun.^{40,55-56} JNK is a subgroup of the mitogen activated protein kinases (MAPK) and is responsible for inflammatory/immune response, apoptosis, cell proliferation, and cell motility.⁵⁷⁻⁶⁰ Dysregulation of these pathways has been implicated with tumorigenesis.⁶¹

The catalytically active PKD can also enter the nucleus, phosphorylate class II HDAC's (5 and 7)⁶²⁻⁶⁷ and trigger their nuclear exocytosis.⁴¹ HDAC's have been shown to be important in transcription and cardiac muscle contraction. Moreover, class II HDAC's can silence protein expression through DNA methylation.⁶⁸ In certain tumor types PKD is downregulated as a result of this gene silencing.^{21-22,69-70} Dysregulation of PKD can cause cardiac hypertrophy and heart failure, and is one reason why PKD is being targeted as an upstream effector of HDAC export.^{67,71-74}

PKD has been demonstrated to be important in cell migration and invasion events that lead to the metastasis of cancer. PKD plays a key role in the regulation of protein transport from the trans Golgi network (TGN) to the cell surface.⁷⁵⁻⁷⁷ PKD has been shown to mitigate cell motility through phosphorylation of proteins involved in cell migration/invasion, including slingshot-1-like (SSH1L),²⁵ cortactin,⁷⁸⁻⁸¹ and Par-1.⁸² Phosphorylated SSH1L can further bind to the 14-3-3 protein, which results in the release of F-actin into the cytosol. The release of F-actin then feeds into the cofilin remodeling of membranes of migrating cells.^{17,83-87} PKD also inhibits F-actin remodeling by phosphorylation of RIN1, which activates c-Abl. c-Abl then alters the conformation of the adaptor protein Cullin-RING ubiquitin ligases (CRL), preventing activation of the F-actin remodeling proteins and disrupting cell motility.⁵⁰ PKD has also been associated

with the regulation of spatial memory through the stabilization of F-actin in dendritic spines.⁸⁸ PKD also regulates matrix-metalloproteinases (MMP's) that are responsible for the degradation of the extracellular matrix (ECM).⁸⁹⁻⁹⁰ These MMP's have been shown to play an important role in the metastasis of multiple cancers.^{25,91-95} Recently, PKD1 has been shown to regulate focal adhesions, attachment sites connecting cells to the ECM, through the localization of $\alpha v \beta 3$ integrin and phosphatidylinositol-4-phosphate 5-kinase type-1 gamma (PIP5K1 γ).⁹⁶ PKD isoforms 1 and 3 have been found to regulate the cell cycle through microtubule modulation during mitosis.⁹⁷

PKD can also be activated as a response to oxidative stress through a PKC dependent Src-Abl pathway.⁹⁸⁻¹⁰⁰ PKD is phosphorylated at the PH domain, which allows for further phosphorylation on the CRD followed by PKC δ phosphorylation of the activation loop.^{38,98,101-104} Phosphorylated PKD can phosphorylate the IKK complex that signals Nf- κ B to induce expression for manganese superoxide dismutase (MnSOD) from the mitochondria, which then quenches ROS in the cytosol.^{100,102,105}

Each of these pathways plays an important role in either cell survival or cell death and for this reason PKD represents a complex but viable target for cancer therapy.

1.1.1 Small Molecule Inhibitors of PKD

The ATP binding domain of PKD was the target of early PKD inhibitors.¹⁰⁶ Unfortunately, the ATP binding domain is highly conserved within the kinome and was the main downfall of early PKD inhibitors because they were non-selective and inhibited other kinases, resulting in off target effects. Over the past 15 years, potent PKD-selective inhibitors have been developed

targeting both the ATP binding domain and allosteric sites. In general, most ATP-competitive inhibitors are less kinase-selective due to the highly conserved nature of ATP binding sites.¹⁰⁶

One of the earliest known PKD inhibitors, staurosporine (Figure 1.2), has low nanomolar PKD inhibition but also inhibits numerous other kinases, including protein kinase C (PKC), protein kinase A (PKA), and CAMK II.¹⁰⁷ Recently, fluorescein-staurosporine conjugates have been synthesized for their use as tools to monitor binding of other ATP competitive inhibitors.¹⁰⁸ The staurosporine type inhibitors including Gö 6976 (Figure 1.2) have been well studied for their kinase activity and exhibit low nanomolar inhibition of both PKC and PKD.^{33,107,109-111}

The stilbene resveratrol was found to inhibit many proteins including PKD and required high micromolar concentrations for any observable inhibition effect (Figure 1.2). Resveratrol has been extensively studied as a cancer preventative and therapeutic but is limited due to its poor solubility, low bioavailability, and photochemical stability.¹¹² Despite these limiting factors, several formulations and analogs of resveratrol have been developed for the treatment of cancer and various diseases.¹¹² The flavonol, quercetin, was found to have low micromolar inhibition of PKD and PKC in addition to a number of other proteins and has been well studied for its use in the prevention and treatment of cancer (Figure 1.2).¹¹³ The polysulfonylated naphthylurea, Suramin, was initially used for the treatment of sleeping sickness and parasitic diseases and later found to be an effective activator of PKD (Figure 1.2).¹¹⁴ Based on its ability to decrease tumor growth, Suramin has been advanced into a number of clinical trials including a combination treatment with paclitaxel in a phase I/II clinical trial for metastatic breast cancer (NCT00054028), a phase II clinical trial in combination with docetaxel for the treatment of non-small cell lung cancer (NCT01671332), a phase I clinical trial for bladder cancer (NCT00006476), and a phase III clinical trial for the treatment of castration resistant prostate

cancer (NCT00002723) (Figure 1.2). The marine-derived macrolactone bryostatin 1 was shown to activate PKD and PKC leading to alterations in cell aggregation and proliferation through localization of β -catenin.¹¹⁵ Bryostatin 1 has been used in numerous (>40) clinical trials for the treatment of cancer, HIV, and Alzheimer's disease.¹¹⁶⁻¹¹⁷

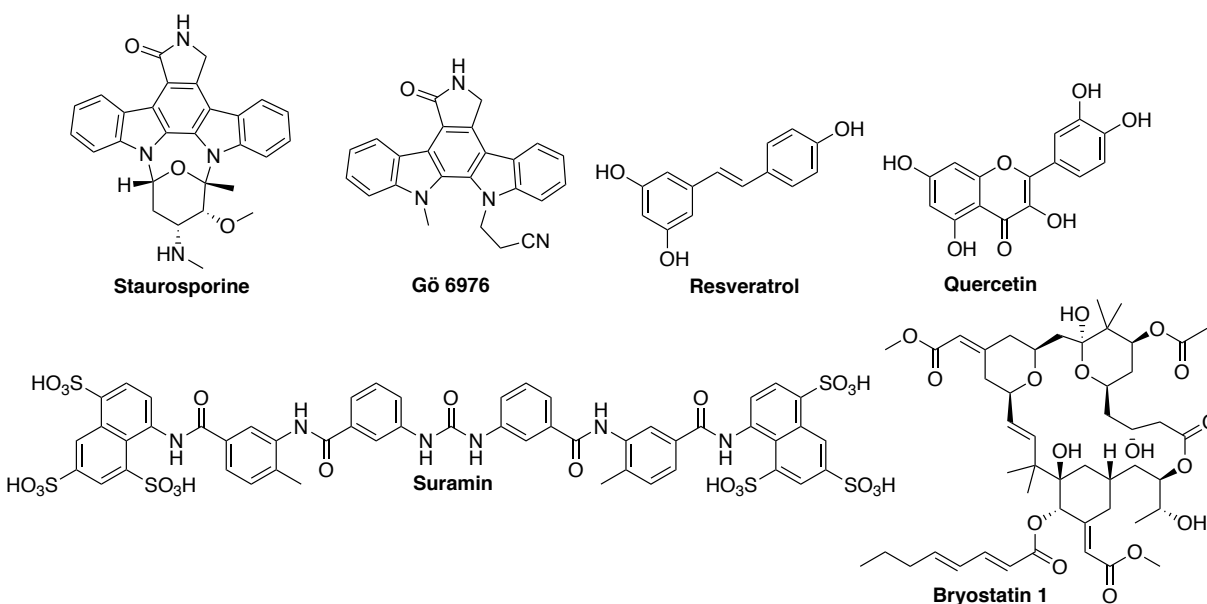


Figure 1.2. Early PKD modulators.

The novel 3,5-diarylazole **1.1** was identified from a HTS against PKD1 and had moderate kinase inhibition (PKD1 $IC_{50} = 2.3 \mu M$).¹¹⁸ Subsequent structural optimization of **1.1** afforded compound **1.2** a potent, selective, and orally bioavailable inhibitor of PKD. Analog **1.2** exhibited modest isoform selectivity with a 9-fold and 3-fold selectivity for PKD1 over PKD2 and PKD3 respectively along with >1000-fold selectivity against a panel of 230 kinases.¹¹⁸ PK data for **1.2** indicates that there is moderate oral bioavailability (38%) with a short plasma half-life (1.2 h). Combined, the selectivity, activity, and PK data for **1.2** make it a viable target for further optimization.

The 2,6-naphthyridines, developed by Novartis, have emerged as novel PKD inhibitors (Figure 1.3).¹¹⁹⁻¹²⁰ The 2,6-naphthyridine inhibitor **1.3** was identified in a HTS and shown to be

ATP-competitive PKC/PKD inhibitor. A series of modified 2,6-naphthyridines was used to investigate PKD as a possible therapeutic target for cardiac hypertrophy, since PKD is a downstream effector of nuclear export of class II HDAC's.^{41,67,73-74,121-122} Subsequent SAR studies led to the orally available **1.4**, which was shown to block phosphorylation of PKD and nuclear export of class II HDAC's (Figure 1.3).¹¹⁹ Additionally, when **1.4** was administered in 2 rat cardiac hypertrophy disease models it was found to have no effect. Unfortunately, it was unclear whether this was the result of PKD inhibition by **1.4** or the ability of **1.4** to also inhibit glycogen synthase kinase 3 β (GSK3 β), which is known for its role in antihypertrophy.¹²³ An Using molecular modeling and conformational analysis, the 2,6-naphthyridine core was truncated to a bipyridyl.¹¹⁹⁻¹²⁰ Further optimization produced a new lead, BPKDi, a potent pan-PKD inhibitor that inhibits autophosphorylation of PKD and provides increased retention of HDAC4 and HDAC5 in cardiomyocytes (Figure 1.3).¹²⁰ In a PK panel in rats, BPKDi performed poorly due to high clearance, low solubility, and poor bioavailability. Attempts to improve the PK parameters were met with compounds less active or selective against PKD. To assess the *in vivo* activity, BPKDi was administered sc daily at 5 mg/kg in two rat models with no reduction in cardiac hypertrophy was observed. When higher doses of BPKDi were administered, a significant increase in blood pressure was observed, however, adequate plasma concentrations were reached at this dosing concentration. The lack of *in vivo* activity for these compounds ultimately led to their discontinuation as targets for the treatment of hypertrophy.

Cancer Research Technologies (CRT) produced the potent, orally available pan-PKD inhibitor CRT0066101 (Figure 1.3).²¹ CRT0066101 was shown to have single-digit nanomolar pan-PKD activity *in vitro*. In a human pancreatic cancer tumor xenograft model, CRT0066101 was administered orally daily at 80 mg/kg for 28 days halting tumor growth completely.²¹ In rat

pancreatic acinar cells, CRT0066101 promoted apoptosis and decreased necrosis in pancreatic cells.^{23,124} In malignant brain tumor cells, glioblastoma multiforme, CRT0066101 decreased cell migration and invasion events through inhibition of PKD2.¹²⁵ CRT0066101 was antiproliferative *in vitro* in low micromolar concentrations against multiple colorectal cancer cell lines.¹²⁶ Subsequent administration of CRT0066101 in HCT116 xenograft nude mice displayed significant inhibition of tumor growth.¹²⁶ When used in combination with Regorafenib, CRT0066101 demonstrated a synergistic effect on the inhibition and cell proliferation in metastatic colorectal cancer.¹²⁷ Additionally, CRT0066101 has also been shown to inhibit estrogen receptor negative breast cancer both *in vitro* and *in vivo*.¹⁹ CRT0066101 remains a promising inhibitor of PKD for the treatment of cancer. In addition to CRT0066101, CRT also developed the pyrazine benzamide CRT5, which was a potent selective pan-PKD inhibitor ($IC_{50} = 1.5$ nM) and decreased VEGF-induced endothelial migration, cell proliferation, and tubulogenesis (Figure 1.3).¹²⁸

The pyrazolo[3,4-d]pyrimidine 3-IN-PP1 was identified from a recent SAR of 1-NM-PP1, a previously known inhibitor of Src and calcium dependent kinases,^{15,129-130} as a potent (*in vitro* $IC_{50} = 33$ nM) pan-PKD inhibitor (Figure 1.3).¹³¹ Based on the interesting trends with the SAR, 3-IN-PP1 was proposed to have an alternate binding mode in the ATP binding pocket of PKD with the structure flipped 180° compared to other classically modeled kinase inhibitors.¹³¹ 3-IN-PP1 is a promising new inhibitor that has potential for further structural development. Recently, the pyrazolo[3,4-d]pyrimidine **1.5** was identified as a low nanomolar pan-PKD inhibitor from a novel LC-MS based kinase screening technique (Figure 1.3).¹³² This HTS technique allows for the rapid proteome profiling of new inhibitors of protein kinases and other purine-binding proteins.¹³³⁻¹³⁴

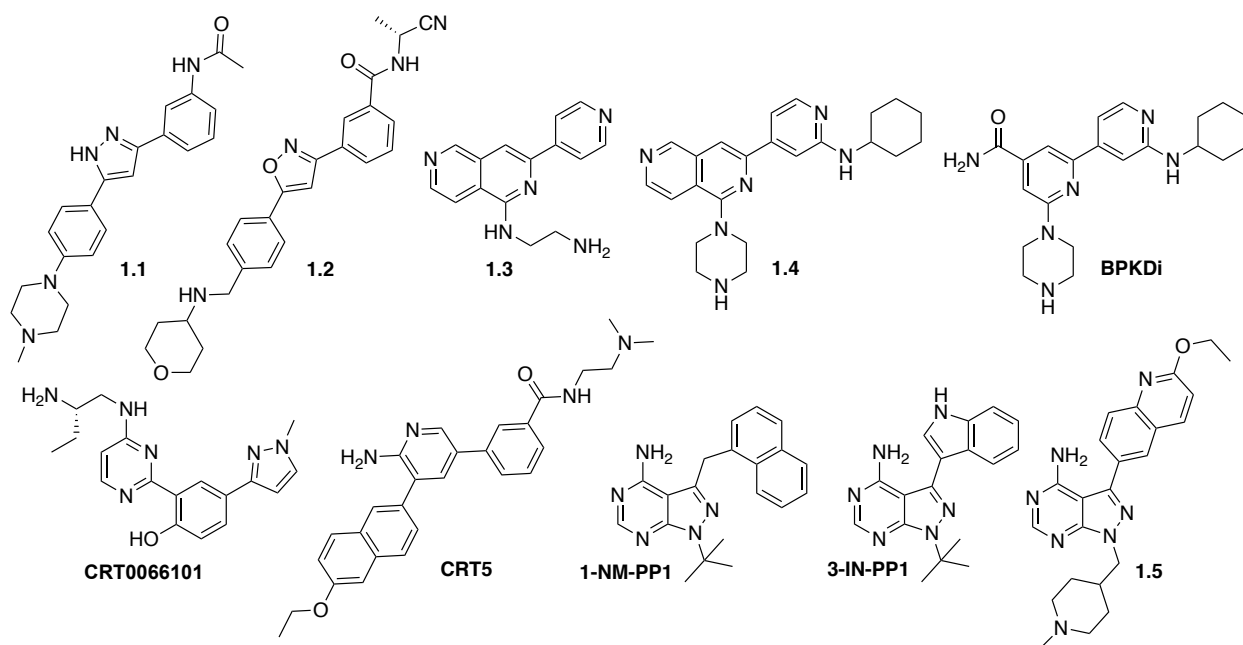


Figure 1.3. Recent inhibitors of PKD.

1.1.2 Small Molecule Inhibitors of PKD: Previous Work in the Wipf Group

Over the past 10 years, the Wipf group has been attracted to developing small molecule inhibitors of PKD as a potential target for cancer therapy. A library screen of the NIH SMRL produced the first potent PKD specific inhibitor CID 755673 with an *in vitro* IC_{50} of 180 nM (Figure 1.4).¹³⁵ Previous work in the Wipf group aimed to improve potency of CID755673 which led to the synthesis of the more potent kb-NB142-70 with an *in vitro* IC_{50} of 28 nM.¹³⁵⁻¹³⁷ CID755673 and kb-NB142-70 were effective in reducing prostate and colorectal cancer cell proliferation and migration *in vitro*.^{126,138} Unfortunately, no therapeutic effect was observed when kb-NB142-70 was administered to mice bearing PC-3 xenografts.¹³⁸ Subsequent PK analysis of kb-NB142-70 revealed that it had a plasma half-life of 6 min that can correlate directly to poor *in vivo* efficacy. Attempts to improve the metabolic stability of kb-NB142-70 resulted in kmg-NB4-23 that was slightly less potent with an *in vitro* IC_{50} of 124 nM (Figure

1.4). Unfortunately, the poor solubility of kmg-NB4-23 (<0.4 mg/mL) prevented the *in vivo* biological characterization of this compound. The benzoxoloazepinolones were found to bind non-competitively with ATP indicating a potential alternative binding mode or location. An allosteric inhibitor may exhibit increased kinase selectivity making this scaffold a viable lead for further development.

SD-208 was identified from a targeted kinase inhibitor library screen and was found to be a potent, selective, orally bioavailable ATP-competitive inhibitor of PKD *in vitro* and *in vivo* (Figure 1.4).¹³⁹ A subsequent SAR of SD-208 revealed key binding interactions were required for potency in PKD and did not result in any analogs with increased potency. Finally, Ro139 was identified from a HTS campaign and was found to have low nanomolar activity against PKD *in vitro* (Figure 1.4).¹⁴⁰ Subsequent analog synthesis and biological characterization by WST-1 assay¹⁴¹ revealed that analogs of Ro139 were selective towards rectal carcinoma RKO cells with low micromolar inhibition.

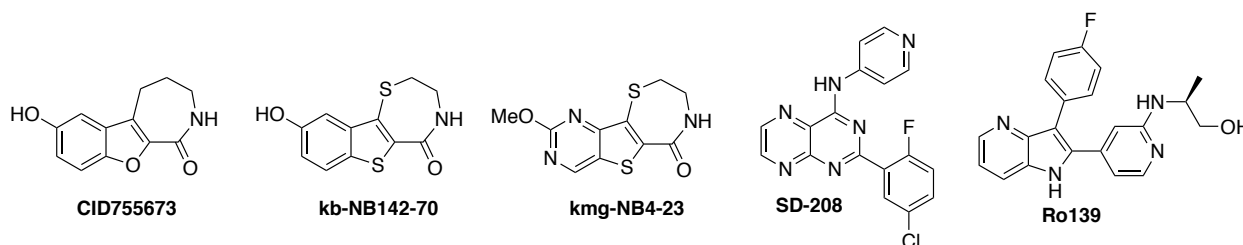


Figure 1.4. PKD inhibitors developed in the Wipf Group.

1.2 RESULTS AND DISCUSSION

The pyrazolopyrimidine 1-naphthyl-PP1 (PP1) was identified as a novel ATP competitive pan-PKD inhibitor (Figure 1.5).¹⁵ Initially, PP1 was developed for analog specific mutants of src

kinases.¹²⁹ This scaffold was used to probe the ATP binding sites of gatekeeper mutant proteins that provide a more accessible binding pocket for new inhibitors.^{129,142} PP1 has been shown to be highly selective for PKD over PKC and other members of the CAMK family.¹⁵ To validate the analog specific mutant approach, PP1 was tested against the gatekeeper mutant of PKD that had been transfected and overexpressed in human embryonic kidney (HEK293) cells. **PP1** showed a 12-fold increase in activity from the wild type to the mutant. This suggests that the mutant PKD could be used to assess structural modifications of PP1 to develop a more potent PKD inhibitor as shown by Bishop and coworkers.¹⁴² Additionally, **PP1** derivatives are active in mutants of ERK1/2 containing a single amino acid alteration.¹⁴³ PP1 is a potent pan-PKD inhibitor that has an IC₅₀ of 155 nM and has been shown to inhibit growth and cell proliferation in prostate cancer (PC3 cells).¹⁵ We envisioned 4 zones of modification around the **PP1** core to identify the substituent effect on the biological activity (Figure 1.5).

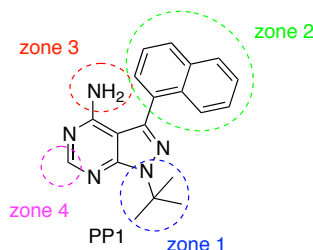
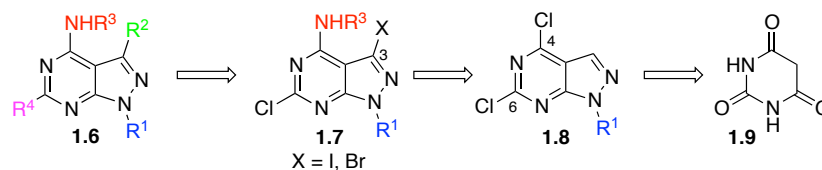


Figure 1.5. Zones of structural modification around PP1 core.

1.2.1 Synthesis of Pyrazolo[3,4-d]pyrimidine-Based Analogs

Our synthetic approach to the PP1 analogs utilized a late stage Suzuki cross coupling at halogenated C-3 with a variety of aryl boronic acids. We proposed that intermediate **1.7** could be formed by nucleophilic aromatic substitution with an amine at C-4 and subsequent halogenation

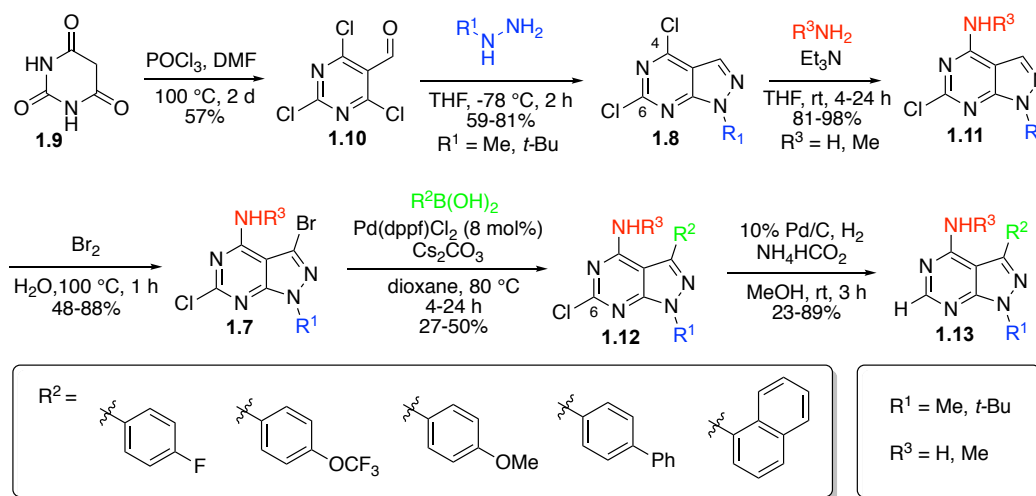
at C-3. Precursor **1.8** could be readily formed by a Vilsmeier-Haack reaction and hydrazine cyclization of commercially available barbituric acid **1.9** (Scheme 1.1).



Scheme 1.1. Retrosynthetic approach to PP1 analogs.

The synthesis of PP1 and its analogs began with the tandem Vilsmeier-Haack chlorination and formylation reaction on commercially available barbituric acid (**1.9**) to give the trichloropyrimidine **1.10** in moderate yields.¹⁴⁴ Condensation and cyclization with methyl or *t*-butyl hydrazine afforded the pyrazolo[3,4-d]pyrimidines **1.8** in good yields. Initially, the cyclization with *t*-butyl hydrazine hydrochloride was low yielding due to poor solubility of the *t*-butyl hydrazine hydrochloride salt in THF at -78 °C. Attempts to freebase the hydrazine to improve the reaction were unsuccessful. After screening several solvents and solvent combinations, it was determined that addition of a solution of the hydrazine hydrochloride in acetonitrile to a THF solution of pyrimidine affords the desired product **1.8** in good yields. Regioselective aminolysis of **1.8** at the C4-position with ammonia or methylamine gave amines **1.11** in great yields. Initial attempts to iodinate at C-3 to form the 3-iodo intermediate with iodine, Barluenga's reagent, or *N*-iodosuccinimide were unsuccessful.¹⁵ Gratifyingly, treatment with bromine afforded 3-bromo-pyrazolopyrimidines **1.7** in good yields. The C-3 bromide **1.7** was functionalized via a Suzuki cross coupling using a variety of aryl boronic acids to give the arylated compounds **1.12**. The low yields in some cases are the result of the arylation at both C-3 and C-6 to afford diarylated products. Finally, the 6-chloro substituent was reduced via a catalytic hydrogen transfer reaction to give the desired products **1.13** in poor to excellent yields

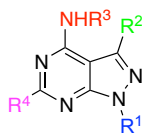
(Scheme 1.2). Overall PP1 and 17 analogs were prepared with varying substitution at the pyrazole nitrogen R¹, aryl ring at R², amine R³, and C-6 position.



Scheme 1.2. Synthesis of PP1 analogs.

1.2.2 Biological Activity of PP1 Analogs

The *in vitro* PKD1 inhibition for PP1 and analogs was determined at 1 μ M using a radiometric kinase assay.¹⁵ The 17 analogs of PP1 showed that the PKD binding pocket was very resistant to structural modifications of the parent structure (Table 1.1). Modifying R₁ from a bulky *t*-butyl to a smaller methyl group resulted in a 50% loss in activity (entry 7). Replacement of the naphthyl group at R₂ with other aryl substituents also eliminated PKD activity. Analogs with methylation at R₃ were completely inactive and further confirmed the importance of the hydrogen bonding interactions within the binding pocket.¹²⁹ Electrophilic analogs (R₄=Cl) were also completely inactive. Unfortunately, the PP1 analog with a 6-chloro substitution was never synthesized and therefore no direct comparison can be made about the chloro substitution on activity of PP1. Based on the steep SAR observed, this series was deprioritized in favor of new cores.

Table 1.1. *In vitro* radiometric kinase inhibition assay for PP1 analogs against PKD1.¹⁵

Entry	Compound	Structure				PKD1 % inhibition ^a
		R ¹	R ²	R ³	R ⁴	
1	PP1	<i>t</i> -butyl	1-naphthyl	H	H	80% (PP1)
2	1.13a	<i>t</i> -butyl	1-naphthyl	methyl	H	<10%
3	1.13b	<i>t</i> -butyl	(4-MeO)phenyl	H	H	<10%
4	1.13c	<i>t</i> -butyl	(4-MeO)phenyl	methyl	H	<10%
5	1.13d	<i>t</i> -butyl	(4-F)phenyl	H	H	<10%
6	1.13e	<i>t</i> -butyl	(4-Ph)phenyl	H	H	<10%
7	1.13f	methyl	1-naphthyl	H	H	32%
8	1.13g	methyl	1-naphthyl	methyl	H	<10%
9	1.13h	methyl	(4-MeO)phenyl	H	H	<10%
10	1.13i	methyl	(4-MeO)phenyl	methyl	H	<10%
11	1.12h	methyl	(4-MeO)phenyl	H	Cl	<10%
12	1.12i	methyl	(4-MeO)phenyl	methyl	Cl	<10%
13	1.13j	methyl	(4-CF ₃ O)phenyl	methyl	H	<10%
14	1.12j	methyl	(4-CF ₃ O)phenyl	methyl	Cl	<10%
15	1.13k	methyl	(4-F)phenyl	methyl	H	<10%
16	1.12k	methyl	(4-F)phenyl	methyl	Cl	<10%
17	1.13l	methyl	(4-Ph)phenyl	methyl	H	<10%
18	1.12l	methyl	(4-Ph)phenyl	methyl	Cl	<10%

^aPKD1 %inhibition was determined at 1 μ M concentration as previously described.^{15,140}

1.3 CONCLUSIONS

PP1 was identified in an initial library screen and was found to be a potent PKD inhibitor with selectivity against similar kinases.¹⁴⁰ To validate the initial results, PP1 was resynthesized and 17 analogs were prepared to probe the effect of substitution around the PP1 core (Figure 1.3). Unfortunately, we discovered that the PKD binding pocket was very resistant to our structural modifications. The limited SAR produced compounds with no activity or poor activity, with PP1 remaining the most active analog (Table 1.1). The parent PP1 blocked 50% of PKD activity at

100 nM. A subsequent assay of PP1 against closely related kinases PKC α , PKC δ , and CAMKII α had shown no inhibition even at concentrations as high as 10 μ M. Although all new analogs of PP1 were inactive, PP1 was established as a potent pan-PKD inhibitor having antitumor activity in prostate cancer cells.¹⁵

2.0 SYNTHESIS OF BOTULINUM NEUROTOXIN A METALLOPROTEASE INHIBITORS

2.1 INTRODUCTION

The *Clostridium* genus of gram-positive bacteria includes several human pathogens that are well known for their toxicity, including *C. botulinum* (botulism), *C. tetani* (tetanus),¹⁴⁵⁻¹⁴⁷ and *C. perfringens* (clostridial necrotizing enteritis).¹⁴⁸⁻¹⁴⁹ The toxicity of *C. botulinum* is due to botulinum neurotoxins (BoNT's), which are a family of proteins consisting of eight serotypes (A-H).¹⁵⁰⁻¹⁵⁴ The resulting disease, botulism, is characterized by flaccid muscle paralysis, leading to respiratory failure and death. Of the eight serotypes, BoNT/A is the most potent neurotoxin with an LD₅₀ of less than 1 ng/kg.¹⁵⁵ There are five subtypes of BoNT/A (1-5) that contain unique characteristics.¹⁵⁶⁻¹⁵⁷ In 1942, methods to effectively purify crystalline BoNT/A were developed leading to its use in the treatment of muscle disorders and increasing its potential for use in biological warfare.¹⁵⁸⁻¹⁶⁴ Today, BoNT's are classified by the CDC as a class A biothreat.¹⁶⁵ Even with early detection, effective treatments of BoNT intoxication are limited and prophylactic. Several low-dose injectable forms of BoNT/A (Botox, Dysport, Xeomin) and BoNT/B (Myobloc) have been approved by the FDA for the treatment of a number of neuromuscular, urological, pain, and cosmetic disorders.^{146-147,155,166-195}

BoNT's are metalloproteases¹⁹⁶ that consist of a 100 kDa heavy-chain (HC) and a 50 kDa light-chain (LC), both linked by a single disulfide bond (Figure 2.1).¹⁹⁷⁻²⁰⁰ The HC contains two 50 kDa domains, the *C*-terminal binding domain (HC_C) and the *N*-terminal translocation domain (HC_N). The LC is the catalytic domain containing zinc in the active site. Toxicity arises after disulfide cleavage, which enables release of the LC into the intracellular membrane.²⁰¹

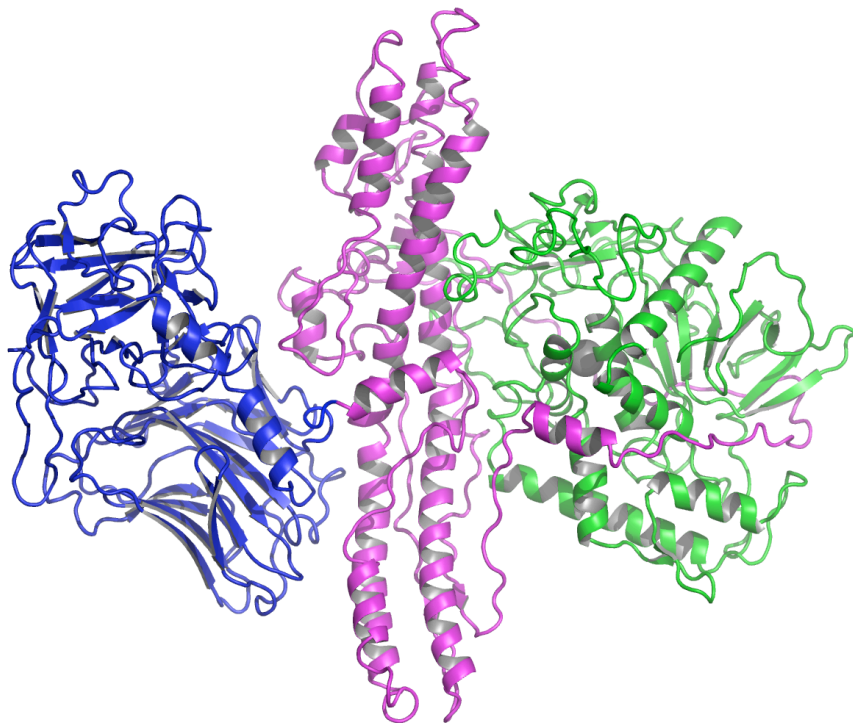


Figure 2.1. Structure of BoNTA (PDB: 3BTA) rendered in PyMol, HC_C (Blue), HC_N (Pink), LC (green), catalytic Zn (grey).

There are four main methods of BoNT intoxication including ingestion, wound, intentional intoxication (bioterrorism), or unintentional intoxication (side effect of therapeutic treatment).²⁰²⁻²⁰³ Ingestion is the most common form of intoxication and occurs only with a preformed complex BoNT that consists of three components: BoNT, hemagglutinins (HAs; three HA-70, three HA-17, and six HA-33), and “non-toxic” non-hemagglutinin (NTNHA) also referred to as “non-toxic” neurotoxin associated proteins (NAP's). The complex provides heat

and hydrolytic stability as well as aid in intestinal absorption.²⁰⁴⁻²⁰⁸ The HA and NTNH proteins are shed as BoNT circulates through the blood stream.²⁰³ Homogeneous BoNT shows remarkable stability and rapid distribution in the bloodstream.²⁰³ BoNT localizes at neuromuscular junctions (NMJ) where the heavy chain (HC_c) binds to extracellular membrane gangliosides (Figure 2.2).²⁰⁹⁻²¹¹ Once bound to the membrane, BoNT triggers a recycling of synaptic vesicle membrane proteins (SV2) that cause endocytosis of the BoNT.²¹² The newly formed vesicle is acidified by an ATP activated proton pump, which causes the translocation domain HC_n to insert into the vesicle membrane.²¹³⁻²¹⁴ The translocation domain HC_n opens a pore within the vesicle that facilitates the extension of the LC out of the vesicle and into the cytosol.^{145,214} Recently, it has been shown that the stability of the HC/LC complex under acidic pH increases and that under an acidic pH the LC interacts and permeates the anionic phospholipid bilayer.²¹⁵ Once exposed to the cytosol, the disulfide bond is reduced,²¹⁴ releasing the free LC into the cytosol. The LC of BoNT then facilitates hydrolysis of the soluble *N*-ethylmaleimide-sensitive factor attachment protein receptor (SNARE) proteins that facilitate pore formation along the synaptic membrane and are crucial in releasing the neurotransmitter acetylcholine into the synaptic cleft. There are three SNARE proteins that are targeted by the different serotypes of BoNT's: vesicle associated membrane proteins (VAMP also known as synaptobrevin) are targeted by BoNT B,²¹⁶ D,²¹⁷ F,²¹⁸ and G,¹⁹⁷ synaptosomal associated protein of 25 kDa (SNAP-25) is targeted by BoNT A, C, and E,²¹⁹⁻²²⁰ and syntaxin is targeted by BoNT C.^{202,221} BoNT/A cleaves SNAP-25 at Gln¹⁹⁷ and Arg¹⁹⁸ to produce a very stable truncated peptide that will not form the SNARE complex responsible for membrane fusion, thus inhibiting the release of acetylcholine into the NMJ (Figure 2.2).²²²⁻²²³

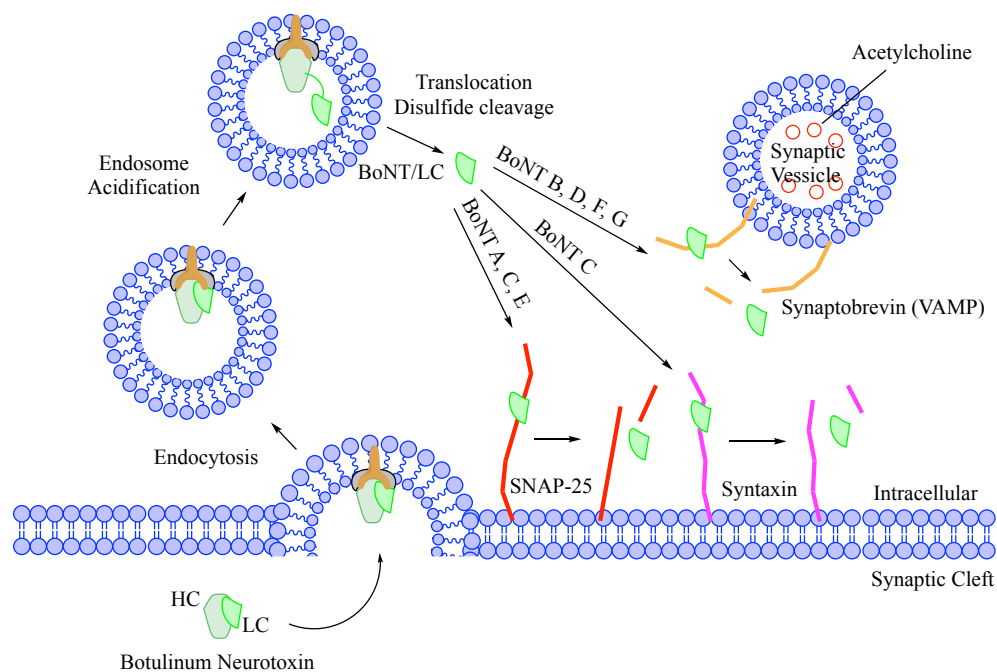
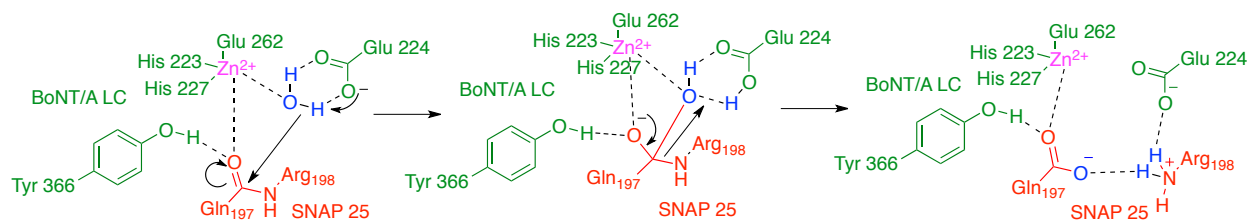


Figure 2.2. Mechanism of BoNT intoxication.^{191,202}

The mechanism of zinc-mediated hydrolysis is exemplified by the reaction of SNAP-25 with the LC of BoNT/A. Cleavage begins with coordination of the catalytic zinc, to the carbonyl of the amide, thereby activating the amide toward hydrolysis. Water then adds into the amide to form a tetrahedral intermediate that is stabilized by the catalytic zinc and adjacent Tyr³⁶⁶ residue. Subsequent elimination of the amine generates Gln¹⁹⁷ acid (Scheme 2.1).²²²



Scheme 2.1. Mechanism of SNAP-25 hydrolysis.²²³

To date, the only approved treatments of BoNT's are vaccines (antitoxins). In 2013, the Botulism Antitoxin Heptavalent (BAT) was approved by the FDA and is the current standard of care for BoNT intoxication of adults.¹⁹¹ These vaccines work as prophylactic treatments and only remain effective for a few months to one year.²²⁴ In addition, the vaccines are expensive to

produce (ca. \$2100/dose), and are made from equine botulinum antitoxin that has been shown to have adverse effects in ~10% of the population.^{191,225} The monoclonal antibodies produced by vaccines are only effective if applied before exposure to the toxin as the toxins have been found in the motor neurons within minutes to hours after exposure.²²⁶ Due to the lack of a readily available treatment of BoNT's and the possibility of a widespread bioterrorism event, the development of a small molecule inhibitor of BoNT/A LC is highly desirable.

2.1.1 Peptide Based Inhibitors of BoNT's

Initial inhibitors of the LC were peptides and peptidomimetics that mimic the truncated SNAP-25 (amino acids 187-206) and have been primarily used as chemical probes and in assay development for the measurement of inhibition of BoNT's.²²⁷⁻²³⁴ Early work by Schmidt and Bostian used a truncated SNAP-25 (amino acids 187-206) to monitor the proteolytic activity of BoNT/A LC. After screening a number of truncated peptides it was discovered that the relative size and sequence of the truncated peptide was important and that the 17-mer had the highest k_{cat} .^{227,235} Schmidt and Stafford developed a HTS FRET (fluorescence resonance energy transfer) assay that uses the modified SNAP-25 fragment SNRTRIDEAN[dnpK]RA[daciaC]RML as a FRET substrate.²³⁶ The FRET substrate for this assay tends to suffer from photodegradation or fluorescence quenching and is usually run along with HPLC analysis to eliminate false positives.²³⁶⁻²³⁹ Janda and coworkers developed another HTS that relies on a modified SNAP-25 fragment (FITC)-TRIDEANQRATK(DABCYL)M known as SNAPtide, which is more resistant to photodegradation and has higher bench stability.²⁴⁰⁻²⁴³ When using SNAPtide as a FRET substrate the N-terminal fluorophore, fluorescein isothiocyanate (FITC), is quenched by the C-terminal 4-((4-dimethylamino)phenyl)azo) benzoic acid (DABCYL).²⁴³ These substrates are also

used in HPLC assays to measure the extent of proteolysis of the truncated peptide that can be directly correlated to a ligand binding affinity or IC_{50} .

In the search for more potent and specific small molecule non-peptidic inhibitors (SMNPI's) of BoNT/A, extensive work has focused on using computational models of the binding site and known SAR to probe for a more potent or specific structure. Based on the previous work on modified SNAP-25 fragments by Schmidt and coworkers, the pseudo-peptide mpp-RATKM (Figure 2.3) was developed. It was initially identified through a cysteine scan of a SNAP-25 (187-203) fragment and further optimized through SAR to provide a mpp-RATKM that had a K_i of 300 nM.^{228-229,231,244} Burnett and coworkers used this pseudo-peptide along with conformational and docking studies of a library of previously known active compounds to elucidate the pharmacophore of BoNT/A LC (Figure 2.3).^{202,238,244-247}

Compound I1 was derived from the SNAP-25 fragment QRATKML and is the most potent non-zinc chelating peptide mimetic to date.²²² In the Wipf lab, several peptidomimetics have also been previously synthesized as a hybrid of RRG²⁴⁸ and I1 resulting in 3 new peptides with K_i 's ranging from 0.3 μ M to 1 μ M.²³³ Further development of these peptides has led to cyclic peptides analogs.²⁴⁹ Unfortunately, even shorter peptides suffer from high polar surface areas (>300), which could cause limited cell permeability that may lead to a poor therapeutic profile. The shorter tetrapeptide (RRGC) could be a potential lead compound for further backbone modifications as it has the lowest MW of all truncated peptides and a promising K_i of 160 nM. Compound RRG²⁴⁸ was shown to be protective and non-toxic to chick motor neurons at 600 μ M along with an intracellular stability over 24 hours (Figure 2.3).

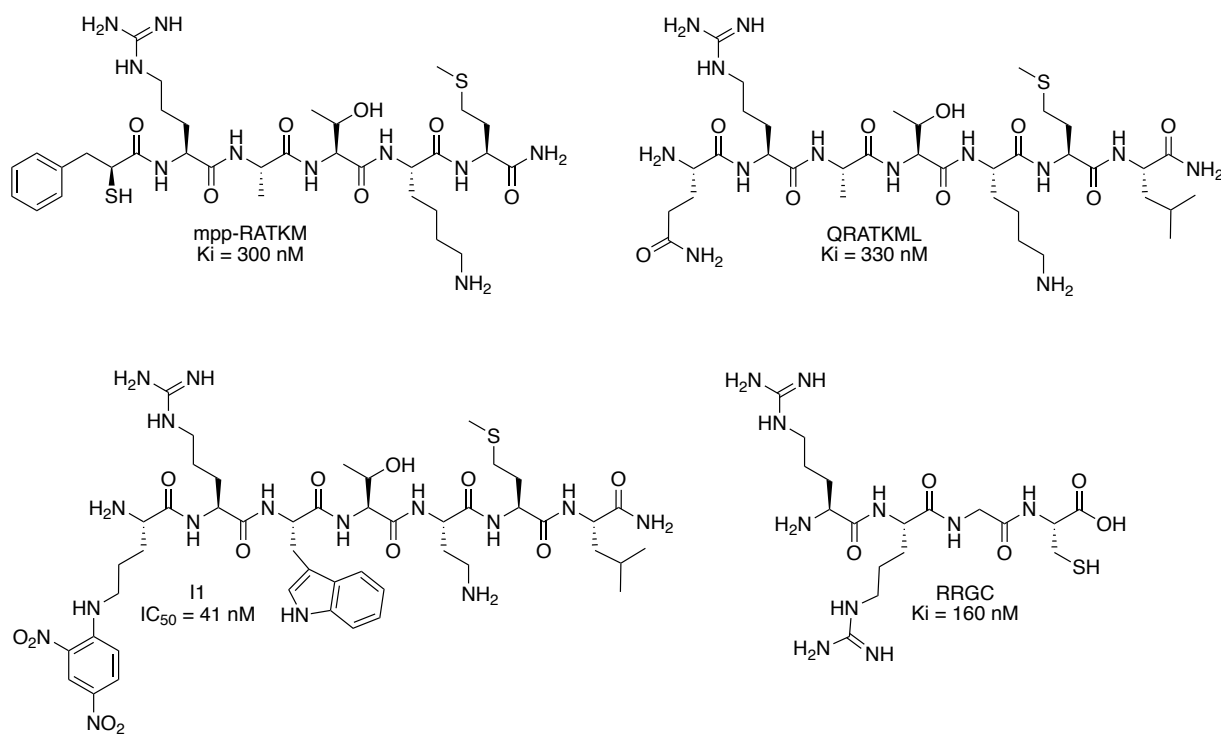


Figure 2.3. Structures of peptide-like inhibitors of BoNT/A.

2.1.2 Small Molecule Inhibitors of BoNT's

As peptides often suffer from high metabolism and low absorption, significant efforts have been made toward pinpointing a small molecule non-peptidic inhibitor of BoNT. As a result a variety of small molecule scaffolds have emerged in the literature for the treatment of BoNT over the past 30 years.

Hydroxamic acids have emerged as very potent inhibitors of BoNT LC. The catalytic domain has been cocrystallized to elucidate their binding mode, showing that the hydroxamic acids chelate zinc in the active site.²⁵⁰⁻²⁵² The earliest potent (< 1 μ M) nonpeptidic hydroxamic acid inhibitor **2.1** was identified from a screen of a small library of hydroxamic acids (Figure 2.4).^{239,252-253} Hydroxamic acid **2.1** had a promising *in vitro* IC_{50} of 0.4 μ M but was found to be toxic in neuroblastoma N2a cells at 5 μ M. Subsequently, in two separate mouse studies, **2.1** did

not show significant protection in BoNT intoxicated mice versus the controls.²⁵³⁻²⁵⁶ *In silico* screening of 2.5 million hydroxamic acid derivatives led to the discovery of **2.2** that demonstrated low μM *in vitro* activity and promising *in vivo* survival with 60% survival compared to the control after 48 h.²⁵⁷⁻²⁵⁸ Despite concerns due to hydroxamic acids being flagged as potentially concerning functionalities, several examples of FDA approved drugs contain this moiety.²⁵⁹⁻²⁶¹

Covalent inhibitors of BoNT/A LC have also been investigated, which act by binding to the free Cys¹⁶⁵ produced by disulfide bond reduction during the release of the LC into the cytosol.²⁶²⁻²⁶³ These compounds are noncompetitive inhibitors of BoNT and covalently bind through the Michael acceptor acrylonitrile. Compound **2.3** was identified from a 70,000 compound library screen and was further optimized to **2.4** that had shown increased selectivity for BoNT/A LC in a chick neuronal cell-based assay (Figure 2.4). IC_{50} values for **2.3** and **2.4** were calculated using a HTS FRET assay and verified using an HPLC assay.²³⁵⁻²³⁶ Advantages of these selective covalent inhibitors include increased biochemical efficiency since their binding is not in equilibrium and can outcompete endogenous ligand binding at lower concentrations as exhibited by numerous FDA approved covalent drugs. Unfortunately, the possible off target effects of these covalent inhibitors include alkylation or reaction with glutathione, which could lead to potential toxicity.²⁶⁴

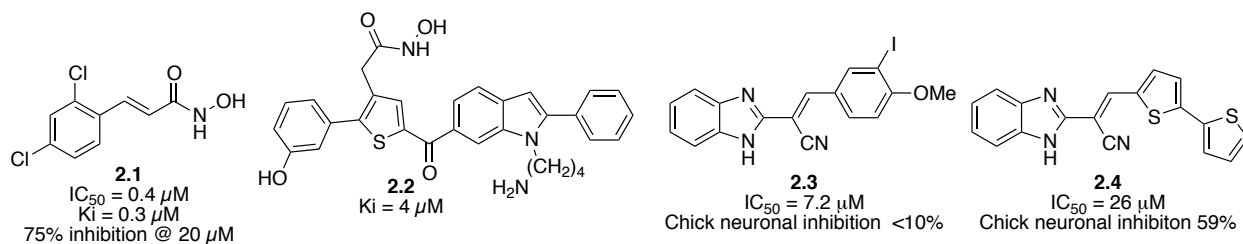


Figure 2.4. Hydroxamic acid and covalent inhibitors of BoNT.

The antimalarial aminochloroquinolines (ACQ) have also been explored as inhibitors of BoNT's (Figure 2.5). Compound **2.5** (also known as Q2-15) was discovered from a HTS of the NCI diversity set of a variety of ACQ containing substrates.²³⁸ In particular, **2.5** was shown to inhibit BoNTA with an IC₅₀ of 11 μM. More recently a series of hybrid structures such as **2.6** were synthesized and found to have submicromolar IC₅₀ of 0.3 μM in an *in vitro* assay. Although compounds such as **2.6** show submicromolar *in vitro* inhibition of BoNT they suffer from high MW and LogP, which raises concerns regarding aqueous solubility and potentially short half-lives *in vivo*.

The quinolinol **2.7** was discovered as a result of several iterations of virtual screening, hit validation, and safety evaluations (Figure 2.5).²⁶⁵ Compound **2.7** was shown to be efficacious both in *in vitro* with 97% inhibition of BoNTA/LC at 20 μM and *ex vivo* in a mouse phrenic nerve diaphragm assay (MPNHDA) by significantly slowing the onset of muscle paralysis at 10 μM. Recently, two independent efforts to optimize this scaffold yielded **2.8**²⁶⁶ and **2.9**.²⁶⁷ A small SAR of the quinolinol **2.7** afforded compound **2.8** with an improved *in vitro* IC₅₀ of 0.6 μM and slowed the onset of muscle paralysis at 20 μM in the MPNHDA assay.²⁶⁶ A crude library screen of sulfonylated quinolinols, hit validation, and SAR optimization yielded sulfonamide **2.9** with a similar *in vitro* efficacy to **2.7** (1.6 μM) and slowed the onset of muscle paralysis at 20 μM in the MPNHDA assay.²⁶⁷ Interestingly, inhibition kinetics of quinolinol **2.9** have shown that the inhibition is uncompetitive with respect to SNAP-25 binding.²⁶⁷ These compounds containing the quinolinol moiety remain interesting scaffolds in the pursuit of inhibitors of BoNT as they display promising physiochemical properties and show low μM activity in both *in vitro* and *ex vivo* assays (Figure 2.5).

Finally, NSC 240898 displayed a dose-dependent protection of SNAP-25 in chick spinal motor neurons with low cytotoxic effects even at 40 μM (Figure 2.5).²⁴⁴ Based on its biological activity and low cytotoxicity, NSC 240898 is an attractive target for further development.

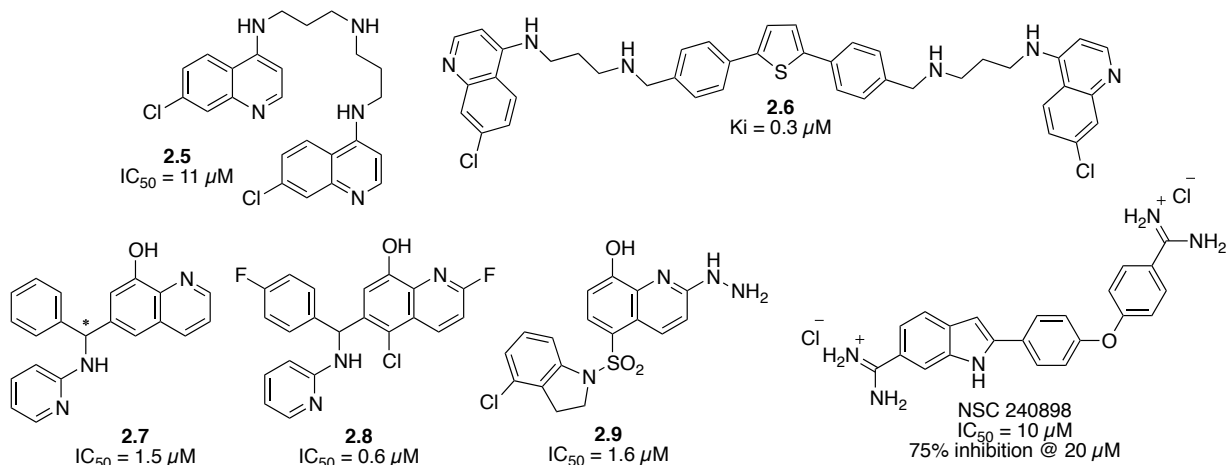


Figure 2.5. Other small molecule non-peptidic inhibitors of BoNT.

2.1.3 Structure-Activity Relationship of NSC 240898: Previous Work in the Wipf Group

Despite the dose-dependent protection of SNAP-25 and low cytotoxicity of NSC 240898, its activity against BoNT was relatively poor ($\text{IC}_{50} = 10 \mu\text{M}$). In an effort to enhance the potency and learn more about the BoNT binding pocket, Wipf and coworkers investigated the SAR around NSC 240898 with structural modifications on the indole, diaryl ether, and polar end groups.²⁶⁸ The structure was divided into 5 major structural zones for modification (Figure 2.6).

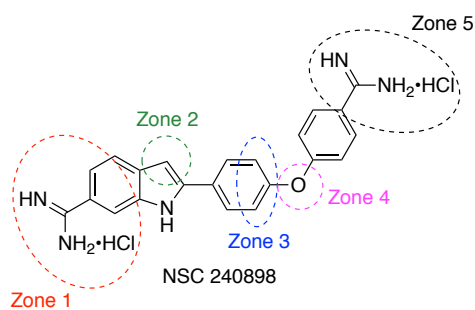
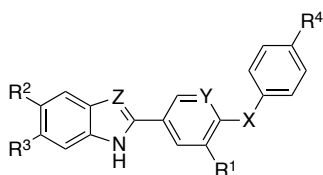


Figure 2.6. Zones for structural modifications of NSC 240898.

The SAR of the NSC 240898 scaffold showed a number of modifications that could be tolerated within the binding site (Table 2.1). Position R¹ in zone 3 tolerated functionalization with -OMe and -Cl, with the resulting analogs achieving similar potency to the parent scaffold NSC 240898. This indicates that there is an available pocket in the binding site that allows minor variations in steric bulk without a loss in potency. The diaryl thioether linkage was found to increase potency, which is most likely due to the smaller bond angle leading to closer proximity of the terminal imidazolines for hydrogen bonding with Glu⁵⁶. Interestingly, NSC 377363 (Table 2.1, entry 15) with a NH in place of the diaryl ether was equipotent to NSC 240898 demonstrating that both a hydrogen bond donor and hydrogen bond acceptor are tolerated in the binding site. Alternating R² and R³ with amidine (Am) and imidazoline (Im) substituents showed some flexibility in the binding site, but substitution at R₃ was more potent. The terminal substituents R³ and R⁴ could tolerate either the bis-Am or bis-Im, however, neutral (nitriles, CF₃) or acidic functionalities (tetrazoles) were inactive (Table 2.1).²⁶⁸⁻²⁶⁹ The basic Am or Im functionality likely interacts through hydrogen bonding within the binding site. Finally, shortening the distance between the two polar contacts or removing a polar contact led to a decrease in potency. Not only did this SAR reveal new electrostatic and steric information about the BoNTA/LC binding site it also led to the identification of compound **2.10** (Table 2.1, entry 13), as a new more potent lead structure.

Table 2.1. Structure-activity relationship of NSC 240898.²⁶⁸

Entry	Structure ^b							% BoNT/A LC inhibition ^a
	X	Y	Z	R ¹	R ²	R ³	R ⁴	
1	O	CH	N	H	H	Am	Am	24.7 (±1.5)
2	O	CH	N	H	H	Im	Im	34.8 (±1.4)
3	O	CH	CH	H	Am	H	Am	58.8 (± 3.3)
4	O	CH	CH	H	Im	H	Im	51.4 (± 4.6)
5	O	CH	CH	H	H	Am	CF ₃	25.2 (± 3.4)
6	O	CH	CH	H	H	Im	CF ₃	43.3 (± 7.2)
7	O	CH	CH	Cl	H	Am	Am	64.4 (± 2.1)
8	O	CH	CH	Cl	H	Im	Im	64.8 (± 4.4)
9	O	CH	CH	OMe	H	Am	Am	58.0 (± 6.7)
10	O	CH	CH	OMe	H	Im	Im	69.8 (± 1.8)
11	O	N	CH	H	H	Am	Am	52.7 (± 5.5)
12	O	N	CH	H	H	Im	Im	46.1 (± 1.2)
13	S	CH	CH	H	H	Am	Am	80.3 (± 6.7)
14	S	CH	CH	H	H	Im	Im	67.3 (± 3.6)
15	NH	CH	CH	H	H	Am	Am	70
15	O	CH	CH	H	H	CN	CN	NI ^c
16	O	CH	CH	H	H	Tet	Tet	NI ^c
17	O	CH	CH	H	H	Am	Am	73.5 (± 7.5) ^d

^ainhibition of BoNTA/LC at 20 μM using the assay as previously described.^{247,268} ^bTet, tetrazole; Am, Amidine; Im, Imidazoline; ^cNI, no inhibition; ^dNSC 240898.

2.2 RESULTS AND DISCUSSION

With only a modest improvement in efficacy from NSC 240898, compound **2.10** remained a viable target for the further optimization of efficacy, solubility, and metabolic stability. To further optimize **2.10** we constrained the diaryl thioether into an eight membered ring in an attempt to increase solubility and potency. Additionally we also investigated the 1,2,4-triazine as

a substitution for the imidazoline rings of **2.10** as imidazolines pose a potential metabolic risk through hydrolysis or oxidation.

2.2.1 Synthesis of 3-(4,5-Dihydro-1*H*-imidazol-2-yl)-9-(6-(4,5-dihydro-1*H*-imidazol-2-yl)-1*H*-indol-2-yl)-6,7-dihydro-5*H*-dibenzo[*b,g*][1,5]thiazocine

The previous SAR of NSC 240898²⁶⁸ revealed that the diaryl thioether increased activity versus the parent compound due to the decreased bond angle of the aryl rings. It was also noted that steric bulk could be tolerated around the diaryl ether (Table 2.1). Conformationally constrained analogs of **2.10** were proposed to further increase binding affinity, solubility, and drug-likeness.²⁷⁰ The thiazocinone and thiazocine inhibitors take advantage of the tight thioether bond angle, and further constraint into the 8-membered ring greatly reduces the entropic penalty of binding and potentially enhancing binding site interactions of the polar end caps. These analogs also have additional hydrogen bond donor and acceptor functionality that may lead to increased binding interactions in the active site. The thiazocinone analogs **2.11-2.14** were previously synthesized by Drs. Igor Opsenica and Jared Hammill (Figure 2.7).

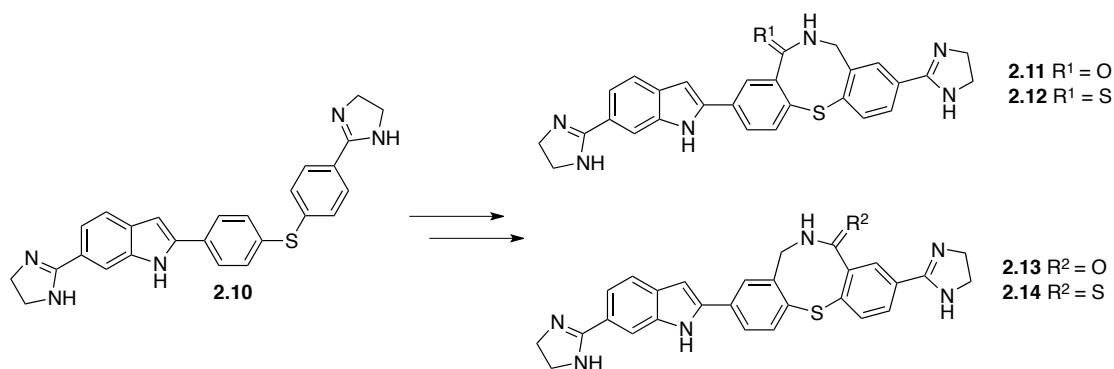


Figure 2.7. Structures of **2.10**, lactam, and thiolactam analogs.

The diaryl bond angle and conformation of the eight-membered ring mimic the binding mode of NSC 240898 (Figure 2.8). Smaller rings produce relatively planar conformations,²⁷¹ while larger rings increase steric bulk and are conformationally more labile.

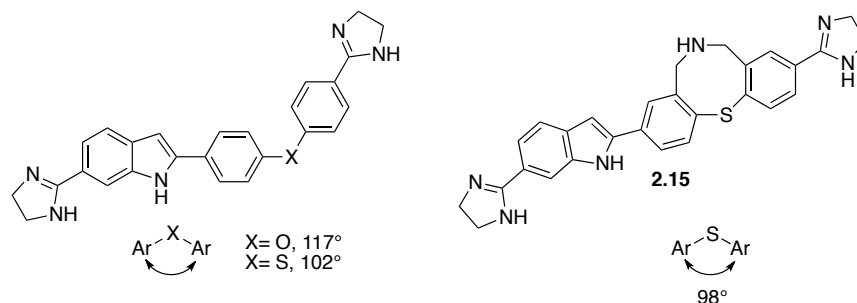
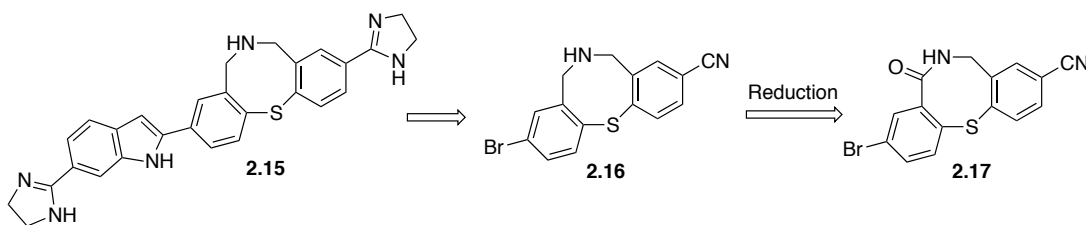


Figure 2.8. Bond angle of diaryl (thio)ether linkage.²⁷²

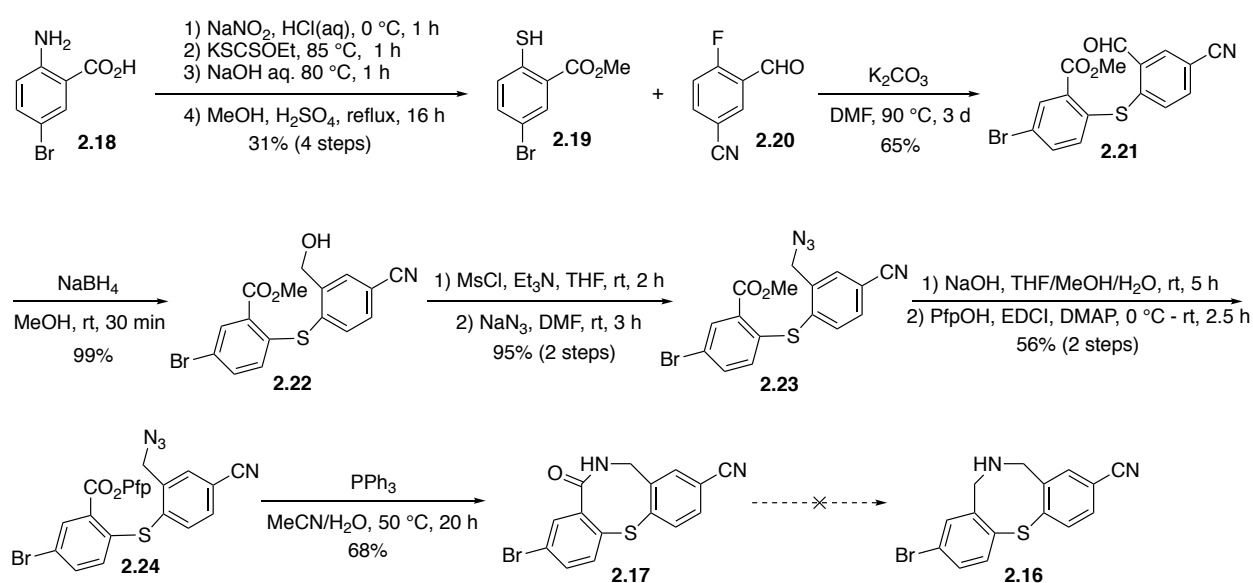
The thiazocine variant of **2.10** was the final member of this constrained series to be synthesized. Initially, we envisioned that we could access the thiazocine through a late stage reduction of the lactam **2.17** a common building block in the synthesis of the previous thiazocinone inhibitors **2.11-2.14** (Scheme 2.2).



Scheme 2.2. Retrosynthetic approach to common intermediate lactam **2.17**.

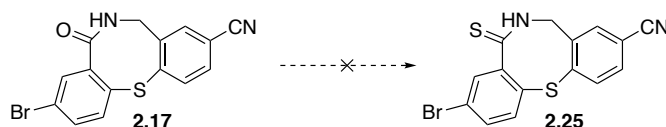
The synthesis of the key lactam intermediate **2.17** began with the condensation of thiol **2.19** with fluorobenzonitrile **2.20** to form **2.22**. Thiol **2.19** can easily be prepared by diazotization of aniline **2.18** followed by displacement of the diazo intermediate using potassium *O*-ethyl xanthate.²⁷³ The resulting xanthate ester is hydrolyzed to form the thiol. The carboxylic acid of **2.19** was esterified to afford the methyl ester **2.19**.²⁷⁴ The aldehyde **2.21** was reduced using sodium borohydride and the resulting alcohol **2.22** was mesylated and displaced with sodium azide. The methyl ester **2.23** was saponified then subjected to a Steglich esterification with

pentafluorophenol (Pfp) to deliver Pfp ester **2.24**. An intramolecular Staudinger ligation was used to prepare the corresponding lactam **2.17** in good yield (Scheme 2.3). Attempts to reduce the lactam using transition metal catalysis with silanes, Hantzsch ester hydride reductions, borohydride reductions, and borane methyl sulfide reductions were unsuccessful and yielded complex mixtures of products, dehalogenation, or overreduction.²⁷⁵⁻²⁷⁷ Using zinc triflate and TMDS afforded the product, but reaction mixtures were very difficult to purify due to the solubility and polarity of the free amine **2.16**.²⁷⁸



Scheme 2.3. Synthesis of thiazocinone **2.17**.

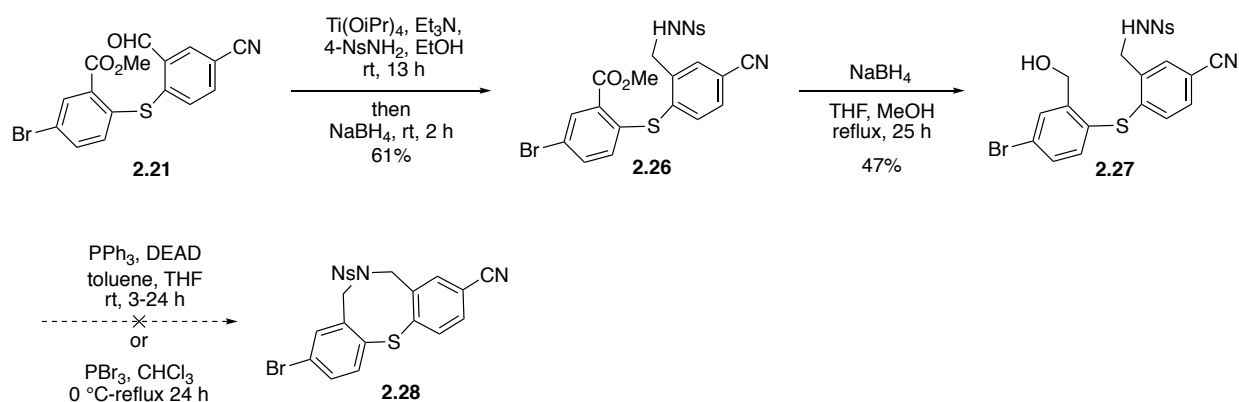
Due to the difficulty of reduction of the amide **2.17**, the thioamide **2.25** was pursued as a synthetic target (Scheme 2.4). Thioamides can be reduced with the use of mild reducing agents like Raney-Ni,²⁷⁹ or via *S*-alkylation and reduction using metal borohydrides.²⁸⁰ Unfortunately, forming the thioamide was unsuccessful using a number of precedented methods, including Lawesson's and Belleau's reagents or P₄S₁₀.²⁸¹⁻²⁸²



Scheme 2.4. Attempted synthesis of thiolactam **2.25**.

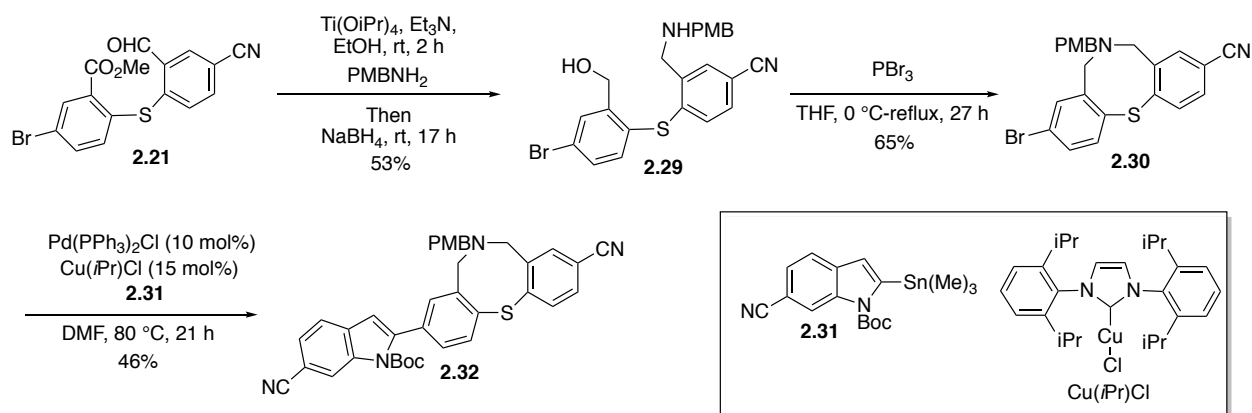
Dibenzo[*b,g*][1,5]thiazocines such as the desired intermediate **2.16** have been previously constructed by two main routes: the reduction of the corresponding lactam using LAH²⁸³⁻²⁸⁴ or via an alkylation approach.²⁸⁵⁻²⁸⁸ Since LAH reductions were not tolerated on this system due to the presence of the nitrile, an alkylation approach was explored. It has been shown that medium sized rings could be formed through a Mitsunobu reaction using an *N*-4-nitrophenylsulfonyl (nosyl, Ns) protected amino alcohol.²⁸⁸

Initially, we synthesized the *N*-nosyl thiazocine precursor **2.27** to determine if the Mitsunobu cyclization would be successful on our substrate. The synthesis of **2.28** began from aldehyde **2.21** (Scheme 2.5). Attempts at a classical reductive amination using STAB were unsuccessful due to slow imine formation.²⁸⁹ Preforming the imine by CeCl₃,²⁹⁰ TiCl₄,²⁹¹ or Bronsted acid catalysis²⁹² was also unsuccessful. Gratifyingly, the formation of *N*-nosyl protected amine **2.26** proved successful when aldehyde **2.21** was subjected to a titanium(IV)isopropoxide mediated condensation with *p*-nitrobenzenesulfonamide, followed by sodium borohydride reduction. The ester **2.26** was then further reduced to the amino alcohol **2.27**. Unfortunately, neither the Mitsunobu or PBr₃ cyclization of compound **2.27** were successful in obtaining the *N*-nosyl thiazocine **2.28**. This was most likely due to the fact that our system is more strained than what had been previously used by Kan et al. for the Mitsunobu cyclization²⁸⁸ and the sulfonamide was not nucleophilic enough to displace the benzylic bromide formed under the PBr₃ conditions.



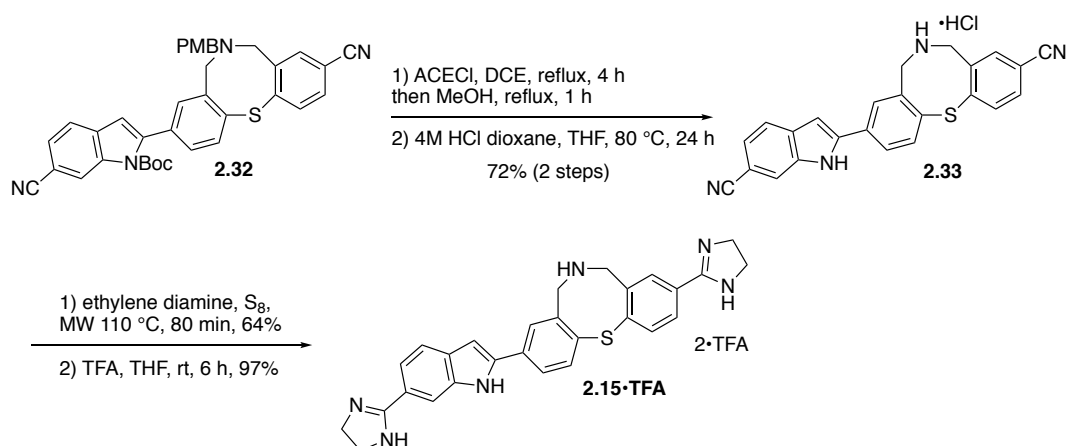
Scheme 2.5. Synthetic approach to *N*-nosyl thiazocine **2.28**.

To affect a cyclization, the protected amine was modified to a *p*-methoxybenzylamine, which is more nucleophilic and should be readily removed at the end of the synthesis. Combining the aldehyde **2.21** and *p*-methoxybenzylamine with titanium(IV)isopropoxide and an excess of sodium borohydride, delivered amino alcohol **2.29** in a one-pot reaction, albeit in modest yield (Scheme 2.6). Sequential reductions of the unreacted ester of **2.29** to the amino alcohol **2.29** were low yielding. In attempts to form the thiazocine ring **2.30**, only PBr_3 ²⁸⁷ was successful. The literature PBr_3 conditions²⁸⁷ using chloroform as a solvent afforded clean product on small scale, however, our large scale reactions were plagued by a chloroform adduct side product. Gratifyingly, when the solvent was changed to THF at a concentration of 10 mM, the cyclization proceeded in good yield. The thiazocine core **2.30** was coupled to indole stannane **2.31** via a Stille cross coupling to afford **2.32**.²⁹³ The temperature of the coupling proved critical to the reaction yield as Boc removal could be observed by NMR analysis at 100 °C. Indole stannane **2.31** was prepared by a Boc-protection of 6-cyanoindole followed by metalation of the 2-position and quenching with trimethyltin chloride.



Scheme 2.6. Synthesis of coupling product **2.32**.

Following the successful synthesis of the coupling product **2.32**, PMB removal conditions were explored. The PMB protecting group removal by conventional methods proved unsuccessful. Catalytic hydrogenation²⁹⁴ only returned starting material, while acidic conditions such as TFA or HCl led to decomposition and facilitated hydrolysis of the nitriles. Oxidative conditions using DDQ led to PMB deprotection with undesired oxidation of the thioether. TMSI²⁹⁵ and TBSOTf provided an excellent method for Boc deprotection; however, the PMB group remained intact. Chlorosulfonyl isocyanate (CSI) provided the bis-deprotection product along with a number of other undesired products. Instead, the PMB protecting group was removed using α -chloroethylchloroformate (ACECI) to afford the PMB-deprotected thiazocine in good yield.²⁹⁶ Boc deprotection of the indole was accomplished by heating in 4 M HCl in dioxane at 80 °C due to the insolubility of the compound in THF or 1,4-dioxane at rt. The HCl salt **2.33** was used for the formation of the imidazolines **2.15** using elemental sulfur, ethylene diamine, and microwave irradiation.²⁹⁷ Thiazocine **2.15** was obtained as a bis TFA salt, and was submitted to the USAMRIID for biological testing (Scheme 2.7).



Scheme 2.7. Completion of the synthesis of **2.15•TFA**.

2.2.2 Biological Activity of Thiazocine Analogs

Following the completion of the synthesis of **2.15•TFA**, a sample was tested for BoNT inhibition using a variant of the SNAPtide HPLC assay at the USAMRIID. We discovered that the activity of **2.15•TFA** was very similar to **2.10**, further confirming that we are able to introduce steric bulk without significant penalties to the activity (Table 2.2).²⁶⁸ However, this also indicates that **2.15•TFA** has not gained any favorable binding interactions within the large binding pocket of BoNT/LC. Additionally, it is possible that introduction of the thiazocine may have perturbed the imidazoline orientation in the binding site leading to a less favorable interactions that cause a slight decrease in activity.

Table 2.2. Biological activity of NSC 240898 analogs.

Entry	Compound	BoNT IC_{50}^a (μM)
1	2.10	5.2 ± 0.1
2	2.15•TFA	6.3 ± 2.9
3	NSC 240898	10.7 ± 0.5

^a IC_{50} 's were determined using the previously described SNAPtide HPLC assay.²⁴² Data were collected using duplicate data points over two independent assays.

2.2.3 Synthesis of 1,2,5,6-Tetrahydro-1,2,4-triazines

In addition to replacing the diarylthioether in **2.10** with a thiazocine ring to generate compound **2.15** we wanted to substitute the imidazoline rings as they are prone to hydrolysis and metabolic oxidation (Figure 2.9). Based on a previous SAR study, the bis-imidazole analogs were found to be inactive because they tend to have other binding modes to chelate Zn.²⁴⁶ 1,2,5,6-Tetrahydro-1,2,4-triazines (1,2,4-triazines) represented an attractive alternative to the imidazoline functionality as they maintain a similar pKa while displaying increased hydrolytic stability.²⁹⁸⁻³⁰⁰ Thus, a new analog containing terminal bis-1,2,4-triazine moieties should retain the potency of the parent compound without being rendered inactive by metabolic oxidation, as even the oxidation product has a similar pKa to the parent compound.(Figure 2.9).

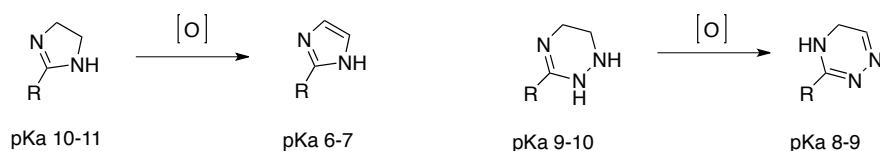


Figure 2.9. Effect of oxidation on pKa of imidazolines vs 1,2,4-triazines.

The Wipf group has been interested in constructing 1,2,4-triazines for many years as they are a key structural component of the furanosteroid natural product noelaquinone (Figure 2.10).³⁰¹⁻³⁰² Wipf and coworkers' previous synthesis of the DEF fragment of noelaquinone resulted in the development of a new method to form 1,2,4-triazines through an intramolecular Staudinger *aza*-Wittig (SAW) reaction.³⁰³ The SAW reaction is a useful tool for the synthesis of heterocyclic compounds and natural products.³⁰⁴ It combines the Staudinger phosphazine ylide formation with the *aza*-Wittig addition to a carbonyl group.³⁰⁵⁻³⁰⁹

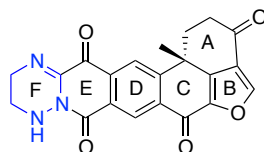
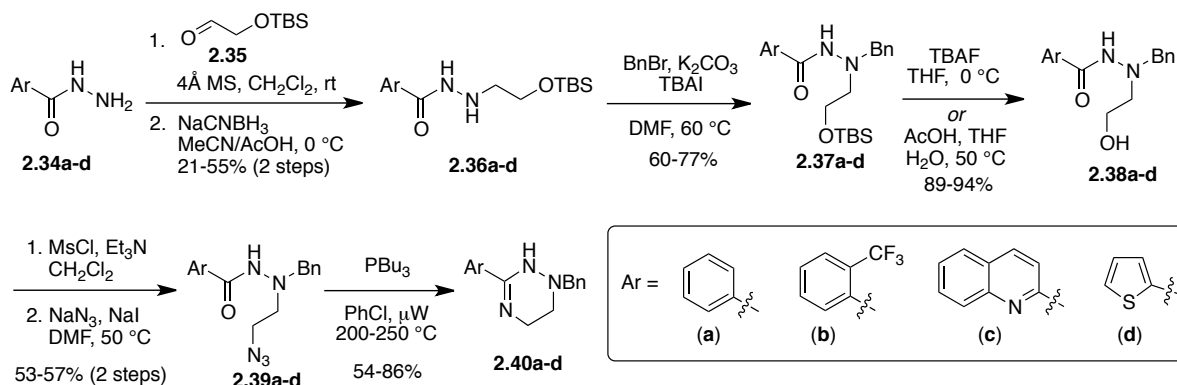


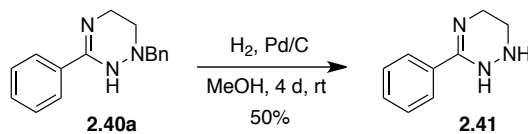
Figure 2.10. Structure of noelaquinone.

Initial routes to form the 1,2,4-triazines in the Wipf group were pioneered by former students Dhezi Fu and David Amantini. These linear approaches began with a reductive amination of aldehyde **2.35** on various aromatic hydrazides **2.34a-2.34d**. Benzoylation and TBS deprotection afforded alcohols **2.38a-2.38d**. A subsequent mesylation, azidation, and SAW cyclization afforded the triazines **2.40a-2.40d** in good yields (Scheme 2.8).



Scheme 2.8. Linear synthesis of 1,2,4-triazines.

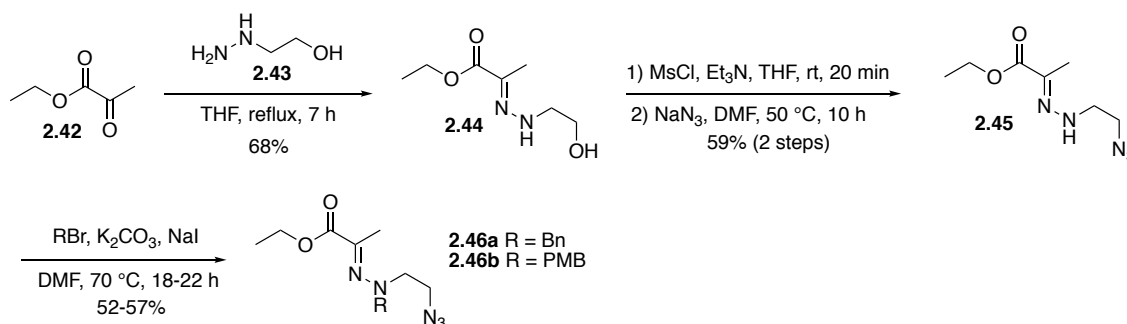
Fu and Amantini also explored the deprotection of the benzyl group on **2.40a** and found that catalytic hydrogen conditions over 4 days the product was obtained in modest yields without reduction of the C=N bond (Scheme 2.9).



Scheme 2.9. Depbenzylation of triazine **2.40a**.

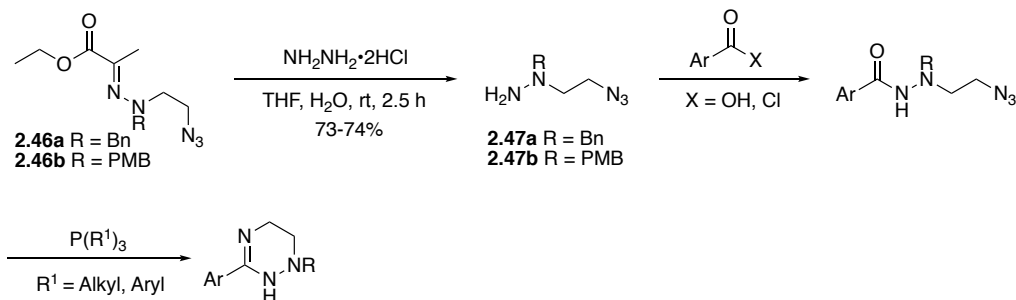
A more convergent approach was developed by converting the hydrazine to the stable hydrazone, which can be unmasked prior to coupling with carboxylic acid or acid chloride

moieties.³⁰³ The synthesis of hydrazones **2.45a** and **2.45b** began with the condensation of hydrazinoethanol (**2.43**) onto ethyl pyruvate (**2.42**) to provide the hydrazone **2.44** (Scheme 2.10). The alcohol **2.44** was mesylated and displaced using sodium azide. The corresponding azidohydrazone **2.45** was protected with BnBr or PMBBBr to afford the shelf-stable azidohydrazone precursors **2.46a** and **2.46b** respectively. The pyruvate hydrazone **2.46b** was previously prepared on 45 g scale and found to be bench stable for months with no noticeable decomposition according to ¹H NMR.



Scheme 2.10. Synthesis of hydrazones **2.46a** and **2.46b**.

Hydrazine exchange of hydrazones **2.46a-2.46b** afforded the desired *N*(2)-protected hydrazines **2.47a-2.47b** in good yields. Using peptide coupling conditions or the acyl chloride, hydrazides can be formed in varying yields. The corresponding hydrazide can then undergo cyclization via a SAW reaction to form the 1,2,4-triazine (Scheme 2.11).

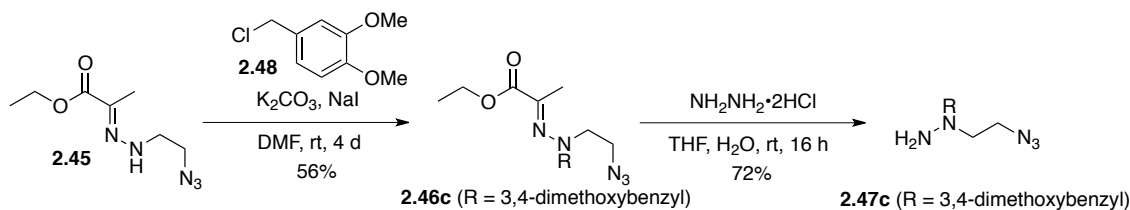


Scheme 2.11. Synthetic route to 1,2,4-triazines.

2.2.3.1 Screening and Optimization of 1,2,4-Triazines

To simulate the formation of the 1,2,4-triazine on a more complex system and to further expand the substrate scope we synthesized several new triazine systems. In addition to expanding the substrate scope we also developed a new hydrazine with a more labile protecting group to allow for milder deprotection conditions.

We synthesized a novel 3,4-dimethoxybenzyl protected hydrazine **2.47c** that should be more acid-labile than the corresponding PMB-protected derivative. In a similar synthetic sequence to previous hydrazines we arrived at azide intermediate **2.45**. Alkylation with 3,4-dimethoxybenzyl chloride afforded hydrazone **2.46c** in modest yields. Deprotection using hydrazine afforded our desired hydrazine **2.47c** in good yields (Scheme 2.12).



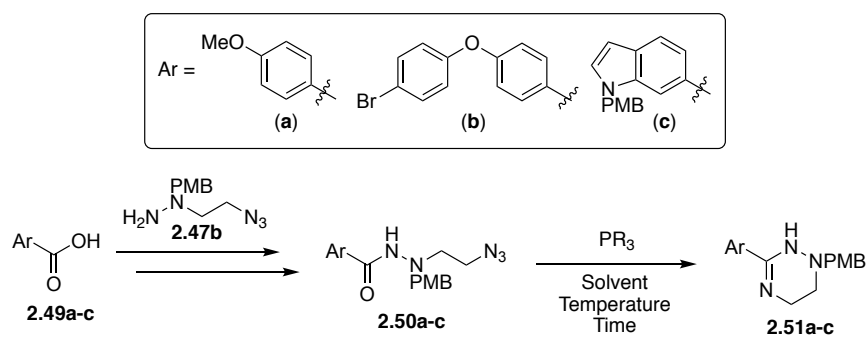
Scheme 2.12. Synthesis of 3,4-dimethoxybenzyl protected hydrazine **2.47c**.

Since low molecular weight compounds with a high N to C ratio are potentially explosive,³¹⁰ we also determined the thermal stability of azidohydrazines **2.47b** and **2.47c** by differential scanning calorimetry (DSC) to establish the safety profile of these compounds. Gratifyingly, we found that compounds **2.47b** and **2.47c** were stable up to 150 °C and did not undergo complete decomposition until >200 °C.

Azidohydrazine **2.47b** was acylated directly via the acyl chloride or by peptide coupling conditions with the aromatic carboxylic acid. The corresponding hydrazides **2.50a-2.50c** were subjected to the SAW conditions to afford the *N*-protected 1,2,4-triazines **2.51a-2.51c** in this convergent synthesis (Table 2.3). While the SAW reaction generally proceeded with acceptable

to good yields using *tri-n*-butyl phosphine, we used the conversion of **2.50a** to **2.51a** to explore the scope of the variation of phosphines, solvents, temperature, and reaction times (Table 2.3). A solvent switch to 1,2-dichlorobenzene provided similar yields to chlorobenzene. Using aromatic phosphines such as P(Ph)₃ or PMe(Ph)₂ afforded the product in decreased yield and were difficult to separate from the corresponding phosphine oxides via chromatography. Finally, using P(Me)₃, the SAW reaction provided modest yields but the corresponding water soluble phosphine oxide was readily separable from the triazine product.

Table 2.3. Screening of conditions for SAW cyclization.

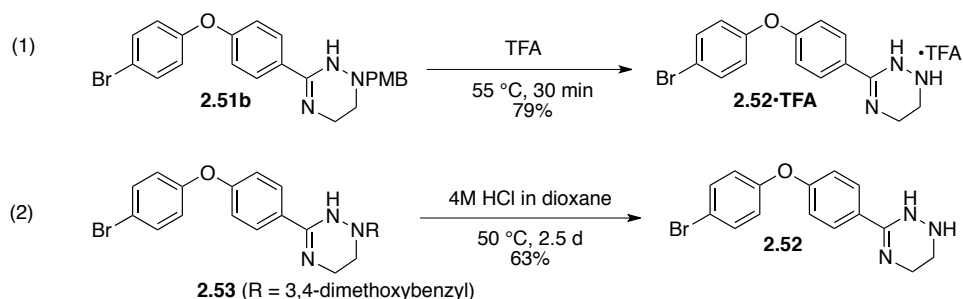


Entry	PR ₃	Solvent	Temperature/time ^c	Yield
1	P(<i>n</i> -Bu) ₃	<i>o</i> -1,2-dichlorobenzene	MW, 180 °C, 1 h	47%
2	P(<i>n</i> -Bu) ₃	PhCl	MW, 180 °C, 1.5 h	41%
3	P(<i>n</i> -Bu) ₃	PhCl	MW, 180 °C, 2 h	50%
4	P(Ph) ₃	PhCl	MW, 180 °C, 1 h	42% ^a
5	P(Ph) ₃	PhCl	MW, 180 °C, 1.5 h	38% ^a
6	P(Ph) ₃	PhCl	150 °C, 12 h	dec.
7	PMe(Ph) ₂	PhCl	MW, 180 °C, 1.5 h	37% ^b
8	PMe(Ph) ₂	PhCl	MW, 180 °C, 2 h	42% ^b
9	P(Me) ₃	PhCl	MW, 180 °C, 1 h	38%
10	P(Me) ₃	PhCl	MW, 180 °C, 1.5 h	29%; dec.

^aProduct contains P(Ph)₃O; ^bproduct contains PMe(Ph)₂O; ^call reactions used a 50 mg scale of **2.50a**

With the triazine substrates in hand, we investigated the removal of the PMB and 3,4-DMB protecting group. The PMB proved difficult to remove. The use of reductive conditions

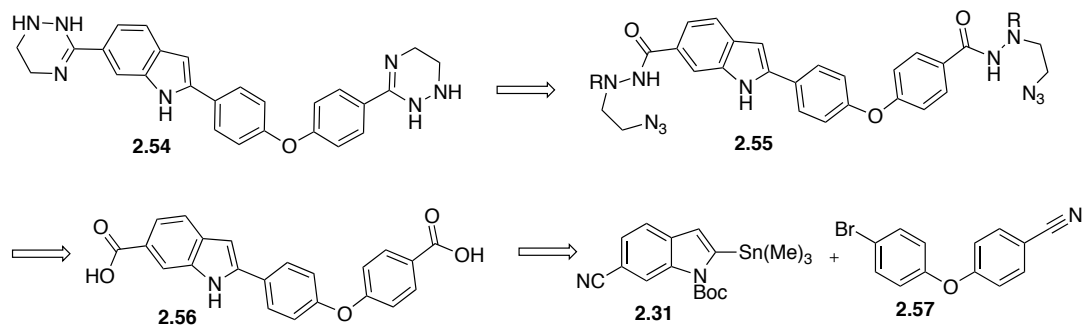
(H₂, Pd/C) returned only starting material, oxidative conditions (CAN) led to deprotection and partial oxidation of the triazine, and strongly acidic conditions (TfOH/TFA/anisole) led to decomposition. Finally, the PMB deprotection of **2.51b** was accomplished using neat TFA at 55 °C for 30 min, followed by a basic aqueous work up, to afford the deprotected triazine **2.52•TFA** in good yields (Scheme 2.13). For the deprotection of the 3,4-dimethoxybenzyl analog **2.53**, we discovered that 4 M HCl in dioxane at 50 °C for 2.5 days afforded the product **2.52** in modest yields after column chromatography.



Scheme 2.13. Deprotection of PMB and 3,4-dimethoxybenzyl protecting groups.

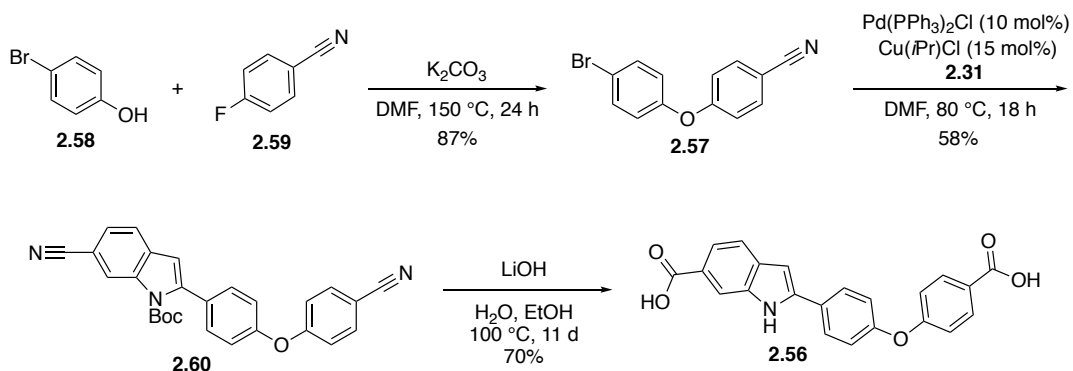
2.2.3.2 Efforts Towards the Synthesis of 6-(1,2,5,6-Tetrahydro-1,2,4-triazin-3-yl)-2-(4-(4-(1,2,5,6-tetrahydro-1,2,4-triazin-3-yl)phenoxy)phenyl)-1H-indole

To test our hypothesis that these 1,2,4-triazines could be used as isosteres of the metabolically labile imidazoline moiety, we proposed to synthesize an analog of **2.10** that contained the 1,2,4-triazines in place of the imidazolines. Our retrosynthetic approach to compound **2.54** features a double SAW cyclization of diazide **2.55** to form the bis-triazine rings of **2.54** (Scheme 2.14). We proposed that amide coupling of the diacid to our hydrazine building blocks **2.47a-2.47c** would give our hydrazide **2.55**. The diacid precursor can be formed via a Stille coupling of stannane **2.31** and aryl bromide **2.57**.



Scheme 2.14. Retrosynthetic approach to **2.54**.

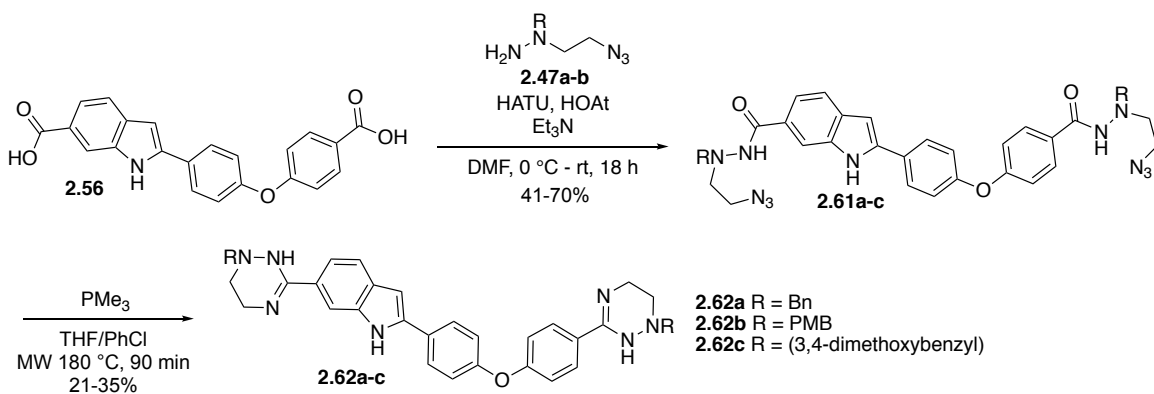
The synthesis of the bis-1,2,4-triazine analog **2.54** began with the condensation of 4-bromophenol (**2.58**) and 4-fluorobenzonitrile (**2.59**) to form the diarylether **2.57**. The indole stannane **2.31** was installed via a Stille cross coupling to give nitrile **2.60** that was subsequently hydrolyzed over 11 days to afford the Boc-protected diacid **2.56** in good yields (Scheme 2.15).



Scheme 2.15. Synthesis of diacid **2.56**.

Diacid **2.56** was coupled to the freshly deprotected hydrazines **2.47a-2.47c** using HATU/HOAt to provide the bis-hydrazides **2.61a-2.61c** in modest yields (Scheme 2.16).³¹¹ Previous attempts to couple the hydrazine via the acid chloride, or by activation with EDCI/HOBt, DEPC, DPPA, or PyBrOP were unsuccessful, very low yielding, or gave complex mixtures of products. The bishydrazides **2.61a-2.61c** were subjected to the original SAW reaction conditions (PhCl, PBU₃), but the reaction was unsuccessful. Although in the model system it was found that either PMe₃ or PBU₃ gave the best yield and, in the case of PMe₃, the

phosphine oxide was easier to remove (Table 2.3), the conditions didn't translate to the synthesis of **2.54**. When PMe_3 (1 M in toluene) or $\text{P}(\text{Bu})_3$ were used in PhCl, the reaction only afforded trace product. It was found that the solubility of the starting material/bisphosphazine ylide in PhCl/toluene was poor and the compound would precipitate out of solution during the reaction. We found that by using PMe_3 as a 1 M solution in THF, the bis-1,2,4-triazines **2.62a-2.62c** were formed in low yields. $\text{PMe}_3/\text{PhCl}/\text{THF}$ provided the best results for the SAW cyclization as it kept the phosphazine ylide in solution during the reaction. At this point, the remaining step involved the removal of the protecting groups. Attempts at removing the Bn protecting groups on **2.62a** through hydrogenation were unsuccessful even after 1 week with 50 mol% Pd/C. Unfortunately, the deprotection conditions previously identified for the removal of the PMB protecting group used on **2.62b** afforded the deprotected product **2.54** as a 1:1:1 mixture with the monodeprotected products (Scheme 2.16). Attempts to resubject the mixtures or drive the reactions to completion were unsuccessful, as the reactions seem to stop at a mixture of partial deprotection or lead to decomposition. We propose that, based on the lack of reactivity and product mass distribution, the indole was scavenging the cation intermediates formed in the deprotection. Using cation scavengers (Et_3SiH , anisole, and thioanisole) did not appear to improve the ratio of products. The 3,4-dimethoxybenzyl protected compound **2.62c** also proved resistant to deprotection conditions.



Scheme 2.16. Synthesis of protected bis-1,2,4-triazines **2.62a-2.62c**.

Although the deprotection of the 1,2,4-triazines was unsuccessful, possible alternatives to the benzyl protecting groups include the 2-(trimethylsilyl)ethoxymethyl (SEM) or the 2,3,6-trimethyl-4-methoxybenzenesulfonamide (Mtr) protecting groups. The SEM protecting group is a viable option as it can be deprotected using TBAF³¹²⁻³¹⁵ or Lewis and Bronsted acids,³¹⁶⁻³¹⁸ and is easily installed using SEMCl. The Mtr protecting group has been used in peptide synthesis for the protection of the ϵ -amino function of lysine using Mtr-Cl and is readily cleaved using either (0.15 M) methane sulfonic acid in a mixture of TFA and thioanisole³¹⁹ at room temperature in 2 h or 1 M HBF₄ in TFA at room temperature for 20 min.³²⁰⁻³²¹ The Mtr functionality has also been shown to be stable to Staudinger ligation conditions and is lipophilic, and therefore may aid to increase solubility during the SAW cyclization.³²²

2.3 CONCLUSIONS

In summary, we have successfully synthesized the final analog (**2.15•TFA**) of the thiazocine-based inhibitor series (Figure 2.7). Initial attempts to use the common thiazocinone intermediate **2.17** from the synthesis of the previous analogs were unsuccessful (Scheme 2.2). Therefore, we

developed a novel procedure to form the thiazocine through an activated ring closure using a PMB protected amine (Scheme 2.6). This analog will provide additional evidence for the hypothesis that constraining the diarylthioether will provide more favorable hydrogen bonding interactions within the binding site of BoNT/A LC.

Additionally, the first bis-triazine was synthesized in an attempt to use 1,2,4-triazine as isosteres of cyclic amidines. To date we have been unsuccessful in the deprotection of **2.62** after many attempts to remove the Bn, PMB, and 3,4-dimethoxybenzyl protecting groups. In addition to our work on the bis-triazine analog, we have further developed the scope of a convergent method for the synthesis of 1,2,4-triazines using newly developed azidohydrazine reagents. Hydrazines **2.47b** and **2.47c** were also shown to be thermally stable up to 150 °C by DSC analysis.

3.0 SYNTHESIS OF ANTAGONISTS OF THE NUCLEAR ANDROGEN RECEPTOR FOR THE TREATMENT OF CASTRATION-RESISTANT PROSTATE CANCER

3.1 INTRODUCTION

The androgen receptor (AR) is a 110-kDa ligand-inducible transcription factor that is a member of the nuclear steroid receptor family.³²³ AR is responsible for normal prostate function, and plays a key role in the progression of prostate cancer (PCa). In humans, the AR gene is located on the q-arm of the X-chromosome and is comprised of eight coding exons (Figure 3.1).³²⁴ Genetic disorders associated with AR include androgen-insensitivity syndrome, spinal and bulbar muscular atrophy (SBMA), hypogonadism, benign prostatic hyperplasia (BPH), and PCa.³²⁵ PCa is the third deadliest cancer in men with 161,000 new cases and 27,000 deaths expected in 2017, and is typically diagnosed through measurement of prostate-specific antigen (PSA) in the blood serum, rectal examination, or biopsy.³²⁶ PSA in blood serum is an indication that the prostatic epithelium has been disrupted as a result of hyperplasia of the prostate. Unfortunately, PSA levels in serum can also be the result of BPH, infection, or chronic inflammation. New PCa specific biomarkers are under investigation to reduce false positives associated with current detection techniques.³²⁷⁻³³¹

The AR structure consists of four functional domains: the N-terminal domain (NTD), DNA binding domain (DBD), hinge region, and ligand-binding domain (LBD).³³²⁻³³³ The NTD

is the largest and least conserved domain in AR that contains activation function-1 (AF-1), transcription activation units (TAU) 1 and 5, and contains polyglutamine and polyglycine repeats that are involved in regulating AR transcriptional activity by influencing the interaction with other receptor regions and altering the tertiary structure of the receptor.³³⁴⁻³³⁵ The DBD is highly conserved and contains two zinc fingers that are responsible for DNA recognition, binding, and stabilization.^{333,336} The nuclear localizing sequence (NLS) is a short overlapping segment between the DBD and the hinge region that functions in nuclear translocation of the androgen-activated AR.³³⁷ The hinge region modulates the conformational changes associated with androgen activation and contains a site for phosphorylation.³³⁸ The LBD binds to androgens, heat shock proteins (HSP's), and transcriptional co-activators and also contains the activation function-2 (AF-2) that stabilizes AR allowing the NTD to interact with co-regulators (Figure 3.1).^{333,339}

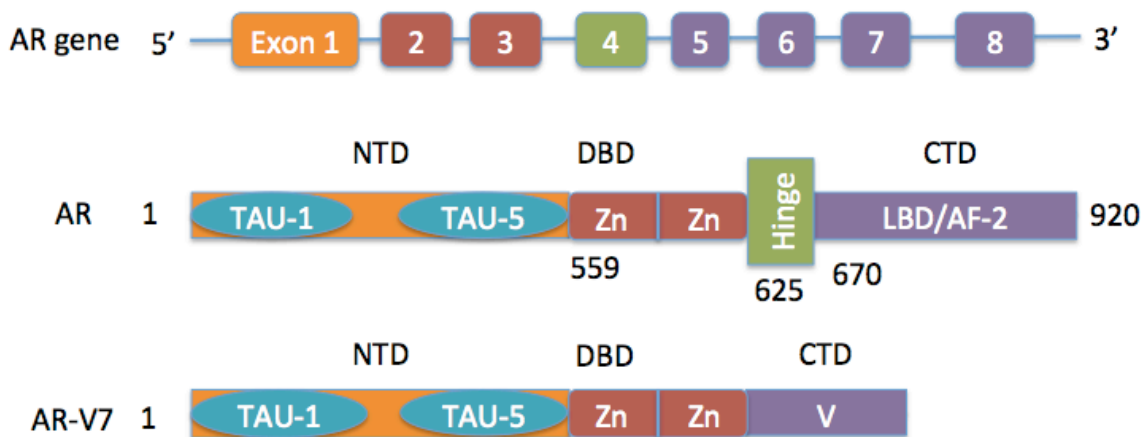


Figure 3.1. AR gene and functional domains.^{323,325,340-341}

Normal transcriptional activity of AR involves the binding of androgens to the LBD and translocation of AR to the nucleus for transcription. In the absence of ligands, the LBD localizes AR to the cytosol through binding to HSPs (HSP 90, HSP 70, HSP 56, and p23) that maintain its inactive form.^{323,342-343} The androgen testosterone is produced by the testes (ca. 90-95%) with a

small portion produced by the adrenal gland (ca. 5-10%), which is transported to AR-positive cells by sex hormone binding globulin (SHBG) and is subsequently reduced to DHT by 5 α -reductase. When DHT binds to the LBD, the HSPs are displaced. This ligand-bound AR undergoes homo-dimerization and phosphorylation that results in a conformational change, exposing the NLS, which then undergoes translocation to the nucleus.³⁴³ The nuclear translocated AR-dimer then binds to androgen response elements (AREs), short DNA sequences in the promoter or enhancer regions of target genes, as well as non-ARE associated upstream promoters of genes.³⁴⁴⁻³⁴⁵ The AR-ARE complex then binds to co-activators and co-repressors to form the co-regulator complex that can either up- or downregulate transcription (Figure 3.1).³⁴⁶ Dysregulation of these signaling pathways has been tied to the progression of PCa.

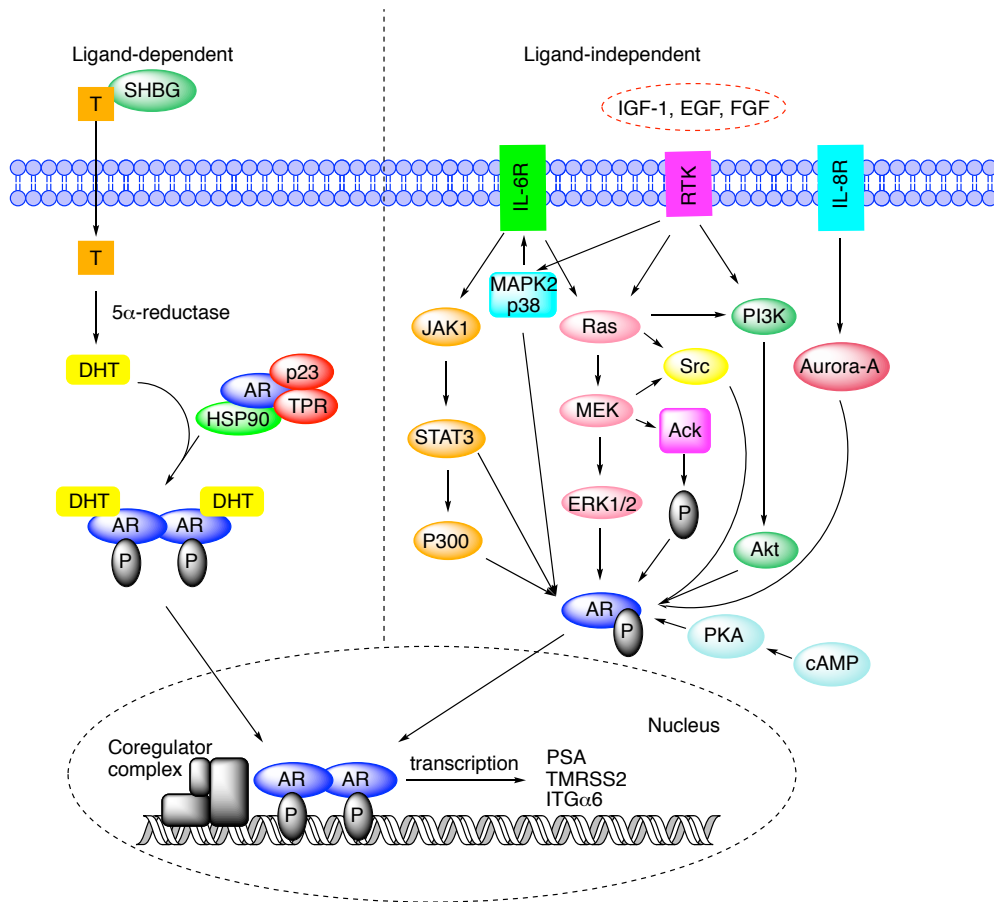


Figure 3.2. Signaling pathways of AR.^{323,325,340,343}

At prognosis, 80-90% of PCa are androgen dependent therefore initial therapies of PCa focus on androgen deprivation therapy (ADT) a treatment that was first developed in 1941 by Huggins and Hodges.³⁴⁷ ADT is achieved using luteinizing hormone-releasing hormone (LHRH) agonists in combination with antiandrogens and is accompanied by a number of side effects.³⁴⁸ Unfortunately, AR mutations occur causing androgen insensitivity and independence that result in PCa advancing to its lethal stage of castration-resistant prostate cancer, CRPC (formerly known as hormone-refractory prostate cancer).^{323,349} The mechanism of CRPC progression is associated with several androgen-dependent and androgen-independent signaling pathways of the AR.³⁵⁰ Therefore, blocking AR signaling is an attractive therapeutic target for the treatment of CRPC.

AR overexpression has been observed in CRPC cell lines as a result of increased mRNA transcription or AR gene amplification.³⁵¹⁻³⁵² Androgen insensitivity is thought to develop as a result of ADT, where mutations in the AR LBD will allow for more promiscuous ligand binding resulting in activation by other endogenous hormones (estrogen, progesterone, cortisone) and even antiandrogens such as flutamide.^{333,353} Mutations in the NTD and DBD could influence nuclear localization, co-regulator binding affinity, and transcription.³⁵⁴ Co-regulators of AR are proteins that activate (co-activators) or repress (co-repressors) the transcriptional activity of AR. Overexpression of the co-activators SRC-1 and TIF-2 have been associated with the progression of CRPC as they facilitate ligand binding to AR, resulting in increased nuclear concentrations of AR.³⁵⁵

De novo androgen synthesis is another mechanism of CRPC progression. Interestingly, testosterone levels in CRPC tumor cells are four times higher compared to primary tumors even with low serum testosterone levels caused by ADT.³²³ This is a result of gene upregulation in the

testosterone biosynthetic pathway that leads to testosterone synthesis from cholesterol, and the adrenal androgen dehydroepiandrosterone (DHEA).³⁵⁶⁻³⁶⁰

AR splice variants (AR-V's) emerge from insertions or deletions of exons and more than 20 AR-V's have been characterized in prostate cancer cell lines.³²³ Usually, exons 5 and 7 are deleted by RNA splicing factors producing a transcriptionally active AR that lacks the LBD (Figure 3.1).³⁶¹⁻³⁶² In particular, AR-V7 is the most common AR-V found in CRPC cell lines and in place of a LBD or hinge region contains a short variable amino acid sequence (Figure 3.1).³⁶³ Typically found localized in the nucleus, AR-V7 is important in the regulation of target genes involved in cancer cell proliferation.³⁶³⁻³⁶⁵ Another splice variant, AR-V3 undergoes SRC phosphorylation of the Y⁵³⁴ on the NTD resulting in nuclear translocation.³⁶⁵ Overexpression of AR-V7 in patients was correlated to poor clinical outcome, as patients encountered rapid resistance to current antiandrogens such as enzalutamide.³⁶⁵⁻³⁶⁶ Interestingly, AR-V's are found in CRPC cell lines that also express full length AR, and typical treatments of AR were ineffective suggesting that AR-V's can maintain AR transcriptional activity in low androgen environments.^{323,362} Additionally, AR-V's can also undergo homodimerization and even heterodimerization with full-length AR, and that dimerization was required for transcription.³⁶⁷ AR-V's have been identified as markers for hormonal resistance and in combination with monitoring PSA levels can allow for early detection of the progression of CRPC.³⁶⁸⁻³⁶⁹

Ligand independent signaling of AR is also responsible for downstream genomic regulation. Growth factor dysregulation can lead to alterations in downstream pathways such as the PI3K/AKT pathway that leads to phosphorylation of AR, resulting in increased nuclear translocation and transcriptional activity.^{12,370-372} Mutations in the receptor tyrosine kinase pathway (HER2) promote cell growth and survival, and have been associated with progression of

CRPC through the activation of Akt.³⁷³⁻³⁷⁵ In PCa, AR can also activate NF- κ B in the absence of androgens, which leads to cell proliferation.³⁷⁶⁻³⁷⁷

Unfortunately, all PCa patients will eventually progress to the incurable lethal CRPC stage in which current treatments are only effective in extending patient life by several months. Therefore, there is an urgent need for new therapeutics for the treatment of CRPC.

3.1.1 Treatments of PCa and CRPC

While ADT is used as a treatment for PCa, it is ineffective towards CRPC. New treatments have been developed mainly focused on using antiandrogen antagonists of AR. These antiandrogens bind to AR and halt its transcriptional activity. Several FDA approved antiandrogens are now available with additional treatments currently in phase II and phase III clinical trials. Structurally, antiandrogens can be divided into two classes: steroidal and nonsteroidal. In addition to antiandrogens, taxanes and radiopharmaceuticals have also been approved for the treatment of CRPC.

Steroidal antiandrogens are competitive inhibitors of androgens (testosterone and DHT) that also reduce plasma levels of androgens and the release of luteinizing hormone.³⁷⁸ Discovered in 1967, cyproterone acetate (CPA) was one of the first reported steroidal antiandrogens (Figure 3.3).³⁷⁹ In patients, CPA was less effective (13% increased risk of death) than the nonsteroidal antiandrogen flutamide (8% increased risk of death). In addition to the common side effects of ADT, CPA has also been shown to reduce hormonal flares associated with LHRH agonists when used as a combination therapy.³⁸⁰⁻³⁸¹ Unfortunately, CPA has a very limited effect against CRPC.³⁸²

Flutamide was the first widely used nonsteroidal antiandrogen. The biologically active form hydroxyl-flutamide is a result of metabolic oxidation and has a half-life of ~5 hours that requires three daily doses (Figure 3.3).³⁸² Apart from the common side effects of antiandrogens therapies, flutamide has been found to cause severe diarrhea in 10-20% of the patients that ultimately results in the discontinuation of treatment.³⁸³ In addition, flutamide has also been shown to disrupt liver function in a small subset of patients that was resolved with discontinuing treatment.³⁸³ Although flutamide is effective in the treatment of PCa, large doses are required (750 mg/day) and several undesired side effects make it less desirable than current treatments.

Nilutamide was the second most widely used antiandrogen for clinical use and has a half-life of ~38 hours enabling its administration via a once daily dose (Figure 3.3).³⁸² Similar to flutamide, nilutamide is also heavily metabolized in the liver due to the presence of the nitroaniline functionality, but does not require metabolism to get to its active form as observed with flutamide. It has been used in combination with LHRH agonists to prevent hormonal flares. Several side effects have been noted in patients that have used nilutamide including delayed adaption to dark, alcohol intolerance, pneumonitis, and nausea.³⁸³

The orally available bicalutamide (Casodex®) was approved by the FDA in 1995 and is one of the current standards of care for the treatment of both non-metastatic and metastatic CRPC (Figure 3.3). Interestingly, bicalutamide is marketed as the racemic drug even though the *S*-enantiomer is rapidly metabolized and cleared while the *R*-enantiomer is significantly more active and metabolically stable in plasma for up to a week.³⁸² Bicalutamide dosed at 150 mg/day is well tolerated compared to nilutamide and flutamide as common side effects include breast pain, gynaecomastia, loss of libido, and hot flashes.³⁸⁴

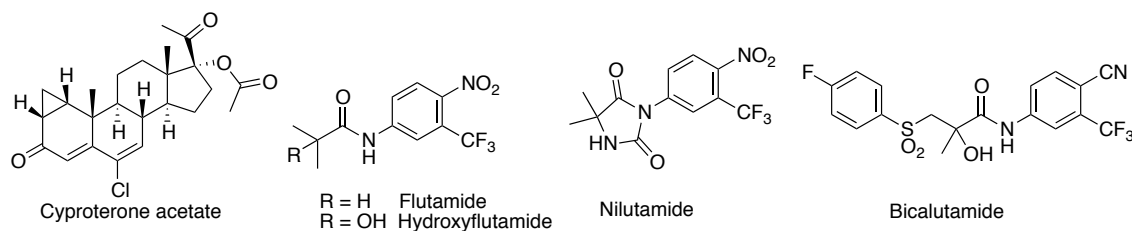


Figure 3.3. 1st generation antiandrogens.

The thiohydantoin enzalutamide (Xtandi®; formerly known as MDV3100) was approved by the FDA in 2012. It is an orally available antagonist of AR with a half-life of 1 week that acts by inhibiting AR nuclear translocation and by reducing the transcriptional activity of AR (Figure 3.4).³⁸⁵ Patients with CRPC treated with enzalutamide displayed decreased levels of PSA. A recent double-blind study comparing the efficacy and safety of enzalutamide and bicalutamide in both metastatic and non-metastatic CRPC revealed that patients treated with enzalutamide had 19.4 months progression-free survival whereas patients treated with bicalutamide had progression-free survival of only 5.7 months.³⁸⁶ Side effects of enzalutamide usually include fatigue, nausea, diarrhea, musculoskeletal pain, hot flashes, and headache.³⁸⁷⁻³⁸⁸ Enzalutamide also presents a small risk of seizure, as it was shown to inhibit GABA-A currents *in vitro*.³⁸⁹ Unfortunately, patients with CRPC develop resistance to enzalutamide after 3-5 months.³⁹⁰

A more recent thiohydantoin, apalutamide (formerly known as ARN-509) is a new investigational drug currently in phase II and phase III clinical trials for its use in combination with bicalutamide (NCT02531516), abiraterone acetate (NCT02789878), or radiation (NCT02531516) (Figure 3.4). Similar to enzalutamide, apalutamide also inhibits nuclear translocation of AR and reduces transcriptional activity, but has been shown to be more effective *in vivo*.³⁹¹ Additionally, apalutamide has shown low CNS penetration and therefore poses less of a risk for seizures than enzalutamide.³⁸⁹

Abiraterone acetate inhibits the enzyme CYP17, which blocks the production of androgens, reducing levels to less than 1 ng/dL,³⁹² and when used in combination with prednisone has been shown to improve progression-free and overall survival by an average of 16 months vs. 11 months with only prednisone (Figure 3.4).³⁹³ Side effects of abiraterone acetate include fluid retention, hypokalemia, and hypertension.³⁹⁴⁻³⁹⁵ When used in combination with glucocorticoids, cardiac disorders, and abnormal liver function were also observed.^{393,395}

The taxanes, docetaxel and carbazitaxel³⁹⁶ are also FDA approved treatments of CRPC and act through tubulin stabilization and cell cycle arrest (Figure 3.3). Unfortunately, docetaxel suffers from a high affinity to P-glycoprotein (P-gp), which leads to a decrease in intracellular docetaxel concentrations and promotes resistance. Further structural optimization led to carbazitaxel, the dimethoxy analog of docetaxel, which has decreased P-gp affinity and is effective towards docetaxel-resistant tumors.³⁹⁷ In a recent study, taxanes were also found to be effective in patients with CRPC with detectable AR-V. Levels of PSA in these patients was reduced ~41%.³⁹⁸

Radium-223 dichloride (Xofigo®; formerly known as Alpharadin™) was approved by the FDA in 2013 for the treatment of CRPC that has metastasized to the bone by acting as a calcium mimetic.³⁹⁹⁻⁴⁰⁰ Other radiotherapy previously used was external beam radiotherapy for the management of localized PCa.⁴⁰¹

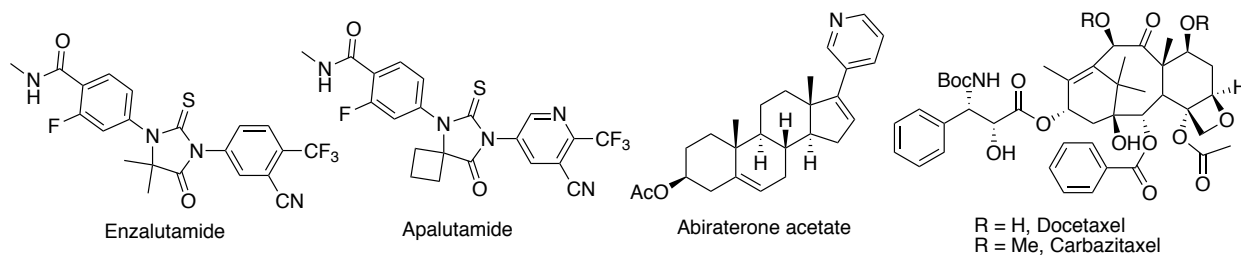


Figure 3.4. 2nd generation treatments of CRPC.

Several new scaffolds have emerged in the literature over the past few years as potential treatments of CRPC. The tropinol **3.1** was found to have stronger antagonistic behavior than bicalutamide with an 87% reduction in luciferase activity at 1 μ M (Figure 3.5). In addition to the activity against wild-type AR, compound **3.1** also showed promising antiandrogen activity in the two most common AR mutants.⁴⁰² The oxabicyclic compound BMS-641988 was identified from a recent SAR and was found to have high binding affinity to AR ($K_i = 1.7$ nM) acting as a potent antagonist *in vitro* ($IC_{50} = 16$ nM). In addition to *in vitro* activity, BMS-641988 was also efficacious in the CWR22-BMSLD1 xenograft model that has shown resistance to bicalutamide and flutamide. Based on its promising PK/PD profile, BMS-641988 was advanced into clinical development.⁴⁰³ Efforts to improve the chemical stability of BMS-641988 led to the discovery of the bicyclic sultam **3.2**, which was also found to have high affinity for AR ($K_i = 5$ nM) and potent antagonist activity *in vitro* ($IC_{50} = 57$ nM). With a promising PK/PD profile, **3.2** was tested in human tumor xenograft studies where poor oral exposure was observed and was possibly due to high metabolism.⁴⁰⁴ Ultimately, this result led to the discontinuation of **3.2**. Physachenolide C was identified from a HTS of a library of natural products and further structural optimization of the 17β -hydroxywithanolides for stability and potency. This analog is capable of reducing PSA expression, has nanomolar potency to both AR-positive and AR-negative cell lines, and was shown to be active in human tumor xenograft models. It is proposed that physachenolide C acts via sensitizing tumor necrosis factor-related apoptosis-inducing ligand (TRAIL) to induce apoptosis.⁴⁰⁵ The chlorohydrin EPI-002 and its analogs have been shown to inhibit AR-transcriptional activity through covalently binding to the AR-NTD (Figure 3.5).^{335,406} Using high resolution solution NMR spectroscopy, Salvatella and coworkers have also shown that EPI-002 analogs interact with TAU-5 of the AR-NTD (Figure 3.5).⁴⁰⁷ In a VCaP

human tumor xenograft model, EPI-002 was effective in reducing tumor volume.³³⁵ A prodrug of EPI-002, EPI-506 (not shown), is currently in phase (I/II) clinical trials (NCT02606123) for the treatment of patients with metastatic CRPC.⁴⁰⁸ The cyanobacteria metabolite sintokamide A (SINT1) has also been found to inhibit AR through binding to the AF-1 region of the NTD. Additionally, SINT1 has been shown to have low cytotoxicity and also inhibit AR-Vs.⁴⁰⁹⁻⁴¹⁰ Binding to the AR-NTD represents a novel mechanism of action to treat CRPC that potentially avoids the mechanisms of resistance commonly found with other antiandrogens, such as point mutations in the LBD and splice variants.

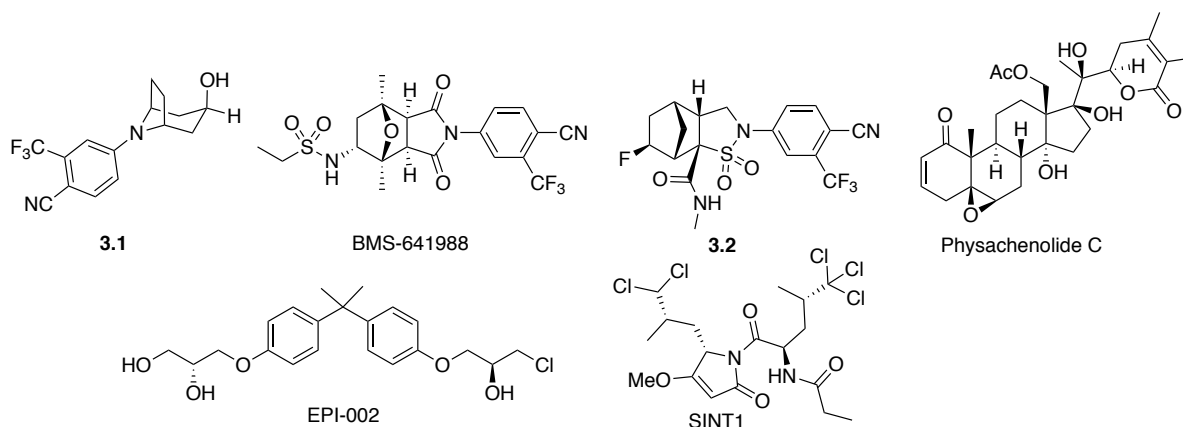


Figure 3.5. Recent inhibitors of the AR.

3.1.2 High Throughput Screen and Structure Activity Relationship: Previous Work in the Wipf Group

Although a number of treatments available treatments for CRPC, they eventually become ineffective as the cancer develops resistance. One therapeutic avenue that has not been developed is to block the nuclear localization of AR, therefore removing transcriptional activity of AR and blocking the progression of the cancer. In an effort to identify a viable treatment of CRPC, Wang and coworkers developed a high throughput screen to identify small molecules that

selectively reduce the nuclear localization of AR in CRPC cells.⁴¹¹ Using a GFP labeled AR (GFP-AR) transfected into C4-2 CRPC cells and fluorescence visualization, 219,000 compounds from the National Institutes of Health (NIH) molecular libraries screening centers network (MLSCN) were screened at a concentration of 20 μ M. After screening and hit validation, 3 compounds were identified that were selective towards GFP-AR with no inhibition of nuclear localization of GFP labeled glucocorticoid receptor (GFP-GR) or GFP labeled estrogen receptor (GFP-ER) and low micromolar potency in C4-2 CRPC cells (Figure 3.6). The structurally similar compounds **3.3** and **3.4** inhibited nuclear localization of GFP-AR in C4-2 cells and localized GFP-AR to the cytosol. Interestingly, compound **3.5** decreased nuclear GFP-AR without increasing cytoplasmic levels of GFP-AR. This indicates an overall downregulation of AR expression and potential inhibition of the activity of AR. Western blot analysis of C4-2 cells treated with **3.5** indicated that AR and PSA protein levels were reduced even at concentrations as low as 2 μ M, suggesting that **3.5** can inhibit AR signaling. The three compounds identified from this HTS have structures that are very unique compared to androgens and known AR antagonists and as a result may have a different mechanism of action. These mechanisms could involve direct inhibition of AR or an indirect inhibition targeting AR cofactors.⁴¹¹ All three HTS hits demonstrated low micromolar potency with low cytotoxicity in AR negative cell lines. However, structural analogs of **3.3** and **3.4** were found to have antifungal activity, thus raising concerns about potential off-target effects.⁴¹² The scaffold of **3.5** did not show any precedence for biological activity and thus was a more attractive target for further investigations. Cell proliferation was inhibited in the AR-positive prostate cancer cell lines LNCAP, C4-2, LAPC4, 22Rv1, and CWR-R1 that were treated with **3.5** at 1 μ M and no cell death was observed at 10 mM in AR-negative cell lines. A C4-2 mouse xenograft tumor model treated with **3.5** showed

tumor growth inhibition with no decrease in the body weight in the mice further indicating little to no cytotoxicity.

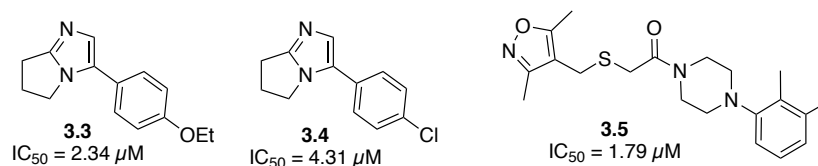


Figure 3.6. Hits identified from HTS.

Based on the promising biological activity and low cytotoxicity of **3.5**, Wipf and coworkers probed the structure-activity relationship of **3.5** by dividing the structure into 5-zones for structural modification: the aryl substitution pattern (zone 1), piperazine modifications (zone 2), carbonyl replacements (zone 3), thioether substitution (zone 4), and variations at the 3,5-dimethylisoxazole (3,5-DMI) ring (zone 5) (Figure 3.7).³⁴⁹

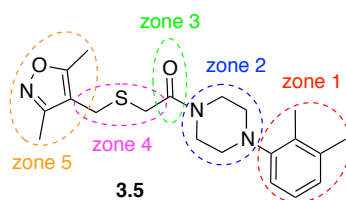
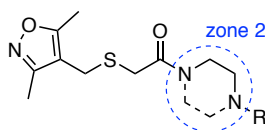
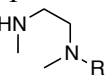
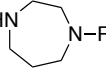
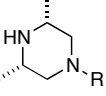
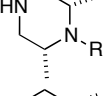
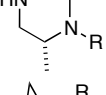
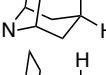
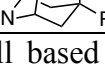


Figure 3.7. Zone of structural modification.

The analogs were biologically characterized by a Dual-Glo luciferase system in the presence of 1 nM of the synthetic androgen R1881 in C4-2-PSA-rl cells and were compared to the initial HTS hit **3.5** (EC_{50} 7.3 μM) and enzalutamide (EC_{50} 1.1 μM) (Table 3.1). Initially, amides **3.6a-p** were synthesized to probe structural changes in zones 1 and 2 to determine the effect of substitution around the aryl and piperazine rings. Small modifications on the aryl ring in zone 1 revealed that monomethyl substitution in the 3- and 4-positions resulted in a loss of activity. The 2-methyl analog **3.6b** had 2-fold loss in activity compared to **3.5**. Removal of the methyl groups resulted in a complete loss in activity. Additional steric bulk was also tolerated where the bulky naphthyl substitution of **3.6g** was also active (EC_{50} 11.1 μM). Electron

withdrawing aryl substituents (2-CN, **3.6e**, and 2-F, **3.6f**) were also moderately active ($EC_{50} \sim 12 \mu\text{M}$), however, the analog with the electron-donating 2-OMe, **3.6h**, was completely inactive, possibly due to an increase in the aniline-nitrogen pK_a . As multiple benzylic methyl groups are a potential metabolic liability, the 2-methyl substitution was used for further SAR investigations. Several analogs with more flexible or constrained amine linkers were prepared to probe the SAR around the piperazine in zone 2. The flexible *N,N'*-dimethylethylenediamine linker in **3.6i** and the homopiperazine **3.6j** had decreased activity. The 2,6-dimethylpiperazines **3.6l** and **3.6m** were also 2-fold less active than **3.5**. The more constrained 2,6-dimethylpiperazine analog **3.4k** resulted in increased activity, with a 2-fold improvement on **3.5**. The bridged bicyclic [3.2.1] systems **3.6o** and **3.6p** improved the activity slightly from **3.6b** with EC_{50} 's around $8 \mu\text{M}$ (Table 3.1).

Table 3.1. Structural modifications in zones 1 and 2.

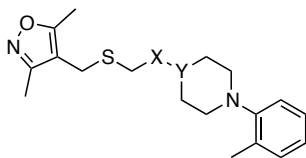
Entry	Compound	Structure		EC ₅₀ (μM) ^a
		Zone 2	R	
1	3.5	Piperazine	(2,3-Me)Ph	7.3 ± 2.5 ^d
2	enzalutamide	-	-	1.1 ± 0.5 ^e
3	3.6a	Piperazine	Ph	>25 ^b
4	3.6b	Piperazine	(2-Me)Ph	14.5 ± 3.2 ^c
5	3.6c	Piperazine	(3-Me)Ph	>25 ^b
6	3.6d	Piperazine	(4-Me)Ph	>25 ^b
7	3.6e	Piperazine	(2-CN)Ph	12.0 ± 1.6 ^c
8	3.6f	Piperazine	(2-F)Ph	12.6 ± 7.7 ^c
9	3.6g	Piperazine	1-naphthyl	11.1 ± 5.3 ^c
10	3.6h	Piperazine	(2-MeO)Ph	>25 ^b
11	3.6i		(2-Me)Ph	18.4 ± 9.2 ^c
12	3.6j		(2-Me)Ph	11.1 ± 3.3 ^b
13	3.6k		(2-Me)Ph	3.1 ± 1.1 ^b
14	3.6l		Ph	14.7 ± 4.4 ^b
15	3.6m		(3-Me)Ph	16.6 ± 4.8 ^c
16	3.6o		(2-Me)Ph	7.7 ± 1.6 ^c
17	3.6p		(2-Me)Ph	7.9 ± 2.8 ^b

^aEC₅₀'s were determined using a cell based luciferase assay as previously described.³⁴⁹ EC₅₀ refers to the concentration that results in 50% inhibition of PSA-luciferase activity. Each EC₅₀ was calculated using GraphPad Prism and is the average ± stdev of at least two independent experiments using triplicate determinations at each concentration for each experiment; *n* = number of assay repeats: ^b*n* = 2, ^c*n* = 3, ^d*n* = 4, ^e*n* = 6.

For the investigation of zone 3, the piperazine and 2-Me-Ph substitution were retained for comparison. Interestingly, the amide was found to not be necessary for activity, as the reduced

analog **3.7b** maintained activity (Table 3.2). The sulfonamide **3.7a** was also as active as the initial hit **3.5** whereas the urea **3.7c** and carbamate **3.7d** were completely inactive.

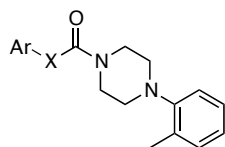
Table 3.2. Modifications to amide of zone 3.



Entry	Compound	Structure		EC ₅₀ (μM) ^a
		X	Y	
1	3.7a	SO ₂	N	7.2 ± 2.7 ^d
2	3.7b	CH ₂	N	10.8 ± 5.7 ^c
3	3.7c		N	>25 ^b
4	3.7d		CH	>25 ^d

^aEC₅₀'s were determined using a cell based luciferase assay as previously described.³⁴⁹ EC₅₀ refers to the concentration that results in 50% inhibition of PSA-luciferase activity. Each EC₅₀ was calculated using GraphPad Prism and are the average ± stdev of at least two independent experiments using triplicate determinations at each concentration for each experiment; *n* = number of assay repeats: ^b*n* = 2, ^c*n* = 3, ^d*n* = 4.

Finally zones 4 and 5 were investigated. The thioether linker was oxidized to sulfoxide **3.8a** and sulfone **3.8b** resulting in analogs with very poor or decreased activity, confirming that the biological activity was not a result of *S*-oxidation (Table 3.3). Substitution of the thioether with oxygen and *N*-Me resulted in a complete loss in activity. It was found that a phenyl ring could be used in place of the 3,5-DMI (**3.8d**) with no significant decrease in activity. Additionally, activity was sustained when using an all-carbon linker in place of the thioether (**3.8f**). Removing a carbon from the thioether linker **3.8g** deleted all activity. The *E*-alkene **3.8h**, *trans*-cyclopropane **3.8i**, and alkyne **3.8j** were also inactive. In contrast, the *Z*-alkene **3.8k** was found to have similar activity to **3.6b** (EC₅₀ ~13 μM). Gratifyingly, the corresponding *cis*-cyclopropane **3.8l** had greatly improved activity over the initial hit **3.5** with an EC₅₀ of 2.9 μM.

Table 3.3. Structural modifications in zones 4 and 5.

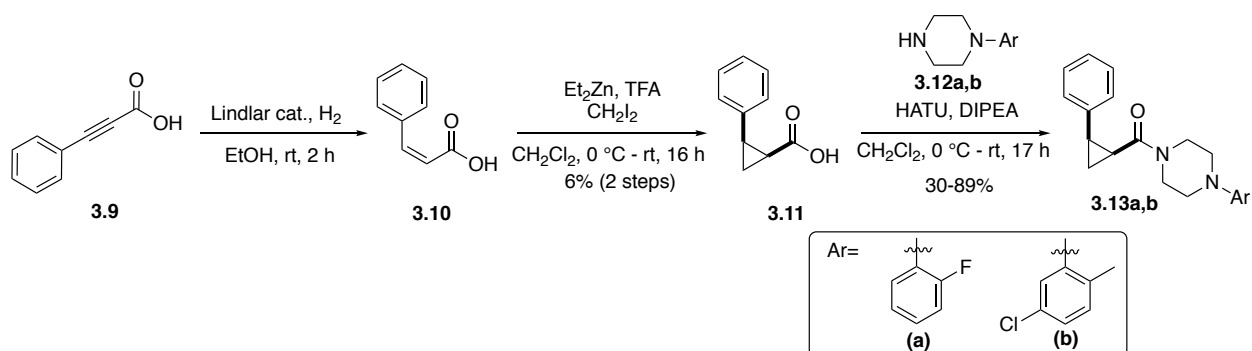
Entry	Compound	Structure		EC ₅₀ (μM) ^a
		X	Ar	
1	3.5^e		3,5-DMT ^f	7.3 ± 2.5 ^d
2	3.6b		3,5-DMT ^f	14.5 ± 3.2 ^c
3	3.8a		3,5-DMT ^f	>25 ^c
4	3.8b		3,5-DMT ^f	16.1 ± 3.3 ^c
5	3.8c		3,5-DMT ^f	>25 ^c
6	3.8d		Ph	13.7 ± 0.8 ^c
7	3.8e		Ph	>25 ^c
8	3.8f		Ph	14.4 ± 3.7 ^c
9	3.8g		Ph	>25 ^b
10	3.8h		Ph	>25 ^b
11	3.8i		Ph	>25 ^c
12	3.8j		Ph	20.3 ± 11.6 ^b
13	3.8k		Ph	12.7 ± 0.8 ^b
14	3.8l		Ph	2.9 ± 1.0 ^c

^aEC₅₀'s were determined using a cell based luciferase assay as previously described.³⁴⁹ EC₅₀ refers to the concentration that results in 50% inhibition of PSA-luciferase activity. Each EC₅₀ was calculated using GraphPad Prism and are the average ± stdev of at least two independent experiments using triplicate determinations at each concentration for each experiment; *n* = number of assay repeats: ^b*n* = 2, ^c*n* = 3, ^d*n* = 4. ^epiperazine *N*-aryl group is 2,3-Me-Ph. ^f3,5-DMT, 3,5-dimethylisoxazole.

3.2 RESULTS AND DISCUSSION

After identifying the *cis*-cyclopropane **3.8l** as a key component of our pharmacophore, we sought to further develop the scaffold in order to increase its potency. We had previously discovered

that the *N*-aryl substitutions with 2-F and 5-Cl-2-Me showed a modest increase in biological activity. Our plan was to combine these substitutions with the cyclopropyl amide side chain to see if a similar trend in activity was observed. Initially, we attempted to generate the *cis*-cyclopropane carboxylic acid **3.11** as building block for a convergent synthesis of new analogs (Scheme 3.1). The synthesis began with a hydrogenation of phenylpropionic acid **3.9** using a Lindlar catalyst to afford the *cis*-alkene **3.10**. A Simmons-Smith cyclopropanation afforded the *cis*-cyclopropane carboxylic acid **3.11** in poor yield after recrystallization.⁴¹³ The carboxylic acid was then used in a HATU-mediated amide coupling with commercially available piperazines **3.12a** and **3.12b** to afford amides **3.13a** and **3.13b**.



Scheme 3.1. Synthesis of cyclopropane analogs **3.13a** and **3.13b**.

To further improve these analogs, we decided to introduce a 4-fluoro substitution on the unsubstituted aryl ring to reduce the potential for metabolic oxidation (Figure 3.8).⁴¹⁴

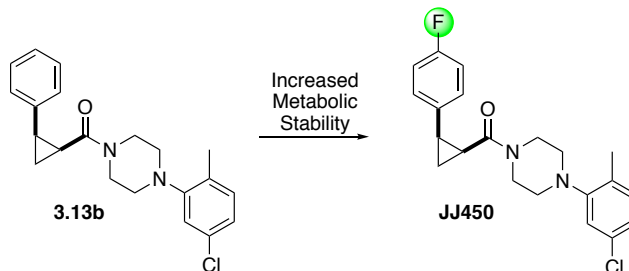
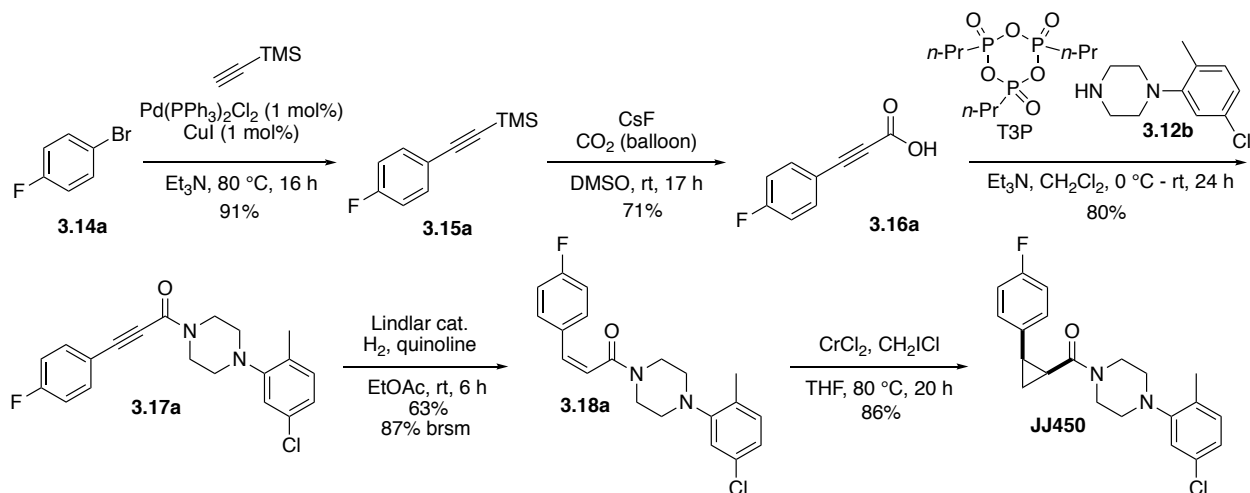


Figure 3.8. Proposed fluorine substitution for increased metabolic stability.

We first needed to synthesize 4-fluorophenylpropionic acid (**3.16a**), as it wasn't readily available from commercial sources (Scheme 3.2). Initial attempts to directly couple propionic acid with 4-bromofluorobenzene were messy, difficult to purify, and low yielding. Exploring an alternative stepwise approach previously described by Kondo et al., we first coupled TMS-acetylene to the aryl bromide **3.14a**. Concomitant desilylation and decarboxylation mediated by CsF under an atmosphere of CO₂ provided the carboxylic acid **3.15a** in excellent yields.⁴¹⁵ A T3P mediated amide coupling gave amide **3.17a** that was subsequently reduced under Lindlar hydrogenation conditions to the *cis*-alkene **3.18a** in excellent yields. This reaction is typically stopped prematurely as the alkene is readily separated by chromatography from the alkyne starting material but not the over-reduced alkane, which can be observed with long reaction times. We have also found the Pd/BaSO₄ quinoline catalyst system works well for the reduction of the alkyne to the *cis*-alkene.⁴¹⁶ Finally, the *cis*-alkene **3.18** was subjected to chromium mediated Simmons-Smith cyclopropanation conditions to give the cyclopropane **JJ450** in good yield. Other attempts to form the cyclopropane using samarium and diiodomethane were very low yielding with incomplete conversion of the starting material.⁴¹⁷ This route has been optimized for multigram-scale synthesis of **JJ450** and used to prepare more than 20 g of **JJ450**. Analysis of **JJ450** by inductively coupled plasma optical emission spectroscopy (ICP-OES) and chromium levels were measured at 1.3 ppm (1.3 mg/L) with no detectable amount of lead. Chromium (II) is readily oxidized to chromium (III), which has been found to be an essential nutrient with low toxicity by oral administration by the EPA and FDA. According to USP<232> the permissible daily exposure (PDE) is 11,000 μg/day and 1,100 μg/day for oral and parenteral exposure respectively. The environmental protection agency (EPA) set the maximum contaminant level of chromium in drinking water to 100 μg/L (100 ppb).⁴¹⁸



Scheme 3.2. Synthesis of **JJ450**.

In order to determine if a specific binding site is being engaged by our analogs, we separated racemic **JJ450** by semi-preparative chiral SFC using a Chiralpak IC column (25 x 1 cm) and 20% methanol as the modifier. The absolute configuration of the enantiomers were initially assigned based on the specific rotation of similar compounds in the literature,⁴¹⁹ and were later confirmed by single crystal X-ray diffraction of (1*R*,2*S*)-**JJ450** (Figure 3.9).

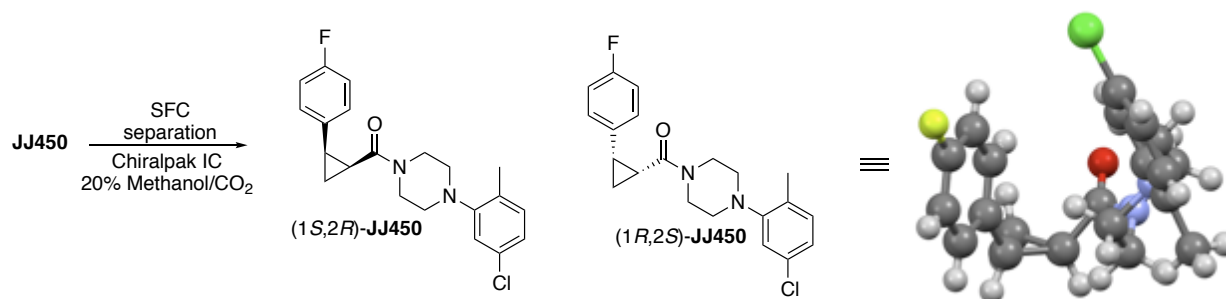
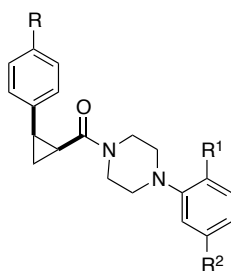


Figure 3.9. Resolution of racemic **JJ450** and crystal structure of (1*R*,2*S*)-**JJ450**.

3.2.1 Biological Data

Our therapeutic goal was to discover a potent, orally bioavailable modulator of AR with preclinical efficacy in CRPC in both *in vitro* and *in vivo* tumor models. Following the synthesis

of analogs **3.13a**, **3.13b**, and **JJ450**, the Wang lab characterized their biological activity in a PSA luciferase assay (Table 3.4). The assay utilizes a Dual-Glo luciferase system in the presence of 1 nM of the synthetic androgen R1881 in C4-2-PSA-rl cells. In this Dual-Glo luciferase system, the relative luciferase activity is calculated as the quotient of androgen-induced PSA-firefly/Renilla luciferase and as the PSA promoter activity correlates to AR transcriptional activity, inhibition of AR will result in decrease PSA-luciferase activity.³⁴⁹ The EC₅₀'s were calculated using GraphPad Prism and are highly dependent on the type of curve fit used for analysis. The biological activities were compared to the cyclopropane **3.8I** and enzalutamide (EC₅₀ 1.1 μM, Table 3.4, entry 7). The cyclopropane derivative **3.13a** with a 2-F-Ph ring was found to be equipotent to the 2-Me-Ph analog **3.8I**. Interestingly, compound **3.13b** (R₂=Cl) was three-fold more potent than **3.8I** and **JJ450** was equipotent to **3.8I**. Gratifyingly, chiral resolution of **JJ450** (EC₅₀ 2.7 μM, entry 4) provided a more potent enantiomer (*1S,2R*)-**JJ450** (EC₅₀ 1.7 μM, entry 5) and the ca. 10-fold less potent (*1R,2S*)-**JJ450** (EC₅₀ 15.2 μM, entry 6), which supports a specific binding mode at a still to be defined AR binding site.

Table 3.4. Biological activity of *cis*-cyclopropane analogs.

Entry	Compound	Structure			EC ₅₀ (μM) ^a
		R	R ¹	R ²	
1	3.81	H	Me	H	2.9 ± 1.0 ^c
2	3.13a	H	F	H	2.6 ± 1.6 ^b
3	3.13b	H	Me	Cl	0.9 ± 0.9 ^b
4	JJ450	F	Me	Cl	2.7 ± 1.1 ^d
5	(1 <i>S</i> ,2 <i>R</i>)- JJ450	F	Me	Cl	1.7 ± 0.2 ^c
6	(1 <i>R</i> ,2 <i>S</i>)- JJ450	F	Me	Cl	15.2 ± 3.3 ^c
7	enzalutamide	-	-	-	1.1 ± 0.5 ^e

^aEC₅₀'s were determined using a cell based luciferase assay as previously described.³⁴⁹ EC₅₀ refers to the concentration that results in 50% inhibition of PSA-luciferase activity. Each EC₅₀ was calculated using GraphPad Prism, and are the average ± stdev of at least two independent assays using triplicate determinations at each concentration for each experiment; *n* = number of assay repeats: ^b*n* = 2, ^c*n* = 3, ^d*n* = 4, ^e*n* = 5.

An initial mouse PK panel of **JJ450** proved promising as **JJ450** showed some oral bioavailability (23%), *t*_{1/2} (IV) of 1.3 h, clearance of 68 mL/min/kg, and steady state volume of distribution (*V*_{ss}) of 0.7 L/kg. The plasma concentrations were quantifiable until 8 h after dosing C57BL/6 mice with 10 mg/kg **JJ450** by IV and OG method of administration (Table 3.5). Comparison of **JJ450** with data for the FDA approved enzalutamide shows that there is room to improve the PK profile of **JJ450**.³⁹¹

Table 3.5. PK data for **JJ450**.

Entry	Compound ^a	T _{max} [h]	C ₀ /C _{max} [ng/mL]	AUC _{last} [h•ng/ mL]	AUC _{inf} [h•ng/ mL]	t _{1/2} [h]	CL [mL/min /kg]	V _{ss} [L/kg]	%F
1	JJ450 (i.v) ^a	-	6,822.2	2423	2430	1.26	68	2.79	-
2	JJ450 (o.g) ^a	0.25	582.3	559.7	569.2	-	-	-	23.1
3	enzalutamide (o.g) (CD-1 mice) ^b	4.0	19,800	-	212,000	15.8	0.675* (IV)	0.824* (IV)	94.3

^aPharmacokinetic Data was obtained from C57BL/6 mice administered with **JJ450** at 10 mg/kg by o.g or i.v as denoted. ^bData for enzalutamide was obtained from ref³⁹¹.

The metabolic stability in mouse liver microsomes (MLM), rat liver microsomes (RLM), and human liver microsomes (HLM) was determined at 30 and 60 min (Table 3.6). It appears that mouse and rats have rapid metabolism of **JJ450** (t_{1/2} = 10 min) while HLM metabolism is much slower. The microsome stability was also determined for both enantiomers. These are relatively similar with half-lives in MLM of 6.21 min and 7.48 min for the (1*S*,2*R*)-**JJ450** and (1*R*,2*S*)-**JJ450** enantiomers respectively. In comparison, for enzalutamide (Table 3.6, entry 5) almost no metabolism is present in RLM after 30 min.⁴²⁰

Table 3.6. Liver microsome data for **JJ450** and enzalutamide.

Entry	Compound ^a	MLM ^b	RLM ^b	HLM ^b
1	JJ450 (30 min)	8%	1%	85%
2	JJ450 (60 min)	3%	0%	59%
3	(1 <i>S</i> ,2 <i>R</i>)- JJ450 (60 min)	0.3%	-	27%
4	(1 <i>R</i> ,2 <i>S</i>)- JJ450 (60 min)	0.4%	-	8%
5	enzalutamide (30 min) ⁴²⁰	-	98%	-

^aInitial compound concentrations were 1 μM. ^bLiver microsome data is reported as the % compound remaining a time point (X) and were measured in the presence of NADPH. MLM, mouse liver microsomes; RLM, rat liver microsomes, HLM, human liver microsomes.

From these studies, **JJ450** emerged as a potent lead analog from our SAR. Despite having decreased activity compared to **3.13b**, we proposed that **JJ450** would have an increased metabolic stability *in vivo* due to the presence of the 4-fluoro substitution and was taken forward as a promising lead for further biological testing. The initial xenograft studies were performed in

the Wang lab using racemic **JJ450** (Figure 3.10). **JJ450** was screened in three human tumor mouse xenograft models LNCaP, VCaP, and 22Rv1. Nude SCID mice bearing LNCaP xenografts were administered **JJ450** once daily by oral gavage (o.g) or intraperitoneal (i.p) at two concentrations (10 mg/kg o.g, 10 mg/kg i.p, and 75 mg/kg o.g) (Figure 3.10, (A)). Lower concentrations (10 mg/kg) administered by o.g had begun to show increased tumor growth around 30 days while the i.p (10 mg/kg) had shown almost no tumor growth until day 40. Interestingly, the highest dose of **JJ450** (75 mg/kg) o.g had no tumor growth until day 50 (Figure 3.10, A). **JJ450** was administered to nude SCID mice bearing the more aggressive 22Rv1 tumors, which are resistant towards enzalutamide, at 10 mg/kg and 75 mg/kg i.p (Figure 3.10, B). Although **JJ450** was able to slow the progression of the 22Rv1 tumor, the rapid tumor growth combined with the poor metabolism may have contributed to its ineffectiveness in this tumor model. Finally, a comparison study of **JJ450** and enzalutamide (MDV3100) in a VCaP xenograft model shows **JJ450** to be more effective than enzalutamide with only a small increase in tumor volume (Figure 3.10, C). In all of these xenograft models, mice administered **JJ450** showed no sign of weight loss indicating low cytotoxicity. Additionally, no adverse effects were observed in mice administered with a single dose of either 225 mg/kg or 375 mg/kg. Interestingly, a subsequent *in vivo* experiment using the separated enantiomers of **JJ450** revealed that (1*R*,2*S*)-**JJ450** was more efficacious, directly contrasting the *in vitro* result. We are still unsure as to the reason for this activity difference from the *in vitro* to *in vivo*.

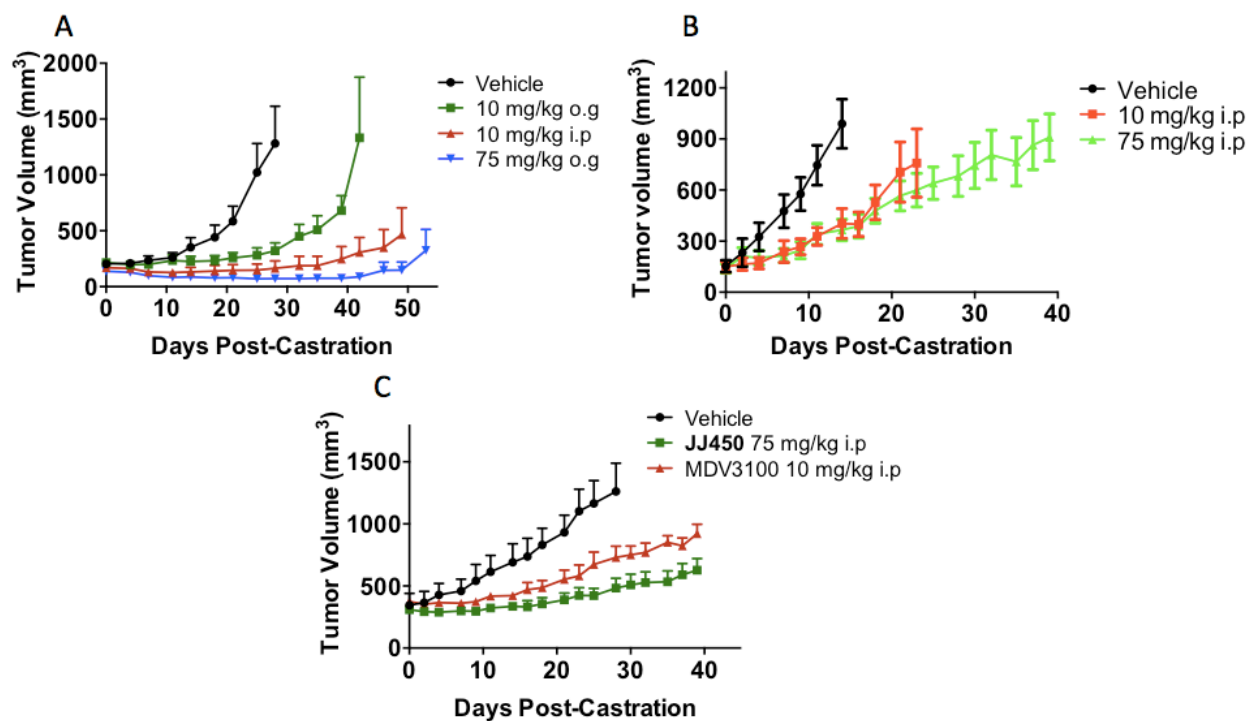
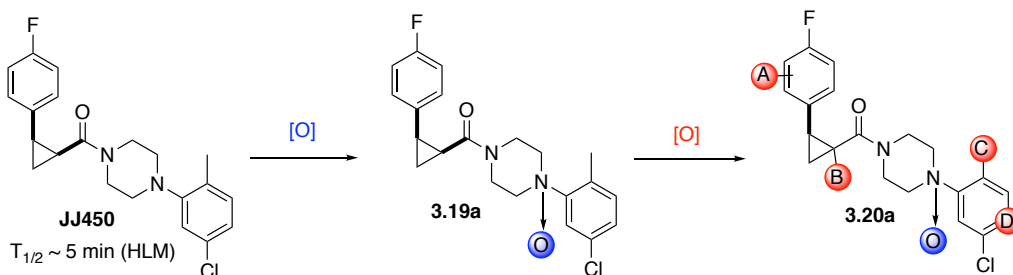


Figure 3.10. Effect of **JJ450** on LNCaP, 22Rv1, and VCaP s.c. tumor xenografts in nude SCID mice.⁴²¹

To further understand the metabolism of **JJ450**, HLM were incubated with **JJ450** and LCMS analysis of the microsomal fractions indicated two oxidation events were occurring. Our initial hypothesis was first *N*-oxidation of the aniline nitrogen to give *N*-oxide **3.20** (Scheme 3.3). We proposed that the second oxidation could occur in several other locations including the fluorinated aryl ring (A), next to the amide (B), the benzylic methyl group (C), and the 4-position of the aniline (D).



Scheme 3.3. Proposed metabolic oxidation and hotspots on **JJ450**.

3.2.2 Improving the Metabolic Stability of JJ450

With **JJ450** as our new starting point, we wanted to further improve its metabolic stability. Drug metabolism is an important factor to consider for further development of lead compounds as it plays a key role in toxicity, oral bioavailability, dosing. Several strategies have been developed to block or replace metabolically labile sites that include decreasing lipophilicity, introducing conformational constraint, introducing steric hindrance, tuning electronics, and altering stereochemistry.⁴²² Cytochrome P450s (CYP's) are responsible for most oxidative metabolism, which increases the polarity facilitating faster elimination. Liver microsomes serve as an *in vitro* model to predict CYP metabolism. Fluorine and fluorinated functional groups (CF₃, and SF₅) are commonly employed to block metabolically labile C-H bonds, decrease electron density of aromatic rings, increase lipophilicity, and lower the pKa of adjacent heteroatoms. In particular, we aimed to block several potentially metabolically labile sites on **JJ450** that included the benzylic methyl and aniline nitrogen (zone 1), the cyclopropane (zone 2), and the aryl ring (zone 3) (Figure 3.11). Additionally, as lipophilic compounds are more prone to CYP metabolism, we were also interested in decreasing the lipophilicity of **JJ450** through incorporation of heterocycles in zones 1 and 3 (Figure 3.11).

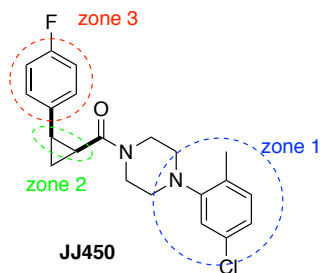
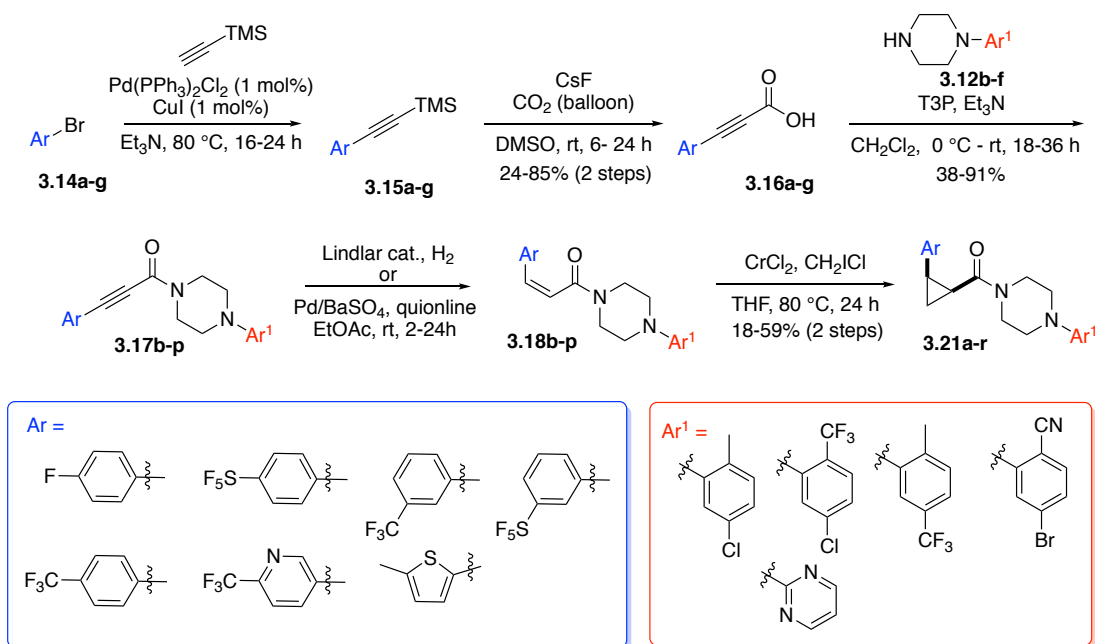


Figure 3.11. Proposed zones of structural modification.

The synthesis of new analogs were carried out in a similar fashion to **JJ450** and began with a Sonogashira coupling of commercially available aryl bromides **3.14a-3.14g** with TMS

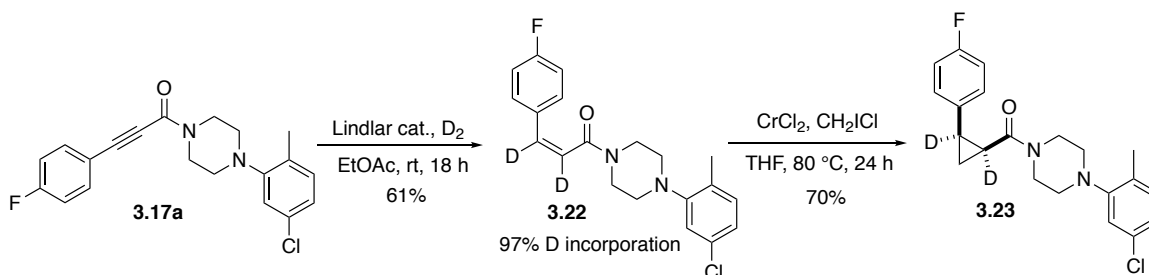
acetylene followed by treatment with CsF under an atmosphere of CO₂ to give the corresponding carboxylic acids **3.16a-3.16g** in good yields (Scheme 3.3). A subsequent T3P coupling of carboxylic acids **3.16b-3.16r** with *N*-arylated piperazines **3.12b-3.12f** afforded amides **3.17b-3.17r**. Hydrogenation was accomplished using either Lindlar catalyst or Pd/BaSO₄ with quinoline to afford the *cis*-alkenes **3.18b-3.18r** that were subjected to the chromium cyclopropanation conditions to afford *cis*-cyclopropanes **3.21a-3.21r**.



Scheme 3.4. Synthetic route to analogs of **JJ450**.

In addition to analogs with varying aryl substitutions, we prepared an analog containing a deuterium substituted cyclopropane ring. If the metabolic oxidation is a result of oxidation on the cyclopropane we should see a decrease in metabolic rate due to the primary kinetic isotope effect. The synthesis began with a Lindlar reduction of **3.17a** under an atmosphere of D₂ to afford the deuterated-*cis*-alkene **3.22** in excellent yields that was subsequently subjected to the Simmons-Smith cyclopropanation conditions to afford the desired deuterio-cyclopropane **3.23** (Scheme 3.4). Interestingly, we had also attempted to form the deuterio-*cis*-alkene using D₂O and

gold nanoparticle catalysis under a high pressure atmosphere of CO as previously described by Cao et al.,⁴²³ but, were unable to reproduce the reported pressures (400 psi) and therefore had low conversions and deuterium incorporation.



Scheme 3.5. Synthesis of deuterocyclopropane **3.23**.

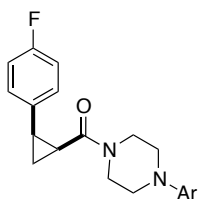
In total 19 analogs of **JJ450** were synthesized. Several of these racemic analogs were further resolved into their component enantiomers by semi-preparative chiral SFC chromatography. The absolute configurations of the separated enantiomers were assigned through a combination of circular dichroism (CD) and specific rotation analysis. Since the separated enantiomers retain the same *cis*-cyclopropane substitution pattern of the parent compound (1*R*,2*S*)-**JJ450**, the absolute configurations of the separated enantiomers were assigned by comparison to the specific rotation of (1*R*,2*S*)-**JJ450**, whose absolute configuration had been previously assigned by X-ray crystallography. Additionally, these analogs displayed consistent cotton effects in the circular dichroism (CD) spectra of enantiomers with matching specific rotation signs to (1*S*,2*R*)-**JJ450** and (1*R*,2*S*)-**JJ450** (See Appendix B).

3.2.3 Biological Data of **JJ450** Analogs: Cell Data and Metabolism

Following the synthesis of the 43 analogs of **JJ450**, their biological activity was determined in a PSA luciferase assay using a Dual-Glo luciferase system in the presence of 1 nM of the synthetic androgen R1881 in C4-2-PSA-rl cells.³⁴⁹ The EC₅₀'s were calculated using GraphPad Prism and

are preliminary. The biological activities were compared to **JJ450** (EC₅₀ 2.7 μM, Table 3.7, entry 1). Deuteration of the cyclopropane did not have any significant effect on the activity or the metabolism, indicating that the oxidation is possibly not on the cyclopropane but on one of the aryl rings. Substituents on the piperazines with aryl groups replacing the benzylic methyl or chloro with a trifluoromethyl were met with slight loss in activity with no effect on the metabolism. Unfortunately, the pyrimidine aryl functionality was met with a complete loss in activity as it has one of the most promising cLogD values of 2.25.

Table 3.7. Biological activity and liver microsome data for 4-fluoro substituted analogs.

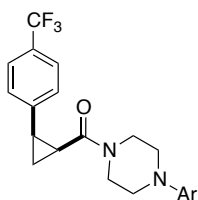


Entry	Compound	Structure Ar	EC ₅₀ (μM) ^a	cLogD ^e	MLM ^f	HLM ^f
1	JJ450	2-Me-5-Cl-Ph	2.7 ± 1.1 ^d	4.6	-	-
2	(1 <i>S</i> ,2 <i>R</i>)- JJ450	2-Me-5-Cl-Ph	1.7 ± 0.2 ^c	4.6	0.3%	27%
3	(1 <i>R</i> ,2 <i>S</i>)- JJ450	2-Me-5-Cl-Ph	15.2 ± 3.3 ^c	4.6	0.4%	8%
4	3.23	2-Me-5-Cl-Ph	2.2 ± 0.3 ^b	4.6	-	-
5	(1 <i>S</i> ,2 <i>R</i>)- 3.23	2-Me-5-Cl-Ph	1.9 ± 0.5 ^b	4.6	0.2%	28%
6	(1 <i>R</i> ,2 <i>S</i>)- 3.23	2-Me-5-Cl-Ph	14.3 ± 0.2 ^b	4.6	0.5%	9%
7	3.21a^g	2-Me-5-CF ₃	6.3 ± 3.0 ^b	4.9	-	-
8	(1 <i>S</i> ,2 <i>R</i>)- 3.21a^g	2-Me-5-CF ₃	2.5 ± 1.9 ^b	4.9	0.8%	31%
9	(1 <i>R</i> ,2 <i>S</i>)- 3.21a^g	2-Me-5-CF ₃ -Ph	9.4 ± 1.4 ^b	4.9	7%	26%
10	3.21b	2-CF ₃ -5-Cl-Ph	4.9 ± 0.9 ^b	5.0	-	-
11	3.21c		>25 ^b	2.3	-	-
12	(1 <i>S</i> ,2 <i>R</i>)- 3.21c		>25 ^b	2.3	-	-
13	(1 <i>R</i> ,2 <i>S</i>)- 3.21c		>25 ^b	2.3	-	-

^aEC₅₀'s were determined using a cell based luciferase assay as previously described.³⁴⁹ EC₅₀ refers to the concentration that results in 50% inhibition of PSA-luciferase activity. Each EC₅₀ was calculated using GraphPad Prism, and are the average of at least one independent assays using triplicate determinations at each concentration for each experiment where noted; *n* = number of assay repeats: ^b*n* = 2, ^c*n* = 3, ^d*n* = 4. ^ecLogD were calculated using InstantJchem. ^fLiver microsome data is reported as the % compound remaining at 60 min and were measured in

the presence of NADPH. MLM, mouse liver microsomes; HLM, human liver microsomes.
^gCompound was synthesized by Dr. Keita Takubo.

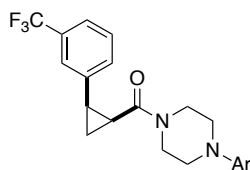
The 4-trifluoromethyl substitution of the arylcyclopropane resulted in an overall 2 to 3-fold decrease in activity and an overall increase in microsome stability, possibly due to an increased in steric bulk and decreased electron density on the aryl ring respectively. The parent **3.21d** (2-Me-5-Cl-Ph) appears to have poor metabolism (Table 3.8, entries 1-3) while the trifluoromethyl substitutions afford a 20-fold increase in microsome stability over **JJ450**. In particular, analog (1*S*,2*R*)-**3.21f** (Table 3.8, entry 8) had a promising half-life of 1.5 h with an EC₅₀ of ~12 μM. Interestingly, compound **3.21g** with the 2-CN-5-Br-Ph substitution led to a significant decrease in activity contrary to what we had previously observed for compound **3.6e** in our original SAR (Table 3.8, entries 10-12). Additionally, these trifluoromethyl substituted analogs also are significantly lipophilic (cLogD ~5-6), possibly limiting their utility in animal and human studies.

Table 3.8. Biological activity and liver microsome data for 4-trifluoromethyl substituted analogs.

Entry	Compound	Structure	EC ₅₀ (μM) ^a	cLogD ^d	MLM ^e	HLM ^e
		Ar				
1	3.21d^f	2-Me-5-Cl-Ph	6.6 ± 1.7 ^c	5.4	-	-
2	(1 <i>S</i> ,2 <i>R</i>)- 3.21d^f	2-Me-5-Cl-Ph	8.4 ± 3.6 ^c	5.4	11%	45%
3	(1 <i>R</i> ,2 <i>S</i>)- 3.21d^f	2-Me-5-Cl-Ph	23.1 ± 2.6 ^c	5.4	14%	5%
4	3.21e^f	2-Me-5-CF ₃ -Ph	11.9 ± 2.1 ^c	5.6	-	-
5	(1 <i>S</i> ,2 <i>R</i>)- 3.21e^f	2-Me-5-CF ₃ -Ph	12.1 ± 4.5 ^c	5.6	49%	58%
6	(1 <i>R</i> ,2 <i>S</i>)- 3.21e^f	2-Me-5-CF ₃ -Ph	15.5 ± 5.7 ^c	5.6	48%	23%
7	3.21f	2-CF ₃ -5-Cl-Ph	9.1 ± 0.8 ^c	5.7	-	-
8	(1 <i>S</i> ,2 <i>R</i>)- 3.21f	2-CF ₃ -5-Cl-Ph	12.0 ^b	5.7	60% (t _{1/2} = 1.5 h)	65%
9	(1 <i>R</i> ,2 <i>S</i>)- 3.21f	2-CF ₃ -5-Cl-Ph	>25 ^b	5.7	34%	51%
10	3.21g	2-CN-5-Br-Ph	>25 ^c	4.9	-	-
11	(1 <i>S</i> ,2 <i>R</i>)- 3.21g	2-CN-5-Br-Ph	23.4 ± 3.5 ^c	4.9	-	-
12	(1 <i>R</i> ,2 <i>S</i>)- 3.21g	2-CN-5-Br-Ph	>25 ^c	4.9	-	-

^aEC₅₀'s were determined using a cell based luciferase assay as previously described.³⁴⁹ EC₅₀ refers to the concentration that results in 50% inhibition of PSA-luciferase activity. Each EC₅₀ was calculated using GraphPad Prism, and are the average ± stdev of at least one independent assay using triplicate determinations at each concentration for each experiment where noted; *n* = number of assay repeats: ^b*n* = 1, ^c*n* = 2. ^dcLogD were calculated using InstantJchem. ^eLiver microsome data is reported as the % compound remaining at 60 min and were measured in the presence of NADPH. MLM, mouse liver microsomes; HLM, human liver microsomes. ^fCompound was synthesized by Dr. Keita Takubo.

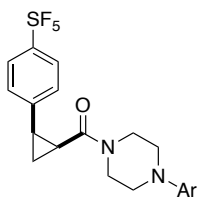
Analogues containing the 3-trifluoromethyl substitution also showed a slight decrease in activity (ca. 2-fold) compared to the 4-F analogs, exhibiting a similar trend to analogues containing the 4-trifluoromethyl substitution (Table 3.9). In contrast, the 3-substituted analogues were not as metabolically stable as the 4-substituted analogues with a ca. 5-fold decrease in stability.

Table 3.9. Biological activity and liver microsome data for 3-trifluoromethyl substituted analogs.

Entry	Compound	Structure	EC ₅₀ (μM) ^a	cLogD ^d	MLM ^e	HLM ^e
		Ar				
1	3.21h	2-Me-5-Cl-Ph	3.3 ± 0.8 ^c	5.4	-	-
2	(1 <i>S</i> ,2 <i>R</i>)- 3.21h	2-Me-5-Cl-Ph	3.6 ± 0.2 ^b	5.4	0.2%	1%
3	(1 <i>R</i> ,2 <i>S</i>)- 3.21h	2-Me-5-Cl-Ph	6.3 ± 1.8 ^b	5.4	0.9%	4%
4	3.21i	2-Me-5-CF ₃ -Ph	7.7 ± 2.1 ^b	5.6	-	-
5	3.21j	2-CF ₃ -5-Cl-Ph	3.4 ± 2.3 ^b	5.7	12%	34%

^aEC₅₀'s were determined using a cell based luciferase assay as previously described.³⁴⁹ EC₅₀ refers to the concentration that results in 50% inhibition of PSA-luciferase activity. Each EC₅₀ was calculated using GraphPad Prism, and are the average ± stdev of two independent assay using triplicate determinations at each concentration for each experiment where noted; *n* = number of assay repeats: ^b*n* = 2, ^c*n* = 3. ^dcLogD were calculated using InstantJchem. MLM, mouse liver microsomes; HLM, human liver microsomes. ^eLiver microsome data is reported as the % compound remaining at 60 min and were measured in the presence of NADPH.

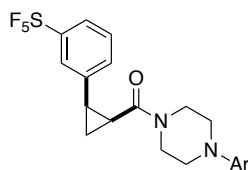
Similar to its trifluoromethyl counterpart, the 4-pentafluorosulfanyl substitution led to a global 3-fold decrease in activity but an overall increase in microsome stability (Table 3.10). In particular, analog (1*S*,2*R*)-**3.21i** (Table 3.10, entry 5) had a half-life in liver microsomes ~3 h with an EC₅₀ of 11 μM. Unfortunately, these analogs are even more lipophilic than the trifluoromethyl analogs with cLogDs ~6-7 that could also limit their utility in animal and human studies.

Table 3.10. Biological activity and liver microsome data for 4-pentafluorosulfanyl substituted analogs.

Entry	Compound	Structure	EC ₅₀ (μM) ^a	cLogD ^d	MLM ^e	HLM ^e
		Ar				
1	3.21k	2-Me-5-Cl-Ph	11.4 ± 1.6 ^c	6.5	-	-
2	(1 <i>S</i> ,2 <i>R</i>)- 3.21k	2-Me-5-Cl-Ph	8.2 ± 4.0 ^b	6.5	24%	3%
3	(1 <i>R</i> ,2 <i>S</i>)- 3.21k	2-Me-5-Cl-Ph	18.9 ± 4.4 ^b	6.5	40%	53%
4	3.21l	2-Me-5-CF ₃ -Ph	7.8 ± 4.3 ^b	6.9	-	-
5	(1 <i>S</i> ,2 <i>R</i>)- 3.21l	2-Me-5-CF ₃ -Ph	9.1 ± 2.7 ^b	6.9	80%	77%
6	(1 <i>R</i> ,2 <i>S</i>)- 3.21l	2-Me-5-CF ₃ -Ph	21.3 ± 2.8 ^b	6.9	66%	30% (t _{1/2} = 3 h)

^aEC₅₀'s were determined using a cell based luciferase assay as previously described.³⁴⁹ EC₅₀ refers to the concentration that results in 50% inhibition of PSA-luciferase activity. Each EC₅₀ was calculated using GraphPad Prism, and are the average ± stdev of two independent assay using triplicate determinations at each concentration for each experiment where noted; *n* = number of assay repeats: ^b*n* = 2, ^c*n* = 3. ^dcLogD were calculated using InstantJchem. ^eLiver microsome data is reported as the % compound remaining at 60 min and were measured in the presence of NADPH. MLM, mouse liver microsomes; HLM, human liver microsomes.

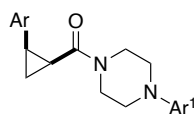
The 3-pentafluorosulfanyl analogs were ca. 2-fold more potent compared to the 4-pentafluorosulfanyl analogs, but did not perform as well in the liver microsomes (Table 3.11). Even with the modest recovery of activity, the aqueous solubility will also be a concern for these analogs.

Table 3.11. Biological activity and liver microsome data for 3-pentafluorosulfanyl substituted analogs.

Entry	Compound	Structure	EC ₅₀ (μM) ^a	cLogD ^c	MLM ^d	HLM ^d
		Ar				
1	3.21m	2-Me-5-Cl-Ph	4.6 ± 0.8 ^b	5.4	-	-
2	3.21n	2-Me-5-CF ₃ -Ph	5.7 ± 0.3 ^b	6.9	-	-
3	(1 <i>S</i> ,2 <i>R</i>)- 3.21n	2-Me-5-CF ₃ -Ph	9.9 ± 1.4 ^b	6.9	6%	4%
4	(1 <i>R</i> ,2 <i>S</i>)- 3.21n	2-Me-5-CF ₃ -Ph	7.1 ± 1.8 ^b	6.9	35%	11%

^aEC₅₀'s were determined using a cell based luciferase assay as previously described.³⁴⁹ EC₅₀ refers to the concentration that results in 50% inhibition of PSA-luciferase activity. Each EC₅₀ was calculated using GraphPad Prism, and are the average ± stdev of at least two independent assays using triplicate determinations at each concentration for each experiment where noted; *n* = number of assay repeats: ^b*n* = 2. ^ccLogD were calculated using InstantJchem. ^dLiver microsome data is reported as the % compound remaining at 60 min and were measured in the presence of NADPH. MLM, mouse liver microsomes; HLM, human liver microsomes.

Interestingly, the trifluoromethyl pyridine **3.21o** (Table 3.12, entries 1-3) was found to be less active and less stable in microsomes. Additionally, it appears that (1*R*,2*S*)-**3.21o** is slightly more potent than the (1*S*,2*R*)-**3.21o**, which is opposite from what is observed with other **JJ450** analogs. In contrast, the thiophene **3.21p-3.21r** was similar potency to **JJ450** with all substitutions on the piperazine. This is promising as smaller 5-membered heterocycles seem to recover the activity lost with introduction of bulky para-substituents as previously observed with the SF₅ and CF₃ substitutions.

Table 3.12. Biological activity and liver microsome data for heteroaryl substituted analogs.

Entry	Compound	Structure		EC ₅₀ (μM) ^a	cLogD ^d	MLM ^e	HLM ^e
		Ar	Ar ¹				
1	3.21o		2-Me-5-CF ₃ -Ph	20.8 ± 6.0 ^c	4.8	-	-
2	(1 <i>S</i> ,2 <i>R</i>)- 3.21o		2-Me-5-CF ₃ -Ph	18.0 ± 1.7 ^b	4.8	35%	39%
3	(1 <i>R</i> ,2 <i>S</i>)- 3.21o		2-Me-5-CF ₃ -Ph	13.6 ± 1.8 ^b	4.8	24%	6%
4	3.21p		2-Me-5-Cl-Ph	2.2 ± 0.5 ^c	5.0	-	-
5	3.21q		2-Me-5-CF ₃ -Ph	4.1 ± 0.3 ^c	5.3	-	-
6	3.21r		2-CF ₃ -5-Cl-Ph	2.0 ± 0.1 ^b	5.4	-	-

^aEC₅₀'s were determined using a cell based luciferase assay as previously described.³⁴⁹ EC₅₀ refers to the concentration that results in 50% inhibition of PSA-luciferase activity. Each EC₅₀ was calculated using GraphPad Prism, and are the average ± stdev of at least two independent assays using triplicate determinations at each concentration for each experiment where noted; *n* = number of assay repeats: ^b*n* = 2, ^c*n* = 3. ^dcLogD were calculated using InstantJchem. ^eLiver microsome data is reported as the % compound remaining at 60 min and were measured in the presence of NADPH.

In summary, 43 analogs were synthesized, and the SAR evaluated 3 zones of modifications of our lead compound **JJ450** (Figure 3.12). We gained further understanding about the environment that these compounds bind. Zone 1 modifications showed that the 2,5-aryl substitutions with Cl or CF₃ were well tolerated, while other modifications appeared to cause significant loss in activity. Limited substitutions were performed in zone 2 and deuterio-**JJ450** was found to have similar activity to the parent compound. In zone 4, increasing the steric bulk of the *para* or *meta*-substituent reduced activity, and only the thiophene maintained activity comparable to **JJ450**.

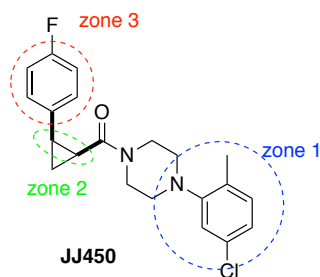
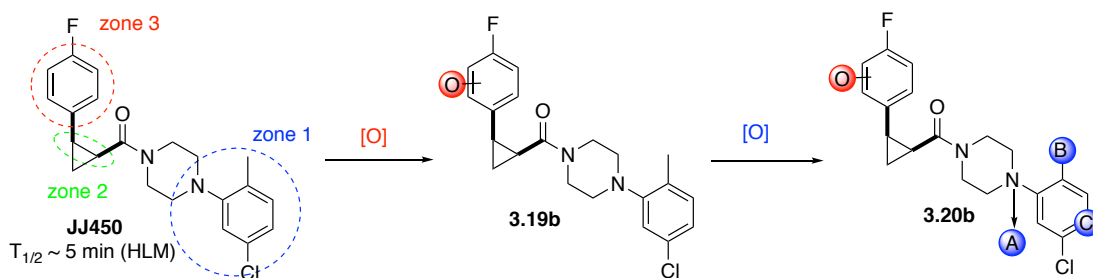


Figure 3.12. Zones of structural modification on **JJ450**.

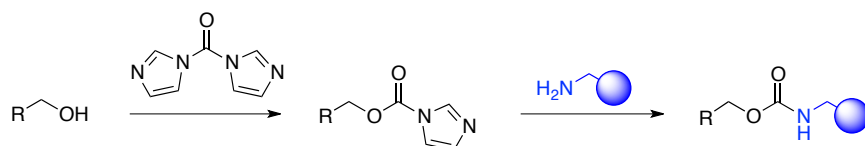
Our primary aim of these 3 zones of structural modifications was to increase the stability of the parent compound **JJ450** in liver microsomes, a predictive model for phase 1 metabolism (Scheme 3.6). In zone 1, the 2-CF₃-5-Cl and 2-Me-5-CF₃ substitution only afforded modest increase in stability. The deuterium labeling in zone 2 resulted in no overall effect on the metabolism indicating that this is not a major or initial site of metabolism. Finally, modifications in zone 3 were shown to be the most influential in increasing the microsomal stability indicating that this is our primary site of metabolism. The most significant increase in microsomal stability was noted in compounds containing a *para*-CF₃ or SF₅. Gratifyingly, compound **3.211** was found to have a half-life of ~3 h in liver microsomes, a ~40-fold increase in stability from the parent **JJ450**. Additionally, given this data we must reconsider our initial hypothesis of the metabolic oxidation of **JJ450**. The major metabolic liability appears to be the fluorinated aryl ring (Scheme 3.6). The second metabolic liability is found at the aniline ring where fluorinated substituents were found to slightly improve the microsomal stability.



Scheme 3.6. Revised sites of metabolism on **JJ450**.

3.2.4 Synthesis of Chemical Probes to Elucidate the Mechanism of Action

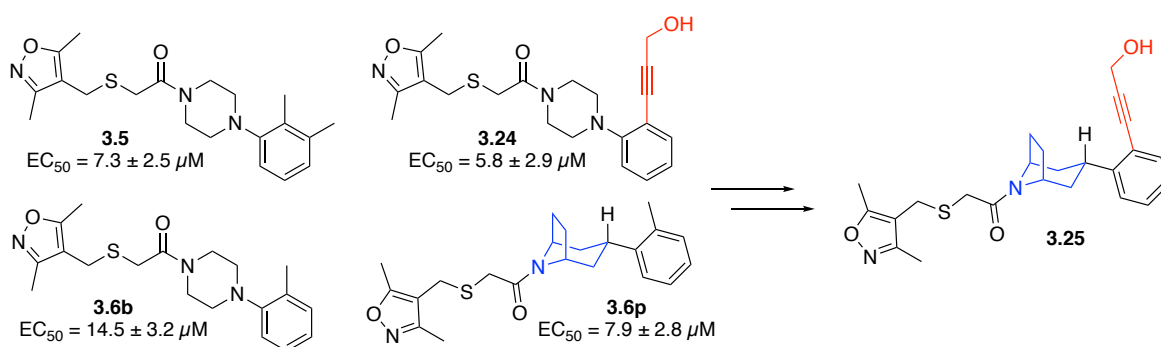
In addition to developing new and more potent inhibitors of CRPC with increased metabolic stability, we also wanted to develop small molecules to probe the mechanism of action of our lead compounds. Several methods have been developed using small-molecule-based affinity reagents to identify cellular targets.⁴²⁴⁻⁴²⁵ They require an effective conjugation protocol as well as methods for affinity purification. There are three main methods for target pull-down using small molecules that include immobilization onto agarose beads, conjugation to biotin, or photoaffinity labeling. In particular, many agarose beads are commercially available or readily tuned to have a variety of functionalized surfaces (containing carboxylic acids, amines, alkynes, or azides). There are many methods used for the conjugation step such as peptide coupling of amines and carboxylic acids, reductive amination, or Cu(I)-catalyzed [3+2] cycloaddition. Agarose beads conjugated to active compounds are incubated with whole cell lysates to capture potential target proteins. Schreiber and coworkers developed a method to conjugate alcohol-containing small molecules to agarose beads that uses CDI to form an activated carbamate that can then undergo conjugation to an agarose bead functionalized with amine linkers (Scheme 3.7).⁴²⁶



Scheme 3.7. Bead conjugation of alcohol-containing molecules.

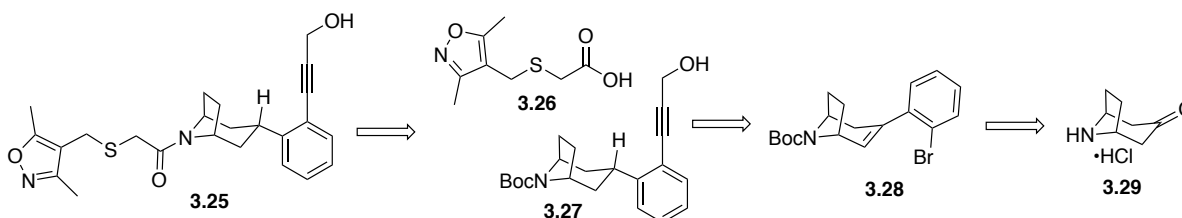
Previously, we identified **3.24** as a new analog that was slightly more potent than the original HTS hit **3.5** and contained a propargyl alcohol handle that could be coupled to an agarose bead to form a derivative for pull-down studies. The bridged bicyclic [3.2.1] analogs

such as **3.6p** were of interest as both diastereomers were equipotent indicating that structural bulk could be tolerated around the piperazine as well as a 2-fold increase in potency from the 2-MePh analog **3.6b**. We proposed that a hybrid structure of **3.24** and the bridged bicyclic [3.2.1] analog **3.6p** would yield a 2-fold increase in binding affinity compared to **3.24**. This more potent analog **3.25** would be better suited for conjugation to agarose beads and a subsequent pull-down study (Scheme 3.8).



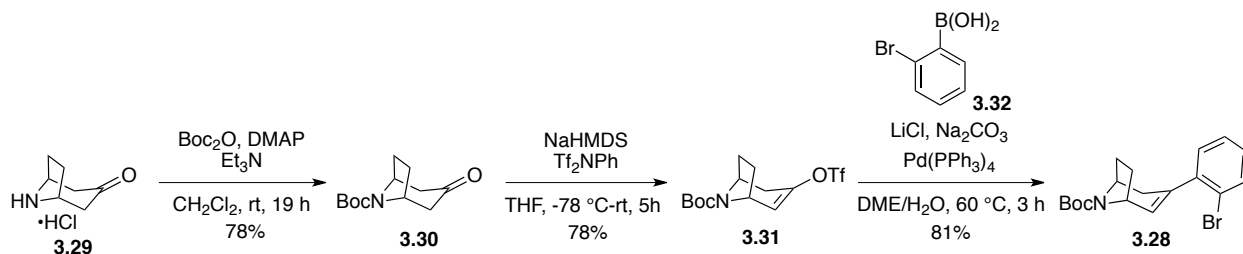
Scheme 3.8. Initial proposed analog **3.25** for affinity labeling.

Our retrosynthetic approach to **3.25** features a late stage coupling of amine **3.27** to commercially available carboxylic acid **3.26** (Scheme 3.9). We proposed hydrogenation of the styrene **3.28** followed by a Sonogashira coupling to install the key propargyl alcohol side chain. We envisioned that styrene **3.28** could be constructed from commercially available nortropinone hydrochloride **3.29** via a Boc-protection, enolization and vinyl triflate formation, and a Suzuki cross coupling.



Scheme 3.9. Retrosynthetic approach to analog **3.25**.

The synthesis of the styrene intermediate **3.28** began with Boc-protection of commercially available nortropinone hydrochloride (**3.29**) followed by enolization with NaHMDS and trapping of the enolate with Comins' reagent to afford the vinyl triflate **3.31** (Scheme 3.10). A Suzuki coupling of vinyl triflate **3.31** and boronic acid **3.32** afforded the 2-bromostyrene **3.28** in good yields.

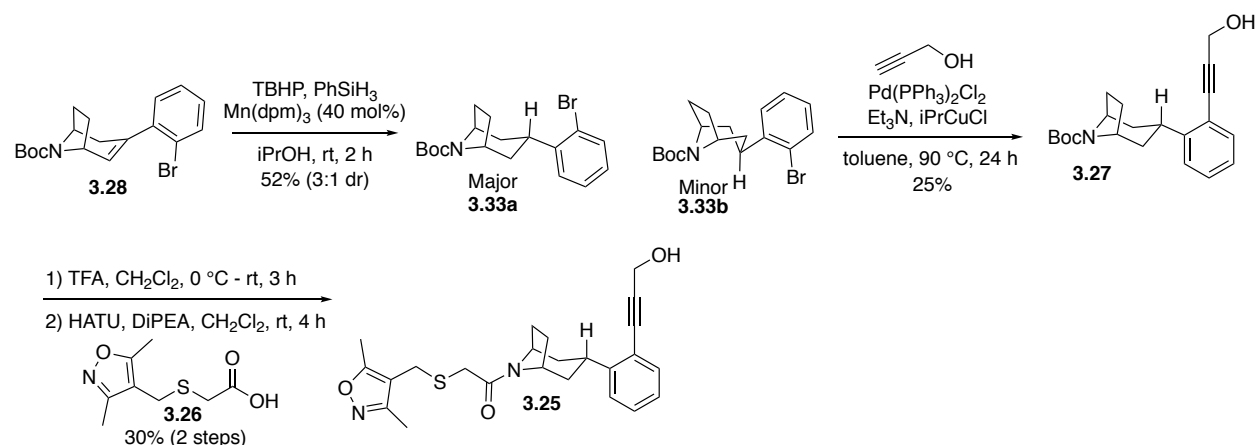


Scheme 3.10. Synthesis of styrene **3.28**.

Our next focus was to reduce the alkene in the presence of the aryl bromide. We screened many reaction conditions for this reduction including PtO₂, and diimide reductions; however, all attempts were unsuccessful due to overreduction of the alkene and aryl bromide or lack of reactivity.⁴²⁷⁻⁴²⁹ In the case of the diimide reductions, a large excess of reagents was required to see even trace reduction. Gratifyingly, we discovered that the hydrogen atom transfer hydrogenation conditions, previously developed by Shenvi, were successful on our substrate to afford the product **3.33** in modest yields as a 3:1 mixture of diastereomers **3.33a** and **3.33b** (Scheme 3.11).⁴³⁰⁻⁴³¹ Using the mixture of diastereomers, we moved forward with the Sonogashira cross coupling. Using CuI, other sources of Pd, or a protected propargyl alcohol afforded only trace product. Ultimately, we found that we could use (*i*Pr)CuCl²⁹³ (*vide infra*) to give a single diastereomer of propargyl alcohol **3.27** in manageable yields with only trace amounts (<5%) of the minor diastereomer as separable products by chromatography. Additionally, using the styrene for the Sonogashira coupling was also unsuccessful and protodemetalation was the major pathway observed. Finally, Boc-deprotection of **3.27** and

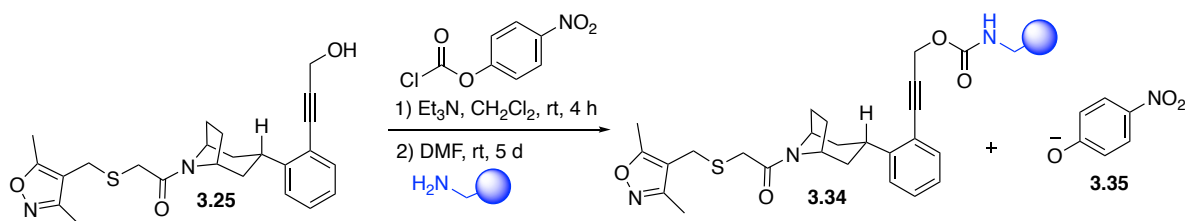
coupling to commercially available carboxylic acid **3.26** afforded amide **3.25** in modest yields.

The poor yield in the coupling is the result of over acylation of the propargyl alcohol.



Scheme 3.11. Synthesis of **3.25**.

For the conjugation of **3.25** to the agarose beads, we had initially tried using CDI to form the activated carbamate but found it difficult to quantify by LCMS and IR. We modified our procedure for the use of 4-nitrophenylchloroformate to form the activated carbonate that releases the highly colored 4-nitrophenolate anion **3.35** upon amine conjugation in DMF at rt for 5 days with gentle inversion (Scheme 3.12).



Scheme 3.12. Conjugation of **3.25** to agarose beads.

After washing of the beads, we were able to see several characteristic IR shifts compared to a blank bead sample. In particular, we can see a small alkyne stretch around 2050 cm⁻¹ and significant changes in the fingerprint region (Figure 3.13).

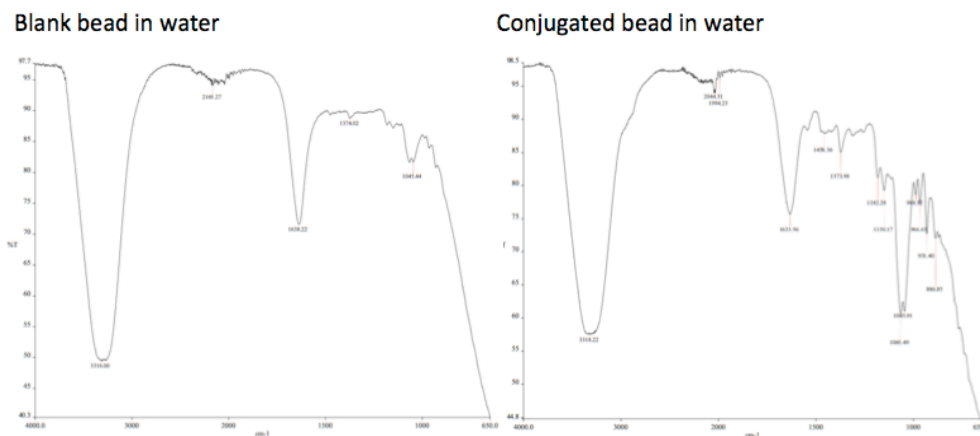


Figure 3.13. Comparison of the IR spectra of the unconjugated blank bead to the conjugated bead.

In addition to **3.25**, we also wanted to synthesize an analog **3.36** with a longer flexible linker to prevent any potential interference of the agarose bead with binding of the inhibitor and to avoid any nonspecific binding interactions (Figure 3.14). Initial attempts at the Sonogashira coupling with a PEG-alkyne were unsuccessful and instead we used a Heck coupling to install an ester as a more flexible handle for conjugation. We proposed that the benzyl ester could be selectively cleaved in the presence of the internal ester and the corresponding carboxylic acid can be used in an amide coupling for conjugation.

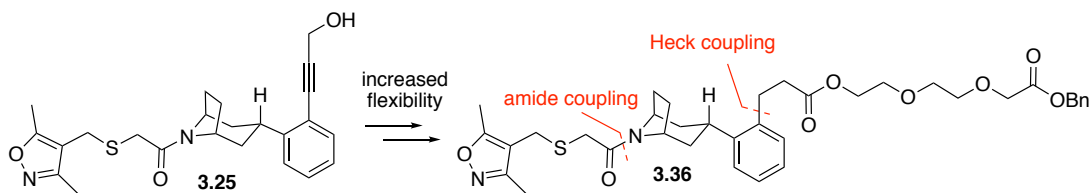
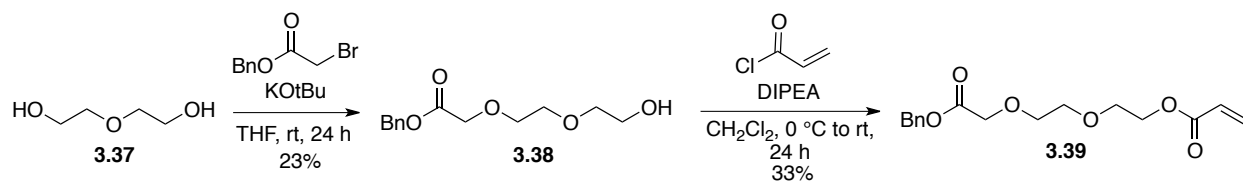


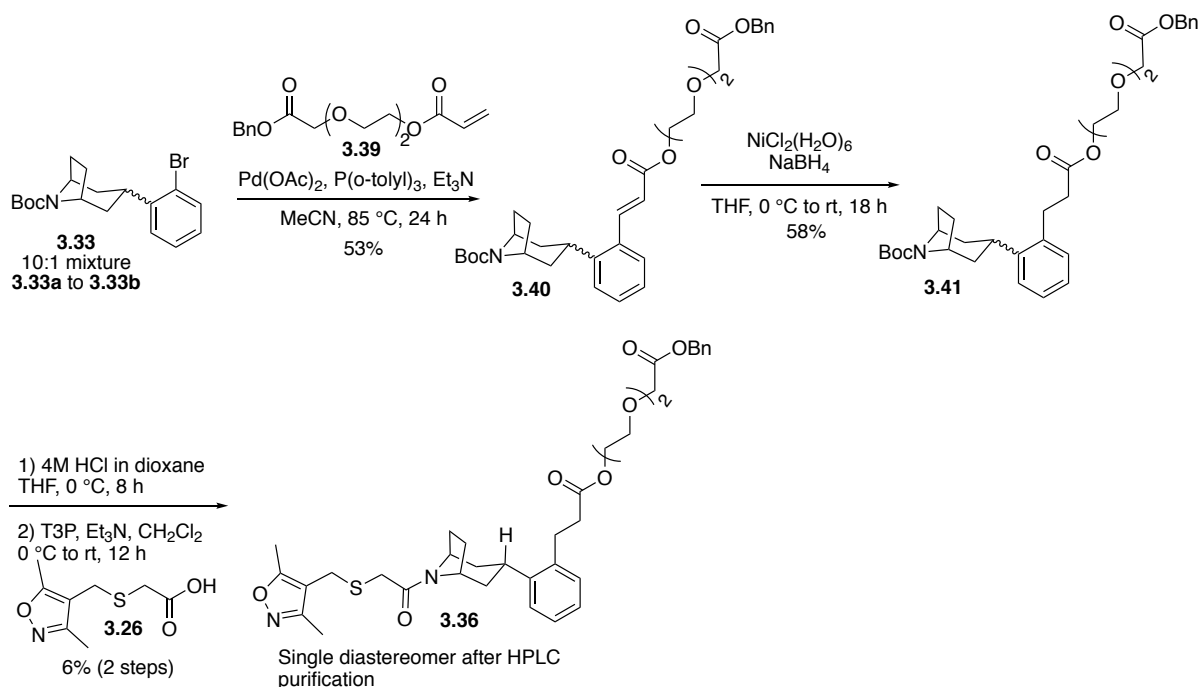
Figure 3.14. Proposed flexible linker modifications to **3.25**.

For a convergent approach we synthesized the acrylate PEG linker **3.29** for the Heck coupling (Scheme 3.13). The synthesis of **3.29** began from the monoalkylation of diethylene glycol (DEG, **3.37**) to afford benzyl ester **3.38** in poor yields. The terminal alcohol of **3.38** was acylated with acryloyl chloride to afford acrylate **3.39** in poor yields.



Scheme 3.13. Synthesis of acrylate linker **3.39**.

The acrylate side chain was coupled to the previously prepared bromide diastereomers **3.33** (enriched to a 10:1 mixture of **3.33a**:**3.33b** by chromatography) via a Heck coupling (Scheme 3.14). In contrast to the Sonogashira coupling, both diastereomers participate in the Heck coupling to give the alkene **3.40** as a similar mixture of diastereomers. Selective reduction of the $\alpha\beta$ -unsaturated ester **3.40** in the presence of the benzyl ether was accomplished using nickel mediated conjugate reduction. Other attempts using Pd/C also resulted in competitive cleavage of the OBn ester. Boc-deprotection and coupling to carboxylic acid **3.26** afforded **3.36** as a mixture of diastereomers that could be separated by preparative HPLC to afford poor yields of **3.26** as a single diastereomer. In preparation for conjugation, we looked to selectively cleave the benzyl ester in the presence of the internal ester. Unfortunately, the benzyl ester could not readily be cleaved by hydrogenation using Pd/C due to the presence of the thioether with no reactivity observed. Saponification in alcoholic solvents only afforded a mixture of transesterified products. We were delighted to find that tetrabutyl ammonium hydroxide (TBAH) selectively cleaved the benzyl ester in modest yields. Unfortunately, on large scale we encountered problems with the stability of these compounds during the conjugate reduction of **3.40** to **3.41**, where we observed reduction of the internal ester and loss of the PEG linker. As a result of this we wanted to modify the linker to have increased stability.



Scheme 3.14. Synthesis of **3.36**.

We hypothesized that a major source of instability was the presence of the internal ester. Therefore, we proposed analog **3.42**, which would contain an ether in place of the ester (Figure 3.15). We anticipated that this analog could be synthesized using a late stage amide coupling of carboxylic acid **3.26** and an amine precursor that can presumably be constructed by a Heck coupling with ethyl acrylate and then reduced to the propyl alcohol that can be alkylated with a PEG linker.

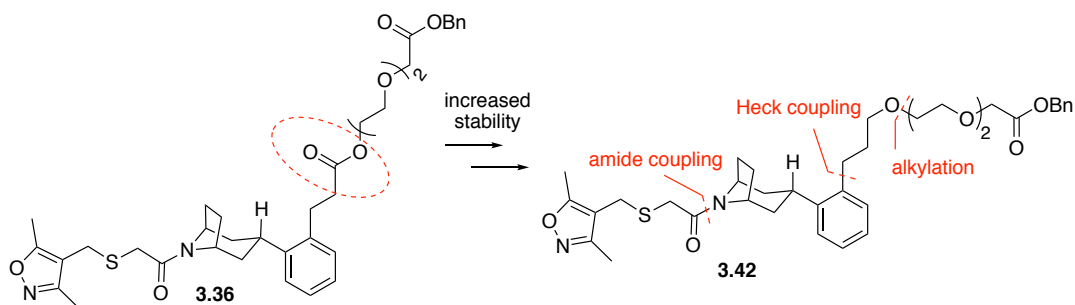
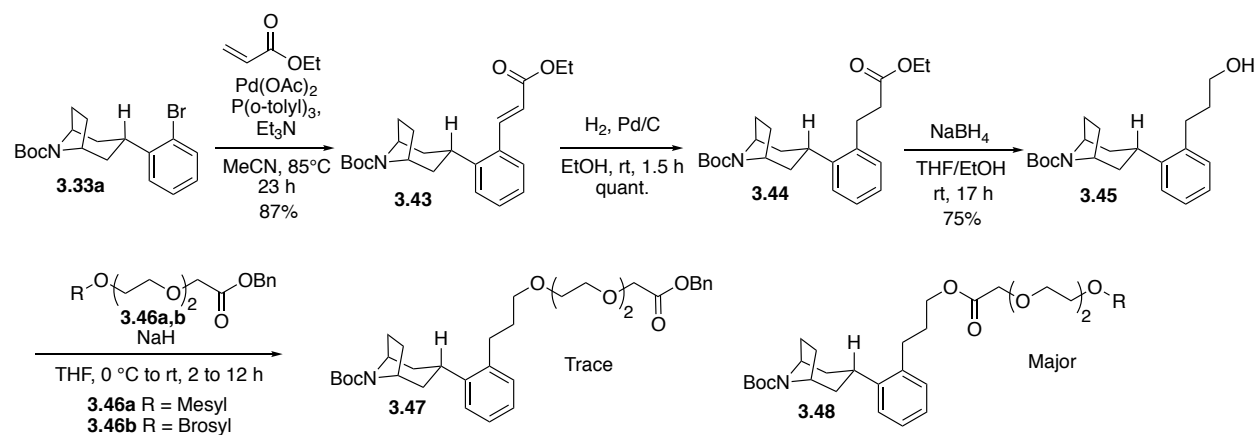


Figure 3.15. Proposed structural modifications to improve chemical stability.

Given the difficulty encountered in separating the diastereomers at the final step, we optimized the chromatographic separation after the reduction of alkene **3.28** to yield pure diastereomer **3.33a**, which, under Heck coupling conditions with ethyl acrylate, gave ester **3.43** in excellent yields (Scheme 3.15). Hydrogenation of the alkene **3.43** followed by reduction of the ester afforded alcohol **3.45**. Unfortunately, displacement of the activated mesylate and brosylate only afforded the transesterified product **3.48** with only trace amounts of the ether **3.47**.



Scheme 3.15. Synthetic approach to ether intermediate **3.47**.

To circumvent issues of reactivity we decided to synthesize an analog of **3.36** containing an amide in place of the internal ester (Figure 3.16). This more stable variant containing a readily saponified aromatic ester will reduce problems of chemical intractability encountered with previous substrates. We envisioned the synthesis of this analog could be through a late stage amide coupling of an amine linker and the carboxylic acid of **3.44**.

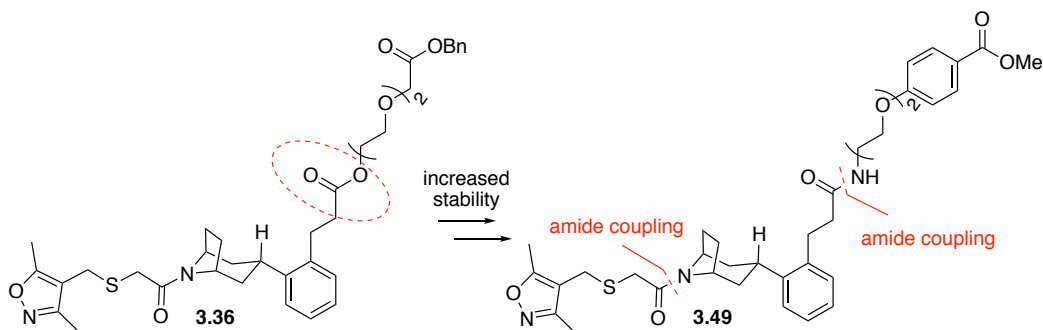
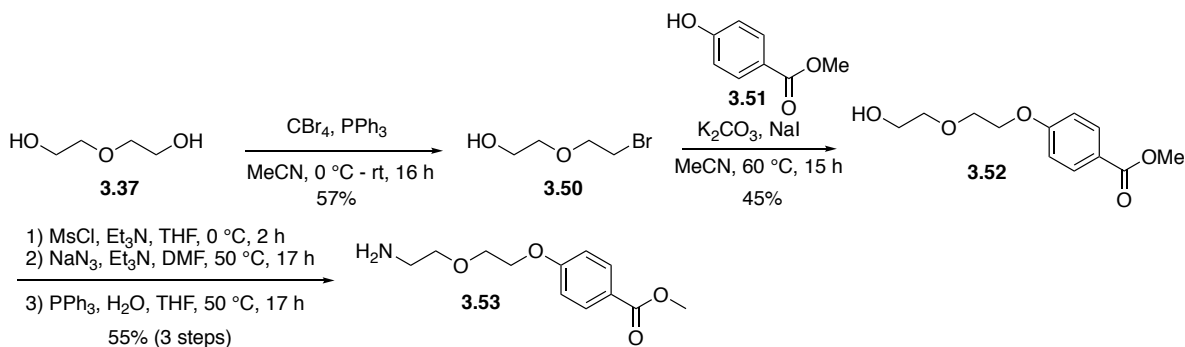


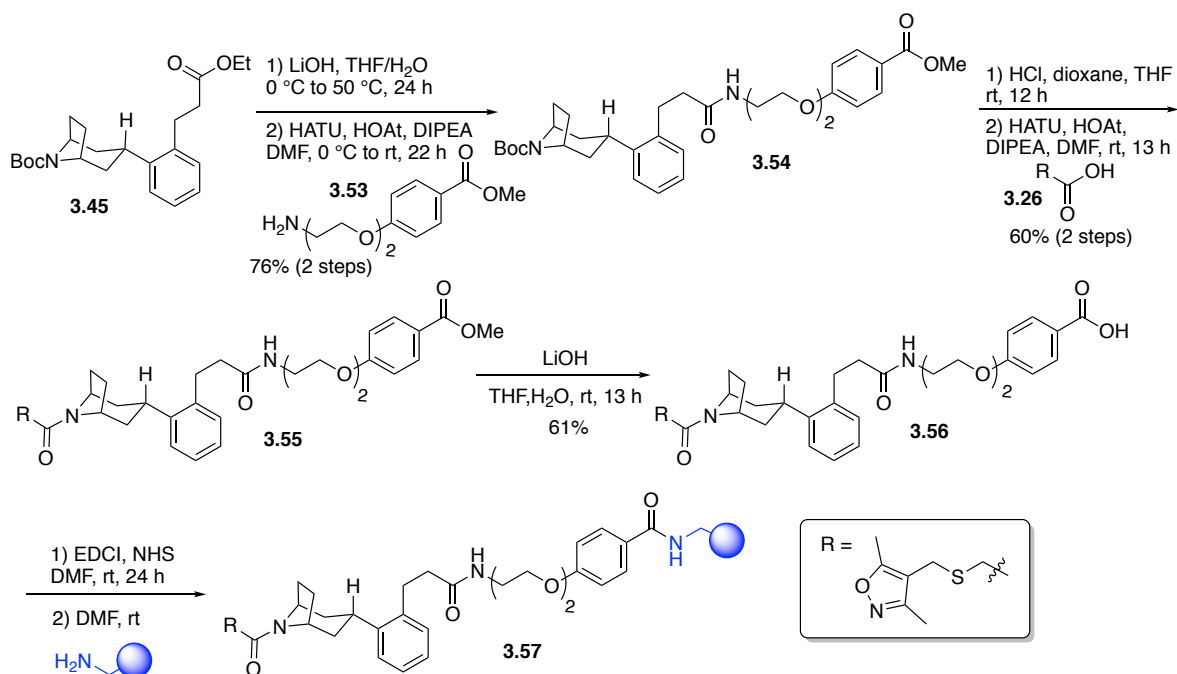
Figure 3.16. Proposed amide bead precursor **3.49**.

The synthesis of the amine linker **3.53** began with an Appel bromination of DEG (**3.37**) and displacement of the bromide with methyl paraben (**3.51**) to afford ester **3.52** (Scheme 3.16). The terminal alcohol of **3.52** was activated as the mesylate, displaced with sodium azide, and reduced under Staudinger reduction conditions to afford amine **3.53**.



Scheme 3.16. Synthesis of amine linker **3.53**.

The previously synthesized ester **3.45** was hydrolyzed and coupled to the amine linker **3.53** to afford the amide **3.54** (Scheme 3.17). Deprotection of the Boc group and coupling with the commercially available carboxylic acid **3.26** gave the amide **3.55** in modest yields. Saponification of the methyl ester of **3.55** gave the carboxylic acid that was activated as the *N*-hydroxysuccinimide (NHS) ester and conjugated to the Carboxylink® agarose beads to afford the affinity labeled **3.57**.



Scheme 3.17. Synthesis and conjugation of analog **3.55**.

In addition to the bridged bicyclic [3.2.1] analogs we also wanted to append a cyclopropane side chain in place of the thioether of **3.24** to test if we will see a similar increase in efficacy when attached to a piperazine containing a propargyl alcohol linker (Figure 3.17).

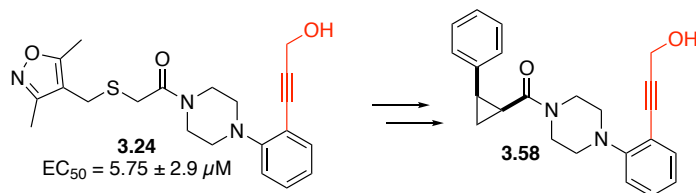
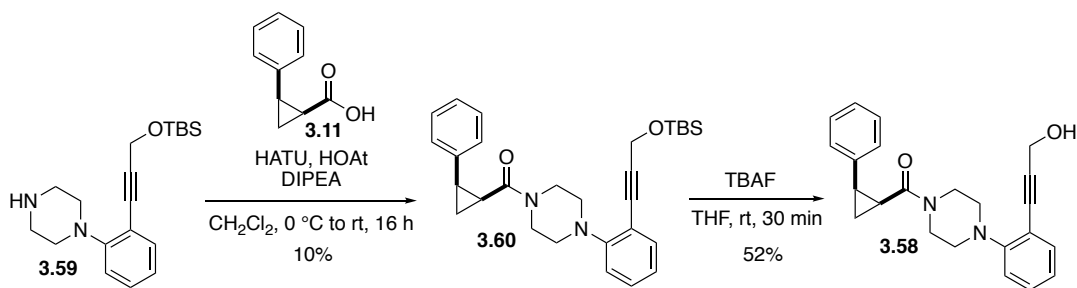


Figure 3.17. Proposed cyclopropane analog **3.58**.

The synthesis of the cyclopropane analog **3.58** began with a T3P coupling of cyclopropane carboxylic acid **3.11** and piperazine **3.59** that was previously prepared by Dr. Mustafa Kazancioglu to afford the amide **3.60** in poor yields (Scheme 3.18). The low yield in the coupling is possibly due to some decomposition of piperazine **3.59** after storage as the free base. A final TBS deprotection of **3.60** afforded the desired propargyl alcohol **3.58** in modest yields.



Scheme 3.18. Synthesis of cyclopropane analog affinity labeling precursor **3.58**.

3.2.5 Biological Activity of Analogs for Affinity Labeling

Following the synthesis of the analogs for affinity labeling, their biological activity was determined using a PSA luciferase assay using a Dual-Glo luciferase system in the presence of 1 nM of the synthetic androgen R1881 in C4-2-PSA-rl cells. The preliminary EC_{50} 's were calculated using GraphPad Prism. Gratifyingly, analog **3.27** was 2-fold more active compared to the alkyne **3.24** further supporting our hypothesis that the bridged bicyclic [3.2.1] system results in a 2-fold increase in activity (Table 3.13). The analog with the longer linker **3.55** was significantly less active than hybrid **3.25**. We are not sure if this is the result of a longer linker or the more flexible propyl side chain compared to the propargyl linker. Surprisingly, the cyclopropyl analog of **3.58** was 3-fold less active than **3.24** with the thioether side chain. With the promising activity of **3.25**, the conjugated beads were carried forward into whole cell pull-down assay.

Table 3.13. Biological activity of affinity precursors.

Entry	Compound	EC_{50} (μ M) ^a
1	3.24	5.8 ± 2.9^b
2	3.25	2.8 ± 1.0^b
3	3.55	11.1 ± 4.3^b
4	3.58	14.9 ± 9.1^b

^a EC_{50} 's were determined using a cell based luciferase assay as previously described.³⁴⁹ EC_{50} refers to the concentration that results in 50% inhibition of PSA-luciferase activity. Each EC_{50}

was calculated using GraphPad Prism, and are the average \pm stdev of two independent assays using triplicate determinations at each concentration for each experiment.

A subsequent pull-down experiment conducted in the Wang lab using C4-2 whole cell lysates. Cell lysates were precleared with acetylated control beads and incubated with or without 50-fold **3.5**. Levels of AR were detected using electrophoresis followed by western immunoblotting experiments with an anti-AR antibody. Using the control beads in the presence or absence of **3.5** there is no observed pull-down of AR. In contrast, using **3.34** beads resulted in AR pull-down. Additionally, compound **3.5** was found to competitively block the AR pull-down of the **3.34** beads.

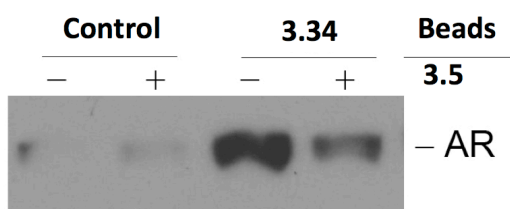


Figure 3.18. Affinity purification of AR from C4-2 whole cell lysate using immobilized **3.34**.

3.3 CONCLUSIONS

In conclusion, compound **3.5** was discovered in a HTS to reduce endogenous levels of AR in both the cytoplasm and the nucleus. An SAR of **3.5** was established using 5 zones of structural diversification that resulted in the synthesis of **JJ450** a new, more potent analog than the initial HTS hit **3.5** that contained a *cis*-cyclopropane in place of the potentially metabolically labile thioether side chain. **JJ450** was administered to nude mice bearing s.c. prostate cancer (LnCaP, VCaP, 22Rv1) xenografts via o.g and i.p to determine the *in vivo* efficacy. Gratifyingly, **JJ450** was found to have modest therapeutic efficacy with no toxicity in the xenograft models and was

even more efficacious than enzalutamide in a comparison study. A resolution of **JJ450** afforded the separated enantiomers, which were unambiguously assigned by X-ray crystallography. A preliminary xenograft study using the separated enantiomers indicated that the (1*R*,2*S*)-**JJ450** was more efficacious *in vivo*, contrary to the trend observed with the *in vitro* data. It was determined that **JJ450** had a poor metabolic half-life in liver microsomes and in an effort to improve metabolic stability 43 analogs were synthesized with varying substituents to decrease metabolism and increase half-life. Although increased potency was not achieved, we identified compound **3.211** that was 40-fold more stable in liver microsomes compared to the parent **JJ450** with only a 3-fold decrease in activity. A subsequent xenograft study is currently underway using the resolved enantiomers of **3.211**.

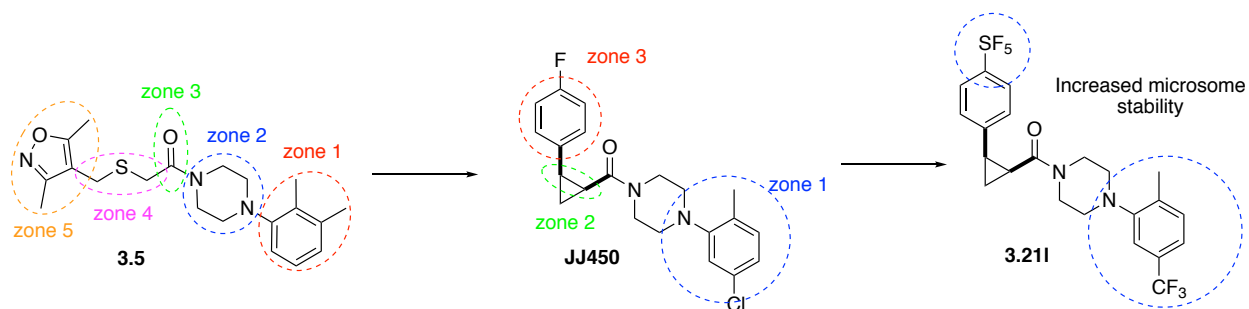


Figure 3.19. Structural improvements leading to compound **3.211**.

Several analogs were synthesized as probes for the determination of mechanism of action. In particular, we discovered that **3.25**, a structural hybrid of **3.6p** and **3.24** had an EC_{50} of 2.8 μ M that was conjugated to an agarose bead through a carbamate linker. Additionally, an analog of **3.55** containing a longer linker was synthesized and was found to have a 3-fold reduction in activity, and was also conjugated to the agarose beads for comparison to **3.25**. Interestingly, we found that the cyclopropyl side chain performed poorly on the analogs containing the propargyl alcohol linker when compared to those containing the thioether side chain. This indicated that the more flexible thioether allows for better binding with the more

rigid alkyne handle. A preliminary pull-down assay using bead conjugate **3.34** revealed that AR was retained by the affinity reagent **3.34** and was competitively blocked by **3.5**.

4.0 EFFORTS TOWARDS THE TOTAL SYNTHESIS OF 9- DESMETHYLPLEUROTIN

4.1 INTRODUCTION

The natural product pleurotin was first isolated from the fungus *Pleurotus griseus* in 1947. In preliminary biological evaluations it was found to inhibit *Staphylococcus aureus* along with several other gram-positive bacteria.⁴³² Although the structure of pleurotin was unknown at the time of isolation, Kavanagh and coworkers were able to determine several structural characteristics by chemical degradation studies.⁴³² The full structure was eventually elucidated in 1974 by NMR and later confirmed in 1981 by X-Ray crystallography.⁴³³⁻⁴³⁴ Pleurotin has also been isolated from the fungus *Hohenbuehelia geogenius* and has demonstrated moderate antitumor activity against Ehrlich ascites carcinoma, L-1210 lymphoid leukemia and a spontaneous mammary tumor in mice.⁴³⁵⁻⁴³⁶ More recently, pleurotin has been shown to inhibit bacterial peptidoglycan biosynthesis, a potential target for resistant infections.⁴³⁷ Synthetically challenging structural features of the complex hexacyclic framework of pleurotin includes a redox labile *para*-quinone moiety with two adjacent β -leaving groups, and the presence of 8 contiguous stereocenters (Figure 4.1).

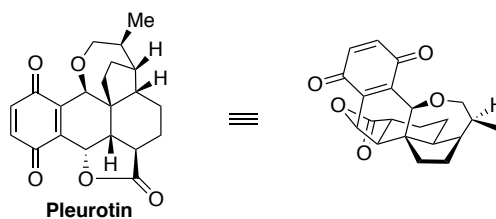


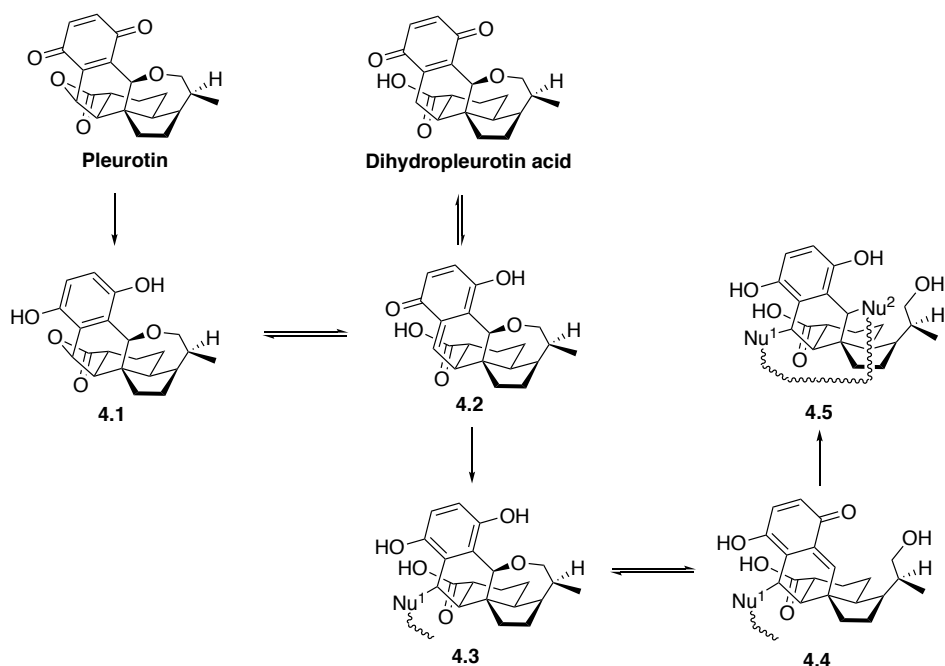
Figure 4.1. Structure of pleurotin.

Although pleurotin performed poorly in the National Cancer Institute (NCI) 60 cancer cell line panel having a GI_{50} of 20 μ M and no selectivity toward tissue type, it has been a target of interest for many years as it is a potent irreversible inhibitor of the thioredoxin-thioreductase (Trx/TrxR) system ($IC_{50} = 170$ nM).⁴³⁸⁻⁴⁴⁰ The Trx/TrxR system is important for the regulation of reactive oxygen species (ROS) and various redox processes, synthesis of deoxyribonucleotides, growth factor signaling, cytokine function, and protein biosynthesis.⁴⁴¹ The TrxR's contain a selenocysteine, which is essential for their redox activity.⁴⁴¹ In hypoxic tumors, Trx-1 is over-expressed leading to increasing levels of hypoxia-inducible factor-1 α (HIF-1 α). The hypoxia-activated transcription factor HIF-1 is the heterodimer of HIF-1 α and HIF-1 β and is responsible for the transcription of genes leading to angiogenesis, cell proliferation and survival, vasculogenesis, glucose metabolism, and iron homeostasis.⁴⁴²⁻⁴⁴³ The activity of the HIF-1 complex is directly correlated to levels of HIF-1 α , and pleurotin has been shown to reduce levels of HIF-1 α and decrease HIF-1 transactivation both *in vitro* and *in vivo* through inhibition of TrxR.⁴³⁹ Since hypoxia is a common feature that promotes the survival and metastasis of most cancerous tumors, a therapeutic treatment that targets hypoxic tumors is highly desirable.

In 2006, the NCI expressed renewed interest in pleurotin as a cancer therapeutic; however, the short supply of pleurotin largely limited further development. Previous isolations from *Hohenbuehelia atrocaerulea* were extremely low yielding (1-2 mg/L) and took over 2

months. Shipley and coworkers optimized a fermentation process of *H. atrocaerulea* to afford ~300 mg/L over 5 weeks resulting in the isolation of more than 10 g of pleurotin. Due to the long fermentation times, this optimization was accomplished over 5 years.⁴⁴⁰

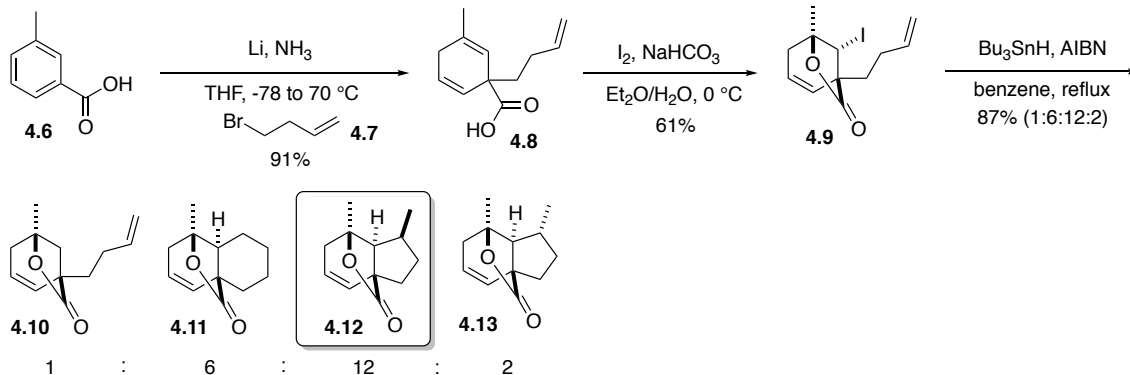
Like many of the redox active natural products, the proposed mechanism of action of pleurotin is through bioreductive alkylation⁴⁴⁴ and cross-linking of TrxR. In hypoxic cells, pleurotin can undergo a 2-electron reduction to the hydroquinone leukopleurotin **4.1** that can β -eliminate to the intermediate quinone methide **4.2**, a highly reactive Michael acceptor (Scheme 4.1). Quinone methide **4.2** can either tautomerise to dihydropleurotin acid, a proposed intermediate in the biosynthetic pathway, or be trapped with a nucleophile to afford the intermediate hydroquinone **4.3**. A subsequent β -elimination of the oxacycloheptane ether of **4.3** unveils a second quinone methide **4.4** that can undergo nucleophilic trapping to afford the hydroquinone **4.5**. Interestingly, bioreductive alkylating agents have been found to be selective for hypoxic tumor cells, and this is a mechanism of action observed with a number of FDA approved cancer treatments, including mitomycin C, which is used in combination therapies for the treatment of various solid tumors.⁴⁴⁵



Scheme 4.1. Proposed bioreductive alkylation mechanism of pleurotin.

4.1.1 Previous Syntheses: Hart

The first total synthesis of (\pm)-pleurotin was accomplished by Hart and coworkers in 1989 and was inspired by a novel radical cyclization methodology developed by their group to form perhydroindans (Scheme 4.2). In their initial report, the radical cyclization precursor **4.9** was prepared from a Birch reduction of *m*-toluic acid, alkylation with 4-bromo-1-butene (**4.7**), and a subsequent iodolactonization of intermediate **4.8**.⁴⁴⁶⁻⁴⁴⁷ Treating intermediate **4.9** with azobisisobutyronitrile (AIBN) and tributyltin hydride delivered a mixture of products with perhydroindan **4.12** as the major component of the mixture.



Scheme 4.2. Hart's initial radical cyclization discovery.

To showcase their chemistry, Hart and coworkers identified pleurotin as an appropriate synthetic target as its core contains the perhydroindan skeleton (Figure 4.2).

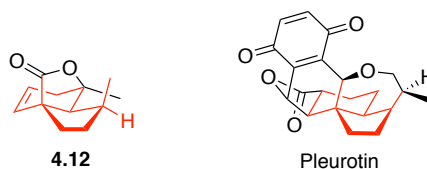
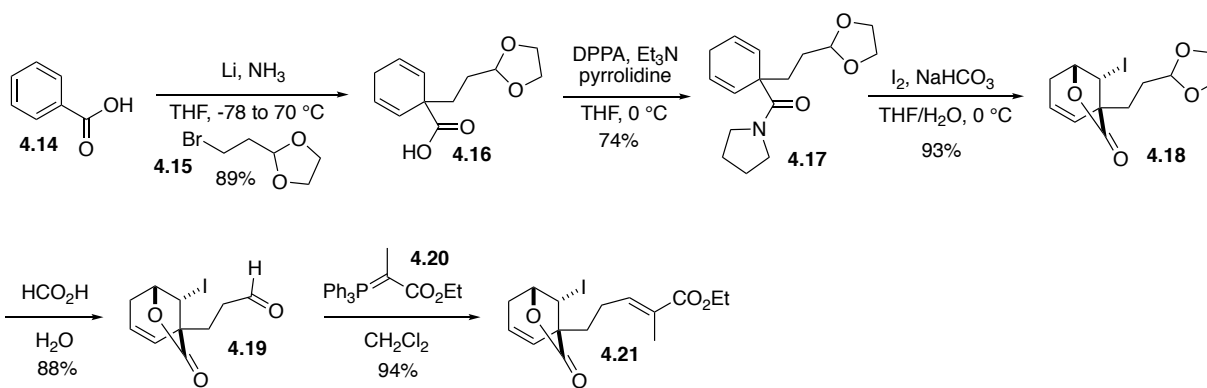


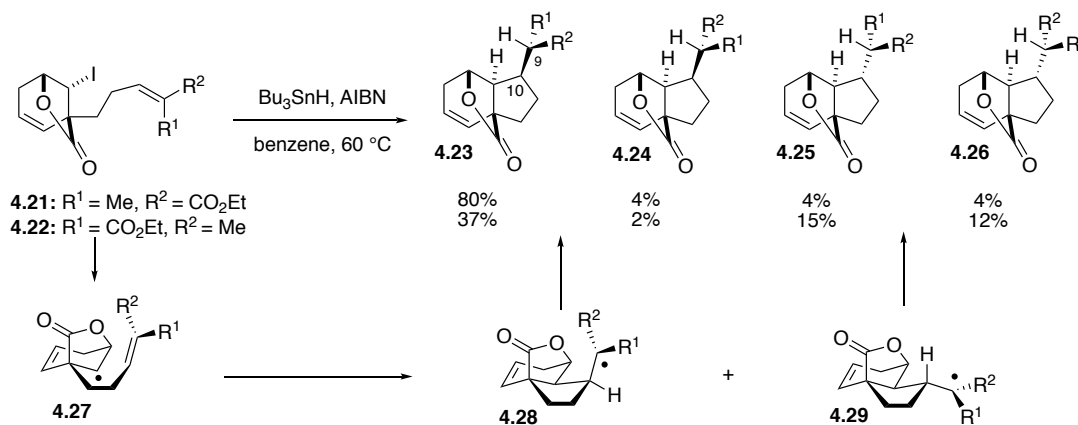
Figure 4.2. Perhydroindan scaffold **4.12** and pleurotin.

The first portion of their synthesis focused on the preparation of the key radical cyclization precursor **4.21**. The synthesis of **4.21** began with a Birch reduction of benzoic acid (**4.14**) and alkylation with bromide **4.15** (Scheme 4.3). Iodolactonization of carboxylic acid **4.16** resulted in decomposition and, instead, this transformation was accomplished using the amide **4.17**. The acetal **4.18** was deprotected with aqueous formic acid and then subjected to a Wittig olefination with ylide **4.20** to deliver the radical cyclization precursor **4.21** in excellent yields as a single diastereomer.⁴⁴⁶⁻⁴⁴⁹



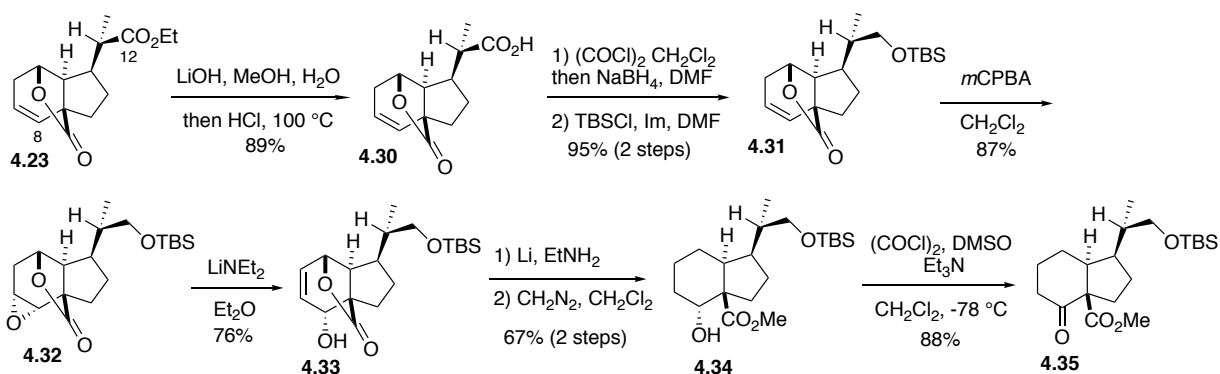
Scheme 4.3. Synthesis of radical cyclization precursor **4.21**.

Gratifyingly, the radical cyclization of **4.21** proceeded with high diastereoselectivity giving almost complete conversion to **4.23** (Scheme 4.4). To test whether the olefin geometry was responsible for the observed selectivity, the olefin with opposite geometry **4.22** was synthesized and subjected to the same reaction conditions. Interestingly, a similar ratio of **4.23** to **4.24** was obtained albeit in diminished yields. This indicated that while the alkene geometry influences the stereochemistry at C10, it is not responsible for the selectivity at C9. After conducting subsequent experiments where the alkene substituents were varied, they concluded that the stereochemistry at C9 is the result of a dipolar interaction between the two carbonyl groups.⁴⁴⁹



Scheme 4.4. Hart's radical cyclization.

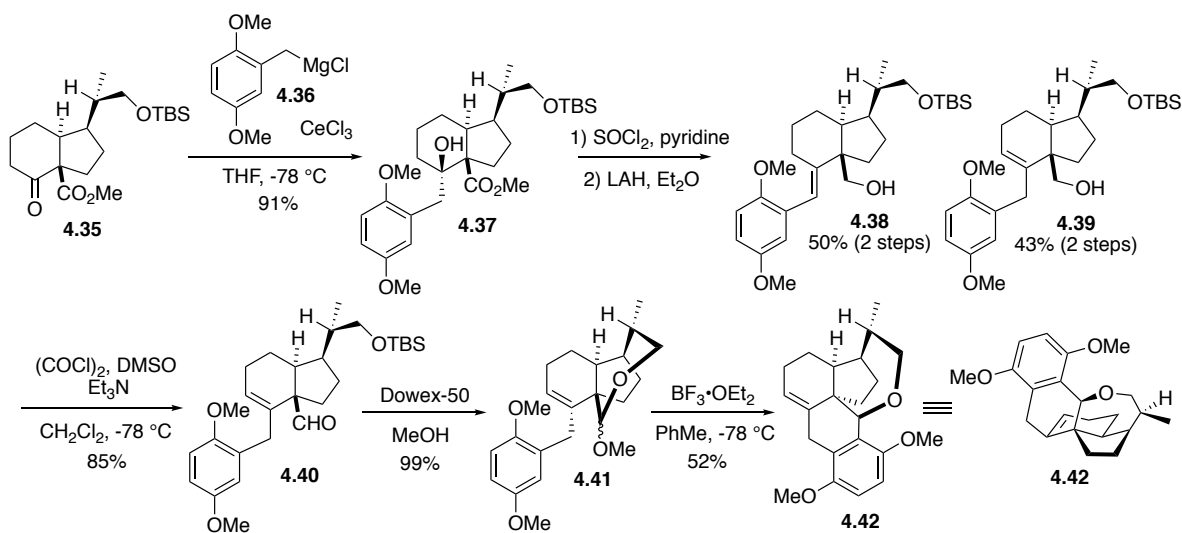
With ample amounts of the radical cyclization product in hand, they turned their attention to modifying the oxidation states at C8 and C12 (Scheme 4.5). As the lactone is also susceptible to reduction, the ester of **4.23** was reduced over 2 steps. First, **4.23** was hydrolyzed using aqueous lithium hydroxide to form the diacid. Subsequent treatment with acid regenerated the lactone in **4.30**. The carboxylic acid was reduced by treatment with oxalyl chloride to form the acid chloride and then sodium borohydride to give an intermediate alcohol that was TBS protected to give **4.31** in excellent yields. Interestingly, the reduction of ester **4.23** to the alcohol can also be achieved in a single step using LAH in 95% yield, which is most likely due to the steric crowding of the lactone. Epoxidation of alkene **4.31** followed by lithium diethylamide mediated rearrangement of the epoxide gave the corresponding allylic alcohol **4.33**. Birch reduction of the allylic ester **4.33** resulted in opening of the lactone and a subsequent methylation with diazomethane gave the methyl ester **4.34**. Finally, Swern oxidation of the alcohol **4.34** afforded the ketone **4.35** in good yields. It was also noted that starting from **4.31**, the epoxide opening, reduction, and esterification could give **4.34** in a one-pot procedure with 59% overall yield.



Scheme 4.5. Synthesis of ketone **4.35**.

With the ketone **4.35** in hand, Hart then focused on the formation of the oxacycloheptane ring and the pentacyclic core. Transmetalation of 2,5-dimethoxybenzyl magnesium chloride **4.36**

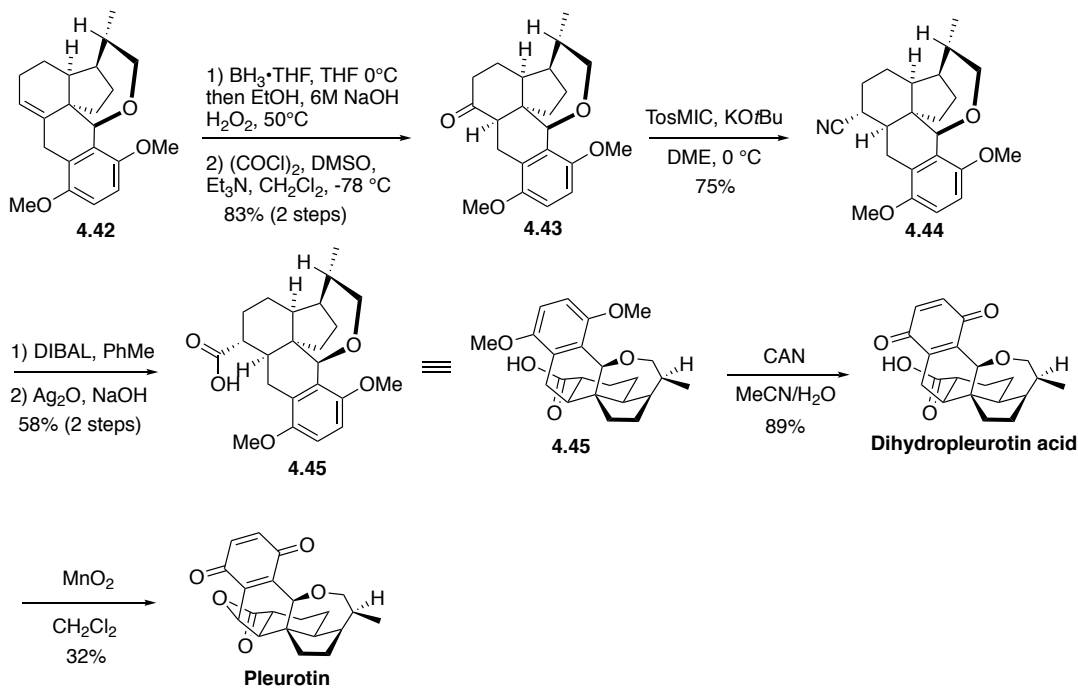
with cerium(III) followed by addition of the resulting organocerium reagent to ketone **4.35** afforded the alcohol **4.37** as a single diastereomer (Scheme 4.6). Subsequent elimination of the tertiary alcohol **4.37** afforded alkene isomers as an inseparable 1:1 mixture. The isomers were directly subjected to LAH reduction to give the separable alcohols **4.38** and **4.39**. Oxidation of alcohol **4.39** to aldehyde **4.40** followed by a mild acid catalyzed TBS deprotection of **4.40** using Dowex-50 in methanol provided acetal **4.41**. Treatment of acetal **4.41** with boron trifluoride etherate at low temperature initiated an intramolecular electrophilic aromatic substitution reaction to yield pentacyclic **4.42** in modest yields. Hart noted that performing the cyclization in other solvents at room temperature resulted in the formation of several rearranged products. Furthermore, it was also noted that product **4.42** was susceptible to rearrangement after prolonged exposure to acid.



Scheme 4.6. Synthesis of pentacyclic core **4.42**.

Following the synthesis of the pentacyclic core **4.42**, Hart shifted his attention to the final installation of the lactone ring and the completion of the synthesis of pleurotin. A hydroboration of the alkene **4.42** followed by oxidation afforded an intermediate alcohol that was further oxidized to the ketone **4.43** using a Swern oxidation (Scheme 4.7). A Van Leusen reaction of

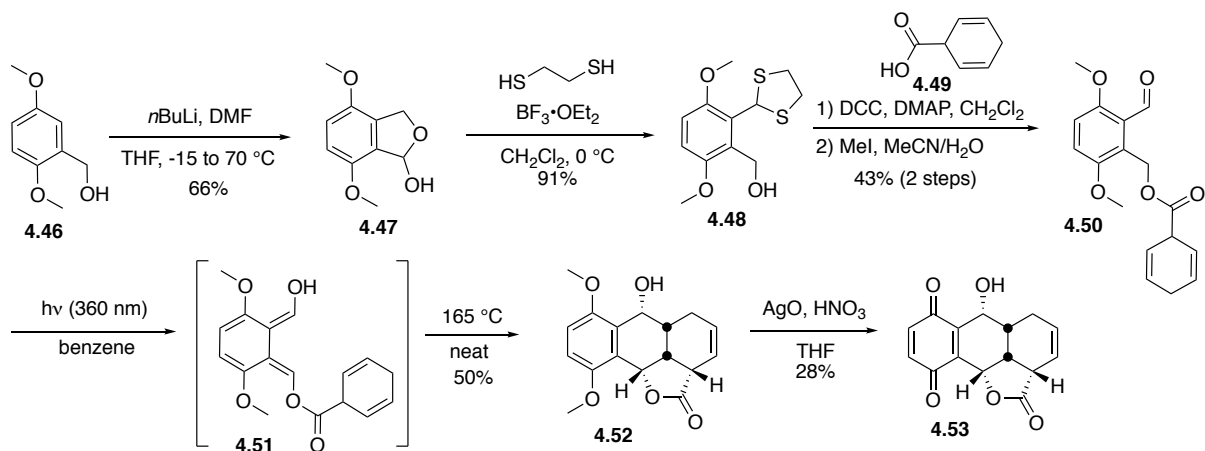
ketone **4.43** with tosylmethyl isocyanide (TosMIC) and KOtBu afforded the homologated nitrile **4.44**. While direct hydrolysis of the nitrile to the carboxylic acid proved problematic, they found that a two step protocol was effective whereby the nitrile was reduced to the corresponding aldehyde with DIBAL-H then oxidized to the carboxylic acid **4.45** with silver (I) oxide. Oxidation of **4.45** with ceric ammonium nitrate (CAN) in aqueous acetonitrile gave dihydropleurotin acid in excellent yields. Initial attempts to oxidize dihydropleurotin acid using amine bases in the presence or absence of oxygen were unsuccessful. Instead, the final oxidation was accomplished by treating dihydropleurotin with an excess of manganese dioxide over 2 days to give pleurotin in 32% yield along with 33% of recovered dihydropleurotin acid. Thus, the first total synthesis of pleurotin was completed in 26 steps and 0.3% overall yield.



Scheme 4.7. Completion of the synthesis of pleurotin.

4.1.2 Synthesis of a Pleurotin Analog: Kraus

In 1993 Kraus and coworkers developed a photoenolization/Diels-Alder approach to an analog of pleurotin.⁴⁵⁰⁻⁴⁵¹ The synthesis began with the formation of the dianion of **4.46**, which underwent formylation with DMF followed by mild hydrolysis to afford lactol **4.47** (Scheme 4.8). Unfortunately, direct acylation of **4.47** with dihydrobenzoic acid (**4.49**) proved unsuccessful and an alternative approach was pursued where thioacetal **4.48** was prepared and readily acylated with dihydrobenzoic acid (**4.49**). Subsequent thioacetal deprotection using MeI in aqueous acetonitrile yielded aldehyde **4.50** in modest yields. With their photoenolization substrate **4.50** in hand, aldehyde **4.50** was subjected to their previously optimized photoenolization conditions to deliver intermediate **4.51**.⁴⁵⁰⁻⁴⁵² Gratifyingly, they found that heating the enolate intermediate **4.51** neat at 165 °C promoted the key intramolecular Diels-Alder (IMDA) reaction to afford the tetracyclic core **4.52** as a single diastereomer in modest yield over two steps. The relative configuration of **4.52** was supported by 2D-NMR analysis and molecular mechanics calculations revealed that *endo* adduct **4.52** was favored over the *exo* adduct by 1.6 kcal/mol. Finally, oxidation of **4.52** to the quinone **4.53** was accomplished using silver (II) oxide and nitric acid in THF.⁴⁵¹



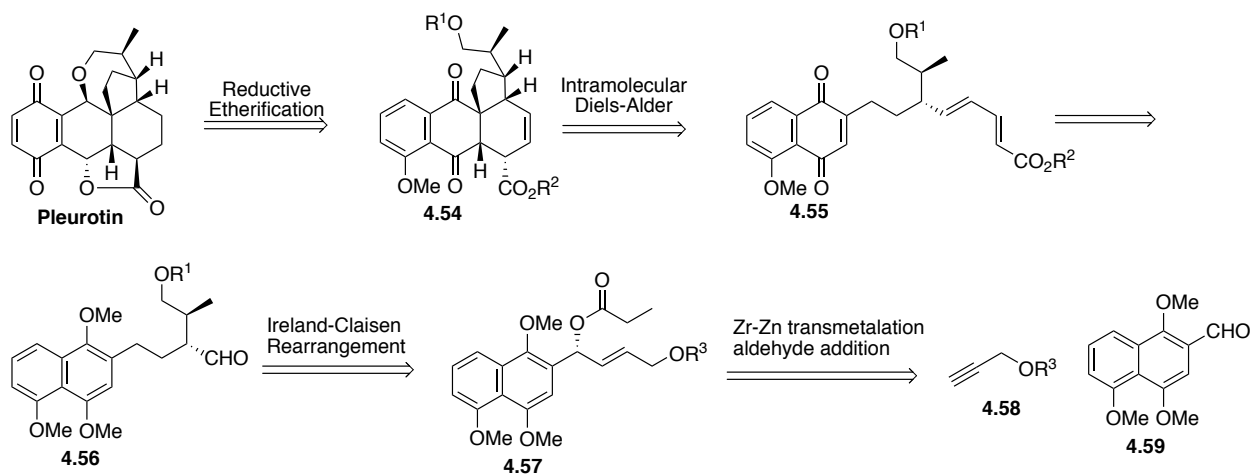
Scheme 4.8. Synthesis of pleurotin analog **4.53**.

Biological testing revealed that quinone **4.53** was active against a SR leukemia cell line ($GI_{50} = 4.67 \mu\text{M}$) and most colon cancer cell lines ($GI_{50} = 22.4 \mu\text{M}$ to $17.0 \mu\text{M}$). These activities are comparable to pleurotin, which has a mean value of GI_{50} of $3.09 \mu\text{M}$ against SR leukemia and $6.76 \mu\text{M}$ against colon cancer cell lines.⁴⁵¹

4.1.3 Previous Synthetic Work: Wipf Group

The Wipf group has ongoing interest in the synthesis and biological evaluation of pleurotin and other quinoid inhibitors of the Trx/TrxR system.⁴⁵³⁻⁴⁵⁷ Early synthetic efforts toward the total synthesis of pleurotin within the Wipf group were pioneered by Drs. Sonia Rodriguez, Shinya Immura, and Stephan Elzner. Retrosynthetically, the original approach to pleurotin featured a late stage reductive etherification to form pleurotin from intermediate **4.54** (Scheme 4.9). Intermediate **4.54** would then be formed by a key IMDA reaction of **4.55**. Diels-Alder precursor **4.55** could be constructed via a Horner Wadsworth Emmons reaction with aldehyde **4.56**, which in turn could be formed from an Ireland-Claisen rearrangement of **4.57**. Lastly, it was envisaged

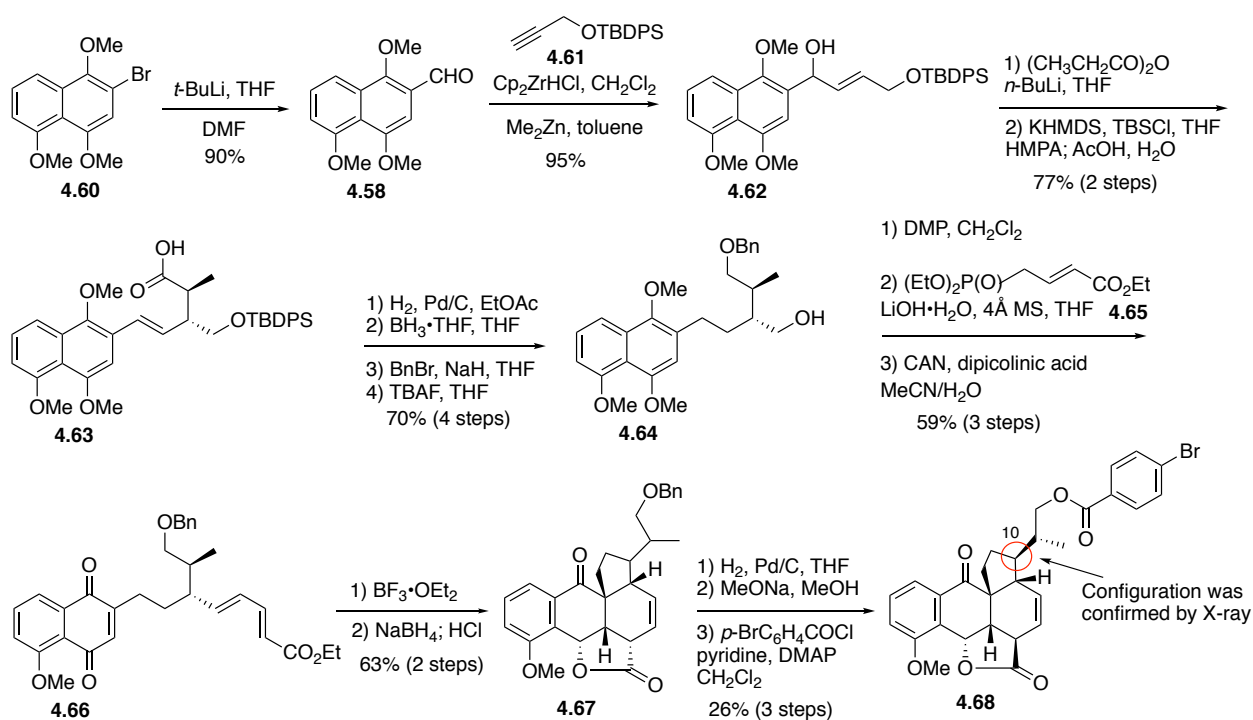
that intermediate **4.57** could be formed by a hydrozirconation-transmetalation-addition sequence of propargyl alcohol **4.58** to aldehyde **4.59**.



Scheme 4.9. Initial retrosynthetic approach to pleurotin.

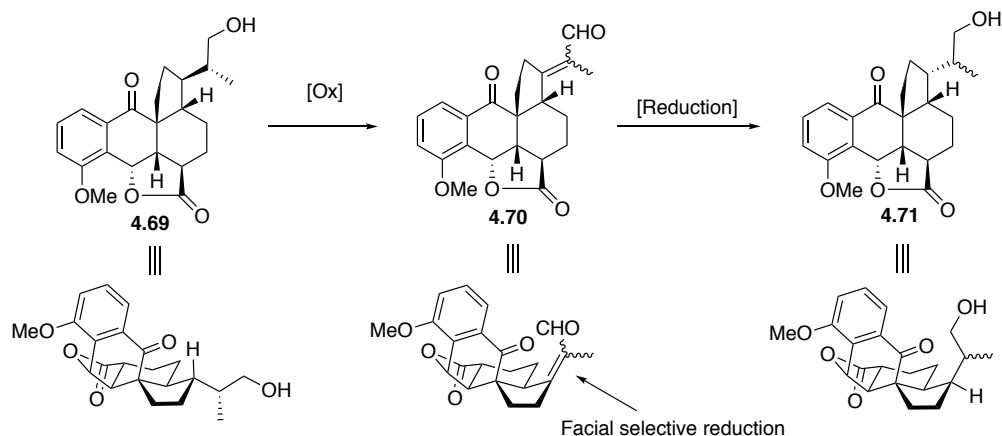
The initial synthetic route used the known bromo-naphthylene **4.60** prepared from 1,5-naphthalenediol in 5 steps.⁴⁵⁸ Lithium-halogen exchange of bromide **4.60** followed by formylation with *N,N'*-dimethylformamide gave the aldehyde **4.59** (Scheme 4.10). Propargyl alcohol **4.61** was subjected to hydrozirconation with Cp_2ZrHCl followed by transmetalation to the corresponding organozinc species. Addition of the resulting alkenylzinc reagent to aldehyde **4.59** afforded the allylic alcohol **4.62** in excellent yields. Acylation of alcohol **4.62** and enolization set the stage for a subsequent Ireland-Claisen rearrangement to produce carboxylic acid **4.63**. Hydrogenation of the alkene **4.63**, followed by reduction of the carboxylic acid, benzylation of the corresponding alcohol, and removal of the TBDPS protecting group gave alcohol **4.64** in excellent yield over 4 steps. Alcohol **4.64** was oxidized to the corresponding aldehyde and treated with phosphonate **4.65** in a HWE reaction to install the diene fragment of **4.66**. The naphthalene was oxidized to the naphthoquinone **4.66** using CAN to deliver the IMDA precursor **4.66**. Gratifyingly, treatment of **4.66** with boron trifluoride etherate yielded the IMDA adduct that was subsequently reduced using sodium borohydride with an acidic workup to give

lactone **4.67** with unknown configuration at C10. To elucidate the configuration at C10, **4.67** was hydrogenated giving both reduction of the alkene and debenzylation in a single step. Epimerization of the intermediate alcohol at C14 under basic conditions afforded the thermodynamically favored *trans* lactone. The free alcohol was then acylated with *p*-bromobenzoyl chloride yielding the crystalline product **4.68** whose structure was confirmed by X-ray crystallographic analysis. Unfortunately, the configuration at C10 was the opposite of the natural product and thus, a route to invert this stereogenic center was pursued.



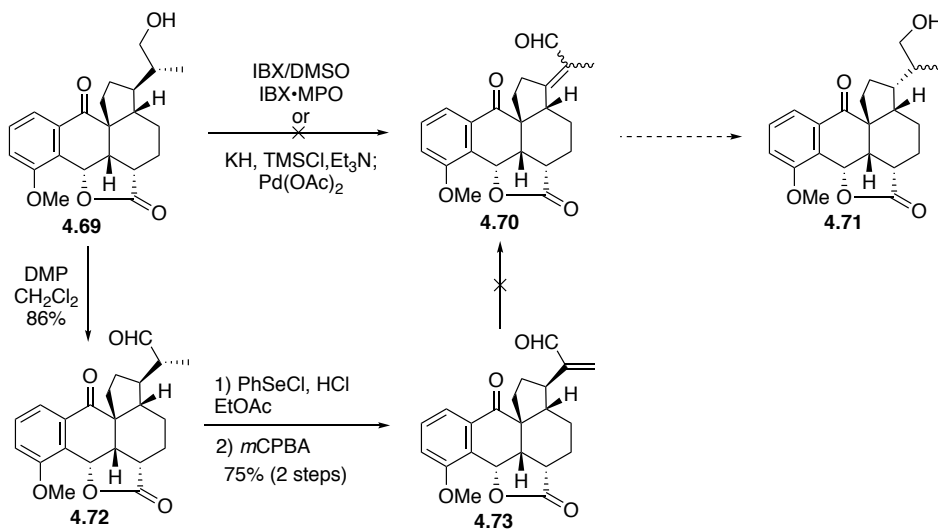
Scheme 4.10. Early synthetic studies towards pleurotin.

The strategy to invert the configuration was to first oxidize the side chain to the α,β -unsaturated aldehyde **4.70** (Scheme 4.11). Based on the caged nature of the structure, it was proposed that a reduction from the least hindered face would yield the desired stereochemistry at C10.



Scheme 4.11. Synthetic approach to side chain inversion.

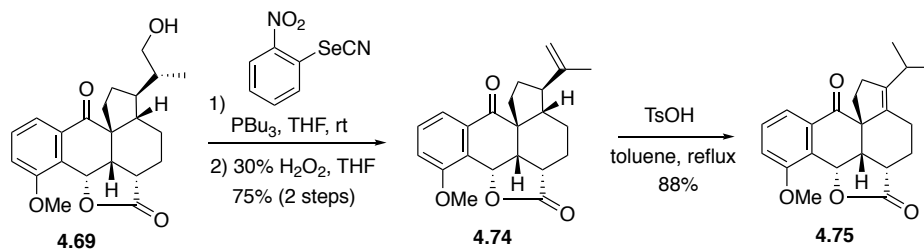
Unfortunately, direct one step oxidations of **4.69** to the α,β -unsaturated aldehyde **4.70** were unsuccessful (Scheme 4.12). Instead a stepwise approach was developed beginning with Dess-Martin periodinane (DMP) oxidation to the aldehyde **4.72**. α -Selenation of **4.72** and oxidative elimination afforded the undesired α,β -unsaturated aldehyde isomer **4.73**. Unfortunately, attempts to isomerize **4.73** to **4.70** did not yield the desired product.



Scheme 4.12. Attempts to invert C10 stereochemistry.

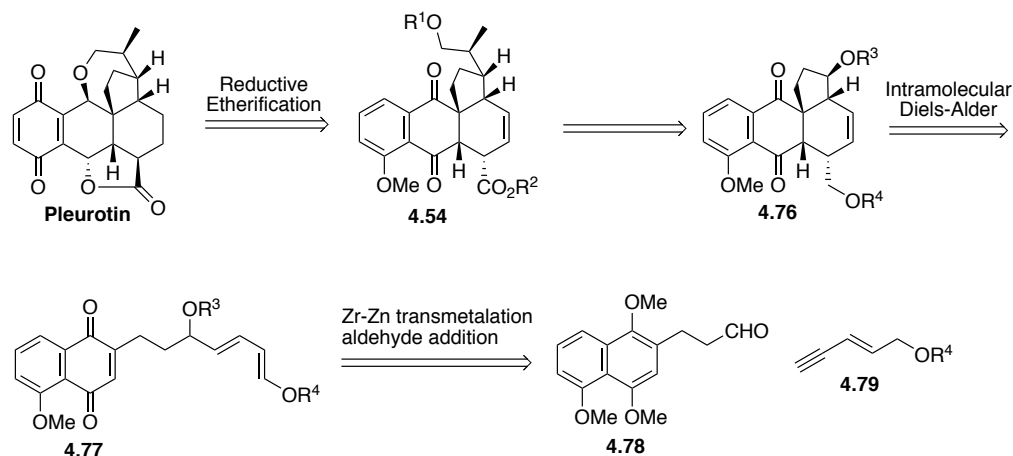
An alternative alcohol elimination/alkene isomerization approach was also investigated (Scheme 4.13). Unfortunately, while the elimination of the alcohol **4.69** proceeded smoothly to afford alkene **4.74** in 75% yield over two steps, all attempts to isomerize the alkene to form the

tetrasubstituted exocyclic olefin failed. Acid mediated conditions resulted in isomerization of the alkene into the ring to give **4.75** and no reaction was observed when **4.74** was subjected to an isomerization with Grubbs catalyst. Given the numerous difficulties encountered in attempts to invert the configuration of the C10 stereocenter, the first-generation route was deprioritized and a second-generation approach was developed.



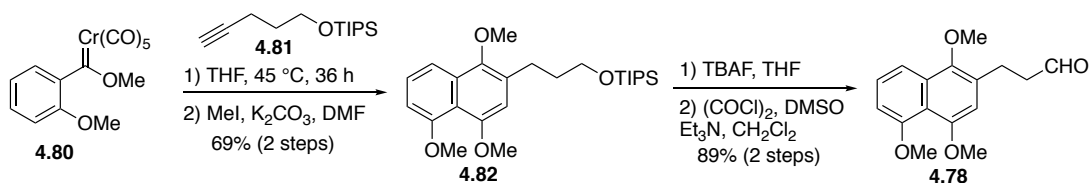
Scheme 4.13. Attempted alkene isomerization.

The second-generation retrosynthetic approach retains the late stage reductive etherification reaction to form pleurotin from intermediate **4.54** (Scheme 4.14). To circumvent the problematic inversion of the C10 stereocenter in the first approach, a key displacement of alcohol **4.76** could be implemented to install the inverted side chain. The tetracyclic core **4.76** would be formed via an IMDA reaction in an analogous manner to the previous route. It was envisioned that the Diels-Alder precursor **4.77** could be formed via a hydrozirconation/transmetalation of alkyne **4.79** and addition to aldehyde **4.78**.



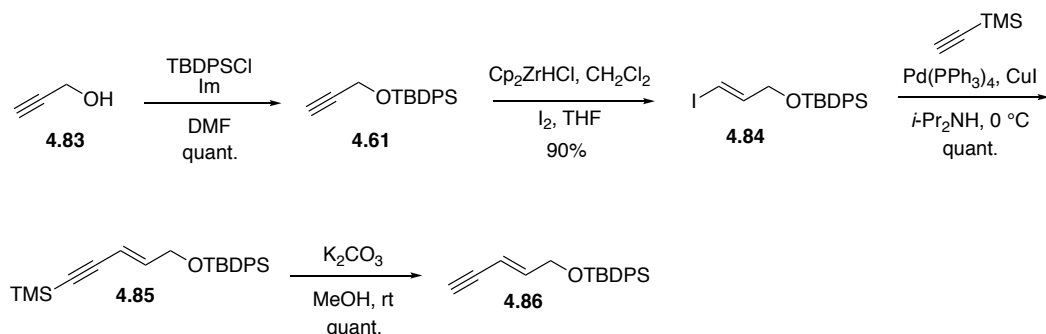
Scheme 4.14. 2nd generation retrosynthetic approach to pleurotin.

The 4-step synthesis of aldehyde **4.78** began with a Dötz benzannulation of triisopropylsilyl (TIPS) protected 1-pentynol **4.81** and the chromium Fischer carbene **4.80** followed by methylation of the naphthol intermediate to produce **4.82** (Scheme 4.15). TBAF desilylation of **4.82** and Swern oxidation of the intermediate alcohol gave aldehyde **4.78** in excellent yields.



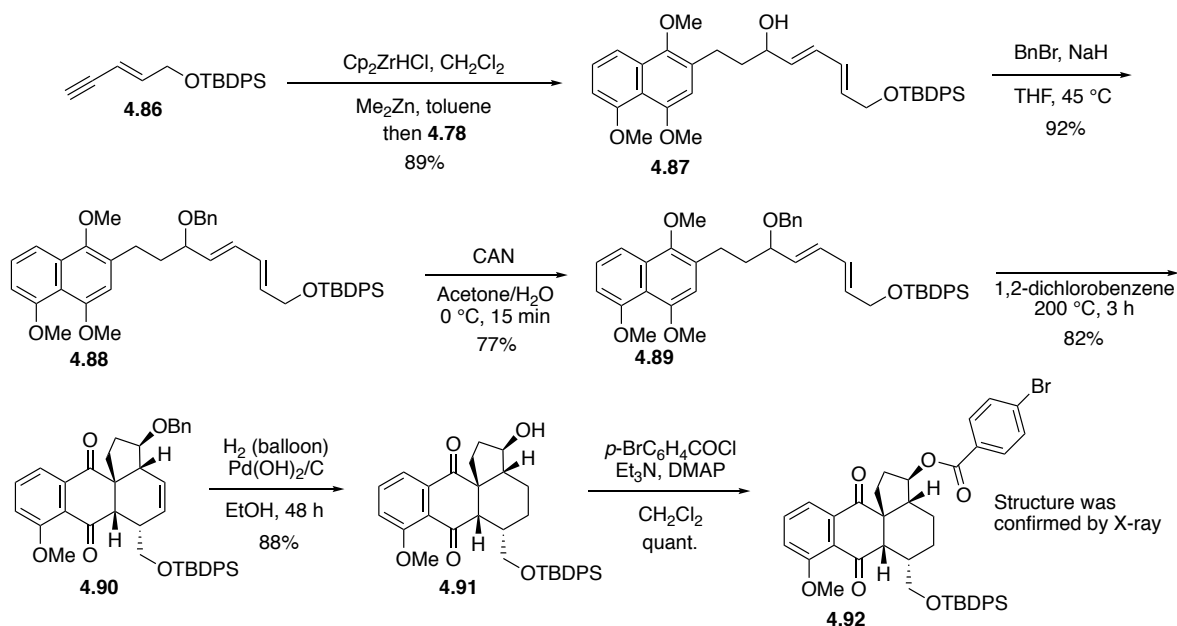
Scheme 4.15. Synthesis of naphthalene **4.78**.

The synthesis of alkyne fragment **4.86** was accomplished in 4 steps and began with the silylation of propargyl alcohol (**4.83**). Hydrozirconation/iodination of alkyne **4.61** afforded the *E*-vinyl iodide that was coupled to TMS-acetylene using Sonogashira coupling conditions to give alkyne **4.85**. Desilylation of alkyne **4.85** afforded the desired enyne **4.86**.



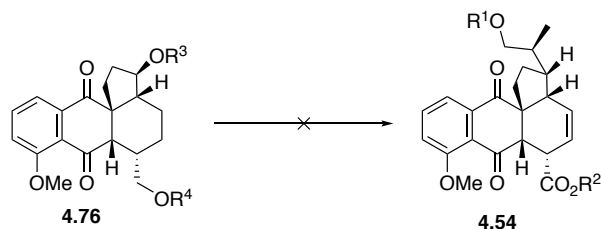
Scheme 4.16. Synthesis of enyne fragment **4.86**.

Hydrozirconation of alkyne **4.86** followed by transmetalation, and addition to aldehyde **4.78** went smoothly in 89% to give the diene **4.87** (Scheme 4.17). Benzoylation of the allylic alcohol **4.87** and oxidation using CAN gave key naphthoquinone **4.88** setting the stage for pivotal IMDA reaction. In contrast to the IMDA of the previous route, the Lewis acid catalyzed reaction was unsuccessful. Instead, the IMDA was accomplished thermally by heating **4.88** at 200 °C for 3 h to afford the product **4.90** as a single diastereomer in excellent yields. One-pot hydrogenation of the alkene and debenzoylation gave alcohol **4.91**. Acylation of **4.91** produced the crystalline ester **4.92** that was unambiguously assigned by X-ray analysis.



Scheme 4.17. Synthesis of alcohol **4.91**.

Unfortunately, all attempts to install the side chain on **4.76** or cyclize the oxacycloheptane ring were unsuccessful, forcing alteration of the synthetic strategy to install and invert the C10 side chain in a third generation approach (Scheme 4.18).



Scheme 4.18. Attempts at installation of the side chain at C10.

4.2 RESULTS AND DISCUSSION

4.2.1 Retrosynthetic analysis

Given the difficulties encountered in inverting the C10 configuration in the presence of the C9 methyl group, we envisioned that we could initially develop a synthetic route to 9-desmethylpleurotin and subsequently develop a late stage introduction of the methyl group at C9 (Figure 4.3).

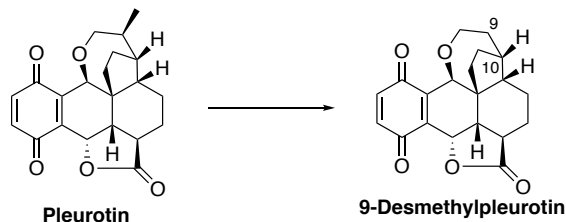
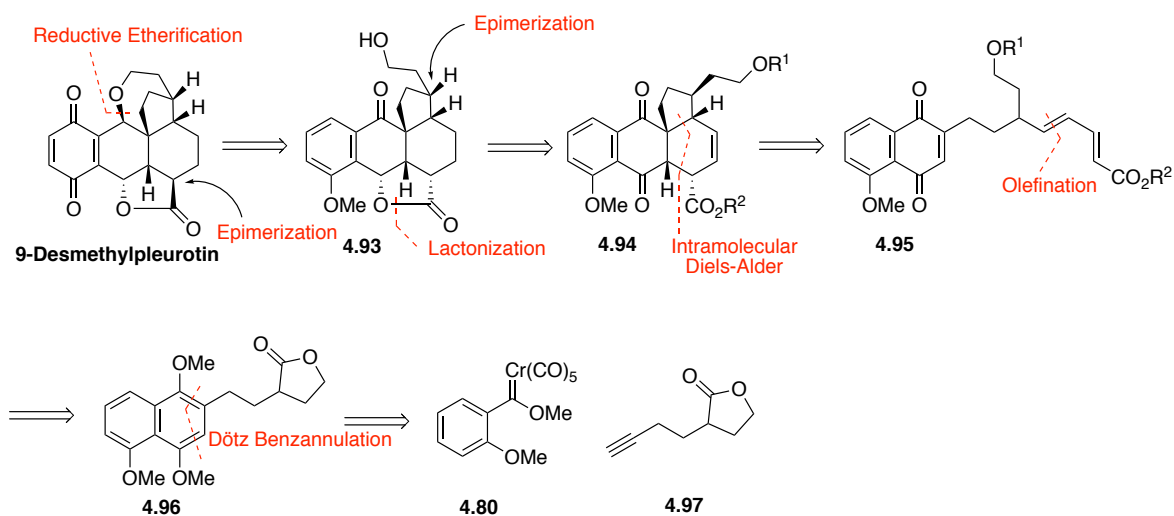


Figure 4.3. Proposed model system of pleurotin, 9-desmethylpleurotin.

Our third generation retrosynthesis of 9-desmethylpleurotin is outlined in Scheme 4.19. Our approach retains the late stage reductive etherification to close the oxacycloheptane ring. We

expect lactone epimerization will deliver the desired *trans* lactone from **4.93**. Inversion of the C10 stereocenter leads retrosynthetically to Diels-Alder precursor **4.94**. In the absence of the C9 methyl group, we envisioned a more facile inversion of the C10 configuration in **4.94**. Analogous to previous routes, we propose that **4.94** can be formed via an IMDA reaction from the diene naphthaquinone **4.95**. The naphthalene **4.95** would be constructed using a Dötz benzannulation of the chromium Fischer carbene **4.80** and lactone **4.97**. We envisioned that butyrolactone **4.97** would serve as an easy handle for the construction of the diene fragment in **4.95**.

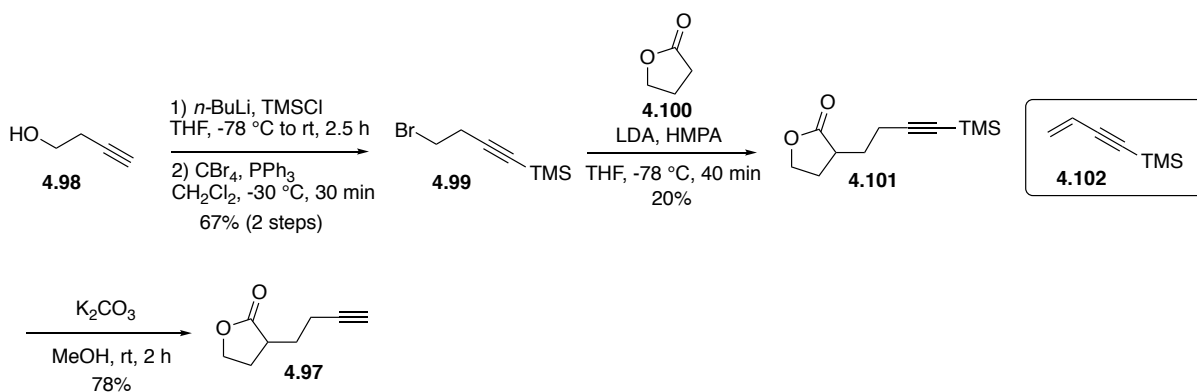


Scheme 4.19. Retrosynthetic approach to 9-desmethylpleurotin.

4.2.2 Approach 1: Synthesis of γ -Butyrolactone **4.97**

Our initial approach to synthesize lactone fragment **4.97** was based on a direct α -alkylation of the γ -butyrolactone (**4.100**) (Scheme 4.20). Synthesis of bromide **4.99** began with the TMS protection of the dianion of 1-butynol (**4.98**), mild hydrolysis of the TMS ether, and a subsequent Appel bromination.⁴⁵⁹⁻⁴⁶¹ Many reaction conditions (solvents, temperature, times,

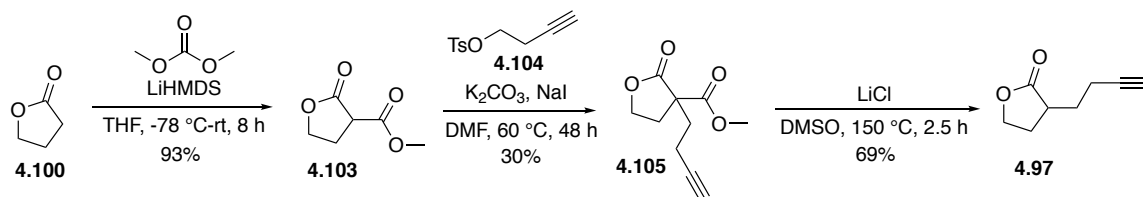
bases, additives) were screened for the alkylation of **4.100** including the use of the iodide as the coupling partner. Unfortunately, all conditions resulted in little or no formation of the desired product. Enyne **4.102** was identified as the main byproduct in many cases. At best, the desired product **4.101** was formed in 20% yield along with elimination byproduct **4.102** using LDA/HMPA enolization conditions. However, attempts to scale up this reaction were met with even lower yields of **4.101**.



Scheme 4.20. Initial synthetic route to alkyne **4.97**.

Given the difficulty in obtaining meaningful quantities of lactone **4.101**, we investigated alternate approaches to form lactone **4.97**. Hoping to circumvent the issue of base mediated elimination that dominated the alkylation of **4.100**, we designed a new approach using activated lactone **4.103** (Scheme 4.21). We reasoned that alkylation of **4.103** should be favored using a mild base, hopefully avoiding the undesired elimination pathway that predominated under strongly basic conditions. The activated lactone **4.103** was rapidly synthesized by acylation of **4.100** with dimethyl carbonate.⁴⁶² With facile access to **4.103** we began to investigate alkylation conditions. After screening a variety of alkylating agents, we determined that the tosylate **4.104** was superior over the corresponding mesylate, bromide, or iodide in both synthetic tractability as well as performance in the reaction. Additionally, after screening a number of bases, solvents, and additives, it was determined that K₂CO₃, NaI in DMF at 60 °C proved optimal; however, on

scale the maximum yield was 30%. Even with a low yield we had enough of this material to test subsequent transformations in the synthesis. The alkylated product **4.105** was subjected to Krapcho decarboxylation conditions to give our desired lactone **4.97**.

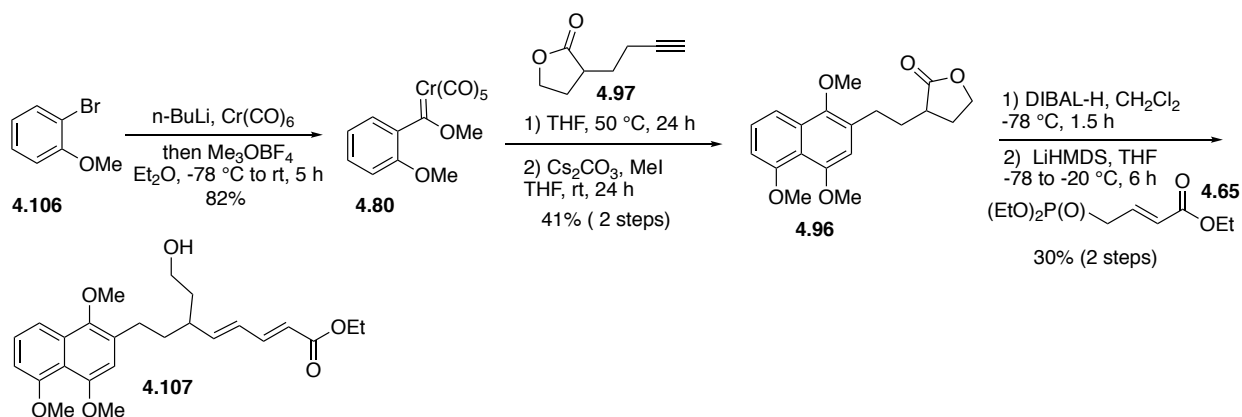


Scheme 4.21. Synthesis of alkyne **4.97**.

4.2.3 Approach 1: Investigation of the Key Dötz Benzannulation and IMDA Sequence

Using Lactone **4.97**

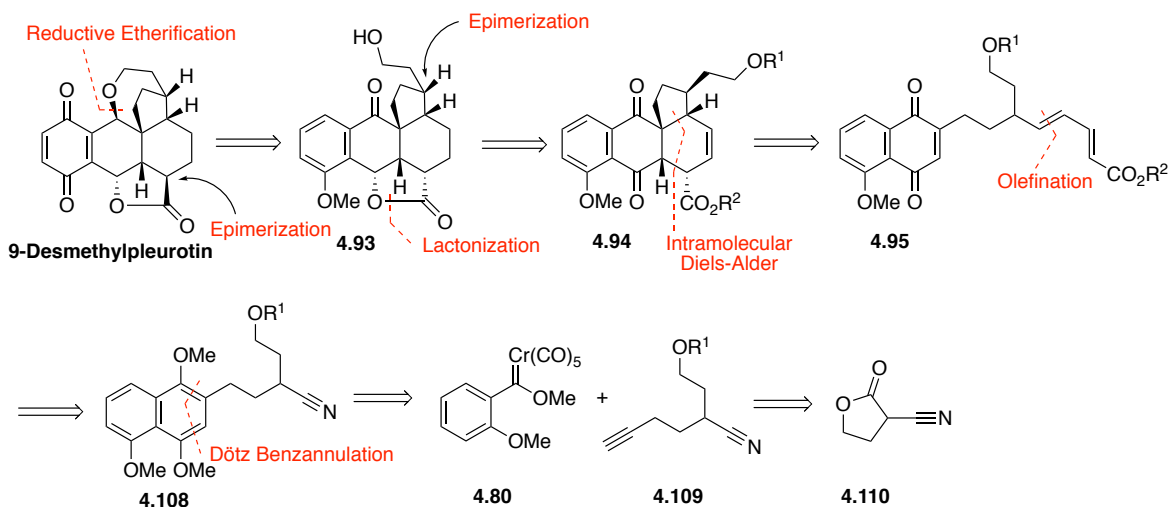
The chromium Fischer carbene **4.80** was prepared using a one-pot literature protocol starting with lithium-halogen exchange of 2-bromoanisole (**4.106**), addition of the resulting anion to chromium hexacarbonyl, and methylation using Meerwein's reagent (Scheme 4.22).⁴⁶³ Subjecting lactone **4.97** to the Dötz benzannulation yielded naphthalene **4.96** in a modest yield of 41%. Attempts to optimize this reaction were unsuccessful in increasing the overall yield past 41% and the reaction profile was generally complex. Other methylating reagents such as dimethyl sulfate resulted in multiple methylations of the naphthalene substrate **4.96**. Reduction of the lactone **4.96** to the corresponding lactol worked well using DIBAL-H,⁴⁶⁴ however, the subsequent HWE reaction with phosphonate **4.65** proved low yielding, forming diene **4.107** in 30% over 2 steps.⁴⁶⁵



Scheme 4.22. Synthesis of diene **4.107**.

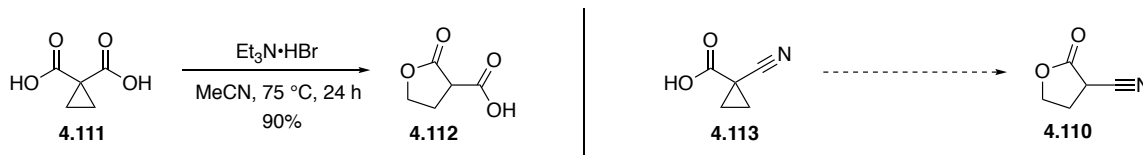
4.2.4 Approach 2: Synthesis of γ -Butyrolactone **4.110**.

We reasoned that the presence of the free primary alcohol could be interfering in the diene formation sequence, contributing to the low isolated yield of **4.107**. Therefore, we decided to protect it prior to installation of the diene fragment. In order to introduce a protecting group, we needed to redesign the lactone precursor. In this second-generation approach, we envisioned that **4.95** could be synthesized from the nitrile **4.108** (Scheme 4.23). We reasoned that using a smaller activating substituent on the γ -butyrolactone would increase yields by decreasing steric hindrance in the enolate formation and alkylation. The nitrile was an ideal choice since it is smaller in size compared to the methyl ester, electron-withdrawing, and can be converted to the necessary aldehyde by treatment with DIBAL-H. Analogous to the previous routes, naphthalene **4.108** could be synthesized via a Dötz benzannulation of carbene **4.80** and alkyne **4.109**. Alkyne **4.109** can be prepared from the lactone **4.110**.



Scheme 4.23. 2nd Generation retrosynthesis of 9-desmethylpleurotin.

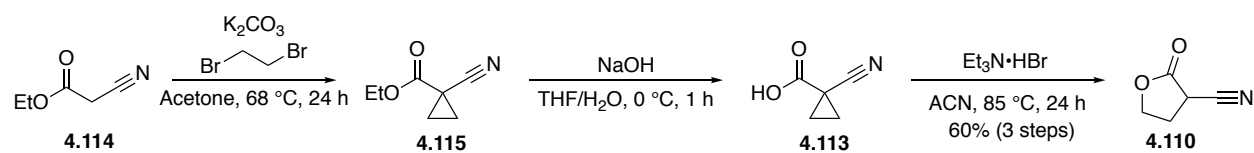
An extensive search of the literature yielded only three methods for the synthesis of α -cyanosubstituted γ -butyrolactones.⁴⁶⁶⁻⁴⁶⁸ Unfortunately, these literature protocols did not appear amenable to a scalable synthesis of this building block due to low yields or safety concerns. Instead, we discovered a method developed by Rao *et al.* for the rearrangement of cyclopropane-1,1-dicarboxylic acid **4.111** with triethylammonium bromide to deliver 2-carboxy- γ -butyrolactone **4.112** (Scheme 4.24).⁴⁶⁹ Encouraged by Rao's work we wanted to see if this transformation could be applied to a cyano-substituted cyclopropane **4.113**.



Scheme 4.24. Proposed synthesis of cyano-substituted lactone.

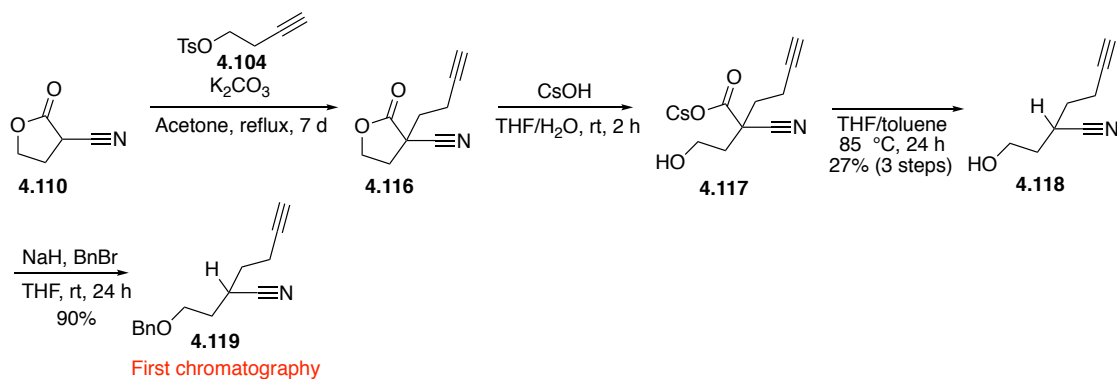
The synthesis of cyclopropane **4.113** began with alkylation of ethylcyanoacetate (**4.114**) with 1,2-dibromoethane to give cyclopropane ester **4.115** (Scheme 4.25). Saponification of ester **4.115** afforded carboxylic acid **4.113** that, gratifyingly, rearranged upon treatment with triethylammonium bromide to give the desired lactone **4.110**. This reaction sequence is highly scalable and has been carried out on upwards of 370 g scale with no incident. This sequence is

also appealing as it does not require any chromatography, and the only purification step is a distillation to purify lactone **4.110**. Additionally, we demonstrated that the triethylammonium bromide can be recovered after lactonization and recycled up to 7 times with no detectable loss in yield. We were also interested in determining if this rearrangement could be carried out catalytically in the presence of a metal ion or Lewis acid. After screening numerous additives, it was found that 5 mol% of either sodium iodide or magnesium iodide effectively promoted the rearrangement. A 10 g scale test reaction with NaI gave 77% isolated yield of the desired lactone **4.110**.



Scheme 4.25. Synthesis of lactone **4.110**.

With ample amounts of lactone **4.110** in hand, alkylation of **4.110** with tosylate **4.104** proceeded smoothly (Scheme 4.26). On large scale (100 g), mechanical stirring in the lactone alkylation greatly improved the overall yield of the sequence. Lactone hydrolysis and decarboxylation were screened using a number of bases solvents and temperatures. When lithium or sodium hydroxide were used for the hydrolysis of lactone **4.116**, the corresponding decarboxylation required high temperatures (~150 °C) and resulted in low yields and mixtures of products. We were delighted to find that when cesium hydroxide was used in the hydrolysis, the corresponding decarboxylation occurred under milder conditions in a mixture of THF and toluene to afford highly pure alcohol **4.118**. Lastly, the benzylation of the primary alcohol afforded the desired intermediate **4.119**, which was purified using the first chromatographic purification of the synthesis.



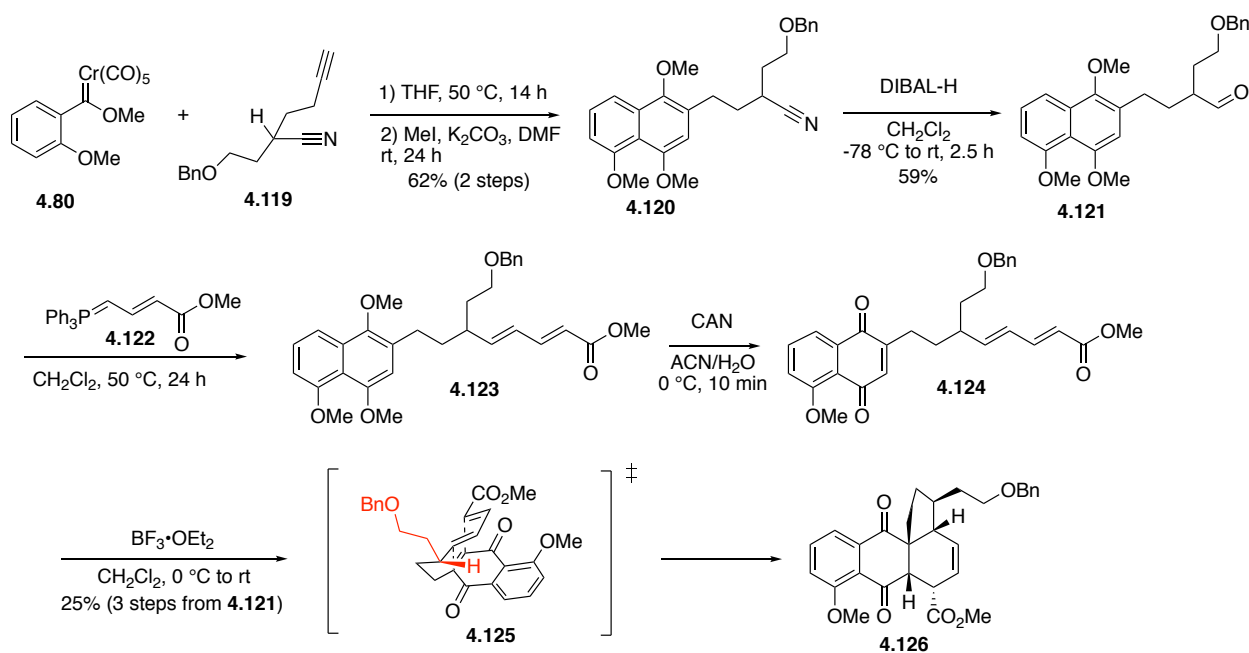
Scheme 4.26. Synthesis of alkyne **4.119**.

4.2.5 Approach 2: Investigation of the Key Dötz Benzannulation and IMDA Sequence

Using Nitrile **4.119**

After successfully preparing the alkyne **4.119**, we shifted our attention to the Dötz benzannulation and the IMDA (Scheme 4.27). Carbene **4.80** was combined with the previously prepared alkyne **4.119** and heated at 50 °C for 14 h to give a naphthol intermediate that was subsequently methylated with methyl iodide in DMF to give **4.120**. Performing the methylation in THF or acetone led to incomplete conversion and lower yields of the methylation product. The DIBAL-H reduction of nitrile **4.120** to the corresponding aldehyde was sluggish at low temperatures and required warming to room temperature to give even modest conversion. Interestingly, the reduction proved highly sensitive to the solvent in the commercial DIBAL solution. A 1.2 M solution of DIBAL in toluene was far superior to a 1.0 M solution of DIBAL in hexanes. The intermediate aldehyde **4.121** was treated with phosphorus ylide **4.122** in a Wittig olefination to give diene **4.123** in modest yields.⁴⁷⁰ Additionally, this transformation has also been accomplished under HWE conditions using phosphonate **4.65** with LiOH in THF to give the diene product in comparable yields. Oxidation of the naphthalene **4.123** with CAN to the

naphthoquinone yielded the Diels-Alder precursor **4.124**.⁴⁷¹ Unfortunately, the yields for the CAN oxidation dropped significantly on scales larger than 1 g. Encouraged by the initial work on this transformation (*vide infra*), **4.124** was treated with boron trifluoride etherate at low temperature to yield Diels-Alder product **4.126** as a single diastereomer in modest yields. Using the TBS or TBDPS protected alcohol in the IMDA reaction resulted in low yields (~20%) of only the desilylated product. Additionally, the yields were much lower in other solvents such as THF or toluene.



Scheme 4.27. Dötz and IMDA reaction sequence.

Given the stereochemical outcome of the Diels-Alder reaction to **4.126** we propose that the IMDA proceeds via the *endo*-transition state **4.125** with the side chain placed away from the plane of the dienophile, thus minimizing any destabilizing $A^{1,3}$ interactions (Figure 4.4). This result is similar to previous results on related systems such as **4.67**. The alternate *endo*-transition state **4.127** is destabilized by an $A^{1,3}$ strain between the side chain R and the plane of the diene, resulting in a 2-3 kcal/mol destabilization versus **4.125**.⁴⁷² Houk and coworkers used

DFT calculations to study the effect of BF_3 on the rate and stereoselectivity of IMDA reactions of cycloalkenones, and have shown, in their system, that the *endo* pathway is favored over the *exo* pathway by ~ 2.8 kcal/mol.⁴⁷³ Furthermore, both *exo*-transition states **4.128** and **4.129** contain a combination of destabilizing $A^{1,3}$ interactions. Therefore, we propose that all alternative transition states are higher in energy than **4.125**.

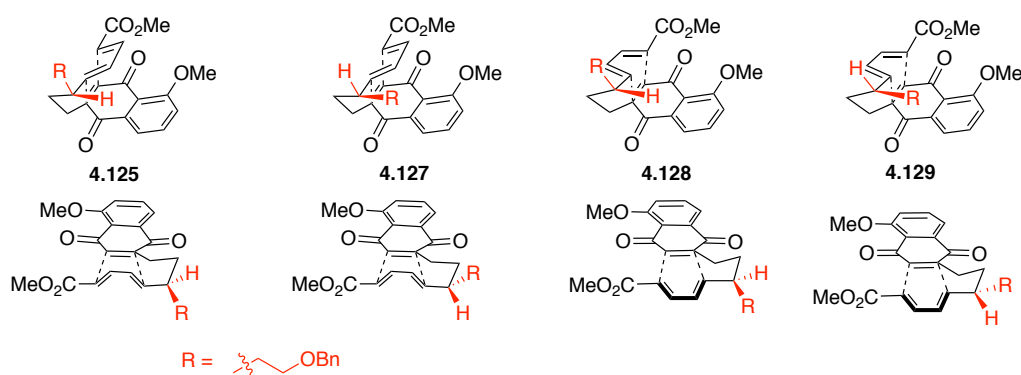
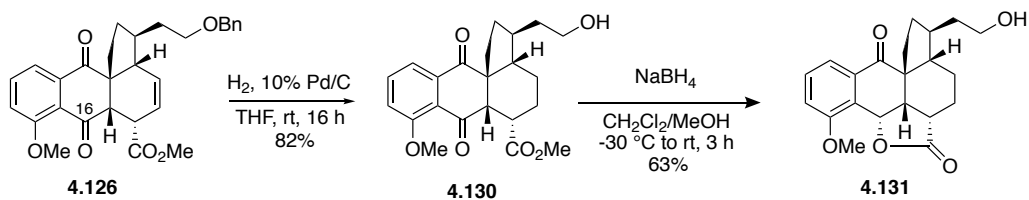


Figure 4.4. Diels-Alder transition state models.

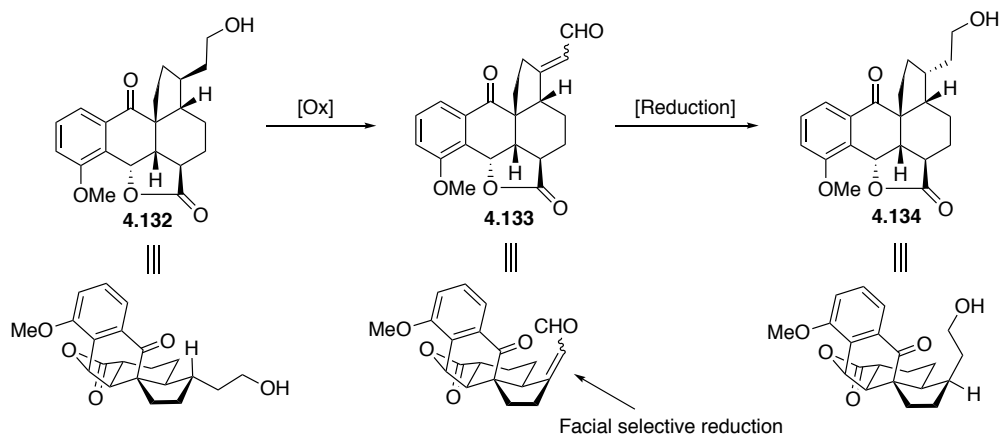
The Diels-Alder product **4.126** was subjected to one-pot hydrogenation conditions to reduce the alkene and cleave the benzyl ether to give the alcohol **4.130** (Scheme 4.28). A subsequent selective reduction of the ketone and acidic workup yielded lactone **4.131**. The selectivity for *cis*-lactone formation is governed by hydride addition to the more accessible convex face. Interestingly, if this sequence is used in the reverse order, the alkene is prone to a base mediated conjugation with the ester. A conjugate reduction of the resulting α,β -unsaturated ester can be accomplished using NiBH_4 and affords the thermodynamically favored *trans*-fused lactone.



Scheme 4.28. Synthesis of lactone 4.131.

4.2.6 End Game: Progress Toward the C10 Inversion Sequence and Preliminary Investigation Into the Reductive Etherification to Deliver the Hexacyclic Core of 9-Desmethylpleurotin

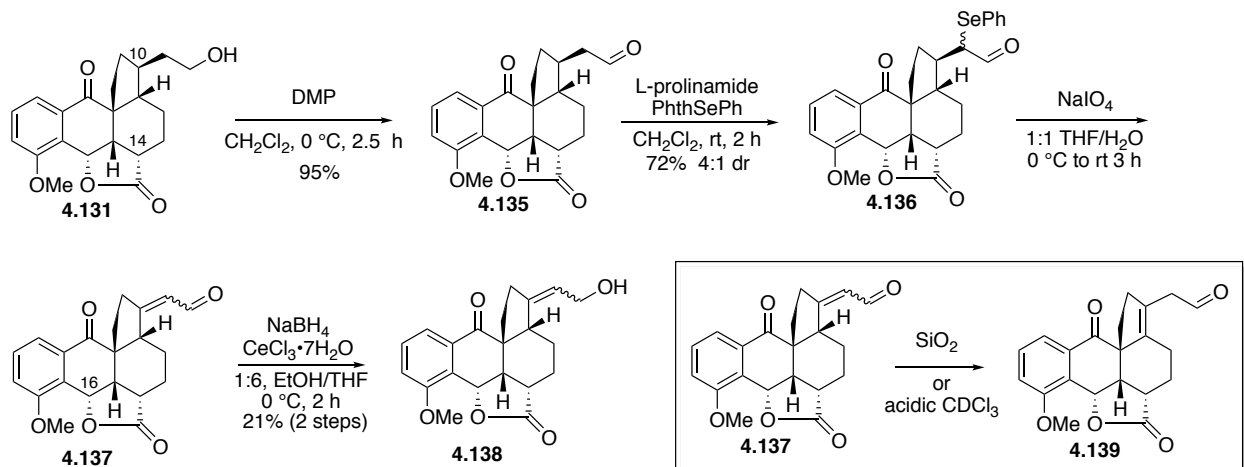
With the tetracyclic core successfully synthesized, we turned our attention to the challenging C10 inversion sequence. We intended to employ the groups' first-generation strategy to accomplish the inversion by converting the alcohol 4.132 to the enal 4.133 followed by a selective reduction to give 4.134 (Scheme 4.29).



Scheme 4.29. Proposed inversion of side chain configuration.

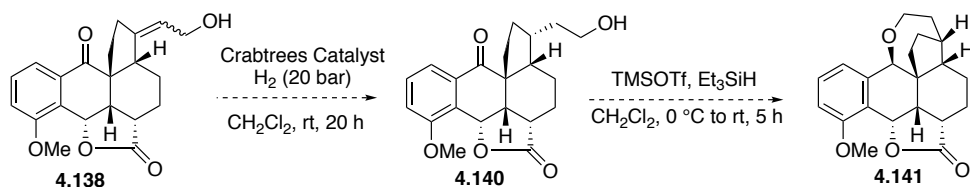
Our initial studies were performed on the undesired C14 epimer, which we reasoned could be epimerized at a later stage to the desired *trans*-configuration. The inversion of the C10 side chain on the undesired C14 epimer began with a Dess-Martin oxidation of the alcohol 4.131 to give the aldehyde 4.135 in excellent yields (Scheme 4.30). Selenation under standard

conditions using PhSeCl and acid resulted in a complex mixture of products. However, we discovered a mild enamine catalyzed selenation using L-prolinamide and *N*-(phenylseleno)phthalimide (PhthSePh) to give selenide **4.136** in 72% yield as a 4:1 mixture of diastereomers.⁴⁷⁴ Using DL-proline affords the same mixture of diastereomers in similar yields indicating that this transformation is highly substrate controlled. Next, several oxidants were screened for the elimination of selenide **4.136**, including sodium periodate, tetrabutyl ammonium periodate (TBAIO₄), and manganese monoprophthalate (MMPP).⁴⁷⁵ The sodium periodate reaction proved optimal, proceeding with the cleanest reaction profile. The intermediate enal **4.137** was highly prone to isomerization; therefore, this product was directly subjected to a Luche reduction to give allylic alcohol **4.138**.



Scheme 4.30. Progress towards the inversion of the C10 configuration.

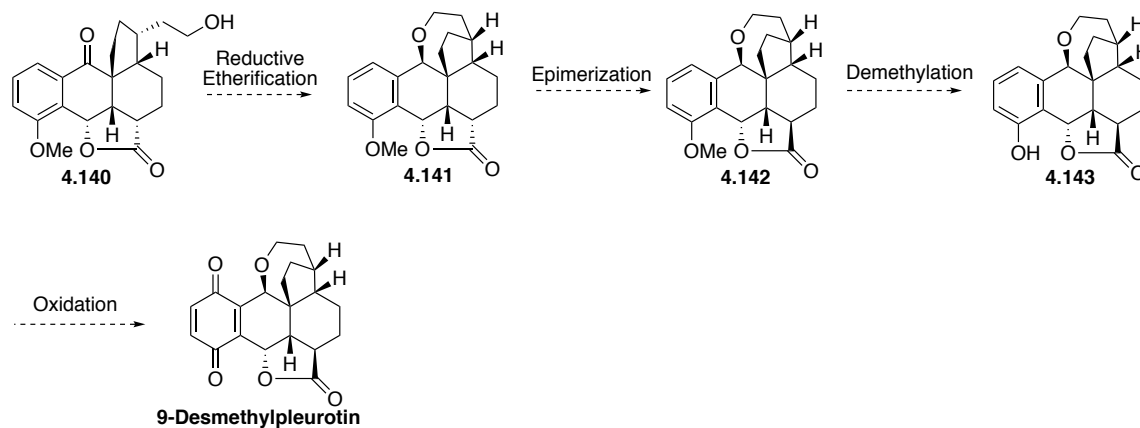
While attempts to reduce **4.138** using Pd/C resulted in a mixture of C16 benzylic cleavage products, we found that hydrogenation using Crabtree's catalyst gave the desired saturated alcohol **4.140** by crude ¹HNMR and LCMS. The crude alcohol products were directly subjected to reductive etherification conditions using TMSOTf and triethylsilane and a HRMS match by LCMS indicated formation of the desired product **4.141** (Scheme 4.31).⁴⁷⁶



Scheme 4.31. Reduction of allylic alcohol **4.139** and reductive etherification to **4.142**.

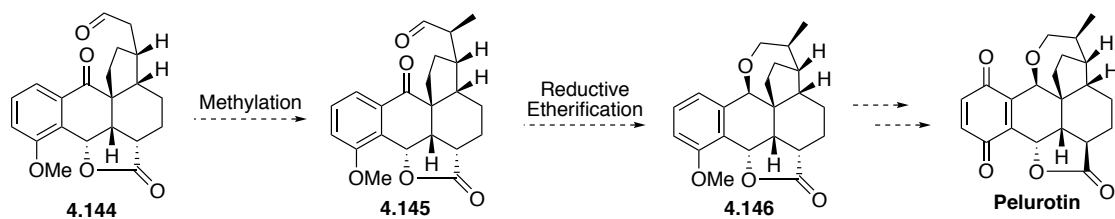
4.2.7 Future Directions

Following the reductive etherification, we plan to epimerize at C14, demethylate the phenol, and oxidize to the quinone to give 9-desmethylpleurotin (Scheme 4.32).



Scheme 4.32. Proposed endgame for the synthesis of 9-desmethylpleurotin.

After the completion of 9-desmethylpleurotin, we propose that we can perform a late stage methylation of aldehyde **4.144** (Scheme 4.33). Using the proposed reductive etherification/demethylation/oxidation sequence outlined in Scheme 4.32 we can arrive at the desired pleurotin.



Scheme 4.33. Proposed synthesis of pleurotin by late stage methylation.

4.3 CONCLUSIONS

We have developed a third generation approach to pleurotin and a first generation approach to 9-desmethylpleurotin. This strategy utilizes a key IMDA reaction to afford the tetracyclic core of pleurotin and sets three of the required seven stereocenters. Progress has been made toward completing the challenging inversion sequence to correct the C10 side chain configuration that proved a significant synthetic challenge in previous routes. We have demonstrated that the saturated alcohol side chain with the incorrect C10 configuration can be oxidized to the enal and then subsequently reduced to the allylic alcohol. Synthetic investigations to reduce the allylic alcohol **4.138** to the saturated alcohol **4.140** and complete the inversion sequence were promising. Upon completion of 9-desmethylpleurotin, we can potentially access pleurotin via a late stage methylation.

5.0 EXPERIMENTAL PART

5.1 GENERAL EXPERIMENTAL

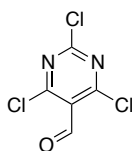
Moisture and air-sensitive reactions were performed under N₂ or Ar atmosphere and glassware used for these reactions was flamed dried and cooled under N₂ or Ar prior to use. All moisture sensitive reactions were performed using syringe-septum cap techniques under an atmosphere of dry N₂ or Ar. Reactions carried out below 0 °C employed a dry ice/acetone bath or a cryocool and an isopropanol bath. THF and Et₂O were distilled from sodium/benzophenone ketyl. DMF and CH₂Cl₂ were distilled from CaH₂. Anhydrous 1,4-dioxane, dimethylsulfoxide, and dimethylformamide were purchased from Acros (Sure/Seal bottle) and used as received. Et₃N was distilled from CaH₂ and stored over KOH. Toluene was purified by passage through an activated alumina filtration system. Melting points were determined using a Mel-Temp II instrument and are not corrected. Infrared spectra were determined using a Smiths Detection IdentifyIR FT-IR spectrometer. High-resolution mass spectra were obtained on a Micromass UK Limited, Q-TOF Ultima API, Thermo Scientific Exactive Orbitrap LC-MS. ¹H and ¹³C NMR spectra were obtained on Bruker Advance 300 MHz, 400 MHz, 500 MHz, 600 MHz, or 700 MHz instruments. Chemical shifts (δ) were reported in parts per million with the residual solvent peak used as an internal standard, δ ¹H/¹³C (Solvent): 7.26/77.00 (CDCl₃); 2.05/29.84 (acetone-d₆); 2.50/39.52 (DMSO-d₆), 3.31/49.00 (CD₃OD); and are tabulated as follows: chemical shift,

multiplicity (s = singlet, bs = broad singlet, d = doublet, bd = broad doublet, t = triplet, app t = apparent triplet, q = quartet, m = multiplet), number of protons, and coupling constant(s). ^{13}C NMR spectra were obtained at 75 MHz, 100 MHz, 125 MHz, 150 MHz, or 175 MHz using a proton-decoupled pulse sequence and are tabulated by observed peak. ^{19}F NMR spectra were obtained at 376 MHz or 470 MHz using a proton-decoupled pulse sequence, are tabulated by observed peak, and are uncorrected. CDCl_3 was filtered through dried basic alumina prior to use. Thin-layer chromatography was performed using pre-coated silica gel 60 F254 plates (EMD, 250 μm thickness) and visualization was accomplished with a 254 nm UV light and by staining with a PMA solution (5 g of phosphomolybdic acid in 100 mL of 95% EtOH), Vaughn's reagent (4.8 g of $(\text{NH}_4)_6\text{Mo}_7\text{O}_{24}\cdot 4\text{H}_2\text{O}$ and 0.2 g of $\text{Ce}(\text{SO}_4)_2$ in 100 mL of a 3.5 N H_2SO_4 solution) or a KMnO_4 solution (1.5 g of KMnO_4 and 1.5 g of K_2CO_3 in 100 mL of a 0.1% NaOH solution). Chromatography on SiO_2 (Silicycle, Silia-P Flash Silica Gel or SiliaFlash® P60, 40-63 μm) was used to purify crude reaction mixtures. Automated column chromatography was done using an Isco Combiflash Rf. Concentrating under reduced pressure refers to the use of rotary evaporator connected to a PIAB Lab Vac H40 to remove solvent. Final products were of >95% purity as analyzed by RP HPLC (Alltech Prevail C-18, 100 \times 4.6 mm, 1 mL/min, CH_3CN , H_2O and 0.1% TFA) with UV (210, 220 and 254 nm), ELS (nebulizer 45 $^\circ\text{C}$, evaporator 45 $^\circ\text{C}$, N_2 flow 1.25 SLM), and MS detection using a Thermo Scientific Exactive Orbitrap LC-MS (ESI positive). All other materials were obtained from commercial sources and used as received.

Safety Note: All organic azides and azide waste products should be considered toxic as well as potentially explosive and must be handled and stored with care. Avoid using halogenated solvents when performing reactions involving sodium azide, in addition to using halogenated solvents in reaction workup. Avoid quenching/manipulating/treating sodium azide reactions with

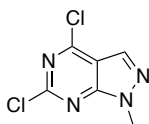
acid, as generation of trace amounts of hydrazoic acid (HN₃) may result in an explosion. In general, a safety shield must be used when conducting reactions involving either sodium azide or organic azide derivatives.

5.2 CHAPTER 1 EXPERIMENTAL PART



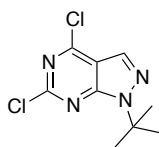
1.10

2,4,6-Trichloropyrimidine-5-carbaldehyde (1.10).¹⁴⁴ *N,N*-Dimethylformamide (4.85 mL, 62.5 mmol) was added dropwise to phosphorus oxychloride (25.1 mL, 269 mmol) at 0 °C. Barbituric acid (**1.9**, 5.00 g, 62.5 mmol) was then added portion-wise over 1 h, and the resulting suspension was stirred in a pre-equilibrated oil bath at 90 °C for 2 d. The reaction mixture was concentrated under reduced pressure and a H₂O-ice mixture (50 mL) was slowly added to the residue in an ice bath. The yellow precipitate that formed was filtered, washed with a H₂O-ice mixture (3 x 10 mL), dissolved in CH₂Cl₂ (100 mL) and washed with brine (30 mL) and satd. aqueous NaHCO₃ (30 mL). The organic extract was dried (MgSO₄) and concentrated under reduced pressure to give **1.10** (4.70 g, 22.3 mmol, 57%) as a pale yellow solid: ¹H NMR (400 MHz, CDCl₃) δ 10.40 (s, 1 H); ¹³C NMR (100 MHz, CDCl₃) δ 184.6, 164.0, 161.5, 160.9, 159.9, 122.9.



1.8a

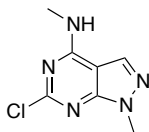
4,6-Dichloro-1-methyl-1*H*-pyrazolo[3,4-*d*]pyrimidine (1.8a).¹⁴⁴ A solution of 2,4,6-trichloropyrimidine-5-carbaldehyde (**1.10**, 1.00 g, 4.73 mmol) in dry THF (10 mL) at -78 °C was treated with a solution of methyl hydrazine (0.26 mL, 4.73 mmol) in dry THF (2 mL) dropwise followed by Et₃N (2.0 mL, 14.2 mmol). The resulting mixture was stirred for 1.5 h at -78 °C, warmed to rt, and concentrated under reduced pressure. The crude residue was purified by chromatography on SiO₂ (hexanes/EtOAc, 8:2) to give **1.8a** (0.570 g, 2.81 mmol, 59 %) as a colorless solid: Mp 88.9-90.9 °C; IR (neat) 3110, 1588, 1545, 1371, 1299, 1127 cm⁻¹; ¹H NMR (400 MHz, CDCl₃) δ 8.12 (s, 1 H), 4.10 (s, 3 H); ¹³C NMR (100 MHz, CDCl₃) δ 156.5, 155.4, 154.2, 132.3, 112.6, 34.6.



1.8b

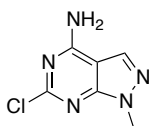
1-(*t*-Butyl)-4,6-dichloro-1*H*-pyrazolo[3,4-*d*]pyrimidine (1.8b).¹⁴⁴ A solution of 2,4,6-trichloropyrimidine-5-carbaldehyde (**1.10**, 1.00 g, 4.73 mmol) in dry CH₂Cl₂ (20 mL) at -78 °C under Ar was treated with a solution of *t*-butyl hydrazine hydrochloride (0.631 g, 4.73 mmol) and Et₃N (2.0 mL, 14.2 mmol) in dry CH₃CN (30 mL) dropwise. The mixture was stirred for 2 h at -78 °C where analysis by TLC (hexanes/EtOAc, 4:1) indicated the SM was consumed. SiO₂ was added and the reaction was concentrated under reduced pressure and was purified by chromatography on SiO₂ (solid load, hexanes/EtOAc, 8:1) to give **1.8b** (0.937 g, 3.82 mmol, 81%) as a colorless solid: IR (neat) 3118, 2984, 2934, 1582, 1525, 1320, 1230, 1208, 1152 cm⁻¹; ¹H NMR (400 MHz, CDCl₃) δ 8.08 (s, 1 H), 1.80 (s, 9 H); ¹³C NMR (100 MHz, CDCl₃) δ 155.1,

155.0, 153.6, 130.8, 113.7, 61.9, 29.0; HRMS (ESI) m/z calcd for $C_9H_{10}Cl_2N_4$ ($[M+H]^+$) 245.0361, found 245.0357.



1.11a

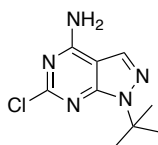
6-Chloro-*N*,1-dimethyl-1*H*-pyrazolo[3,4-*d*]pyrimidin-4-amine (1.11a). To a solution of 4,6-dichloro-1-methyl-1*H*-pyrazolo[3,4-*d*]pyrimidine (**1.8a**, 0.300 g, 1.48 mmol) in dry THF (15 mL) was added methylamine hydrochloride (0.110 g, 1.55 mmol), followed by freshly distilled Et_3N (1.0 mL, 7.38 mmol). The reaction mixture was stirred at rt for 2 d, concentrated under reduced pressure, and the residue was dissolved in EtOAc (100 mL), washed with H_2O (3 x 75 mL), dried ($MgSO_4$) and concentrated under reduced pressure. The crude product was purified by chromatography on SiO_2 (hexanes/EtOAc, 2:1) to give **1.11a** (0.267 g, 1.35 mmol, 91%) as a colorless solid: Mp 239.3-240.4 °C; IR (neat) 3230, 3105, 1614, 1579, 1316, 1128, 930 cm^{-1} ; 1H NMR (400 MHz, $DMSO-d_6$) δ 8.70 (bs, 1 H), 8.03 (s, 1 H), 3.83 (s, 3 H), 2.95 (d, J = 4.4 Hz, 3 H); ^{13}C NMR (100 MHz, $DMSO-d_6$) δ 157.4, 157.2, 153.3, 131.6, 99.3, 33.7, 27.1; HRMS (ESI) m/z calcd for $C_7H_8ClN_5$ ($[M+H]^+$) 198.0546, found 198.0551.



1.11b

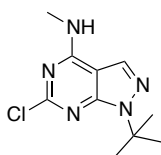
6-Chloro-1-methyl-1*H*-pyrazolo[3,4-*d*]pyrimidin-4-amine (1.11b). Ammonia gas was bubbled for 15 min through a suspension of 4,6-dichloro-1-methyl-1*H*-pyrazolo[3,4-*d*]pyrimidine (**1.8a**, 0.300 g, 1.48 mmol) in dry THF (48 mL). The mixture was stirred at rt for 8 h, concentrated under reduced pressure, and the residue was dissolved in EtOAc (30 mL),

washed with H₂O (3 x 15 mL), dried (MgSO₄) and concentrated under reduced pressure. The crude product was purified by chromatography on SiO₂ (hexanes/EtOAc, 1:1 to EtOAc) to give **1.11b** (0.220 g, 1.20 mmol, 81%) as a colorless solid: Mp 265-275 °C; IR (neat) 3308, 3099, 2920, 1657, 1599, 1561, 1187 cm⁻¹; ¹H NMR (400 MHz, DMSO-d₆) δ 8.24 (bs, 1 H), 8.11 (bs, 1 H), 8.05 (s, 1 H), 3.83 (s, 3 H); ¹³C NMR (100 MHz, DMSO-d₆) δ 158.6, 157.3, 153.9, 132.1, 98.9, 33.6; HRMS (ESI) *m/z* calcd for C₆H₆ClN₅ ([M+H]⁺) 184.0390, found 184.0381.



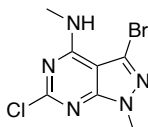
1.11c

1-(*t*-Butyl)-6-chloro-1H-pyrazolo[3,4-*d*]pyrimidin-4-amine (1.11c). Ammonia gas was bubbled through a suspension of 1-(*t*-butyl)-4,6-dichloro-1H-pyrazolo[3,4-*d*]pyrimidine (**1.8b**, 0.800 g, 3.26 mmol) in THF (100 mL) for 20 min. A white precipitate started to form after several minutes and the resulting mixture was stirred at rt for 24 h, concentrated under reduced pressure, and the residue was dissolved in EtOAc (250 mL), washed with H₂O (3 x 75 mL), dried (MgSO₄) and concentrated under reduced pressure to give **1.11c** (0.740 g, 3.19 mmol, 98%) as a colorless solid which was used in the next step without further purification: Mp 272-274 °C; IR (neat) 3297, 3135, 2971, 2932, 1644, 1592, 1469, 1366, 1236, 1171 cm⁻¹; ¹H NMR (400 MHz, DMSO-d₆) δ 8.17 (bs, 1 H), 8.03 (s, 2 H), 1.65 (s, 9 H); ¹³C NMR (100 MHz, DMSO-d₆) δ 158.7, 156.0, 153.5, 130.6, 100.3, 59.6, 28.7; HRMS (ESI) *m/z* calcd for C₉H₁₂ClN₅ ([M+H]⁺) 226.0859, found 226.0882.



1.11d

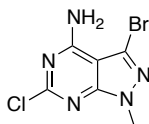
1-(*t*-Butyl)-6-chloro-*N*-methyl-1*H*-pyrazolo[3,4-*d*]pyrimidin-4-amine (1.11d). A solution of 1-(*t*-butyl)-4,6-dichloro-1*H*-pyrazolo[3,4-*d*]pyrimidine (**1.8b**, 0.800 g, 3.26 mmol) in THF (24 mL) at rt under Ar was treated with methylamine hydrochloride (0.230 g, 3.43 mmol) and Et₃N (2.30 mL, 16.3 mmol). The reaction mixture was stirred at rt for 24 h, concentrated under reduced pressure, dissolved in EtOAc (75 mL), washed with H₂O (3 x 30 mL), dried (MgSO₄) and concentrated under reduced pressure. The residue was purified by chromatography on SiO₂ (hexanes/EtOAc, 2:1) to give **1.11d** (0.700 g, 2.93 mmol, 90%) as a colorless solid: Mp 160.7-161.9 °C; IR (neat) 3236, 3133, 2947, 1579, 1428, 1361, 1310, 1282, 1124, 1075 cm⁻¹; ¹H NMR (400 MHz, DMSO-*d*₆) δ 8.63 (bd, *J* = 4.4 Hz, 1 H), 8.02 (s, 1 H), 2.93 (d, *J* = 4.4 Hz, 3 H), 1.65 (s, 9 H); ¹³C NMR (100 MHz, DMSO-*d*₆) δ 157.3, 156.1, 152.8, 130.0, 100.7, 59.7, 28.7, 27.0; HRMS (ESI) *m/z* calcd for C₁₀H₁₄ClN₅ ([M+H]⁺) 240.1016, found 240.1006.



1.7a

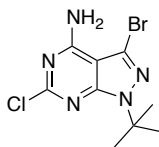
3-Bromo-6-chloro-*N*,1-dimethyl-1*H*-pyrazolo[3,4-*d*]pyrimidin-4-amine (1.7a). A mixture of 6-chloro-*N*,1-dimethyl-1*H*-pyrazolo[3,4-*d*]pyrimidin-4-amine (**1.11a**, 0.260 g, 1.31 mmol) and Br₂ (0.21 mL, 3.92 mmol) in H₂O (90 mL) was stirred at rt for 1 h and heated at 100 °C for 2 h. The reaction mixture was cooled to rt and extracted with EtOAc (3 x 75 ml), washed with 5% aqueous NaHSO₃ solution (100 mL) and brine (75 mL), dried (MgSO₄) and concentrated under reduced pressure to give **1.7a** (0.318 g, 1.15 mmol, 88%) as a colorless solid, which was used in the next step without further purification: Mp 246.9-248.0 °C; IR (neat) 3407, 2939, 1606, 1567, 1325, 1200 cm⁻¹; ¹H NMR (400 MHz, CDCl₃) δ 6.14 (bs, 1 H), 3.94 (s, 3 H),

3.20 (d, $J = 4.8$ Hz, 3 H); ^{13}C NMR δ 159.3, 157.4, 154.8, 116.8, 99.3, 34.4, 28.1; HRMS (ESI) m/z calcd for $\text{C}_7\text{H}_7\text{BrClN}_5$ ($[\text{M}+\text{H}]^+$) 275.9652, found 275.9652.



1.7b

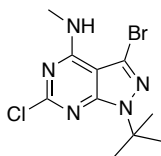
3-Bromo-6-chloro-1-methyl-1H-pyrazolo[3,4-*d*]pyrimidin-4-amine (1.7b). A mixture of 6-chloro-1-methyl-1H-pyrazolo[3,4-*d*]pyrimidin-4-amine (**1.11b**, 0.196 g, 1.07 mmol) and Br_2 (0.23 mL, 4.27 mmol) in H_2O (5 mL) was stirred at rt for 1 h and at 100 °C for an additional 1 h. The reaction mixture was cooled to rt, extracted with EtOAc (3 x 15 mL), and washed with 5% aqueous NaHSO_3 solution (10 mL) and brine (15 mL). The organic layer was dried (MgSO_4) and concentrated under reduced pressure. The residue was purified by chromatography on SiO_2 (hexanes/EtOAc, 1:1) to give **1.7b** (0.113 g, 0.431 mmol, 40%) as a colorless solid: Mp 285-295 °C; IR (neat) 3451, 3282, 3125, 1586, 1552, 1248, 1189 cm^{-1} ; ^1H NMR (400 MHz, DMSO-d_6) δ 8.53 (bs, 1 H), 7.28 (bs, 1 H), 3.81 (s, 3 H); ^{13}C NMR (100 MHz, DMSO-d_6) δ 157.9 (2 C), 154.8, 117.3, 98.5, 34.0; HRMS (ESI) m/z calcd for $\text{C}_6\text{H}_6\text{ClN}_5$ ($[\text{M}+\text{H}]^+$) 262.9573, found 262.9593.



1.7c

3-Bromo-1-(*t*-butyl)-6-chloro-1H-pyrazolo[3,4-*d*]pyrimidin-4-amine (1.7c). A mixture of 1-(*t*-butyl)-6-chloro-1H-pyrazolo[3,4-*d*]pyrimidin-4-amine (**1.11c**, 0.100 g, 0.440 mmol) and Br_2 (50 μL , 0.890 mmol) in H_2O (5 mL) was stirred at rt for 1 h and then at 100 °C for 30 min. In

order to increase the solubilizing power of the reaction mixture, EtOAc (3 mL) was added, and the resulting solution was heated at reflux for an additional 15 min. The two layers were separated and the aqueous phase was extracted with EtOAc (3 x 7.5 mL). The combined organic extracts were washed with 5% aqueous NaHSO₃ solution (10 mL), brine (15 mL), dried (MgSO₄) and concentrated under reduced pressure. The crude residue was purified by chromatography on SiO₂ (CH₂Cl₂ to CH₂Cl₂:EtOAc, 1:1) to give **1.7c** (0.110 g, 0.371 mmol, 84%) as a light yellow solid: Mp 225-226°C; IR (neat) 3450, 3282, 2971, 2919, 2718, 1651, 1634, 1584, 1543, 1461, 1234, 1174, 1131 cm⁻¹; ¹H NMR (400 MHz, CDCl₃) δ 6.05 (bs, 2 H), 1.74 (s, 9 H); ¹³C NMR (100 MHz, CDCl₃) δ 157.6, 157.1, 154.7, 115.8, 100.1, 61.9, 29.1; HRMS (ESI+) *m/z* calcd for C₉H₁₁BrClN₅ ([M+H]⁺) 303.9965, found 303.9983.

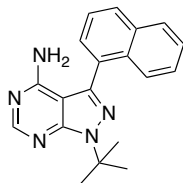


1.7d

3-Bromo-1-(*t*-butyl)-6-chloro-*N*-methyl-1*H*-pyrazolo[3,4-*d*]pyrimidin-4-amine

(1.7d). A mixture of 1-(*t*-butyl)-6-chloro-*N*-methyl-1*H*-pyrazolo[3,4-*d*]pyrimidin-4-amine (**1.11d**, 0.120 g, 0.500 mmol) and Br₂ (50 μL, 1.00 mmol) in H₂O (3 mL) was stirred at rt for 1 h, treated with EtOAc (1 mL), and heated at reflux for an additional 1 h. Additional EtOAc (3 mL) was added and the reaction mixture was heated at reflux for 15 min. Analysis by TLC (hexanes/EtOAc, 2:1) indicated the SM was consumed, the layers were separated and the aqueous phase was extracted with EtOAc (3 x 8 mL). The combined organic layers were washed with 5% aqueous NaHSO₃ solution (10 mL), brine (15 mL), dried (MgSO₄) and concentrated under reduced pressure. The crude residue was purified by automated chromatography on SiO₂ (12 g column, liquid load CH₂Cl₂, stepwise gradient, 100% hexanes to 100% EtOAc over 15

min) to give **1.7d** (0.130 g, 0.355 mmol, 71%) as a colorless solid: Mp 106.8-108.4 °C; IR (neat) 3413, 2982, 2934, 1609, 1553, 1364, 1322, 1217, 1133 cm⁻¹; ¹H NMR (400 MHz, CDCl₃) δ 6.12 (bs, 1 H), 3.18 (d, *J* = 4.8 Hz, 3 H), 1.73 (s, 9 H); ¹³C NMR (100 MHz, CDCl₃) δ 157.7, 157.3, 154.2, 114.9, 100.2, 61.7, 29.1, 27.9; HRMS (ESI) *m/z* calcd for C₁₀H₁₃BrClN₅ ([M+H]⁺) 318.0121, found 318.0110.

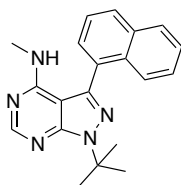


PP1

1-(*tert*-Butyl)-3-(naphthalen-1-yl)-1*H*-pyrazolo[3,4-*d*]pyrimidin-4-amine (PP1).^{1,2,3} A solution of dichloro[1,1'-bis(diphenylphosphino)ferrocene]palladium(II)-CH₂Cl₂ adduct (0.0182 g, 0.0200 mmol) in freshly distilled and degassed 1,4-dioxane (2 mL) was treated with 3-bromo-1-(*t*-butyl)-6-chloro-1*H*-pyrazolo[3,4-*d*]pyrimidin-4-amine (**1.7c**, 0.0750 g, 0.250 mmol), Cs₂CO₃ (0.122 g, 0.370 mmol) and 1-naphthylboronic acid (0.0500 g, 0.300 mmol). The flask was sealed and the reaction mixture was stirred at 100 °C for 2 d, filtered through Celite, and concentrated under reduced pressure. The crude residue was purified by chromatography on SiO₂ (hexanes/EtOAc, 6:1) to give a mixture of 1-(*t*-butyl)-6-chloro-3-(naphthalen-1-yl)-1*H*-pyrazolo[3,4-*d*]pyrimidin-4-amine and starting material (3:1, 0.0436 g) as an off-white solid.

A solution of this mixture (0.0400 g, 0.0825 mmol), 5% Pd/C (1.08 g, 0.460 mmol) and NH₄HCO₂ (0.0430 g, 0.680 mmol) in MeOH (8 mL) was stirred at rt for 10 min, purged with H₂ for 30 min and stirred under and atmosphere of H₂ (balloon) for 26 h. The reaction mixture was filtered through Celite, washed (CH₂Cl₂ (10 mL)), and concentrated under reduced pressure. The crude residue was purified by chromatography on SiO₂ (hexanes/EtOAc, 4:1) to give **PP1**

(0.00594 g, 0.0187 mmol, 7.6% (2 steps), 95% purity by LC-MS) as a colorless solid: ^1H NMR (400 MHz, CDCl_3) δ 8.39 (bs, 1 H), 7.98 (d, $J = 8.0$ Hz, 1 H), 7.94 (t, $J = 6.6$ Hz, 1 H), 7.67 (d, $J = 6.6$ Hz, 1 H), 7.61 (d, $J = 8.0$ Hz, 1 H), 7.85-7.49 (m, 2 H), 5.00 (bs, 2 H), 1.89 (s, 9 H); ^{13}C NMR (100 MHz, CDCl_3) δ 157.6, 154.7, 153.9, 134.0, 131.8, 130.6, 129.6, 128.4, 128.4, 127.1, 126.5, 125.6, 125.5, 60.6, 29.3; HRMS (ESI) m/z calcd for $\text{C}_{19}\text{H}_{19}\text{N}_5$ ($[\text{M}+\text{H}]^+$) 318.1719, found 318.1698.



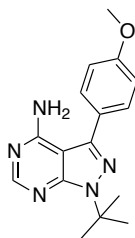
1.13a

1-(*tert*-Butyl)-*N*-methyl-3-(naphthalen-1-yl)-1*H*-pyrazolo[3,4-*d*]pyrimidin-4-amine

(1.13a).¹²⁹ To a solution of dichloro[1,1'-bis(diphenylphosphino)ferrocene]palladium (II)- CH_2Cl_2 adduct (0.0174 g, 0.0200 mmol) in freshly distilled and degassed 1,4-dioxane (2 mL) was added 3-bromo-1-(*t*-butyl)-6-chloro-*N*-methyl-1*H*-pyrazolo[3,4-*d*]pyrimidin-4-amine (**1.7d**, 0.0750 g, 0.240 mmol) and Cs_2CO_3 (0.116 g, 0.350 mmol) and the resulting mixture was stirred for 10 min, and treated with 1-naphthylboronic acid (0.0500 g, 0.280 mmol). The flask was sealed, heated to 100 °C for 42 h, and the reaction mixture was filtered through Celite. The filtrate was concentrated under reduced pressure. The residue was purified by automated chromatography on SiO_2 (12 g column, liquid load CH_2Cl_2 , stepwise gradient, 100% hexanes to 100% EtOAc over 15 min) to give a mixture of 1-(*t*-butyl)-6-chloro-*N*-methyl-3-(naphthalen-1-yl)-1*H*-pyrazolo[3,4-*d*]pyrimidin-4-amine and starting material (3:1, 0.0318 g) as an off-white solid.

A solution of this mixture (0.0318 g, 0.0652 mmol), 10% Pd/C (0.0154 g, 0.130 mmol) and NH_4HCO_2 (0.0328 g, 0.521 mmol) in MeOH (5 mL) was stirred at rt for 30 min, purged with

H₂ for 15 min and stirred under an atmosphere of H₂ (balloon) for 22 h. The reaction mixture was filtered through Celite and the filtrate was concentrated under reduced pressure. The residue was purified by preparative TLC on SiO₂ (hexanes/EtOAc, 5:1) to give **1.13a** (0.00485 g, 0.0146 mmol, 6.2% (2 steps), 100% purity by LC-MS) as a clear oil which crystallized upon standing at rt for ~1 h: Mp 152.4-156.3 °C; IR (neat) 3437, 3044, 2975, 2926, 1597, 1558, 1312, 1243, 1079, cm⁻¹; ¹H NMR (400 MHz, CDCl₃) δ 8.47 (s, 1 H), 7.97 (dd, *J* = 14.4, 8.0 Hz, 2 H), 7.90 (d, *J* = 8.0 Hz, 1 H), 7.65-7.50 (m, 4 H), 4.71 (bs, 1 H), 2.86 (d, *J* = 4.8 Hz, 3 H), 1.88 (s, 9 H); ¹³C NMR (100 MHz, CDCl₃) δ 157.6, 154.7, 153.3, 139.7, 134.1, 131.9, 129.5, 128.4, 128.3, 127.0, 126.5, 125.7, 125.5, 101.7, 60.4, 29.3, 27.6; HRMS (ESI) *m/z* calcd for C₂₀H₂₁N₅ ([M+H]⁺) 332.1875, found 332.1863.

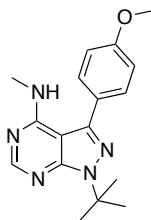


1.13b

1-(*t*-Butyl)-3-(4-methoxyphenyl)-1*H*-pyrazolo[3,4-*d*]pyrimidin-4-amine (1.13b). A solution of dichloro[1,1'-bis(diphenylphosphino)ferrocene]palladium (II)-CH₂Cl₂ adduct (0.0180 g, 0.0200 mmol) in freshly distilled and degassed 1,4-dioxane (2 mL) was treated with 3-bromo-1-(*t*-butyl)-6-chloro-1*H*-pyrazolo[3,4-*d*]pyrimidin-4-amine (**1.7c**, 0.0750 g, 0.250 mmol) and Cs₂CO₃ (0.122 g, 0.370 mmol). The reaction mixture was stirred for 10 min and 4-methoxybenzeneboronic acid (0.0450 g, 0.300 mmol) was added. The flask was sealed and the solution was stirred at 100 °C for 20 h, filtered through Celite and concentrated under reduced pressure. The residue was purified by automated chromatography on SiO₂ (4 g column, liquid load CH₂Cl₂, stepwise gradient, 100% hexanes to 100% EtOAc over 15 min) to give a mixture of

1-(*t*-butyl)-6-chloro-3-(4-methoxyphenyl)-1*H*-pyrazolo[3,4-*d*]pyrimidin-4-amine and starting material (20:1, 0.0480 g) as an off-white solid.

A solution of this mixture (0.0200 g, 0.0571 mmol), 10% Pd/C (0.0857 g, 0.0700 mmol) and NH₄HCO₂ (0.0228 g, 0.360 mmol) in MeOH (2 mL) was stirred at rt for 30 min, purged with H₂ for 15 min and stirred under H₂ for 28 h. The reaction mixture was filtered through Celite and the filtrate was concentrated under reduced pressure. The residue was purified by chromatography on SiO₂ (hexanes/EtOAc, 6:1) to give **1.13b** (0.0140 g, 0.0486 mmol, 48% (2 steps), 96% purity by LC-MS) as a colorless solid: ¹H NMR (400 MHz, CDCl₃) δ 8.34 (s, 1 H), 7.61 (d, *J* = 8.6 Hz, 1 H), 7.04 (d, *J* = 8.6 Hz, 1 H), 5.51 (bs, 2 H), 3.87 (s, 3 H), 1.83 (s, 9 H); ¹³C NMR (100 MHz, CDCl₃) δ 160.1, 157.8, 154.4, 154.1, 141.9, 129.9, 126.1, 114.7, 99.7, 60.3, 55.4, 29.2; HRMS (ESI) *m/z* calcd for C₁₆H₁₉N₅O ([M+H]⁺) 298.1668, found 298.1649.



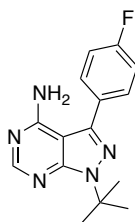
1.13c

1-(*t*-Butyl)-3-(4-methoxyphenyl)-*N*-methyl-1*H*-pyrazolo[3,4-*d*]pyrimidin-4-amine

(1.13c). A solution of dichloro[1,1'-bis(diphenylphosphino)ferrocene]palladium (II)-CH₂Cl₂ adduct (0.0016 g, 0.0157 mmol) in freshly distilled and degassed 1,4-dioxane (2 mL) was treated with 3-bromo-1-(*t*-butyl)-6-chloro-*N*-methyl-1*H*-pyrazolo[3,4-*d*]pyrimidin-4-amine (**1.7d**, 0.0500 g, 0.157 mmol), and Cs₂CO₃ (0.0774 g, 0.235 mmol). The resulting mixture was stirred for 10 min and 4-methoxybenzeneboronic acid (0.0286 g, 0.188 mmol) was added. The flask was sealed and heated at 80 °C for 11 h and at 100 °C for an additional 4 h. The reaction mixture was filtered through Celite and the filtrate was concentrated under reduced pressure. The residue was

purified by automated chromatography on SiO₂ (4 g column, liquid load CH₂Cl₂, stepwise gradient, 100% hexanes to 100% EtOAc over 15 min) to give a mixture of 1-(*t*-butyl)-6-chloro-3-(4-methoxyphenyl)-*N*-methyl-1*H*-pyrazolo[3,4-*d*]pyrimidin-4-amine and starting material (20:1, 0.0275 g) as an off-white solid.

A solution of this mixture (0.0145 g, 0.0381 mmol), 10% Pd/C (0.0074 g, 0.0629 mmol) and NH₄HCO₂ (0.0159 g, 0.250 mmol) in MeOH (5 mL) was stirred at rt for 30 min, purged with H₂ for 15 min and stirred under H₂ for 25 h. The reaction mixture was filtered through Celite, and the filtrate was concentrated under reduced pressure. The residue was purified by chromatography on SiO₂ (hexanes/EtOAc, 4:1) to give **1.13c** (0.00760 g, 0.0245 mmol, 30% (2 steps), 100% purity by LC-MS) as a clear oil which crystallized to a colorless solid after ~1 h: Mp 89.3-91.2 °C; IR (neat) 3439, 2977, 2930, 1596, 1560, 1517, 1314, 1245, 1033 cm⁻¹; ¹H NMR (400 MHz, CDCl₃) δ 8.43 (s, 1 H), 7.57 (d, *J* = 8.8 Hz, 2 H), 7.05 (d, *J* = 8.8 Hz, 2 H), 5.29 (bd, *J* = 4.6 Hz, 1 H), 3.88 (s, 3 H), 3.21 (d, *J* = 4.6 Hz, 3 H), 1.82 (s, 9 H); ¹³C NMR (100 MHz, CDCl₃) δ 160.0, 157.8, 154.5, 153.5, 141.3, 129.9, 126.4, 114.7, 100.0, 60.1, 55.4, 29.2, 27.7; HRMS (ESI) *m/z* calcd for C₂₀H₂₁N₅ ([M+H]⁺) 312.1824, found 312.1814.

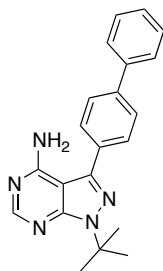


1.13d

1-(*tert*-Butyl)-3-(4-fluorophenyl)-1*H*-pyrazolo[3,4-*d*]pyrimidin-4-amine (1.13d). A solution of dichloro[1,1'-bis(diphenylphosphino)ferrocene]palladium (II)-CH₂Cl₂ adduct (0.0182 g, 0.0200 mmol) in freshly distilled and degassed 1,4-dioxane (2 mL) was treated with 3-bromo-1-(*t*-butyl)-6-chloro-1*H*-pyrazolo[3,4-*d*]pyrimidin-4-amine (**1.7c**, 0.0750 g, 0.250 mmol) and

Cs₂CO₃ (0.0122 g, 0.370 mmol). The resulting mixture was stirred for 10 min and 4-fluorobenzeneboronic acid (0.0400 g, 0.290 mmol) was added. The reaction was heated at 100 °C for 20 h, filtered through Celite and the filtrate was concentrated under reduced pressure. The crude residue was purified by automated chromatography on SiO₂ (4 g column, liquid load CH₂Cl₂, stepwise gradient, 100% hexanes to 100% EtOAc over 15 min) to give a mixture of 1-(*t*-butyl)-6-chloro-3-(4-fluorophenyl)-1*H*-pyrazolo[3,4-*d*]pyrimidin-4-amine and starting material (10:1, 0.0540 g) as an off-white solid.

A solution of this mixture (0.0180 g, 0.0512 mmol), 10% Pd/C (0.0800 g, 0.0700 mmol) and NH₄HCO₂ (0.0200 g, 0.340 mmol) in MeOH (2 mL) was stirred at rt for 15 min, purged with H₂ for 15 min and stirred under H₂ for 28 h. The reaction mixture was filtered through Celite and the filtrate was concentrated under reduced pressure. The residue was purified by chromatography on SiO₂ (hexanes/EtOAc, 6:1) to give **1.13d** (0.00410 g, 0.0144 mmol, 18% (2 steps), 93% purity by LC-MS) as a colorless solid: ¹H NMR (400 MHz, CDCl₃) δ 8.36 (s, 1 H), 7.68 (dd, *J* = 8.2, 5.2 Hz, 2 H), 7.23 (t, *J* = 8.2 Hz, 2 H), 5.37 (bs, 2 H), 1.83 (s, 9 H); ¹³C NMR (100 MHz, CDCl₃) δ 163.1 (d, *J*_{CF} = 247 Hz), 157.7, 154.6, 154.3, 141.0, 130.4 (d, *J*_{CF} = 8.3 Hz), 129.9 (d, *J*_{CF} = 3.1 Hz), 129.2, 128.6, 116.3 (d, *J*_{CF} = 22 Hz), 99.7, 60.5, 29.2; HRMS (ESI) *m/z* calcd for C₁₅H₁₆FN₅ ([M+H]⁺) 286.1468, found 286.1452.

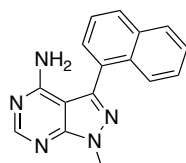


1.13e

3-([1,1'-Biphenyl]-4-yl)-1-(*tert*-butyl)-1*H*-pyrazolo[3,4-*d*]pyrimidin-4-amine (1.13e).

To a solution of dichloro[1,1'-bis(diphenylphosphino)ferrocene]palladium (II)-CH₂Cl₂ adduct (0.0182 g, 0.0200 mmol) in freshly distilled and degassed 1,4-dioxane (2 mL) was added 3-bromo-1-(*t*-butyl)-6-chloro-1*H*-pyrazolo[3,4-*d*]pyrimidin-4-amine (**1.7c**, 0.0750 g, 0.250 mmol), and Cs₂CO₃ (0.122 g, 0.370 mmol). The resulting mixture was stirred for 10 min and 4-phenylbenzeneboronic acid (0.0585 g, 0.300 mmol) was added. The flask was sealed and heated to 100 °C for 21 h. The reaction mixture was filtered through Celite and concentrated under reduced pressure. The residue was purified by automated chromatography on SiO₂ (4 g column, liquid load CH₂Cl₂, stepwise gradient, hexanes to EtOAc over 15 min) to give a mixture of 3-([1,1'-biphenyl]-4-yl)-1-(*t*-butyl)-6-chloro-1*H*-pyrazolo[3,4-*d*]pyrimidin-4-amine and starting material (9:1, 0.0350 g) as an off-white solid.

A solution of this mixture (0.0200 g, 0.0477 mmol), 10% Pd/C (0.0752 g, 0.0600 mmol), and NH₄CO₂ (0.0200 g, 0.320 mmol) in MeOH (2 mL) was stirred at rt for 30 min, purged with H₂ for 15 min and stirred under an atmosphere of H₂ (balloon) for 28 h. The reaction mixture was filtered through Celite and the filtrate was concentrated under reduced pressure. The residue was purified by chromatography on SiO₂ (hexanes/EtOAc, 4:1) to give **1.13e** (0.00890 g, 0.0260 mmol, 19% (2 steps), 94% purity by LC-MS) as a colorless solid: ¹H NMR (400 MHz, CDCl₃) δ 8.38 (s, 1 H), 7.78 (d, *J* = 8.4 Hz, 2 H), 7.75 (d, *J* = 8.4 Hz, 2 H), 7.65 (d, *J* = 7.6 Hz, 2 H), 7.48 (t, *J* = 7.6 Hz, 2 H), 7.39 (t, *J* = 7.6 Hz, 1 H), 5.84 (bs, 3 H), 1.86 (s, 9 H); ¹³C NMR (100 MHz, CDCl₃) δ 157.7, 154.5, 154.3, 141.6 (2 C), 140.3, 132.6, 128.9, 128.9, 127.9, 127.7, 127.0, 99.7, 60.5, 29.2; HRMS (ESI) *m/z* calcd for C₂₁H₂₁N₅ ([M+H]⁺) 344.1875, found 344.1858.

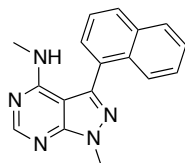


1.13f

1-Methyl-3-(naphthalen-1-yl)-1H-pyrazolo[3,4-*d*]pyrimidin-4-amine (1.13f). A solution of dichloro[1,1'-bis(diphenylphosphino)ferrocene]palladium (II)-CH₂Cl₂ adduct (0.0098 g, 0.0100 mmol) in freshly distilled and degassed 1,4-dioxane was treated with 3-bromo-6-chloro-1-methyl-1H-pyrazolo[3,4-*d*]pyrimidin-4-amine (**1.7b**, 0.0500 g, 0.190 mmol) and Cs₂CO₃ (0.0900 g, 0.0300 mmol). The reaction mixture was stirred for 10 min and 1-naphthylboronic acid (0.0393 g, 0.230 mmol) was added. The solution was continuously degassed by purging with N₂ over the course of the addition of reagent. The vial was capped and the solution was stirred at 80 °C for 34 h and at 100 °C for an additional 12 h, and filtered through Celite. The filtrate was concentrated under reduced pressure and the residue was purified by chromatography on SiO₂ (hexanes/EtOAc, 2:1) to give a mixture of 6-chloro-1-methyl-3-(naphthalen-1-yl)-1H-pyrazolo[3,4-*d*]pyrimidin-4-amine and starting material (6:1, 0.0180 g) as an off-white solid.

A solution of this mixture (0.00420 g, 0.00857 mmol), 5% Pd/C (0.0819 g, 0.0300 mmol) and NH₄HCO₂ (0.0087 g, 0.140 mmol) in MeOH (1 mL) was stirred at rt for 10 min, purged with H₂ for 30 min and stirred under H₂ for 22 h. The reaction mixture was filtered through Celite, which was rinsed with CH₂Cl₂ (4 mL), and the combined filtrate was concentrated under reduced pressure. The crude residue was purified by chromatography on SiO₂ (hexanes/EtOAc, 6:1) to give **1.13f** (0.00370 g, 0.0133 mmol, 17 % (2 steps), 96% purity by LC-MS) as a colorless solid: Mp 210-212 °C; IR (neat) 3465, 3299, 3220, 2937, 1631, 1565, 1513, 1312, 1269 cm⁻¹; ¹H NMR (400 MHz, CDCl₃) δ 8.43 (s, 1 H), 8.01-7.92 (m, 3 H), 7.67-7.52 (m, 4 H), 5.11 (bs, 2 H), 4.16 (s, 3 H); ¹³C NMR (100 MHz, CDCl₃) δ 157.6, 156.2, 154.3, 142.4, 133.9, 131.5, 130.0, 129.8,

128.6, 128.4, 127.3, 126.6, 125.5, 125.3, 100.3, 34.0; HRMS (ESI) m/z calcd for $C_{16}H_{13}N_5$ ($[M+H]^+$) 276.1249, found 276.1242.

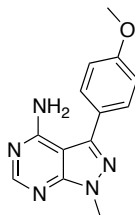


1.13g

***N*,1-Dimethyl-3-(naphthalen-1-yl)-1*H*-pyrazolo[3,4-*d*]pyrimidin-4-amine (1.13g).** A solution of $Pd_2(dba)_3$ (0.0176 g 0.0200 mmol) and PA-Ph (0.0087 g, 0.0300 mmol) in degassed 1,4-dioxane (1.7 mL) was stirred at rt for 10 min, treated with 3-bromo-6-chloro-*N*,1-dimethyl-1*H*-pyrazolo[3,4-*d*]pyrimidin-4-amine (**1.7a**, 0.0750 g, 0.270 mmol), Cs_2CO_3 (0.133 g, 0.410 mmol) and 1-naphthylboronic acid (0.0560 g, 0.330 mmol) and stirred in a pre-equilibrated oil bath at 100 °C for 25 h. The reaction mixture was filtered through Celite and the filtrate was concentrated under reduced pressure. The residue was purified by chromatography on SiO_2 (hexanes/EtOAc, 4:1) to give a mixture of 6-chloro-*N*,1-dimethyl-3-(naphthalen-1-yl)-1*H*-pyrazolo[3,4-*d*]pyrimidin-4-amine and starting material (10:1, 0.0340 g) as an off-white solid.

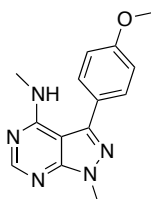
A solution of this mixture (0.0080 g, 0.0182 mmol), 10% Pd/C (0.0400 g, 0.0400 mmol) and NH_4HCO_2 (0.0093 g, 0.150 mmol) in MeOH (1 mL) was stirred at rt for 30 min, purged with H_2 for 15 min and stirred under H_2 for 27 h. The reaction mixture was filtered through Celite and the filtrate was concentrated under reduced pressure. The residue was purified by chromatography on SiO_2 (hexanes/EtOAc, 6:1) to give **1.13g** (0.00330 g, 0.0113 mmol, 18% (2 steps)) as a colorless solid: Mp 154.2-155.6 °C; IR (neat) 3438, 3045, 2939, 1599, 1569, 1312, 1269 cm^{-1} ; 1H NMR (400 MHz, $CDCl_3$) δ 8.51 (s, 1 H), 7.99 (dd, $J = 16.0, 8.0$ Hz, 2 H), 7.90 (d, $J = 8.0$ Hz, 2 H), 7.70-7.50 (m, 4 H), 4.76 (bs, 1 H), 4.15 (s, 3 H), 2.89 (d, $J = 4.8$ Hz, 3 H); ^{13}C NMR (100 MHz, $CDCl_3$) δ 157.5, 156.3, 153.7, 141.8, 134.0, 131.6, 130.3, 129.8, 128.5, 128.3,

127.2, 126.6, 125.5, 125.4, 100.5, 34.0, 27.7; HRMS (ESI) m/z calcd for $C_{17}H_{14}ClN_5$ ($[M+H]^+$) 290.1406, found 290.1385.



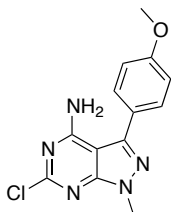
1.13h

3-(4-Methoxyphenyl)-1-methyl-1H-pyrazolo[3,4-*d*]pyrimidin-4-amine (1.13h). A mixture of 6-chloro-3-(4-methoxyphenyl)-1-methyl-1H-pyrazolo[3,4-*d*]pyrimidin-4-amine (**1.12h**, 0.0132 g, 0.0500 mmol), 5% Pd/C (0.162 g, 0.0700 mmol) and NH_4HCO_2 (0.0172 g, 0.270 mmol) in MeOH (3 mL) was stirred at rt for 10 min, purged with H_2 for 10 min and stirred under H_2 for 22 h. The reaction mixture was filtered through Celite, which was washed with CH_2Cl_2 (4 mL), and the combined filtrate was concentrated under reduced pressure. The residue was purified by chromatography on SiO_2 (hexanes/EtOAc, 6:1) to give **1.13h** (0.00435 g, 0.0170 mmol, 37 %, 100% purity by LC-MS) as a colorless solid: Mp 185-188 °C IR (neat) 3468, 3071, 2926, 2851, 1647, 1581, 1568, 1322, 1288, 1249, 1172 cm^{-1} ; 1H NMR (400 MHz, $CDCl_3$) δ 8.40 (s, 1 H), 7.62 (d, $J = 8.8$ Hz, 2 H), 7.06 (d, $J = 8.8$ Hz, 2 H), 5.48 (bs, 2 H), 4.07 (s, 3 H), 3.88 (s, 3 H); ^{13}C NMR (100 MHz, $CDCl_3$) δ 160.3, 157.8, 156.0, 154.5, 144.0, 129.7, 125.5, 114.8, 98.4, 55.4, 33.8; HRMS (ESI) m/z calcd for $C_{13}H_{13}N_5O$ ($[M+H]^+$) 256.1198, found 256.1181.



1.13i

3-(4-Methoxyphenyl)-*N*,1-dimethyl-1*H*-pyrazolo[3,4-*d*]pyrimidin-4-amine (1.13i). A mixture of 6-chloro-3-(4-methoxyphenyl)-*N*-methyl-1*H*-pyrazolo[3,4-*d*]pyrimidin-4-amine (**1.12i**, 0.0080 g, 0.0300 mmol), 10% Pd/C (0.0500 g, 0.100 mmol) and NH₄HCO₂ (0.0010 g, 0.160 mmol) in MeOH (0.8 mL) was stirred at rt for 30 min, purged with H₂ for 15 min and stirred under H₂ for 24 h. The reaction mixture was filtered through Celite and the filtrate was concentrated under reduced pressure. The residue was dissolved in EtOAc (1 mL), washed with H₂O (2 x 1 mL), dried (MgSO₄), and concentrated under reduced pressure. The crude residue was purified by chromatography on SiO₂ (hexanes/EtOAc, 1:2) to give **1.13i** (0.0053 g, 0.0196 mmol, 74%) as a colorless solid: Mp 110.2-111.6 °C; IR (neat) 3442, 2935, 1591, 1567, 1526, 1496, 1246 cm⁻¹; ¹H NMR (400 MHz, CDCl₃) δ 8.46 (s, 1 H) 7.56 (d, *J* = 8.4 Hz, 2 H), 7.06 (d, *J* = 8.4 Hz, 2 H), 5.37 (bs, 1 H), 4.05 (s, 3 H), 3.89 (s, 3 H), 3.09 (d, *J* = 4.8 Hz, 3 H); ¹³C NMR (100 MHz, CDCl₃) δ 160.2, 157.8, 156.0, 153.9, 143.5, 129.6, 125.8, 114.8, 98.6, 55.4, 33.7, 27.8; HRMS (ESI) *m/z* calcd for C₁₄H₁₄ClN₅O ([M+H]⁺) 270.1355, found 270.1351.

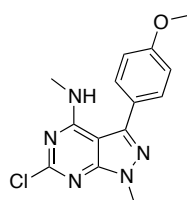


1.12h

6-Chloro-3-(4-methoxyphenyl)-1-methyl-1*H*-pyrazolo[3,4-*d*]pyrimidin-4-amine

(1.12h). A solution of dichloro[1,1'-bis(diphenylphosphino)ferrocene]palladium (II)-CH₂Cl₂ adduct (0.0099 g, 0.0100 mmol) in freshly distilled and degassed 1,4-dioxane (2 mL) was stirred for 10 min, treated with 3-bromo-6-chloro-1-methyl-1*H*-pyrazolo[3,4-*d*]pyrimidin-4-amine (**1.7b**, 0.0500 g, 0.190 mmol), Cs₂CO₃ (0.0900 g, 0.290 mmol), and 4-methoxybenzeneboronic acid (0.0350 g, 0.230 mmol) and stirred at 80 °C for 20 h and at 100 °C for an additional 4 h.

The reaction mixture was filtered through Celite and the filtrate was concentrated under reduced pressure. The residue was purified by chromatography on SiO₂ (hexanes/EtOAc, 1:1) to give **1.12h** (0.0137 g, 0.0473 mmol, 25%) as a colorless solid: Mp >250 °C; IR (neat) 3465, 3288, 3070, 3001, 2835, 1648, 1586, 1504, 1450, 1251, 1038 cm⁻¹; ¹H NMR (400 MHz, CDCl₃) δ 7.59 (d, *J* = 8.4 Hz, 2 H), 7.06 (d, *J* = 8.4 Hz, 2 H), 5.72 (bs, 2 H), 4.03 (s, 3 H), 3.88 (s, 3 H); ¹³C NMR (100 MHz, CDCl₃) δ 160.5, 158.2, 157.9, 155.6, 144.4, 129.5, 124.9, 114.9, 97.1, 55.4, 34.1; HRMS (ESI) *m/z* calcd for C₁₃H₁₂ClN₅O ([M+H]⁺) 290.0809, found 290.0799.

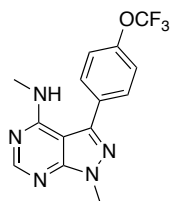


1.12i

6-Chloro-3-(4-methoxyphenyl)-*N*,1-dimethyl-1*H*-pyrazolo[3,4-*d*]pyrimidin-4-amine

(1.12i). A solution of Pd₂(dba)₃ (0.0176 g 0.0200 mmol) and PA-Ph (0.0079 g, 0.0300 mmol) in degassed 1,4-dioxane (1 mL) was stirred for 10 min, treated with 3-bromo-6-chloro-*N*,1-dimethyl-1*H*-pyrazolo[3,4-*d*]pyrimidin-4-amine (**1.7a**, 0.0748 g, 0.270 mmol), Cs₂CO₃ (0.133 g, 0.410 mmol) and 4-methoxybenzeneboronic acid (0.0390 g 0.270 mmol), and stirred at 50 °C for 24 h. The reaction mixture was filtered through Celite and the filtrate was concentrated under reduced pressure. The crude residue was purified by preparative TLC on SiO₂ (hexanes/EtOAc, 3:7) to give **1.12i** (0.0284 g, 0.0935 mmol, 35%, 100% purity by LC-MS) as a colorless solid: Mp 159.3-160.9 °C; IR (neat) 3349, 2957, 1601, 1569, 1496, 1246, 1209, 1172 cm⁻¹; ¹H NMR (400 MHz, CDCl₃) δ 7.54 (d, *J* = 8.8 Hz, 2 H), 7.06 (d, *J* = 8.8 Hz, 2 H), 5.51 (bs, 1 H), 4.01 (s, 3 H), 3.89 (s, 3 H), 3.09 (d, *J* = 4.8 Hz, 3 H); ¹³C NMR (100 MHz, CDCl₃) δ 160.3, 158.2, 157.9,

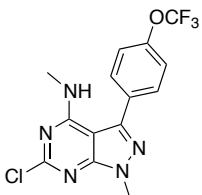
154.8, 143.6, 129.4, 125.1, 114.8, 97.2, 55.3, 33.8, 27.9; HRMS (ESI) m/z calcd for $C_{14}H_{14}ClN_5O$ ($[M+H]^+$) 304.0965, found 304.0974.



1.13j

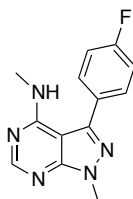
N,1-Dimethyl-3-(4-(trifluoromethoxy)phenyl)-1*H*-pyrazolo[3,4-*d*]pyrimidin-4-amine

(11). A solution of 6-chloro-*N*,1-dimethyl-3-(4-(trifluoromethoxy)phenyl)-1*H*-pyrazolo[3,4-*d*]pyrimidin-4-amine (**1.12j**, 0.0081 g, 0.0200 mmol), 5% Pd/C (0.0800 g, 0.0300 mmol) and NH_4HCO_2 (0.0085 g, 0.140 mmol) in MeOH (2 mL) was stirred at rt for 30 min, purged with H_2 for 15 min and stirred under H_2 for 19 h. The reaction mixture was filtered through Celite and the filtrate was concentrated under reduced pressure. The residue was dissolved in EtOAc (1 mL), washed with H_2O (2 x 1 mL), dried ($MgSO_4$) and concentrated under reduced pressure. The crude residue was purified by chromatography on SiO_2 (hexanes/EtOAc, 6:1) to give **1.13j** (0.00651 g, 0.0201 mmol, 89%, 91% purity by LC-MS) as a colorless solid: Mp 101.5-103.3 °C; IR (neat) 3452, 2943, 1592, 1568, 1249, 1219, 1204, 1161, 1103 cm^{-1} ; 1H NMR (400 MHz, $CDCl_3$) δ 8.49 (s, 1 H), 7.69 (d, $J = 8.4$ Hz, 2 H), 7.39 (d, $J = 8.4$ Hz, 2 H), 5.25 (bd, $J = 2.4$ Hz, 1 H), 4.10 (s, 3 H), 3.12 (d, $J = 5.2$ Hz, 3 H); ^{13}C NMR (100 MHz, $CDCl_3$) δ 157.6, 156.1, 154.1, 149.7, 142.1, 132.6, 129.9, 129.4, 128.4, 121.8, 120.4 (q, $J_{CF} = 257$ Hz), 98.6, 33.9, 28.0; HRMS (ESI) m/z calcd for $C_{14}H_{11}ClF_3N_5O$ ($[M-H]^-$) 324.1072, found 324.1078.



1.12j

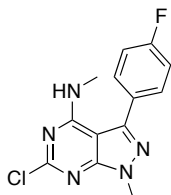
6-Chloro-*N*,1-dimethyl-3-(4-(trifluoromethoxy)phenyl)-1*H*-pyrazolo[3,4-*d*]pyrimidin-4-amine (1.12j). A solution of Pd₂(dba)₃ (0.0176 g, 0.0200 mmol) and dppf (0.0090 g, 0.0160 mmol) in freshly distilled and degassed 1,4-dioxane (1.7 mL) was stirred for 10 min, treated with 3-bromo-6-chloro-*N*,1-dimethyl-1*H*-pyrazolo[3,4-*d*]pyrimidin-4-amine (**1.7a**, 0.0750 g, 0.270 mmol), Cs₂CO₃ (0.133 g, 0.410 mmol), and 4-trifluoromethoxybenzeneboronic acid (0.0670 g, 0.330 mmol), and stirred at 100 °C for 2 d, filtered through Celite, and the filtrate was concentrated under reduced pressure. The crude residue was purified by chromatography on SiO₂ (hexanes/EtOAc, 4:1) to give **1.12j** (0.0270 g, 0.0753 mmol, 28%, 100% purity by LC-MS) as a colorless solid: Mp 115.3-119.1 °C; IR (neat) 3444, 2944, 1593, 1567, 1246, 1202, 1155 cm⁻¹; ¹H NMR (400 MHz, CDCl₃) δ 7.66 (d, *J* = 8.4 Hz, 2 H), 7.38 (d, *J* = 8.4 Hz, 2 H), 5.40 (bs, 1 H), 4.00 (s, 3 H), 3.11 (d, *J* = 4.8 Hz, 3 H); ¹³C NMR (100 MHz, CDCl₃) δ 158.5, 157.9, 155.2, 149.9, 142.4, 131.7, 129.8, 121.7, 120.4 (q, *J*_{CF} = 257 Hz), 97.3, 34.1, 28.2; HRMS (ESI) *m/z* calcd for C₁₄H₁₁ClF₃N₅O ([M-H]⁻) 356.0526, found 356.0521.



1.13k

3-(4-Fluorophenyl)-*N*,1-dimethyl-1*H*-pyrazolo[3,4-*d*]pyrimidin-4-amine (1.13k). A solution of 6-chloro-3-(4-fluorophenyl)-*N*-methyl-1*H*-pyrazolo[3,4-*d*]pyrimidin-4-amine (**1.12k**, 0.0120 g, 0.0400 mmol), 10% Pd/C (0.0580 g, 0.0490 mmol) and NH₄HCO₂ (0.0053 g, 0.0800 mmol) in MeOH (1 mL) was stirred at rt for 30 min, purged with H₂ for 15 min and stirred under

an atmosphere of H₂ (balloon) for 24 h. The reaction mixture was filtered through Celite and the filtrate was concentrated under reduced pressure. The residue was dissolved in EtOAc (1 mL), washed with H₂O (2 x 1 mL), dried (MgSO₄), filtered, and concentrated under reduced pressure. The crude residue was purified by chromatography on SiO₂ (hexanes/EtOAc, 1:1 to 1:4) to give **1n** (0.0080 g, 0.0311 mmol, 76%, 96% purity by LC-MS) as a colorless solid: Mp 111.8-114.5 °C; IR (neat) 3446, 2941, 1588, 1567, 1522, 1494, 1312, 1265, 1220 cm⁻¹; ¹H NMR (400 MHz, CDCl₃) δ 8.47 (s, 1 H), 7.62 (dd, *J* = 8.4, 5.2 Hz, 2 H), 7.23 (t, *J* = 8.4 Hz, 2 H), 5.26 (bs, 1 H), 4.06 (s, 3 H), 3.10 (d, *J* = 4.8 Hz, 3 H); ¹³C NMR (100 MHz, CDCl₃) δ 163.2 (d, *J*_{CF} = 248 Hz), 157.6, 156.1, 154.0, 142.6, 130.2 (d, *J*_{CF} = 8.2 Hz), 129.2 (d, *J*_{CF} = 3.2 Hz), 116.4 (d, *J*_{CF} = 22 Hz), 98.6, 33.8, 27.9; HRMS (ESI) *m/z* calcd for C₁₃H₁₂FN₅ ([M+H]⁺) 258.1155, found 258.1150.

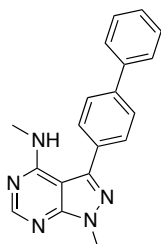


1.12k

6-Chloro-3-(4-fluorophenyl)-*N*,1-dimethyl-1*H*-pyrazolo[3,4-*d*]pyrimidin-4-amine

(1.12k). A solution of Pd₂(dba)₃ (0.0176 g, 0.0200 mmol) and PA-Ph (0.0079 g, 0.0300 mmol) in 1,4-dioxane (1 mL) was stirred for 10 min, treated with 3-bromo-6-chloro-*N*,1-dimethyl-1*H*-pyrazolo[3,4-*d*]pyrimidin-4-amine (**1.7a**, 0.0748 g, 0.270 mmol), Cs₂CO₃ (0.133 g, 0.410 mmol) and 4-fluorobenzeneboronic acid (0.0420 g, 0.300 mmol), and stirred at 60 °C for 22 h and at 100 °C for an additional 4 h. The reaction mixture was filtered through Celite and the filtrate was concentrated under reduced pressure. The crude residue was purified by chromatography on SiO₂ (hexanes/EtOAc, 5:1) to give **1.12k** (0.0210 g, 0.0734 mmol, 27%, 100% purity by LC-MS) as a

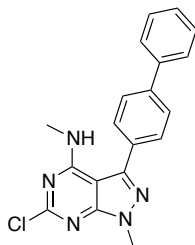
colorless solid: Mp 189.9-192.3 °C; IR (neat) 3438, 2943, 1597, 1569, 1526, 1493, 1347, 1260 cm^{-1} ; ^1H NMR (400 MHz, CDCl_3) δ 7.60 (dd, $J = 8.4, 5.6$ Hz, 2 H), 7.20-7.30 (m, 2 H), 5.40 (bs, 1 H), 4.02 (s, 3 H), 3.11 (d, $J = 4.8$ Hz, 3 H); ^{13}C NMR (100 MHz, CDCl_3) δ 163.4 (d, $J_{\text{CF}} = 248$ Hz), 158.5, 158.0, 155.1, 142.9, 130.2 (d, $J_{\text{CF}} = 8.2$ Hz), 129.2 (d, $J_{\text{CF}} = 3.4$ Hz), 116.7 (d, $J_{\text{CF}} = 21.4$ Hz), 97.4, 34.1, 28.2; HRMS (ESI) m/z calcd for $\text{C}_{13}\text{H}_{11}\text{ClFN}_5$ ($[\text{M}+\text{H}]^+$) 292.0765, found 292.0788.



1.131

3-([1,1'-Biphenyl]-4-yl)-N,1-dimethyl-1H-pyrazolo[3,4-d]pyrimidin-4-amine (1.131).

A solution of 3-([1,1'-biphenyl]-4-yl)-6-chloro-N,1-dimethyl-1H-pyrazolo[3,4-d]pyrimidin-4-amine (**1.121**, 0.0200 g, 0.0500 mmol), 10% Pd/C (0.0850 g, 0.0725 mmol) and NH_4HCO_2 (0.0183 g, 0.290 mmol) in MeOH (2 mL) was stirred at rt for 30 min, purged with H_2 for 30 min and stirred under H_2 for 22 h. The reaction mixture was filtered through Celite and the filtrate was concentrated under reduced pressure. The crude residue was purified by chromatography on SiO_2 (hexanes/EtOAc, 6:1) to give **1.131** (0.0128 g, 0.0404 mmol, 84%, 100% purity by LC-MS) as a colorless solid: Mp 190.8-192.3 °C; IR (neat) 3439, 3027, 2937, 1590, 1566, 1487, 1264 cm^{-1} ; ^1H NMR (400 MHz, CDCl_3) δ 8.49 (s, 1 H), 7.78-7.71 (m, 4 H), 7.66 (d, $J = 7.6$ Hz, 2 H), 7.49 (t, $J = 7.6$ Hz, 2 H), 7.40 (t, $J = 7.2$ Hz, 1 H), 5.46 (bd, $J = 4.0$ Hz, 1 H), 4.08 (s, 3 H), 3.12 (d, $J = 4.8$ Hz, 3 H); ^{13}C NMR (100 MHz, CDCl_3) δ 157.7, 156.0, 154.0, 143.3, 141.8, 140.1, 132.4, 128.9, 128.7, 128.0, 127.8, 127.1, 98.7, 33.8, 27.9; HRMS (ESI) m/z calcd for $\text{C}_{13}\text{H}_{11}\text{ClFN}_5$ ($[\text{M}+\text{H}]^+$) 316.1562, found 316.1571.

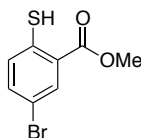


1.12I

3-([1,1'-Biphenyl]-4-yl)-6-chloro-*N*,1-dimethyl-1*H*-pyrazolo[3,4-*d*]pyrimidin-4-amine (1.12I). A solution of Pd₂(dba)₃ (0.0176 mg, 0.0200 mmol) and dppf (0.0098 g, 0.0160 mmol) in distilled and degassed 1,4-dioxane (1.7 mL) was stirred for 10 min, treated with 3-bromo-6-chloro-*N*,1-dimethyl-1*H*-pyrazolo[3,4-*d*]pyrimidin-4-amine (**1.7a**, 0.0750 g, 0.270 mmol), Cs₂CO₃ (0.133 g, 0.410 mmol) and 4-phenylbenzeneboronic acid (0.0640 g, 0.330 mmol), and stirred at 100 °C for 21 h. The reaction mixture was filtered through Celite and the filtrate was concentrated under reduced pressure. The crude residue was purified by chromatography on SiO₂ (hexanes/EtOAc, 4:1) to give **1.12I** (0.0470 g, 0.136 mmol, 50%) as a colorless solid: Mp 211.9-213.8 °C; IR (neat) 3435, 3058, 1593, 1569, 1485, 1347, 1260 cm⁻¹; ¹H NMR (400 MHz, CDCl₃) δ 7.77-7.66 (m, 4 H), 7.65 (d, *J* = 7.6 Hz, 2 H), 7.48 (t, *J* = 7.2 Hz, 2 H), 7.40 (t, *J* = 7.2 Hz, 1 H), 5.61 (bs, 1 H), 4.02 (s, 3 H), 3.11 (d, *J* = 6.0 Hz, 3 H); ¹³C NMR (100 MHz, CDCl₃) δ 158.4, 158.0, 155.1, 143.6, 142.0, 139.9, 131.8, 128.9, 128.6, 128.1, 127.8, 127.0, 97.3, 34.0, 28.1; HRMS (ESI) *m/z* calcd for C₁₉H₁₆ClN₅ (M-H)⁻ 350.1172, found 350.1165.

5.3 CHAPTER 2 EXPERIMENTAL PART

5.3.1 Synthesis of Thiazocine Inhibitor 2.15

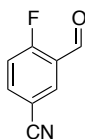


2.19

Methyl 5-bromo-2-mercaptobenzoate (2.19).²⁷³⁻²⁷⁴ To a cooled (0-5 °C) stirring solution of 2-amino-5-bromobenzoic acid (**2.18**, 1.00 g, 4.49 mmol), NaOH (0.180 g, 4.49 mmol), and NaNO₂ (0.310 g, 4.49 mmol) in H₂O (6 mL) was slowly treated with a solution of concentrated HCl (12.4 mL) in H₂O (21.5 mL). The resulting mixture was stirred at 0 °C for 1 h, and then neutralized with potassium acetate (1.47 g). This solution was added to a solution of potassium O-ethylxanthate (2.23 g, 13.6 mmol) in H₂O (6 mL) which was preheated to 90 °C. The mixture was stirred at the same temperature for 30 min, cooled to 0 °C and acidified with conc. HCl. The aqueous phase was decanted from the resulting semisolid sludge. This was dissolved in 10% aqueous NaOH (5 mL), and heated to 85 °C for 2 h. To this mixture was added portionwise NaHSO₃ (0.42 g), and the mixture was heated to 85 °C for 10 min. The mixture was filtered, cooled to 0 °C, and acidified with conc. HCl. The precipitate was collected by filtration and washed with H₂O. The moist cake was dissolved in THF/EtOAc, washed with brine, dried (Na₂SO₄), and concentrated under reduced pressure to give crude product as a yellow solid. This material was used for the next reaction without further purification.

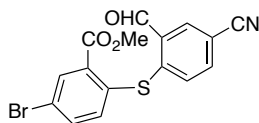
A mixture of crude 5-bromo-2-mercaptobenzoic acid (1.05 g, 4.49 mmol) and conc. H₂SO₄ (0.45 mL) in MeOH (10 mL) was heated to reflux for 16 h, concentrated under reduced

pressure, diluted with ice-H₂O, and extracted with EtOAc. The combined organic layers were washed with brine, dried (Na₂SO₄), and concentrated under reduced pressure. The crude residue was purified by chromatography on SiO₂ (hexanes:EtOAc, 10:1) to give **2.19** (0.338 g, 1.37 mmol, 31%) as a yellow solid: ¹H NMR (300 MHz, CDCl₃) δ 8.12 (d, *J* = 2.1 Hz, 1 H), 7.41 (dd, *J* = 8.6, 2.1 Hz, 1 H), 7.18 (d, *J* = 8.6 Hz, 1 H), 4.80 (s, 1 H), 3.93 (s, 3 H); ¹³C NMR (75 MHz, CDCl₃) δ 166.0, 137.5, 135.2, 134.3, 132.1, 127.2, 117.7, 52.5.



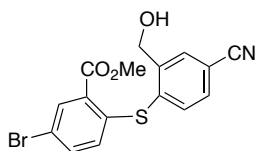
2.20

4-Fluoro-3-formylbenzonitrile (2.20).⁴⁷⁷ A solution of 5-bromo-2-fluorobenzaldehyde (4.00 g, 19.3 mmol) in DMF (4 mL) was treated with CuCN (2.10 g, 23.2 mmol) and the mixture was heated at 100 °C for 2 h, and at 130 °C for 18 h. The mixture was cooled to rt, treated with a solution of FeCl₃ (13.0 g) in conc. HCl (4 mL) and H₂O (16 mL). The mixture was heated at 70-80 °C for 20 min. The aqueous layer was extracted with CH₂Cl₂ (3 x 80 mL). The combined organic layers were washed with brine, dried (Na₂SO₄), filtered, and concentrated under reduced pressure. The crude residue was purified by chromatography on SiO₂ (hexanes/EtOAc, 9:1) to give **2.20** (1.52 g, 10.2 mmol, 53%) as a colorless solid: ¹H NMR (400 MHz, CDCl₃) δ 10.34 (s, 1 H), 8.19 (d, *J* = 6.0 Hz, 1 H), 7.90 (m, 1 H), 7.35 (t, *J* = 9.0 Hz, 1 H); ¹³C NMR (100 MHz, CDCl₃) δ 184.7 (d, *J*_{CF} = 6.0 Hz), 167.5 (d, *J*_{CF} = 266.0 Hz), 139.4 (d, *J*_{CF} = 11.0 Hz), 133.4 (d, *J*_{CF} = 3.0 Hz), 124.8 (d, *J*_{CF} = 9.0 Hz), 118.3 (d, *J*_{CF} = 22.0 Hz), 116.7, 109.7 (d, *J*_{CF} = 4.0 Hz).



2.21

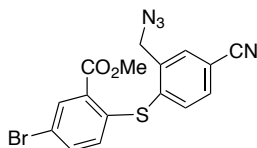
Methyl 5-bromo-2-((4-cyano-2-formylphenyl)thio)benzoate (2.21) A solution of methyl 5-bromo-2-mercaptobenzoate (**2.19**, 1.68 g, 6.80 mmol) and 5-cyano-2-fluorobenzaldehyde (**2.20**, 0.940 g, 6.18 mmol) in DMF (24 mL) was treated with K₂CO₃ (1.28 g, 9.27 mmol) and the reaction was heated to 90 °C for 3 d, cooled to rt, poured onto a mixture of EtOAc (150 mL) and H₂O (150 mL) and the mixture was extracted with EtOAc (2 x 100 mL). The combined organic layers were washed with brine, dried (Na₂SO₄), filtered, and concentrated under reduced pressure. The crude residue was purified by chromatography on SiO₂ (hexanes/EtOAc, 9:1 to hexanes/EtOAc, 4:1) to give **2.21** (1.51 g, 4.01 mmol, 65%) as a light yellow solid: Mp 108-110 °C; IR (neat) 3115, 3083, 3070, 3059, 2945, 2837, 2227, 1739, 1672, 1596, 1569, 1534, 1458, 1430, 1282, 1221 cm⁻¹; ¹H NMR (300 MHz, CDCl₃) δ 10.31 (s, 1 H), 8.18 (d, *J* = 1.8 Hz, 1 H), 8.13 (d, *J* = 2.2 Hz, 1 H), 7.68 (dd, *J* = 8.4, 1.8 Hz, 1 H), 7.57 (dd, *J* = 8.4, 2.1 Hz, 1 H), 7.27 (d, *J* = 8.4 Hz, 1 H), 7.06 (d, *J* = 8.4 Hz, 1 H), 3.88 (s, 3 H); ¹³C NMR (75 MHz, CDCl₃) δ 189.2, 165.2, 145.6, 136.2, 135.9, 135.0, 134.9, 134.5, 134.3, 133.9, 133.5, 132.8, 122.4, 111.4, 52.8; HRMS (ESI) *m/z* calcd for C₁₆H₁₁BrNO₃S ([M+H]⁺) 375.9643, found 375.9668. Note: characterization was taken from Dr. Igor Opsenica's final postdoctoral research report.



2.22

Methyl 5-bromo-2-((4-cyano-2-(hydroxymethyl)phenyl)thio)benzoate (2.22). To a stirred solution of methyl 5-bromo-2-((4-cyano-2-formylphenyl)thio)benzoate (**2.21**, 1.40 g, 3.72 mmol) in dry MeOH (60 mL) was added NaBH₄ (0.154 g, 4.09 mmol) and the mixture was stirred at rt for 30 min where analysis by TLC (hexanes/EtOAc, 7:3) indicated the starting

material had been consumed. The reaction was concentrated under reduced pressure, and the residue was diluted with EtOAc (80 mL) and 10% HCl aq. (15 mL), and the aqueous layer was extracted with EtOAc (80 mL). The combined organic layers were washed with brine, dried (Na₂SO₄), filtered, and concentrated under reduced pressure. The residue was triturated with Et₂O to give **2.22** (1.39 g, 3.67 mmol, 99%) as a colorless solid: Mp 76-77 °C; IR (neat) 3515, 3088, 2945, 2235, 1711, 1456, 1446, 1301, 1236 cm⁻¹; ¹H NMR (400 MHz, CDCl₃) δ 8.18 (d, *J* = 2.2 Hz, 1 H), 7.94 (s, 1 H), 7.56 (dd, *J* = 8.0, 1.6 Hz, 1 H), 7.47 (d, *J* = 8.0 Hz, 1 H), 7.41 (dd, *J* = 8.6, 2.2 Hz, 1 H), 6.64 (d, *J* = 8.6 Hz, 1 H), 4.77 (s, 2 H), 3.92 (s, 3 H); ¹³C NMR (100 MHz, CDCl₃) δ 165.4, 145.1, 138.0, 136.8, 135.6, 135.5, 134.2, 131.6, 131.3, 130.1, 129.8, 119.7, 118.2, 113.1, 62.1, 52.7; HRMS (ESI) *m/z* calcd for C₁₆H₁₃BrNO₃S ([M+H]⁺) 377.9800, found 377.9820. Note: characterization was taken from Dr. Igor Opsenica's final postdoctoral research report.

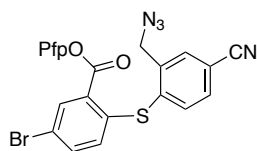


2.23

Methyl 2-((2-(azidomethyl)-4-cyanophenyl)thio)-5-bromobenzoate (2.23). To a solution of methyl 5-bromo-2-((4-cyano-2-(hydroxymethyl)phenyl)thio)benzoate (**2.22**, 1.00 g, 2.64 mmol) in CH₂Cl₂ (30 mL) under Ar at 0 °C was added Et₃N (0.56 mL, 3.97 mmol) and MsCl (0.23 mL, 2.91 mmol). The cooling bath was removed and the solution was stirred at rt for 2 h. The reaction mixture was poured into CH₂Cl₂ (40 mL) washed with H₂O (10 mL), dried (Na₂SO₄), and concentrated under reduced pressure to give the mesylate as a crude intermediate.

A mixture of the above crude mesylate and sodium azide (0.868 g, 13.2 mmol) in DMF (10 mL) under an Ar atmosphere was stirred at rt for 3 h, poured onto EtOAc (100 mL), washed

with H₂O (30 mL) and brine, dried (Na₂SO₄) and concentrated under reduced pressure to give **2.23** (1.01 g, 2.51 mmol, 95%) as a tan solid: Mp 121-122 °C; IR (neat) 3096, 3070, 3001, 2950, 2240, 2127, 2089, 1704, 1450, 1437, 1295, 1243 cm⁻¹; ¹H NMR (400 MHz, CDCl₃) δ 8.15 (d, *J* = 2.4 Hz, 1 H), 7.82 (s, 1 H), 7.61 (dd, *J* = 8.0, 2.0 Hz, 1 H), 7.53 (d, *J* = 8.0 Hz, 1 H), 7.44 (dd, *J* = 8.4, 2.4 Hz, 1 H), 6.64 (d, *J* = 8.4 Hz, 1 H), 4.58 (s, 2 H), 3.94 (s, 3 H); ¹³C NMR (100 MHz, CDCl₃) δ 165.3, 140.1, 138.4, 137.5, 135.8, 135.7, 134.3, 132.4, 132.3, 130.2, 130.1, 120.0, 117.8, 113.2, 52.7, 52.0; HRMS (ESI) *m/z* calcd for C₁₆H₁₂BrN₄O₂S ([M+H]⁺) 402.9864, found 402.9897. Note: characterization was taken from Dr. Igor Opsenica's final postdoctoral research report.

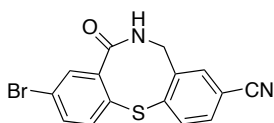


2.24

Perfluorophenyl 2-((2-(azidomethyl)-4-cyanophenyl)thio)-5-bromobenzoate (2.24) A solution of methyl 2-((2-(azidomethyl)-4-cyanophenyl)thio)-5-bromobenzoate (**2.23**, 0.800 g, 1.98 mmol) in MeOH (20 mL) and THF (20 mL) was treated with 1 M aqueous NaOH (18 mL). The solution was stirred for 5 h at rt, concentrated under reduced pressure and acidified to pH 2 with 1 M aqueous HCl, extracted with EtOAc (100 mL), dried (Na₂SO₄), and concentrated under reduced pressure to give crude 2-((2-(azidomethyl)-4-cyanophenyl)thio)-5-bromobenzoic acid that was used in next reaction without purification.

A solution of 2-((2-(azidomethyl)-4-cyanophenyl)thio)-5-bromobenzoic acid (0.700 g, 1.80 mmol) in CH₂Cl₂ (60 mL) was treated with Pfp-OH (0.331 g, 1.80 mmol), EDCI (0.518 g, 2.70 mmol) and DMAP (0.0220 g, 0.180 mmol) at 0 °C. The mixture was warmed at rt for 2.5 h, poured onto H₂O (50 mL), and extracted with CH₂Cl₂ (2 x 100 mL). The combined organic

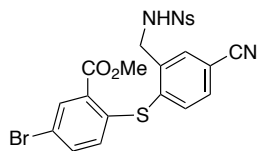
layers were washed with Brine, dried (Na_2SO_4), and concentrated under reduced pressure. The crude residue was purified by chromatography on SiO_2 (hexanes/EtOAc, 9:1) to give **2.24** (0.619 g, 1.12 mmol, 56% (2 steps)) as a colorless solid: Mp 160-163 °C; IR (neat) 3089, 2938, 2235, 2103, 1750, 1517, 1454, 1214 cm^{-1} ; ^1H NMR (400 MHz, CDCl_3) δ 8.41 (d, $J = 2.0$ Hz, 1 H), 7.85 (s, 1 H), 7.66 (dd, $J = 8.0, 2.0$ Hz, 1 H), 7.59-7.56 (m, 2 H), 6.71 (d, $J = 8.4$ Hz, 1 H), 4.59 (s, 2 H); ^{13}C NMR (100 MHz, CDCl_3) δ 160.5, 142.2 (m, C-F coupling), 140.9 (m, C-F coupling), 140.6, 140.2 (m, C-F coupling), 140.1, 139.0 (C-F coupling), 137.4, 137.2, 137.0 (m, C-F coupling), 136.2, 135.3, 132.6, 132.5, 130.3, 126.2, 124.7 (m, C-F coupling), 120.1, 117.6, 113.9, 52.0; HRMS (ESI) m/z calcd for $\text{C}_{21}\text{H}_9\text{BrF}_5\text{N}_4\text{O}_2\text{S}$ ($[\text{M}+\text{H}]^+$) 554.9550, found 554.9534. Note: characterization was taken from Dr. Igor Opsenica's final postdoctoral research report.



2.17

9-Bromo-7-oxo-6,7-dihydro-5H-dibenzo[*b,g*][1,5]thiazocine-3-carbonitrile (2.17). A solution of perfluorophenyl 2-((2-(azidomethyl)-4-cyanophenyl)thio)-5-bromobenzoate (**2.24**, 0.500 g, 0.900 mmol) in MeCN (48 mL) and H_2O (12 mL) was treated with PPh_3 (0.286 g, 1.08 mmol) at rt. The mixture was stirred at 50 °C for 20 h. During reaction a precipitate formed. The reaction mixture was concentrated under reduced pressure and filtered. The solid was washed with CH_2Cl_2 and acetone. The solid by NMR still contained trace PPh_3 oxide and was sonicated in acetone and decanted several times to give **2.17** (0.212 g, 0.614 mmol, 68%) as a colorless solid: Mp >250 °C; IR (neat) 3309, 3227, 3102, 2228, 1661, 1469, 1447, 1404, 1342 cm^{-1} ; ^1H NMR (400 MHz, DMSO-d_6) δ 8.46 (t, $J = 6.8$ Hz, 1 H), 7.81-7.72 (m, 4 H), 7.68-7.63 (m, 2 H), 4.20-4.10 (m, 2 H); ^{13}C NMR (100 MHz, DMSO-d_6) δ 169.7, 144.3, 139.4, 138.0, 137.2, 134.5,

134.1, 131.7, 130.7, 130.1, 125.3, 123.6, 118.2, 109.6, 45.0; HRMS (ESI) m/z calcd for $C_{15}H_{10}BrN_2OS$ ($[M+H]^+$) 344.9697, found 344.9669. Note: characterization was taken from Dr. Igor Opsenica's final postdoctoral research report.



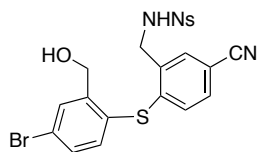
2.26

Methyl

5-bromo-2-((4-cyano-2-((4-

nitrophenylsulfonamido)methyl)phenyl)thio)benzoate (2.26). A solution of methyl 5-bromo-2-((4-cyano-2-formylphenyl)thio)benzoate (**2.21**, 0.500 g, 1.33 mmol) in absolute EtOH (10 mL) was treated titanium(IV)isopropoxide (2.45 mL, 7.97 mmol), 4-nitrobenzenesulfonamide (0.537 g, 2.66 mmol), Et₃N (0.37 mL, 2.66 mmol) and stirred at rt for 13 h. NaBH₄ (0.101 g, 2.66 mmol) was added and the mixture stirred for additional 2 h at rt, diluted with aqueous ammonium hydroxide (5 mL). The resulting inorganic precipitate was removed by filtration, washed with EtOAc (50 mL) and H₂O (10 mL). The organic layer was separated washed with 1 M aqueous HCl, brine, dried (Na₂SO₄), filtered, and concentrated under reduced pressure. The crude residue was purified by chromatography on SiO₂ (hexanes/EtOAc, 2:1) to give **2.26** (0.455 g, 0.808 mmol, 61%) as a colorless solid: Mp 138.7-141.5 °C; IR (neat) 3312, 3103, 2952, 2229, 1709, 1527, 1340, 1303, 1247, 1171, 1159, 818, 734 cm⁻¹; ¹H NMR (400 MHz, CDCl₃) δ 8.29 (dd, $J = 2.2, 9.2$ Hz, 2 H), 8.12 (d, $J = 2.4$ Hz, 1 H), 7.95 (dd, $J = 2.2, 9.2$ Hz, 2 H), 7.73 (d, $J = 1.8$ Hz, 1 H), 7.52 (dd, $J = 1.8, 8.4$ Hz, 1 H), 7.49 (dd, $J = 1.8, 8.4$ Hz, 1 H), 7.34 (d, $J = 7.8$ Hz, 1 H), 6.73 (d, $J = 7.8$ Hz, 1 H), 5.52 (bt, $J = 6.2$ Hz, 1 H), 4.28 (d, $J = 6.2$ Hz, 2 H), 3.91 (s, 3 H); ¹³C NMR (100 MHz, CDCl₃) δ 165.2, 150.1, 145.5, 139.4, 139.3, 136.2, 135.9, 134.8, 134.6,

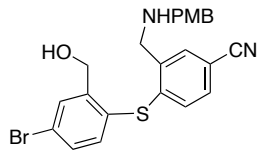
133.5, 132.5, 131.6, 130.4, 128.3, 124.3, 120.9, 117.5, 112.9, 52.9, 45.1; HRMS (ESI) m/z calcd for $C_{22}H_{16}N_3O_6BrS_2$ ($[M+Na]^+$) 583.9562, found 583.9558.



2.27

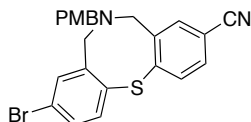
N-(2-((4-Bromo-2-(hydroxymethyl)phenyl)thio)-5-cyanobenzyl)-4-

nitrobenzenesulfonamide (2.27) A solution of methyl 5-bromo-2-((4-cyano-2-((4-nitrophenylsulfonamido)methyl)phenyl)thio)benzoate (**2.26**, 0.250 g, 0.445 mmol) in dry THF (16 mL) was treated with $NaBH_4$ (0.168 g, 4.45 mmol) and the mixture was refluxed for 30 min followed by the addition of MeOH (8 mL) and the solution was refluxed for 25 h, cooled to rt, and concentrated under reduced pressure. The residue was diluted with EtOAc (50 mL) and washed with 10% HCl aq. (10 mL). The aqueous layer was extracted with EtOAc (50 mL). The combined organic layers were washed with brine, dried (Na_2SO_4) and concentrated under reduced pressure. The crude residue was purified by chromatography on SiO_2 (hexanes/EtOAc, 2:1) to give **2.27** (0.110 g, 0.207 mmol, 47%) as a colorless amorphous solid: IR (neat) 3525, 3320, 3142, 2928, 2229, 1685, 1596, 1528, 1411, 1348, 1142, 1090, 1033, 736 cm^{-1} ; 1H NMR (400 MHz, $CDCl_3$) δ 8.31 (d, $J = 8.8$ Hz, 2 H), 8.01 (d, $J = 8.8$ Hz, 2 H), 7.74 (d, $J = 1.8$ Hz, 1 H), 7.56 (d, $J = 1.8$ Hz, 1 H), 7.46 (dd, $J = 1.8, 8.4$ Hz, 1 H), 7.49 (dd, $J = 1.8, 8.4$ Hz, 1 H), 7.32 (dd, $J = 1.8, 8.4$ Hz, 1 H), 7.19 (d, $J = 8.2$ Hz, 1 H), 6.77 (d, $J = 8.2$ Hz, 1 H), 5.30 (bt, $J = 6.2$ Hz, 1 H), 4.60 (s, 2 H), 4.30 (d, $J = 6.2$ Hz, 2 H); ^{13}C NMR (100 MHz, $CDCl_3$) δ 150.1, 145.5, 145.4, 142.4, 136.9, 135.0, 132.7, 132.3 (2 C), 132.1, 128.5, 128.3, 127.0, 125.1, 124.4, 118.0, 109.7, 62.5, 44.7; HRMS (ESI) m/z calcd for $C_{21}H_{16}N_3O_5BrS_2$ ($[M]^+$) 534.9694, found 534.9688.



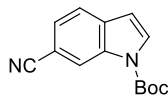
2.29

4-((4-Bromo-2-(hydroxymethyl)phenyl)thio)-3-(((4-methoxybenzyl)amino)methyl)benzonitrile (2.29) A solution of methyl 5-bromo-2-((4-cyano-2-formylphenyl)thio)benzoate (**2.21**, 0.300 g, 0.797 mmol) in absolute EtOH (8 mL) was treated with titanium(IV)isopropoxide (0.612 mL, 1.99 mmol), 4-methoxybenzylamine (0.219 g, 1.59 mmol), Et₃N (0.22 mL, 1.59 mmol) and stirred at rt for 2 h. Analysis by ¹H NMR (300 MHz, CDCl₃) indicated that the aldehyde had been consumed, NaBH₄ (0.0603 g, 1.59 mmol) was added and the mixture stirred for 17 h where analysis by TLC (hexanes/EtOAc, 1:1) indicated the imine intermediate had been consumed. The reaction was diluted with aqueous ammonium hydroxide (5 mL). The resulting inorganic precipitate was filtered off washed with EtOAc (30 mL) and H₂O (10 mL), and the organic layer separated. The aqueous layer was extracted with EtOAc (2 x 20 mL) and the combined organic layers were washed with satd. aqueous NaHCO₃, brine, and dried (Na₂SO₄). The crude residue was purified by chromatography on SiO₂ (hexanes/EtOAc, 2:1 to hexanes/EtOAc, 1:2 w/ 3% Et₃N) to give **2.29** (0.196 g, 0.418 mmol, 53%) as a colorless solid: Mp 125.7-128.6 °C; IR (neat) 3262, 3006, 2870, 2833, 2220, 1592, 1510, 1454, 1238, 1174, 1070, 1031, 822, 736 cm⁻¹; ¹H NMR (400 MHz, CDCl₃) δ 7.76 (s, 1 H), 7.66 (s, 1 H), 7.48 (d, *J* = 8.0 Hz, 1 H), 7.32 (d, *J* = 8.2 Hz, 2 H), 7.28-7.24 (m, 3 H), 6.90 (d, *J* = 8.2 Hz, 2 H), 6.80 (d, *J* = 8.0 Hz, 1 H), 4.61 (s, 2 H), 3.89 (s, 2 H), 3.82 (s, 3 H), 3.80 (s, 2 H); ¹³C NMR (100 MHz, CDCl₃) δ 158.9, 146.1, 143.0, 139.1, 137.5, 132.2, 132.0, 131.8, 131.5, 131.1, 129.4, 128.0, 127.9, 124.7, 118.6, 113.9, 113.8, 62.6, 55.3, 52.9, 50.2; HRMS (ESI) *m/z* calcd for C₂₃H₂₂N₂O₂Br ([M+H]⁺) 469.0580, found 469.0575.



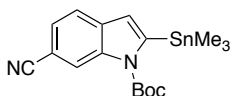
2.30

9-Bromo-6-(4-methoxybenzyl)-6,7-dihydro-5H-dibenzo[*b,g*][1,5]thiazocine-3-carbonitrile (2.30). A solution of 4-((4-bromo-2-(hydroxymethyl)phenyl)thio)-3-(((4-methoxybenzyl)amino)methyl)benzonitrile (**2.29**, 0.100 g, 0.213 mmol) in dry THF (20 mL) at 0 °C, was treated with phosphorus tribromide (13.5 μ L, 0.142 mmol), stirred at 0 °C for 2 h, heated at reflux for 27 h, cooled to rt, diluted with H₂O (5 mL), and made basic with solid K₂CO₃. The organic layer was separated and the aqueous layer was extracted with EtOAc (3 x 20 mL). The combined organic layers were washed with brine, dried (Na₂SO₄), filtered, and concentrated under reduced pressure. The crude residue was purified by chromatography on SiO₂ (hexanes/EtOAc, 3:1 w/ 5% Et₃N) to give **2.30** (0.0624 g, 0.138 mmol, 65%) as a colorless solid: Mp 149.6-152.8 °C; IR (neat) 3064, 3003, 2949, 2833, 2803, 2227, 1614, 1514, 1463, 1253, 1174, 1092, 1046, 815, 746 cm⁻¹; ¹H NMR (400 MHz, DMSO-d₆, 100 °C) δ 7.75 (d, *J* = 8.0 Hz, 1 H), 7.65 (d, *J* = 8.0 Hz, 1 H), 7.58 (d, *J* = 7.6 Hz, 1 H), 7.47 (d, *J* = 7.6 Hz, 1 H) 7.41 (s, 1 H), 7.21 (d, *J* = 7.6 Hz, 1 H), 6.93 (d, *J* = 7.6 Hz, 1 H), 4.13 (s, 4 H), 4.79 (s, 3 H), 3.42 (s, 2 H); ¹³C NMR (100 MHz, DMSO-d₆, 100 °C) δ 165.2, 150.1, 145.5, 139.4, 139.3, 136.2, 135.9, 134.8, 134.6, 133.5, 132.5, 131.6, 130.4, 128.3, 124.3, 120.9, 117.5, 112.9, 52.9, 45.1; HRMS (ESI) *m/z* calcd for C₂₃H₂₀N₂OBrS ([M+H]⁺) 451.0474, found 451.0482.



1-(*tert*-Butoxycarbonyl)-1H-indole-6-carbonitrile⁴⁷⁸ A solution of 6-cyanoindole (4.00 g, 28.1 mmol) and Boc-anhydride (7.68 g, 35.2 mmol) in anhydrous CH₂Cl₂ (45 mL) at rt was

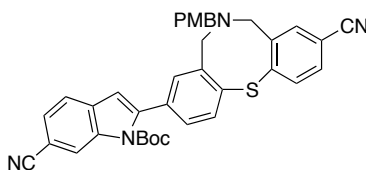
treated with DMAP (0.0530 g, 0.422 mmol) stirred for 3 h, diluted with ice H₂O (200 mL). The organic layer was separated and the aqueous layer was extracted with CH₂Cl₂ (200 mL). The combined organic layers were washed with 0.5M aqueous HCl (50 mL), brine (100 mL) and H₂O (200 mL), and dried (MgSO₄). The solution was filtered through a pad of SiO₂ (CH₂Cl₂) and the combined filtrates were concentrated under reduced pressure. The product was crystallized from cold EtOH/hexanes (1:1) to give 1-(*tert*-butoxycarbonyl)-1*H*-indole-6-carbonitrile (6.15 g, 25.4 mmol, 90%) as a colorless solid: ¹H NMR (500 MHz, CDCl₃) δ 8.51 (bs, 1 H), 7.77 (bs, 1 H), 7.64 (d, *J* = 8.0 Hz, 1 H), 7.48 (d, *J* = 8.0 Hz, 1 H), 6.64 (d, *J* = 3.5 Hz, 1 H), 1.70 (s, 9 H); ¹³C NMR (125 MHz, CDCl₃) δ 148.9, 134.2, 133.8, 129.2, 125.7, 121.7, 119.7, 107.2, 107.1, 85.0, 28.1.



2.31

1-(*tert*-Butoxycarbonyl)-2-(trimethylstannyl)-1*H*-indole-6-carbonitrile⁴⁷⁸ (**2.31**). A solution of distilled *i*Pr₂NH (2.21 mL, 15.5 mmol) in anhydrous THF (15 mL) at -78 °C was treated with *n*-BuLi (2.5 M in hexanes)(5.40 mL, 13.4 mmol) dropwise. The solution was allowed to warm to 0 °C briefly then cooled back down to -78 °C. The solution was then cannulated dropwise into a solution, cooled to -78 °C, of 1-(*tert*-butoxycarbonyl)-1*H*-indole-6-carbonitrile (2.50 g, 10.3 mmol) and trimethyltin chloride (2.50 g, 12.4 mmol) in THF (30 mL) while keeping the temperature below -40 °C. The reaction mixture was stirred at -78 °C for 30 min then warmed to rt and left to stir for 22 h. After quenching the reaction with H₂O (5 mL), the reaction mixture was concentrated under reduced pressure. The crude residue was dissolved in Et₂O (250 mL), washed with 10% KF solution (50 mL) and H₂O, dried (Na₂SO₄), filtered, and concentrated under reduced pressure to give **2.31** (3.82 g, 9.43 mmol, 91%) as a colorless solid,

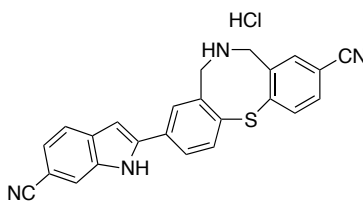
which was used immediately in the next reaction: ^1H NMR (300 MHz, CDCl_3) δ 8.25 (bs, 1 H), 7.59 (d, $J = 8.1$ Hz, 1 H), 7.44 (dd, $J = 8.1, 0.9$ Hz, 1 H), 6.79 (t, $J = 8.6$ Hz, 1 H), 1.74 (s, 9 H), 0.35 (t, $J_{\text{Sn-H}} = 28.8$ Hz, 9 H).



2.32

***tert*-Butyl 6-cyano-2-(9-cyano-6-(4-methoxybenzyl)-6,7-dihydro-5H-dibenzo[*b,g*][1,5]thiazocin-3-yl)-1H-indole-1-carboxylate (2.32)** A solution of 9-bromo-6-(4-methoxybenzyl)-6,7-dihydro-5H-dibenzo[*b,g*][1,5]thiazocine-3-carbonitrile (**2.30**, 0.500 g, 1.11 mmol) and *tert*-butyl 6-cyano-2-(trimethylstannyl)-1H-indole-1-carboxylate (**2.31**, 0.769 g, 1.33 mmol) in dry degassed DMF (10 mL) was treated with $\text{Pd}(\text{PPh}_3)_2\text{Cl}_2$ (0.0778 g, 0.111 mmol) and $(i\text{Pr})\text{CuCl}^{293}$ (0.0810 g, 0.166 mmol) at rt. The reaction mixture was heated to 80 °C for 21 h where analysis by LCMS indicated that the SM was consumed. The reaction mixture was poured onto H_2O (20 mL) and extracted EtOAc (3 x 75 mL). The combined organic layers were washed with satd. aqueous NaHCO_3 (10 mL), brine (10 mL), dried (Na_2SO_4), filtered, and concentrated under reduced pressure. The crude residue was purified by chromatography on SiO_2 (hexanes to hexanes/EtOAc, 3:1 w/ 5% Et_3N). The product was sonicated with methanol and pelleted by centrifugation. The supernatant was removed and this process was repeated twice, and the product was dried under high vacuum to give **2.32** (0.312 g, 0.509 mmol, 46%) as a colorless solid. Due to the removal of the Boc group during high temperature NMR analysis this product was carried onto the Boc-deprotection: Characteristic ^1H NMR peaks, ^1H NMR (400 MHz, DMSO-d_6 , 82 °C) δ 8.44 (s, 1 H), 7.82 (t, $J = 8.2$ Hz, 2 H), 7.76 (d, $J = 8.0$ Hz, 1 H), 7.70 (d, $J = 8.0$ Hz, 1 H), 7.64 (d, $J = 8.2$ Hz, 1 H), 7.45-7.43 (m, 2 H), 7.24-7.22 (m, 3 H), 6.92 (d, $J = 8.2$

Hz, 2 H), 6.88 (s, 1 H), 4.18 (s, 4 H), 3.77 (s, 3 H), 3.47 (s, 2 H), 1.30 (s, 9 H); HRMS (ESI) m/z calcd for $C_{37}H_{33}N_4O_3S$ ($[M+H]^+$) 613.2268, found 613.2267.

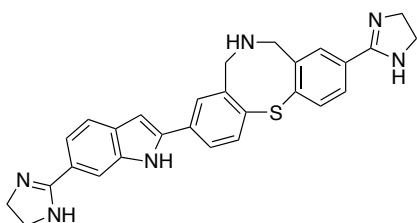


2.33

9-(6-Cyano-1H-indol-2-yl)-6,7-dihydro-5H-dibenzo[b,g][1,5]thiazocine-3-carbonitrile hydrochloride (2.33). A solution of tert-butyl 6-cyano-2-(9-cyano-6-(4-methoxybenzyl)-6,7-dihydro-5H-dibenzo[b,g][1,5]thiazocin-3-yl)-1H-indole-1-carboxylate (**2.33**, 0.150 g, 0.245 mmol) in dry 1,2-dichloroethane (4 mL) cooled to 0 °C was treated with α -chloroethylchloroformate (54 μ L, 0.201 mmol) and stirred for 30 min at 0 °C. The reaction was heated to 90 °C for 4 h at which point analysis by LCMS indicated the starting material had been consumed. The reaction was concentrated under reduced pressure, dissolved in dry MeOH (2 mL), and heated to reflux for 1 h. The resulting precipitate was collected by vacuum filtration and washed with Et_2O to give tert-butyl 6-cyano-2-(9-cyano-6,7-dihydro-5H-dibenzo[b,g][1,5]thiazocin-3-yl)-1H-indole-1-carboxylate hydrochloride (0.106 g, 0.201 mmol) as a colorless solid. The product was taken on to the next deprotection with no further purification.

A solution of tert-butyl 6-cyano-2-(9-cyano-6,7-dihydro-5H-dibenzo[b,g][1,5]thiazocin-3-yl)-1H-indole-1-carboxylate hydrochloride (0.0200 g, 0.0378 mmol) in 4M HCl in dioxane (1 mL) was stirred in a sealed tube at 0 °C for 20 min, warmed to rt for 4 h, and heated at 80 °C for 20 h. The reaction had turned green and was diluted with Et_2O (10 mL). The resulting precipitate was collected by vacuum filtration and washed with Et_2O (20 mL), and dried under high vacuum

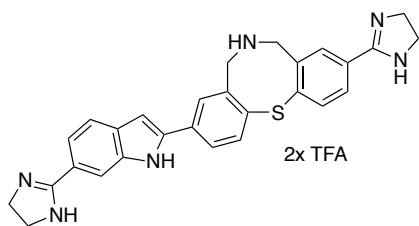
to give **2.33** (0.0130 g, 0.0331 mmol, 72% (2 steps)) as a green solid: Mp 290 °C (decomp.); IR (neat) 3541, 3458, 2937, 2729, 2608, 2216, 1735, 1596, 1458, 1314, 1254, 1221, 1117, 1055, 870, 818 cm⁻¹; ¹H NMR (400 MHz, DMSO-d₆, 100 °C) δ 12.16 (s, 1 H), 8.20 (s, 1 H), 8.00 (m, 2 H), 7.85-7.79 (m, 5 H), 7.72 (d, *J* = 8.0 Hz, 1 H), 7.31 (d, *J* = 8.0 Hz, 1 H), 7.09 (s, 1 H), 4.51 (s, 2 H), 4.43 (s, 2 H); ¹³C NMR (100 MHz, DMSO-d₆, 100 °C) δ 143.7, 139.6, 137.3, 135.8, 134.7, 132.6, 132.0, 131.2, 130.9, 126.7, 121.7, 120.7, 119.6, 117.0, 115.5, 110.3, 103.0, 100.2; HRMS (ESI) *m/z* calcd for C₂₄H₁₇N₄S ([M+H]⁺) 393.1168, found 393.1172.



2.15

3-(4,5-Dihydro-1H-imidazol-2-yl)-9-(6-(4,5-dihydro-1H-imidazol-2-yl)-1H-indol-2-yl)-6,7-dihydro-5H-dibenzo[b,g][1,5]thiazocine (2.15). A solution of 9-(6-cyano-1H-indol-2-yl)-6,7-dihydro-5H-dibenzo[b,g][1,5]thiazocine-3-carbonitrile (**30**, 0.0200 g, 0.0466 mmol) in ethylenediamine (1.0 mL) was treated with sulfur (0.0056 g, 0.0932 mmol). The reaction was irradiated in the microwave for 80 min at 110 °C, poured onto H₂O, filtered, and the resulting solid was washed with H₂O, Et₂O, and dried under high vacuum to give **2.15** (0.0142 g, 0.0297 mmol, 64%) as a brown orange solid: Mp 233 °C (decomp.); IR (neat) 3217, 2926, 2875, 1599, 1551, 1445, 1396, 1370, 1342, 1281, 1113, 1090, 1034, 984, 784, 708 cm⁻¹; ¹H NMR (400 MHz, DMSO-d₆, 100 °C) δ 11.45 (bs, 1 H), 7.91 (s, 1 H), 7.78 (s, 1 H), 7.72-7.63 (m, 5 H), 7.55 (s, 2 H), 6.92 (s, 1 H), 4.22 (s, 2 H), 4.18 (s, 2 H), 3.69 (s, 4 H), 3.63 (s, 4 H); ¹³C NMR (100 MHz, DMSO-d₆, 100 °C) δ 164.4, 162.4, 143.5, 142.5, 138.6, 138.2, 136.3, 135.0, 132.3, 131.9, 131.3,

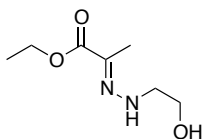
130.6, 130.0, 129.4, 127.5, 125.8, 124.1, 118.9, 118.5, 110.2, 99.1, 51.8, 49.2, 48.4; HRMS (ESI) m/z calcd for $C_{28}H_{27}N_6S$ ($[M+H]^+$) 479.2012, found 479.2007.



2.15•TFA

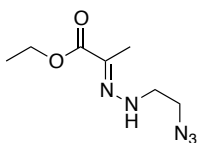
3-(4,5-Dihydro-1H-imidazol-2-yl)-9-(6-(4,5-dihydro-1H-imidazol-2-yl)-1H-indol-2-yl)-6,7-dihydro-5H-dibenzo[*b,g*][1,5]thiazocine bis(2,2,2-trifluoroacetate) (2.15•TFA). A suspension of 3-(4,5-dihydro-1H-imidazol-2-yl)-9-(6-(4,5-dihydro-1H-imidazol-2-yl)-1H-indol-2-yl)-6,7-dihydro-5H-dibenzo[*b,g*][1,5]thiazocine (**2.15**, 0.0400 g, 0.0836 mmol) in THF (0.5 mL) was treated with a solution of TFA in THF (100 μ L, 4 M) and the reaction mixture was vigorously stirred at rt for 18 h, concentrated under reduced pressure, and co-evaporated with hexanes. The resulting solid was suspended in Et₂O and pelleted by centrifugation. The supernatant was removed and the solid was dried under high vacuum to give **2.15•TFA** (0.0572 g, 0.0809 mmol, 97%, 98.5% pure by ELSD) as a tan solid: Mp 272 °C (decomp.); IR (neat) 3210, 3094, 2753, 1664, 1609, 1482, 1426, 1370, 1289, 1197, 1174, 1130, 1034, 824, 798, 719 cm^{-1} ; ¹H NMR (400 MHz, DMSO-*d*₆, 100 °C) δ 12.06 (bs, 1 H), 10.14 (bs, 1 H), 8.05-8.03 (m, 2 H), 7.96-7.79 (m, 6 H), 7.58 (dd, $J = 8.4, 1.8$ Hz, 1 H), 7.12 (d, $J = 1.8$ Hz, 1 H), 4.40 (s, 2 H), 4.28 (s, 2 H), 4.07 (s, 4 H), 4.05 (s, 4 H); ¹³C NMR (100 MHz, DMSO-*d*₆, 100 °C) δ 166.0, 163.9, 158.3, 157.9, 150.3, 150.1, 147.8, 144.7, 140.7, 136.0, 134.7, 132.6, 132.1, 128.6, 126.6, 121.2, 120.2, 118.7, 114.4, 112.2, 100.3, 44.2, 43.9; HRMS (ESI) m/z calcd for $C_{28}H_{27}N_6S$ ($[M+H]^+$) 479.2012, found 479.2007.

5.3.2 Synthesis of 1,2,4-Triazines



2.44

(E)-Ethyl 2-(2-(2-hydroxyethyl)hydrazono)propanoate (2.44).³⁰³ A solution of ethyl pyruvate (**2.42**, 3.64 mL, 32.7 mmol) in THF (40 mL) was treated with a solution of 2-hydroxyethylhydrazine (**2.43**, 3.00 mL, 44.7 mmol) in EtOH (0.5 mL). This mixture was heated at reflux for 7 h, concentrated under reduced pressure, diluted with H₂O (30 mL) and EtOAc (30 mL), partitioned, and the aqueous layer was extracted with EtOAc (3 x 40 mL). The combined organic layers were washed with brine, dried (Na₂SO₄), and concentrated under reduced pressure. The crude residue was purified by chromatography on SiO₂ (100% EtOAc) to give **2.44** (3.90 g, 22.4 mmol, 68%) as a pale yellow oil: ¹H NMR (300 MHz, CDCl₃) δ 4.25 (q, *J* = 7.2 Hz, 2 H), 3.84 (dd, *J* = 5.1, 4.5 Hz, 2 H), 3.56 (dd, *J* = 5.1, 4.5 Hz, 2 H), 1.93 (s, 3 H), 1.31 (t, *J* = 7.2 Hz, 3 H); ¹³C NMR (75 MHz, CDCl₃) δ 164.9, 132.6, 62.3, 61.0, 52.1, 14.3, 10.0.

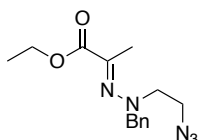


2.45

(E)-Ethyl 2-(2-(2-azidoethyl)hydrazono)propanoate (2.45).³⁰³ A solution of (*E*)-Ethyl 2-(2-(2-hydroxyethyl)hydrazono)propanoate (**2.44**, 6.35 g, 36.5 mmol) and Et₃N (7.87 mL, 56.0 mmol) in THF (60 mL) was treated with MsCl (3.54 mL, 45.7 mmol). This mixture was stirred at rt for 20 min, diluted with satd. aqueous NaHCO₃ (80 mL) and H₂O (50 mL), and extracted with Et₂O (3 x 125 mL). The combined organic layers were dried (Na₂SO₄), and concentrated

under reduced pressure to give the crude mesylate as a yellow oil that was used without further purification.

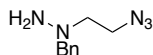
The crude oil was dissolved in DMF (30 mL), treated with NaN₃ (7.14 g, 110. mmol) and heated to 50 °C behind a blast shield for 10 h where analysis by TLC (hexanes/EtOAc, 1:1) indicated that the mesylate intermediate was completely consumed. The reaction was cooled to rt, diluted with H₂O (60 mL) and brine (40 mL) and extracted with EtOAc (4 x 100 mL). The combined organic layers were washed with H₂O (50 mL), brine (2 x 100 mL), dried (Na₂SO₄), filtered, and concentrated under reduced pressure. The crude residue was purified by chromatography on SiO₂ (hexanes to hexanes/EtOAc, 2:1 gradient with 1% Et₃N) to give **2.45** (4.25 g, 21.4 mmol, 59% (2 steps)) as a yellow oil: ¹H NMR (300 MHz, CDCl₃) δ 5.83 (bs, 1 H), 4.29 (q, *J* = 7.2 Hz, 2 H), 3.84 (dd, *J* = 9.9, 5.1 Hz, 2 H), 3.56 (dd, *J* = 9.9, 5.1 Hz, 2 H), 1.96 (s, 3 H), 1.33 (t, *J* = 7.2 Hz, 3 H). ¹³C NMR (75 MHz, CDCl₃) δ 164.8, 113.7, 61.1, 51.2, 49.7, 14.3, 10.3.



2.46a

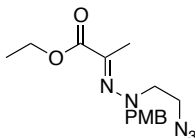
Ethyl (*E*)-2-(2-(2-azidoethyl)-2-benzylhydrazineylidene)propanoate (2.46a).³⁰³ A solution of (*E*)-ethyl 2-(2-(2-azidoethyl)hydrazono)propanoate (**2.45**, 1.00 g, 5.02 mmol) in dry DMF (28 mL) was treated with K₂CO₃ (1.39 g, 10.0 mmol), NaI (0.752 g, 5.02 mmol), and benzyl bromide (1.80 mL, 15.1 mmol), heated at 70 °C behind a blast shield for 18 h, cooled to rt, diluted with H₂O (15 mL), and extracted with EtOAc (3 x 20 mL). The combined organic layers were washed with H₂O (20 mL), brine (20 mL), dried (Na₂SO₄), filtered and concentrated under reduced pressure. The crude residue was purified by chromatography on SiO₂ (hexanes to

hexanes/EtOAc, 1:1 with 1% NEt₃) to give **2.46a** (0.832 g, 2.88 mmol, 57%) as a golden oil: ¹H NMR (300 MHz, CDCl₃) δ 7.37-7.29 (m, 5 H), 4.33 (q, *J* = 7.2 Hz, 2 H), 4.08 (s, 3 H), 3.34 (t, *J* = 5.5 Hz, 2 H), 3.23 (t, *J* = 5.5 Hz, 2 H), 2.22 (s, 3 H), 1.36 (t, *J* = 7.2 Hz, 3 H);



2.47a

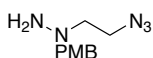
1-(2-azidoethyl)-1-benzylhydrazine (2.47a).³⁰³ A solution of (*E*)-ethyl 2-(2-(2-azidoethyl)-2-benzylhydrazono)propanoate (**2.46a**, 1.30 g, 4.49 mmol) in THF (20 mL) and H₂O (6 mL) at rt was treated with hydrazine dihydrochloride (1.41 g, 13.5 mmol). This mixture was stirred at rt for 5 h, treated with solid Na₂CO₃, filtered through a cotton plug, washed (EtOAc), and concentrated under reduced pressure. The resulting oil was immediately purified by chromatography on SiO₂ (hexanes/EtOAc, 1:1 with 1% Et₃N) to give **2.47a** (0.634 g, 3.31 mmol, 74%) as an unstable colorless oil: ¹H NMR (300 MHz, CDCl₃) δ 7.38-7.29 (m, 5 H), 3.76 (s, 2 H), 3.49 (t, *J* = 5.7 Hz, 2 H), 2.77 (t, *J* = 5.7 Hz, 2 H).



2.46b

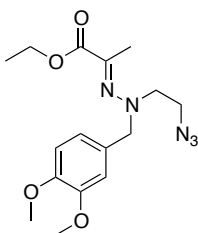
(*E*)-Ethyl 2-(2-(2-azidoethyl)-2-(4-methoxy benzyl)hydrazono)propanoate (2.46b).³⁰³ A solution of (*E*)-ethyl 2-(2-(2-azidoethyl)hydrazono)propanoate (**2.45**, 4.20 g, 21.1 mmol) in DMF (50 mL) was treated with K₂CO₃ (5.83 g, 42.2 mmol), NaI (3.16 g, 21.1 mmol), and freshly prepared paramethoxybenzyl bromide (9.2 mL, 12.7 g, 63.3 mmol). The mixture was heated at 70 °C behind a blast shield for 22 h, cooled to rt, diluted with H₂O (100 mL) and extracted with EtOAc (3 x 100 mL). The combined organic layers were washed with H₂O (100 mL), brine (100 mL), dried (Na₂SO₄), and concentrated under reduced pressure. The crude

residue was purified by chromatography on SiO₂ (hexanes to hexanes/EtOAc, 2:1 gradient with 1% Et₃N) to give **2.46b** (3.49 g, 10.9 mmol, 52%) as a golden oil: ¹H NMR (300 MHz, CDCl₃) δ 7.27 (d, *J* = 8.4 Hz, 2 H), 6.89 (d, *J* = 8.4 Hz, 2 H), 4.29 (q, *J* = 7.2 Hz, 2 H), 4.00 (s, 2 H), 3.79 (s, 3 H), 3.31 (t, *J* = 5.5 Hz, 2 H), 3.20 (t, *J* = 5.5 Hz, 2 H), 2.22 (s, 3 H), 1.35 (t, *J* = 7.2 Hz, 3 H); ¹³C NMR (75 MHz, CDCl₃) δ 164.6, 158.9, 152.6, 129.4, 128.3, 113.8, 61.4, 60.0, 55.5, 55.0, 49.4, 15.7, 14.0.



2.47b

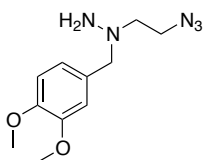
1-(2-Azidoethyl)-1-(4-methoxybenzyl)hydrazine (2.47b).³⁰³ A solution of (*E*)-ethyl 2-(2-(2-azidoethyl)-2-(4-methoxy benzyl)hydrazono)propanoate (**2.46b**, 0.150 g, 0.470 mmol) in THF (2 mL) and H₂O (1 mL) at rt was treated with hydrazine dihydrochloride (0.148 g, 1.41 mmol), stirred at rt for 2 h, treated with solid Na₂CO₃, and concentrated under reduced pressure. The crude residue was immediately purified by chromatography on SiO₂ (hexanes/EtOAc, 1:2 with 1% Et₃N) to give **2.47b** (0.0761 g, 0.344 mmol, 73%) as an unstable, colorless oil: ¹H NMR (300 MHz, CDCl₃) δ 7.26 (d, *J* = 8.6 Hz, 2 H), 6.89 (d, *J* = 8.6 Hz, 2 H), 3.81 (s, 3 H), 3.67 (s, 2 H), 3.48 (t, *J* = 5.6 Hz, 2 H), 2.74 (t, *J* = 5.6 Hz, 2 H); ¹³C NMR (75 MHz, CDCl₃) δ 130.3, 114.0, 66.9, 58.5, 55.3, 44.7.



2.46c

(E)-Ethyl 2-(2-(2-azidoethyl)-2-(3,4-dimethoxybenzyl)hydrazono)propanoate (2.46c).

A solution of (*E*)-ethyl 2-(2-(2-azidoethyl)hydrazono)propanoate (**2.45**, 13.7 g, 68.8 mmol) in DMF (138 mL) was treated 4-(chloromethyl)-1,2-dimethoxybenzene (32.1 g, 138 mmol), KI (34.3 g, 206 mmol), and K₂CO₃ (28.5 g, 206 mmol). The reaction mixture was stirred at rt for 2 d, diluted with H₂O (500 mL) and extracted with EtOAc (3 x 250 mL). The combined organic layers were washed with H₂O (300 mL), brine (300 mL), dried (Na₂SO₄), filtered, and concentrated under reduced pressure. The crude residue was purified by chromatography on SiO₂ (hexanes/EtOAc, 5:1 with 1% Et₃N) to give **2.46c** (22.5 g, 57.9 mmol, 84%) as a yellow oil: IR (CHCl₃) 2921, 2848, 2097, 1708, 1590, 1512, 1462, 1258, 1234, 1135, 1025, 803 cm⁻¹; ¹H NMR (300 MHz, CDCl₃) δ 6.94-6.81 (m, 3 H), 4.31 (q, *J* = 7.2 Hz, 2 H), 3.99 (s, 2 H), 3.87 (m, 6 H), 3.31 (t, *J* = 5.4 Hz, 2 H), 3.22 (t, *J* = 5.4 Hz, 2 H), 2.20 (s, 3 H), 1.34 (t, *J* = 7.2 Hz, 3 H); ¹³C NMR (75 MHz, CDCl₃) δ 164.6, 152.9, 149.0, 148.4, 128.9, 120.4, 111.1, 110.8, 61.5, 60.4, 55.7, 55.6, 49.4, 15.8, 14.0; HRMS (ESI) *m/z* calcd for C₁₆H₂₄N₅O₂ ([M+H]⁺) 350.1823, found 350.1832.

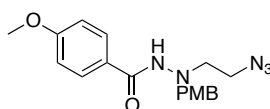


2.47c

1-(2-Azidoethyl)-1-(3,4-dimethoxybenzyl)hydrazine (2.47c). A solution of (*E*)-ethyl 2-(2-(2-azidoethyl)-2-(3,4-methoxy benzyl)hydrazono)propanoate (**2.46c**, 1.00 g, 2.86 mmol) in THF (40 mL) and H₂O (2 mL) at 25 °C was treated with hydrazine dihydrochloride (0.901 g, 8.59 mmol). The reaction mixture was stirred at rt for 24 h, treated with solid Na₂CO₃, filtered and washed with EtOAc, concentrated under reduced pressure. The crude residue was purified by chromatography on SiO₂ (EtOAc/hexanes, 3:2 with 1% Et₃N) to give **2.47c** (0.515 g, 2.05

mmol, 72%) as yellow oil: IR (CH₂Cl₂) 3426, 2934, 2831, 2097, 1696, 1590, 1512, 1450, 1260, 1232, 1135, 1025, 764 cm⁻¹; ¹H NMR (300 MHz, CDCl₃) δ 6.99 (s, 1 H), 6.82 (bd, *J* = 0.9 Hz, 2 H), 3.90 (s, 3 H), 3.88 (s, 3 H), 3.72 (s, 2 H), 3.49 (t, *J* = 5.6 Hz, 2 H), 2.79 (t, *J* = 5.6 Hz, 2 H); ¹³C NMR (75 MHz, CDCl₃) δ 149.3, 148.6, 121.1, 111.8, 110.9, 67.1, 58.5, 55.9, 48.4; HRMS (ESI) *m/z* calcd for C₁₁H₁₈N₅O₂ ([M+H]⁺) 252.1455, found 252.1458.

5.3.3 Synthesis of Triazine Analogs 2.51a-c

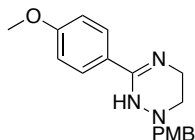


2.50a

***N'*-(2-Azidoethyl)-*N'*-(4-methoxybenzyl)benzohydrazide (2.50a).** A solution of 4-methoxybenzoic acid (**2.49a**, 0.250 g, 1.64 mmol) in CH₂Cl₂ (10 mL) was cooled to 0 °C and treated with oxalyl chloride (0.16 mL, 1.81 mmol) and DMF (2 drops). The reaction mixture was stirred at rt for 2 h, concentrated under reduced pressure and used without further purification.

A solution of 4-methoxybenzoyl chloride, prepared above, in CH₂Cl₂ (8 mL) was cooled to 0 °C and treated with a solution of 1-(2-azidoethyl)-1-(4-methoxybenzyl)hydrazine (**2.47b**, 0.400 g, 1.81 mmol) in CH₂Cl₂ (1.0 mL), and Et₃N (0.69 mL, 4.93 mmol). The reaction mixture was allowed to warm to rt for 20 h, diluted with satd. aqueous NaHCO₃ (2 mL), and extracted with CH₂Cl₂ (3 x 10 mL). The combined organic layers were dried (Na₂SO₄), filtered, and concentrated under reduced pressure. The crude residue was washed with hexanes and filtered to give **2.50a** (0.436 g, 1.23 mmol, 75%) as a colorless solid that was used without further purification: Mp 90.4-91.8 °C; IR (neat) 3251, 2833, 2114, 2089, 1640, 1605, 1504, 1459, 1252,

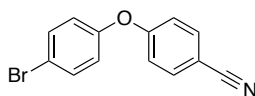
1171, 1023, 820, 768 cm^{-1} ; ^1H NMR (400 MHz, CDCl_3) δ 7.54 (d, $J = 8.4$ Hz, 2 H), 7.27 (d, $J = 8.4$ Hz, 2 H), 7.01 (bs, 1 H), 6.88 (d, $J = 6.8$ Hz, 2 H), 6.85 (d, $J = 6.8$ Hz, 2 H), 4.22 (s, 2 H), 3.83 (s, 3 H), 3.79 (s, 3 H), 3.42 (t, $J = 5.6$ Hz, 2 H); 3.34 (t, $J = 5.6$ Hz, 2 H); ^{13}C NMR (100 MHz, CDCl_3) δ 166.9, 162.4, 159.2, 130.6, 128.6, 125.7, 113.9, 59.6, 55.4, 55.2, 54.3, 49.0; HRMS (ESI) m/z calcd for $\text{C}_{18}\text{H}_{22}\text{N}_5\text{O}_3$ ($[\text{M}+\text{H}]^+$) 356.1717, found 356.1715.



2.51a

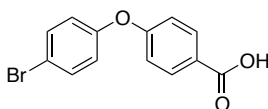
1-(4-Methoxybenzyl)-3-(4-methoxyphenyl)-1,2,5,6-tetrahydro-1,2,4-triazine (2.51a).

A flame-dried microwave vial containing a solution of *N'*-(2-azidoethyl)-4-methoxy-*N'*-(4-methoxybenzyl)benzohydrazide (**2.50a**, 0.0500 g, 0.141 mmol) in dry *o*-1,2-dichlorobenzene (4 mL) was treated with $\text{P}(n\text{-Bu})_3$ (0.139 mL, 0.563 mmol). The reaction mixture was irradiated in the microwave at 180 $^\circ\text{C}$ for 1 h, treated with Et_3N (0.1 mL) and then applied directly to a 4g silica cartridge and purified by automated chromatography on SiO_2 (gradient, 100% hexanes to 100% EtOAc over 15 min) to give **2.51a** (0.0206 g, 0.0662 mmol, 47%) as a tan solid: Mp 115.5-119.8 $^\circ\text{C}$; IR (hexanes) 3410, 1609, 1508, 1491, 1446, 1351, 1238, 1172, 1025, 988, 843, 762 cm^{-1} ; ^1H NMR (400 MHz, CDCl_3) δ 7.56 (d, $J = 8.8$ Hz, 2 H), 7.37 (d, $J = 8.8$ Hz, 2 H), 6.87 (dd, $J = 8.8, 2.0$ Hz, 4 H), 4.13 (s, 2 H), 3.81 (s, 6 H), 3.54 (bs, 2 H), 2.70 (t, $J = 5.0$ Hz, 2 H); ^{13}C NMR (100 MHz, CDCl_3) δ 160.2, 158.8, 144.8, 130.6, 130.1, 128.1, 126.8, 113.7, 113.5, 63.3, 55.3, 55.2, 45.0, 41.7; HRMS (ESI) m/z calcd for $\text{C}_{18}\text{H}_{21}\text{N}_3\text{O}_2$ ($[\text{M}+\text{H}]^+$) 312.1707, found 312.1695.



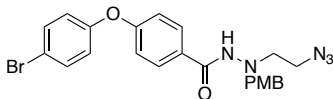
2.57

4-(4-Bromophenoxy)benzonitrile (2.57).⁴⁷⁹ A solution of 4-bromophenol (**2.58**, 4.00 g, 22.7 mmol) and 4-fluorobenzonitrile (**2.59**, 3.05 g, 24.9 mmol) in DMF (22 mL) was treated with K₂CO₃ (3.46 g, 23.8 mmol) and the mixture was stirred for 10 min at rt, then heated at 150 °C under nitrogen for 24 h, cooled to rt, poured onto ice and stirred for 10 min. A tan solid formed and was collected by vacuum filtration and washed with H₂O. The solid was dissolved in CH₂Cl₂, dried (Na₂SO₄), and concentrated. The residue was recrystallized with EtOH to give **2.57** (5.41 g, 19.8 mmol, 87%) as a tan crystalline solid: ¹H NMR (500 MHz, CDCl₃) δ 7.61 (d, *J* = 8.0 Hz, 2 H), 7.52 (d, *J* = 8.0 Hz, 2 H), 7.01 (d, *J* = 8.5 Hz, 2 H), 6.95 (d, *J* = 8.5 Hz, 2 H); ¹³C NMR (125 MHz, CDCl₃) δ 161.0, 154.0, 134.1, 133.2, 121.9, 118.5, 118.0, 117.8, 106.3.



2.49b

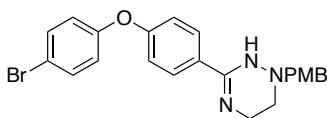
4-(4-Bromophenoxy)benzoic acid (2.49b). A solution of 4-(4-bromophenoxy)benzonitrile (**2.57**, 0.300 g, 1.09 mmol) in EtOH (4 mL) and H₂O (1 mL) was treated with anhydrous LiOH (0.786 g, 32.8 mmol). The reaction was heated to reflux for 3 d, cooled to rt, acidified to pH 2 with 1 M aqueous HCl and the resulting precipitate was collected by vacuum filtration and washed with H₂O. The solid was then suspended in toluene and methanol and concentrated under reduced pressure to give **2.49b** (0.297 g, 1.01 mmol, 93%) as a colorless solid: ¹H NMR (500 MHz, DMSO-*d*₆) δ 7.93 (d, *J* = 8.0 Hz, 2 H), 7.59 (d, *J* = 8.0 Hz, 2 H), 7.05 (d, *J* = 7.8 Hz, 2 H), 7.00 (d, *J* = 7.8 Hz, 2 H); ¹³C NMR (125 MHz, CDCl₃) δ 166.6, 160.4, 154.6, 133.1, 131.7, 125.7, 122.0, 117.5, 116.4; HRMS (ESI) *m/z* calcd for C₁₃H₁₀O₃Br ([M+H]⁺) 292.9808, found 292.9806.



2.50b

N'-(Azidoethyl)-4-(4-bromophenoxy)-*N'*-(4-methoxybenzyl)benzohydrazide (2.50b).

According to the procedure used to prepare compound **2.50a**, **2.49b** was converted to crude **2.50b**, which was purified by chromatography on SiO₂ (hexanes/EtOAc, 1:1) to give pure **2.50b** (0.328 g, 0.661 mmol, 55%) as a viscous oil that solidified in the freezer at -20 °C to a pale yellow solid: Mp 98.2-101.8 °C; IR (neat) 3310, 2958, 2101, 2076, 1653, 1603, 1512, 1495, 1478, 1232, 1174, 1010, 943, 869, 777 cm⁻¹; ¹H NMR (300 MHz, CDCl₃) δ 7.55 (d, *J* = 8.4 Hz, 2 H), 7.45 (d, *J* = 8.7 Hz, 2 H), 7.28 (d, *J* = 8.4 Hz, 1 H), 7.13 (bs, 1 H), 6.94-6.83 (m, 6 H), 4.21 (s, 2 H), 3.78 (s, 3 H), 3.42 (bd, *J* = 5.3 Hz, 2 H), 3.35 (bd, *J* = 5.3 Hz, 2 H); ¹³C NMR (75 MHz, CDCl₃) δ 166.6, 160.1, 159.2, 155.1, 132.9, 130.5, 128.9, 128.5, 128.3, 121.3, 117.9, 116.9, 113.9, 59.6, 55.2, 54.3, 49.1; HRMS (ESI) *m/z* calcd for C₂₃H₂₃N₅O₃Br ([M+H]⁺) 496.0979, found 469.0969.

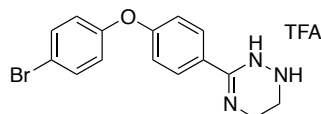


2.51b

3-(4-(4-Bromophenoxy)phenyl)-1-(4-methoxybenzyl)-1,2,5,6-tetrahydro-1,2,4-

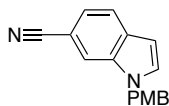
triazine (2.51b). According to the procedure used to prepare compound **2.51a**, **2.50b** was converted to crude **2.51b**, which was purified by chromatography on SiO₂ (hexanes/EtOAc, 2:1 with 1% Et₃N) to give **2.51b** (0.0288 g, 0.0637 mmol, 63%) as a tan solid: Mp 180.3-184.1 °C; IR (neat) 3450, 3040, 2939, 2814, 1610, 1579, 1510, 1482, 1247, 1238, 1167, 1033, 839, 818, 733 cm⁻¹; ¹H NMR (400 MHz, CDCl₃) δ 7.62 (d, *J* = 8.8 Hz, 2 H), 7.43 (d, *J* = 8.8 Hz, 2 H), 7.37

(d, $J = 8.8$ Hz, 1 H), 6.97 (d, $J = 8.4$ Hz, 2 H), 6.89-6.86 (overlapping doublets, $J = 8.8, 8.4$ Hz, 4 H), 4.14 (s, 2 H), 3.81 (s, 3 H), 3.56 (bd, $J = 2.4$ Hz, 2 H), 2.73 (t, $J = 5.0$ Hz, 2 H); ^{13}C NMR (100 MHz, CDCl_3) δ 158.8, 157.4, 156.2, 132.7, 130.6, 129.8, 127.2, 120.5, 118.7, 115.9, 113.6, 63.2, 55.2, 44.9, 41.6; HRMS (ESI) m/z calcd for $\text{C}_{23}\text{H}_{23}\text{N}_3\text{O}_2\text{Br}$ ($[\text{M}+\text{H}]^+$) 452.0968, found 452.0953.



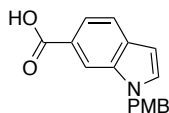
2.52•TFA

3-(4-(4-Bromophenoxy)phenyl)-1,2,5,6-tetrahydro-1,2,4-triazine (2.52•TFA) A solution of 3-(4-(4-bromophenoxy)phenyl)-1-(4-methoxybenzyl)-1,2,5,6-tetrahydro-1,2,4-triazine (**2.51b**, 0.0080 g, 0.0177 mmol) in TFA (0.2 mL) was warmed to 55 °C for 30 min. The reaction was diluted with satd. aqueous NaHCO_3 (2.0 mL) and extracted with EtOAc (3 x 5 mL). The combined organic layers were dried (Na_2SO_4), filtered, and concentrated under reduced pressure to give **2.52•TFA** (0.00621 g, 0.0139 mmol, 79%) as a pale yellow amorphous solid: IR (CH_2Cl_2) 3290, 2923, 2848, 1609, 1495, 1478, 1336, 1236, 1109, 1081, 1033, 736 cm^{-1} ; ^1H NMR (400 MHz, MeOD-d_4) δ 7.60 (d, $J = 8.8$ Hz, 2 H), 7.50 (d, $J = 8.8$ Hz, 2 H), 7.00 (d, $J = 8.8$ Hz, 1 H), 6.95 (d, $J = 8.8$ Hz, 2 H), 3.55 (t, $J = 5.0$ Hz, 2 H), 3.09 (t, $J = 5.0$ Hz, 2 H); ^{13}C NMR (100 MHz, MeOD-d_4) δ 159.6, 157.5, 150.7, 134.0, 131.3, 129.0, 122.0, 119.4, 117.2, 42.1, 41.2; HRMS (ESI) m/z calcd for $\text{C}_{15}\text{H}_{15}\text{N}_3\text{OBr}$ ($[\text{M}+\text{H}]^+$) 332.0393, found 332.0383.



1-(4-Methoxybenzyl)-1H-indole-6-carbonitrile⁴⁸⁰ A solution of 6-cyanoindole (0.800 g, 5.63 mmol) in THF (10 mL) at 0 °C was treated with NaH (60% dispersion in mineral oil) (0.472

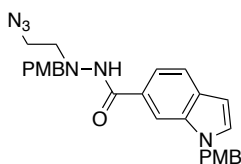
g, 11.8 mmol) and stirred for 20 min at 0 °C followed by the addition of a solution of 4-methoxybenzyl bromide (1.25 g, 6.19 mmol) in THF (2 mL) dropwise. The reaction was stirred at 0 °C for 1 h, rt for 1 h, cooled to 0 °C, diluted with H₂O (1.0 mL), and concentrated under reduced pressure. The residue was dissolved in EtOAc (50 mL), washed with H₂O (5 mL), brine, dried (Na₂SO₄), filtered, and concentrated under reduced pressure. The residue was purified by chromatography on SiO₂ (hexanes/EtOAc, 2:1 w/ 2% Et₃N) to give 1-(4-methoxybenzyl)-1*H*-indole-6-carbonitrile (0.575 g, 2.19 mmol, 39%) as a colorless solid: Mp 94.1-96.6 °C; IR (neat) 3128, 2958, 2932, 2218, 1610, 1510, 1465, 1446, 1349, 1314, 1247, 1174, 1025, 813, 738 cm⁻¹; ¹H NMR (400 MHz, CDCl₃) δ 7.67 (d, *J* = 8.0 Hz, 2 H), 7.62 (s, 1 H), 7.31 (bs, 2 H), 7.07 (d, *J* = 7.8 Hz, 2 H), 6.86 (d, *J* = 7.8 Hz, 2 H), 6.60 (s, 1 H), 5.25 (s, 2 H), 3.78 (s, 3 H); ¹³C NMR (100 MHz, CDCl₃) δ 159.3, 134.8, 131.8, 128.1 (2 C), 122.2, 121.6, 120.6, 114.6, 114.2, 103.9, 102.3, 55.2, 49.9; HRMS (ESI) *m/z* calcd for C₁₇H₁₅N₂O ([M+H]⁺) 263.1179, found 263.1181.



2.49c

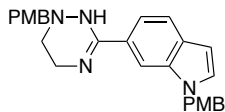
1-(4-Methoxybenzyl)-1*H*-indole-6-carboxylic acid (2.49c) A solution of 1-(4-methoxybenzyl)-1*H*-indole-6-carbonitrile (0.100 g, 0.381 mmol) in EtOH (3.0 mL) and H₂O (3.0 mL) was treated with anhydrous LiOH (0.183 g, 7.62 mmol), and heated at reflux for 4 d, concentrated, suspended in H₂O (5.0 mL), and acidified to pH 2 using conc. HCl. The resulting precipitate was collected by vacuum filtration and dried under high vacuum to give **2.49c** (0.0980 g, 0.348 mmol, 91%) as an off-white solid: Mp 157.6-159.7 °C; IR (neat) 3107, 2962, 2636, 1672, 1612, 1508, 1463, 1286, 1234, 1174, 1019, 826, 809, 768, 736 cm⁻¹; ¹H NMR (400 MHz, CDCl₃) δ 8.25 (s, 1 H), 7.93 (dd, *J* = 8.4, 1.2 Hz, 1 H), 7.72 (d, *J* = 8.4 Hz, 1 H), 7.32 (d, *J*

= 3.2 Hz, 1 H), 7.14 (d, $J = 8.7$ Hz, 2 H), 6.89 (d, $J = 8.7$ Hz, 2 H), 6.63 (d, $J = 3.2$ Hz, 1 H), 5.36 (s, 2 H), 3.81 (s, 3 H); ^{13}C NMR (75 MHz, CDCl_3) δ 173.3, 159.2, 153.5, 133.0, 131.6, 128.8, 128.3, 122.3, 121.0, 120.5, 114.2, 112.7, 102.1, 55.2 (2 C), 49.6; HRMS (ESI) m/z calcd for $\text{C}_{17}\text{H}_{15}\text{NO}_3$ ($[\text{M}+\text{H}]^+$) 282.1125, found 282.1126.



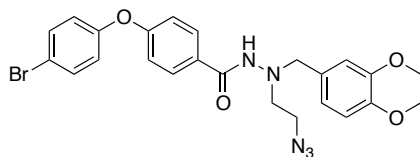
2.50c

***N'*-(2-Azidoethyl)-*N'*,1-bis(4-methoxybenzyl)-1*H*-indole-6-carbohydrazide (2.50c).** A solution of 1-(4-methoxybenzyl)-1*H*-indole-6-carboxylic acid (**2.49c**, 0.0750 g, 0.267 mmol) in CH_2Cl_2 (1 mL) was treated with 1-(2-azidoethyl)-1-(4-methoxybenzyl)hydrazine (**2.47b**, 0.0590 g, 0.267 mmol), DIPEA (0.14 mL, 0.800 mmol), hydroxybenzotriazole (0.0735 g, 0.533 mmol), and EDCI (0.0767 g, 0.400 mmol) and stirred at rt 2 d, diluted with CH_2Cl_2 (10 mL) and washed with a mixture of H_2O (2.0 mL) and satd. aqueous NaHCO_3 (5 mL). The combined organic layers were dried (Na_2SO_4), filtered and concentrated under reduced pressure. The crude residue was purified by chromatography on SiO_2 (hexanes/ EtOAc , 1:1 w/ 2% Et_3N) to give **2.50c** (0.0692 g, 0.143 mmol, 54%) as a colorless solid: Mp 110.6-114.4 $^\circ\text{C}$; IR (neat) 3174, 3061, 2829, 2099, 1642, 1610, 1549, 1510, 1301, 1243, 1228, 1176, 1034, 822, 725 cm^{-1} ; ^1H NMR (400 MHz, CDCl_3) δ 7.81 (s, 1 H), 7.64 (d, $J = 8.4$ Hz, 1 H), 7.36 (d, $J = 7.6$ Hz, 2 H), 7.28 (d, $J = 11.6$ Hz, 2 H), 7.11 (d, $J = 7.6$ Hz, 2 H), 6.90 (t, $J = 7.6$ Hz, 4 H), 6.59 (s, 1 H), 5.28 (s, 2 H), 4.30 (s, 2 H), 3.81 (s, 6 H), 3.47 (bs, 2 H), 3.42 (bs, 2 H); ^{13}C NMR (100 MHz, CDCl_3) δ 168.3, 159.2, 159.1, 137.7, 131.3, 130.6 (2 C), 128.8, 128.7, 128.3, 126.5, 120.7, 117.2, 114.2, 113.8, 109.6, 101.8, 59.6, 55.2, 55.1, 54.3, 49.5, 49.0; HRMS (ESI) m/z calcd for $\text{C}_{27}\text{H}_{29}\text{N}_6\text{O}_3$ ($[\text{M}+\text{H}]^+$) 485.2296, found 485.2292.



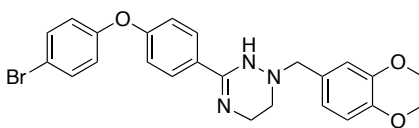
2.51c

1-(4-Methoxybenzyl)-6-(1-(4-methoxybenzyl)-1,2,5,6-tetrahydro-1,2,4-triazin-3-yl)-1H-indole (2.51c). A solution of *N'*-(2-azidoethyl)-*N'*,1-bis(4-methoxybenzyl)-1H-indole-6-carbohydrazide (**2.50c**, 0.0400 g, 0.0826 mmol) in PhCl (4.0 mL) (sparged with Ar for 20 min) was treated with a solution of P(Me)₃ (1 M solution in toluene, 0.25 mL, 0.248 mmol) and irradiated in the microwave at 180 °C for 1 h. The reaction was applied directly to a column pre-equilibrated with hexanes and purified by chromatography on SiO₂ (hexanes/EtOAc, 1:3 w/ 5% Et₃N) to give **2.51c** (0.0198 g, 0.0449 mmol, 55%) as a yellow oil: IR (neat) 3383, 2951, 2833, 1609, 1510, 1461, 1355, 1241, 1174, 1023, 1007, 818, 759, 701 cm⁻¹; ¹H NMR (400 MHz, CDCl₃) δ 7.66 (s, 1 H), 7.59 (d, *J* = 8.0 Hz, 1 H), 7.39-7.36 (m, 3 H), 7.11 (d, *J* = 3.6 Hz, 1 H), 7.06 (d, *J* = 8.8 Hz, 2 H), 6.87 (d, *J* = 8.6 Hz, 2 H), 6.83 (d, *J* = 8.6 Hz, 2 H), 6.50 (d, *J* = 3.6 Hz, 1 H), 5.27 (s, 2 H), 4.16 (s, 2 H), 3.80 (s, 3 H), 3.77 (s, 3 H), 3.56 (bs, 2 H), 2.72 (t, *J* = 5.0 Hz, 2 H); ¹³C NMR (100 MHz, CDCl₃) δ 159.1, 158.8, 136.2, 130.6, 130.2, 129.4 (2 C), 129.1, 128.2, 120.7, 117.3, 114.1, 113.5, 107.2, 101.6, 63.3, 55.2 (2 C), 49.4, 45.1, 41.9; HRMS (ESI) *m/z* calcd for C₂₇H₂₉N₄O₂ ([M+H]⁺) 441.2285, found 441.2283.



***N'*-(2-Azidoethyl)-4-(4-bromophenoxy)-*N'*-(3,4-dimethoxybenzyl)benzohydrazide.** A solution of 4-(4-bromophenoxy)benzoic acid (**2.49b**, 0.600 g, 2.05 mmol), HATU (1.17 g, 3.07 mmol), and HOAt (0.418 g, 3.07 mmol) in DMF (18 mL) cooled to 0 °C was treated with DIPEA (1.4 mL, 8.19 mmol) and stirred at 0 °C for 1 h. The reaction was treated, at 0 °C, with a

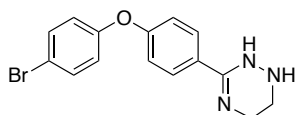
solution of 1-(2-azidoethyl)-1-(3,4-dimethoxybenzyl)hydrazine (**2.47c**, 0.955 g, 2.66 mmol) in DMF (2 mL). The reaction was allowed to warm to rt for 24 h, diluted with EtOAc (200 mL) and satd. aqueous NaHCO₃ (200 mL). The layers were separated and the aqueous layer was extracted with EtOAc (2 x 150 mL). The combined organic layers were washed with brine (2 x 150 mL), dried (Na₂SO₄) and concentrated under reduced pressure. The residue was purified twice by automated chromatography on SiO₂ (12 g column, liquid load with CH₂Cl₂, hexanes to hexanes/EtOAc, 1:1) to give *N'*-(2-azidoethyl)-4-(4-bromophenoxy)-*N'*-(3,4-dimethoxybenzyl)benzohydrazide (1.01 g, 1.91 mmol, 93%) as a pale yellow oil: IR (CH₂Cl₂) 3303, 2952, 2097, 1650, 1512, 1478, 1260, 1230, 1156, 1025, 837 cm⁻¹; ¹H NMR (400 MHz, Acetone-d₆) δ 8.76 (s, 1 H), 7.78 (dt, *J* = 9.4, 2.4 Hz, 1 H), 7.57 (dt, *J* = 9.4, 2.8 Hz, 2 H), 7.16 (d, *J* = 1.6 Hz, 1 H), 7.03-6.98 (m, 4 H), 6.87-6.81 (m, 2 H), 4.21 (s, 2 H), 3.76 (s, 3 H), 3.75 (s, 3 H), 3.44 (dd, *J* = 6.5, 4.7 Hz, 2 H), 3.33 (dd, *J* = 6.5, 4.7 Hz, 2 H); ¹³C NMR (100 MHz, Acetone-d₆) δ 166.4, 160.3, 156.6, 150.2, 149.6, 133.8, 131.4 (2 C), 130.2, 122.2, 121.8, 118.7, 117.0, 113.6, 112.1, 60.9, 56.0 (2 C), 55.9, 49.5; HRMS (ESI) *m/z* calcd for C₂₄H₂₅BrN₅O₄ ([M+H]⁺) 526.1084, found 526.1085.



2.53

3-(4-(4-Bromophenoxy)phenyl)-1-(3,4-dimethoxybenzyl)-1,2,5,6-tetrahydro-1,2,4-triazine (2.53**).** To two flame-dried 20 mL microwave vials each containing a solution of *N'*-(2-azidoethyl)-4-(4-bromophenoxy)-*N'*-(3,4-dimethoxybenzyl)benzohydrazide (0.400 g, 0.760 mmol) in freshly distilled and degassed PhCl (16 mL) was added PMe₃ (1 M in THF) (1.5 mL, 1.52 mmol). The mixture was first warmed in an oil bath (preheated to 60 °C) for 30 min until

the evolution of gas had ceased. The microwave vial was sealed and heated at 180 °C for 2 h in the microwave. TLC analysis (hexanes/EtOAc, 1:2) showed the starting material had been consumed. The reactions were combined and the pale yellow solution was loaded directly onto a SiO₂ column preequilibrated with hexanes w/ 2 % Et₃N followed by chromatography on SiO₂ (hexanes/EtOAc, 1:1) to give **2.53** (0.409 g, 0.848 mmol, 56%) as a colorless solid: Mp 88.3-92.1 °C; IR (CH₂Cl₂) 3323, 2831, 1607, 1512, 1476, 1240, 1165, 1030, 834, 734 cm⁻¹; ¹H NMR (400 MHz, MeOD-d₄) δ 7.65 (dt, *J* = 9.2, 2.5 Hz, 2 H), 7.50 (dt, *J* = 9.6, 2.8 Hz, 2 H), 7.08 (d, *J* = 1.8 Hz, 1 H), 7.00 (dt, *J* = 9.2, 2.5 Hz, 2 H), 6.97-6.90 (m, 4 H), 4.05 (s, 2 H), 3.84 (s, 3 H), 3.82 (s, 3 H), 3.49 (t, *J* = 5.0 Hz, 2 H), 2.69 (t, *J* = 5.0 Hz, 2 H); ¹³C NMR (100 MHz, MeOD-d₄) δ 159.3, 157.6, 150.3, 149.9, 149.4, 134.0, 131.8, 131.2, 129.1, 123.2, 122.0, 119.4, 117.1, 114.3, 112.6, 64.0, 56.5, 56.4, 46.4, 42.0; HRMS (ESI) *m/z* calcd for C₂₄H₂₅BrN₃O₃ ([M+H]⁺) 482.1074, found 482.1071.

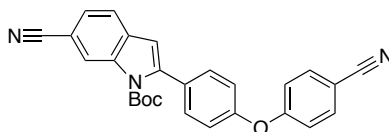


2.52

3-(4-(4-Bromophenoxy)phenyl)-1,2,5,6-tetrahydro-1,2,4-triazine (2.52). (deprotection of 3,4-dimethoxybenzyl protected triazine) A solution of 3-(4-(4-bromophenoxy)phenyl)-1-(3,4-dimethoxybenzyl)-1,2,5,6-tetrahydro-1,2,4-triazine (**2.53**, 0.0500 g, 0.104 mmol) in 4 M HCl in dioxane (2.5 mL) was heated at 50 °C for 2.5 d, diluted with Et₂O (20 mL) and the resulting precipitate was pelleted in the centrifuge and the supernatant removed and repeated 2 times. The resulting pellet was suspended in EtOAc (20 mL) and basified with 1 M NaOH (3 mL). The layers were separated and the aqueous layer was further extracted with EtOAc (2 x 10 mL). The combined organic layers were dried (Na₂SO₄), filtered and concentrated under reduced pressure.

The crude residue was purified by automated chromatography on SiO₂ (4 g column, liquid load CH₂Cl₂, gradient 100% CH₂Cl₂ to 10% MeOH/CH₂Cl₂; product eluted at 10% MeOH:CH₂Cl₂) to give **2.52** (0.0217 g, 0.0653 mmol, 63%) as a tan/orange waxy solid: IR (CH₂Cl₂) 3293, 2951, 1622, 1579, 1478, 1336, 1234, 1165, 1068, 749 cm⁻¹; ¹H NMR (400 MHz, CDCl₃) δ 7.55 (dt, *J* = 9.2, 2.4 Hz, 2 H), 7.43 (dt, *J* = 9.4, 2.7 Hz, 2 H), 6.96 (dt, *J* = 9.2, 2.4 Hz, 2 H), 6.88 (dt, *J* = 9.4, 2.7 Hz, 2 H), 4.53 (bs, 1 H), 3.64 (t, *J* = 4.9 Hz, 2 H), 3.17 (t, *J* = 4.9 Hz, 2 H); ¹³C NMR (100 MHz, CDCl₃) δ 157.6, 156.0, 145.3, 132.7, 130.6, 127.0, 120.7, 118.6, 116.0, 41.9, 40.4; HRMS (ESI) *m/z* calcd for C₁₅H₁₅BrN₃O ([M+H]⁺) 332.0393, found 332.0388.

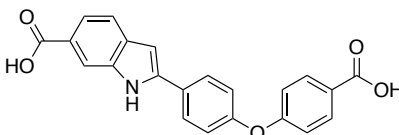
5.3.4 Synthesis of 6-(1,2,5,6-Tetrahydro-1,2,4-triazin-3-yl)-2-(4-(4-(1,2,5,6-tetrahydro-1,2,4-triazin-3-yl)phenoxy)phenyl)-1H-indole



2.60

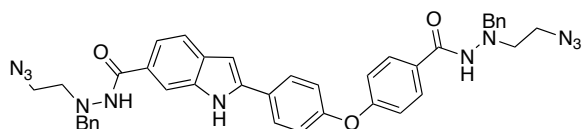
tert-Butyl 6-cyano-2-(4-(4-cyanophenoxy)phenyl)-1H-indole-1-carboxylate (2.60). A solution of 4-(4-bromophenoxy)benzonitrile (**2.57**, 0.750 g, 2.74 mmol) and tert-butyl 6-cyano-2-(trimethylstannyl)-1H-indole-1-carboxylate (**2.31**, 1.77 g, 3.28 mmol) in dry degassed DMF (15 mL) was treated with Pd(PPh₃)₂Cl₂ (0.192 g, 0.274 mmol) and (*i*Pr)CuCl²⁹³ (0.200 g, 0.410 mmol) at rt, heated to 80 °C for 18 h, cooled to rt, poured into H₂O (30 mL) and extracted with Et₂O (3 x 80 mL). The combined organic layers were washed with H₂O, brine, dried (Na₂SO₄), filtered, and concentrated under reduced pressure. The residue was purified by chromatography SiO₂ (gradient hexanes to hexanes/EtOAc, 5:1). The product was triturated/sonicated with methanol then decanted to give **2.60** (0.694 g, 1.59 mmol, 58%) as a colorless solid: ¹H NMR

(300 MHz, DMSO- d_6) δ 8.44 (bs, 1 H), 7.89 (d, $J = 8.4$ Hz, 2 H), 7.82 (d, $J = 8.3$ Hz, 1 H), 7.67 (d, $J = 8.3$ Hz, 1 H), 7.61 (d, $J = 8.4$ Hz, 2 H), 7.26 (d, $J = 8.4$ Hz, 2 H), 7.16 (d, $J = 8.4$ Hz, 2 H), 6.90 (s, 1 H), 1.33 (s, 9 H); ^{13}C NMR (75 MHz, DMSO- d_6) δ 160.6, 154.7, 148.8, 142.8, 135.7, 134.6, 132.2, 130.8, 129.8, 126.1, 121.8, 119.7, 119.6, 118.8, 118.5, 118.3, 109.7, 105.9, 105.5, 84.8, 27.0; HRMS (ESI) m/z calcd for $\text{C}_{23}\text{H}_{14}\text{N}_3\text{O}_3$ ($[\text{M}-t\text{Bu}+\text{H}]^+$) 380.1030, found 380.1024.



2.56

2-(4-(4-Carboxyphenoxy)phenyl)-1H-indole-6-carboxylic acid (2.56). A solution of *tert*-butyl 6-cyano-2-(4-(4-cyanophenoxy)phenyl)-1H-indole-1-carboxylate (**2.60**, 0.500 g, 1.15 mmol) in a mixture of EtOH (125 mL) and H₂O (125 mL) was treated with LiOH monohydrate (1.45 g, 34.5 mmol). The reaction mixture was heated to reflux for 11 d, cooled to rt and filtered. The filtrate was acidified with 1 M HCl to pH 2 and the resulting precipitate was collected by vacuum filtration, and washed with a small amount of H₂O. Toluene was added to the solid and concentrated under reduced pressure to give **2.56** (0.298 g, 0.799 mmol, 70%) as an off-white solid: Mp >350 °C; IR (MeOH) 3437, 3070, 2665, 1681, 1599, 1491, 1417, 1291, 1260, 1230, 1200, 837, 790, 771 cm^{-1} ; ^1H NMR (400 MHz, DMSO- d_6) δ 12.72 (bs, 2 H), 11.89 (s, 1 H), 8.02-7.96 (m, 5 H), 7.60 (dd, $J = 10.4, 76.0$ Hz, 2 H), 7.25 (d, $J = 6.6$ Hz, 2 H), 7.10 (d, $J = 6.6$ Hz, 2 H), 6.99 (s, 1 H); ^{13}C NMR (100 MHz, DMSO- d_6) δ 168.1, 166.6, 160.6, 155.1, 140.3, 136.3, 132.0, 131.7, 128.0, 127.3, 123.4, 120.3, 119.4, 117.5, 113.1, 98.9; HRMS (ESI) m/z calcd for $\text{C}_{22}\text{H}_{16}\text{NO}_5$ ($[\text{M}+\text{H}]^+$) 374.1023, found 374.1008.

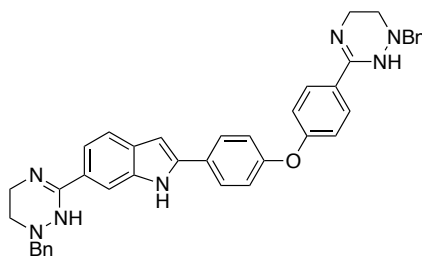


2.61a

N'-(2-Azidoethyl)-2-(4-(4-(2-(2-azidoethyl)-2-

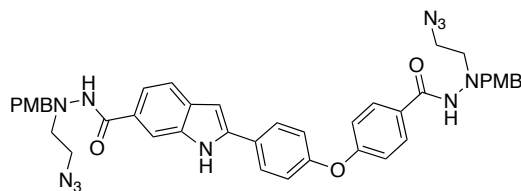
benzylhydrazinecarbonyl)phenoxy)phenyl)-*N'*-benzyl-1*H*-indole-6-carbohydrazide (**2.61a**).

A solution of 2-(4-(4-carboxyphenoxy)phenyl)-1*H*-indole-6-carboxylic acid (**2.56**, 0.200 g, 0.536 mmol), HATU (0.713 g, 1.87 mmol), and HOAt (0.219 g, 1.61 mmol) in DMF (4.0 mL) cooled to 0 °C was treated with DIPEA (0.60 mL, 3.21 mmol) and stirred at 0 °C for 2 h where the color had changed from a brown yellow to a brown orange. The reaction mixture was treated with a solution of 1-(2-azidoethyl)-1-benzylhydrazine (**2.47a**, 0.615 g, 3.21 mmol) in DMF (1.5 mL), warmed to rt, and stirred for 2 d, diluted with EtOAc (75 mL) and satd. aqueous NaHCO₃ (100 mL). The layers were separated and the aqueous layer was extracted with EtOAc (2 x 75 mL). The combined organic layers were washed with satd. aqueous NaHCO₃ (50 mL), brine (2 x 50 mL), dried (Na₂SO₄) and concentrated under reduced pressure. The crude residue was purified by chromatography on SiO₂ (hexanes/EtOAc, 1:4 w/ 2% Et₃N) followed by filtration through basic alumina (hexanes/EtOAc, 1:2 to hexanes/EtOAc, 1:4) to give **2.61a** (0.158 g, 0.220 mmol, 41%) as a pale yellow foam: IR (CH₂Cl₂) 3259, 2925, 2854, 2096, 1644, 1599, 1489, 1458, 1238, 1171, 752 cm⁻¹; ¹H NMR (500 MHz, Acetone-d₆) δ 10.92 (bs, 1 H), 8.81 (bs, 1 H), 8.71 (bs, 1 H), 7.93-7.90 (m, 2 H), 7.87 (s, 1 H), 7.80-7.78 (m, 2 H), 7.53 (d, *J* = 8.0 Hz, 1 H), 7.47-7.43 (m, 5 H), 7.29 (td, *J* = 7.4, 2.0 Hz, 5 H), 7.25-7.21 (m, 2 H), 7.16-7.13 (m, 2 H), 7.05-7.02 (m, 2 H), 6.91 (dd, *J* = 2.0, 0.7 Hz, 1 H), 4.34 (s, 2 H), 4.30 (s, 2 H), 3.50-3.46 (m, 4 H), 3.37 (td, *J* = 10.4, 4.4 Hz, 4 H) ; ¹³C NMR (125 MHz, Acetone-d₆) δ 168.1, 166.4, 163.3, 160.7, 157.1, 140.8, 139.3, 139.1, 137.7, 132.5, 130.2, 129.9 (2 C), 129.2, 129.0, 128.7, 128.0, 120.8, 120.4, 119.5, 118.7, 111.9, 99.9 (2 C), 61.2, 61.1, 55.8 (2 C), 49.8, 49.7; HRMS (ESI) *m/z* calcd for C₄₀H₃₈N₁₁O₃ ([M+H]⁺) 720.3154, found 720.3151.



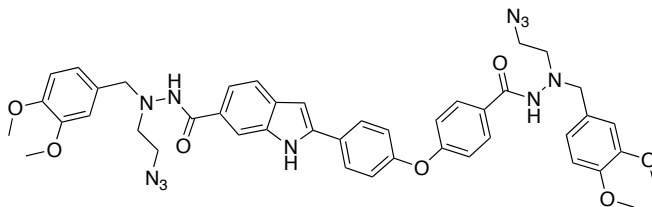
2.62a

6-(1-Benzyl-1,2,5,6-tetrahydro-1,2,4-triazin-3-yl)-2-(4-(4-(1-benzyl-1,2,5,6-tetrahydro-1,2,4-triazin-3-yl)phenoxy)phenyl)-1*H*-indole (2.62a). A solution of **2.61a** (0.130 g, 0.181 mmol) in degassed PhCl (14 mL) and THF (1 mL) was treated with a solution of PMe₃ (1 M solution in THF, 1.08 mL, 1.08 mmol) and the reaction was warmed to 50 °C for 2 h under an atmosphere of nitrogen. The reaction vessel was sealed and heated to 180 °C for 2 h. The resulting yellow solution was applied directly to a column of SiO₂ (equilibrated with hexanes w/ 3% Et₃N) and purified by chromatography on SiO₂ (hexanes to 4:1 EtOAc/Acetone w/ 3% Et₃N), and chromatographed on basic Al₂O₃ (EtOAc/Acetone, 2:1) to give **2.62a** (0.0239 g, 0.0378 mmol, 21%) as a pale yellow foam: IR (Acetone) 3657, 2990, 2889, 1611, 1489, 1382, 1242, 1153, 1072, 956, 821 cm⁻¹; ¹H NMR (400 MHz, Acetone-d₆) δ 10.71 (bs, 1 H), 7.88-7.85 (m, 2 H), 7.81 (s, 1 H), 7.78-7.74 (m, 2 H), 7.50-7.44 (m, 6 H), 7.32 (t, *J* = 7.6 Hz, 4 H), 7.26-7.23 (m, 2 H), 7.11-7.08 (m, 2 H), 7.04-7.00 (m, 2 H), 6.83 (bs, 1 H), 5.78 (bs, 1 H), 5.72 (bs, 1 H), 4.14 (s, 2 H), 4.13 (s, 2 H), 3.58-3.53 (m, 4 H), 2.73-2.70 (m, 4 H); ¹³C NMR (100 MHz, Acetone-d₆) δ 158.1, 157.6, 145.5, 143.7, 139.8, 139.6, 139.4, 138.1, 132.1, 130.6, 130.5, 130.0 (2 C), 128.9, 128.8, 127.7, 127.6, 127.5, 120.2, 120.0, 119.1, 118.4, 108.9, 99.6, 64.3, 64.2, 46.4, 46.2, 42.4, 42.3; HRMS (ESI) *m/z* calcd for C₄₀H₃₈N₇O ([M+H]⁺) 632.3132, found 632.3136.



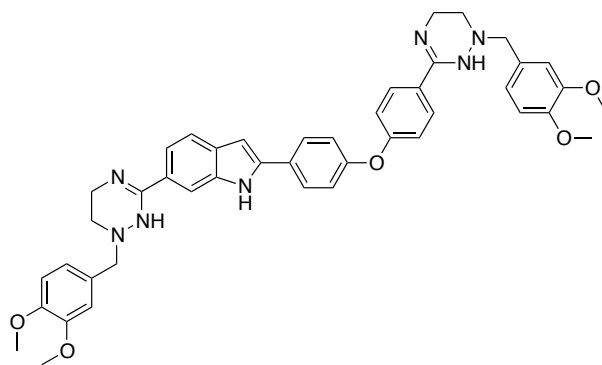
2.61b

***N'*-(2-azidoethyl)-2-(4-(4-(2-(2-azidoethyl)-2-(4-methoxybenzyl)hydrazinecarbonyl)phenoxy)phenyl)-*N'*-(4-methoxybenzyl)-1*H*-indole-6-carbohydrazide (2.61b).** A solution of 2-(4-(4-carboxyphenoxy)phenyl)-1*H*-indole-6-carboxylic acid (**2.56**, 0.100 g, 0.268 mmol) in CH₂Cl₂ (5 mL) was treated with PyBrOP (0.375 g, 0.804 mmol), 1-(2-azidoethyl)-1-(4-methoxybenzyl)hydrazine (**2.47b**, 0.148 g, 0.670 mmol) and DIPEA (0.37 mL, 2.14 mmol). The solution was stirred at rt for 17 h, poured onto H₂O (5 mL), and extracted with EtOAc (3 x 5 mL). The combined organic layers were and washed with 5% NaHCO₃, brine, dried (Na₂SO₄) and concentrated under reduced pressure. The crude residue was purified by chromatography on SiO₂ (hexanes/EtOAc, 1:1 with 5% Et₃N) to give **2.61b** (0.0512 g, 0.0657 mmol, 25%) as a light yellow solid: Mp 73.6-77.9 °C; IR (neat) 3241, 2930, 2093, 1642, 1610, 1510, 1487, 1454, 1301, 1234, 1171, 1031, 822 cm⁻¹; ¹H NMR (400 MHz, CDCl₃) δ 9.96 (bs, 1 H), 8.00 (s, 1 H), 7.77 (d, *J* = 8.4 Hz, 2 H), 7.57-7.53 (overlapping doublets, *J* = 8.4, 7.6 Hz, 3 H), 7.30-7.20 (m, 6 H), 7.02 (d, *J* = 8.8 Hz, 2 H), 6.95 (d, *J* = 8.8 Hz, 2 H), 6.84-6.77 (m, 5 H), 4.20 (s, 2 H), 4.18 (s, 2 H), 3.76 (s, 3 H), 3.73 (s, 3 H), 3.44-3.35 (m, 4 H), 3.32 (dd, *J* = 6.0, 5.2 Hz, 2 H), 3.27 (dd, *J* = 6.0, 5.2 Hz, 2 H); ¹³C NMR (100 MHz, CDCl₃) δ 168.3, 166.7, 160.2, 159.1 (2 C), 155.8, 140.4, 136.6, 132.0, 130.6, 130.5, 128.9, 128.4, 128.3, 128.1 (2 C), 127.3, 126.4, 120.1, 120.0, 118.0, 117.7, 113.8, 111.4, 99.4, 59.9, 59.7, 55.2 (2 C), 54.4, 49.0 (2 C); HRMS (ESI) *m/z* calcd for C₄₂H₄₂N₁₁O₅ ([M+H]⁺) 780.3365, found 780.3350.



2.61c

***N'*-(2-Azidoethyl)-2-(4-(4-(2-(2-azidoethyl)-2-(3,4-dimethoxybenzyl)hydrazinecarbonyl)phenoxy)phenyl)-*N'*-(3,4-dimethoxybenzyl)-1*H*-indole-6-carbohydrazide (2.61c).** A solution of 2-(4-(4-carboxyphenoxy)phenyl)-1*H*-indole-6-carboxylic acid (**2.56**, 0.0500 g, 0.134 mmol) in DMF (1.5 mL) was treated with HATU (0.204 g, 0.536 mmol), 1-(2-azidoethyl)-1-(3,4-dimethoxybenzyl)hydrazine (**2.47c**, 0.135 g, 0.536 mmol) and DIPEA (0.240 mL, 1.34 mmol). The reaction mixture was stirred at rt for 17 h, diluted with H₂O, and stirred at rt for 5 min, extracted with EtOAc (3 x 10 mL). The combined organic layers were washed with H₂O, satd. aqueous NaHCO₃, brine, dried (Na₂SO₄), filtered, and concentrated under reduced pressure. The crude residue was purified by chromatography on SiO₂ (hexanes/EtOAc, 1:6 to EtOAc with 2% Et₃N) to give **2.61c** (0.0429 g, 0.0511 mmol, 38%) as an off-white foam: IR (neat) 3277, 2930, 2833, 2095, 1646, 1596, 1512, 1487, 1452, 1232, 1156, 1025, 727 cm⁻¹; ¹H NMR (300 MHz, CDCl₃) δ 9.86 (s, 1 H), 7.93 (s, 1 H), 7.75 (d, *J* = 8.4 Hz, 2 H), 7.57-7.50 (m, 3 H), 7.37 (s, 1 H), 7.27 (s, 1 H), 7.20 (d, *J* = 8.1 Hz, 1 H), 7.03-6.93 (m, 6 H), 6.86-6.71 (m, 5 H), 4.21 (bd, *J* = 4.2 Hz, 4 H), 3.82 (s, 3 H), 3.79 (s, 6 H), 3.74 (s, 3 H), 3.42-3.34 (m, 8 H); ¹³C NMR (75 MHz, CDCl₃) δ 168.4, 166.8, 160.2, 155.9, 149.0, 148.5, 140.4, 136.6, 132.0, 129.2, 128.9, 128.2, 128.0, 127.3, 126.5, 121.6, 121.4, 120.0, 118.1, 117.8, 112.4, 112.3, 111.3, 111.0, 99.4, 60.0, 55.8, 54.6, 48.9; HRMS (ESI) *m/z* calcd for C₄₄H₄₆N₁₁O₇ ([M+H]⁺) 840.3576, found 840.3574.



2.62c

6-(1-(3,4-Dimethoxybenzyl)-1,2,5,6-tetrahydro-1,2,4-triazin-3-yl)-2-(4-(4-(1-(3,4-dimethoxybenzyl)-1,2,5,6-tetrahydro-1,2,4-triazin-3-yl)phenoxy)phenyl)-1H-indole (2.62c).

Two flame-dried microwave vials each containing a solution of *N*⁷-(2-azidoethyl)-2-(4-(4-(2-(2-azidoethyl)-2-(3,4-dimethoxybenzyl)hydrazinecarbonyl)phenoxy)phenyl)-*N*⁷-(3,4-dimethoxybenzyl)-1*H*-indole-6-carbohydrazide (**2.61c**, 0.200 g, 0.238 mmol) in THF (6 mL) and chlorobenzene (12 mL) were sparged with Ar for 20 min, treated with PMe_3 (1 M solution in THF, 1.43 mL, 1.43 mmol) and heated at 180 °C in the microwave for 1 h. The two solutions were combined and concentrated under reduced pressure. The residue was dissolved in CH_2Cl_2 (100 mL) and washed with H_2O , brine, dried (Na_2SO_4), filtered, and concentrated under reduced pressure. The crude residue was purified by chromatography on SiO_2 (100% hexanes to MeOH/EtOAc, 1:9 with 2% Et_3N) to give **2.62c** (0.0947 g, 0.126 mmol, 27%) as a pale yellow foam: IR (CH_2Cl_2) 3419, 3268, 2992, 2947, 2880, 1668, 1603, 1512, 1488, 1462, 1352, 1236, 1156, 1025, 843, 735 cm^{-1} ; ^1H NMR (500 MHz, CDCl_3) δ 9.50 (s, 1 H), 7.89 (s, 1 H), 7.61 (d, J = 8.5 Hz, 2 H), 7.56 (d, J = 8.5 Hz, 2 H), 7.49 (d, J = 8.5 Hz, 1 H), 7.30 (dd, J = 8.0, 1.0 Hz, 1 H), 7.04 (d, J = 1.5 Hz, 1 H), 6.98 (dd, J = 9.0, 2.0 Hz, 4 H), 6.94-6.89 (m, 2 H), 6.82 (d, J = 8.0 Hz, 1 H), 6.77 (d, J = 8.0 Hz, 1 H), 6.66 (d, J = 1.0 Hz, 1 H), 4.70 (bs, 1 H), 4.47 (s, 1 H), 4.14 (s, 4 H), 3.87 (s, 6 H), 3.83 (s, 3 H), 3.77 (s, 3 H), 3.56-3.52 (m, 4 H), 2.77 (t, J = 4.8 Hz, 2 H),

2.73 (t, $J = 4.8$ Hz, 2 H); ^{13}C NMR (125 MHz, CDCl_3) δ 157.6, 156.7, 148.8, 148.3, 148.2, 147.0, 144.5, 138.9, 136.9, 130.8, 130.6 (2 C), 130.1, 128.8, 127.7, 127.1, 126.9, 121.6 (2 C), 120.0, 119.1, 118.7, 117.4, 112.5, 112.4, 110.8, 109.1, 99.1, 63.8, 63.7, 55.9, 55.8, 45.5, 45.1, 41.7, 46.6; HRMS (ESI) m/z calcd for $\text{C}_{44}\text{H}_{46}\text{N}_7\text{O}_5$ ($[\text{M}+\text{H}]^+$) 752.3555, found 752.3537.

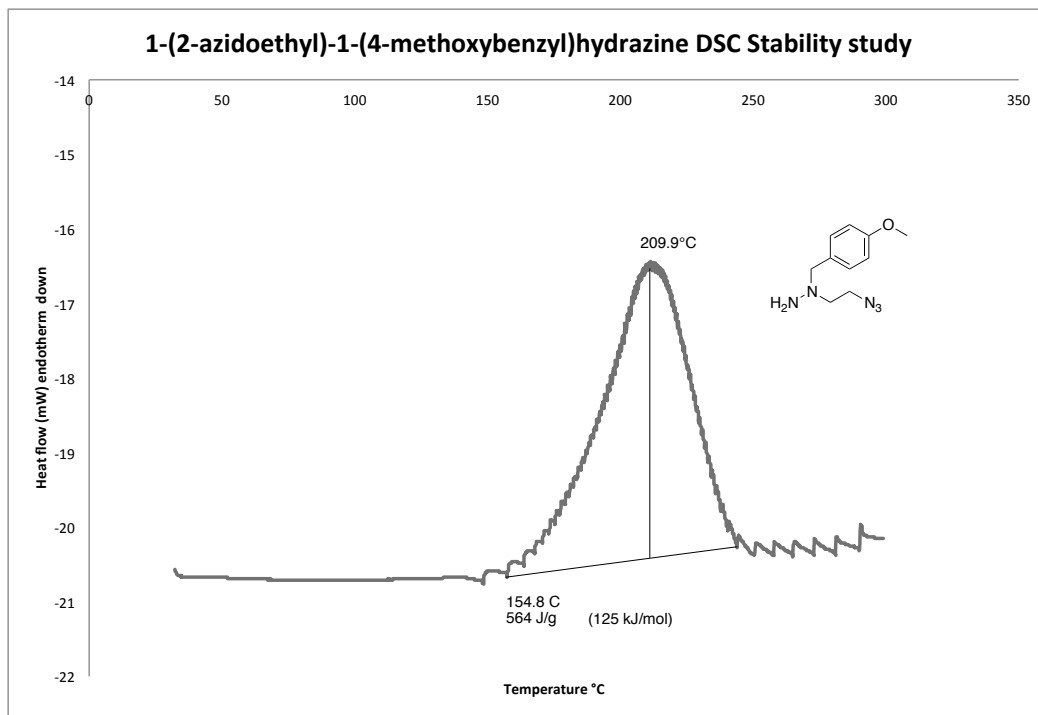
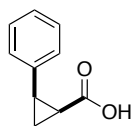


Figure 5.1. DSC thermogram for **2.47b**.

Table 5.1. DSC data for hydrazines **2.47b** and **2.47c**.

Compound	Onset (°C)	Peak (°C)	Energy J/g	Energy kJ/mol
2.47b	154.8	209.9	564.4	124.8
2.47c	185.3	238.5	490.7	123.7
Trityl azide	167.9	198.0	612.5	174.6

5.4 CHAPTER 3 EXPERIMENTAL PART

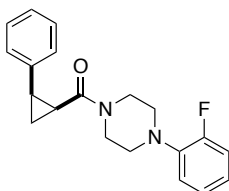


3.11

(1*RS*,2*SR*)-2-Phenylcyclopropanecarboxylic acid (3.11).⁴¹³ A solution of 3-phenylpropionic acid (**3.9**, 1.60 g, 10.9 mmol) and quinoline (4.1 mL, 34.1 mmol) in EtOH (80 mL) at rt was treated with Lindlar catalyst (5% Pd on CaCO₃, lead poisoned, 1.17 g, equivalent to 5 mol% Pd). The flask was evacuated and back-filled with H₂ (3x) using a balloon. The resulting suspension was stirred for 20 h, filtered through a short pad of Celite, washed (EtOAc), and concentrated under reduced pressure. The residue was dissolved in ether and washed with 1 M aqueous HCl. The organic phase was dried (Na₂SO₄), filtered, and concentrated under reduced pressure to give a mixture of *cis*-cinnamic acid (**3.10**) and *trans*-cinnamic acid (ratio 5:1, 0.527 g, 3.56 mmol) as a brown liquid.

A solution of Et₂Zn (1 M in CH₂Cl₂, 1.1 mL Et₂Zn in 10.5 mL CH₂Cl₂, 10.5 mmol) was diluted with CH₂Cl₂ (8.0 mL) and treated with a solution of TFA (0.78 mL, 10.5 mmol) in CH₂Cl₂ (6.0 mL) at 0 °C under an Ar atmosphere, stirred for 20 min, treated with a solution of CH₂I₂ (0.85 mL, 10.5 mmol) in CH₂Cl₂ (6.0 mL) stirred for 20 min and treated with a solution of *cis/trans*-cinnamic acid (0.520 g, 3.51 mmol) in CH₂Cl₂ (10 mL) was added to the mixture. The reaction was stirred at rt for 16 h, diluted with satd. aqueous NH₄Cl, extracted with Et₂O, dried (MgSO₄), filtered, and concentrated under reduced pressure. The crude residue was purified by automated chromatography on SiO₂ (12 g column, liquid load CH₂Cl₂, gradient 100% hexanes to 30% EtOAc/hexanes) and, following recrystallization (toluene), to give **3.11** (0.0690 g, 0.591

mmol, 6% (2 steps)) as colorless needles: ^1H NMR (500 MHz, CDCl_3) δ 11.35 (bs, 1 H), 7.23-7.16 (m, 5 H), 2.58 (q, $J = 8.3$ Hz, 1 H), 1.99 (dd, $J = 8.3, 6.3$ Hz, 1 H), 1.62 (q, $J = 6.3$ Hz, 1 H), 1.34-1.29 (m, 1 H); ^{13}C NMR (125 MHz, CDCl_3) δ 177.4, 135.9, 129.2, 127.9, 126.7, 26.6, 21.4, 12.0.

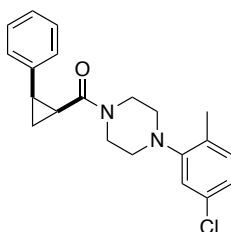


3.13a

(4-(2-fluorophenyl)piperazin-1-yl)((1*S*,2*R*)-2-phenylcyclopropyl)methanone

(3.13a). A solution of (1*S*,2*R*)-2-phenylcyclopropanecarboxylic acid (**3.11**, 0.0260 g, 0.160 mmol) and HATU (0.0914 g, 0.240 mmol) in CH_2Cl_2 (1 mL) was cooled to 0 °C and treated with DIPEA (83 μL , 0.481 mmol) warmed to rt over 45 min, cooled to 0 °C and treated with a solution of 1-2-fluorophenyl piperazine (**3.12a**, 0.0318 g, 0.176 mmol) in CH_2Cl_2 (0.5 mL) and stirred at rt for 17 h, diluted with H_2O and washed with EtOAc (2×10 mL). The combined organic layers were washed with 1 M aqueous NaHSO_4 , satd. aqueous NaHCO_3 , dried (Na_2SO_4), and concentrated under reduced pressure. The crude residue was purified by automated chromatography on SiO_2 (4g column, liquid load CH_2Cl_2 , gradient 100% hexanes to 100% EtOAc) to give **3.13a** (0.0463 g, 0.0143 mmol, 89%) a light orange oil: IR (CH_2Cl_2) 3005, 2895, 1635, 1489, 1458, 1431, 1223, 1206, 1033, 749, 695 cm^{-1} ; ^1H NMR (400 MHz, CDCl_3) δ 7.26-7.22 (m, 2 H), 7.15-7.12 (m, 3 H), 7.04-6.98 (m, 2 H), 6.97-6.92 (m, 1 H), 6.70 (dt, $J = 8.8, 1.6$ Hz, 1 H), 3.88 (app dt, $J = 13.2, 3.6$ Hz, 1 H), 3.72 (app dt, $J = 13.2, 4.0$ Hz, 1 H), 3.60 (ddd, $J = 12.0, 8.8, 3.2$ Hz, 1 H), 3.32 (ddd, $J = 12.0, 8.4, 2.8$ Hz, 1 H), 2.97-2.94 (m, 2 H), 2.48-2.36 (m, 2 H), 2.21-2.12 (m, 2 H), 1.86 (dd, $J = 12.8, 5.6$ Hz, 1 H), 1.34 (ddd, $J = 8.4, 8.4, 5.2$ Hz, 1 H); ^{13}C

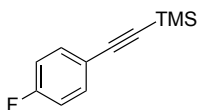
NMR (100 MHz, CDCl₃) δ 167.1, 155.6 (d, J_{CF} = 244.0 Hz), 139.6 (d, J_{CF} = 9.0 Hz), 137.5, 128.1, 127.3, 126.3, 124.4 (d, J_{CF} = 4.0 Hz), 122.9 (d, J_{CF} = 32.0 Hz), 119.0 (d, J_{CF} = 3.0 Hz), 116.1 (d, J_{CF} = 21 Hz), 50.7, 50.3, 45.2, 41.8, 24.3, 24.0, 10.5; HRMS (ESI) m/z calcd for C₂₀H₂₂FN₂O ([M+H]⁺) 325.1711, found 325.1711.



3.13b

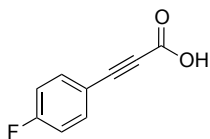
(4-(5-chloro-2-methylphenyl)piperazin-1-yl)((1SR,2RS)-2-phenylcyclopropyl)methanone (3.13b). A solution of (1SR,2RS)-2-phenylcyclopropanecarboxylic acid (**3.11**, 0.0260 g, 0.160 mmol) and HATU (0.0914 g, 0.240 mmol) in CH₂Cl₂ (1 mL) was cooled to 0 °C and treated with DIPEA (83 μ L, 0.481 mmol) and warmed to rt over 45 min. The solution was cooled to 0 °C again and added a solution of 1-(5-chloro-2-methylphenyl)piperazine (**3.12b**, 0.0372 g, 0.176 mmol) in CH₂Cl₂ (0.5 mL) and stirred at rt for 17 h, diluted with H₂O and washed with EtOAc (2 \times 10 mL). The combined organic layers were washed with 1 M aqueous NaHSO₄, satd. aqueous NaHCO₃, dried (Na₂SO₄), and concentrated. The crude residue was purified by automated chromatography on SiO₂ (4g column, liquid load CH₂Cl₂, gradient 100% hexanes to 100% EtOAc) to give the **3.13b** (0.0169 g, 0.0476 mmol, 30%) a light orange oil: IR (CH₂Cl₂) 3018, 2913, 1635, 1487, 1458, 1431, 1223, 1206, 1033, 697 cm⁻¹; ¹H NMR (400 MHz, CDCl₃) δ 7.31-7.28 (m, 2 H), 7.22 (tt, J = 7.2, 1.6 Hz, 1 H), 7.18-7.15 (m, 2 H), 7.05 (d, J = 8.2 Hz, 1 H), 6.94 (dd, J = 8.2, 2.0 Hz, 1 H), 6.63 (d, J = 2.0 Hz, 1 H), 3.96 (app d, J = 12.8 Hz, 1 H), 3.76 (app d, J = 12.8 Hz, 1 H), 3.54-3.48 (m, 1 H), 3.22-3.16 (m, 1 H), 2.70-2.66 (m, 2 H), 2.45 (ddd, J = 9.2, 9.2, 7.2 Hz, 1 H), 2.21-2.13 (m, 5 H), 1.95-

1.89 (m, 1 H), 1.86 (dd, $J = 12.8, 6.0$ Hz, 1 H), 1.36 (ddd, $J = 8.4, 8.4, 5.6$ Hz, 1 H); ^{13}C NMR (100 MHz, CDCl_3) δ 167.3, 152.0, 137.7, 131.9, 131.7, 131.1, 128.3, 127.4, 126.6, 123.5, 119.9, 51.6, 45.6, 42.2, 24.6, 24.1, 17.3, 10.7; HRMS (ESI) m/z calcd for $\text{C}_{21}\text{H}_{24}\text{ClN}_2\text{O}$ ($[\text{M}+\text{H}]^+$) 355.1572, found 355.1570.



3.15a

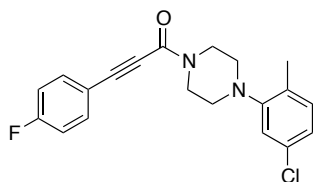
((4-Fluorophenyl)ethynyl)trimethylsilane (3.15a).^{415,481} A solution of $\text{Pd}(\text{PPh}_3)_2\text{Cl}_2$ (0.361 g, 0.514 mmol), CuI (0.0979 g, 0.514 mmol), and 4-fluorobromobenzene (**3.14a**, 5.66 mL, 51.4 mmol) in Et_3N (110 mL) was sparged with Ar for 15 min and treated with (trimethylsilyl)acetylene (10.9 mL, 77.1 mmol) and the solution was sparged with Ar for 5 min. The reaction mixture was heated to 80 °C for 16 h, cooled to rt, filtered through Celite, washed (Et_2O) until the washes appeared colorless, and the combined filtrates were concentrated under reduced pressure. The crude residue was purified by chromatography on SiO_2 (hexanes) to give **3.15a** (9.03 g, 47.0 mmol, 91%) as a pale orange oil: ^1H NMR (300 MHz, CDCl_3) δ 7.47-7.42 (m, 2 H), 6.99 (t, $J = 8.7$ Hz, 2 H), 0.25 (s, 9 H); ^{13}C NMR (75 MHz, CDCl_3) δ 162.6 (d, $J_{\text{CF}} = 244.5$ Hz), 133.9 (d, $J_{\text{CF}} = 8.3$ Hz), 119.3 (d, $J_{\text{CF}} = 4.0$ Hz), 115.5 (d, $J_{\text{CF}} = 21.8$ Hz), 104.0, 93.8, -0.07.



3.16a

3-(4-Fluorophenyl)propionic acid (3.16a).⁴¹⁵ CsF (4.74 g, 31.2 mmol) was loaded into an oven-dried 250-mL round bottom flask in a glovebox. The flask was removed from the

glovebox, attached to a CO₂ balloon, equipped with a magnetic stirrer and a septum, and filled with anhydrous DMSO (60 mL). Neat ((4-fluorophenyl)ethynyl)trimethylsilane (**3.15a**, 5.00 g, 26.0 mmol) was added dropwise. The reaction mixture was stirred under an atmosphere of CO₂ at rt for 17 h, diluted with H₂O (600 mL) and washed with CH₂Cl₂ (2 × 150 mL). The aqueous layer was acidified at 0 °C to pH 1 with 6 M aqueous HCl and then extracted with Et₂O (3 × 200 mL). The combined organic layers were dried (MgSO₄), filtered, and concentrated under reduced pressure to give **3.16a** (3.02 g, 18.4 mmol, 71%) as an orange solid: ¹H NMR (400 MHz, Acetone-d₆) δ 11.74 (bs, 1 H), 7.71 (dd, *J* = 8.6, 5.6 Hz, 2 H), 7.26 (t, *J* = 8.6 Hz, 2 H); ¹³C NMR (100 MHz, Acetone-d₆) δ 164.8 (d, *J*_{CF} = 249.0 Hz), 154.7, 136.1 (d, *J*_{CF} = 9.0 Hz), 117.1 (d, *J*_{CF} = 22.5 Hz), 84.6, 81.8.

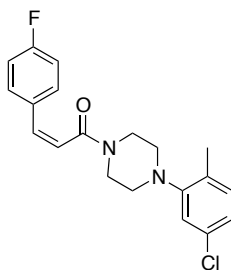


3.17a

1-(4-(5-Chloro-2-methylphenyl)piperazin-1-yl)-3-(4-fluorophenyl)prop-2-yn-1-one

(3.17a). A solution of 3-(4-fluorophenyl)propionic acid (**3.16a**, 3.00 g, 18.3 mmol) and 1-(5-chloro-2-methylphenyl)piperazine (**3.12b**, 4.62 g, 21.9 mmol) in anhydrous CH₂Cl₂ (180 mL) at 0 °C was treated with Et₃N (6.35 mL, 45.7 mmol), followed by dropwise addition of T3P (50 wt.% solution in EtOAc, 19.4 mL, 27.4 mmol). The reaction mixture was stirred at 0 °C for 30 min, warmed to rt for 24 h, diluted with CH₂Cl₂ (200 mL), washed with 1 M aqueous HCl (150 mL), dried (MgSO₄), filtered, and concentrated under reduced pressure. The residue was purified by chromatography on SiO₂ (hexanes/EtOAc, 2:1) to give **3.17a** (5.22 g, 14.6 mmol, 80%) as an off white solid: Mp 138.7-140.4 °C; IR (neat) 2924, 2216, 1625, 1596, 1504, 1443, 1431, 1219,

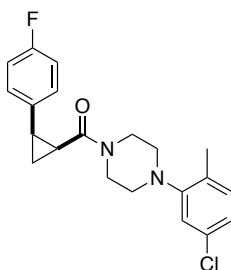
1038, 837 cm^{-1} ; ^1H NMR (300 MHz, CDCl_3) δ 7.55 (dd, $J = 7.5, 5.4$ Hz, 2 H), 7.12-6.94 (m, 5 H), 3.96 (app t, $J = 4.8$ Hz, 2 H), 3.82 (app t, $J = 4.8$ Hz, 2 H), 2.95 (app t, $J = 4.8$ Hz, 2 H), 2.87 (app t, $J = 4.8$ Hz, 2 H), 2.28 (s, 3 H); ^{13}C NMR (75 MHz, CDCl_3) δ 163.5 (d, $J_{\text{CF}} = 250.5$ Hz), 153.0, 151.7, 134.5 (d, $J_{\text{CF}} = 9.0$ Hz), 132.1, 131.8, 130.9, 123.7, 119.8, 116.4 (d, $J_{\text{CF}} = 3.8$ Hz), 116.0 (d, $J_{\text{CF}} = 22.5$ Hz), 89.9, 80.9, 51.9, 51.3, 47.4, 41.8, 17.3; HRMS (ESI) m/z calcd for $\text{C}_{20}\text{H}_{19}\text{ClFON}_2$ ($[\text{M}+\text{H}]^+$) 357.1164, found 357.1165.



3.18a

(Z)-1-(4-(5-Chloro-2-methylphenyl)piperazin-1-yl)-3-(4-fluorophenyl)prop-2-en-1-one (3.18a). A solution of 1-(4-(5-chloro-2-methylphenyl)piperazin-1-yl)-3-(4-fluorophenyl)prop-2-yn-1-one (5.00 g, 14.0 mmol) in dry EtOAc (140 mL) was treated with Lindlar catalyst (5% Pd on CaCO_3 , lead poisoned, 0.298 g, equivalent to 1 mol% Pd) and quinoline (0.83 mL, 7.01 mmol). The reaction vessel was placed under vacuum, backfilled with H_2 (balloon, 2x) and allowed to stir under an atmosphere of H_2 for 6 h. Analysis by TLC (2:1, hexanes/EtOAc) indicated that **3.17a** had been mostly consumed. The reaction mixture was filtered through Celite, washed (EtOAc), and the combined filtrates were washed with 1 M aqueous HCl, dried (MgSO_4), filtered, and concentrated under reduced pressure. The crude residue was purified by chromatography on SiO_2 (hexanes/EtOAc, 1:1) to give **3.18a** (3.15 g, 8.78 mmol, 63%, 87% brsm) as a colorless solid: IR (neat) 2913, 2239, 1616, 1506, 1437, 1223, 837, 725 cm^{-1} ; ^1H NMR (400 MHz, CDCl_3) δ 7.41-7.36 (m, 2 H), 7.08-7.02 (m, 3 H), 6.96 (dd, J

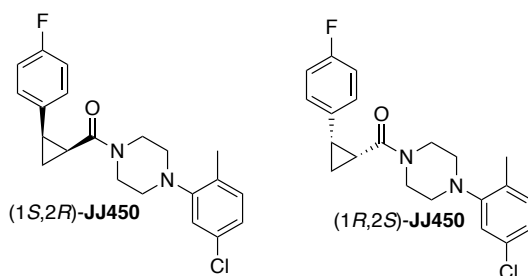
= 8.1, 2.1 Hz, 1 H), 6.80 (d, $J = 2.1$ Hz, 1 H), 6.66 (d, $J = 12.5$ Hz, 1 H), 6.05 (d, $J = 12.5$ Hz, 1 H), 3.80 (t, $J = 5.0$ Hz, 2 H), 3.49 (t, $J = 5.0$ Hz, 2 H), 2.80 (t, $J = 5.0$ Hz, 2 H), 2.53 (t, $J = 5.0$ Hz, 2 H), 2.21 (s, 3 H); ^{13}C NMR (100 MHz, CDCl_3) δ 167.3, 162.7 (d, $J_{\text{CF}} = 247.0$ Hz), 151.7, 132.6, 132.0, 131.8, 131.5 (d, $J_{\text{CF}} = 4.0$ Hz), 132.1, 131.8, 130.9, 130.2 (d, $J_{\text{CF}} = 9.0$ Hz), 123.6, 122.7, 119.6, 115.6 (d, $J_{\text{CF}} = 22$ Hz), 51.4, 51.2, 46.5, 41.5, 17.3; HRMS (ESI) m/z calcd for $\text{C}_{20}\text{H}_{21}\text{ClFON}_2$ ($[\text{M}+\text{H}]^+$) 359.1321, found 359.1329.



JJ450

(4-(5-Chloro-2-methylphenyl)piperazin-1-yl)((1RS,2SR)-2-(4-fluorophenyl)cyclopropyl)methanone (JJ450). THF (90 mL) was degassed by sparging with Ar for 60 min and treated at rt under Ar atmosphere with anhydrous CrCl_2 (6.43 g, 51.8 mmol) followed by (*Z*)-1-(4-(5-Chloro-2-methylphenyl)piperazin-1-yl)-3-(4-fluorophenyl)prop-2-en-1-one (**3.18a**, 3.10 g, 8.64 mmol) and CH_2I_2 (3.36 mL, 43.2 mmol). The reaction mixture was stirred for 20 h at 80 °C, cooled to rt, diluted with 1 M aqueous HCl (300 mL) and extracted with EtOAc (3 x 300 mL). The combined organic layers were filtered through a plug of basic Al_2O_3 , and concentrated under reduced pressure. The crude residue was purified by chromatography on SiO_2 (1:1, hexanes/EtOAc) to give an oil that was further purified twice by chromatography on basic Al_2O_3 (hexanes/EtOAc, 1:1) to give **JJ450** (2.76 g, 7.41 mmol, 86%) as a clear oil that solidified after storage on high vacuum: Mp 78.2-80.4 °C (hexanes); IR (CH_2Cl_2) 2936, 1637, 1592, 1510, 1487, 1435, 1223, 1033, 837, 815 cm^{-1} ; ^1H NMR (400 MHz, CDCl_3) δ 7.16-7.11 (m,

2 H), 7.07 (dd, $J = 8.1, 0.5$ Hz, 1 H), 7.00-6.94 (m, 3 H), 6.73 (d, $J = 2.1$ Hz, 1 H), 3.81-3.76 (m, 1 H), 3.71-3.60 (m, 2 H), 3.36 (ddd, $J = 12.4, 8.8, 3.1$ Hz, 1 H), 2.79-2.71 (m, 2 H), 2.45 (td, $J = 8.8, 7.0$ Hz, 1 H), 2.35-2.29 (m, 1 H), 2.26-2.16 (m, 5 H), 1.83 (dt, $J = 7.0, 5.6$ Hz, 1 H), 1.35 (td, $J = 8.8, 5.6$ Hz, 1 H); ^{13}C NMR (100 MHz, CDCl_3) δ 167.2, 161.7 (d, $J_{\text{CF}} = 244.0$ Hz), 151.9, 133.1 (d, $J_{\text{CF}} = 3.0$ Hz), 132.0, 131.8, 130.9, 129.1 (d, $J_{\text{CF}} = 8.0$ Hz), 123.6, 119.7, 115.0 (d, $J_{\text{CF}} = 21.0$ Hz), 51.8, 51.6, 45.6, 42.2, 23.8, 23.5, 17.3, 10.7; HRMS (ESI) m/z calcd for $\text{C}_{21}\text{H}_{23}\text{ClFON}_2$ ($[\text{M}+\text{H}]^+$) 373.1477, found 373.1478.



Racemic (4-(5-chloro-2-methylphenyl)piperazin-1-yl)((1*S*,2*R*)-2-(4-fluorophenyl)cyclopropyl)methanone (**JJ450**) was separated on a SFC Chiralpak-IC semiprep (250 x 10 mm) column (20% MeOH, 6 mL/min, 220 nM, P=100) to give (4-(5-chloro-2-methylphenyl)piperazin-1-yl)((1*S*,2*R*)-2-(4-fluorophenyl)cyclopropyl)methanone ((1*S*,2*R*)-**JJ450**) (retention time 13.1 min) as a colorless viscous oil (100% purity by ELSD): $[\alpha]_{\text{D}}^{20} -164.3$ (c 1.34, MeOH); ^1H NMR (300 MHz, CDCl_3) δ 7.17-7.10 (m, 2 H), 7.07 (d, $J = 8.1$ Hz, 1 H), 7.02-6.94 (m, 3 H), 6.72 (d, $J = 2.1$ Hz, 1 H), 3.83-3.75 (m, 1 H), 3.72-3.58 (m, 2 H), 3.39-3.31 (m, 1 H), 2.81-2.69 (m, 2 H), 2.45 (td, $J = 8.6, 6.9$ Hz, 1 H), 2.36-2.25 (m, 1 H), 2.25-2.15 (m, 5 H), 1.83 (dt, $J = 6.9, 5.6$ Hz, 1 H), 1.35 (td, $J = 8.6, 5.6$ Hz, 1 H); HRMS (ESI) m/z calcd for $\text{C}_{21}\text{H}_{23}\text{ClFON}_2$ ($[\text{M}+\text{H}]^+$) 373.1477, found 373.1476. The enantiomeric excess was >99.9% ee (SFC Chiralpak-IC (250 x 4.6 mm); 20% MeOH, 220 nM, 2 mL/min; retention time: 9.8 min).

(4-(5-Chloro-2-methylphenyl)piperazin-1-yl)((1*R*,2*S*)-2-(4-fluorophenyl)cyclopropyl)methanone ((1*S*,2*R*)-**JJ450**) (retention time 16.5 min) was obtained as a colorless viscous oil (100% purity by ELSD): $[\alpha]_D^{20} +167.1$ (*c* 1.27, MeOH); $^1\text{H NMR}$ (300 MHz, CDCl_3) δ 7.17-7.10 (m, 2 H), 7.07 (d, $J = 8.1$ Hz, 1 H), 7.01-6.94 (m, 3 H), 6.72 (d, $J = 2.1$ Hz, 1 H), 3.82-3.74 (m, 1 H), 3.71-3.60 (m, 2 H), 3.39-3.30 (m, 1 H), 2.81-2.68 (m, 2 H), 2.45 (td, $J = 8.6, 7.0$ Hz, 1 H), 2.35-2.26 (m, 1 H), 2.25-2.15 (m, 5 H), 1.83 (dt, $J = 7.0, 5.6$ Hz, 1 H), 1.35 (td, $J = 8.6, 5.6$ Hz, 1 H); HRMS (ESI) m/z calcd for $\text{C}_{21}\text{H}_{23}\text{ClFON}_2$ ($[\text{M}+\text{H}]^+$) 373.1477, found 373.1476. The enantiomeric excess was >99.9% ee (SFC Chiralpak-IC (250 x 4.6 mm); 20% MeOH, 220 nM, 2 mL/min; retention time: 12 min).

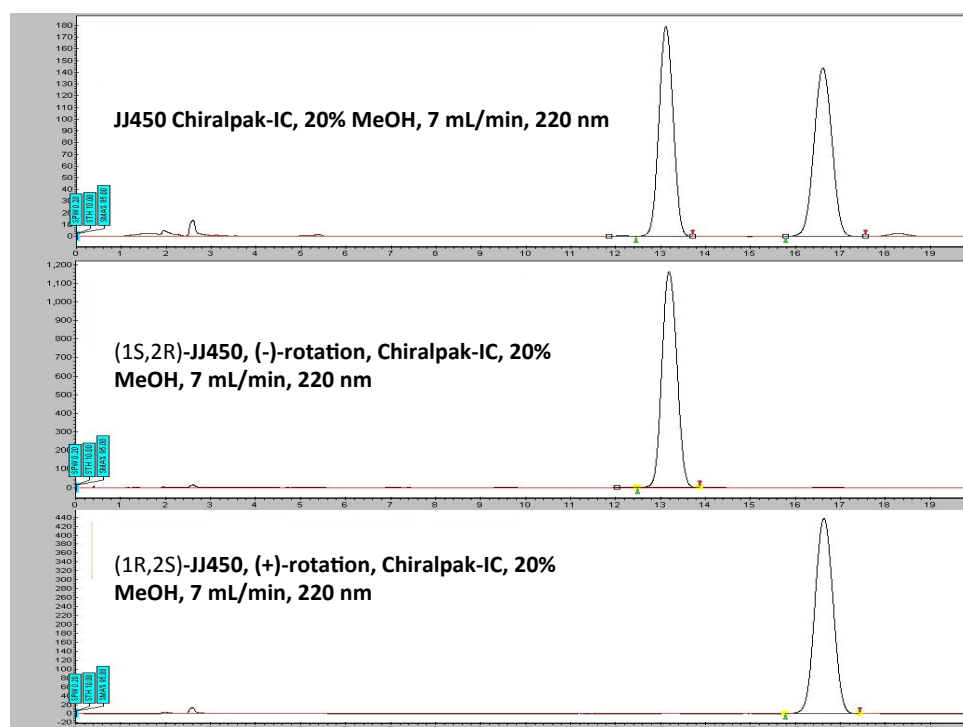
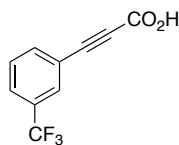


Figure 5.2. SFC chromatograms for **JJ450** and separated enantiomers.

5.4.1 Synthesis of JJ450 Analogs

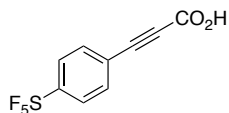


3.16b

3-(3-(Trifluoromethyl)phenyl)propionic acid (3.16b).^{415,482-483} A solution of Pd(PPh₃)₂Cl₂ (0.0306 g, 0.0436 mmol), CuI (0.00829 g, 0.0436 mmol), and 3-bromobenzotrifluoride **3.14b** (0.62 mL, 4.36 mmol) in Et₃N (8.7 mL) was sparged with Ar for 15 min and treated with (trimethylsilyl)acetylene (0.93 mL, 6.53 mmol) and sparged for an additional 2 min, heated to 80 °C for 16 h, cooled to rt, filtered through Celite, washed (Et₂O) until the washes appeared colorless and the filtrate was concentrated under reduced pressure. The crude residue was purified by chromatography on SiO₂ (hexanes) to give the trimethyl((3-(trifluoromethyl)phenyl)ethynyl)silane (**3.15b**, 1.03 g, 4.24 mmol) as a pale yellow oil.

A solution of CsF (0.775 g, 5.10 mmol) in dry DMSO (6.5 mL) under an atmosphere of CO₂ (balloon) at rt was treated with a solution of trimethyl((3-(trifluoromethyl)phenyl)ethynyl)silane (**3.15b**, 1.03 g, 4.25 mmol) dropwise and the reaction was stirred under CO₂ at rt for 17 h. The reaction mixture was diluted with H₂O (80 mL) and extracted with CH₂Cl₂ (2 × 25 mL). The aqueous layer was acidified (> pH 1) with 6 M aqueous HCl at 0 °C and extracted with Et₂O (3 × 25 mL). The combined organic layers were dried (MgSO₄), concentrated under reduced pressure, and dried under high vacuum to give **3.16b** (0.774 g, 3.62 mmol, 83% (2 steps)) as a pale tan orange waxy solid: ¹H NMR (400 MHz, Acetone-d₆) δ 11.85 (bs, 1 H), 7.95-7.87 (m, 3 H), 7.36 (t, *J* = 7.4 Hz, 1 H); ¹³C NMR (100 MHz,

Acetone-d₆) δ 154.3, 137.1, 131.7 (q, J_{CF} = 33.0 Hz), 130.0 (q, J_{CF} = 3.8 Hz), 128.1 (q, J_{CF} = 3.4 Hz), 124.5 (q, J_{CF} = 272.0 Hz), 121.7, 83.6, 82.9.

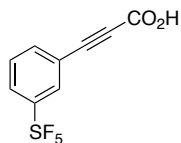


3.16c

3-(4-(Pentafluoro- λ 6-sulfaneyl)phenyl)propionic acid (3.16c). A solution of Pd(PPh₃)₂Cl₂ (0.0365 g, 0.0519 mmol), CuI (0.0100 g, 0.0519 mmol), and (4-bromophenyl)pentafluoro- λ 6-sulfane (**3.14c**, 1.50 g, 5.19 mmol) in Et₃N (11 mL) was sparged with Ar for 10 min, treated with (trimethylsilyl)acetylene (1.10 mL, 7.79 mmol), sparged with Ar for 5 min, heated to 80 °C for 22 h, cooled to rt, filtered through Celite, washed (Et₂O) until the washes appeared colorless, and the combined filtrates were concentrated under reduced pressure. The crude residue was purified by chromatography on SiO₂ (hexanes) to give **3.15c** (1.32 g, 4.40 mmol) as a pale yellow oil.

A solution of CsF (0.801 g, 5.27 mmol) in dry DMSO (3 mL) under CO₂ (balloon) at rt was treated with a solution of trimethyl((4-(pentafluoro- λ 6-sulfaneyl)phenyl)ethynyl)silane (**3.15c**, 1.32 g, 4.40 mmol) in DMSO (5.8 mL) dropwise and the reaction was stirred under CO₂ at rt for 25 h, diluted with H₂O (90 mL) and extracted with CH₂Cl₂ (2 \times 50 mL). The aqueous layer was acidified (> pH 1) with 6 M aqueous HCl at 0 °C and extracted with Et₂O (3 \times 50 mL). The combined organic layers were washed with H₂O (50 mL), dried (MgSO₄), concentrated under reduced pressure, and dried under high vacuum to give **3.16c** (0.338 g, 1.24 mmol, 24% (2 steps)) as light brown solid: Mp 156.5–159.6 °C; IR (CHCl₃) 2979, 2876, 2577, 2235, 1677, 1416, 1298, 1217, 886, 829, 751 cm⁻¹; ¹H NMR (400 MHz, CDCl₃) δ 10.00 (bs, 1 H), 7.82 (dt, J = 9.0, 2.0 Hz, 2 H), 7.73 (d, J = 9.0 Hz, 2 H); ¹³C NMR (100 MHz, CDCl₃) δ 157.7, 155.2 (quint,

$J_{CF} = 19.0$ Hz), 133.3, 126.5 (quint, $J_{CF} = 4.0$ Hz), 122.7, 85.9, 81.7; ^{19}F NMR (376 MHz, CDCl_3) δ 82.6 (quint, $J = 150.5$ Hz, 1 F), 62.3 (d, $J = 150.3$ Hz, 4 F); HRMS (ESI) m/z calcd for $\text{C}_9\text{H}_4\text{O}_2\text{F}_5\text{S}$ ($[\text{M}-\text{H}]^-$) 270.9858, found 270.9858.

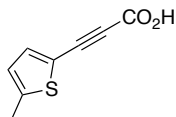


3.16d

3-(3-(Pentafluoro- λ 6-sulfaneyl)phenyl)propionic acid (3.16d). A solution of $\text{Pd}(\text{PPh}_3)_2\text{Cl}_2$ (0.0365 g, 0.0519 mmol), CuI (0.0100 g, 0.0519 mmol), and (3-bromophenyl)pentafluoro- λ 6-sulfane (**3.14d**, 1.50 g, 5.19 mmol) in Et_3N (11 mL) was sparged with Ar for 10 min, treated with (trimethylsilyl)acetylene (1.10 mL, 7.79 mmol), sparged with Ar for 5 min heated to 80 °C for 22 h, cooled to rt, filtered through Celite, washed (Et_2O) until the washes appeared colorless. The combined filtrates were concentrated under reduced pressure. The crude residue was purified by chromatography on SiO_2 (hexanes) to give **3.15d** (1.29 g, 4.29 mmol) as a yellow oil.

A solution of CsF (0.783 g, 5.15 mmol) in dry DMSO (3 mL) under CO_2 (balloon) at rt was treated a solution of trimethyl((3-(pentafluoro- λ 6-sulfaneyl)phenyl)ethynyl)silane (**3.15d**, 1.29 g, 4.30 mmol) in DMSO (5.6 mL) dropwise and the reaction was stirred under CO_2 at rt for 25 h. The reaction mixture was diluted with H_2O (90 mL) and extracted with CH_2Cl_2 (2×50 mL). The aqueous layer was acidified ($> \text{pH } 1$) with 6 M aqueous HCl at 0 °C and then extracted with Et_2O (3×50 mL). The combined organic layers were washed with H_2O (50 mL), dried (MgSO_4), concentrated under reduced pressure, and further dried under high vacuum to give **3.16d** (0.935 g, 3.43 mmol, 66% (2 steps)) as tan solid: Mp 121.1-124.4 °C; IR (CHCl_3) 2831, 2218, 1688, 1479, 1426, 1214, 831, 791, 768, 680 cm^{-1} ; ^1H NMR (400 MHz, CDCl_3) δ 10.92 (s,

1 H), 8.01 (t, $J = 2.0$ Hz, 1 H), 7.87 (ddd, $J = 8.0, 2.0, 0.9$ Hz, 1 H), 7.75 (d, $J = 8.0$ Hz, 1 H), 7.54 (t, $J = 8.0$ Hz, 1 H); ^{13}C NMR (100 MHz, CDCl_3) δ 158.1, 153.8 (quint, $J_{\text{CF}} = 19.0$ Hz), 135.9, 130.7 (quint, $J_{\text{CF}} = 5.0$ Hz), 129.3, 128.4 (quint, $J_{\text{CF}} = 4.0$ Hz), 120.2, 86.2, 81.0; ^{19}F NMR (376 MHz, CDCl_3) δ 82.5 (quint, $J = 150.4$ Hz, 1 F), 62.5 (d, $J = 150.4$ Hz, 4 F); HRMS (ESI) m/z calcd for $\text{C}_9\text{H}_4\text{O}_2\text{F}_5\text{S}$ ($[\text{M}-\text{H}]^-$) 270.9858, found 270.9856.

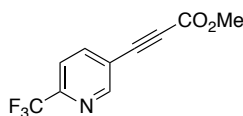


3.16e

3-(5-Methylthiophen-2-yl)propionic acid (3.16e).^{484-485 486} A solution of $\text{Pd}(\text{PPh}_3)_2\text{Cl}_2$ (0.0615 g, 0.0877 mmol), CuI (0.0167 g, 0.0877 mmol), and 2-bromo-5-methyl thiophene (**3.14e**, 1.00 mL, 8.77 mmol) in Et_3N (17.5 mL) sparged with Ar for 15 min and treated with (trimethylsilyl)acetylene (1.9 mL, 13.2 mmol) and the mixture was further sparged for 2 min, heated to 80 °C for 17 h, cooled to rt, filtered through Celite, washed (Et_2O) until the washes appeared colorless and the filtrate was concentrated under reduced pressure. The crude residue was purified by chromatography on SiO_2 (hexanes) to give the **3.15e** (1.06 g, 5.47 mmol) as a pale yellow oil.

To solution of CsF (0.994 g, 6.54 mmol) in dry DMSO (8 mL) under an atmosphere of CO_2 (balloon) at rt was added a solution of trimethyl((5-methylthiophen-2-yl)ethynyl)silane (**3.15e**, 1.06 g, 5.45 mmol) dropwise and the reaction was stirred under CO_2 at rt for 17 h. The reaction mixture was diluted with H_2O (100 mL) and extracted with CH_2Cl_2 (2×25 mL). The aqueous layer was acidified ($> \text{pH } 1$) with 6 M aqueous HCl at 0 °C and extracted with Et_2O (3×25 mL). The combined organic layers were washed with brine (50 mL), dried (MgSO_4), filtered, and concentrated under reduced pressure to give **3.16e** (0.571 g, 3.44 mmol, 39% (2 steps)) as a

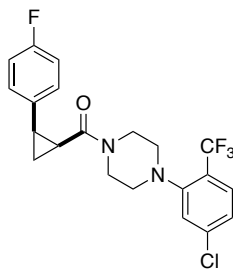
brown solid: ^1H NMR (300 MHz, CDCl_3) δ 10.14 (bs, 1 H), 7.36 (d, $J = 3.3$ Hz, 1 H), 6.73 (dd, $J = 3.3$ Hz, 1 H), 2.52 (s, 3 H).



Methyl 3-(6-(trifluoromethyl)pyridin-3-yl)propiolate. To two flasks each containing a solution of $\text{Pd}(\text{PPh}_3)_2\text{Cl}_2$ (0.0466 g, 0.0664 mmol), CuI (0.0126 g, 0.0664 mmol), and 5-bromo-2-trifluoromethyl pyridine (**3.14f**, 1.50 g, 6.64 mmol) in Et_3N (13 mL) sparged with Ar for 10 min followed by addition of (trimethylsilyl)acetylene (1.4 mL, 9.96 mmol) and sparged with Ar for 2 min. The resulting mixtures were heated to 80 °C for 16 h where analysis by TLC (hexanes/ EtOAc , 4:1) indicated that the SM had been consumed. After cooling the reaction to rt, the reactions were combined, the solution was filtered through Celite, which was washed with Et_2O (100 mL) until the washes appeared colorless. The filtrate was concentrated under reduced pressure. The crude residue was purified by chromatography on SiO_2 (hexanes/ EtOAc , 9:1) to give **3.15f** (3.37 g, 13.9 mmol) as orange/brown waxy solid.

A solution of CsF (2.52 g, 16.6 mmol) in DMSO (20 mL) under CO_2 at rt was treated with a solution of 2-(trifluoromethyl)-5-((trimethylsilyl)ethynyl)pyridine (**3.15f**, 3.37 g, 13.9 mmol) in DMSO (7 mL) dropwise and the reaction was stirred under CO_2 (balloon) at rt for 5 h, treated with MeI (0.95 mL, 15.2 mmol) was added and the solution was stirred for 1 h at rt. The reaction mixture was diluted with H_2O (200 mL), brine (100 mL) and extracted with Et_2O (3 \times 150 mL). The combined organic layers were washed with H_2O (100 mL), dried (MgSO_4), and concentrated under reduced pressure. The crude product was purified by chromatography on SiO_2 (hexanes/ EtOAc , 4:1) to give methyl 3-(6-(trifluoromethyl)pyridin-3-yl)propiolate (1.87 g, 8.17 mmol, 59% (2 steps)) as tan solid: Mp 98.2-99.7 °C; IR (neat) 2962, 2233, 1712, 1433,

1337, 1242, 1127, 1085, 864, 745 cm^{-1} ; ^1H NMR (400 MHz, CDCl_3) δ 8.87 (s, 1 H), 8.04 (ddd, J = 8.0, 1.2, 0.6 Hz, 1 H), 7.71 (d, J = 8.0 Hz, 1 H), 3.86 (s, 3 H); ^{13}C NMR (100 MHz, CDCl_3) δ 153.4, 153.1, 148.6 (q, J_{CF} = 35.5 Hz), 141.2, 121.0 (q, J_{CF} = 274.4 Hz), 120.1 (q, J_{CF} = 2.8 Hz), 120.0, 84.7, 80.7, 53.2; ^{19}F NMR (376 MHz, CDCl_3) δ -68.3 (s, 3 F); HRMS (ESI) m/z calcd for $\text{C}_{10}\text{H}_7\text{F}_3\text{NO}_2$ ($[\text{M}+\text{H}]^+$) 230.0423, found 230.0422.



3.21b

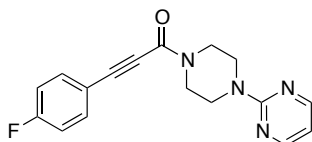
(4-(5-Chloro-2-(trifluoromethyl)phenyl)piperazin-1-yl)((1RS,2SR)-2-(4-fluorophenyl)cyclopropyl)methanone (3.21b). A solution of 3-(4-fluorophenyl)propionic acid (**3.16a**, 0.0800 g, 0.487 mmol) and 1-(5-chloro-2-(trifluoromethyl)phenyl)piperazinehydrochloride (**3.12b**, 0.142 g, 0.536 mmol) in CH_2Cl_2 (4.9 mL) at 0 °C was treated Et_3N (0.27 mL, 1.95 mmol). The cooled solution was treated with T3P (50% solution in EtOAc) (0.52 mL, 0.73 mmol) dropwise and the reaction was stirred at 0 °C for 30 min, warmed to rt for 24 h, diluted with CH_2Cl_2 (30 mL), washed with H_2O (20 mL), satd. aqueous NaHCO_3 (20 mL), dried (MgSO_4), filtered, and concentrated under reduced pressure. The crude material was purified by automated chromatography on SiO_2 (4g column, liquid load CH_2Cl_2 , gradient 100% hexanes to 30% EtOAc/hexanes) to give **3.17b** (0.140 g, 0.341 mmol) as a colorless solid.

A solution of 1-(4-(5-chloro-2-(trifluoromethyl)phenyl)piperazin-1-yl)-3-(4-fluorophenyl)prop-2-yn-1-one (**3.17b**, 0.140 g, 0.341 mmol) in EtOAc (3.4 mL) was treated with

Lindlar catalyst (5% Pd on CaCO₃, lead poisoned, 0.0363 g, equivalent to 5 mol% Pd). The reaction was placed under a balloon of H₂ (3 vacuum/backfill cycles) and stirred at rt for 2 d. TLC (hexanes/EtOAc, 2:1) indicated that the SM had been mostly consumed. The reaction was filtered through Celite (eluting with EtOAc (10 mL)) and the combined filtrates were concentrated under reduced pressure. The crude residue was purified by automated chromatography on SiO₂ (4g column, 100% hexanes to 40% EtOAc/hexanes, product eluted at 20% EtOAc/hexanes) to give **3.18b** (0.0510 g, 0.124 mmol) as a colorless solid.

A solution of CrCl₂ (0.0911 g, 0.741 mmol) and (Z)-1-(4-(5-chloro-2-(trifluoromethyl)phenyl)piperazin-1-yl)-3-(4-fluorophenyl)prop-2-en-1-one (**3.18b**, 0.0510 g, 0.124 mmol) in dry degassed THF (1.2 mL) was sparged with Ar for 5 min and treated with CH₂ICl (0.071 mL, 0.618 mmol) at rt, stirred for 2 d at 80 °C, cooled to rt, diluted with EtOAc (50 mL) and washed with 1 M aqueous HCl (3 x 20 mL). The organic layer was dried (MgSO₄), filtered and concentrated under reduced pressure. The crude residue was purified by automated chromatography on SiO₂ (4g column, liquid load CH₂Cl₂, 100% hexanes to 30% EtOAc/hexanes, product eluted at 20% EtOAc/hexanes), filtered through basic Al₂O₃ (CH₂Cl₂/EtOAc, 1:1) and concentrated under reduced pressure. The resulting oil was recrystallized from a mixture of hexanes/cyclohexane (1:1), the crystals were washed with hexanes and dried under high vacuum to give **3.21b** (0.0238 g, 0.0558 mmol, 11% (3 steps) (100% purity by ELSD)) as a colorless solid: Mp 101.0-103.2 °C; IR (CH₂Cl₂) 2917, 1639, 1513, 1418, 1308, 1225, 1126, 1085, 1031, 838 cm⁻¹; ¹H NMR (400 MHz, CDCl₃) δ 7.45 (dd, *J* = 8.4, 0.6 Hz, 1 H), 7.25-7.22 (m, 1 H), 7.16-7.11 (m, 2 H), 7.00 (d, *J* = 1.8 Hz, 1 H), 6.99-6.93 (m, 2 H), 3.92-3.86 (m, 1 H), 3.79-3.73 (m, 1 H), 3.67 (ddd, *J* = 12.6, 8.6, 3.2 Hz, 1 H), 3.37 (ddd, *J* = 12.6, 9.0, 3.2 Hz, 1 H), 3.01-2.95 (m, 2 H), 2.49-2.39 (m, 2 H), 2.31-2.25 (m, 1 H), 2.19 (ddd, *J* = 9.0, 8.6, 5.8 Hz, 1 H), 1.83 (dt, *J*

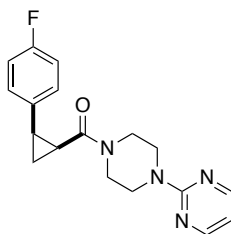
= 6.8, 5.8 Hz, 1 H), 1.36 (td, $J = 8.6, 5.6$ Hz, 1 H); ^{13}C NMR (100 MHz, CDCl_3) δ 167.2, 161.6 (d, $J_{\text{CF}} = 245.1$ Hz), 149.1, 132.5, 131.1, 130.1 (q, $J_{\text{CF}} = 32.7$ Hz), 129.1, 129.0, 123.6 (q, $J_{\text{CF}} = 272.2$ Hz), 120.8 (q, $J_{\text{CF}} = 3.8$ Hz), 117.2 (q, $J_{\text{CF}} = 3.8$ Hz), 115.0 (d, $J_{\text{CF}} = 21.3$ Hz), 51.3, 51.0, 45.3, 41.9, 23.9, 23.5 10.7; ^{19}F NMR (376 MHz, CDCl_3) δ -62.6 (s, 3 F), -116.4 (s, 1 F); HRMS (ESI) m/z calcd for $\text{C}_{21}\text{H}_{20}\text{ClF}_4\text{N}_2\text{O}$ ($[\text{M}+\text{H}]^+$) 427.1195, found 427.1192.



3.17c

3-(4-Fluorophenyl)-1-(4-(pyrimidin-2-yl)piperazin-1-yl)prop-2-yn-1-one (3.17c). A solution of 3-(4-fluorophenyl)propionic acid (**3.16a**, 0.150 g, 0.914 mmol) and 2-(1-piperazinyl)pyrimidine (**3.12f**, 0.188 g, 0.841 mmol) in CH_2Cl_2 (9.1 mL) at 0 °C was treated with Et_3N (0.51 mL, 3.66 mmol). The cooled solution was treated with T3P (50% solution in EtOAc) (1.0 mL, 1.37 mmol) dropwise and the reaction was stirred at 0 °C for 30 min, warmed to rt for 16 h, diluted with CH_2Cl_2 (30 mL), washed with H_2O (20 mL), dried (MgSO_4), filtered, and concentrated under reduced pressure. The crude material was purified by automated chromatography on SiO_2 (4g column, liquid load CH_2Cl_2 , gradient 100% hexanes to 100% EtOAc) to give **3.17c** (0.223 g, 0.719 mmol, 79%) as a colorless solid: Mp 168.4-170.8 °C; IR (CH_2Cl_2) 2859, 2217, 1618, 1585, 1506, 1435, 1355, 1261, 1227, 980, 838, 732 cm^{-1} ; ^1H NMR (400 MHz, CDCl_3) δ 8.34 (d, $J = 4.6$ Hz, 2 H), 7.56 (dd, $J = 8.8, 5.3$ Hz, 2 H), 7.08 (t, $J = 8.8$ Hz, 2 H), 6.56 (t, $J = 4.6$ Hz, 1 H), 3.95-3.93 (m, 2 H), 3.88 (app dd, $J = 6.6, 3.4$ Hz, 4 H), 3.76 (app dd, $J = 6.6, 4.1$ Hz, 2 H); ^{13}C NMR (100 MHz, CDCl_3) δ 163.6 (d, $J_{\text{CF}} = 253.0$ Hz), 161.4, 157.8, 153.1, 134.6 (d, $J_{\text{CF}} = 8.7$ Hz), 116.4 (d, $J_{\text{CF}} = 3.6$ Hz), 116.1 (d, $J_{\text{CF}} = 22.1$ Hz), 110.6,

90.0, 80.8, 46.8, 44.0, 43.3, 41.5; ^{19}F NMR (376 MHz, CDCl_3) δ -107.3 (s, 1 F); HRMS (ESI) m/z calcd for $\text{C}_{17}\text{H}_{16}\text{FN}_4\text{O}$ ($[\text{M}+\text{H}]^+$) 311.1303, found 311.1301.

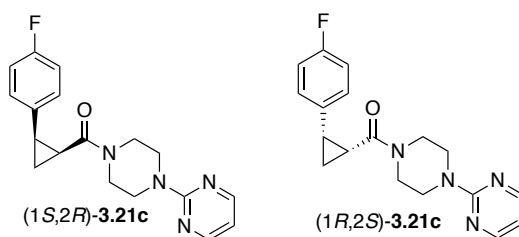


3.21c

((1*RS*,2*SR*)-2-(4-Fluorophenyl)cyclopropyl)(4-(pyrimidin-2-yl)piperazin-1-yl)methanone (3.21c). A solution of 3-(4-fluorophenyl)-1-(4-(pyrimidin-2-yl)piperazin-1-yl)prop-2-yn-1-one (**3.17c**, 0.200 g, 0.644 mmol) in EtOAc (6.4 mL) was treated with Lindlar catalyst (5% Pd on CaCO_3 , lead poisoned, 0.0685 g, equivalent to 5 mol% Pd). The reaction vessel was placed under vacuum and backfilled with H_2 (balloon, 4x) and stirred for 18 h at rt, filtered through Celite, washed (EtOAc), and the combined filtrates were concentrated under reduced pressure. The crude residue was purified by automated chromatography on SiO_2 (4g column, gradient 100% hexanes to 40% EtOAc/hexanes) to give **3.18c** (0.211 g, 0.676 mmol) as a colorless solid.

A solution of CrCl_2 (0.472 g, 3.84 mmol) and (Z)-3-(4-fluorophenyl)-1-(4-(pyrimidin-2-yl)piperazin-1-yl)prop-2-en-1-one (**3.18c**, 0.200 g, 0.640 mmol) in dry degassed THF (6.4 mL) (previously sparged with Ar for 15 min) was treated with CH_2I_2 (0.37 mL, 3.20 mmol) and further sparged with Ar for 2 min. The reaction mixture was stirred for 20 h at 80 °C, cooled to rt, diluted with EtOAc (10 mL), filtered through a plug of basic Al_2O_3 (EtOAc), and concentrated under reduced pressure. The crude material was purified by automated chromatography on SiO_2 (4g column, liquid load CH_2Cl_2 , gradient 100% hexanes to 60% EtOAc/hexanes) to give **3.21c** (0.128 g, 0.392 mmol, 61% (2 steps) (100% purity by ELSD)) as a colorless solid: Mp 141.9-

145.3 °C; IR (CH₂Cl₂) 2922, 1636, 1583, 1510, 1432, 1359, 1224, 1027, 981, 837, 797 cm⁻¹; ¹H NMR (400 MHz, CDCl₃) δ 8.28 (d, *J* = 4.6 Hz, 2 H), 7.12 (dd, *J* = 8.7, 5.3 Hz, 2 H), 6.92 (t, *J* = 8.7 Hz, 2 H), 6.50 (t, *J* = 4.6 Hz, 1 H), 4.00 (dt, *J* = 13.3, 4.4 Hz, 1 H), 3.93 (dt, *J* = 13.0, 4.4 Hz, 1 H), 3.76 (ddd, *J* = 13.0, 5.1, 3.6 Hz, 1 H), 3.66 (dt, *J* = 13.0, 4.4 Hz, 1 H), 3.53 (ddd, *J* = 13.0, 8.8, 3.6 Hz, 1 H), 3.26 (ddd, *J* = 13.0, 8.8, 3.4 Hz, 1 H), 3.13 (ddd, *J* = 13.0, 8.8, 3.6 Hz, 1 H), 3.00 (ddd, *J* = 13.0, 8.8, 3.6 Hz, 1 H), 2.49-2.43 (m, 1 H), 2.18 (ddd, *J* = 9.2, 8.4, 5.8 Hz, 1 H), 1.83 (q, *J* = 5.8 Hz, 1 H), 1.34 (td, *J* = 8.4, 5.8 Hz, 1 H); ¹³C NMR (100 MHz, CDCl₃) δ 167.3, 161.7 (d, *J*_{CF} = 244.9 Hz), 161.3, 157.7, 133.0, 129.0 (d, *J*_{CF} = 8.0 Hz), 115.0 (d, *J*_{CF} = 21.3 Hz), 110.3, 45.0, 43.8, 43.4, 41.6, 23.9, 23.5, 10.6; ¹⁹F NMR (470 MHz, CDCl₃) δ -116.4 (s, 1 F); HRMS (ESI) *m/z* calcd for C₁₈H₂₀FN₄O ([M+H]⁺) 327.1616, found 327.1616.



Racemic ((1*RS*,2*SR*)-2-(4-fluorophenyl)cyclopropyl)(4-(pyrimidin-2-yl)piperazin-1-yl)methanone (**3.21c**) was separated on a SFC Chiralpak-IC semiprep (250 x 10 mm) column (30% Methanol/CO₂, 7 mL/min, *p* = 100 bar, 90 μL injection, 20 mg/mL in MeOH) to give ((1*S*,2*R*)-2-(4-fluorophenyl)cyclopropyl)(4-(pyrimidin-2-yl)piperazin-1-yl)methanone ((1*S*,2*R*)-**3.21c**) (retention time 7.63 min) as a colorless solid (100% purity by ELSD): [α]_D¹⁷ -207.0 (*c* 0.53, MeOH); ¹H NMR (300 MHz, CDCl₃) δ 8.28 (d, *J* = 4.6 Hz, 1 H), 7.12 (dd, *J* = 8.6, 5.3 Hz, 1 H), 6.92 (t, *J* = 8.6 Hz, 1 H), 6.50 (t, *J* = 4.6 Hz, 1 H), 4.02-3.91 (m, 2 H), 3.79-3.73 (m, 1 H), 3.69-3.64 (m, 1 H), 3.56-3.48 (m, 2 H), 3.29-3.21 (m, 1 H), 3.16-3.08 (m, 1 H), 2.98 (ddd, *J* = 12.6, 9.0, 3.7 Hz, 1 H), 2.51-2.42 (m, 1 H), 2.18 (ddd, *J* = 9.0, 8.4, 6.0, 1 H), 1.83 (q, *J* = 5.6 Hz,

1 H), 1.35 (td, $J = 8.4, 5.6$ Hz, 1 H). The enantiomeric excess was >99.9% ee (SFC Chiralpak-IC (250 x 10 mm); 30% Methanol:CO₂, 7 mL/min, $p = 100$ bar, 220 nm; retention time: 8.0 min).

((1*R*,2*S*)-2-(4-Fluorophenyl)cyclopropyl)(4-(pyrimidin-2-yl)piperazin-1-yl)methanone ((1*R*,2*S*)-**3.21c**) (retention time 8.61 min) was obtained as a colorless solid (100% purity by ELSD): $[\alpha]^{17}_D +213.2$ (c 0.54, MeOH); ¹H NMR (300 MHz, CDCl₃) δ 8.28 (d, $J = 4.6$ Hz, 2 H), 7.12 (dd, $J = 8.6, 5.3$ Hz, 2 H), 6.92 (t, $J = 8.6$ Hz, 2 H), 6.50 (t, $J = 4.6$ Hz, 1 H), 4.02-3.90 (m, 2 H), 3.79-3.73 (m, 1 H), 3.69-3.62 (m, 1 H), 3.57-3.48 (m, 2 H), 3.30-3.21 (m, 1 H), 3.16-3.08 (m, 1 H), 2.98 (ddd, $J = 13.0, 9.0, 3.5$ Hz, 1 H), 2.47 (td, $J = 9.0, 6.0$ Hz, 1 H), 2.18 (ddd, $J = 9.0, 8.4, 6.0$ Hz, 1 H), 1.83 (q, $J = 5.6$ Hz, 1 H), 1.35 (td, $J = 8.4, 5.6$ Hz, 1 H). The enantiomeric excess was >99.9% ee (SFC Chiralpak-IC (250 x 10 mm); 30% Methanol:CO₂, 7 mL/min, $p = 100$ bar, 220 nm; retention time: 9.0 min).

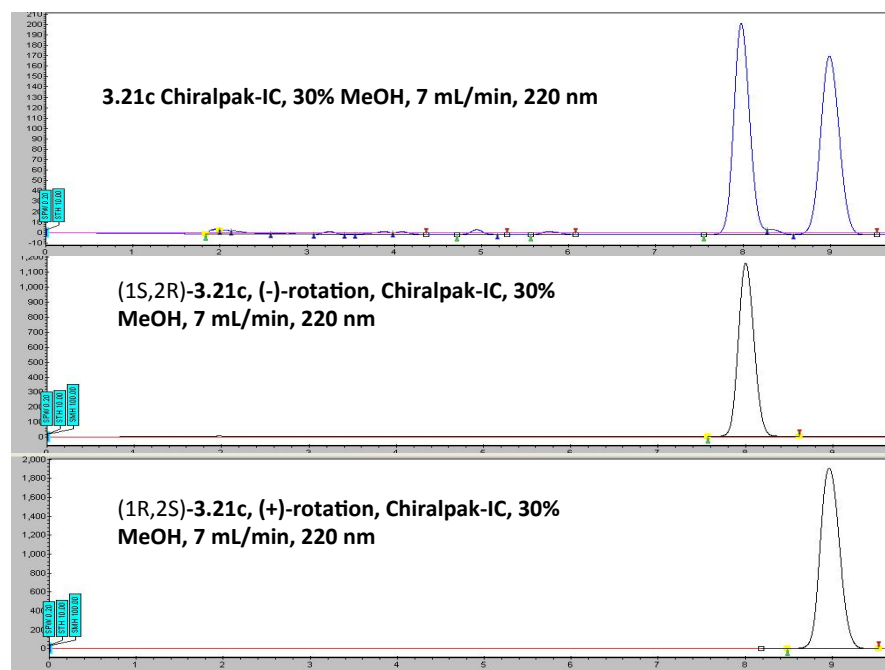
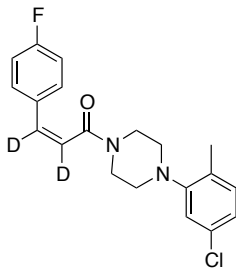
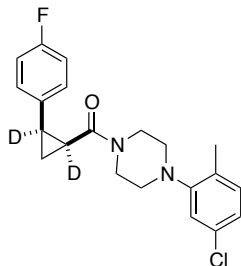


Figure 5.3. SFC chromatograms for **3.21c** and separated enantiomers.



3.22

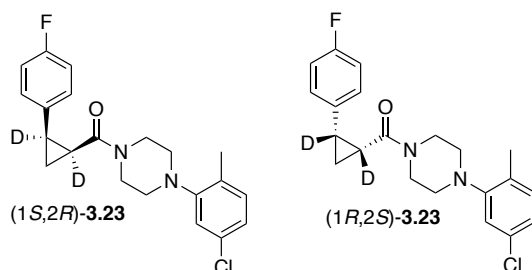
(Z)-1-(4-(5-Chloro-2-methylphenyl)piperazin-1-yl)-3-(4-fluorophenyl)prop-2-en-1-one-2,3-d2 (3.22). A solution of 1-(4-(5-chloro-2-methylphenyl)piperazin-1-yl)-3-(4-fluorophenyl)prop-2-yn-1-one (**3.17a**, 0.150 g, 0.140 mmol) in anhydrous EtOAc (4.2 mL) was treated with Lindlar catalyst (5% Pd on CaCO₃, lead poisoned, 0.0447 g, 0.0210 mmol, equivalent to 5 mol% Pd). The reaction was placed under a balloon of D₂ (3 vacuum/backfill cycles) and stirred vigorously at rt for 24 h, filtered through Celite, washed (EtOAc), and concentrated under reduced pressure. The crude residue was purified by automated chromatography on SiO₂ (4 g column, liquid load with CH₂Cl₂, gradient 100% hexanes to 30% EtOAc:hexanes, product eluted at 25% EtOAc:hexanes) to give **3.22** (0.0919 g, 0.255 mmol, 61%, 97% deuterium incorporation) as a colorless solid: Mp 122.1-124.8 °C; IR (CH₂Cl₂) 2918, 2819, 1628, 1595, 1505, 1432, 1222, 1022, 852, 817, 735 cm⁻¹; ¹H NMR (400 MHz, CDCl₃) δ 7.39 (dd, *J* = 8.6, 5.4 Hz, 2 H), 7.07-7.01 (m, 3 H), 6.95 (dd, *J* = 8.2, 2.0 Hz, 1 H), 6.79 (d, *J* = 2.0 Hz, 1 H), 3.79 (bs, 2 H), 3.48 (t, *J* = 5.0 Hz, 2 H), 2.80 (t, *J* = 5.0 Hz, 2 H), 2.52 (t, *J* = 5.0 Hz, 2 H), 2.20 (s, 3 H); ¹³C NMR (100 MHz, CDCl₃) δ 167.2, 162.6 (d, *J* = 249.3 Hz), 151.7, 132.1 (t, *J*_{CD} = 23.6 Hz), 132.0, 131.7, 131.4 (d, *J*_{CF} = 3.2 Hz), 130.8, 130.2 (d, *J*_{CF} = 8.1 Hz), 123.6, 122.2 (t, *J*_{CD} = 24.2 Hz), 119.5, 115.6 (d, *J*_{CF} = 21.4 Hz), 51.4, 51.1, 46.5, 41.4 17.3; ¹⁹F NMR (376 MHz, CDCl₃) δ -112.0 (s, 1 F); HRMS (ESI) *m/z* calcd for C₂₀H₁₉D₂ClFN₂O ([M+H]⁺) 361.1446, found 361.1446



3.23

(4-(5-Chloro-2-methylphenyl)piperazin-1-yl)((1RS,2SR)-2-(4-fluorophenyl)cyclopropyl-1,2-d2)methanone (3.23). A solution of CrCl_2 (0.225 g, 1.83 mmol) and (4-(5-chloro-2-methylphenyl)piperazin-1-yl)(2-(4-fluorophenyl)cyclopropyl-1,2-d2)methadone (**3.22**, 0.110 g, 0.305 mmol) in dry degassed THF (3 mL) was treated with CH_2I_2 (0.18 mL, 1.52 mmol) and sparged with Ar for 2 min. The reaction mixture was stirred for 24 h at 80 °C, cooled to rt, diluted with EtOAc (50 mL), and washed with 1 M HCl (3 x 20 mL). The organic layer was dried (MgSO_4), filtered and concentrated under reduced pressure. The crude residue was purified by automated chromatography on SiO_2 (4g column, liquid load CH_2Cl_2 , gradient 100% hexanes to 40% EtOAc/hexanes) to give a yellow oil that was filtered through basic Al_2O_3 ($\text{CH}_2\text{Cl}_2/\text{EtOAc}$, 1:1) concentrated under reduced pressure to a clear oil that was triturated in minimal cyclohexane to give a colorless solid that was dried under high vacuum to give **3.23** (0.0799 g, 0.213 mmol, 70% (100% purity by ELSD)) as a colorless solid: Mp 100.2-102.7 °C; IR (CH_2Cl_2) 2917, 1632, 1512, 1431, 1221, 1032, 818, 729 cm^{-1} ; ^1H NMR (400 MHz, CDCl_3) δ 7.16-7.11 (m, 2 H), 7.06 (d, $J = 8.2$ Hz, 1 H), 7.00-6.94 (m, 3 H), 6.71 (d, $J = 2.0$ Hz, 1 H), 3.81-3.77 (m, 1 H), 3.72-3.59 (m, 2 H), 3.37-3.31 (m, 1 H), 2.79-2.69 (m, 2 H), 2.33-2.28 (m, 1 H), 2.24-2.20 (m, 4 H), 1.81 (d, $J = 5.4$ Hz, 1 H), 1.32 (d, $J = 5.4$ Hz, 1 H); ^{13}C NMR (100 MHz, CDCl_3) δ 167.2, 161.5 (d, $J_{\text{CF}} = 244.7$ Hz), 151.8, 133.0 (d, $J_{\text{CF}} = 3.1$ Hz), 131.9, 131.7, 130.9, 129.0 (d, $J_{\text{CF}} = 7.7$ Hz), 123.5, 119.6, 114.9 (d, $J_{\text{CF}} = 21.3$ Hz), 51.7, 51.5, 45.5, 42.1, 23.4

(t, $J_{CD} = 25.4$ Hz), 23.0 (t, $J_{CD} = 24.6$ Hz) 17.3, 10.4; ^{19}F NMR (376 MHz, CDCl_3) δ -116.3 (s, 1 F); HRMS (ESI) m/z calcd for $\text{C}_{21}\text{H}_{21}\text{D}_2\text{ClFN}_2\text{O}$ ($[\text{M}+\text{H}]^+$) 375.1603, found 375.1602.



Racemic

(4-(5-chloro-2-methylphenyl)piperazin-1-yl)((1*RS*,2*SR*)-2-(4-

fluorophenyl)cyclopropyl-1,2-*d*2)methanone (**3.23**) was separated on a SFC Chiralpak-IC semiprep (250 x 10 mm) column (30% Methanol: CO_2 , 7 mL/min, $p = 100$ bar, 220 nm) injection volume 90 μL , 20 mg/mL) to give (4-(5-chloro-2-methylphenyl)piperazin-1-yl)((1*S*,2*R*)-2-(4-fluorophenyl)cyclopropyl-1,2-*d*2)methanone ((1*S*,2*R*)-**3.23**) (retention time 7.58 min) as a colorless viscous oil (100% purity by ELSD): $[\alpha]_{\text{D}}^{18} -152.0$ (c 0.70, MeOH); ^1H NMR (300 MHz, CDCl_3) δ 7.16-7.12 (m, 2 H), 7.07 (d, $J = 8.1$ Hz, 1 H), 7.01-6.94 (m, 3 H), 6.72 (d, $J = 1.8$ Hz, 1 H), 3.82-3.76 (m, 1 H), 3.74-3.58 (m, 2 H), 3.39-3.31 (m, 1 H), 2.80-2.69 (m, 2 H), 2.80-2.69 (m, 2 H), 2.35-2.17 (m, 5 H), 1.82 (d, $J = 5.4$ Hz, 1 H), 1.33 (d, $J = 5.4$ Hz, 1 H). The enantiomeric excess was >99.9% ee (SFC Chiralpak-IC (250 x 10 mm); 30% Methanol: CO_2 , 7 mL/min, $p = 100$ bar, 220 nm; retention time: 7.8 min).

(4-(5-Chloro-2-methylphenyl)piperazin-1-yl)((1*R*,2*S*)-2-(4-fluorophenyl)cyclopropyl-1,2-*d*2)methanone ((1*S*,2*R*)-**3.23**) (retention time 9.28 min) was obtained as a colorless viscous oil (100% purity by ELSD): $[\alpha]_{\text{D}}^{19} +154.0$ (c 0.66, MeOH); ^1H NMR (300 MHz, CDCl_3) δ 7.17-7.10 (m, 2 H), 7.07 (d, $J = 8.2$ Hz, 1 H), 7.02-6.94 (m, 3 H), 6.72 (d, $J = 2.0$ Hz, 1 H), 3.83-3.74 (m, 1 H), 3.73-3.58 (m, 2 H), 3.39-3.31 (m, 1 H), 2.80-2.69 (m, 2 H), 2.36-2.18 (m, 5 H), 1.82 (d, $J = 5.4$ Hz, 1 H), 1.33 (d, $J = 5.4$ Hz, 1 H). The enantiomeric excess was >99.9% ee (SFC

Chiralpak-IC (250 x 10 mm); 30% Methanol:CO₂, 7 mL/min, p = 100 bar, 220 nm; retention time: 9.6 min).

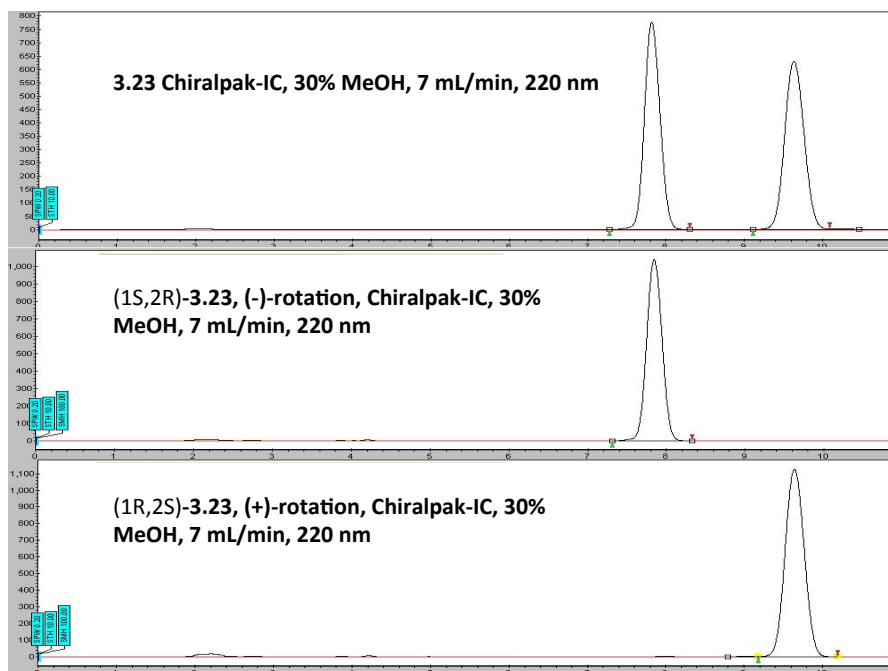
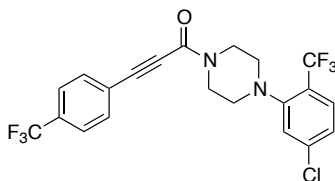


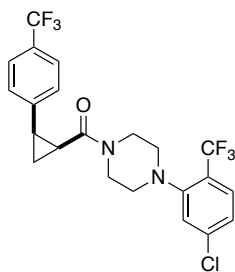
Figure 5.4. SFC chromatograms for **3.23** and separated enantiomers.



3.17d

1-(4-(5-Chloro-2-(trifluoromethyl)phenyl)piperazin-1-yl)-3-(4-(trifluoromethyl)phenyl)prop-2-yn-1-one (3.17d). A solution of 3-(4-(trifluoromethyl)phenyl)propionic acid (**3.16h**, 0.100 g, 0.467 mmol) and 1-(5-chloro-2-(trifluoromethyl)phenyl)piperazinehydrochloride (**3.12b**, 0.155 g, 0.514 mmol) in CH₂Cl₂ (4.7 mL) cooled to 0 °C was treated with Et₃N (0.26 mL, 1.87 mmol). The cooled solution was treated with T3P (50 wt. % solution in EtOAc, 0.49 mL, 0.701 mmol) dropwise and the reaction

was stirred at 0 °C for 30 min and allowed to warm to rt for 16 h, diluted with CH₂Cl₂ (30 mL) and washed with H₂O (20 mL), satd. aqueous NaHCO₃ (20 mL), dried (MgSO₄), filtered, and concentrated under reduced pressure. The crude material was purified by automated chromatography on SiO₂ (4g column, liquid load CH₂Cl₂, hexanes to 30% EtOAc/hexanes), to give **3.17d** (0.161 g, 0.350 mmol, 75%) as a colorless solid: Mp 145.8-148.8 °C; IR (CH₂Cl₂) 2928, 2827, 2223, 1634, 1596, 1432, 1322, 1310, 1122, 1107, 1033, 844 cm⁻¹; ¹H NMR (400 MHz, CDCl₃) δ 7.65 (app q, *J* = 7.3 Hz, 4 H), 7.58 (d, *J* = 8.4 Hz, 1 H), 7.28-7.24 (m, 2 H), 3.96 (app t, *J* = 5.0 Hz, 2 H), 3.84 (app t, *J* = 5.0 Hz, 2 H), 3.00 (app t, *J* = 5.0 Hz, 2 H), 2.94 (app t, *J* = 5.0 Hz, 2 H); ¹³C NMR (100 MHz, CDCl₃) δ 152.5, 138.8, 132.5, 131.6 (q, *J*_{CF} = 33.0 Hz), 128.5 (q, *J*_{CF} = 5.4 Hz), 125.7 (q, *J*_{CF} = 29.4 Hz), 125.7, 125.4 (q, *J*_{CF} = 3.7 Hz), 124.7, 124.1, 123.5 (q, *J*_{CF} = 270.8 Hz, 2 C), 89.0, 82.7, 53.6, 52.7, 47.3, 41.8; ¹⁹F NMR (376 MHz, CDCl₃) δ -60.3 (s, 3 F), -63.1 (s, 3 F); HRMS (ESI) *m/z* calcd for C₂₁H₁₆ClF₆N₂O ([M+H]⁺) 461.0850, found 461.0847.



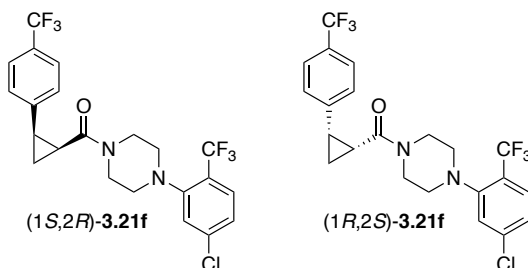
3.21f

(4-(5-Chloro-2-(trifluoromethyl)phenyl)piperazin-1-yl)((1R,2SR)-2-(4-(trifluoromethyl)phenyl)cyclopropyl)methanone (3.21f). A solution of 1-(4-(5-chloro-2-(trifluoromethyl)phenyl)piperazin-1-yl)-3-(4-(trifluoromethyl)phenyl)prop-2-yn-1-one (**3.17d**, 0.127 g, 0.276 mmol) in EtOAc (2.8 mL) was treated with quinoline (0.16 mL, 1.38 mmol) and 5% Pd/BaSO₄ (0.0059 g, equivalent to 1 mol% Pd). The reaction was placed under and

atmosphere of H₂ (balloon) (3 vacuum/backfill cycles) and stirred at rt for 1.5 h, filtered through Celite, washed (EtOAc), and the combined filtrates were washed with 1 M aqueous HCl (10 mL), dried (MgSO₄), filtered, and concentrated under reduced pressure. The crude residue was purified by automated chromatography on SiO₂ (4 g column, liquid load CH₂Cl₂, gradient 100% hexanes to 30% EtOAc/hexanes; product eluted at 20% EtOAc) to give **3.18d** (0.114 g, 0.246 mmol) as a colorless solid.

A solution of CrCl₂ (0.182 g, 0.148 mmol) and (Z)-1-(4-(5-chloro-2-(trifluoromethyl)phenyl)piperazin-1-yl)-3-(4-(trifluoromethyl)phenyl)prop-2-en-1-one (**3.18d**, 0.114 g, 0.246 mmol) in dry degassed THF (2.5 mL) was sparged with Ar for 15 min, treated with CH₂ICl (0.14 mL, 1.23 mmol), heated for 2 d at 80 °C. The reaction was cooled to rt, diluted with EtOAc (50 mL) and washed with 1 M aqueous HCl (3 x 20 mL). The organic layer was dried (MgSO₄), filtered and concentrated under reduced pressure. The crude residue was purified by automated chromatography on SiO₂ (4g column, liquid load CH₂Cl₂, gradient 100% hexanes to 30% EtOAc/hexanes, product eluted at 20% EtOAc/hexanes), filtered through basic Al₂O₃ (CH₂Cl₂/EtOAc, 1:1), concentrated, and dried under high vacuum to give **3.21f** (0.0681 g, 0.143 mmol, 52% (2 steps) (100% purity by ELSD)) as a colorless solid: Mp 138.0-139.9 °C; IR (CH₂Cl₂) 3014, 2825, 1641, 1596, 1326, 1309, 1116, 1031, 844 cm⁻¹; ¹H NMR (400 MHz, CDCl₃) δ 7.56 (d, *J* = 8.2 Hz, 2 H), 7.51 (d, *J* = 8.5 Hz, 1 H), 7.29 (d, *J* = 8.2 Hz, 2 H), 7.19 (dd, *J* = 8.5, 1.4 Hz, 1 H), 6.89 (d, *J* = 1.4 Hz, 1 H), 3.95 (bd, *J* = 12.4 Hz, 1 H), 3.73 (bd, *J* = 12.4 Hz, 1 H), 3.54 (bt, *J* = 10.0 Hz, 1 H), 3.21 (bt, *J* = 10.0 Hz, 1 H), 2.74 (bt, *J* = 10.0 Hz, 2 H), 2.50 (td, *J* = 8.9, 7.1 Hz, 1 H), 2.29-2.19 (m, 2 H), 1.98 (bt, *J* = 8.9 Hz, 1 H), 1.92 (q, *J* = 6.2 Hz, 1 H), 1.43 (td, *J* = 8.4, 5.6 Hz, 1 H); ¹³C NMR (100 MHz, CDCl₃) δ 166.5, 152.7, 142.1, 138.9, 128.8 (q, *J*_{CF} = 32.6 Hz), 128.4 (q, *J*_{CF} = 5.8 Hz), 127.9, 125.7 (q, *J*_{CF} = 30.2 Hz), 125.6, 125.0 (q, *J*_{CF} =

3.7 Hz), 124.6 (q, $J_{CF} = 273.0$ Hz), 124.4, 123.6 (q, $J_{CF} = 272.9$ Hz), 53.7, 52.9, 45.5, 42.1, 24.7, 23.9, 11.2; ^{19}F NMR (376 MHz, CDCl_3) δ -60.4 (s, 3 F), -62.2 (s, 3 F); HRMS (ESI) m/z calcd for $\text{C}_{22}\text{H}_{20}\text{ClF}_6\text{N}_2\text{O}$ ($[\text{M}+\text{H}]^+$) 477.1163, found 477.1160.



Racemic (4-(5-chloro-2-(trifluoromethyl)phenyl)piperazin-1-yl)((1*RS*,2*SR*)-2-(4-(trifluoromethyl)phenyl)cyclopropyl)methanone (**3.21f**) was separated on a SFC Chiralpak-IC semiprep (250 x 10 mm) column (25% Methanol: CO_2 , 7 mL/min, $p = 100$ bar, 220 nm) injection volume 90 μL , 20 mg/mL) to give 4-(5-chloro-2-(trifluoromethyl)phenyl)piperazin-1-yl)((1*S*,2*R*)-2-(4-(trifluoromethyl)phenyl)cyclopropyl)methanone ((1*S*,2*R*)-**3.21f**) (retention time 3.57 min) as a colorless viscous oil (100% purity by ELSD): $[\alpha]_{\text{D}}^{19} -106.6$ (c 0.68, MeOH); ^1H NMR (300 MHz, CDCl_3) δ 7.57 (d, $J = 8.1$ Hz, 2 H), 7.52 (d, $J = 8.4$ Hz, 1 H), 7.29 (d, $J = 8.1$ Hz, 2 H), 7.20 (d, $J = 8.4$ Hz, 1 H), 6.88 (d, $J = 0.9$ Hz, 1 H), 3.98-3.93 (m, 1 H), 3.76-3.70 (m, 1 H), 3.54 (ddd, $J = 12.3, 9.3, 3.0$ Hz, 2 H), 3.21 (ddd, $J = 12.3, 9.3, 3.0$ Hz, 2 H), 2.76-2.71 (m, 2 H), 2.51 (td, $J = 9.3, 7.2$ Hz, 1 H), 2.30-2.18 (m, 2 H), 2.00-1.89 (m, 2 H), 1.44 (td, $J = 8.4, 5.7$ Hz, 1 H). The enantiomeric excess was >99.9% ee (SFC Chiralpak-IC (250 x 10 mm); 25% Methanol: CO_2 , 7 mL/min, $p = 100$ bar, 220 nm; retention time: 3.8 min).

(4-(5-Chloro-2-(trifluoromethyl)phenyl)piperazin-1-yl)((1*R*,2*S*)-2-(4-(trifluoromethyl)phenyl)cyclopropyl)methanone ((1*S*,2*R*)-**3.21f**) (retention time 4.20 min) was obtained as a colorless viscous oil (100% purity by ELSD): $[\alpha]_{\text{D}}^{19} +111.1$ (c 0.71, MeOH); ^1H NMR (300 MHz, CDCl_3) δ 7.57 (d, $J = 8.1$ Hz, 2 H), 7.52 (d, $J = 8.4$ Hz, 1 H), 7.29 (d, $J = 8.1$

Hz, 2 H), 7.20 (d, $J = 8.4$ Hz, 1 H), 6.88 (s, 1 H), 3.99-3.93 (m, 1 H), 3.76-3.70 (m, 1 H), 3.58-3.49 (m, 1 H), 3.25-3.16 (m, 1 H), 2.76-2.71 (m, 2 H), 2.51 (q, $J = 9.6$ Hz, 1 H), 2.30-2.18 (m, 2 H), 2.00-1.89 (m, 2 H), 1.44 (td, $J = 8.4, 5.6$ Hz, 1 H). The enantiomeric excess was >99.9% ee (SFC Chiralpak-IC (250 x 10 mm); 25% Methanol:CO₂, 7 mL/min, p = 100 bar, 220 nm; retention time: 4.1 min).

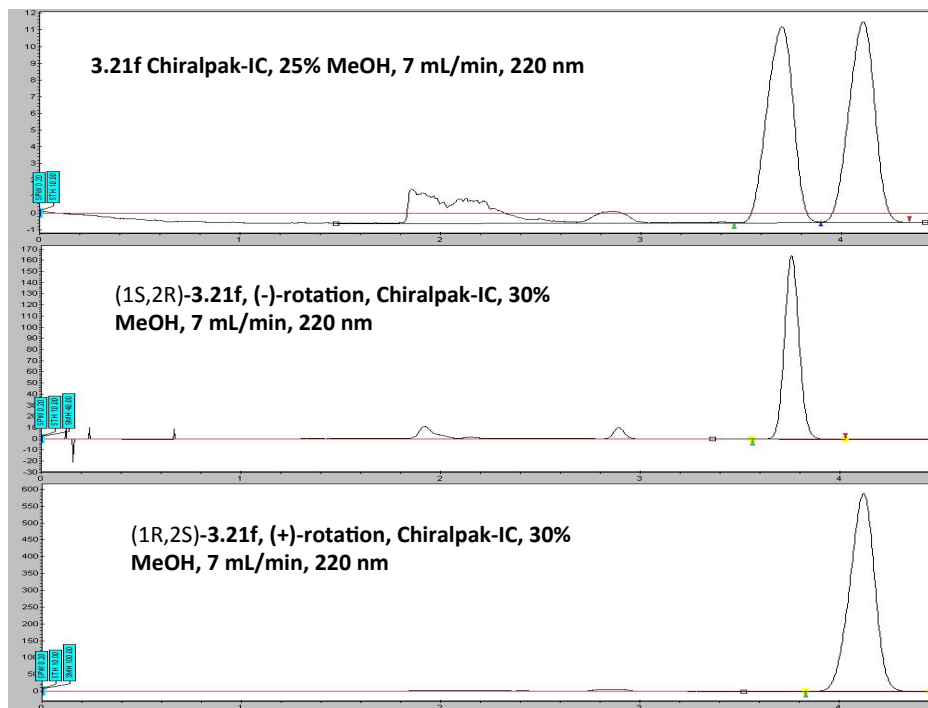
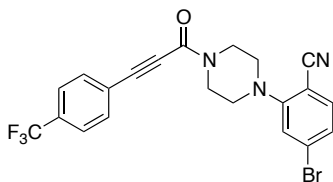


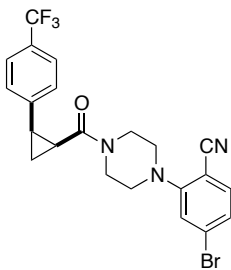
Figure 5.5. SFC chromatograms for **3.21f** and separated enantiomers.



3.17e

4-Bromo-2-(4-(3-(4-(trifluoromethyl)phenyl)propioloyl)piperazin-1-yl)benzonitrile (3.17e). A solution of 3-(4-trifluoromethylphenyl)propionic acid (**3.16h**, 0.400 g, 1.87 mmol) and 4-bromo-2-(piperazin-1-yl)benzonitrile hydrochloride (**3.12e**, 0.735 g, 2.43 mmol) in CH₂Cl₂ (19

mL) at 0 °C was treated Et₃N (1.0 mL, 7.47 mmol). The cooled solution was treated with T3P (50% solution in EtOAc) (2.0 mL, 2.80 mmol) dropwise and the reaction was stirred at 0 °C for 30 min, warmed to rt for 16 h, diluted with EtOAc (80 mL) and washed with H₂O (20 mL), satd. aqueous NaHCO₃ (20 mL), dried (MgSO₄), filtered, and concentrated under reduced pressure. The crude residue was purified by chromatography on SiO₂ (hexanes/EtOAc, 1:1), to give **3.17e** (0.784 g, 1.70 mmol, 91%) as a pale yellow solid: Mp 176.3-179.1 °C; IR (CH₂Cl₂) 2824, 2222, 1626, 1583, 1432, 1324, 1163, 1129, 1107, 1035, 949, 928, 846, 816 cm⁻¹; ¹H NMR (500 MHz, CDCl₃) δ 7.66 (dd, *J* = 7.8 Hz, 4 H), 7.45 (d, *J* = 8.0 Hz, 1 H), 7.22 (dd, *J* = 8.0, 1.6 Hz, 1 H), 7.15 (d, *J* = 1.6 Hz, 1 H), 4.05 (t, *J* = 5.0 Hz, 2 H), 3.91 (t, *J* = 5.0 Hz, 2 H), 3.31 (t, *J* = 5.0 Hz, 2 H), 3.22 (t, *J* = 5.0 Hz, 2 H); ¹³C NMR (125 MHz, CDCl₃) δ 155.6, 152.6, 135.1, 132.6, 131.8 (q, *J*_{CF} = 32.8 Hz), 128.8, 125.9, 125.5 (q, *J*_{CF} = 3.8 Hz), 124.0, 123.5 (q, *J*_{CF} = 272.5 Hz), 122.7, 117.4, 105.1, 89.3, 82.5, 52.0, 50.7, 47.0, 41.5; ¹⁹F NMR (470 MHz, CDCl₃) δ -63.1 (s, 3 F); HRMS (ESI) *m/z* calcd for C₂₁H₁₆BrF₃N₃O ([M+H]⁺) 462.0423, found 462.0423.

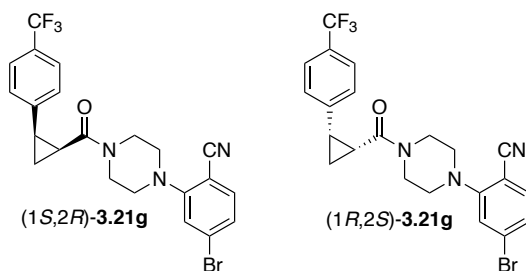


3.21g

4-Bromo-2-(4-((1RS,2SR)-2-(4-(trifluoromethyl)phenyl)cyclopropane-1-carbonyl)piperazin-1-yl)benzonitrile (3.21g). A solution of 4-bromo-2-(4-(3-(4-(trifluoromethyl)phenyl)propioloyl)piperazin-1-yl)benzonitrile (**3.17e**, 0.750 g, 1.62 mmol) in EtOAc (16 mL) was treated with Lindlar catalyst (5% Pd on CaCO₃, lead poisoned, 0.691 g, equivalent to 20 mol% Pd). The reaction was placed under a balloon of H₂ (3 vacuum/backfill

cycles) and stirred at rt for 3 d, filtered through Celite, washed (EtOAc), and the combined filtrates were concentrated under reduced pressure. The crude residue was purified by chromatography on SiO₂ (hexanes/EtOAc, 1:4) to give **3.18e** (0.318 g, 0.685 mmol) as a tan foam.

A solution of CrCl₂ (0.477 g, 0.899 mmol) and (Z)-4-bromo-2-(4-(3-(4-(trifluoromethyl)phenyl)acryloyl)piperazin-1-yl)benzotrile (**3.18e**, 0.300 g, 0.646 mmol) in dry degassed THF (6.5 mL) was sparged with Ar for 5 min and treated with CH₂ICl (0.37 mL, 3.23 mmol) at rt, stirred for 2 d at 80 °C, cooled to rt, diluted with EtOAc (150 mL) and washed with 1 M aqueous HCl (3 x 50 mL). The organic layer was dried (MgSO₄), filtered and concentrated under reduced pressure. The crude residue was purified by chromatography on SiO₂ (hexanes/EtOAc, 1:9) to give a colorless oil that was filtered through basic Al₂O₃ (EtOAc) concentrated and further dried under high vacuum to give **3.21g** (0.148 g, 0.309 mmol, 20% (2 steps) (100% purity by ELSD)) as a colorless oil: IR (CH₂Cl₂) 2833, 2222, 1642, 1583, 1484, 1436, 1326, 1228, 1116, 1069, 844 cm⁻¹; ¹H NMR (400 MHz, CDCl₃) δ 7.52 (d, *J* = 8.5 Hz, 2 H), 7.38 (d, *J* = 8.0 Hz, 1 H), 7.27 (d, *J* = 8.5 Hz, 2 H), 7.17 (dd, *J* = 8.0, 1.5 Hz, 1 H), 6.90 (d, *J* = 1.5 Hz, 1 H), 3.93 (dt, *J* = 13.0, 3.5 Hz, 1 H), 3.78 (dt, *J* = 13.0, 3.5 Hz, 1 H), 3.67 (ddd, *J* = 13.0, 9.0, 3.0 Hz, 1 H), 3.35 (ddd, *J* = 13.0, 9.0, 3.0 Hz, 1 H), 3.18-3.15 (m, 1 H), 3.08-3.06 (m, 1 H), 2.55-2.45 (m, 2 H), 2.29-2.24 (m, 2 H), 1.92 (q, *J* = 6.0 Hz, 1 H), 1.43 (td, *J* = 8.0, 6.0 Hz, 1 H); ¹³C NMR (125 MHz, CDCl₃) δ 166.8, 155.7, 141.8, 135.0, 128.8, 128.8 (q, *J*_{CF} = 32.6 Hz), 127.9, 125.7, 125.1 (q, *J*_{CF} = 3.6 Hz), 124.1 (q, *J*_{CF} = 271.8 Hz), 122.4, 117.5, 105.0, 52.1, 50.8, 45.2, 41.7, 24.5, 24.1, 11.2; ¹⁹F NMR (376 MHz, CDCl₃) δ -62.3 (s, 3 F); HRMS (ESI) *m/z* calcd for C₂₂H₂₀BrF₃N₃O ([M+H]⁺) 478.0736, found 478.0734.



Racemic 4-bromo-2-(4-((1*RS*,2*SR*)-2-(4-(trifluoromethyl)phenyl)cyclopropane-1-carbonyl)piperazin-1-yl)benzonitrile (**3.21g**) was separated on a SFC Chiralpak-IC semiprep (250 x 10 mm) column (25% Methanol/CO₂, 7 mL/min, 220nm, p =100 bar, 20 mg/mL in MeOH) to give 4-bromo-2-(4-((1*S*,2*R*)-2-(4-(trifluoromethyl)phenyl)cyclopropane-1-carbonyl)piperazin-1-yl)benzonitrile ((1*S*,2*R*)-**3.21g**) (retention time 10.5 min) as a colorless solid (100% purity by ELSD): $[\alpha]_{\text{D}}^{19} -144.1$ (*c* 1.31, MeOH); ¹H NMR (300 MHz, CDCl₃) δ 7.52 (d, *J* = 8.1 Hz, 2 H), 7.39 (d, *J* = 8.1 Hz, 1 H), 7.27 (d, *J* = 8.1 Hz, 2 H), 7.17 (dd, *J* = 8.1, 1.5 Hz, 1 H), 6.90 (d, *J* = 1.5 Hz, 1 H), 3.95-3.89 (m, 1 H), 3.76-3.67 (m, 2 H), 3.38-3.33 (m, 1 H), 3.16-3.04 (m, 2 H), 2.56-2.45 (m, 2 H), 2.27 (td, *J* = 8.7, 6.0 Hz, 2 H), 1.92 (q, *J* = 6.0 Hz, 1 H), 1.44 (td, *J* = 8.4, 5.5 Hz, 1 H). The enantiomeric excess was >99.9% ee (SFC Chiralpak-IC (250 x 10 mm); 25% MeOH, 7 mL/min, 220nm, p = 100 bar; retention time: 10.8 min).

4-Bromo-2-(4-((1*R*,2*S*)-2-(4-(trifluoromethyl)phenyl)cyclopropane-1-carbonyl)piperazin-1-yl)benzonitrile ((1*R*,2*S*)-**3.21g**) (retention time 11.6 min) was obtained as a colorless solid (100% purity by ELSD): $[\alpha]_{\text{D}}^{19} +135.8$ (*c* 1.43, MeOH); ¹H NMR (300 MHz, CDCl₃) δ 7.52 (d, *J* = 8.1 Hz, 2 H), 7.39 (d, *J* = 8.1 Hz, 1 H), 7.29 (s, 2 H), 7.17 (dd, *J* = 8.1, 1.5 Hz, 1 H), 6.90 (d, *J* = 1.5 Hz, 1 H), 3.93-3.90 (m, 1 H), 3.78-3.67 (m, 2 H), 3.38-3.33 (m, 1 H), 3.17-3.04 (m, 2 H), 2.56-2.43 (m, 2 H), 2.27 (td, *J* = 8.7, 6.0 Hz, 2 H), 1.92 (q, *J* = 6.0 Hz, 1 H), 1.44 (td, *J* = 8.4, 5.6 Hz, 1 H). The enantiomeric excess was >99.9% ee (SFC Chiralpak-IC (250 x 10 mm); 25% MeOH, 7 mL/min, 220nm, p = 100 bar; retention time: 11.8 min).

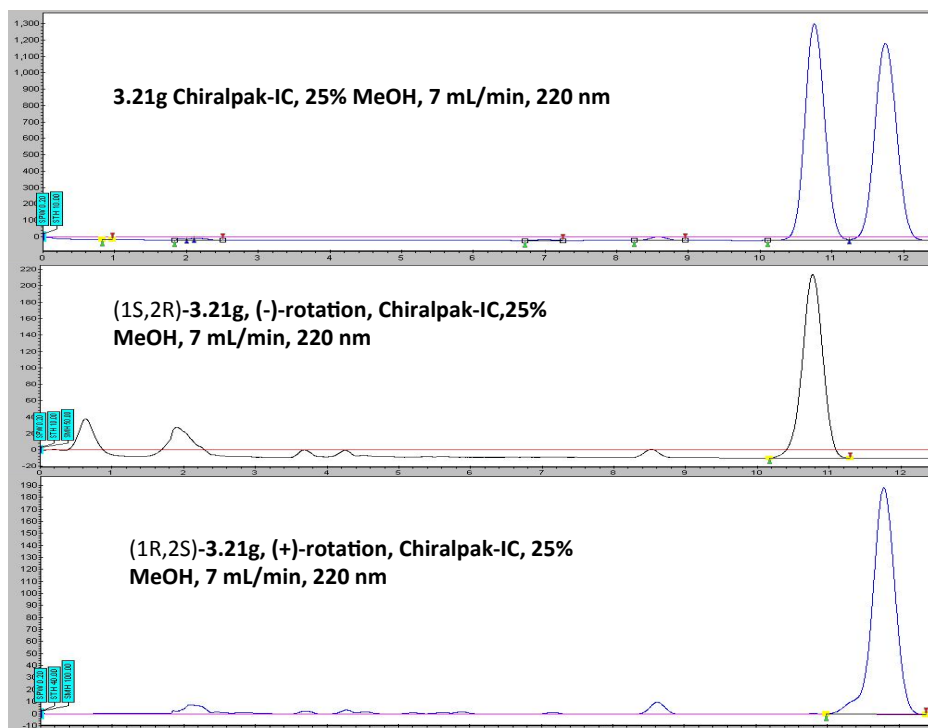
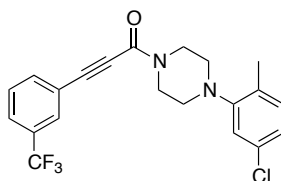


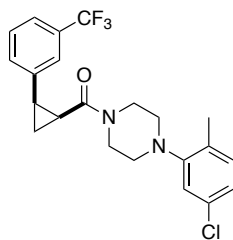
Figure 5.6. SFC chromatograms for **3.21g** and separated enantiomers.



3.17f

1-(4-(5-Chloro-2-methylphenyl)piperazin-1-yl)-3-(3-(trifluoromethyl)phenyl)prop-2-yn-1-one (3.17f). A solution of 3-(3-(trifluoromethyl)phenyl)propionic acid (**3.16b**, 0.0750 g, 0.350 mmol) and 1-(5-chloro-2-methylphenyl)piperazine hydrochloride (**3.12b**, 0.104 g, 0.420 mmol) in CH_2Cl_2 (3.5 mL) cooled to 0 °C was treated with Et_3N (0.15 mL, 1.05 mmol). The cooled solution was treated with T3P (50 wt. % solution in EtOAc 0.37 mL, 0.525 mmol) dropwise and the reaction was stirred at 0 °C for 30 min, warmed to rt for 16 h, diluted with CH_2Cl_2 (30 mL), washed with 1 M aqueous HCl (20 mL), dried (MgSO_4), filtered, and concentrated under reduced pressure. The crude material was purified by automated

chromatography on SiO₂ (4g column, liquid load CH₂Cl₂, gradient 100% hexanes to 40% EtOAc/hexanes) to give **3.17f** (0.106 g, 0.261 mmol, 75%) as a colorless solid: Mp 130.3-132.8 °C; IR (CH₂Cl₂) 2820, 2218, 2161, 1631, 1489, 1435, 1201, 1128, 1041, 805, 695 cm⁻¹; ¹H NMR (400 MHz, CDCl₃) δ 7.81 (s, 1 H), 7.74 (d, *J* = 7.8 Hz, 1 H), 7.68 (d, *J* = 7.8 Hz, 1 H), 7.52 (t, *J* = 7.8 Hz, 1 H), 7.12 (d, *J* = 8.1 Hz, 1 H), 7.00 (dd, *J* = 8.1, 2.1 Hz, 1 H), 6.96 (d, *J* = 2.1 Hz, 1 H), 3.98 (app t, *J* = 5.0 Hz, 2 H), 3.84 (app t, *J* = 5.0 Hz, 2 H), 2.98 (app t, *J* = 5.0 Hz, 2 H), 2.90 (app t, *J* = 5.0 Hz, 2 H), 2.29 (s, 3 H); ¹³C NMR (100 MHz, CDCl₃) δ 152.6, 151.6, 135.4, 132.1, 131.8, 131.2 (q, *J*_{CF} = 33.0 Hz), 130.9, 129.17, 129.0 (q, *J*_{CF} = 4.1 Hz), 126.6 (q, *J*_{CF} = 3.6 Hz), 123.8, 123.5 (q, *J*_{CF} = 272.5 Hz), 121.4, 119.8, 88.9, 82.1, 51.9, 51.3, 47.4, 41.9; HRMS (ESI) *m/z* calcd for C₂₁H₁₉ClF₃N₂O ([M+H]⁺) 407.1133, found 407.1130.

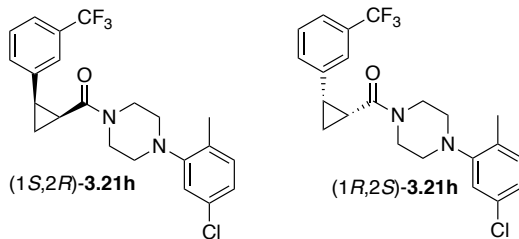


3.21h

(4-(5-Chloro-2-methylphenyl)piperazin-1-yl)((1RS,2SR)-2-(3-(trifluoromethyl)phenyl)cyclopropyl)methanone (3.21h). A solution of 1-(4-(5-chloro-2-methylphenyl)piperazin-1-yl)-3-(3-(trifluoromethyl)phenyl)prop-2-yn-1-one (**3.17f**, 0.100 g, 0.246 mmol) in EtOAc (2.5 mL) was added Lindlar catalyst (5% Pd on CaCO₃, lead poisoned, 0.0105 g, equivalent to 2 mol% Pd) and quinoline (0.015 mL, 0.123 mmol). The reaction vessel was placed under vacuum and backfilled with H₂ (balloon, 4x) stirred for 3.5 h at rt, filtered through Celite, washed (EtOAc), and the combined filtrates were washed with 1 M aqueous HCl, dried (Na₂SO₄), filtered, and concentrated under reduced pressure. The crude residue was purified by automated chromatography on SiO₂ (4g column, liquid load CH₂Cl₂, 10%

EtOAc/hexanes to 40% EtOAc/hexanes) to give **3.18f** (0.0932 g, 0.228 mmol, 93%) as a colorless solid.

A solution of CrCl₂ (0.105 g, 0.851 mmol) and (*Z*)-1-(4-(5-chloro-2-methylphenyl)piperazin-1-yl)-3-(3-(trifluoromethyl)phenyl)prop-2-en-1-one (**3.18f**, 0.0580 g, 0.142 mmol) in dry degassed THF (1.4 mL) was treated with CH₂ICl (82 uL, 0.709 mmol) and the mixture was sparged with Ar for 2 min, heated for 20 h at 80 °C, cooled to rt, diluted with Et₂O (50 mL) and washed with 1 M HCl (3 x 20 mL). The organic layer was dried (MgSO₄), filtered and concentrated under reduced pressure. The crude material was purified by automated chromatography on SiO₂ (4g column, liquid load CH₂Cl₂, 100% hexanes to 40% EtOAc/hexanes) to give a clear oil that filtered through basic Al₂O₃ (CH₂Cl₂/EtOAc, 1:1), recrystallized from hot cyclohexane the mother liquor was decanted and the crystals were washed with hexanes (2 x 1 mL) and dried under high vacuum to give **3.21h** (0.0356 g, 0.0842 mmol, 55% (2 steps) (100% purity by ELSD)) as colorless needles: Mp 115.6-117.4 °C; IR (CH₂Cl₂) 2914, 2820, 1639, 1593, 1490, 1437, 1225, 1161, 1123, 1074, 806 cm⁻¹; ¹H NMR (400 MHz, CDCl₃) δ 7.49-7.48 (m, 2 H), 7.40 (t, *J* = 8.0 Hz, 1 H), 7.32 (d, *J* = 8.0 Hz, 1 H), 7.06 (d, *J* = 8.0 Hz, 1 H), 6.95 (dd, *J* = 8.0, 2.1 Hz, 1 H), 6.67 (d, *J* = 2.1 Hz, 1 H), 3.86 (dt, *J* = 13.0, 2.9 Hz, 1 H), 3.74 (dt, *J* = 13.0, 3.2 Hz, 1 H), 3.62-3.56 (m, 1 H), 3.26 (ddd, *J* = 12.4, 9.0, 3.2 Hz, 1 H), 2.79-2.70 (m, 2 H), 2.53 (td, *J* = 9.0, 6.9 Hz, 1 H), 2.26 (ddd, *J* = 9.0, 8.4, 5.9 Hz, 1 H), 2.20 (s, 3 H), 2.10 (ddd, *J* = 11.2, 9.0, 2.4 Hz, 1 H), 1.91 (app q, *J* = 5.8 Hz, 1 H), 1.41 (td, *J* = 8.4, 5.8 Hz, 1 H); ¹³C NMR (100 MHz, CDCl₃) δ 166.7, 151.7, 138.7, 131.9, 131.8, 130.9, 130.5, 130.5 (d, *J*_{CF} = 32.2 Hz) 128.7, 125.1 (d, *J*_{CF} = 4.0 Hz), 124.2 (d, *J*_{CF} = 272.2 Hz), 123.6, 123.3 (d, *J*_{CF} = 3.7 Hz), 119.6, 51.7, 51.6, 45.5, 42.2, 24.1, 23.9, 17.3, 10.8; ¹⁹F NMR (376 MHz, CDCl₃) δ -62.4 (s, 3 F); HRMS (ESI) *m/z* calcd for C₂₂H₂₃ClF₃N₂O ([M+H]⁺) 423.1446, found 423.1443.



Racemic (4-(5-chloro-2-methylphenyl)piperazin-1-yl)((1*R*,2*S*)-2-(3-(trifluoromethyl)phenyl)cyclopropyl)methanone (**3.21h**) was separated on a SFC Chiralpak-IC semiprep (250 x 10 mm) column (30% Methanol:CO₂, 7 mL/min, p = 100 bar, 220 nm) injection volume 90 μL, 20 mg/mL) to give (4-(5-chloro-2-methylphenyl)piperazin-1-yl)((1*S*,2*R*)-2-(3-(trifluoromethyl)phenyl)cyclopropyl)methanone ((1*S*,2*R*)-**3.21h**) (retention time 4.82 min) as a colorless viscous oil (100% purity by ELSD): [α]¹⁹_D -133.5 (*c* 0.70, MeOH); ¹H NMR (300 MHz, CDCl₃) δ 7.48 (bs, 2 H), 7.41 (t, *J* = 8.0 Hz, 1 H), 7.33 (d, *J* = 7.4 Hz, 1 H), 7.06 (d, *J* = 8.1 Hz, 1 H), 6.95 (dd, *J* = 8.1, 2.0 Hz, 1 H), 6.67 (d, *J* = 2.0 Hz, 1 H), 3.89-3.82 (m, 1 H), 3.78-3.71 (m, 1 H), 3.63-3.55 (m, 1 H), 3.31-3.23 (m, 1 H), 2.79-2.69 (m, 2 H), 2.53 (td, *J* = 8.4, 7.2 Hz, 1 H), 2.30-2.07 (m, 6 H), 1.92 (q, *J* = 5.4 Hz, 1 H), 1.41 (td, *J* = 8.4, 5.4 Hz, 1 H). The enantiomeric excess was >99.9% ee (SFC Chiralpak-IC (250 x 10 mm); 30% Methanol:CO₂, 7 mL/min, p = 100 bar, 220 nm; retention time: 5.0 min).

(4-(5-Chloro-2-methylphenyl)piperazin-1-yl)((1*R*,2*S*)-2-(3-(trifluoromethyl)phenyl)cyclopropyl)methanone ((1*R*,2*S*)-**3.21h**) (retention time 5.57 min) was obtained as a colorless viscous oil (100% purity by ELSD): [α]¹⁹_D +133.1 (*c* 0.65, MeOH); ¹H NMR (300 MHz, CDCl₃) δ 7.48 (bs, 2 H), 7.41 (t, *J* = 8.0 Hz, 1 H), 7.33 (d, *J* = 8.0 Hz, 1 H), 7.06 (d, *J* = 8.0 Hz, 1 H), 6.95 (dd, *J* = 8.0, 2.0 Hz, 1 H), 6.67 (d, *J* = 2.0 Hz, 1 H), 3.90-3.82 (m, 1 H), 3.78-3.70 (m, 1 H), 3.64-3.55 (m, 1 H), 3.31-3.23 (m, 1 H), 2.80-2.69 (m, 2 H), 2.53 (td, *J* = 8.4, 6.8 Hz, 1 H), 2.30-2.07 (m, 6 H), 1.92 (q, *J* = 5.4 Hz, 1 H), 1.41 (td, *J* = 8.4, 5.4 Hz, 1 H).

The enantiomeric excess was >99.9% ee (SFC Chiralpak-IC (250 x 10 mm); 30% Methanol:CO₂, 7 mL/min, p = 100 bar, 220 nm; retention time: 5.7 min).

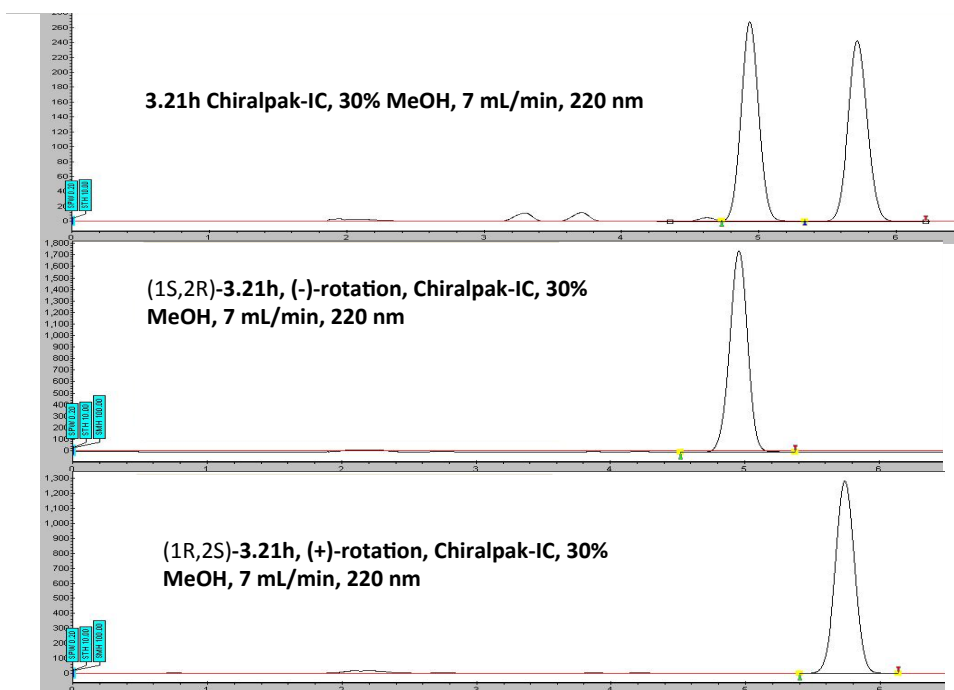
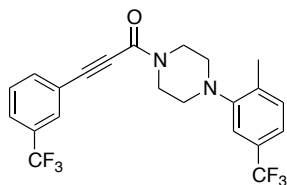


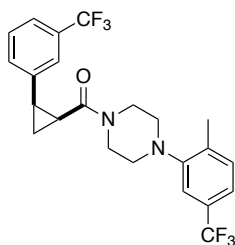
Figure 5.7. SFC chromatograms for **3.21h** and separated enantiomers.



3.17g

1-(4-(2-Methyl-5-(trifluoromethyl)phenyl)piperazin-1-yl)-3-(3-(trifluoromethyl)phenyl)prop-2-yn-1-one (3.17g). A solution of 3-(3-(trifluoromethyl)phenyl)propionic acid (**3.16b**, 0.0763 g, 0.356 mmol) and 1-(2-methyl-5-(trifluoromethyl)phenyl)piperazine hydrochloride (**3.12c**, 0.100 g, 0.356 mmol) in CH₂Cl₂ (3.6 mL) cooled to 0 °C was treated with Et₃N (0.20 mL, 1.42 mmol). The cooled solution was treated with T3P (50 wt. % solution in EtOAc, 0.38 mL, 0.534 mmol) dropwise and the reaction

was stirred at 0 °C for 30 min, warmed to rt for 16 h, diluted with CH₂Cl₂ (30 mL), washed with 1 M aqueous HCl (20 mL), dried (MgSO₄), filtered, and concentrated under reduced pressure. The crude residue was purified by automated chromatography on SiO₂ (4g column, liquid load CH₂Cl₂, gradient 100% hexanes to 40% EtOAc/hexanes), to give **3.17g** (0.0819 g, 0.186 mmol, 52%) as a pink solid: Mp 121.8-125.2 °C; IR (CH₂Cl₂) 2924, 2217, 1633, 1436, 1333, 1310, 1166, 1076, 1042, 695 cm⁻¹; ¹H NMR (400 MHz, CDCl₃) δ 7.81 (s, 1 H), 7.74 (d, *J* = 7.8 Hz, 1 H), 7.67 (d, *J* = 7.8 Hz, 1 H), 7.52 (t, *J* = 7.8 Hz, 1 H), 7.30 (d, *J* = 8.1 Hz, 1 H), 7.26 (d, *J* = 8.1 Hz, 1 H), 7.22 (s, 1 H), 4.00 (app t, *J* = 5.0 Hz, 2 H), 3.86 (app t, *J* = 4.8 Hz, 2 H), 3.03 (app t, *J* = 5.0 Hz, 2 H), 2.93 (app t, *J* = 5.0 Hz, 2 H), 2.39 (s, 3 H); ¹³C NMR (100 MHz, CDCl₃) δ 152.6, 150.9, 136.8, 135.4, 135.4, 131.5, 131.2 (q, *J*_{CF} = 33.0 Hz), 129.2 (s), 129.0 (q, *J*_{CF} = 32.2 Hz), 129.0 (q, *J*_{CF} = 3.9 Hz), 126.6 (q, *J*_{CF} = 3.7 Hz), 124.0 (q, *J*_{CF} = 272.0 Hz), 123.4 (q, *J*_{CF} = 272.3 Hz), 121.3, 120.5 (q, *J*_{CF} = 3.8 Hz), 88.9, 82.0, 51.8, 51.3, 47.4, 41.9, 17.9; ¹⁹F NMR (376 MHz, CDCl₃) δ -62.3 (s, 3 F), -63.0 (s, 3 F); HRMS (ESI) *m/z* calcd for C₂₂H₁₉F₆N₂O ([M+H]⁺) 441.1396, found 441.1391.



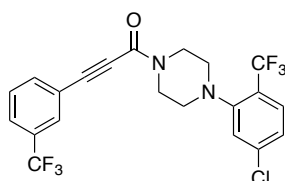
3.21i

(4-(2-Methyl-5-(trifluoromethyl)phenyl)piperazin-1-yl)((1RS,2SR)-2-(3-(trifluoromethyl)phenyl)cyclopropyl)methanone (3.21i). A solution of 1-(4-(2-methyl-5-(trifluoromethyl)phenyl)piperazin-1-yl)-3-(3-(trifluoromethyl)phenyl)prop-2-yn-1-one (**3.17g**, 0.0800 g, 0.182 mmol) in EtOAc (1.8 mL) was treated with Lindlar catalyst (5% Pd on CaCO₃, lead poisoned, 0.0193 g, equivalent to 5 mol% Pd). The reaction was placed under a balloon of

H₂ (3 vacuum/backfill cycles) and stirred at rt for 2 d, filtered through Celite, washed (EtOAc), and concentrated under reduced pressure. The crude residue was purified by automated chromatography on SiO₂ (4g column, liquid load CH₂Cl₂, gradient 100% hexanes to 40% EtOAc/hexanes, product eluted at 10% EtOAc/hexanes) to give the **3.18g** (0.0572 g, 0.129 mmol) as clear/tan viscous oil.

A solution of CrCl₂ (0.0955 g, 0.777 mmol) and (Z)-1-(4-(2-methyl-5-(trifluoromethyl)phenyl)piperazin-1-yl)-3-(3-(trifluoromethyl)phenyl)prop-2-en-1-one (**3.18g**, 0.0573 g, 0.130 mmol) in dry degassed THF (1.3 mL) was sparged with Ar for 5 min and treated with CH₂ICl (75 uL, 0.648 mmol) at rt and under Ar atmosphere, heated for 20 h at 80 °C, cooled to rt, diluted with Et₂O (50 mL), and washed with 1 M aqueous HCl (3 x 20 mL). The organic layer was dried (MgSO₄), filtered and concentrated under reduced pressure. The crude material was purified by automated chromatography on SiO₂ (4g column, liquid load CH₂Cl₂, gradient 100% hexanes to 40% EtOAc/hexanes) to give a clear oil that was filtered through basic Al₂O₃ (CH₂Cl₂/EtOAc, 1:1), recrystallized from CH₂Cl₂/hexanes (ca. 1:5) the mother liquor was decanted and the clear colorless cubes were washed with hexanes (2 x 1 mL) and dried under high vacuum to give **3.21i** (0.0115 g, 0.0252 mmol, 14% (2 steps) (100% purity by ELSD)) as a colorless solid: Mp 113.4-116.8 °C; IR (CH₂Cl₂) 2914, 2824, 1641, 1418, 1328, 1309, 1163, 1121, 1073 cm⁻¹; ¹H NMR (400 MHz, CDCl₃) δ 7.47 (bd, *J* = 7.1 Hz, 2 H), 7.41 (t, *J* = 7.8 Hz, 1 H), 7.33 (d, *J* = 7.8 Hz, 1 H), 7.24 (s, 2 H), 6.92 (s, 1 H), 3.94 (d, *J* = 12.2 Hz, 1 H), 3.79 (d, *J* = 12.2 Hz, 1 H), 3.58 (ddd, *J* = 12.2, 9.2, 3.0 Hz, 1 H), 3.24 (ddd, *J* = 12.2, 9.2, 2.6 Hz, 1 H), 2.77 (td, *J* = 12.2, 3.7 Hz, 2 H), 2.53 (td, *J* = 9.2, 7.0 Hz, 1 H), 2.29 (s, 3 H), 2.28-2.18 (m, 2 H), 2.11-2.05 (m, 1 H), 1.92 (q, *J* = 6.0 Hz, 1 H), 1.42 (td, *J* = 8.5, 6.0 Hz, 1 H); ¹³C NMR (100 MHz, CDCl₃) δ 166.7, 151.1, 138.8, 136.9, 131.4, 130.6 (q, *J*_{CF} = 31.2 Hz), 130.5, 129.1 (q, *J*_{CF} = 32.1

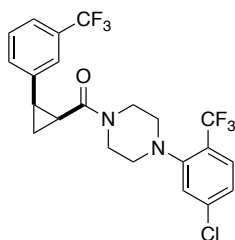
Hz), 128.7, 125.1 (q, $J_{CF} = 3.7$ Hz), 124.2 (q, $J_{CF} = 272.3$ Hz, 2 C), 123.2 (q, $J_{CF} = 3.8$ Hz), 120.4 (q, $J_{CF} = 3.8$ Hz), 116.1 (q, $J_{CF} = 3.7$ Hz), 51.7 (2 C), 45.6, 42.2, 24.2, 24.0, 17.8, 10.9; ^{19}F NMR (376 MHz, CDCl_3) δ -62.4 (s, 3 H), -62.6 (s, 3 H); HRMS (ESI) m/z calcd for $\text{C}_{22}\text{H}_{23}\text{F}_6\text{N}_2\text{O}$ ($[\text{M}+\text{H}]^+$) 457.1709, found 457.1704.



3.17h

1-(4-(5-Chloro-2-(trifluoromethyl)phenyl)piperazin-1-yl)-3-(3-(trifluoromethyl)phenyl)prop-2-yn-1-one (3.17h). A solution of 3-(3-(trifluoromethyl)phenyl)propionic acid (**3.16b**, 0.100 g, 0.467 mmol) and 1-(5-chloro-2-(trifluoromethyl)phenyl)piperazinehydrochloride (**3.12d**, 0.155 g, 0.514 mmol) in CH_2Cl_2 (4.7 mL) cooled to 0 °C was treated with Et_3N (0.26 mL, 1.87 mmol). The cooled solution was treated with T3P (50 wt. % solution in EtOAc , 0.49 mL, 0.701 mmol) dropwise and the reaction was stirred at 0 °C for 30 min, warmed to rt for 16 h, diluted with CH_2Cl_2 (30 mL), washed with H_2O (20 mL), satd. aqueous NaHCO_3 (20 mL), dried (MgSO_4), filtered, and concentrated under reduced pressure. The crude residue was purified by automated chromatography on SiO_2 (4g column, liquid load CH_2Cl_2 , gradient 100% hexanes to 30% EtOAc /hexanes) to give the crude product that was recrystallized from hot EtOH . The supernatant was removed and the crystals were washed with hexanes and then dried under high vacuum to give **3.17h** (0.168 g, 0.365 mmol, 78%) as a colorless solid: Mp 87.6-91.2 °C; IR (CH_2Cl_2) 2921, 2827, 2222, 1633, 1596, 1436, 1332, 1309, 1121, 1034, 695 cm^{-1} ; ^1H NMR (400 MHz, CDCl_3) δ 7.78 (s, 1 H), 7.71 (d, $J = 7.8$ Hz, 1 H), 7.65 (d, $J = 8.5$ Hz, 1 H), 7.56 (d, $J = 8.5$ Hz, 1 H), 7.50 (t, $J = 7.8$ Hz, 1 H),

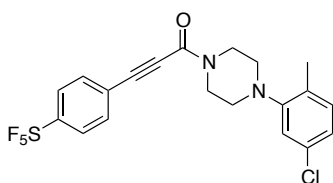
7.26-7.22 (m, 2 H), 3.95 (app t, $J = 5.0$ Hz, 2 H), 3.81 (app t, $J = 5.0$ Hz, 2 H), 2.99 (app t, $J = 5.0$ Hz, 2 H), 2.92 (app t, $J = 5.0$ Hz, 2 H); ^{13}C NMR (100 MHz, CDCl_3) δ 152.6, 138.8, 135.4, 131.2 (q, $J_{\text{CF}} = 33.0$ Hz), 129.2, 129.0 (q, $J_{\text{CF}} = 3.7$ Hz), 128.6 (q, $J_{\text{CF}} = 5.4$ Hz), 126.6 (q, $J_{\text{CF}} = 3.7$ Hz), 125.8 (q, $J_{\text{CF}} = 29.5$ Hz), 125.7, 124.7, 123.5 (q, $J_{\text{CF}} = 273.0$ Hz), 123.2 (q, $J_{\text{CF}} = 272.5$ Hz), 121.3, 88.9, 82.0, 53.6, 52.7, 47.4, 41.8; ^{19}F NMR (376 MHz, CDCl_3) δ -60.3 (s, 3 F), -63.0 (s, 3 F); HRMS (ESI) m/z calcd for $\text{C}_{21}\text{H}_{16}\text{ClF}_6\text{N}_2\text{O}$ ($[\text{M}+\text{H}]^+$) 461.0850, found 461.0849.



(4-(5-Chloro-2-(trifluoromethyl)phenyl)piperazine-1-yl)(2-(3-(trifluoromethyl)phenyl)cyclopropyl)methanone (3.21j). A solution of 1-(4-(5-chloro-2-(trifluoromethyl)phenyl)piperazine-1-yl)-3-(3-(trifluoromethyl)phenyl)prop-2-yn-1-one (**3.17h**, 0.0684 g, 0.148 mmol) in EtOAc (1.5 mL) was treated with Lindlar catalyst (5% Pd on CaCO_3 , lead poisoned, 0.0158 g, equivalent to 5 mol% Pd). The reaction was placed under a balloon of H_2 (3 vacuum/backfill cycles) and stirred at rt for 3 d, filtered through Celite, washed (EtOAc), and the combined filtrates were concentrated under reduced pressure. The crude residue was purified by automated chromatography on SiO_2 (4g column, liquid load CH_2Cl_2 , gradient 100% hexanes to 40% EtOAc/hexanes) to give **3.18h** (0.0512 g, 0.111 mmol) as a colorless solid.

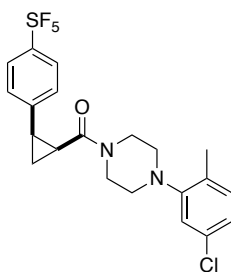
A solution of CrCl_2 (0.816 g, 0.940 mmol) and (*Z*)-1-(4-(5-chloro-2-(trifluoromethyl)phenyl)piperazine-1-yl)-3-(3-(trifluoromethyl)phenyl)prop-2-en-1-one (**3.18h**, 0.0512 g, 0.111 mmol) in dry degassed THF (1.6 mL) was sparged with Ar for 5 min and treated with CH_2I_2 (0.064 mL, 0.553 mmol) at rt, heated for 2 d at 80 °C, cooled to rt, diluted with EtOAc (50 mL), and washed with 1 M aqueous HCl (3 x 20 mL). The organic layer was dried

(MgSO₄), filtered and concentrated under reduced pressure. The crude residue was purified by automated chromatography on SiO₂ (4g column, liquid load CH₂Cl₂, gradient 100% hexanes to 30% EtOAc/hexanes, product eluted at 20% EtOAc/hexanes) to give a clear oil that was filtered through basic Al₂O₃ (eluting with 1:1 CH₂Cl₂/EtOAc), concentrated under reduced pressure, and dried under high vacuum to give **3.21j** (0.0409 g, 0.0858 mmol, 59% (2 steps) (100% purity by ELSD)) as a clear colorless oil: IR (CH₂Cl₂) 2918, 1641, 1596, 1437, 1327, 1120, 1032, 809, 702 cm⁻¹; ¹H NMR (400 MHz, CDCl₃) δ 7.54-7.50 (m, 3 H), 7.44 (t, *J* = 8.0 Hz, 1 H), 7.34 (d, *J* = 8.0 Hz, 1 H), 7.20 (dd, *J* = 8.5, 1.4 Hz, 1 H), 6.87 (d, *J* = 1.6 Hz, 1 H), 4.02 (d, *J* = 13.0 Hz, 1 H), 3.80 (d, *J* = 13.0 Hz, 1 H), 3.51 (ddd, *J* = 12.8, 9.8, 3.0 Hz, 1 H), 3.13 (ddd, *J* = 12.5, 9.8, 2.7 Hz, 1 H), 2.73 (td, *J* = 7.7, 3.6 Hz, 2 H), 2.52 (td, *J* = 9.0, 7.0 Hz, 1 H), 2.25 (ddd, *J* = 9.0, 8.4, 6.0 Hz, 1 H), 2.21-2.15 (m, 1 H), 1.97-1.90 (m, 2 H), 1.42 (td, *J* = 8.4, 6.0 Hz, 1 H); ¹³C NMR (100 MHz, CDCl₃) δ 166.6, 152.7, 138.9, 138.7, 130.6 (q, *J*_{CF} = 32.1 Hz), 130.5, 128.7, 128.3 (q, *J*_{CF} = 5.4 Hz), 125.8 (q, *J*_{CF} = 29.4 Hz), 125.6, 125.1 (q, *J*_{CF} = 3.8 Hz), 124.6, 124.2 (q, *J*_{CF} = 272.4 Hz), 123.5 (q, *J*_{CF} = 272.9 Hz), 123.2 (q, *J*_{CF} = 3.7 Hz), 53.5, 53.0, 45.5, 42.1, 24.3, 23.9, 10.9; ¹⁹F NMR (376 MHz, CDCl₃) δ -60.4 (s, 3 F), -62.4 (s, 3 F); HRMS (ESI) *m/z* calcd for C₂₂H₂₀ClF₆N₂O ([M+H]⁺) 477.1163, found 477.1166.



1-(4-(5-Chloro-2-methylphenyl)piperazine-1-yl)-3-(4-(pentafluoro-λ6-sulfanyl)phenyl)prop-2-yn-1-one (3.17i). A solution of 3-(4-(pentafluoro-λ6-sulfanyl)phenyl)propionic acid (**3.16c**, 0.100 g, 0.367 mmol) and 1-(1-(5-chloro-2-methylphenyl)piperazine hydrochloride (**3.12b**, 0.0999 g, 0.404 mmol) in CH₂Cl₂ (3.7 mL)

cooled to 0 °C was treated with Et₃N (0.20 mL, 1.47 mmol). The cooled solution was treated with T3P (50 wt. % solution in EtOAc, 0.39 mL, 0.551 mmol) dropwise and the reaction was stirred at 0 °C for 30 min, warmed to rt for 16 h, diluted with EtOAc (30 mL), washed with H₂O (20 mL), satd. aqueous NaHCO₃ (20 mL), dried (MgSO₄), filtered, and concentrated under reduced pressure. The crude residue was purified by automated chromatography on SiO₂ (4g column, liquid load CH₂Cl₂, gradient 100% hexanes to 30% EtOAc/hexanes), to give **3.17i** (0.127 g, 0.272 mmol, 74%) as a pale yellow foam: IR (CHCl₃) 2981, 2222, 1627, 1490, 1432, 1275, 832, 792, 727 cm⁻¹; ¹H NMR (400 MHz, CDCl₃) δ 7.76 (d, *J* = 8.8 Hz, 2 H), 7.64 (d, *J* = 8.8 Hz, 2 H), 7.11 (d, *J* = 8.1 Hz, 1 H), 6.99 (dd, *J* = 8.1, 2.1 Hz, 1 H), 6.95 (d, *J* = 2.1 Hz, 1 H), 3.96 (app t, *J* = 5.0 Hz, 2 H), 3.84 (app t, *J* = 5.0 Hz, 2 H), 2.97 (app t, *J* = 5.0 Hz, 2 H), 2.89 (app t, *J* = 5.0 Hz, 2 H), 2.29 (s, 3 H); ¹³C NMR (100 MHz, CDCl₃) δ 154.4 (quint, *J*_{CF} = 18.3 Hz), 152.4, 151.6, 132.4, 132.1, 131.9, 131.0, 126.2 (quint, *J*_{CF} = 4.6 Hz), 124.1, 123.8, 119.8, 88.2, 83.2, 51.9, 51.3, 47.4, 42.0, 17.3; ¹⁹F NMR (376 MHz, CDCl₃) δ 83.0 (quint, *J* = 150.3 Hz, 1 F), 62.4 (d, *J* = 150.3 Hz, 4 F); HRMS (ESI) *m/z* calcd for C₂₀H₁₉ClF₅N₂OS ([M+H]⁺) 465.0821, found 465.0819.



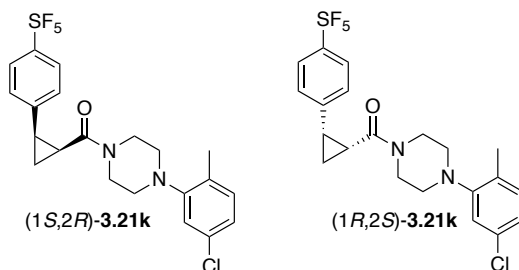
3.21k

(4-(5-Chloro-2-methylphenyl)piperazin-1-yl)((1*RS*,2*SR*)-2-(4-(pentafluoro-λ6-sulfaneyl)phenyl)cyclopropyl)methanone (3.21k). A solution of 1-(4-(5-chloro-2-methylphenyl)piperazin-1-yl)-3-(4-(pentafluoro-λ6-sulfaneyl)phenyl)prop-2-yn-1-one (**3.17i**,

0.0850 g, 0.183 mmol) in EtOAc (1.8 mL) was treated with Lindlar catalyst (5% Pd on CaCO₃, lead poisoned, 0.0195 g, equivalent to 5 mol% Pd). The reaction was placed under a balloon of H₂ (3 vacuum/backfill cycles) and stirred at rt for 2 d, filtered through Celite, washed (EtOAc), and the combined filtrates were concentrated under reduced pressure. The crude residue was purified by automated chromatography on SiO₂ (4g column, liquid load CH₂Cl₂, gradient 100% hexanes to 40% EtOAc/hexanes, product eluted at 35% EtOAc/hexanes) to give **3.18i** (0.0811 g, 0.174 mmol) as a colorless solid.

A solution of CrCl₂ (0.126 g, 1.03 mmol) and (*Z*)-1-(4-(5-chloro-2-methylphenyl)piperazin-1-yl)-3-(4-(pentafluoro- λ 6-sulfaneyl)phenyl)prop-2-en-1-one (**3.18i**, 0.0800 g, 0.171 mmol) in dry degassed THF (1.7 mL) was sparged with Ar for 5 min and added CH₂ICl (0.10 mL, 0.857 mmol) at rt, heated for 2 d at 80 °C, cooled to rt, diluted with EtOAc (50 mL) and washed with 1 M aqueous HCl (3 x 20 mL). The organic layer was dried (MgSO₄), filtered and concentrated under reduced pressure. The crude residue was purified by automated chromatography on SiO₂ (4g column, liquid load CH₂Cl₂, gradient 100% hexanes to 30% EtOAc/hexanes, product eluted at 30% EtOAc/hexanes) to give a clear oil that was filtered through basic Al₂O₃ (CH₂Cl₂/EtOAc, 1:1), concentrated under reduced pressure, and dried under high vacuum to give **3.21k** (0.0451 g, 0.0938 mmol, 52% (2 steps) (100% purity by ELSD)) as a colorless solid: Mp 169.8-172.0 °C; IR (CH₂Cl₂) 2919, 1639, 1490, 1466, 1438, 1225, 1035, 835, 750 cm⁻¹; ¹H NMR (400 MHz, CDCl₃) δ 7.66 (d, *J* = 8.6 Hz, 2 H), 7.25 (d, *J* = 8.6 Hz, 2 H), 7.06 (dd, *J* = 8.1, 0.4 Hz, 1 H), 6.95 (dd, *J* = 8.1, 2.1 Hz, 1 H), 6.69 (d, *J* = 2.1 Hz, 1 H), 3.82 (bd, *J* = 14.0 Hz, 1 H), 3.70-3.58 (m, 2 H), 3.33 (ddd, *J* = 12.4, 8.9, 3.0 Hz, 1 H), 2.75 (tdd, *J* = 14.0, 7.7, 3.4 Hz, 2 H), 2.50 (td, *J* = 8.9, 7.0 Hz, 1 H), 2.32-2.23 (m, 2 H), 2.20 (s, 3 H), 2.10 (ddd, *J* = 11.1, 8.2, 3.0 Hz, 1 H), 1.91 (q, *J* = 6.3 Hz, 1 H), 1.44 (td, *J* = 8.4, 5.6 Hz, 1 H); ¹³C

NMR (100 MHz, CDCl₃) δ 166.5, 152.1 (quint, $J_{CF} = 17.3$ Hz), 151.6, 141.9, 131.9 (2 C), 130.9, 127.7, 125.7 (quint, $J_{CF} = 4.6$ Hz), 123.7, 119.5, 51.9, 51.5, 45.5, 42.2, 24.6, 23.7, 17.3, 11.3; ¹⁹F NMR (376 MHz, CDCl₃) δ 84.8 (quint, $J = 150.4$ Hz, 1 F), 63.2 (d, $J = 150.4$ Hz, 4 F); HRMS (ESI) m/z calcd for C₂₁H₂₃ClF₅N₂OS ([M+H]⁺) 481.1134, found 481.1134.



Racemic (4-(5-chloro-2-methylphenyl)piperazin-1-yl)((1*RS*,2*SR*)-2-(4-(pentafluoro- λ 6-sulfaneyl)phenyl)cyclopropyl)methanone (**3.21k**) was separated on a SFC Chiralpak-IC semiprep (250 x 10 mm) column (30% Methanol:CO₂, 7 mL/min, $p = 100$ bar, 220 nm) injection volume 90 μ L, 20 mg/mL) to give (4-(5-chloro-2-methylphenyl)piperazin-1-yl)((1*S*,2*R*)-2-(4-(pentafluoro- λ 6-sulfaneyl)phenyl)cyclopropyl)methanone ((1*S*,2*R*)-**3.21k**) (retention time 5.14 min) as a colorless viscous oil (100% purity by ELSD): $[\alpha]_D^{17} -134.2$ (c 0.60, MeOH); ¹H NMR (300 MHz, CDCl₃) δ 7.66 (d, $J = 8.7$ Hz, 2 H), 7.26 (overlap, 2 H), 7.06 (d, $J = 8.1$ Hz, 1 H), 6.96 (dd, $J = 8.1, 1.8$ Hz, 1 H), 6.70 (d, $J = 1.8$ Hz, 1 H), 3.87-3.79 (m, 1 H), 3.73-3.58 (m, 3 H), 3.38-3.31 (m, 1 H), 2.81-2.70 (m, 2 H), 2.50 (q, $J = 8.7$ Hz, 1 H), 2.33-2.24 (m, 2 H), 2.20 (s, 3 H), 2.16-2.08 (m, 1 H), 1.91 (q, $J = 5.7$ Hz, 1 H), 1.44 (td, $J = 8.1, 5.7$ Hz, 1 H). The enantiomeric excess was >99.9% ee (SFC Chiralpak-IC (250 x 10 mm); 30% Methanol:CO₂, 7 mL/min, $p = 100$ bar, 220 nm; retention time: 5.1 min).

(4-(5-Chloro-2-methylphenyl)piperazin-1-yl)((1*R*,2*S*)-2-(4-(pentafluoro- λ 6-sulfaneyl)phenyl)cyclopropyl)methanone ((1*R*,2*S*)-**3.21k**) (retention time 6.57 min) was obtained as a colorless viscous oil (100% purity by ELSD): $[\alpha]_D^{17} +136.3$ (c 0.59, MeOH); ¹H

NMR (300 MHz, CDCl_3) δ 7.66 (d, $J = 8.7$ Hz, 2 H), 7.26-7.24 (m, 2 H), 7.06 (d, $J = 8.4$ Hz, 1 H), 6.96 (dd, $J = 8.4, 1.8$ Hz, 1 H), 6.70 (d, $J = 1.8$ Hz, 1 H), 3.85-3.78 (m, 1 H), 3.67-3.61 (m, 2 H), 3.39-3.30 (m, 1 H), 2.81-2.70 (m, 2 H), 2.50 (q, $J = 8.7$ Hz, 1 H), 2.33-2.24 (m, 2 H), 2.20 (s, 3 H), 2.16-2.10 (m, 1 H), 1.91 (q, $J = 5.7$ Hz, 1 H), 1.44 (td, $J = 8.4, 5.7$ Hz, 2 H). The enantiomeric excess was $>99.9\%$ ee (SFC Chiralpak-IC (250 x 10 mm); 30% Methanol: CO_2 , 7 mL/min, $p = 100$ bar, 220 nm; retention time: 6.5 min).

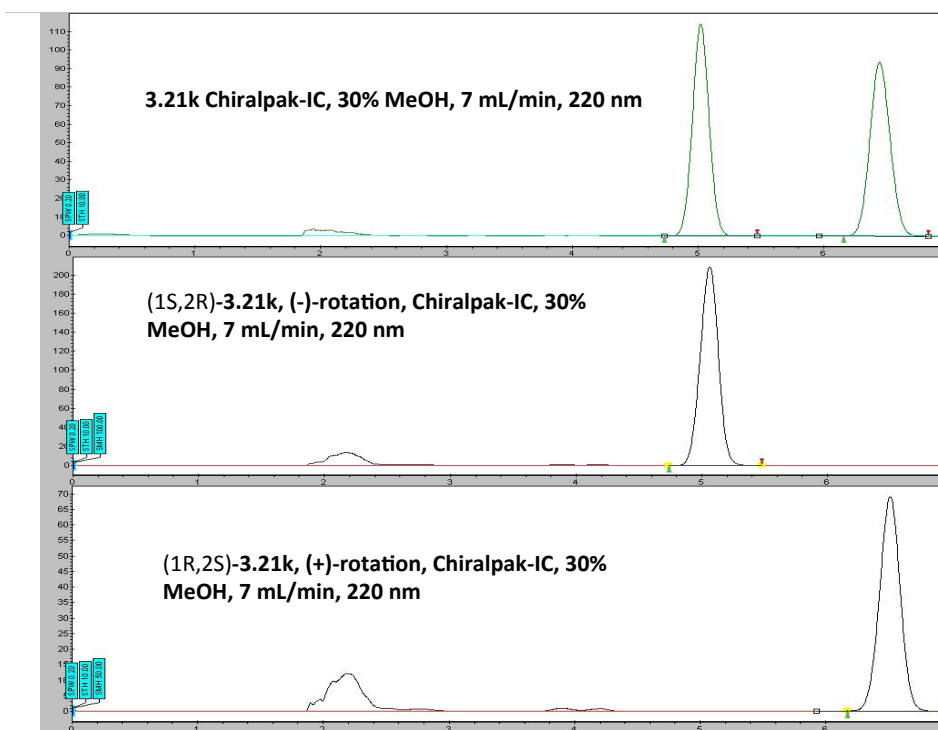
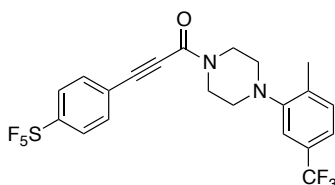


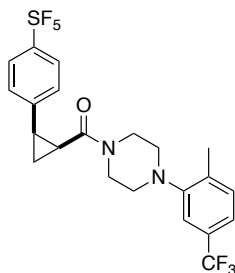
Figure 5.8. SFC chromatograms for **3.21k** and separated enantiomers.



3.17j

1-(4-(2-Methyl-5-(trifluoromethyl)phenyl)piperazin-1-yl)-3-(4-(pentafluoro- λ 6-sulfanyl)phenyl)prop-2-yn-1-one (3.17j). A solution of 3-(4-(pentafluoro- λ 6-

sulfaneyl)phenyl)propionic acid (**3.16c**, 0.100 g, 0.367 mmol) and 1-(2-methyl-5-(trifluoromethyl)phenyl)piperazine hydrochloride (**3.12b**, 0.113 g, 0.404 mmol) in CH₂Cl₂ (3.7 mL) cooled to 0 °C was treated with Et₃N (0.20 mL, 1.47 mmol). The cooled solution was treated with T3P (50 wt. % solution in EtOAc, 0.39 mL, 0.551 mmol) dropwise and the reaction was stirred at 0 °C for 30 min, warmed to rt for 16 h, diluted with EtOAc (30 mL), washed with H₂O (20 mL), satd. aqueous NaHCO₃ (20 mL), dried (MgSO₄), filtered, and concentrated under reduced pressure. The crude residue was purified by automated chromatography on SiO₂ (4g column, liquid load CH₂Cl₂, gradient 100% hexanes to 40% EtOAc/hexanes), to give **3.17j** (0.139 g, 0.278 mmol, 76%) as a tan foam: IR (CH₂Cl₂) 2920, 2222, 1632, 1418, 1340, 1310, 1279, 1122, 839, 793 cm⁻¹; ¹H NMR (400 MHz, CDCl₃) δ 7.75 (d, *J* = 8.8 Hz, 2 H), 7.63 (d, *J* = 8.8 Hz, 2 H), 7.31-7.25 (m, 2 H), 7.21 (s, 1 H), 3.98 (t, *J* = 5.0 Hz, 2 H), 3.85 (app t, *J* = 5.0 Hz, 2 H), 3.02 (app t, *J* = 5.0 Hz, 2 H), 2.92 (app t, *J* = 5.0 Hz, 2 H), 2.38 (s, 3 H); ¹³C NMR (100 MHz, CDCl₃) δ 154.3 (quint, *J*_{CF} = 18.1 Hz), 152.4, 150.9, 136.8, 132.4, 131.5, 129.0 (q, *J*_{CF} = 32.1 Hz), 126.2 (quint, *J*_{CF} = 4.6 Hz), 124.1 (q, *J*_{CF} = 272.1 Hz), 124.0, 120.5 (q, *J*_{CF} = 3.8 Hz), 116.0 (q, *J*_{CF} = 3.6 Hz), 88.2, 83.1, 51.8, 51.3, 47.4, 41.9, 17.8; ¹⁹F NMR (376 MHz, CDCl₃) δ 83.0 (quint, *J* = 150.4 Hz, 1 F), 62.4 (d, *J* = 150.2 Hz, 4 F), -62.3 (s, 3 F); HRMS (ESI) *m/z* calcd for C₂₁H₁₉F₈N₂OS ([M+H]⁺) 499.1085, found 499.1086.

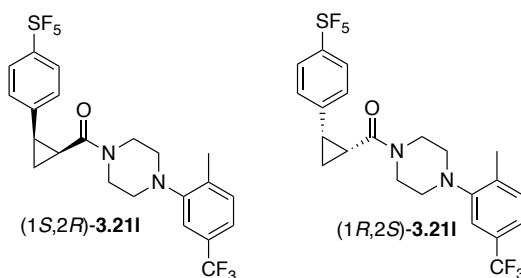


3.21i

(4-(2-Methyl-5-(trifluoromethyl)phenyl)piperazin-1-yl)((1*RS*,2*SR*)-2-(4-(pentafluoro- λ 6-sulfanyl)phenyl)cyclopropyl)methanone (3.211). A solution of 1-(4-(2-methyl-5-(trifluoromethyl)phenyl)piperazin-1-yl)-3-(4-(pentafluorosulfanyl)phenyl)prop-2-yn-1-one (**3.17j**, 0.100 g, 0.201 mmol) in EtOAc (2 mL) was treated with Lindlar catalyst (5% Pd on CaCO₃, lead poisoned, 0.0214 g, equivalent to 5 mol% Pd). The reaction was placed under a balloon of H₂ (3 vacuum/backfill cycles) and stirred at rt for 2 d, filtered through Celite, washed (EtOAc), and the combined filtrates were concentrated under reduced pressure. The crude residue was purified by automated chromatography on SiO₂ (4g column, gradient 100% hexanes to 40% EtOAc/hexanes, product eluted at 30% EtOAc/hexanes) to give **3.18j** (0.0765 g, 0.153 mmol) as a colorless foam.

A solution of CrCl₂ (0.111 g, 0.899 mmol) and (*Z*)-1-(4-(2-methyl-5-(trifluoromethyl)phenyl)piperazin-1-yl)-3-(4-(pentafluoro- λ 6-sulfanyl)phenyl)prop-2-en-1-one (**3.18j**, 0.0750 g, 0.150 mmol) in dry degassed THF (1.5 mL) was sparged with Ar for 5 min, treated with CH₂ICl (0.087 mL, 0.749 mmol) sparged with Ar for 2 min, heated for 2 d at 80 °C, cooled to rt, diluted with EtOAc (50 mL), washed with 1 M aqueous HCl (3 x 20 mL). The organic layer was dried (MgSO₄), filtered and concentrated under reduced pressure. The crude residue was purified by automated chromatography on SiO₂ (4g column, liquid load CH₂Cl₂, gradient 100% hexanes to 30% EtOAc/hexanes, product eluted at 30% EtOAc/hexanes) to give the product as a clear oil that was filtered through basic Al₂O₃ (CH₂Cl₂/EtOAc, 1:1) concentrated to a colorless solid. The solid was recrystallized from hot cyclohexane (2x). The supernatant was removed and the crystals were washed with cyclohexane (2 x 1 mL) and hexanes (2 x 1 mL) and dried under high vacuum to give **3.211** (0.0176 g, 0.0342 mmol, 18% (2 steps) (100% purity by ELSD)) as a colorless solid: Mp 122.1-125.8 °C; IR (CH₂Cl₂) 2919, 1638, 1417, 1338, 1308,

1120, 824, 749 cm^{-1} ; ^1H NMR (400 MHz, CDCl_3) δ 7.65 (d, $J = 8.8$ Hz, 2 H), 7.26-7.24 (m, 5 H), 6.96 (s, 1 H), 3.85 (bd, $J = 13.0$ Hz, 1 H), 3.72-3.60 (m, 2 H), 3.38-3.32 (m, 1 H), 2.86-2.75 (m, 2 H), 2.51 (td, $J = 8.9, 7.0$ Hz, 1 H), 2.32-2.26 (m, 5 H), 2.14 (ddd, $J = 11.0, 8.6, 2.6$ Hz, 1 H), 1.92 (q, $J = 6.2$ Hz, 1 H), 1.45 (td, $J = 8.4, 5.6$ Hz, 1 H); ^{13}C NMR (100 MHz, CDCl_3) δ 166.5, 152.2 (quint, $J_{\text{CF}} = 17.4$ Hz), 150.9, 141.8, 136.7, 131.4, 129.1 (q, $J_{\text{CF}} = 32.1$ Hz), 127.7, 125.7, 125.7 (quint, $J_{\text{CF}} = 4.6$ Hz), 124.0 (q, $J_{\text{CF}} = 271.9$ Hz), 120.4 (q, $J_{\text{CF}} = 3.9$ Hz), 115.7 (q, $J_{\text{CF}} = 3.8$ Hz), 51.9, 51.4, 45.5, 42.2, 24.6, 23.7, 17.9, 11.3; ^{19}F NMR (376 MHz, CDCl_3) δ 84.6 (quint, $J = 149.9$ Hz, 1 F), 63.0 (d, $J = 149.8$ Hz, 4 F), -62.4 (s, 3 F); HRMS (ESI) m/z calcd for $\text{C}_{22}\text{H}_{23}\text{F}_8\text{N}_2\text{OS}$ ($[\text{M}+\text{H}]^+$) 515.1398, found 515.1378.



Racemic (4-(2-methyl-5-(trifluoromethyl)phenyl)piperazin-1-yl)((1*R*S,2*S*R)-2-(4-(pentafluoro- λ 6-sulfaneyl)phenyl)cyclopropyl)methanone (**3.211**) was separated on a SFC Chiralpak-IC semiprep (250 x 10 mm) column (30% Methanol: CO_2 , 7 mL/min, $p = 100$ bar, 220 nm) injection volume (90 μL , 20 mg/mL) to give (4-(2-methyl-5-(trifluoromethyl)phenyl)piperazine-1-yl)((1*S*,2*R*)-2-(4-(pentafluoro- λ 6-sulfaneyl)phenyl)cyclopropyl)methanone ((1*S*,2*R*)-**3.211**) (retention time 3.40 min) as a colorless viscous oil (100% purity by ELSD): $[\alpha]_{\text{D}}^{17} -119.1$ (c 0.79, MeOH); ^1H NMR (300 MHz, CDCl_3) δ 7.66 (d, $J = 8.7$ Hz, 2 H), 7.25 (d, $J = 8.7$ Hz, 3 H), 6.97 (s, 1 H), 3.89-3.80 (m, 1 H), 3.72-3.60 (m, 2 H), 3.40-3.31 (m, 1 H), 2.86-2.74 (m, 2 H), 2.50 (q, $J = 8.4$ Hz, 1 H), 2.33-2.25 (m, 5 H), 2.18-2.12 (m, 1 H), 1.92 (q, $J = 6.0$ Hz, 1 H), 1.44 (td, $J = 8.4, 6.0$ Hz, 1 H). The enantiomeric

excess was >99.9% ee (SFC Chiralpak-IC (250 x 10 mm); 30% Methanol:CO₂, 7 mL/min, p = 100 bar, 220 nm; retention time: 3.3 min).

(4-(2-Methyl-5-(trifluoromethyl)phenyl)piperazine-1-yl)((1*R*,2*S*)-2-(4-(pentafluoro- λ 6-sulfaneyl)phenyl)cyclopropyl)methanone ((1*R*,2*S*)-**3.211**) (retention time 3.65 min) was obtained as a colorless viscous oil (100% purity by ELSD): $[\alpha]_D^{17} +117.0$ (*c* 0.87, MeOH); ¹H NMR (300 MHz, CDCl₃) δ 7.66 (d, *J* = 8.7 Hz, 2 H), 7.26 (d, *J* = 8.7 Hz, 3 H), 6.97 (s, 1 H), 3.88-3.82 (m, 2 H), 3.69-3.63 (m, 3 H), 3.40-3.31 (m, 2 H), 2.89-2.70 (m, 3 H), 2.50 (q, *J* = 8.4 Hz, 2 H), 2.34-2.25 (m, 5 H), 2.20-2.12 (m, 1 H), 1.92 (q, *J* = 6.0 Hz, 1 H), 1.44 (td, *J* = 8.4, 6.0 Hz, 1 H). The enantiomeric excess was >99.9% ee (SFC Chiralpak-IC (250 x 10 mm); 30% Methanol:CO₂, 7 mL/min, p = 100 bar, 220 nm; retention time: 3.7 min).

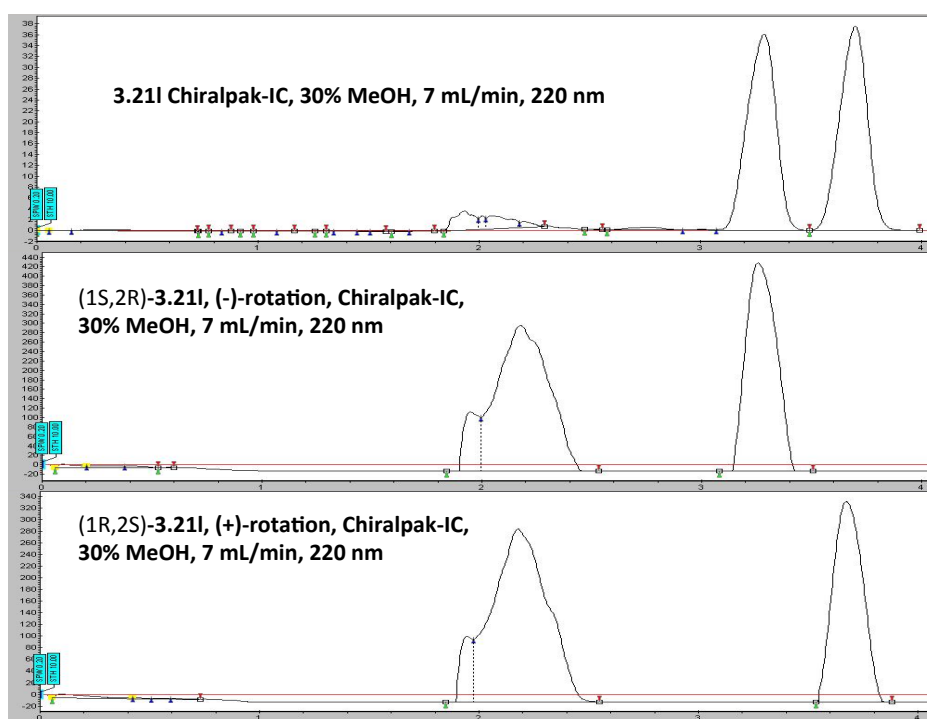
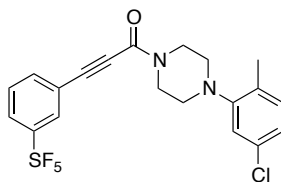
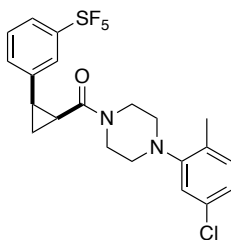


Figure 5.9. SFC chromatograms for **3.211** and separated enantiomers.



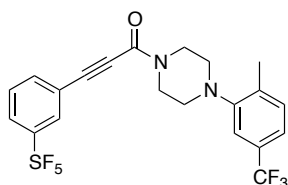
1-(4-(5-Chloro-2-methylphenyl)piperazine-1-yl)-3-(3-(pentafluoro-λ6-sulfaneyl)phenyl)prop-2-yn-1-one (3.17k). A solution of 3-(3-(pentafluoro-λ6-sulfaneyl)phenyl)propionic acid (**3.16d**, 0.100 g, 0.367 mmol) and 1-(1-(5-chloro-2-methylphenyl)piperazine hydrochloride (**3.12b**, 0.0999 g, 0.404 mmol) in CH₂Cl₂ (3.7 mL) cooled to 0 °C was treated with Et₃N (0.20 mL, 1.47 mmol). The cooled solution was treated with T3P (50 wt. % solution in EtOAc, 0.39 mL, 0.551 mmol) dropwise and the reaction was stirred at 0 °C for 30 min and allowed to warm to rt for 16 h. The reaction was diluted with EtOAc (30 mL) and washed with H₂O (20 mL), satd. aqueous NaHCO₃ (20 mL), dried (MgSO₄), filtered, and concentrated under reduced pressure. The crude residue was purified by automated chromatography on SiO₂ (4g column, liquid load CH₂Cl₂, gradient 100% hexanes to 30% EtOAc/hexanes), to give **3.17k** (0.113 g, 0.244 mmol, 66%) as a pale yellow solid: Mp 127.9-133.0 °C; IR (CHCl₃) 2921, 2219, 1627, 1432, 1288, 1223, 1041, 838, 797, 728 cm⁻¹; ¹H NMR (400 MHz, CDCl₃) δ 7.94 (t, *J* = 2.0 Hz, 1 H), 7.80 (ddd, *J* = 8.4, 2.0, 0.8 Hz, 1 H), 7.69 (d, *J* = 7.7 Hz, 1 H), 7.49 (t, *J* = 8.1 Hz, 1 H), 7.11 (d, *J* = 8.1 Hz, 1 H), 6.99 (dd, *J* = 8.1, 2.1 Hz, 1 H), 6.96 (d, *J* = 2.1 Hz, 1 H), 3.97 (app t, *J* = 5.0 Hz, 2 H), 3.84 (app t, *J* = 5.0 Hz, 2 H), 2.98 (app t, *J* = 5.0 Hz, 2 H), 2.89 (app t, *J* = 5.0 Hz, 2 H), 2.29 (s, 3 H); ¹³C NMR (100 MHz, CDCl₃) δ 153.8 (quint, *J*_{CF} = 18.5 Hz), 152.4, 151.6, 135.1, 132.1, 131.9, 131.0, 129.7 (quint, *J*_{CF} = 7.1 Hz), 129.0, 127.3 (quint, *J*_{CF} = 4.5 Hz), 123.8, 121.6, 119.8, 88.4, 82.3, 51.9, 51.3, 47.4, 42.0, 17.3; ¹⁹F NMR (376 MHz, CDCl₃) δ 82.9 (quint, *J* = 150.6 Hz, 1 F), 62.6 (d, *J* = 150.5 Hz, 4 F); HRMS (ESI) *m/z* calcd for C₂₀H₁₉ClF₅N₂OS ([M+H]⁺) 465.0821, found 465.0821.



(4-(5-Chloro-2-methylphenyl)piperazine-1-yl)((1*RS*,2*SR*)-2-(3-(pentafluoro- λ 6-sulfaneyl)phenyl)cyclopropyl)methanone (3.21m). A solution of 1-(4-(5-chloro-2-methylphenyl)piperazine-1-yl)-3-(4-(pentafluorosulfanyl)phenyl)prop-2-yn-1-one (**3.17k**, 0.0930 g, 0.200 mmol) in EtOAc (2 mL) was treated with Lindlar catalyst (5% Pd on CaCO₃, lead poisoned, 0.0213 g, equivalent to 5 mol% Pd). The reaction was placed under a balloon of H₂ (3 vacuum/backfill cycles) and stirred at rt for 3 d, filtered through Celite, washed (EtOAc) and the combined filtrates were concentrated under reduced pressure. The crude residue was purified by automated chromatography on SiO₂ (4g column, liquid load CH₂Cl₂, gradient 100% hexanes to 30% EtOAc/hexanes, product eluted at 20% EtOAc/hexanes) to give **3.18k** (0.0470 g, 0.101 mmol) as a colorless solid.

A solution of CrCl₂ (0.0742 g, 0.604 mmol) and (*Z*)-1-(4-(5-chloro-2-methylphenyl)piperazine-1-yl)-3-(3-(pentafluoro- λ 6-sulfaneyl)phenyl)prop-2-en-1-one (**3.18k**, 0.0470 g, 0.101 mmol) in dry degassed THF (1 mL) was treated with CH₂I₂ (0.058 mL, 0.503 mmol) at rt, heated for 2 d at 80 °C. The reaction was cooled to rt, diluted with EtOAc (50 mL) and washed with 1 M aqueous HCl (3 x 20 mL). The organic layer was dried (MgSO₄), filtered and concentrated under reduced pressure. The crude residue was purified by automated chromatography on SiO₂ (4g column, liquid load CH₂Cl₂, gradient 100% hexanes to 30% EtOAc/hexanes, product eluted at 20% EtOAc/hexanes), filtered through basic Al₂O₃ (CH₂Cl₂/EtOAc, 1:1) concentrated and dried under high vacuum to give **3.21m** (0.0182 g, 0.0378 mmol, 19% (2 steps) (100% purity by ELSD)) as a colorless solid: Mp 112.9-116.1 °C; IR

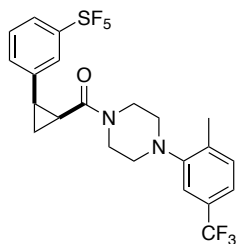
(CH₂Cl₂) 2854, 1640, 1490, 1439, 1225, 1036, 841 cm⁻¹; ¹H NMR (400 MHz, CDCl₃) δ 7.62-7.59 (m, 2 H), 7.38 (t, *J* = 8.1 Hz, 1 H), 7.29 (d, *J* = 7.8 Hz, 1 H), 7.06 (d, *J* = 8.5 Hz, 1 H), 6.95 (dd, *J* = 8.1, 2.1 Hz, 1 H), 6.70 (d, *J* = 2.1 Hz, 1 H), 3.84 (bd, *J* = 12.8 Hz, 1 H), 3.76-3.71 (m, 1 H), 3.61 (ddd, *J* = 12.8, 8.9, 3.2 Hz, 1 H), 3.29 (ddd, *J* = 12.8, 9.0, 3.1 Hz, 1 H), 2.80-2.71 (m, 2 H), 2.53 (td, *J* = 8.9, 6.9 Hz, 1 H), 2.31-2.23 (m, 2 H), 2.20 (s, 3 H), 2.15-2.09 (m, 1 H), 1.91 (q, *J* = 6.2 Hz, 1 H), 1.43 (td, *J* = 8.4, 5.6 Hz, 1 H); ¹³C NMR (100 MHz, CDCl₃) δ 166.6, 153.9 (quint, *J*_{CF} = 16.8 Hz), 151.8, 139.0, 132.0, 131.8, 131.0, 130.2, 128.6, 125.9 (quint, *J*_{CF} = 4.5 Hz), 124.0 (quint, *J*_{CF} = 4.6 Hz), 123.7, 119.7, 51.8, 51.6, 45.6, 42.2, 24.1, 24.0, 17.3, 11.0; ¹⁹F NMR (376 MHz, CDCl₃) δ 84.7 (quint, *J* = 150.1 Hz, 1 F), 62.9 (d, *J* = 149.9 Hz, 4 F); HRMS (ESI) *m/z* calcd for C₂₁H₂₃ClF₅N₂OS ([M+H]⁺) 481.1134, found 481.1133.



3.171

1-(4-(2-Methyl-5-(trifluoromethyl)phenyl)piperazine-1-yl)-3-(3-(pentafluoro-λ6-sulfaneyl)phenyl)prop-2-yn-1-one (3.171). A solution of 3-(3-(pentafluoro-λ6-sulfaneyl)phenyl)propionic acid (**3.16d**, 0.100 g, 0.367 mmol) and 1-(2-methyl-5-(trifluoromethyl)phenyl)piperazine hydrochloride (**3.12c**, 0.113 g, 0.404 mmol) in CH₂Cl₂ (3.7 mL) cooled to 0 °C was treated with Et₃N (0.20 mL, 1.47 mmol). The cooled solution was treated with T3P (50 wt. % solution in EtOAc, 0.39 mL, 0.551 mmol) dropwise and the reaction was stirred at 0 °C for 30 min, warmed to rt for 18 h, diluted with EtOAc (30 mL), washed with H₂O (20 mL), satd. aqueous NaHCO₃ (20 mL), dried (MgSO₄), filtered, and concentrated under reduced pressure. The crude residue was purified by automated chromatography on SiO₂ (4g

column, liquid load CH₂Cl₂, gradient 100% hexanes to 40% EtOAc/hexanes) to give **3.171** (0.150 g, 0.300 mmol, 82%) as a tan foam: IR (CH₂Cl₂) 2919, 2825, 2219, 1629, 1418, 1309, 1152, 1119, 840, 797, 730 cm⁻¹; ¹H NMR (400 MHz, CDCl₃) δ 7.94 (t, *J* = 1.8 Hz, 1 H), 7.81 (dt, *J* = 8.2, 1.1 Hz, 1 H), 7.70 (d, *J* = 7.8 Hz, 1 H), 7.50 (t, *J* = 8.2 Hz, 1 H), 7.29 (q, *J* = 7.8 Hz, 2 H), 7.22 (s, 1 H), 4.00 (app t, *J* = 5.0 Hz, 2 H), 3.87 (app t, *J* = 5.0 Hz, 2 H), 3.04 (app t, *J* = 5.0 Hz, 2 H), 2.94 (app t, *J* = 5.0 Hz, 2 H), 2.39 (s, 3 H); ¹³C NMR (100 MHz, CDCl₃) δ 153.8 (quint, *J*_{CF} = 18.2 Hz), 152.5, 150.9, 136.8, 135.1, 131.6, 129.7 (quint, *J*_{CF} = 4.7 Hz), 129.1 (q, *J*_{CF} = 32.3 Hz), 129.1, 127.4 (quint, *J*_{CF} = 4.7 Hz), 124.1 (q, *J*_{CF} = 271.8 Hz), 121.5, 120.6 (q, *J*_{CF} = 3.9 Hz), 116.1 (q, *J*_{CF} = 3.6 Hz), 88.4, 82.3, 51.9, 51.3, 47.4, 42.0, 17.9; ¹⁹F NMR (376 MHz, CDCl₃) δ 82.9 (quint, *J* = 150.6 Hz, 1 F), 62.6 (d, *J* = 150.4 Hz, 4 F), -62.3 (s, 3 F); HRMS (ESI) *m/z* calcd for C₂₁H₁₉F₈N₂OS ([M+H]⁺) 499.1085, found 499.1086.

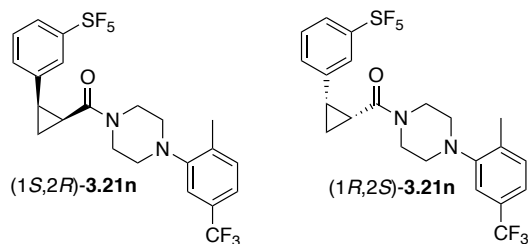


3.21n

(4-(2-Methyl-5-(trifluoromethyl)phenyl)piperazine-1-yl)((1*RS*,2*SR*)-2-(3-(pentafluoro-λ6-sulfaneyl)phenyl)cyclopropyl)methanone (3.21n). A solution of 1-(4-(2-methyl-5-(trifluoromethyl)phenyl)piperazine-1-yl)-3-(3-(pentafluoro-λ6-sulfaneyl)phenyl)prop-2-yn-1-one (**3.171**, 0.100 g, 0.201 mmol) in EtOAc (2 mL) was treated with Lindlar catalyst (5% Pd on CaCO₃, lead poisoned, 0.0214 g, equivalent to 5 mol% Pd). The reaction was placed under a balloon of H₂ (3 vacuum/backfill cycles) and stirred at rt for 2 d, filtered through Celite, washed (EtOAc), and the combined filtrates were concentrated under reduced pressure. The crude residue was purified by automated chromatography on SiO₂ (4g column, liquid load

CH₂Cl₂, gradient 100% hexanes to 40% EtOAc/hexanes, product eluted at 30% EtOAc/hexanes) to give **3.181** (0.0938 g, 0.187 mmol) as a colorless foam.

A solution of CrCl₂ (0.138 g, 1.12 mmol) and (Z)-1-(4-(2-methyl-5-(trifluoromethyl)phenyl)piperazine-1-yl)-3-(3-(pentafluoro-λ⁶-sulfaneyl)phenyl)prop-2-en-1-one (**3.181**, 0.0938 g, 0.187 mmol) in dry degassed THF (1.9 mL) was treated with CH₂ICl (0.11 mL, 0.937 mmol) at rt, sparged for 2 min, heated for 2 d at 80 °C, cooled to rt, diluted with EtOAc (50 mL), and washed with 1 M aqueous HCl (3 x 20 mL). The organic layer was dried (MgSO₄), filtered and concentrated under reduced pressure. The crude residue was purified by automated chromatography on SiO₂ (4g column, liquid load CH₂Cl₂, gradient 100% hexanes to 40% EtOAc/hexanes, product eluted at 30% EtOAc/hexanes), filtered through basic Al₂O₃ (CH₂Cl₂/EtOAc, 1:1), concentrated under reduced pressure, and dried under high vacuum to give **3.21n** (0.0641 g, 0.125 mmol, 62% (2 steps) (100% purity by ELSD)) as a pale yellow oil: IR (CH₂Cl₂) 2917, 1638, 1438, 1417, 1337, 1307, 1120, 835, 758 cm⁻¹; ¹H NMR (400 MHz, CDCl₃) δ 7.62-7.58 (m, 2 H), 7.38 (t, *J* = 7.8 Hz, 1 H), 7.30 (d, *J* = 7.8 Hz, 1 H), 7.24-7.21 (m, 2 H), 6.96 (s, 1 H), 3.93 (d, *J* = 13.0 Hz, 1 H), 3.79 (dt, *J* = 13.0, 3.8 Hz, 1 H), 3.60 (ddd, *J* = 12.6, 9.2, 3.1 Hz, 1 H), 3.25 (ddd, *J* = 12.6, 9.2, 3.0 Hz, 1 H), 2.79 (ddt, *J* = 12.7, 11.9, 3.8 Hz, 2 H), 2.53 (td, *J* = 8.9, 6.9 Hz, 1 H), 2.31-2.20 (m, 5 H), 2.16-2.10 (m, 1 H), 1.92 (q, *J* = 6.2 Hz, 1 H), 1.43 (td, *J* = 8.4, 5.6 Hz, 1 H); ¹³C NMR (100 MHz, CDCl₃) δ 166.5, 153.9 (quint, *J*_{CF} = 16.9 Hz), 151.0, 139.0, 136.8, 131.3, 130.3, 129.0 (q, *J*_{CF} = 33.1 Hz), 128.5, 125.7 (quint, *J*_{CF} = 4.6 Hz), 124.2 (q, *J*_{CF} = 272.0 Hz), 123.9 (quint, *J*_{CF} = 4.6 Hz), 120.3 (q, *J*_{CF} = 3.9 Hz), 115.9 (q, *J*_{CF} = 3.6 Hz), 51.7, 51.6, 45.5, 42.2, 24.0 (2 C), 24.0, 17.8, 10.9; ¹⁹F NMR (376 MHz, CDCl₃) δ 84.5 (quint, *J* = 150.0 Hz, 1 F), 62.7 (d, *J* = 149.8 Hz, 4 F), -62.4 (s, 3 F); HRMS (ESI) *m/z* calcd for C₂₂H₂₃F₈N₂OS ([M+H]⁺) 515.1398, found 515.1380.



Racemic (4-(2-methyl-5-(trifluoromethyl)phenyl)piperazine-1-yl)((1*R*,2*S*)-2-(3-(pentafluoro- λ 6-sulfaneyl)phenyl)cyclopropyl)methanone (**3.21n**) was separated on a SFC Chiralpak-IC semiprep (250 x 10 mm) column (30% Methanol:CO₂, 7 mL/min, p = 100 bar, 220 nm) injection volume 90 μ L, 20 mg/mL) to give (4-(2-methyl-5-(trifluoromethyl)phenyl)piperazin-1-yl)((1*S*,2*R*)-2-(3-(pentafluoro- λ 6-sulfaneyl)phenyl)cyclopropyl)methanone ((1*S*,2*R*)-**3.21n**) (retention time 3.25 min) as a colorless viscous oil (100% purity by ELSD): $[\alpha]_D^{18}$ -104.7 (*c* 0.84, MeOH); ¹H NMR (300 MHz, CDCl₃) δ 7.62-7.58 (m, 2 H), 7.38 (t, *J* = 7.7 Hz, 1 H), 7.31-7.24 (m, 3 H), 6.96 (s, 1 H), 3.94-3.89 (m, 1 H), 3.81-3.75 (m, 1 H), 3.65-3.56 (m, 1 H), 3.31-3.22 (m, 1 H), 2.84-2.74 (m, 2 H), 2.53 (td, *J* = 9.3, 6.9 Hz, 1 H), 2.32-2.21 (m, 5 H), 2.19-2.11 (m, 1 H), 1.93 (q, *J* = 5.7 Hz, 1 H), 1.43 (td, *J* = 8.4, 5.7 Hz, 1 H). The enantiomeric excess was >99.9% ee (SFC Chiralpak-IC (250 x 10 mm); 30% Methanol:CO₂, 7 mL/min, p = 100 bar, 220 nm; retention time: 3.3 min).

(4-(2-Methyl-5-(trifluoromethyl)phenyl)piperazin-1-yl)((1*R*,2*S*)-2-(3-(pentafluoro- λ 6-sulfaneyl)phenyl)cyclopropyl)methanone ((1*R*,2*S*)-**3.21n**) (retention time 3.60 min) was obtained as a colorless viscous oil (100% purity by ELSD): $[\alpha]_D^{18}$ +103.4 (*c* 0.87, MeOH); ¹H NMR (300 MHz, CDCl₃) δ 8.54-7.81 (m, 2 H), 7.62-7.59 (m, 2 H), 7.38 (t, *J* = 7.8 Hz, 1 H), 7.31-7.24 (m, 3 H), 6.96 (s, 1 H), 3.94-3.88 (m, 1 H), 3.81-3.75 (m, 1 H), 3.65-3.56 (m, 1 H), 3.31-3.22 (m, 1 H), 2.84-2.74 (m, 2 H), 2.53 (td, *J* = 9.0, 7.2 Hz, 1 H), 2.32-2.22 (m, 5 H), 2.18-2.11 (m, 1 H), 1.93 (q, *J* = 5.7 Hz, 1 H), 1.43 (td, *J* = 8.4, 5.7 Hz, 1 H); The enantiomeric excess was >99.9% ee

(SFC Chiralpak-IC (250 x 10 mm); 30% Methanol:CO₂, 7 mL/min, p = 100 bar, 220 nm; retention time: 3.6 min).

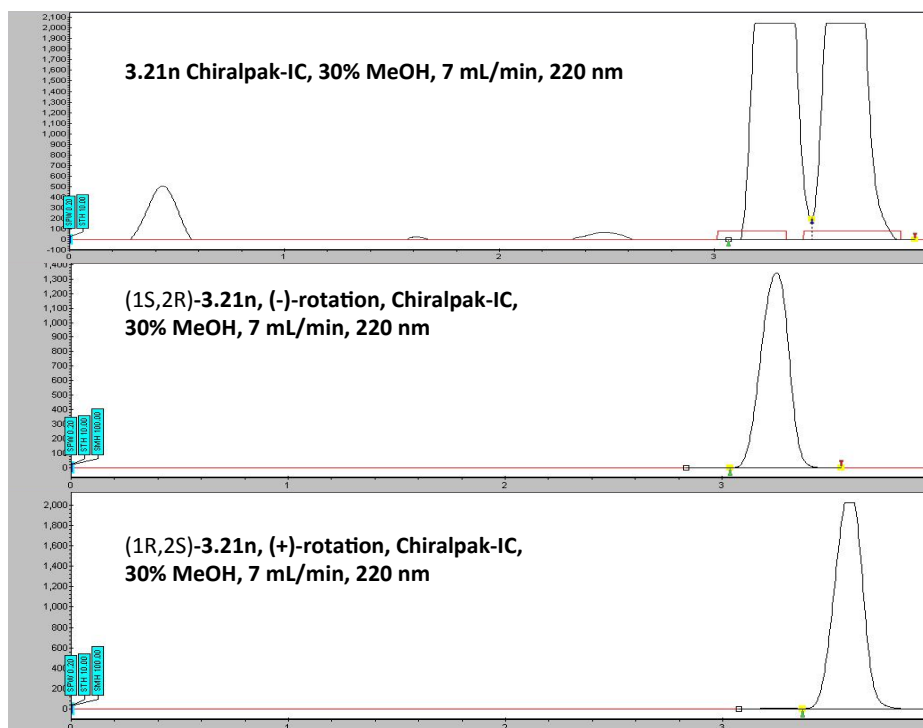
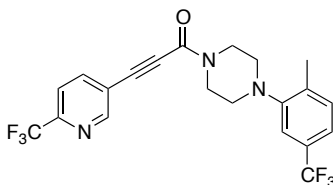


Figure 5.10. SFC chromatograms for **3.21n** and separated enantiomers.

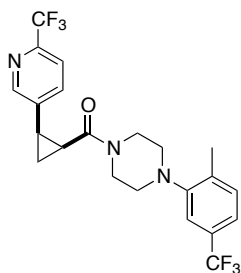


3.17m

1-(4-(2-Methyl-5-(trifluoromethyl)phenyl)piperazin-1-yl)-3-(6-(trifluoromethyl)pyridin-3-yl)prop-2-yn-1-one (3.17m). A solution of methyl 3-(5-chloropyridin-2-yl)propionate (0.500 g, 2.18 mmol) in THF (4 mL) was treated with 2 M NaOH (1.2 mL, 2.40 mmol) and the mixture was stirred at rt for 3 h, acidified with 1 M aqueous HCl, and extracted with EtOAc (3 x 20 mL). The combined organic layers were dried (MgSO₄),

filtered and concentrated under reduced pressure to give **3.16f** (0.422 g, 1.96 mmol) as a colorless solid. This solid was taken on to the coupling reaction with no further purification.

A solution of 3-(6-(trifluoromethyl)pyridin-3-yl)propionic acid (**3.16f**, 0.422 g, 1.96 mmol) and 1-(2-methyl-5-(trifluoromethyl)phenyl)piperazine hydrochloride (**3.12c**, 0.661 g, 2.35 mmol) in CH₂Cl₂ (19 mL) cooled to 0 °C was treated Et₃N (0.83 mL, 5.88 mmol). The cooled solution was treated with T3P (50% solution in EtOAc) (2.1 mL, 2.94 mmol) dropwise and the reaction was stirred at 0 °C for 30 min, warmed to rt for 18 h, diluted with EtOAc (50 mL), washed with H₂O (20 mL), satd. aqueous NaHCO₃ (20 mL), dried (MgSO₄), filtered, and concentrated under reduced pressure. The crude material was purified by chromatography on SiO₂ (hexanes/EtOAc, 1:1) to give **3.17m** (0.781 g, 1.77 mmol, 81% (2 steps)) as a pale yellow solid: Mp 110.7-113.5 °C; IR (CH₂Cl₂) 3652, 2981, 2890, 1635, 1382, 1337, 1240, 1150, 1087, 956 cm⁻¹; ¹H NMR (400 MHz, CDCl₃) δ 8.85 (dd, *J* = 1.6, 0.6 Hz, 1 H), 8.04 (ddd, *J* = 8.2, 1.6, 0.6 Hz, 1 H), 7.72 (dd, *J* = 8.2, 0.6 Hz, 1 H), 7.32-7.26 (m, 2 H), 7.21 (s, 1 H), 3.99 (t, *J* = 5.0 Hz, 2 H), 3.87 (t, *J* = 5.0 Hz, 2 H), 3.04 (t, *J* = 5.0 Hz, 2 H), 2.95 (t, *J* = 5.0 Hz, 2 H), 2.39 (s, 3 H); ¹³C NMR (100 MHz, CDCl₃) δ 152.5, 152.0, 150.8, 148.2 (q, *J*_{CF} = 35.3 Hz), 140.7, 136.8, 131.6, 129.1 (q, *J*_{CF} = 32.3 Hz), 124.1 (q, *J*_{CF} = 272.1 Hz), 121.0 (q, *J*_{CF} = 274.4 Hz), 120.7, 120.6 (q, *J*_{CF} = 3.9 Hz), 120.0 (q, *J*_{CF} = 2.8 Hz), 116.1 (q, *J*_{CF} = 3.6 Hz), 85.6, 51.8, 51.3, 47.4, 42.0, 17.9; ¹⁹F NMR (376 MHz, CDCl₃) δ -62.3 (s, 3 F). -68.2 (s, 3 F); HRMS (ESI) *m/z* calcd for C₂₁H₁₈F₆N₃O ([M+H]⁺) 442.1349, found 442.1345.

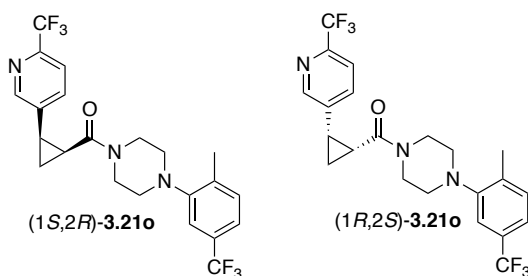


3.21o

(4-(2-Methyl-5-(trifluoromethyl)phenyl)piperazin-1-yl)((1*RS*,2*SR*)-2-(6-(trifluoromethyl)pyridin-3-yl)cyclopropyl)methanone (3.21o). A solution of 1-(4-(2-methyl-5-(trifluoromethyl)phenyl)piperazin-1-yl)-3-(6-(trifluoromethyl)pyridin-3-yl)prop-2-yn-1-one (**3.17m**, 0.720 g, 1.63 mmol) in EtOAc (16 mL) at rt was treated with quinoline (1.0 mL, 8.16 mmol) and 5% Pd/BaSO₄ (0.0347 g, 0.0163 mmol, equivalent to 1 mol% Pd) and the reaction was stirred under an atmosphere of H₂ (3 x backfill cycles) for 4 h. Analysis by TLC (hexanes/EtOAc, 1:1) indicated that the starting material had been mostly consumed. The reaction was filtered (eluting with EtOAc), and the filtrate was washed with 1 M aqueous HCl (3 x 30 mL), dried (Na₂SO₄), filtered and concentrated under reduced pressure. The crude residue was purified by chromatography on SiO₂ (hexanes/EtOAc, 1:1 to EtOAc) to give **3.18m** (0.640 g, 1.44 mmol) as a yellow/orange oil.

A solution of CrCl₂ (1.06 g, 8.66 mmol) and (Z)-1-(4-(2-methyl-5-(trifluoromethyl)phenyl)piperazin-1-yl)-3-(6-(trifluoromethyl)pyridin-3-yl)prop-2-en-1-one (**3.18m**, 0.640 g, 1.44 mmol) in dry degassed THF (14 mL) was sparged with Ar for 5 min and treated with CH₂ICl (0.83 mL, 7.22 mmol) at rt and under Ar atmosphere. The reaction mixture was stirred for 2 d at 80 °C, cooled to rt, diluted with EtOAc (50 mL), and washed with 1 M aqueous HCl (3 x 20 mL). The organic layer was dried (MgSO₄), filtered and concentrated under reduced pressure. The crude material was purified by chromatography on SiO₂ (4:1, EtOAc:hexanes), filtered through basic Al₂O₃ (eluting with EtOAc) concentrated under reduced pressure, and dried under high vacuum to give **3.21o** (0.280 g, 0.612 mmol, 37% (2 steps) (100% purity by ELSD)) as an orange oil: IR (CH₂Cl₂) 2981, 1640, 1418, 1339, 1309, 1166, 1126, 1035, 828 cm⁻¹; ¹H NMR (400 MHz, CDCl₃) δ 8.64 (s, 1 H), 7.60 (t, *J* = 2.0 Hz, 2 H), 7.24 (t, *J* = 2.0

Hz, 2 H), 7.02 (s, 1 H), 3.78-3.65 (m, 3 H), 3.53-3.46 (m, 1 H), 2.92-2.87 (m, 1 H), 2.80-2.75 (m, 1 H), 2.59-2.53 (m, 1 H), 2.47-2.35 (m, 4 H), 2.30 (s, 3 H), 1.95 (q, $J = 5.6$ Hz, 1 H), 1.49 (td, $J = 8.4, 5.6$ Hz, 1 H); ^{13}C NMR (100 MHz, CDCl_3) δ 166.4, 150.8, 150.5, 146.3 (q, $J_{\text{CF}} = 34.8$ Hz), 136.9, 136.7, 135.5, 131.4, 129.1 (q, $J_{\text{CF}} = 32.2$ Hz), 124.1 (q, $J_{\text{CF}} = 272.1$ Hz), 121.6 (q, $J_{\text{CF}} = 273.7$ Hz), 120.4 (q, $J_{\text{CF}} = 3.9$ Hz), 119.8 (q, $J_{\text{CF}} = 2.6$ Hz), 115.9 (q, $J_{\text{CF}} = 3.7$ Hz), 52.0, 51.5, 45.6, 42.3, 23.7, 21.5, 17.9, 11.0; ^{19}F NMR (376 MHz, CDCl_3) δ -62.4 (s, 3 F), -67.8 (s, 3 F); HRMS (ESI) m/z calcd for $\text{C}_{22}\text{H}_{22}\text{F}_6\text{N}_3\text{O}$ ($[\text{M}+\text{H}]^+$) 458.1662, found 458.1660.



Racemic (4-(2-methyl-5-(trifluoromethyl)phenyl)piperazin-1-yl)((1*R*,2*S*)-2-(6-(trifluoromethyl)pyridin-3-yl)cyclopropyl)methanone (**3.21o**) was separated on a SFC Chiralpak-IC semiprep (250 x 10 mm) column (15% Methanol/ CO_2 , 7 mL/min, 220nm, $p = 100$ bar, 20 mg/mL in MeOH) to give (4-(2-methyl-5-(trifluoromethyl)phenyl)piperazin-1-yl)((1*S*,2*R*)-2-(6-(trifluoromethyl)pyridin-3-yl)cyclopropyl)methanone ((1*S*,2*R*)-**3.21o**) (retention time 7.65 min) as a colorless solid (100% purity by ELSD): $[\alpha]_{\text{D}}^{19} -134.8$ (c 0.90, MeOH); ^1H NMR (300 MHz, CDCl_3) δ 8.64 (s, 1 H), 7.60 (s, 2 H), 7.26 (s, 4 H), 7.04 (s, 1 H), 3.75-3.64 (m, 3 H), 3.55-3.47 (m, 1 H), 2.94-2.87 (m, 1 H), 2.82-2.74 (m, 1 H), 2.56 (q, $J = 8.4$ Hz, 1 H), 2.49-2.34 (m, 3 H), 2.31 (s, 3 H), 1.96 (q, $J = 5.8$ Hz, 1 H), 1.50 (td, $J = 8.4, 5.8$ Hz, 1 H). The enantiomeric excess was >99.9% ee (SFC Chiralpak-IC (250 x 10 mm); 15% Methanol: CO_2 , 7 mL/min, $p = 100$ bar, 220 nm; retention time: 7.8 min).

(4-(2-Methyl-5-(trifluoromethyl)phenyl)piperazin-1-yl)((1*R*,2*S*)-2-(6-

(trifluoromethyl)pyridin-3-yl)cyclopropyl)methanone ((1*R*,2*S*)-**3.21o**) (retention time 8.38 min) was obtained as a colorless solid (100% purity by ELSD): $[\alpha]_D^{19} +128.2$ (*c* 1.08, MeOH); ^1H NMR (300 MHz, CDCl_3) δ 8.64 (s, 1 H), 7.60 (s, 2 H), 7.26 (s, 2 H), 7.04 (s, 1 H), 3.77-3.63 (m, 3 H), 3.55-3.47 (m, 1 H), 2.93-2.87 (m, 1 H), 2.81-2.75 (m, 1 H), 2.61-2.52 (m, 1 H), 2.50-2.35 (m, 2 H), 2.31 (s, 3 H), 1.96 (q, $J = 5.8$ Hz, 1 H), 1.50 (td, $J = 8.4, 5.8$ Hz, 1 H). The enantiomeric excess was >99.9% ee (SFC Chiralpak-IC (250 x 10 mm); 15% Methanol:CO₂, 7 mL/min, $p = 100$ bar, 220 nm; retention time: 8.4 min).

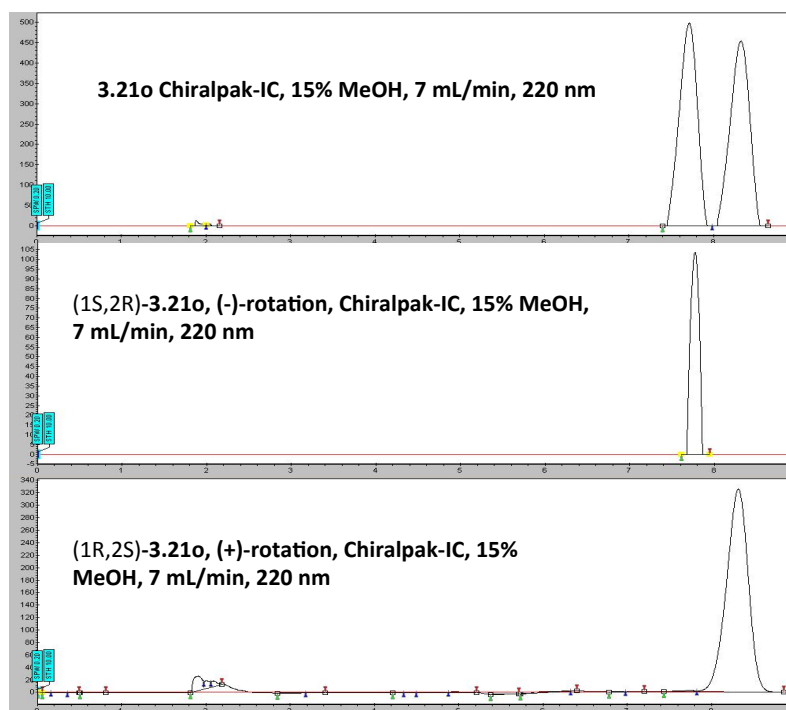
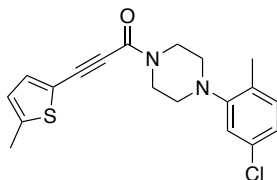
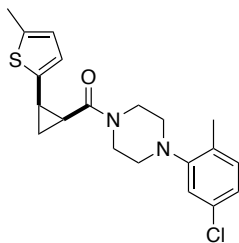


Figure 5.11. SFC chromatograms for **3.21o** and separated enantiomers.



3.17n

1-(4-(5-Chloro-2-methylphenyl)piperazin-1-yl)-3-(5-methylthiophen-2-yl)prop-2-yn-1-one (3.17n). A solution of 3-(5-methylthiophen-2-yl)propionic acid (**3.16e**, 0.0750 g, 0.451 mmol) and 1-(5-chloro-2-methylphenyl)piperazine hydrochloride (**3.12b**, 0.134 g, 0.542 mmol) in CH₂Cl₂ (4.5 mL) cooled to 0 °C was treated with Et₃N (0.19 mL, 1.35 mmol). The cooled solution was treated with T3P (50 wt. % solution in EtOAc, 0.48 mL, 0.677 mmol) dropwise and the reaction was stirred at 0 °C for 30 min, warmed to rt for 16 h, diluted with CH₂Cl₂ (30 mL), washed with 1 M aqueous HCl (20 mL), dried (MgSO₄), filtered, and concentrated under reduced pressure. The crude residue was purified by automated chromatography on SiO₂ (4g column, liquid load CH₂Cl₂, gradient 100% hexanes to 40% EtOAc/hexanes), to give **3.17n** (0.0620 g, 0.173 mmol, 38%) as a colorless solid: Mp 114.4-116.0 °C; IR (CH₂Cl₂) 2919, 2197, 1643, 1593, 1489, 1426, 1224, 1025, 806 cm⁻¹; ¹H NMR (400 MHz, CDCl₃) δ 7.24 (d, *J* = 3.6 Hz, 1 H), 7.10 (d, *J* = 8.1 Hz, 1 H), 6.98 (dd, *J* = 8.1, 1.9 Hz, 1 H), 6.94 (d, *J* = 1.9 Hz, 1 H), 6.69 (dd, *J* = 3.6, 0.8 Hz, 1 H), 3.91 (app t, *J* = 5.0 Hz, 2 H), 3.81 (app t, *J* = 5.0 Hz, 2 H), 2.94 (app t, *J* = 5.0 Hz, 2 H), 2.86 (app t, *J* = 5.0 Hz, 2 H), 2.49 (s, 3 H), 2.28 (s, 3 H); ¹³C NMR (100 MHz, CDCl₃) δ 153.1, 151.7, 145.5, 135.7, 132.0, 131.8, 130.9, 125.8, 123.6, 119.7, 117.4, 85.4, 84.5, 51.8, 51.3, 47.2, 41.8, 17.4, 15.5; HRMS (ESI) *m/z* calcd for C₁₉H₂₀ClN₂OS ([M+H]⁺) 359.0979, found 359.0978.



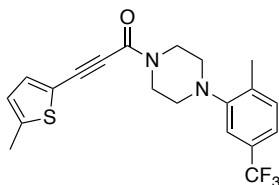
3.21p

(4-(5-Chloro-2-methylphenyl)piperazin-1-yl)((1RS,2SR)-2-(5-methylthiophen-2-yl)cyclopropyl)methanone (3.21p). A solution of 1-(4-(5-chloro-2-methylphenyl)piperazin-1-

yl)-3-(5-methylthiophen-2-yl)prop-2-yn-1-one (**3.17n**, 0.0620 g, 0.173 mmol) in EtOAc (1.7 mL) was treated with Lindlar catalyst (5% Pd on CaCO₃, lead poisoned, 0.00735 g, equivalent to 2 mol% Pd) and quinoline (10 μ L, 0.172 mmol). The reaction was placed under a balloon of H₂ (4 vacuum/backfill cycles) and stirred at rt for 6 h, filtered through Celite, washed (EtOAc), and the combined filtrates were washed with 1 M aqueous HCl, dried (Na₂SO₄), filtered, and concentrated under reduced pressure. The crude residue was purified by automated chromatography on SiO₂ (4g column, liquid load CH₂Cl₂, gradient 10% EtOAc/hexanes to 40% EtOAc/hexanes) to give **3.18n** (0.0263 g, 0.0729 mmol) as a colorless solid.

A solution of CrCl₂ (0.0511 g, 0.416 mmol) and (Z)-1-(4-(5-chloro-2-methylphenyl)piperazin-1-yl)-3-(5-methylthiophen-2-yl)prop-2-en-1-one (**3.18n**, 0.0250 g, 0.0693 mmol) in dry degassed THF (0.7 mL) was sparged with Ar for 5 min and treated with CH₂ICl (40 μ L, 0.346 mmol) at rt, heated for 20 h at 80 °C, cooled to rt, combined, diluted with Et₂O (50 mL), and washed with 1 M aqueous HCl (3 x 20 mL). The organic layer was dried (MgSO₄), filtered and concentrated under reduced pressure. The crude residue was purified by automated chromatography on SiO₂ (4g column, liquid load CH₂Cl₂, gradient 100% hexanes to 40% EtOAc/hexanes), filtered through basic Al₂O₃ (CH₂Cl₂/EtOAc, 1:1), concentrated under reduced pressure and dried under high vacuum to give **3.21p** (0.0154 g, 0.0411 mmol, 25% (2 steps) (100% purity by ELSD)) as a pale yellow oil: IR (CH₂Cl₂) 2918, 1643, 1593, 1490, 1462, 1436, 1226, 1029, 802 cm⁻¹; ¹H NMR (400 MHz, CDCl₃) δ 7.08 (dd, *J* = 8.1, 0.4 Hz, 1 H), 6.97 (dd, *J* = 8.1, 2.1 Hz, 1 H), 6.79 (d, *J* = 2.1 Hz, 1 H), 6.57-6.55 (m, 2 H), 3.96 (d, *J* = 13.0 Hz, 1 H), 3.85 (dt, *J* = 13.0, 3.5 Hz, 1 H), 3.63 (ddd, *J* = 13.0, 8.9, 3.5 Hz, 1 H), 3.34 (ddd, *J* = 13.0, 9.0, 3.2 Hz, 1 H), 2.79 (ddt, *J* = 19.3, 11.2, 4.1 Hz, 2 H), 2.52 (td, *J* = 8.9, 6.8 Hz, 1 H), 2.45-2.36 (m, 5 H), 2.24 (s, 3 H), 2.16 (ddd, *J* = 8.9, 8.2, 6.3 Hz, 1 H), 1.77 (td, *J* = 6.3, 5.6 Hz, 1 H), 1.38

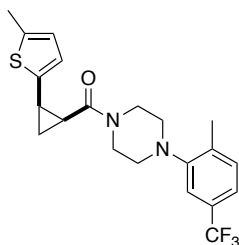
(ddd, $J = 8.9, 8.2, 5.6$ Hz, 1 H). ^{13}C NMR (100 MHz, CDCl_3) δ 167.2, 152.1, 138.2, 137.5, 131.9, 131.7, 131.1, 125.0, 124.1, 123.5, 119.7, 51.8, 51.7, 45.7, 42.4, 24.1, 19.3, 17.3, 15.3, 12.2; HRMS (ESI) m/z calcd for $\text{C}_{19}\text{H}_{24}\text{ClN}_2\text{OS}$ ($[\text{M}+\text{H}]^+$) 375.1292, found 375.1292.



3.17o

1-(4-(2-Methyl-5-(trifluoromethyl)phenyl)piperazin-1-yl)-3-(5-methylthiophen-2-yl)prop-2-yn-1-one (3.17o). A solution of 3-(5-methylthiophen-2-yl)propionic acid (**3.15e**, 0.0592 g, 0.356 mmol) and 1-(2-methyl-5-(trifluoromethyl)phenyl)piperazine hydrochloride (**3.12c**, 0.100 g, 0.356 mmol) in CH_2Cl_2 (3.6 mL) cooled to 0 °C was treated with Et_3N (0.20 mL, 1.42 mmol). The cooled solution was treated with T3P (50 wt. % solution in EtOAc, 0.38 mL, 0.534 mmol) dropwise and the reaction was stirred at 0 °C for 30 min, warmed to rt for 18h, diluted with CH_2Cl_2 (30 mL), washed with 1 M aqueous HCl (20 mL), dried (MgSO_4), filtered, and concentrated under reduced pressure. The crude material was purified by automated chromatography on SiO_2 (4g column, liquid load CH_2Cl_2 , gradient 100% hexanes to 40% EtOAc/hexanes), to give **3.17o** (0.0685, 0.175 mmol, 49%) as a yellow solid. Mp 145.7-149.3 °C; IR (CH_2Cl_2) 2919, 2199, 1635, 1420, 1340, 1309, 1120, 1029, 955, 732 cm^{-1} ; ^1H NMR (400 MHz, CDCl_3) δ 7.31-7.24 (m, 3 H), 7.21 (s, 1 H), 6.69 (dd, $J = 3.6, 0.8$ Hz, 1 H), 3.94 (app t, $J = 5.0$ Hz, 2 H), 3.83 (app t, $J = 5.0$ Hz, 2 H), 3.01 (app t, $J = 5.0$ Hz, 2 H), 2.91 (app t, $J = 5.0$ Hz, 2 H), 2.49 (d, $J = 0.8$ Hz, 3 H), 2.38 (s, 3 H); ^{13}C NMR (100 MHz, CDCl_3) δ 153.2, 151.0, 145.5, 136.8, 135.7, 131.5, 129.0 (q, $J_{\text{CF}} = 32.2$ Hz), 125.9, 124.1 (q, $J_{\text{CF}} = 272.1$ Hz), 120.4 (q, $J_{\text{CF}} = 3.8$ Hz), 117.4, 116.0 (q, $J_{\text{CF}} = 3.6$ Hz), 85.4, 84.5, 51.8, 51.3, 47.3, 41.8, 17.9, 15.5; ^{19}F NMR

(376 MHz, CDCl₃) δ -62.2 (s, 3 F); HRMS (ESI) m/z calcd for C₂₀H₂₀F₃N₂OS ([M+H]⁺) 393.1243, found 393.1241.

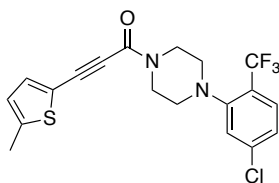


3.21q

(4-(2-Methyl-5-(trifluoromethyl)phenyl)piperazin-1-yl)((1R,2S)-2-(5-methylthiophen-2-yl)cyclopropyl)methanone (3.21q). A solution of 1-(4-(2-methyl-5-(trifluoromethyl)phenyl)piperazin-1-yl)-3-(5-methylthiophen-2-yl)prop-2-yn-1-one (**3.17o**, 0.0650 g, 0.166 mmol) in EtOAc (1.7 mL) was treated with Lindlar catalyst (5% Pd on CaCO₃, lead poisoned, 0.0176 g, equivalent to 5 mol% Pd). The reaction was placed under a balloon of H₂ (3 vacuum/backfill cycles) and stirred at rt for 3 d, filtered through Celite, washed (EtOAc), and the combined filtrates were concentrated under reduced pressure. The crude residue was purified by automated chromatography on SiO₂ (4g column, liquid load CH₂Cl₂, gradient 100% hexanes to 40% EtOAc/hexanes, product eluted at 20% EtOAc/hexanes) to give **3.18o** (0.0443 g, 0.112 mmol) as a colorless solid.

A solution of CrCl₂ (0.105 g, 0.851 mmol) and (Z)-1-(4-(5-chloro-2-methylphenyl)piperazin-1-yl)-3-(3-(trifluoromethyl)phenyl)prop-2-en-1-one (**3.18o**, 0.0420 g, 0.142 mmol) in dry degassed THF (1.1 mL) was sparged with Ar for 5 min and treated with CH₂ICl (62 μ L, 0.532 mmol) at rt, heated for 22 h at 80 °C, cooled to rt, diluted with Et₂O (50 mL), and washed with 1 M aqueous HCl (3 x 20 mL). The organic layer was dried (MgSO₄), filtered and concentrated under reduced pressure. The crude residue was purified by automated chromatography on SiO₂ (4g column, liquid load CH₂Cl₂, 100% hexanes to 40%

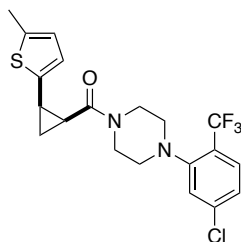
EtOAc/hexanes), filtered through basic Al₂O₃ (CH₂Cl₂/EtOAc, 1:1), concentrated under reduced pressure, and dried under high vacuum to **3.21q** (0.0187 g, 0.0458 mmol, 29% (2 steps) (100% purity by ELSD)) as pale yellow viscous oil: IR (CH₂Cl₂) 2921, 2822, 1639, 1464, 1434, 1417, 1337, 1306, 1116, 1079, 1031, 801 cm⁻¹; ¹H NMR (400 MHz, CDCl₃) δ 7.26 (d, *J* = 8.4 Hz, 1 H), 7.24 (dd, *J* = 8.4, 1.4 Hz, 1 H), 7.04 (s, 1 H), 6.58 (t, *J* = 4.7 Hz, 1 H), 6.55 (dt, *J* = 3.5, 1.0 Hz, 1 H), 4.00 (bd, *J* = 13.0 Hz, 1 H), 3.88 (dt, *J* = 13.0, 3.5 Hz, 1 H), 3.64 (ddd, *J* = 12.4, 9.0, 3.2 Hz, 1 H), 3.34 (ddd, *J* = 13.0, 9.2, 2.9 Hz, 1 H), 2.82 (ddt, *J* = 19.4, 11.6, 3.7 Hz, 2 H), 2.53 (td, *J* = 8.6, 6.6 Hz, 1 H), 2.48-2.40 (m, 1 H), 2.38 (d, *J* = 1.0 Hz, 3 H), 2.34 (s, 3 H), 2.17 (td, *J* = 8.6, 6.6 Hz, 1 H), 1.77 (q, *J* = 6.0 Hz, 1 H), 1.38 (td, *J* = 8.6, 5.3 Hz, 1 H); ¹³C NMR (100 MHz, CDCl₃) δ 167.2, 151.4, 138.3, 137.6, 136.9, 131.4, 128.9 (q, *J*_{CF} = 32.0 Hz), 124.9, 124.3 (q, *J*_{CF} = 272.1 Hz), 124.2, 120.3 (q, *J*_{CF} = 4.0 Hz), 116.0 (q, *J*_{CF} = 3.7 Hz), 51.8, 51.7, 45.7, 42.3, 24.1, 19.4, 17.9, 15.1, 12.3; ¹⁹F NMR (376 MHz, CDCl₃) δ -62.2 (s, 3 F); HRMS (ESI) *m/z* calcd for C₂₁H₂₄F₃N₂OS ([M+H]⁺) 409.1556, found 409.1555.



3.17p

1-(4-(5-Chloro-2-(trifluoromethyl)phenyl)piperazin-1-yl)-3-(5-methylthiophen-2-yl)prop-2-yn-1-one (3.17p). A solution of 3-(5-methylthiophen-2-yl)propionic acid (**3.16e**, 0.0770 g, 0.463 mmol) and 1-(5-chloro-2-(trifluoromethyl)phenyl)piperazine hydrochloride (**3.12d**, 0.153 g, 0.510 mmol) in CH₂Cl₂ (4.6 mL) cooled to 0 °C was treated with Et₃N (0.26 mL, 1.85 mmol). The cooled solution was treated with T3P (50 wt. % solution in EtOAc, 0.49 mL, 0.695 mmol) dropwise and the reaction was stirred at 0 °C for 30 min, warmed to rt for 18

h, diluted with CH₂Cl₂ (30 mL), washed with H₂O (20 mL), satd. aqueous NaHCO₃ (20 mL), dried (MgSO₄), filtered, and concentrated under reduced pressure. The crude material was purified by automated chromatography on SiO₂ (4g column, liquid load CH₂Cl₂, hexanes to 40% EtOAc/hexanes), to give **3.17p** (0.135 g, 0.326 mmol, 70%) as a light orange waxy solid: IR (CH₂Cl₂) 2918, 2200, 1629, 1596, 1425, 1309, 1224, 1144, 1120, 1027, 809 cm⁻¹; ¹H NMR (400 MHz, CDCl₃) δ 7.58 (d, *J* = 8.4 Hz, 1 H), 7.27-7.23 (m, 3 H), 6.69 (dd, *J* = 3.6, 0.8 Hz, 1 H), 3.91 (app t, *J* = 4.9 Hz, 2 H), 3.81 (app t, *J* = 5.0 Hz, 2 H), 2.98 (app t, *J* = 5.0 Hz, 2 H), 2.91 (app t, *J* = 5.0 Hz, 2 H), 2.49 (d, *J* = 0.8 Hz, 3 H); ¹³C NMR (100 MHz, CDCl₃) δ 153.2, 152.7, 152.6, 145.5, 138.8, 135.7, 128.5 (q, *J*_{CF} = 5.4 Hz), 125.9, 125.8 (q, *J*_{CF} = 29.3 Hz), 125.6, 124.7, 123.6 (q, *J*_{CF} = 273.0 Hz), 117.4, 85.4, 84.5, 53.6, 52.8, 47.3, 41.7, 15.5; ¹⁹F NMR (376 MHz, CDCl₃) δ -60.3 (s, 3 F); HRMS (ESI) *m/z* calcd for C₁₉H₁₇ClF₃N₂OS ([M+H]⁺) 413.0697, found 413.0693.



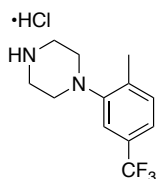
3.21r

(4-(5-Chloro-2-(trifluoromethyl)phenyl)piperazin-1-yl)((1R,2SR)-2-(5-methylthiophen-2-yl)cyclopropyl)methanone (3.21r). A solution of 1-(4-(5-chloro-2-(trifluoromethyl)phenyl)piperazin-1-yl)-3-(5-methylthiophen-2-yl)prop-2-yn-1-one (**3.17p**, 0.112 g, 0.271 mmol) in EtOAc (2.7 mL) was treated with Lindlar catalyst (5% Pd on CaCO₃, lead poisoned, 0.0289 g, equivalent to 5 mol% Pd). The reaction was placed under a balloon of H₂ (3 vacuum/backfill cycles) and stirred at rt for 3 d, filtered through Celite, washed (EtOAc), and the combined filtrates were concentrated under reduced pressure. The crude residue was purified by

automated chromatography on SiO₂ (4g column, liquid load CH₂Cl₂, hexanes to 40% EtOAc/hexanes, product eluted at 20% EtOAc/hexanes) to give **3.18p** (0.0655 g, 0.158 mmol) as a colorless foam.

A solution of CrCl₂ (0.116 g, 0.947 mmol) and (Z)-1-(4-(5-chloro-2-(trifluoromethyl)phenyl)piperazin-1-yl)-3-(5-methylthiophen-2-yl)prop-2-en-1-one (**3.18p**, 0.0655 g, 0.158 mmol) in dry degassed THF (1.6 mL) was sparged with Ar for 5 min and treated with CH₂ICl (0.091 mL, 0.789 mmol) at rt, heated for 2 days at 80 °C, cooled to rt, diluted with EtOAc (50 mL), and washed with 1 M aqueous HCl (3 x 20 mL). The organic layer was dried (MgSO₄), filtered and concentrated under reduced pressure. The crude residue was purified by automated chromatography on SiO₂ (4g column, liquid load CH₂Cl₂, gradient 100% hexanes to 30% EtOAc/hexanes, product eluted at 20% EtOAc/hexanes), filtered through basic Al₂O₃ (CH₂Cl₂/EtOAc, 1:1), and concentrated under reduced pressure. The resulting oil was crystalized from cyclohexane (~0.5 mL at rt), the crystals were washed with hexanes and dried under high vacuum to give **3.21r** (0.0313 g, 0.0730 mmol, 27% (2 steps) (100% purity by ELSD)) as a colorless solid: Mp 84.5-86.8 °C; IR (CH₂Cl₂) 3007, 2920, 1642, 1595, 1464, 1435, 1405, 1308, 1144, 1120, 1031, 825, 803 cm⁻¹; ¹H NMR (400 MHz, CDCl₃) δ 7.54 (d, *J* = 8.5 Hz, 1 H), 7.21 (dd, *J* = 8.5, 1.5 Hz, 1 H), 7.03 (d, *J* = 1.5 Hz, 1 H), 6.61 (dd, *J* = 3.4, 1.0 Hz, 1 H), 6.59 (d, *J* = 3.4 Hz, 1 H), 4.08 (d, *J* = 13.0 Hz, 1 H), 3.87 (d, *J* = 13.0 Hz, 1 H), 3.57 (ddd, *J* = 13.0, 9.4, 3.0 Hz, 1 H), 3.23 (ddd, *J* = 13.0, 9.6, 3.0 Hz, 1 H), 2.78 (tt, *J* = 9.6, 4.7 Hz, 2 H), 2.52 (td, *J* = 8.8, 6.8 Hz, 1 H), 2.46-2.40 (m, 4 H), 2.31-2.25 (m, 1 H), 2.16 (ddd, *J* = 8.8, 8.2, 6.0 Hz, 1 H), 1.77 (q, *J* = 6.0 Hz, 1 H), 1.39 (td, *J* = 8.6, 6.0 Hz, 1 H); ¹³C NMR (100 MHz, CDCl₃) δ 167.1, 153.2, 138.6, 138.5, 137.4, 128.4 (q, *J*_{CF} = 5.4 Hz), 126.0 (q, *J*_{CF} = 28.2 Hz), 125.5, 125.1, 124.8, 124.0, 123.6 (q, *J*_{CF} = 273.0 Hz), 53.6, 53.2, 45.7, 42.4, 24.4, 19.4, 15.3, 12.4; ¹⁹F NMR (376 MHz,

CDCl_3) δ -60.4 (s, 3 F); HRMS (ESI) m/z calcd for $\text{C}_{20}\text{H}_{21}\text{ClF}_3\text{N}_2\text{OS}$ ($[\text{M}+\text{H}]^+$) 429.1010, found 429.1006.

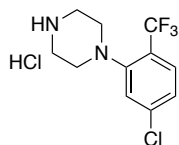


3.12c

1-(2-Methyl-5-(trifluoromethyl)phenyl)piperazine hydrochloride (3.12c). A solution of Boc-piperazine (2.14 g, 11.5 mmol), K₂CO₃ (2.35 g, 20.9 mmol), (racemic)-BINAP (0.671 g, 1.05 mmol), Pd₂(dba)₃ (0.194 g, 0.209 mmol) in dry toluene (105 mL) was sparged with Ar for 20 min, treated with 2-bromo-1-methyl-4-(trifluoromethyl)benzene (2.50 g, 10.5 mmol), and the mixture was heated under Ar at 100 °C for 24 h, cooled to rt, diluted with Et₂O (125 mL), filtered through Celite, washed (Et₂O), and the combined filtrates were concentrated under reduced pressure. The crude residue was purified by chromatography on SiO₂ (hexanes/EtOAc, 9:1) to give tert-butyl 4-(2-methyl-5-(trifluoromethyl)phenyl)piperazine-1-carboxylate (2.49 g, 7.23 mmol) as a orange oil.

A solution of tert-butyl 4-(2-methyl-5-(trifluoromethyl)phenyl)piperazine-1-carboxylate (2.49 g, 7.23 mmol) in THF (3.5 mL) was cooled to 0 °C and treated with 4M HCl in dioxane (9.0 mL, 36.2 mmol) was added and the reaction was stirred at 0 °C for 30 min and then rt for 4 h. The solution was concentrated under reduced pressure and the tan solid was precipitated in Et₂O, filtered off from the solution, washed with Et₂O, dried under vacuum to give the crude product. The crude material was recrystallized from EtOH/hexanes (1:1) to give **3.12c** (1.71 g, 6.10 mmol, 58% (2 steps)) as colorless needles: Mp 296 °C (decomp); IR (CH₂Cl₂) 2939, 2799, 2498, 1610, 1418, 1338, 1307, 1153, 1076, 950, 827 cm⁻¹; ¹H NMR (400 MHz, DMSO-d₆) δ 9.44 (bs, 2 H), 7.42 (d, J = 7.9 Hz, 1 H), 7.35 (dd, J = 7.9, 1.0 Hz, 1 H), 7.25 (d, J = 1.0 Hz, 1 H),

3.22 (dd, $J = 6.2, 3.6$ Hz, 4 H), 3.12 (dd, $J = 6.2, 3.6$ Hz, 4 H), 2.33 (s, 3 H); ^{13}C NMR (100 MHz, DMSO- d_6) δ 150.8, 137.2, 131.9, 127.5 (q, $J_{CF} = 31.6$ Hz), 124.2 (q, $J_{CF} = 272.1$ Hz), 120.1 (q, $J_{CF} = 3.9$ Hz), 115.3 (q, $J_{CF} = 3.8$ Hz), 47.9, 43.1, 17.7; ^{19}F NMR (376 MHz, CDCl_3) δ -60.7 (s, 3 F); HRMS (ESI) m/z calcd for $\text{C}_{12}\text{H}_{16}\text{F}_3\text{N}_2$ ($[\text{M}+\text{H}]^+$) 245.1260, found 245.1261.

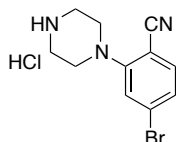


3.12d

1-(5-Chloro-2-(trifluoromethyl)phenyl)piperazine hydrochloride (3.12d). Two flasks each containing a solution Boc-piperazine (1.58 g, 8.48 mmol), K₂CO₃ (1.73 g, 15.4 mmol), (racemic)-BINAP (0.480 g, 0.771 mmol), Pd₂dba₃ (0.142 g, 0.154 mmol) in toluene (8 mL) was sparged with argon for 15 min and treated with 2-bromo-4-chloro-1-(trifluoromethyl)benzene (2.00 g, 7.71 mmol), heated under N₂ at 80 °C for 24 h, cooled to rt, combined, diluted with Et₂O (100 mL) and added Celite and filtered through Celite, washed (Et₂O), and the combined organic layers were concentrated under reduced pressure. The crude residue was purified by chromatography on SiO₂ (hexanes/EtOAc, 9:1) to give 4-(5-chloro-2-(trifluoromethyl)phenyl)piperazine-1-carboxylate (3.12 g, 8.55 mmol) as a orange oil.

A solution of tert-butyl 4-(5-chloro-2-(trifluoromethyl)phenyl)piperazine-1-carboxylate (3.12 g, 8.55 mmol) in THF (8 mL) was treated with 4M HCl in dioxane (10.7 mL, 42.8 mmol), stirred at rt for 18 h, diluted with hexanes (100 mL), and the resulting precipitate was filtered and washed with additional hexanes and Et₂O. The crude material was recrystallized at rt (EtOH/hexanes), crystals were collected by vacuum filtration, washed (hexanes) and dried under high vacuum to give **3.12d** (1.88 g, 6.24 mmol, 41% (2 steps)) as tan solid: Mp 272 °C (decomp); IR (neat) 2947, 2726, 2480, 1599, 1576, 1307, 1118, 1037, 946, 819 cm⁻¹; ^1H NMR

(400 MHz, DMSO- d_6) δ 9.58 (s, 2 H), 7.72 (d, $J = 8.8$ Hz, 1 H), 7.57 (d, $J = 1.6$ Hz, 1 H), 7.46 (dd, $J = 8.8, 1.6$ Hz, 1 H), 3.13 (bs, 8 H); ^{13}C NMR (100 MHz, DMSO- d_6) δ 152.2, 138.3, 129.0 (q, $J = 5.4$ Hz), 125.9, 124.7, 124.2 (q, $J = 29.7$ Hz), 123.7 (q, $J = 273.0$ Hz), 49.6, 43.1; ^{19}F NMR (376 MHz, CDCl_3) δ -59.0 (s, 3 F); HRMS (ESI) m/z calcd for $\text{C}_{11}\text{H}_{13}\text{N}_2\text{ClF}_3$ ($[\text{M}+\text{H}]^+$) 265.0714, found 265.0712.



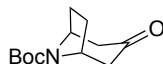
3.12e

4-Bromo-2-(piperazin-1-yl)benzonitrile hydrochloride (3.12e). A suspension of 4-bromo-2-fluorobenzonitrile (2.00 g, 10.0 mmol), 1-boc-piperazine (1.86 g, 10.0 mmol), and Et_3N (1.4 mL, 10.0 mmol) in anhydrous MeCN (5.0 mL) was heated to 110 °C for 21 h, cooled to rt, and concentrated under reduced pressure. The crude residue was purified by chromatography on SiO_2 (hexanes/EtOAc, 9:1) to give tert-butyl 4-(5-bromo-2-cyanophenyl)piperazine-1-carboxylate (3.03 g, 8.27 mmol) as a yellow oil.

A solution of tert-butyl 4-(5-bromo-2-cyanophenyl)piperazine-1-carboxylate (3.03 g, 8.27 mmol) in THF (4 mL) was cooled to 0 °C and treated with 4M HCl in dioxane (10.3 mL, 41.4 mmol), stirred at 0 °C for 30 min, rt for 16 h, diluted with hexanes (200 mL), and the resulting precipitate was collected by vacuum filtration, washed with hexanes, Et_2O , and dried under high vacuum to give **3.12e** (3.82 g, 13.6 mmol, 79% (2 steps)) as a colorless solid: Mp 288 °C (decomp); IR (neat) 2901, 2748, 1459, 1129, 1581, 1411, 1241, 1118, 949, 874 cm^{-1} ; ^1H NMR (400 MHz, MeOD- d_4) δ 7.59 (d, $J = 8.0$ Hz, 1 H), 7.44 (d, $J = 1.6$ Hz, 1 H), 7.37 (dd, $J = 8.0, 1.6$ Hz, 1 H), 3.49 (td, $J = 4.0, 1.2$ Hz, 4 H), 3.44 (td, $J = 4.0, 1.2$ Hz, 4 H); ^{13}C NMR (100

MHz, MeOD-d₄) δ 156.5, 136.4, 129.9, 127.8, 124.2, 118.2, 106.7, 49.6, 44.9; HRMS (ESI) m/z calcd for C₁₁H₁₃N₃Br ([M+H]⁺) 266.0287, found 266.0286.

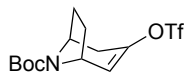
5.4.2 Synthesis of Analogs for Affinity Labeling



3.30

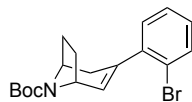
(*tert*-Butyl 3-oxo-8-azabicyclo[3.2.1]octane-8-carboxylate (**3.30**)).³⁴⁹ A solution of nortropinone•HCl (**3.29**, 2.00 g, 12.4 mmol) in a minimum amount of H₂O (6.0 mL) was cooled to 0 °C, treated dropwise with 1 M NaOH (14.8 mL, 14.8 mmol), warmed to rt over 20 min, extracted with CH₂Cl₂ (3 x 40 mL), dried (MgSO₄), filtered, and concentrated under reduced pressure (bath at 23 °C) to give nortropinone **3.29** as the free base (1.54 g, quant.). The colorless oil was used without further purification.

A solution of nortropinone (**3.29**, 1.54 g, 12.3 mmol) in CH₂Cl₂ (50 mL) cooled to 0 °C was treated with Boc anhydride (4.26 mL, 18.6 mmol), DMAP (0.302 g, 2.47 mmol), and Et₃N (7.0 mL, 50.2 mmol). The reaction mixture was allowed to warm to rt and stirred for 19 h, concentrated under reduced pressure, and the residue was diluted with H₂O, extracted with EtOAc (3x), washed with brine, dried (MgSO₄), filtered, and concentrated under reduced pressure. The crude residue was purified by chromatography on SiO₂ (CH₂Cl₂) to give **21a** (2.18 g, 9.68 mmol, 78% (2 steps)) as a pale yellow oil that solidified to an off-white solid upon standing at rt: ¹H NMR (300 MHz, DMSO-d₆) δ 4.34-4.30 (m, 2 H), 2.55 (dt, J = 15.6, 4.2 Hz, 2 H), 2.23 (d, J = 15.6 Hz, 2 H), 2.20 (app s, 1 H), 2.03-1.94 (m, 2 H), 1.60-1.52 (m, 2 H), 1.44 (s, 9 H); ¹³C NMR (75 MHz, DMSO-d₆) δ 207.4, 152.6, 79.2, 52.7, 48.1, 28.0 (2 C).



3.31

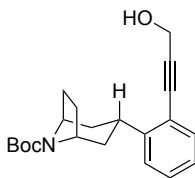
***tert*-Butyl 3-(((trifluoromethyl)sulfonyl)oxy)-8-azabicyclo[3.2.1]oct-2-ene-8-carboxylate (3.31).**³⁴⁹ A solution of NaHMDS (0.895 g, 4.88 mmol) in THF (12 mL) was added dropwise (over 10 min) at -78 °C to a solution of *tert*-butyl 3-oxo-8-azabicyclo[3.2.1]octane-8-carboxylate (**3.30**, 1.00 g, 4.44 mmol) in THF (12 mL). The reaction mixture was stirred at -78 °C for 2 h, treated dropwise (over 20 min) with a solution of PhN(Tf)₂ (1.90 g, 5.33 mmol) in THF (12 mL), stirred for an additional 30 min at -78 °C and then allowed to warm to rt and stirred for 2 h, diluted with 10% aqueous Na₂CO₃ (50 mL), and extracted with Et₂O (2 x 75 mL). The combined organic layers were washed with 10% aqueous Na₂CO₃ solution, dried (MgSO₄), and concentrated under reduced pressure. The crude residue was purified by chromatography on SiO₂ (1:19, EtOAc/hexanes w/ 1% Et₃N) to give **3.31** (1.24 g, 3.47 mmol, 78%) as a clear oil that solidified to a wax upon storage at -20 °C: ¹H NMR (400 MHz, CDCl₃) δ 6.09 (bs, 1 H), 4.54-4.38 (m, 2 H), 3.07-3.02 (m, 1 H), 2.30-2.20 (m, 1 H), 2.11-1.99 (m, 3 H), 2.00-1.97 (m, 2 H), 1.79-1.70 (m, 1 H), 1.45 (s, 9 H).



3.28

(1SR,5RS)-*tert*-Butyl 3-(2-bromophenyl)-8-azabicyclo[3.2.1]oct-2-ene-8-carboxylate (3.28). A solution of Na₂CO₃ (0.860 g, 8.11 mmol), lithium chloride (0.156 g, 3.69 mmol), (1SR,5RS)-*tert*-butyl 3-(((trifluoromethyl)sulfonyl)oxy)-8-azabicyclo[3.2.1]oct-2-ene-8-carboxylate (**3.31**, 1.20 g, 3.69 mmol), and 2-bromobenzenboronic acid (**3.32**, 0.794 g, 3.87 mmol) in DME (36 mL) and H₂O (7 mL) was sparged with Ar for 20 min and treated with

Pd(PPh₃)₄ (0.128 g, 0.111 mmol), sparged with Ar for 2 min, heated to 60 °C for 6 h, cooled to rt, diluted with brine, and extracted with Et₂O (3x). The combined organic layers were dried (Na₂SO₄), and concentrated under reduced pressure. The crude residue was purified by chromatography on SiO₂ (hexanes/EtOAc, 9:1 w/ 1% Et₃N) to give **3.28** (1.08 g, 2.97 mmol, 81%) as a clear oil that solidified to a colorless solid upon storage at -20 °C: Mp 50.2-52.6 °C, IR (neat) 3280, 2971, 1685, 1379, 1327, 1169, 1092, 755 cm⁻¹; ¹H NMR (400 MHz, CDCl₃) δ 7.53 (dd, *J* = 7.8, 1.2 Hz, 1 H), 7.09 (dt, *J* = 7.8, 1.2 Hz, 1 H), 7.12-7.06 (m, 2 H), 5.94-5.92 (m, 1 H), 4.45 (t, *J* = 5.0 Hz, 1 H), 4.38 (dd, *J* = 7.6, 4.4 Hz, 1 H), 2.95 (dt, *J* = 17.2, 2.0 Hz, 1 H), 2.26-2.19 (m, 1 H), 2.14 (s, 1 H), 2.10-1.91 (m, 3 H), 1.49 (s, 9 H); ¹³C NMR (100 MHz, CDCl₃) δ 154.2, 142.5, 136.3, 132.7, 132.0, 129.8, 128.5, 127.2, 122.6, 79.3, 53.1, 52.3, 37.8, 34.5, 29.7, 28.4; HRMS (ESI) *m/z* calcd for C₁₅H₁₇BrNO₂ ([M+H]⁺) 364.0915, found 364.0907.



3.27

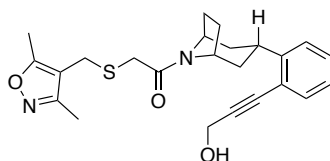
(1*SR*,3*RS*,5*RS*)-tert-Butyl

3-(2-(3-hydroxyprop-1-yn-1-yl)phenyl)-8-

azabicyclo[3.2.1]octane-8-carboxylate (3.27). To four separate flasks each containing a solution of (1*SR*,5*RS*)-tert-butyl 3-(2-bromophenyl)-8-azabicyclo[3.2.1]oct-2-ene-8-carboxylate (**3.28**, 0.150 g, 0.412 mmol) in anhydrous *i*PrOH (2 mL, 0.5 M) under argon and treated with phenylsilane (304 μL, 2.47 mmol) and TBHP (5.5 M solution in decane, 150 μL, 0.824 mmol) and the resulting mixture was sparged with Ar for 10 minutes. Mn(dpm)₃ (0.0249 g, 0.0412 mmol) was then added in one portion and the reaction was then degassed for an additional 30 seconds. The reaction was stirred for 2 h where analysis by LCMS indicated that the SM was completely consumed. The reactions were combined, concentrated under reduced pressure and

purified by automated chromatography on SiO₂ (12 g column, liquid load CH₂Cl₂, isocratic 10% EtOAc/hexanes) to give **3.33** (0.309 g, 0.844 mmol) as a 3:1 mixture of diastereomers as a colorless oil.

A solution of *tert*-butyl (1*SR*,5*RS*)-3-(2-bromophenyl)-8-azabicyclo[3.2.1]octane-8-carboxylate (0.300 g, 0.803 mmol) in dry toluene (6.0 mL) was sparged with Ar for 60 min and treated with propargyl alcohol (0.72 mL, 12.0 mmol), Et₃N (1.70 mL, 12.0 mmol), (*i*Pr)CuCl²⁹³ (0.0587 g, 0.0587 mmol), and Pd(PPh₃)₂Cl₂ (0.0287 g, 0.0040 mmol) further degassed for 5 min and the mixture was stirred 24 h at 90 °C. The reaction was diluted with EtOAc (30 mL) and washed with H₂O (3 x 5 mL), dried (Na₂SO₄), filtered and concentrated under reduced pressure. The crude residue was purified by automated chromatography on SiO₂ (12g column, liquid load CH₂Cl₂, gradient 100% hexanes to 40% EtOAc/hexanes) to give a yellow brown oil that was contaminated with Cu. The oil was then dissolved in hexanes and decanted leaving behind solid Cu. This was repeated 3 times to give **3.27** (0.0695 g, 0.205 mmol, 12% (2 steps)) as a dark yellow oil as a single diastereomer: IR (neat) 3413, 2971, 2865, 1661, 1404, 1364, 1161, 1105, 1029, 757 cm⁻¹; ¹H NMR (300 MHz, CDCl₃) δ 7.36 (dd, *J* = 7.5, 0.9 Hz, 1 H), 7.29-7.24 (m, 1 H), 7.18-7.11 (m, 2 H), 4.47 (t, *J* = 4.5 Hz, 2 H), 4.31-4.21 (m, 3 H), 3.00 (app quint, *J* = 6.3 Hz, 1 H), 2.91-2.82 (m, 1 H), 2.38 (app pent, *J* = 4.5 Hz, 1 H), 2.25-2.14 (m, 1 H), 2.07-1.96 (m, 1 H), 1.76-1.54 (m, 4 H), 1.50 (s, 9 H), 1.01 (t, *J* = 12.9 Hz, 1 H); ¹³C NMR (75 MHz, CDCl₃) δ 155.6, 145.7, 131.4, 128.3, 125.9, 125.6, 122.9, 93.2, 83.1, 79.7, 51.7, 51.3, 51.0, 38.6, 35.6, 32.5, 31.9, 28.5; HRMS (ESI) *m/z* calcd for C₂₁H₂₇NaNO₃ ([M+Na]⁺) 364.1881, found 364.1883.



3.25

2-(((3,5-Dimethylisoxazol-4-yl)methyl)thio)-1-(((1*SR*,3*RS*,5*RS*)-3-(2-(3-hydroxyprop-1-yn-1-yl)phenyl)-8-azabicyclo[3.2.1]octan-8-yl)ethan-1-one (**3.25**). A solution of (1*SR*,3*RS*,5*RS*)-*tert*-butyl 3-(2-(3-hydroxyprop-1-yn-1-yl)phenyl)-8-azabicyclo[3.2.1]octane-8-carboxylate (**3.27** 0.0450 g, 0.0132 mmol) in CH₂Cl₂ (2.5 mL) was treated with TFA (0.2 mL, 2.64 mmol) at 0 °C. After 6 h, the solution was concentrated. The residual oil was dissolved in CH₂Cl₂ and satd. aqueous NaHCO₃, and the aqueous layer was extracted with CH₂Cl₂ (3 x 20 mL). The combined organic layers were dried (Na₂SO₄), filtered and concentrated under reduced pressure to give 3-(2-(((1*SR*,3*RS*,5*RS*)-8-azabicyclo[3.2.1]octan-3-yl)phenyl)prop-2-yn-1-ol (0.0368 g, 0.152 mmol) as a dark red oil that was used without further purification.

A solution of 2-(((3,5-dimethylisoxazol-4-yl)methyl)thio)acetic acid (**3.26**, 0.0584 g, 0.290 mmol), HATU (0.0121 g, 0.319 mmol) and DIPEA (101 µL, 0.580 mmol) in CH₂Cl₂ (1 mL) was stirred for 30 min at 0 °C and treated with a solution of 3-(2-(((1*SR*,3*RS*,5*RS*)-8-azabicyclo[3.2.1]octan-3-yl)phenyl)prop-2-yn-1-ol (0.0350 g, 0.145 mmol) and DIPEA (50 µL, 0.260 mmol) in CH₂Cl₂ (1 mL). The mixture is stirred at rt for 3 h, treated with 1 M NaOH (0.2 mL) and stirred at rt for 2 h. The reaction was diluted with EtOAc, and the layers separated. The organic layer was washed with 1 M aqueous NaHSO₄, satd. aqueous NaHCO₃, dried (Na₂SO₄), and concentrated. The residue was purified by automated chromatography SiO₂ (4g column, liquid load CH₂Cl₂, gradient 50% EtOAc/hexanes to 100% EtOAc) to give **3.25** (0.0182 g, 0.0429 mmol, 30% (2 steps)) as a yellow oil that partially solidified to a waxy off white solid: IR (CH₂Cl₂) 3387, 2924, 2865, 1616, 1448, 1031, 759 cm⁻¹; ¹H NMR (400 MHz, CDCl₃) δ 7.35 (dd, *J* = 8.4, 1.6 Hz, 1 H), 7.26 (dt, *J* = 7.6, 1.2 Hz, 1 H), 7.16-7.13 (m, 2 H), 4.64 (t, *J* = 8.4 Hz, 1 H), 4.47 (ddd, *J* = 16.4, 16.4, 6.0 Hz, 2 H), 4.25 (t, *J* = 8.0 Hz, 1 H), 4.10 (app t, *J* = 5.6 Hz, 1 H),

3.70 (dd, $J = 20.0, 13.6$ Hz, 2 H), 3.23 (dd, $J = 20.0, 14.0$ Hz, 2 H), 3.09 (app quint, $J = 6.0$ Hz, 1 H), 2.91-2.83 (m, 1 H), 2.51-2.44 (m, 1 H), 2.37 (s, 3 H), 2.24 (s, 3 H), 2.23-2.17 (m, 1 H), 2.09-2.00 (m, 1 H), 1.83 (ddd, $J = 9.2, 9.2, 4.4$ Hz, 1 H), 1.74-1.65 (m, 2 H), 1.15 (dt, $J = 13.2, 1.2$ Hz, 1 H); ^{13}C NMR (100 MHz, CDCl_3) δ 168.1, 166.9, 159.7, 145.0, 132.0, 131.4, 128.5, 126.1, 125.6, 122.7, 109.7, 93.4, 83.1, 53.5, 51.2, 50.2, 38.6, 36.6, 33.1, 32.7, 31.0, 24.2, 10.9, 10.0; HRMS (ESI) m/z calcd for $\text{C}_{24}\text{H}_{29}\text{N}_2\text{O}_3\text{S}$ ($[\text{M}+\text{H}]^+$) 425.1893, found 425.1894.

Bead conjugation Conjugation of 3.25 to the Carboxylink Agarose beads

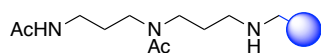
Activation of the alcohol with *p*-nitrophenylchloroformate: A solution of 2-(((3,5-dimethylisoxazol-4-yl)methyl)thio)-1-((1*R*,3*s*,5*S*)-3-(2-(3-hydroxyprop-1-yn-1-yl)phenyl)-8-azabicyclo[3.2.1]octan-8-yl)ethanone (**3.25**, 0.00566 g, 0.0133 mmol) in CH_2Cl_2 (200 μL) was added *p*-nitrophenylchloroformate (0.00403 g, 0.0199 mmol) and Et_3N (3.7 μL , 0.0266 mmol) and the reaction was stirred at rt for 4 hours, diluted with H_2O (50 μL) and stirred for another 10 min where a deep yellow color was noted. The reaction was diluted with CH_2Cl_2 (1 mL) filtered through a small column of Na_2SO_4 and washed (CH_2Cl_2 (1 mL)). The solution was concentrated under reduced pressure to give the product as a clear yellow oil that was dissolved in DMF (400 μL) to give the "**activated alcohol solution**".

Conjugation reaction: A suspension of Carboxylink Coupling Gel (1.0 mL) was washed with DMF (1.0 mL). The tube was capped and the gel resuspended by inverting with gentle shaking. The beads were pelleted in the centrifuge (2 min), the supernatant was removed (pipet). This washing was repeated 3 times and the resulting pellet was treated with the **activated alcohol solution** in DMF, the eppendorf tube was capped and rotated for 5 d at 20 °C then added 5% MES buffer and warmed to 30 °C for 3 d. The gel was pelleted and washed with DMF (3 x 1.0 mL), PBS buffer (3 x 1.0 mL), and (HPLC grade) H_2O (3 x 1.0 mL). Similar to the initial

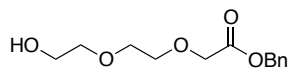
suspension/pelleting/and pipetting. Finally the gel was suspended with 1.0 mL of 0.05% azide solution to give **3.34** conjugated beads.

Quantification: The DMF, phosphate buffer and HPLC H₂O washes were combined and concentrated by centrifugal evaporation in the HT4 (24h@40 °C). The resulting solid was suspended in CH₂Cl₂ and filtered through a plug of cotton. The combined filtrates were concentrated under reduced pressure to give (4.74 mg of a 1:0.5:0.2:0.5 mixture of p-nitrophenol (M=139), activated carbonate (M=589): unknown pdt (M=508): unknown elimination pdt (M=443)). By mass the recovered material was 0.87 mg of p-nitrophenol with the rest comprised of 571 containing material (3.86 mg) was remaining resulting in 1.80 mg (4.24 μmol) of 571 conjugated to bead. (Mass component X/Mass p-nitrophenol)*number of equivalents in ¹HNMR. giving us the ratio by weight of the products as 1:2.1:0.73:1.6 respectively. Adding the values gives us 5.43 and 1/5.43 is the amount of 4.74 mg that contains p-nitrophenol. Subtracting that from the mass and then an overall subtraction from the SM gives us 1.80 mg of SM consumed.

Control beads:

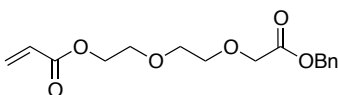


Carboxylink Coupling Gel was washed with DMF (1.0 mL). The eppendorf tube was capped and the gel resuspended by inverting with gentle shaking. The beads were pelleted in the centrifuge tube (2 min), the supernatant was removed (pipet). This washing was repeated 3 times. The pelleted beads were treated with a solution of *N*-acetoxysuccinimide (1 M in DMF, 400 μL) and the eppendorf tube was placed on the rotator for 4 h at rt. After 4 h the gel was washed with DMF (3 x 1 mL), phosphate buffer (pH 7.0) (3 x 1 mL), and H₂O (3 x 1.0 mL (HPLC grade)). The gel was suspended with 1.0 mL of 0.05% azide solution.



3.38

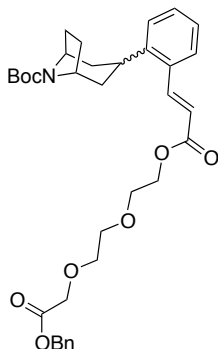
Benzyl 2-(2-(2-hydroxyethoxy)ethoxy)acetate (3.38).⁴⁸⁷ A suspension of tBuOK (2.96 g, 26.4 mmol) in dry THF (70 mL) at 0 °C was treated with di(ethylene)glycol (**3.37**, 4.81 mL, 50.3 mmol) warmed to rt and stirred for 1 h, treated dropwise with a solution of bromobenzoacetate (6.00 g, 4.15 mL, 25.1 mmol) in dry THF (14 mL). The resulting mixture was allowed to stir at rt for 24 h. The mixture was diluted with THF (200 mL) and filtered through Celite, washed (THF), and the filtrate was concentrated under reduced pressure. The crude residue was purified by chromatography on SiO₂ (100% EtOAc) to give **3.38** (1.49 g, 5.86 mmol, 23%) as a pale yellow liquid: ¹H NMR (300 MHz, CDCl₃) δ 7.35 (bs, 5 H), 5.19 (s, 2 H), 4.35-4.28 (m, 2 H), 4.18 (s, 2 H), 3.74-3.70 (m, 10 H), 3.63-3.56 (m, 2 H) 2.09 (bs, 1 H).



3.39

2-(2-(2-(Benzyloxy)-2-oxoethoxy)ethoxy)ethyl acrylate (3.39). A solution of benzyl 2-(2-(2-hydroxyethoxy)ethoxy)acetate (**3.38**, 1.49 g, 5.86 mmol) in dry THF (30 mL) cooled to 0 °C and treated with acryloyl chloride (0.5 mL, 6.15 mmol) and Et₃N (0.91 mL, 6.45 mmol) and stirred at rt for 24 h. The reaction was concentrated under reduced pressure and was dissolved in CH₂Cl₂, successively washed with 5% aqueous HCl, 5% aqueous NaHCO₃, and brine, dried (MgSO₄), and concentrated under reduced pressure. The crude residue was purified by chromatography on SiO₂ (hexanes/EtOAc, 2:1) to give the **3.39** (0.589 g, 1.91 mmol, 33%) as a clear oil: ¹H NMR (400 MHz, CDCl₃) δ 7.37-7.35 (m, 5 H), 6.46 (m, 2 H), 6.39-6.10 (m, 1 H), 5.87-5.79 (m, 1 H), 5.19 (s, 2 H), 4.35-4.29 (m, 4 H), 4.20 (s, 2 H), 3.76-3.69 (m, 8 H); ¹³C NMR

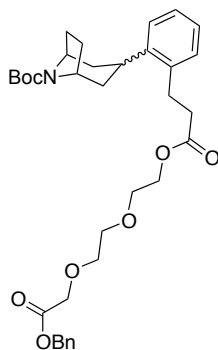
(100 MHz, CDCl₃) δ 170.3, 166.1, 135.4, 131.1, 131.0, 128.6, 128.5, 128.4 (2 C), 128.2, 128.1 (2 C), 73.3, 70.9, 70.7, 69.1, 69.0, 68.9, 68.7, 67.0, 66.5, 63.7, 63.6, 63.5.



3.40

***tert*-Butyl (1*SR*,5*RS*)-3-(2-((*E*)-3,12-dioxo-1-phenyl-2,5,8,11-tetraoxatetradec-13-en-14-yl)phenyl)-8-azabicyclo[3.2.1]octane-8-carboxylate (3.40).** A solution of a 10:1 mixture of **3.33a** and **3.33b** (1*SR*,5*RS*)-*tert*-butyl 3-(2-bromophenyl)-8-azabicyclo[3.2.1]octane-8-carboxylate (**3.33**, 0.215 g, 0.587 mmol) in dry degassed MeCN (3.0 mL) was treated with Pd(OAc)₂ (0.0132 g, 0.0587 mmol), tri(*o*-tolyl)phosphine (0.0295 g, 0.0939 mmol) and Et₃N (215 μ L, 1.53 mmol), followed by 2-(2-(2-(benzyloxy)-2-oxoethoxy)ethoxy)ethyl acrylate (**3.39**, 0.181 g, 0.587 mmol). The reaction mixture was heated at 85 °C for 24 h, cooled to rt, concentrated under reduced pressure, diluted with EtOAc (50 mL), filtered through Celite and the filtrate was concentrated under reduced pressure. The crude residue was purified by automated chromatography on SiO₂ (12 g column, liquid load CH₂Cl₂, gradient, 100% hexanes to 70% EtOAc/hexanes product eluted at 50% EtOAc/hexanes) to give the **3.40** as a 10:1 mixture of diastereomers (0.183 g, 0.308 mmol, 53%) as a light brown/orange oil: IR (CH₂Cl₂) 2962, 2872, 1752, 1711, 1687, 1390, 1310, 1165, 1122, 980, 751 cm⁻¹; Characteristic NMR for the major diastereomer ¹H NMR (300 MHz, CDCl₃) δ 8.04 (d, *J* = 15.7 Hz, 1 H), 7.47 (d, *J* = 7.7 Hz, 1 H), 7.34-7.17 (m, 9 H), 6.34 (d, *J* = 15.7 Hz, 1 H), 5.17 (s, 1 H), 4.62 (s, 1 H), 4.35 (t, *J* =

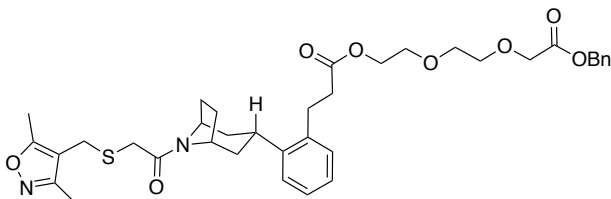
4.5 Hz, 4 H), 4.26 (s, 1 H), 4.21 (s, 2 H), 4.13 (s, 1 H), 3.75 (t, $J = 4.8$ Hz, 6 H), 2.99-2.89 (m, 1 H), 2.50-2.45 (m, 3 H), 2.07 (s, 2 H), 1.70-1.63 (m, 2 H), 1.53 (s, 9 H), 1.46-1.43 (m, 3 H); ^{13}C NMR (75 MHz, CDCl_3) δ 170.1, 166.2, 154.5, 143.8, 142.4, 135.3, 133.4, 129.8, 128.4, 128.2, 127.9, 127.5, 127.1, 126.3, 120.2, 79.2, 73.2, 70.8, 70.5, 69.0, 68.8, 68.5, 66.9, 66.3, 63.6, 63.4, 63.3, 51.3, 50.5, 38.6, 37.7, 32.1, 31.4, 30.4, 28.3; HRMS (ESI) m/z calcd for $\text{C}_{34}\text{H}_{44}\text{NO}_8$ ($[\text{M}+\text{H}]^+$) 594.3061, found 594.3060.



3.41

***tert*-Butyl (1*SR*,5*RS*)-3-(2-(3,12-dioxo-1-phenyl-2,5,8,11-tetraoxatetradecan-14-yl)phenyl)-8-azabicyclo[3.2.1]octane-8-carboxylate (3.41).** A 10:1 diastereomer mixture of (1*SR*,5*RS*)-*tert*-butyl 3-(2-((*E*)-3,12-dioxo-1-phenyl-2,5,8,11-tetraoxatetradec-13-en-14-yl)phenyl)-8-azabicyclo[3.2.1]octane-8-carboxylate (**3.40**, 0.400 g, 0.674 mmol) and $\text{NiCl}_2 \cdot 6\text{H}_2\text{O}$ (0.320 g, 1.35 mmol) in THF (6.7 mL) was treated with NaBH_4 (0.153 g, 4.04 mmol) in portions at 0 °C. Within 5 min gas evolution started and the solution turned black. The reaction was stirred for 6 h where by LCMS it appeared that a small amount of the SM remained so an additional $\text{NiCl}_2 \cdot 6\text{H}_2\text{O}$ (1 eq) and NaBH_4 (2 eq) was added and the reaction was left to stir for 12 h. The reaction was diluted with Et_2O (20 mL) and 1 M aqueous HCl (50 mL), extracted with EtOAc (3×50 mL), and the combined organic layers were washed with satd. aqueous NaHCO_3 (3×30 mL), dried (MgSO_4), and concentrated under reduced pressure. The crude residue was

purified by automated chromatography on SiO₂ (4g column, liquid load CH₂Cl₂, gradient 100% hexanes to 30% hexanes/EtOAc) to give the product as a 10:1 mixture of diastereomers (0.233 g, 0.391 mmol, 58%) as a clear colorless oil: IR (CH₂Cl₂) 2958, 2895, 1733, 1685, 1390, 1163, 1120, 753 cm⁻¹; Characteristic NMR for the major diastereomer ¹H NMR (400 MHz, CDCl₃) δ 7.37-7.33 (m, 6 H), 7.20-7.07 (m, 4 H), 5.18 (s, 1 H), 4.62 (s, 1 H), 4.30 (dd, *J* = 5.4, 4.2 Hz, 2 H), 4.19 (t, *J* = 4.9 Hz, 4 H), 4.13 (s, 1 H), 3.73-3.63 (m, 7 H), 2.95 (t, *J* = 7.8 Hz, 2 H), 2.81-2.74 (m, 1 H), 2.58 (t, *J* = 7.8 Hz, 2 H), 2.46-2.39 (m, 2 H), 2.07 (dd, *J* = 6.4, 4.2 Hz, 2 H), 1.69-1.64 (m, 2 H), 1.49 (s, 9 H), 1.37 (t, *J* = 13.0 Hz, 2 H); ¹³C NMR (100 MHz, CDCl₃) δ 172.4, 170.2, 154.7, 142.5, 137.9, 137.0, 135.3, 129.3, 128.5, 128.4, 128.0, 126.0, 79.1, 73.2, 70.8, 70.5, 69.2, 68.6, 66.9, 66.5, 63.6, 63.5, 63.3, 35.5, 29.4, 28.4, 27.8; HRMS (ESI) *m/z* calcd for C₃₄H₄₆NO₈ ([M+H]⁺) 596.3218, found 596.3220.



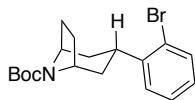
3.36

2-(2-(2-(Benzyloxy)-2-oxoethoxy)ethoxy)ethyl 3-(2-(((1*SR*,3*RS*,5*RS*)-8-(2-(((3,5-dimethylisoxazol-4-yl)methyl)thio)acetyl)-8-azabicyclo[3.2.1]octan-3-yl)phenyl)propanoate (3.36). A solution of (1*SR*,5*RS*)-tert-butyl 3-(2-(3,12-dioxo-1-phenyl-2,5,8,11-tetraoxatetradecan-14-yl)phenyl)-8-azabicyclo[3.2.1]octane-8-carboxylate (**3.41**, 0.122 g, 0.205 mmol) in THF (2 mL) was cooled to 0 °C, treated with 4M HCl in dioxane (1.5 mL, 30 eq) and stirred at 0 °C for 8 h. The solution was concentrated under reduced pressure and the residue was sonicated with Et₂O and hexanes and decanted (3x) leaving behind the product. The product was dried under high vacuum to give 2-(2-(2-(benzyloxy)-2-oxoethoxy)ethoxy)ethyl 3-(2-

((1SR,3RS,5RS)-8-azabicyclo[3.2.1]octan-3-yl)phenyl)propanoate hydrochloride (0.115 g, 0.216 mmol, quant) as a viscous oil that was taken onto the T3P coupling with no further purification.

A solution of 2-(((3,5-dimethylisoxazol-4-yl)methyl)thio)acetic acid (**3.26**, 0.0495 g, 0.246 mmol) and 2-(2-(2-(benzyloxy)-2-oxoethoxy)ethoxy)ethyl 3-(2-((1SR,3RS,5RS)-8-azabicyclo[3.2.1]octan-3-yl)phenyl)propanoate hydrochloride (0.109 g, 0.205 mmol) in CH₂Cl₂ (2 mL), was cooled to 0 °C and treated with Et₃N (86 μL, 0.0622 mmol). The cooled mixture was treated with T3P (50 wt. % solution in EtOAc, 217 μL, 0.307 mmol) and the reaction was warmed to rt, stirred for 12 h, diluted with CH₂Cl₂, and washed with satd. aqueous NH₄Cl, satd. aqueous NaHCO₃, brine, dried (Na₂SO₄), filtered, and concentrated under reduced pressure. The crude material was purified by automated chromatography on SiO₂ (4g column, liquid load CH₂Cl₂, gradient 100% CH₂Cl₂ to 60% CH₂Cl₂/EtOAc, pdt eluted at 15% EtOAc CH₂Cl₂) to give the product as a 3:2 mixture of product:impurity. This mixture was then purified by preparative HPLC (isocratic 16% *i*PrOH/hexanes (Varian Dynamax 250 X 21.4 microsorb 60 - 8 Si 20 mL/ min)) and filtered through a short plug of SiO₂ (2:1, CH₂Cl₂/EtOAc) to give **3.36** as a single diastereomer (0.00850 g, 0.0125 mmol, 6%) as a clear oil: IR (CHCl₃) 2951, 1733, 1629, 1448, 1193, 1144 cm⁻¹; ¹H NMR (600 MHz, CDCl₃) δ 7.37-7.32 (m, 5 H), 7.22-7.18 (m, 2 H), 7.14-7.10 (m, 2 H), 5.17 (s, 2 H), 4.75 (t, *J* = 7.9 Hz, 1 H), 4.18 (t, *J* = 4.7 Hz, 4 H), 3.82 (d, *J* = 14.4 Hz, 1 H), 3.71 (dd, *J* = 5.6, 3.3 Hz, 2 H), 3.64 (dd, *J* = 4.8, 4.2 Hz, 4 H), 3.62 (d, *J* = 14.4 Hz, 1 H), 3.17 (d, *J* = 13.8 Hz, 1 H), 3.03 (d, *J* = 13.8 Hz, 1 H), 2.99-2.95 (m, 3 H), 2.58 (t, *J* = 8.0 Hz, 2 H), 2.54-2.47 (m, 5 H), 2.31 (s, 3 H), 2.17-2.05 (m, 2 H), 1.82-1.73 (m, 2 H), 1.51 (t, *J* = 12.8 Hz, 1 H), 1.46 (t, *J* = 12.8 Hz, 1 H); ¹³C NMR (150 MHz, CDCl₃) δ 172.6, 170.2, 167.0, 166.4, 159.9, 141.9, 138.2, 135.4, 129.3, 128.6, 128.4 (2 C), 127.5, 126.7, 126.3, 110.0, 70.9,

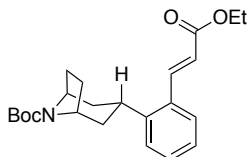
70.5, 69.1, 68.6, 66.5, 63.5, 53.2, 49.2, 40.1, 38.8, 35.7, 32.9, 31.4, 31.1, 29.5, 27.7, 23.6, 11.1, 10.2; HRMS (ESI) m/z calcd for $C_{37}H_{47}O_8N_2S$ ($[M+H]^+$) 679.3048, found 679.3045.



3.33a

tert-Butyl (1SR,3RS,5RS)-3-(2-bromophenyl)-8-azabicyclo[3.2.1]octane-8-carboxylate (3.33a). A solution of (1R,5S)-tert-butyl 3-(2-bromophenyl)-8-azabicyclo[3.2.1]oct-2-ene-8-carboxylate (1.75 g, 4.80 mmol) in anhydrous iPrOH (20 mL, 0.25 M) under argon was treated with phenylsilane (3.6 mL, 28.8 mmol) and TBHP (5.5 M in decane) (1.31 mL, 7.20 mmol) and the resulting mixture was degassed by bubbling argon through the solution for 10 minutes. $Mn(dpm)_3^{431}$ (0.290 g, 0.480 mmol) was added in one portion and the reaction was then degassed for an additional 30 seconds. After 1 h another portion of $Mn(dpm)_3$ (0.290 g, 0.480 mmol) was added and the solution was stirred for another hour. After 1 h another portion $Mn(dpm)_3$ (0.290 g, 0.480 mmol) was added and the solution was stirred for another hour. After stirring for 1 h another portion of $Mn(dpm)_3$ (0.290 g, 0.480 mmol) and the reaction was stirred for 16 h at rt, quenched by SLOW ADDITION of 1 M NaOH (100 mL) at 0 °C and stirred for 15 min, filtered, washed (EtOAc) the layers separated and the aqueous layer was extracted with EtOAc (3 x 100 mL). The combined organic layers were washed with brine, dried ($MgSO_4$), filtered, and concentrated under reduced pressure. The crude residue was purified by chromatography on SiO_2 (hexanes/EtOAc, 9:1) to give the major diastereomer **3.33a** (0.470 g, 1.28 mmol, 27%) as a clear colorless oil. Additionally, a 1:1 mixture of diastereomers was also recovered as mixed fractions (0.327 g, 0.892 mmol, 19%) as a clear colorless oil: Characterization for **3.33a**: IR (CH_2Cl_2) 3280, 2971, 1685, 1379, 1327, 1169, 1092, 755 cm^{-1} ; 1H NMR (400 MHz, $CDCl_3$) δ 7.55 (dd, $J = 7.8, 1.2$ Hz, 1 H), 7.45 (dd, $J = 7.8, 1.2$ Hz, 1 H), 7.35

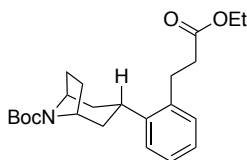
(td, $J = 7.8, 1.2$ Hz, 1 H), 7.13 (td, $J = 7.8, 1.2$ Hz, 1 H), 4.17-4.13 (m, 2 H), 2.90 (tt, $J = 12.0, 6.6$ Hz, 1 H), 2.33-2.32 (m, 2 H), 2.01-1.98 (m, 1 H), 1.96-1.92 (m, 1 H), 1.71-1.67 (m, 2 H), 1.45 (s, 9 H), 1.36 (t, $J = 12.0$ Hz, 2 H); ^{13}C NMR (150 MHz, CDCl_3) δ 153.7, 143.0, 132.5, 129.3, 128.1, 128.1, 123.8, 78.4, 50.8, 50.1, 37.1, 36.4, 33.1, 31.7, 31.1, 28.2; HRMS (ESI) m/z calcd for $\text{C}_{18}\text{H}_{24}\text{BrNNaO}_2$ ($[\text{M}+\text{Na}]^+$) 388.0883, found 388.0880.



3.43

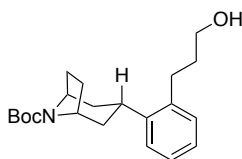
tert-Butyl (1SR,3RS,5RS)-3-(2-((E)-3-ethoxy-3-oxoprop-1-en-1-yl)phenyl)-8-azabicyclo[3.2.1]octane-8-carboxylate (3.43). A solution of (1SR,3RS,5RS)-tert-butyl 3-(2-bromophenyl)-8-azabicyclo[3.2.1]octane-8-carboxylate (**3.33a**, 0.469 g, 1.28 mmol) in dry degassed MeCN (6.4 mL) was treated with $\text{Pd}(\text{OAc})_2$ (0.0287 g, 0.128 mmol), tri(*o*-tolyl)phosphine (0.0643 g, 0.205 mmol), Et_3N (467 μL , 3.33 mmol), and ethyl acrylate (181 μL , 1.66 mmol) and heated 18 h at 85 $^\circ\text{C}$, concentrated under reduced pressure. The residue was diluted with EtOAc (20 mL), filtered through Celite, washed (EtOAc) and the combined filtrates were concentrated under reduced pressure. The crude residue was purified by chromatography on SiO_2 (hexanes/EtOAc, 3:1) to give **3.43** (0.432 g, 1.12 mmol, 87%) as a clear colorless oil: IR (CH_2Cl_2) 2973, 1701, 1691, 1392, 1310, 1172, 1102, 764 cm^{-1} ; ^1H NMR (400 MHz, CDCl_3) δ 8.00 (d, $J = 15.7$ Hz, 1 H), 7.47 (dd, $J = 7.7, 0.9$ Hz, 1 H), 7.33 (td, $J = 7.4, 1.2$ Hz, 1 H), 7.28-7.26 (m, 1 H), 7.20 (td, $J = 7.4, 1.2$ Hz, 1 H), 6.28 (d, $J = 15.7$ Hz, 1 H), 4.37 (bs, 1 H), 4.25 (q, $J = 7.1$ Hz, 3 H), 2.94 (tt, $J = 11.4, 7.3$ Hz, 1 H), 2.53-2.39 (m, 2 H), 2.10-2.05 (m, 2 H), 1.67 (q, $J = 7.3$ Hz, 2 H), 1.52 (s, 9 H), 1.48-1.39 (m, 2 H), 1.34 (t, $J = 7.1$ Hz, 3 H); ^{13}C NMR (100 MHz, CDCl_3) δ 166.5, 154.6, 143.8, 142.0, 133.6, 129.8, 127.7, 127.3, 126.4, 120.9, 79.3, 60.4, 51.4,

50.6, 38.7, 37.8, 32.3, 31.6, 30.6, 28.4, 14.3; HRMS (ESI) m/z calcd for $C_{23}H_{32}O_4N$ ($[M+H]^+$) 386.2326, found 386.2327.



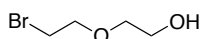
3.44

tert-Butyl (1SR,3RS,5RS)-3-(2-(3-ethoxy-3-oxopropyl)phenyl)-8-azabicyclo[3.2.1]octane-8-carboxylate (3.44). A solution of (1SR,3RS,5RS)-tert-butyl 3-(2-((E)-3-ethoxy-3-oxoprop-1-en-1-yl)phenyl)-8-azabicyclo[3.2.1]octane-8-carboxylate (**3.43**, 0.0500 g, 0.130 mmol) in absolute EtOH (1.3 mL) was treated with 10% Pd/C (0.0138 g, 0.0130 mmol, equivalent to 10 mol% Pd) and stirred under a balloon of H_2 for 1.5 h where analysis by 1H NMR indicated that the alkene had been consumed. The reaction was filtered through basic Al_2O_3 (eluting with EtOAc) to give **3.44** (0.0517 g, 0.133 mmol, quant.) as a clear colorless oil: IR (CH_2Cl_2) 2971, 1732, 1687, 1390, 1564, 1163, 1100, 755 cm^{-1} ; 1H NMR (400 MHz, $CDCl_3$) δ 7.22-7.16 (m, 2 H), 7.14-7.08 (m, 2 H), 4.35 (bs, 1 H), 4.24 (bs, 1 H), 4.10 (q, $J = 7.1$ Hz, 2 H), 2.95 (t, $J = 7.9$ Hz, 2 H), 2.79 (tt, $J = 11.9, 7.1$ Hz, 1 H), 2.56-2.51 (m, 2 H), 2.09-2.07 (m, 2 H), 1.67 (q, $J = 7.4$ Hz, 2 H), 1.50 (s, 9 H), 1.41-1.34 (m, 2 H), 1.22 (t, $J = 7.1$ Hz, 3 H); ^{13}C NMR (100 MHz, $CDCl_3$) δ 172.5, 154.7, 142.5, 138.0, 129.3, 127.6, 126.6, 126.0, 79.1, 60.3, 51.3, 50.6, 39.5 (2 C), 38.6, 35.8, 32.5, 31.8, 29.4, 28.4, 27.9, 14.1; HRMS (ESI) m/z calcd for $C_{23}H_{34}O_4N$ ($[M+H]^+$) 388.2482, found 388.2479.



3.45

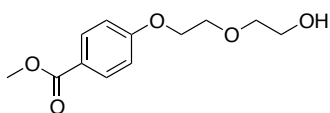
***tert*-Butyl (1*SR*,3*RS*,5*RS*)-3-(2-(3-hydroxypropyl)phenyl)-8-azabicyclo[3.2.1]octane-8-carboxylate (3.45).** A solution of (1*SR*,3*RS*,5*RS*)-*tert*-butyl 3-(2-(3-ethoxy-3-oxopropyl)phenyl)-8-azabicyclo[3.2.1]octane-8-carboxylate (**3.44**, 0.400 g, 1.03 mmol) in THF (8 mL) was treated with NaBH₄ (0.390 g, 10.3 mmol) and stirred for 15 min at rt, treated with absolute ethanol (2 mL) and stirred at rt for 16 h where analysis by TLC (hexanes/EtOAc, 1:1) indicated there was still SM remaining. An additional 2 equiv. of NaBH₄ was added and the reaction was stirred for another 1.5 h where analysis by TLC (hexanes/EtOAc, 1:1) indicated the SM had been consumed. The reaction was cooled to 0 °C and diluted with 1 M aqueous HCl (40 mL), extracted with EtOAc (3 x 30 mL). The combined organic layers were dried (MgSO₄), filtered and concentrated under reduced pressure. The crude residue was purified by chromatography on SiO₂ (hexanes/EtOAc, 1:1) to give **3.45** (0.266 g, 0.771 mmol, 75%) as colorless solid: Mp 99.3-101.7 °C; IR (CH₂Cl₂) 3485, 2971, 1670, 1689, 1407, 1163, 1107, 753 cm⁻¹; ¹H NMR (400 MHz, CDCl₃) δ 7.21-7.08 (m, 4 H), 4.33 (bt, *J* = 7.4 Hz, 1 H), 4.24 (bt, *J* = 7.4 Hz, 1 H), 3.66 (t, *J* = 6.5 Hz, 2 H), 2.83 (tt, *J* = 12.5, 6.5 Hz, 1 H), 2.76-2.67 (m, 2 H), 2.49-2.36 (m, 2 H), 2.17-2.01 (m, 2 H), 1.98-1.86 (m, 1 H), 1.81 (quint, *J* = 7.1 Hz, 2 H), 1.51 (s, 9 H), 1.43-1.32 (m, 2 H); ¹³C NMR (100 MHz, CDCl₃) δ 154.9, 142.3, 139.5, 129.6, 127.5, 126.3, 125.9, 79.2, 62.1, 51.4, 50.7, 39.4, 38.9, 34.6, 32.4 (2 C), 32.0, 29.4, 29.3, 28.5; HRMS (ESI) *m/z* calcd for C₂₁H₃₂O₃N ([M+H]⁺) 346.2377, found 346.2373.



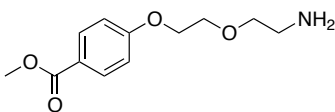
3.50

2-(2-Bromoethoxy)ethanol (3.50).⁴⁸⁸ A solution of diethylene glycol (**3.37**, 1.79 mL, 18.9 mmol) in MeCN (30.0 mL) at rt was treated with carbon tetrabromide (6.88 g, 20.7 mmol), and triphenylphosphine (4.95 g, 18.9 mmol) and the resulting mixture was stirred at rt for 16 h,

diluted with 1 M aqueous NaOH (25 mL) and MeCN, and the mixture was concentrated under reduced pressure. The aqueous residue was extracted with EtOAc (3 × 30 mL), dried (Na₂SO₄), filtered, and concentrated. The crude residue was purified by chromatography on SiO₂ (hexanes/EtOAc, 1:1) to give **3.50** (2.16 g, 10.7 mmol, 57%) as yellow oil contaminated with 16% PPh₃O. This material was carried on with no further purification: ¹H NMR (300 MHz, CDCl₃) δ 3.83 (t, *J* = 6.0 Hz, 2 H), 3.76 (dd, *J* = 5.3, 3.7 Hz, 2 H), 3.63 (dd, *J* = 5.3, 3.7 Hz, 2 H), 3.49 (t, *J* = 6.0 Hz, 2 H), 1.97 (s, 1 H).



Methyl 4-(2-(2-hydroxyethoxy)ethoxy)benzoate (3.52).⁴⁸⁸ A solution of methyl 4-hydroxybenzoate (**3.51**, 2.33 g, 15.3 mmol) in MeCN (80 mL) was treated with K₂CO₃ (4.41 g, 31.9 mmol), NaI (1.91 g, 12.8 mmol), and 2-(2-bromoethoxy)ethanol (**3.50**, 2.16 g, 12.8 mmol) and the resultant mixture was heated to 60 °C 15 h. Then the mixture was diluted with H₂O, extracted with EtOAc. The combined organic layers were dried (Na₂SO₄), filtered, and concentrated under reduced pressure. The crude residue was purified by chromatography on SiO₂ (hexanes/EtOAc, 2:3) to give **3.52** that was contaminated with PPh₃O (15%) (1.62 g, 5.73 mmol, 45%) as a clear/pale-yellow oil: ¹H NMR (300 MHz, CDCl₃) δ 8.01-7.96 (m, 2 H), 6.96-6.91 (m, 2 H), 4.20 (t, *J* = 4.7 Hz, 2 H), 3.91-3.87 (m, 5 H), 3.79-3.75 (m, 2 H), 3.70-3.66 (m, 2 H), 1.80 (s, 1 H).



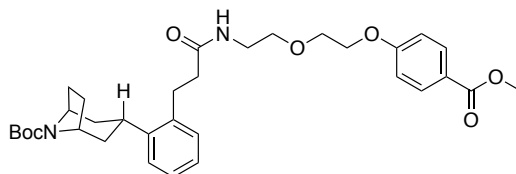
3.53

Methyl 4-(2-(2-aminoethoxy)ethoxy)benzoate (3.53). A solution of methyl 4-(2-(2-hydroxyethoxy)ethoxy)benzoate (**3.52**, 0.300 g, 1.25 mmol) in dry THF (5 mL) at 0 °C was treated Et₃N (193 μ L, 1.37 mmol) followed by MsCl (106 μ L, 1.37 mmol) and stirred at 0 °C for 2 h, diluted with satd. aqueous NaHCO₃ and extracted with Et₂O (3 x 20 mL). The combined organic layers were dried (MgSO₄), filtered, and concentrated under reduced pressure to give the crude mesylate (0.369 g, 1.16 mmol) as a colorless solid.

A solution of the crude mesylate (0.230 g, 0.723 mmol) in DMF (1.5 mL) was treated with Et₃N (0.16 mL, 1.54 mmol) and NaN₃ (0.142 g, 2.18 mmol). This mixture was heated to 50 °C behind a blast shield for 17 h where analysis by TLC (hexanes/EtOAc; 1:1) indicated that the mesylate intermediate was completely consumed. The reaction was cooled to rt, diluted with H₂O (5 mL) and brine (10 mL) and extracted with Et₂O (3 x 10 mL). The combined organic layers were washed with brine, dried (Na₂SO₄), concentrated under reduced pressure to give the crude methyl 4-(2-(2-azidoethoxy)ethoxy)benzoate (0.170 g, 0.449 mmol) as a colorless wax.

To a solution of crude methyl 4-(2-(2-azidoethoxy)ethoxy)benzoate (0.161 g, 1.70 mmol (contaminated with ~30% PPh₃O)) in THF (2 mL) was added triphenyl phosphine (0.223 g, 0.850 mmol) and H₂O (30 μ L, 1.70 mmol) then heated to 50 °C for 17 h, and concentrated under reduced pressure. The residue was dissolved in CH₂Cl₂ and 1 M aqueous HCl (10 mL) and the aqueous layer was washed with CH₂Cl₂ (2x). The aqueous layer was neutralized with solid K₂CO₃ to pH 10. The aqueous layer was washed with CH₂Cl₂ (3 x 30 mL). The combined organic layers were dried (Na₂SO₄), filtered and concentrated under reduced pressure to give **3.53** (0.0893 g, 0.373 mmol, 55% (3 steps)) as a clear oil that solidified in the freezer: Mp ~10-20 °C; (CH₂Cl₂) 3368, 2945, 1707, 1603, 1249, 1169, 1103, 846 cm⁻¹; ¹H NMR (400 MHz, CDCl₃) δ 7.94 (dt, *J* = 9.0, 2.6 Hz, 2 H), 6.90 (dt, *J* = 9.0, 2.6 Hz, 2 H), 4.14 (dd, *J* = 5.4, 4.1 Hz,

2 H), 3.84 (s, 3 H), 3.80 (dd, $J = 5.4, 4.1$ Hz, 2 H), 3.54 (t, $J = 5.4$ Hz, 2 H), 2.85 (bs, 2 H); ^{13}C NMR (100 MHz, CDCl_3) δ 166.7, 162.4, 131.4, 122.6, 114.1, 73.6, 69.2, 67.4, 51.7, 41.7; HRMS (ESI) m/z calcd for $\text{C}_{12}\text{H}_{18}\text{O}_4\text{N}$ ($[\text{M}+\text{H}]^+$) 240.1230, found 240.1229.

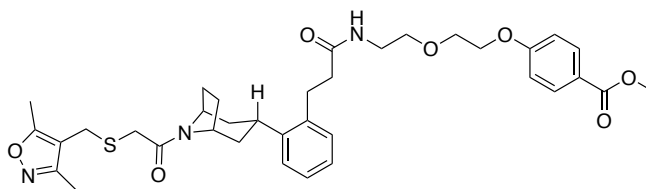


3.54

***tert*-Butyl (1*SR*,3*RS*,5*RS*)-3-(2-(3-((2-(2-(4-(methoxycarbonyl)phenoxy)ethoxy)ethyl)amino)-3-oxopropyl)phenyl)-8-azabicyclo[3.2.1]octane-8-carboxylate (3.54).** A solution of (1*SR*,3*RS*,5*RS*)-*tert*-butyl 3-(2-(3-ethoxy-3-oxopropyl)phenyl)-8-azabicyclo[3.2.1]octane-8-carboxylate (**3.45**, 0.380 g, 0.981 mmol) in THF (4 mL) at 0 °C was treated with 2 M aqueous LiOH (0.98 mL, 1.96 mmol) and the reaction was stirred at 0 °C for 30 min and warmed to rt. A precipitate was noted after addition of the LiOH. The reaction was stirred at rt for 24 h where analysis by TLC (EtOAc) indicated the SM remained. The reaction was heated to 50 °C for 5 h where analysis by TLC (EtOAc) indicated the SM was consumed. The THF was removed under reduced pressure and the aqueous layer was acidified with 1 M aqueous HCl. The aqueous layer was extracted with EtOAc (3 x 20 mL). The combined organic layers were dried (MgSO_4), filtered and concentrated under reduced pressure to give 3-(2-((1*SR*,3*RS*,5*RS*)-8-(*tert*-butoxycarbonyl)-8-azabicyclo[3.2.1]octan-3-yl)phenyl)propanoic acid (0.289 g, 0.804 mmol) as a colorless solid.

A solution of 3-(2-((1*SR*,3*RS*,5*RS*)-8-(*tert*-butoxycarbonyl)-8-azabicyclo[3.2.1]octan-3-yl)phenyl)propanoic acid (0.100 g, 0.278 mmol), HATU (0.127 g, 0.334 mmol), and HOAt (0.0464 g, 0.334 mmol) in DMF (1 mL) at 0 °C was treated with DIPEA (0.19 mL, 1.11 mmol). (The pale yellow solution became dark yellow). After 30 min at 0 °C, a solution of methyl 4-(2-

(2-aminoethoxy)ethoxy)benzoate (**3.53**, 0.0732 g, 0.306 mmol) in DMF (0.4 mL) was added and the reaction mixture was stirred at 0 °C for 1 h, rt for 21 h, diluted with EtOAc (50 mL) and satd. aqueous NaHCO₃ (2 x) and brine, dried (Na₂SO₄) and concentrated under reduced pressure. The crude residue was purified by chromatography on SiO₂ (100% EtOAc) to give **3.54** (0.150 g, 0.259 mmol, 76% (2 steps)) as a colorless foam: IR (CH₂Cl₂) 2969, 1711, 1655, 1603, 1411, 1253, 1167, 1107, 841, 770 cm⁻¹; ¹H NMR (600 MHz, DMSO-d₆) δ 7.91-7.86 (m, 3 H), 7.27 (d, *J* = 7.8 Hz, 1 H), 7.14 (dt, *J* = 7.8, 1.8 Hz, 1 H), 7.08-7.04 (m, 4 H), 4.16 (t, *J* = 4.5 Hz, 2 H), 4.12-4.10 (m, 2 H), 3.81 (s, 3 H), 3.72 (t, *J* = 4.5 Hz, 2 H), 3.44 (t, *J* = 5.9 Hz, 2 H), 3.22-3.17 (m, 2 H), 2.79-2.76 (m, 2 H), 2.67 (tt, *J* = 12.6, 6.5 Hz, 1 H), 2.31-2.26 (m, 4 H), 2.00-1.93 (m, 2 H), 1.72-1.66 (m, 2 H), 1.42 (s, 9 H), 1.37-1.31 (m, 2 H); ¹³C NMR (150 MHz, DMSO-d₆) δ 171.0, 165.8, 162.3, 153.9, 142.2, 138.5, 131.2, 128.8, 127.6, 126.3, 125.7, 121.9, 114.5, 78.3, 69.3, 68.5, 67.4, 51.8, 51.0, 50.3, 38.5, 37.8, 36.6, 31.9, 31.2, 30.7, 28.7, 28.2, 27.6; HRMS (ESI) *m/z* calcd for C₃₃H₄₅O₇N₂ ([M+H]⁺) 581.3221, found 581.3222.



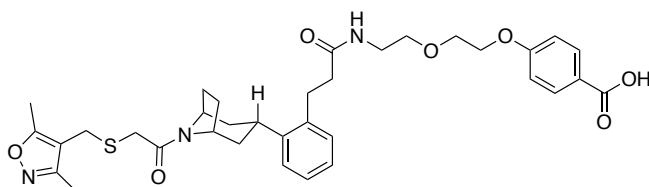
3.55

Methyl 4-(2-(2-(3-(2-((1*S*,3*R*,5*R*)-8-(2-(((3,5-dimethylisoxazol-4-yl)methyl)thio)acetyl)-8-azabicyclo[3.2.1]octan-3-yl)phenyl)propanamido)ethoxy)ethoxy)benzoate (3.55**).** A solution of (1*S*,3*R*,5*R*)-tert-butyl 3-(2-(3-((2-(2-(4-(methoxycarbonyl)phenoxy)ethoxy)ethyl)amino)-3-oxopropyl)phenyl)-8-azabicyclo[3.2.1]octane-8-carboxylate (**3.54**, 0.230 g, 0.396 mmol) in THF (4 mL) was cooled to 0 °C, treated with 4M HCl in dioxane (3.0 mL, 30 eq) and stirred at 0 °C and slowly warmed to rt

for 12 h. The solution was concentrated under reduced pressure and the residue was sonicated with dry THF (4 x 10 mL) and concentrated under reduced pressure each time and dried under high vacuum to give methyl 4-(2-(2-(3-(2-((1SR,3RS,5RS)-8-azabicyclo[3.2.1]octan-3-yl)phenyl)propanamido)ethoxy)ethoxy)benzoate hydrochloride (0.202 g, 0.419 mmol) as a colorless solid that was taken on to the coupling reaction with no further purification.

A solution of 2-(((3,5-dimethylisoxazol-4-yl)methyl)thio)acetic acid (**3.26**, 0.0620 g, 0.308 mmol), HATU (0.141 g, 0.370 mmol), and HOAt (0.0513 g, 0.370 mmol) in DMF (1.5 mL) at 0 °C was treated with DIPEA (214 μ L, 1.23 mmol) and stirred for 20 min at 0 °C where a deep orange solution developed, and treated with a solution of methyl 4-(2-(2-(3-(2-((1SR,3RS,5RS)-8-azabicyclo[3.2.1]octan-3-yl)phenyl)propanamido)ethoxy)ethoxy)benzoate hydrochloride (0.191 g, 0.370 mmol) in DMF (1.6 mL) was added and the reaction was stirred at 0 °C for 30 min and warmed to rt for 12 h. The reaction was diluted with EtOAc (50 mL) and washed with satd. aqueous NaHCO₃ (2 x 20 mL), followed by brine (20 mL), dried (Na₂SO₄), filtered, and concentrated under reduced pressure. The crude material was purified by chromatography on SiO₂ (2% MeOH/EtOAc w/ 2% Et₃N) to give **3.55** (0.122 g, 0.183 mmol, 60% (2 steps)) as a colorless foam: IR (CH₂Cl₂) 2947, 1709, 1603, 1433, 1253, 1167, 1113, 887 cm⁻¹; ¹H NMR (500 MHz, CDCl₃) δ 7.94 (dt, J = 8.8, 2.5 Hz, 2 H), 7.16-7.13 (m, 2 H), 7.10-7.06 (m, 2 H), 6.89 (dt, J = 8.8, 2.5 Hz, 2 H), 6.22 (t, J = 5.5 Hz, 1 H), 4.65 (t, J = 8.0 Hz, 1 H), 4.13 (t, J = 8.0 Hz, 1 H), 4.11 (t, J = 4.5 Hz, 2 H), 3.84 (s, 3 H), 3.77-3.72 (m, 3 H), 3.59-3.54 (m, 3 H), 3.46-3.35 (m, 2 H), 3.19 (d, J = 13.8 Hz, 1 H), 3.06 (d, J = 13.8 Hz, 1 H), 2.97-2.89 (m, 2 H), 2.86 (dt, J = 12.7, 6.1 Hz, 1 H), 2.46-2.39 (m, 5 H), 2.33 (td, J = 8.0, 2.7 Hz, 2 H), 2.26 (s, 3 H), 2.13 (ddt, J = 11.5, 6.9, 4.4 Hz, 1 H), 2.03 (ddt, J = 11.5, 7.6, 3.5 Hz, 1 H), 1.80-1.69 (m, 2 H), 1.44 (td, J = 13.0, 3.5 Hz, 2 H); ¹³C NMR (125 MHz, CDCl₃) δ 172.0, 166.9, 166.8, 166.6,

162.3, 159.7, 141.4, 138.5, 131.5, 129.4, 127.3, 126.6, 126.2, 122.7, 114.0, 109.9, 69.9, 69.1, 67.3, 53.2, 51.7, 49.5, 40.0, 39.1, 38.9, 38.3, 32.6, 32.0, 31.0, 29.5, 28.9, 23.7, 10.9, 10.0; HRMS (ESI) m/z calcd for $C_{36}H_{46}O_7N_3S$ ($[M+H]^+$) 664.3051, found 664.3050.



3.56

4-(2-(2-(3-(2-((1SR,3RS,5RS)-8-(2-(((3,5-Dimethylisoxazol-4-yl)methyl)thio)acetyl)-8-azabicyclo[3.2.1]octan-3-yl)phenyl)propanamido)ethoxy)ethoxy)benzoic acid (3.56). To a solution of methyl 4-(2-(2-(3-(2-((1SR,3RS,5RS)-8-(2-(((3,5-dimethylisoxazol-4-yl)methyl)thio)acetyl)-8-azabicyclo[3.2.1]octan-3-yl)phenyl)propanamido)ethoxy)ethoxy)benzoate (**3.55**, 0.0616 g, 0.0928 mmol) in THF (0.5 mL) and MeOH (0.5 mL) was treated with 2 M aqueous LiOH 4(0.46 mL) and the solution was stirred at rt for 13 h where analysis by TLC (100% EtOAc) indicated the starting material still remained. By TLC there was still a small amount of remaining SM but the reaction was diluted with H₂O (1 mL), washed with Et₂O (2 x 5 mL), and the aqueous layer was acidified to pH 2 with 1 M aqueous HCl at 0 °C. The aqueous layer was extracted with EtOAc (3 x 6 mL). The combined organic layers were dried (MgSO₄), filtered and concentrated under reduced pressure to give **3.56** (0.0367 g, 0.0565 mmol, 61%) as a colorless foam: IR (CH₂Cl₂) 2949, 1702, 1603, 1452, 1249, 1167, 1122, 734 cm⁻¹; ¹H NMR (600 MHz, CDCl₃) δ 7.98 (d, J = 8.7 Hz, 2 H), 7.18-7.09 (m, 4 H), 6.86 (d, J = 8.7 Hz, 2 H), 6.44 (s, 1 H), 4.70 (t, J = 7.5 Hz, 1 H), 4.16 (t, J = 7.5 Hz, 1 H), 4.07 (t, J = 4.4 Hz, 2 H), 3.75 (t, J = 4.4 Hz, 2 H), 3.56 (t, J = 4.4 Hz, 3 H), 3.50-3.47

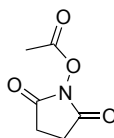
(m, 1 H), 3.37-3.34 (m, 1 H), 3.23-3.20 (m, 1 H), 3.04-2.89 (m, 3 H), 2.50-2.41 (m, 5 H), 2.37-2.32 (m, 2 H), 2.29 (s, 3 H), 2.18-2.06 (m, 2 H), 1.82-1.74 (m, 2 H), 1.51 (t, $J = 12.8$ Hz, 1 H), 1.45 (t, $J = 12.8$ Hz, 1 H); ^{13}C NMR (150 MHz, CDCl_3) δ 172.3, 169.7, 167.2, 162.8, 141.5, 138.8, 132.1, 129.8, 127.4, 126.7, 126.4, 122.4, 114.2, 70.0, 69.3, 67.3, 40.3, 39.2, 39.1, 38.3, 32.7, 31.7, 31.2, 29.5, 29.1, 23.7, 11.1, 10.2; HRMS (ESI) m/z calcd for $\text{C}_{35}\text{H}_{44}\text{O}_7\text{N}_3\text{S}$ ($[\text{M}+\text{H}]^+$) 650.2894, found 650.2888.

Bead conjugation Conjugation of 3.56 to the Carboxylink Agarose beads

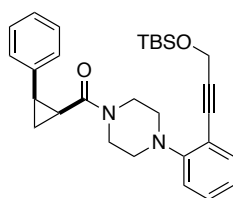
Activation of the carboxylic acid as the NHS ester: A solution of 4-(2-(2-(3-(2-((1R,3s,5S)-8-(2-(((3,5-dimethylisoxazol-4-yl)methyl)thio)acetyl)-8-azabicyclo[3.2.1]octan-3-yl)phenyl)propanamido)ethoxy)ethoxy)benzoic acid (**3.56**, 0.0120 g, 0.0185 mmol) in dry DMF (0.2 mL) was treated with *N*-hydroxysuccinimide (0.0657 g, 0.0554 mmol) followed by EDCI (0.0108 g, 0.0554 mmol). The resulting solution was stirred at rt under an argon atmosphere for 16 h. The reaction was diluted with dry DMF (0.5 mL) to give the **activated ester solution**.

Conjugation reaction: A short (1 cm diameter) column fitted with a magnetic stir bar and a drain cap was loaded suspension of Carboxylink Coupling Gel (1.0 mL) and washed with DMF (5 x 4 mL) allowing the solvent to drain after each addition of DMF. The washed gel was treated with the **activated ester solution** and gently stirred at rt under Ar for 48 h. The beads were transferred to a 1.5 mL eppendorf tube and placed on the little shot rotator for 2 d at rt. The suspension was centrifuged and the DMF was removed via pipet, the pellet was suspended in DMF (1 mL) and centrifuged (5 min in speed vac centrifuge). This washing was repeated 5 times with DMF. The gel was further washed with PBS buffer (3 x 1 mL), and (HPLC grade) water (3 x 1 mL), respectively. Similar method to the DMF washing. The gel was suspended with 1.0 mL

of 0.05% wt. sodium azide solution in HPLC water and stored at 4 °C to give the **3.57** conjugated beads.



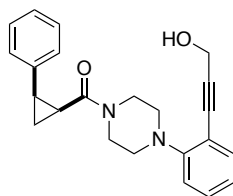
2,5-dioxopyrrolidin-1-yl acetate. (*N*-acetoxysuccinimide).⁴⁸⁹ A solution of *N*-Hydroxysuccinimide (1.00 g, 8.69 mmol) in acetic anhydride (2.5 mL, 26.1 mmol) was stirred at rt for 18 h. A white precipitate had formed and the reaction was cooled to 0 °C and the colorless solid was collected by vacuum filtration and washed with an excess of hexanes to give *N*-acetoxysuccinimide (0.793 g, 5.04 mmol, 58%) as a colorless solid: ¹H NMR (300 MHz, CDCl₃) δ 2.81 (s, 4 H), 2.32 (bd, *J* = 0.9 Hz, 3 H); ¹³C NMR (75 MHz, CDCl₃) δ 169.1, 165.5, 25.5, 17.5.



3.60

(4-(2-(3-((*tert*-Butyldimethylsilyl)oxy)prop-1-yn-1-yl)phenyl)piperazin-1-yl)((1*RS*,2*SR*)-2-phenylcyclopropyl)methanone (3.60). A solution of (1*SR*,2*RS*)-2-phenylcyclopropanecarboxylic acid (**3.11**, 0.0260 g, 0.160 mmol) and HATU (0.0914 g, 0.240 mmol) in CH₂Cl₂ (1 mL), was cooled to 0 °C and treated with DIPEA (83 μL, 0.481 mmol) and warmed to rt over 45 min. The solution was cooled to 0 °C and treated with a solution of 1-(2-(3-((*tert*-butyldimethylsilyl)oxy)prop-1-yn-1-yl)phenyl)piperazine (**3.59**, 0.0583 g, 0.176 mmol) in CH₂Cl₂ (0.5 mL) and stirred at rt 16 h, diluted with H₂O, washed with EtOAc (2 × 10 mL). The combined organic layers were washed with 1 M aqueous NaHSO₄, satd. aqueous NaHCO₃, dried

(Na₂SO₄), and concentrated under reduced pressure. The crude residue was purified twice by automated chromatography SiO₂ column (4g column, liquid load CH₂Cl₂, gradient hexanes/EtOAc, 6:1 to hexanes/EtOAc, 2.5:1) to give **3.60** (0.00763 g, 0.0161 mmol, 10%) as a pale yellow oil: IR (CH₂Cl₂) 2951, 2855, 1640, 1459, 1370, 1251, 1226, 1079, 1027, 833, 777 cm⁻¹; ¹H NMR (500 MHz, CDCl₃) δ 7.36 (dd, *J* = 15.0, 1.5 Hz, 1 H), 7.24-7.19 (m, 3 H), 7.15-7.13 (m, 1 H), 6.92 (dt, *J* = 7.5, 1.0 Hz, 1 H), 4.55 (s, 2 H), 3.93 (bd, *J* = 13.0 Hz, 1 H), 3.76 (app d, *J* = 13.0 Hz, 1 H), 3.60 (ddd, *J* = 12.3, 9.0, 2.5 Hz, 1 H), 3.30 (ddd, *J* = 12.3, 9.0, 3.0 Hz, 1 H), 3.12-3.09 (m, 2 H), 2.47-2.40 (m, 2 H), 2.20-2.13 (m, 2 H), 1.85 (dd, *J* = 12.5, 6 Hz, 1 H), 1.35 (ddd, *J* = 14.0, 8.5, 5.5 Hz, 1 H), 0.93 (s, 9 H), 0.14 (s, 6 H); ¹³C NMR (125 MHz, CDCl₃) δ 167.3, 153.6, 137.6, 133.9, 129.3, 128.1, 127.4, 126.4, 122.1, 117.7, 116.7, 93.2, 82.9, 52.4, 51.4, 50.9, 45.4, 42.0, 25.9, 24.4, 24.1, 18.3, 10.6, -5.1; HRMS (ESI) *m/z* calcd for C₂₉H₃₉SiO₂N₂ ([M+H]⁺) 475.2775, found 475.2769.



(4-(2-(3-Hydroxyprop-1-yn-1-yl)phenyl)piperazin-1-yl)((1R,2SR)-2-phenylcyclopropyl)methanone (3.58). A solution of (4-(2-(3-((tert-butyltrimethylsilyl)oxy)prop-1-yn-1-yl)phenyl)piperazin-1-yl)((1SR,2RS)-2-phenylcyclopropyl)methanone (0.0200 g, 0.0421 mmol) in TBAF (1 M solution in THF) (126 μL, 0.126 mmol) was stirred at rt for 30 min where analysis by TLC (1:1 hexanes/EtOAc) indicated the starting material had been consumed. The reaction was diluted with EtOAc and washed with satd. aqueous NH₄Cl, dried (Na₂SO₄), filtered and concentrated under reduced pressure. The crude residue was purified by chromatography on SiO₂ (1:2, hexanes/EtOAc) to

give the product (0.00784 g, 0.0218 mmol, 52%) as a colorless solid: Mp 121.1-124.3 °C; IR (EtOAc) 3383, 2904, 2820, 1616, 1486, 1437, 1226, 1027, 751, 697 cm⁻¹; ¹H NMR (400 MHz, CDCl₃) δ 7.37 (dd, *J* = 7.6, 1.2 Hz, 1 H), 7.25-7.21 (m, 4 H), 7.16-7.13 (m, 3 H), 6.93 (dt, *J* = 7.6, 1.2 Hz, 1 H), 6.68 (d, *J* = 7.6 Hz, 1 H), 4.51 (d, *J* = 6.0 Hz, 2 H), 3.93 (app d, *J* = 13.0 Hz, 1 H), 3.74 (app d, *J* = 13.0 Hz, 1 H), 3.64-3.61 (m, 1 H), 3.33-3.30 (m, 1 H), 3.11-3.07 (m, 2 H), 2.48-2.41 (m, 2 H), 2.21-2.15 (m, 2 H), 1.84 (q, *J* = 6.2 Hz, 1 H), 1.78 (t, *J* = 6.2 Hz, 1 H), 1.35 (ddd, *J* = 14.0, 8.4, 5.2 Hz, 1 H); ¹³C NMR (100 MHz, CDCl₃) δ 167.4, 153.6, 137.6, 133.9, 129.6, 128.1, 127.3, 126.4, 122.2, 117.8, 116.3, 92.6, 83.9, 51.8, 51.4, 50.9, 45.4, 42.0, 24.5, 24.1, 10.6; HRMS (ESI) *m/z* calcd for C₂₃H₂₅O₂N₂ ([M+H]⁺) 361.1911, found 361.1908.

5.5 CHAPTER 4 EXPERIMENTAL PART

5.5.1 First Approach

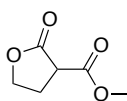


4.99

(4-Bromobut-1-yn-1-yl)trimethylsilane (4.99).⁴⁵⁹⁻⁴⁶¹ A solution of 3-butyn-1-ol (**4.98**, 5.4 mL, 71.3 mmol) in dry THF (200 mL) cooled to -78 °C was treated dropwise with *n*-BuLi (63.0 mL, 2.5M, 157 mmol). Upon the completion of addition the reaction mixture became cloudy. Stirring was continued at -78 °C for 1 h, when freshly distilled TMSCl (27.4 mL, 214 mmol) was added dropwise. The reaction was stirred at -78 for another 15 min. The reaction mixture was allowed to warm to rt and stirred for another 1.5 h when 2 M aqueous HCl (25 mL) was added. The aqueous layer was extracted with EtOAc. The organic layers were combined,

washed with satd. aqueous NaHCO₃, H₂O, brine, dried (Na₂SO₄), filtered and concentrated in vacuo to provide crude 4-(trimethylsilyl)but-3-yn-1-ol (10.2 g, 71.7 mmol) as a clear oil that was taken on to the next step with no further purification.

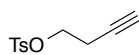
A solution of the crude 4-(trimethylsilyl)but-3-yn-1-ol (10.2 g, 71.7 mmol) in dry CH₂Cl₂ (210 mL) cooled to -30 °C was treated with CBr₄ (30.0 g, 90.3 mmol) in one portion. After stirring for 15 min a solution of PPh₃ (19.7 g, 75.3 mmol) in CH₂Cl₂ (75 mL) was added by cannula. The solution was stirred for 1.5 h at -30 °C and for another 1 h at 0 °C. The crude reaction mixture was filtered through small plug of silica gel, washing with hexanes, and was concentrated until 1/3 of the original volume was left in the flask. Cold hexanes were added to the solution and the solids were suspended, and filtered through Celite and the cake washed with cold hexanes. The filtrate was concentrated under reduced pressure (rotovap bath at 0 °C) and purified by chromatography on SiO₂ (100% hexanes) to give **4.99** (9.86 g, 48.1 mmol, 67% (2 steps)) as a colorless liquid: ¹H NMR (300 MHz, CDCl₃) δ 3.42 (t, *J* = 7.5 Hz, 2 H), 2.77 (t, *J* = 7.5 Hz, 2 H), 0.16 (s, 9 H); ¹³C NMR (75 MHz, CDCl₃) δ 103.2, 87.0, 29.1, 24.3, -0.1.



4.103

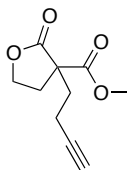
Methyl 2-oxotetrahydrofuran-3-carboxylate (4.103).⁴⁶² A solution of LHMDS (1 M in hexanes, 23.2 mL, 23.2 mmol) in THF (15 mL) was cooled to -78 °C and treated dropwise over 10 min with a solution of γ -butyrolactone (**4.100**, 1.00 g, 11.6 mmol) in THF (12 mL). After stirring for 10 min at -78 °C, the reaction was treated with dimethyl carbonate (1.04 mL, 12.2 mmol). The mixture was allowed to slowly warm to room temperature and stirring was continued for 8 h, poured onto a mixture of conc. HCl (5 mL) and ice (5 g), extracted with EtOAc. The organic layers were combined washed with brine, dried (Na₂SO₄), filtered and

concentrated under reduced pressure to give **4.103** (1.63 g, 10.8 mmol, 93%) as light brown oil. The residue was used in subsequent reactions without further purification: ^1H NMR (300 MHz, CDCl_3) δ 4.41-4.27 (m, 1 H), 4.25-4.19 (m, 1 H), 3.69 (s, 3 H), 3.50 (dt, $J = 8.1, 2.4$ Hz, 1 H) 2.60-2.38 (m, 2 H); ^{13}C NMR (75 MHz, CDCl_3) δ 172.2, 168.1, 67.2, 52.7, 45.5, 26.1.



4.104

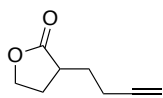
But-3-yn-1-yl 4-methylbenzenesulfonate (4.104).⁴⁹⁰ A solution of 3-butyn-1-ol (5.00 g, 71.3 mmol) in CH_2Cl_2 (71 mL) cooled to 0°C was treated with Et_3N (10.0 mL, 71.3 mmol) and TsCl (12.4 g, 64.9 mmol). The reaction was warmed to rt and stirred for 11 h, diluted with H_2O (100 mL), and the aqueous layer was extracted with CH_2Cl_2 (3×100 mL). The combined organic layers were washed with brine (200 mL), dried (Na_2SO_4) and concentrated under reduced pressure to give **4.104** (14.3 g, 63.9 mmol, 99%) as a light brown oil: ^1H NMR (300 MHz, CDCl_3) δ 7.76 (d, $J = 8.4$ Hz, 2 H), 7.31 (d, $J = 8.4$ Hz, 2 H), 4.05 (dt, $J = 6.9, 1.2$ Hz, 2 H), 2.53-2.48 (m, 2 H), 2.40 (s, 3 H), 1.95 (t, $J = 2.4$ Hz, 2 H); ^{13}C NMR (75 MHz, CDCl_3) δ 144.9, 132.6, 129.7, 127.7, 78.3, 70.6, 67.3, 21.4, 19.2.



4.105

Methyl 3-(but-3-yn-1-yl)-2-oxotetrahydrofuran-3-carboxylate (4.105). A solution of methyl 2-oxotetrahydrofuran-3-carboxylate (**4.103**, 0.100 g, 0.659 mmol) in dry DMF (1.5 mL) at rt was added K_2CO_3 (0.228 g, 1.64 mmol), and NaI (0.247 g, 1.65 mmol). The mixture was stirred for 15 min and a solution of but-3-yn-1-yl 4-methylbenzenesulfonate (**4.104**, 0.177 g,

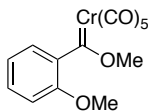
0.791 mmol) in DMF (0.5 mL) was added. After the mixture was stirred at rt for 16 h, and heated to 60 °C for 24 h, cooled to rt, diluted with H₂O and extracted with Et₂O (3 x 20 mL) The organic layers were combined washed with H₂O, brine, dried (MgSO₄), and concentrated under reduced pressure. The residue was purified by automated chromatography on SiO₂ (4g column, liquid load CH₂Cl₂, gradient 100% hexanes to 60% EtOAc/hexanes) to give **4.105** (0.0383 g, 0.195 mmol, 30%) as a colorless oil: IR (CH₂Cl₂) 3286, 2924, 1772, 1732, 1436, 1378, 1213, 1167, 1029 cm⁻¹ ¹H NMR (400 MHz, CDCl₃) δ 4.37-4.33 (m, 2 H), 3.77 (s, 3 H), 2.81-2.75 (m, 1 H), 2.41-2.23 (m, 4 H), 2.08-1.98 (m 1 H), 1.98 (t, *J* = 1.6 Hz, 1 H); ¹³C NMR (100 MHz, CDCl₃) δ 174.1, 169.4, 82.4, 69.5, 66.2, 53.5, 53.2, 32.6, 31.8, 14.4; HRMS (ESI) *m/z* calcd for C₁₀H₁₃O₄ ([M+H]⁺) 197.0808, found 197.0808.



4.97

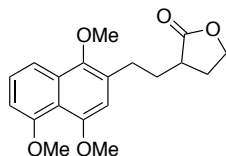
3-(But-3-yn-1-yl)dihydrofuran-2(3H)-one (4.97). A solution of methyl 3-(but-3-yn-1-yl)-2-oxotetrahydrofuran-3-carboxylate (**4.105**, 0.100 g, 0.510 mmol) in wet DMSO (100 uL) was treated with LiCl (0.0432 g, 1.02 mmol) and the mixture was heated to 150 °C in a sandbath for 2.5 h, cooled to rt, diluted with H₂O the extracted with EtOAc (3 x 20 mL). The organic layers were combined washed with H₂O (3 x 20 mL), brine, dried (Na₂SO₄), and concentrated. The crude residue was purified by chromatography on SiO₂ (hexanes/EtOAc, 1:1) to give **4.97** (0.0484 g, 0.350 mmol, 69%) as a clear oil: IR (CH₂Cl₂) 3286, 2919, 1764, 1455, 1377, 1204, 1154, 1024 cm⁻¹; ¹H NMR (400 MHz, CDCl₃) δ 4.33 (td, *J* = 8.8, 2.5 Hz, 1 H), 4.17 (ddd, *J* = 10.0, 9.2, 6.4 Hz, 1 H), 2.70 (dtd, *J* = 10.8, 8.8, 5.2 Hz, 1 H), 2.48-2.37 (m, 2 H), 2.28 (m, *J* = 6.6, 2.6 Hz, 1 H), 2.08 (dddd, *J* = 13.6, 8.0, 6.8, 5.6 Hz, 1 H), 1.99-1.88 (m, 2 H); ¹³C NMR (100

MHz, CDCl₃) δ 178.8, 82.6, 69.4, 66.4, 38.0, 28.9, 28.5, 16.4; HRMS (ESI) m/z calcd for C₈H₁₁O₂ ([M+H]⁺) 139.0754, found 139.0754.



4.80

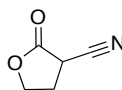
Pentacarbonyl(methoxy(2-methoxyphenyl)methylene)chromium (4.80).⁴⁹¹ A solution of 2-bromoanisole (**4.106**, 3.00 mL, 23.6 mmol) in Et₂O (60 mL) was treated at -50 °C with a solution of *n*-BuLi (2.5 M in hexanes, 10.4 mL, 25.9 mmol) and stirred at -50 °C for 30 min and then at 0 °C for another 30 min. The resulting solution was cannulated to a cold (-20 °C) suspension of chromium hexacarbonyl (6.29 g, 28.3 mmol) in Et₂O (60 mL). The reaction mixture (brown at first and then yellow suspension) was allowed to warm to rt and stirred at rt for 3 h and concentrated under reduced pressure. The residue was dissolved in H₂O, filtered through Celite that was washed (H₂O) and then washed with hexanes. The layers were separated and the aqueous layer was added CH₂Cl₂ (100 mL) (in the separatory funnel) and treated with trimethyloxonium tetrafluoroborate (6.18 g, 40.1 mmol) until acidic pH (the mixture turned red right away). The aqueous layer was further extracted with CH₂Cl₂ (3 x 100 mL) until it was no longer red. The combined organic layers were washed with brine, dried (MgSO₄) and concentrated under reduced pressure. The crude residue was purified by column chromatography on SiO₂ (hexanes/EtOAc, 9:1) to give **4.80** (6.63 g, 19.4 mmol, 82%) as red crystals: ¹H NMR (300 MHz, CDCl₃) δ 7.29 (t, J = 7.5 Hz, 1 H), 7.04 (t, J = 7.5 Hz, 1 H), 6.92 (d, J = 8.4 Hz, 1 H), 6.79 (d, J = 7.5 Hz, 1 H), 4.16 (brs, 3 H), 3.83 (s, 3 H). Note: for best purification column must be preequilibrated with 9:1 hexanes/EtOAc.



4.96

3-(2-(1,4,5-Trimethoxynaphthalen-2-yl)ethyl)dihydrofuran-2(3H)-one (4.96). A solution of the chromium carbene (**4.80**, 1.00 g, 2.78 mmol) and 3-(but-3-yn-1-yl)dihydrofuran-2(3H)-one (**4.97**, 0.460 g, 3.33 mmol) in dry deoxygenated THF (55 mL) and stirred at 50 °C for 36 h. After 36 h, Cs₂CO₃ (2.71 g, 8.33 mmol) and MeI (0.53 mL, 8.33 mmol) were added and the resulting suspension was stirred at rt for 24 h, filtered through Celite, washed (CH₂Cl₂), and the filtrate was concentrated under reduced pressure. The crude residue was purified by chromatography on SiO₂ (hexanes/EtOAc, 2:1) to give **4.96** (0.378 g, 1.14 mmol, 41%) as a red orange oil: IR (CH₂Cl₂) 2930, 2837, 1761, 1597, 1581, 1377, 1260, 1126, 1068, 1021, 755 cm⁻¹; ¹H NMR (400 MHz, CDCl₃) δ 7.64 (dd, *J* = 8.4, 0.8 Hz, 1 H), 7.40 (t, *J* = 8.0 Hz, 1 H), 6.85 (d, *J* = 7.2 Hz, 1 H), 6.67 (s, 1 H), 4.33 (dt, *J* = 8.8, 2.4 Hz, 1 H), 4.13 (dt, *J* = 9.6, 6.8 Hz, 1 H), 3.96 (s, 3 H), 3.94 (s, 3 H), 3.84 (s, 3 H), 2.94-2.89 (m, 2 H), 2.57-2.50 (m, 1 H), 2.47-2.40 (m, 1 H), 2.34-2.26 (m, 1 H), 2.03-1.93 (m, 1 H), 1.88-1.81 (m, 1 H); ¹³C NMR (75 MHz) δ 179.4, 157.4, 153.5, 147.2, 131.4, 129.2, 126.7, 117.4, 114.6, 107.8, 106.1, 66.5, 61.8, 56.9, 56.4, 38.7, 31.1, 28.9, 27.4; HRMS (ESI) *m/z* calcd for C₁₉H₂₃O₅ ([M+H]⁺) 331.1540, found 331.1538.

5.5.2 Second Approach



4.110

2-Oxotetrahydrofuran-3-carbonitrile (4.110).⁴⁹²⁻⁴⁹³ A 3L 3-Necked flask was charged with ethyl 2-cyanoacetate (**4.114**, 370 g, 350 mL, 3.27 mol), 1,2-dibromoethane (509 mL, 5.88 mol) and K₂CO₃ (903 g, 6.54 mol), and acetone (1.3 L), the flask was equipped with a thermometer/thermometer adapter, a mechanical string rod with a teflon stir head and a stir rod condenser, and a reflux condenser. The mixture was mechanically stirred for 24 h at 68 °C (internal temp) reflux. The reaction was monitored by ¹HNMR for the disappearance of the SM singlet at 3.44 ppm (CDCl₃, 300 MHz). The reaction mixture was cooled to rt diluted with EtOAc (0.5 L), filtered, washed (EtOAc (3 L)) until the washes became colorless and the combined filtrates were concentrated in vacuo to afford a crude oil. The oil was dissolved in Et₂O (1 L) and H₂O (500 mL). The organic layer was separated and the aqueous layer was further extracted with Et₂O (2 x 500 mL). The organic layers were combined, dried (MgSO₄), filtered through a fritted filter that was washed with Et₂O (200 mL), and concentrated by rotary evaporation (water bath at 50 °C) to give crude **4.115** (461 g, 2.85 mol, (86% pure contaminated with excess dibromoethane) as a orange oil that was taken on with no further purification to the saponification.

A 4 L Erlenmeyer flask containing a solution of ethyl 1-cyanocyclopropanecarboxylate (**4.115**, 300 g, 1.85 mol) in THF (0.9 L) cooled to 0 °C was treated with NaOH (2M aqueous) (1.9 L, 2 eq) in one portion and the solution was stirred for 1 h at 0 °C where analysis by TLC (1:1 hexanes:EtOAc, KMnO₄) indicated that the starting material was consumed. The reaction was acidified at 0 °C with portion-wise addition of 6 M aqueous HCl (620 mL over 10 min) to a pH of 2 and the aqueous layer was extracted portion-wise with EtOAc (2 x (3 x 500 mL)). The organic layers were combined, dried (MgSO₄), filtered and concentrated in vacuo (water bath at 35 °C). The crude residue was concentrated from hexanes (1 L) to afford the product (191 g, 1.55

mol (90% pure)) as an off-white waxy solid. This solid was taken on to the lactone formation with no further purification.

To a 3L 3-necked flask equipped with a thermometer, mechanical stirrer, and condenser connected to a N₂ bubbler was added 1-cyanocyclopropanecarboxylic acid (**4.113**, 191 g, 1.55 mol), triethylammonium bromide (254 g, 1.39 mol) and dry MeCN (2.5 L) and was heated to 85 °C for 24 h where analysis by ¹H NMR indicated that the cyclopropane had been consumed. The reaction was cooled to rt, concentrated under reduced pressure, the residue was suspended in EtOAc (1 L) and filtered, washed with ethyl acetate (4 x 500 mL) and concentrated in vacuo. The crude residue was purified by short path distillation (165 °C) (internal temp 140 °C) to give **4.110** (138 g, 1.25 mol, 60% (3 steps)) as a pale yellow oil: ¹H NMR (300 MHz, CDCl₃) δ 4.54 (ddd, *J* = 9.3, 8.3, 3.3 Hz, 1 H), 4.35 (td, *J* = 9.3, 6.7 Hz, 1 H), 3.72 (t, *J* = 9.3 Hz, 1 H), 2.81-2.57 (m, 2 H); ¹³C NMR (75 MHz, CDCl₃) δ 168.6, 114.8, 67.3, 31.4, 27.6.

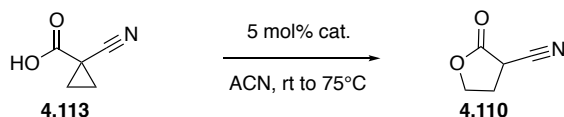
Triethylammonium Hydrobromide. To a 1 L 1-neck flask containing a solution triethylamine (110 mL, 785 mmol) in acetone (0.6 L). The solution was cooled to 0 °C (ice bath) and added HBr (48% aqueous) (89 mL, 785 mmol) dropwise over 30 min. The solution was let stir for 1 h, diluted with Et₂O (400 mL) and the precipitated salt was filtered through a buchner funnel with filterpaper. The solid was washed Et₂O (1.4 L) and dried under vacuum (50 torr) at 45 °C to give the product (62.0 g, 340 mmol, 80%) as a colorless solid: Mp 256-258 (Lit 248)

General procedure for screening conditions in Table 5.2:

A solution 1-cyanocyclopropanecarboxylic acid (**4.110**, 0.0500 g, 0.450 mmol) in dry ACN (3 mL) was added additive (See Table 5.2) (0.0225 mmol, 5 mol%) and stirred at 75 °C for

24, 48, or 72 h and reaction progress was monitored by TLC and ^1H NMR using CDCl_3 as a solvent. Reactions with no product formation after 24 h were not analyzed further.

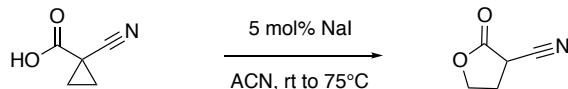
Table 5.2. Screening conditions for lactone formation.



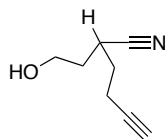
Entry	Conditions and analysis			
	Cat. (5 mol%)	24h 75 °C	48h 75 °C	72h 75 °C
1	NiBr_2^{ab}	12% ^d	30% ^d	50% ^d
2	PtBr_2^{ab}	NR ^d	ND	ND
3	$\text{Rh}_2(\text{OAc})_4^{ab}$	NR ^d	ND	ND
4	$\text{Pd}(\text{PPh}_3)_4^{ab}$	NR ^d	ND	ND
5	I_2^a	NR ^d	ND	ND
6	$\text{Yb}(\text{OTf})_3^a$	NR ^d	ND	ND
7	ZnCl_2^a	NR ^d	ND	ND
8	$\text{Sn}(\text{OTf})_2^a$	NR ^d	ND	ND
9	MgI_2^a	60% ^d	>95% ^d	ND
10	$\text{Ti}(\text{O}i\text{Pr})_4^a$	NR ^d	ND	ND
11	$\text{NiCl}_2 \cdot 6\text{H}_2\text{O}^a$	NR ^d	NR ^d	ND
12	CaCl_2^a	NR ^d	NR ^d	ND
13	CaI_2^a	15% ^d	25% ^d	30% ^d
14	$\text{MnCl}_2 \cdot 4\text{H}_2\text{O}^a$	NR ^d	NR ^d	ND
15	MnBr_2^a	NR ^d	NR ^d	ND
16	Bu_4NBr^a	ND	12%	ND
17	NiI_2^a	ND	76% ^d	ND
18	CuI^a	ND	5% ^d	ND
19	NaI^a	ND	94% ^d	ND
20	NaI^c	ND	77% ^e (42 h)	ND

^a50 mg scale; ^breaction was degassed by sparging with Ar; ^c10 g scale; ^dconversion by ^1H NMR; ^eisolated yield; NR, no reaction; ND, not determined.

Lactonization using sodium iodide:



A solution of 1-cyanocyclopropanecarboxylic acid (**4.113**, 10.0 g, 81.0 mmol) in dry MeCN (162 mL) was treated with NaI (0.607 g, 4.05 mmol) and the reaction was heated to 80 °C for 42 h where analysis by ¹HNMR indicated that the cyclopropane starting material had been consumed. The reaction was concentrated under reduced pressure and the residue was suspended in EtOAc (150 mL), filtered, washed (EtOAc), the filtrates were combined, and concentrated under reduced pressure. The crude residue was purified by short path distillation (150 °C at 0.25 mmHg) (internal temp 120 °C) to give **4.110** (6.97 g, 62.8 mmol, 77%) as an orange oil. NMR data matches what was previously reported for the synthesis of this compound.

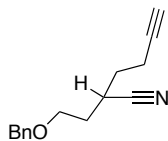


4.118

2-(2-Hydroxyethyl)hex-5-ynenitrile (4.118). A solution of 2-oxotetrahydrofuran-3-carbonitrile (**4.110**, 22.0 g, 198 mmol) in acetone (570 mL) at rt was treated with K₂CO₃ (41.1 g, 297 mmol) and but-3-yn-1-yl 4-methylbenzenesulfonate (**4.104**, 44.4 g, 198 mmol) and the mixture was stirred at 65 °C for 7 days. The reaction was concentrated under reduced pressure and the solid was dissolved in CH₂Cl₂ (300 mL) and H₂O (300 mL) and the layers separated. The aqueous layer was extracted with CH₂Cl₂ (3 x 200 mL). The combined organic layers were dried (MgSO₄), filtered, and concentrated under reduced pressure to give the crude **4.116** (35.4, 86.8 mmol, (40% pure) as a brown oil. This oil was taken on with no further purification.

A solution of 3-(but-3-yn-1-yl)-2-oxotetrahydrofuran-3-carbonitrile (**4.116**, 35.4 g, 86.8 mmol) in THF (30 mL) at rt was treated with aqueous cesium hydroxide (52 mL, 104 mmol, 2 M, 1.2 eq) and stirred at rt for 2 h where analysis by TLC (1:1, hexanes/EtOAc, KMnO₄ Stain) indicated that the SM had been consumed. The reaction was concentrated under reduced pressure (rotovap bath ~25 °C) and washed with EtOAc (3 x 200 mL) and decanted where the washes became colorless. The aqueous layer was concentrated under reduced pressure (Azeotrope with toluene (3 x 100 mL) (rotovap bath at 50 °C) and the product was dried under high vacuum to give crude **4.117** (26.4 g, 84.4 mmol, 97% crude) as a waxy orange solid that was taken on to the decarboxylation with no further purification.

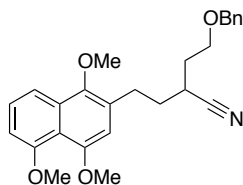
A solution of cesium 2-cyano-2-(2-hydroxyethyl)hex-5-ynoate (**4.117**, 26.4 g, 84.4 mmol) in THF (100 mL) and toluene (50 mL) was heated at 85 °C for 24 h, cooled to rt, and filtered. The solid/oil remaining in the flask was washed with EtOAc (3 x 100 mL) and filtered. The combined filtrates were concentrated under reduced pressure to give **4.118** (7.28 g, 53.1 mmol, 27% (3 steps) as a light orange oil: IR (CH₂Cl₂) 3452, 3288, 2952, 2887, 2239, 1433, 1053, 749 cm⁻¹; ¹H NMR (300 MHz, CDCl₃) δ 3.79-3.69 (m, 2 H), 2.99 (quint, *J* = 7.5 Hz, 1 H), 2.57 (s, 1 H), 2.45-2.28 (m, 2 H), 2.01 (t, *J* = 2.4 Hz, 1 H), 1.88-1.74 (m, 4 H); ¹³C NMR (75 MHz, CDCl₃) δ 121.2, 81.8, 70.0, 59.1, 34.2, 30.7, 27.1, 16.3; HRMS (ESI) *m/z* calcd for C₈H₁₂NO ([M+H]⁺) 138.0913, found 138.0914.



4.119

2-(2-(Benzyloxy)ethyl)hex-5-ynenitrile (4.119). A solution of 2-(2-hydroxyethyl)hex-5-ynenitrile (**4.118**, 7.28 g, 53.1 mmol) in THF (132 mL) at rt was treated with NaH (60%

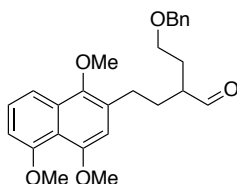
dispersion in mineral oil) (4.67 g, 117 mmol) portion-wise over 5 min with vigorous stirring. After stirring for 20 min the reaction mixture was treated with BnBr (12.7 mL, 106 mmol), stirred at rt for 24 h, diluted with satd. aqueous NH₄Cl, and extracted with EtOAc (3 x 200 mL). The combined organic layers were dried (MgSO₄), filtered, and concentrated under reduced pressure. The crude residue was purified by chromatography on SiO₂ (hexanes/EtOAc, 6:1) to give **4.119** (10.8 g, 47.6 mmol, 90%) as a yellow oil: IR (CHCl₃) 3290, 2889, 2242, 1495, 1452, 1094, 907, 731 cm⁻¹; ¹H NMR (400 MHz, CDCl₃) δ 7.39-7.29 (m, 6 H), 4.54 (d, *J* = 8.0 Hz, 2 H), 3.65 (dd, *J* = 6.3, 5.5 Hz, 2 H), 3.06 (tt, *J* = 8.9, 6.1 Hz, 1 H), 3.06 (tt, *J* = 8.9, 6.1 Hz, 1 H), 2.50-2.35 (m, 2 H), 2.03 (t, *J* = 2.6 Hz, 1 H), 1.95-1.78 (m, 4 H); ¹³C NMR (100 MHz, CDCl₃) δ 137.8, 128.3, 127.7, 127.6, 121.1, 81.8, 73.2, 69.9, 66.7, 32.1, 30.8, 27.5, 16.4; HRMS (ESI) *m/z* calcd for C₁₅H₁₈NO ([M+H]⁺) 228.1383, found 228.1380.



4.120

4-(Benzyloxy)-2-(2-(1,4,5-trimethoxynaphthalen-2-yl)ethyl)butanenitrile (4.120). A solution of pentacarbonyl[methoxy(methoxy-2-phenyl)carben]chromium(IV) (**4.80**, 8.01 g, 21.1 mmol) and 2-(2-(benzyloxy)ethyl)hex-5-ynenitrile (**4.119**, 7.18 g, 31.6 mmol) in dry deoxygenated THF (420 mL) was stirred at 50 °C for 14 h. The reaction was cooled to rt and added dry SiO₂ and concentrated under reduced pressure to a free flowing powder. The crude residue was purified by chromatography on SiO₂ solid load (hexanes/EtOAc, 2:1) to give the naphthol intermediate (8.1 g) that was taken on to the methylation.

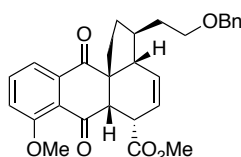
A solution of the naphthol intermediate in dry DMF (42 mL) was treated with MeI (5.3 mL, 84.3 mmol) and K₂CO₃ (11.7 g, 84.3 mmol) and the reaction was stirred at rt 24 h. Analysis by LCMS indicated that the SM appeared to be consumed. The reaction was diluted with H₂O (250 mL) and brine (150 mL) and extracted with Et₂O (3 x 250 mL). The combined organic layers were washed with brine, dried (MgSO₄), filtered, and concentrated under reduced pressure. The crude residue was purified by chromatography on SiO₂ (hexanes/EtOAc, 3:1) to give the product as a red oil. This oil was filtered through basic Al₂O₃ (hexanes/EtOAc, 1:1) to give **4.120** (5.49 g, 13.1 mmol, 62%) as a dark orange oil: IR (CH₂Cl₂) 2930, 2861, 1597, 1581, 1450, 1379, 1260, 1124, 1070, 1003, 734 cm⁻¹; ¹H NMR (500 MHz, CDCl₃) δ 7.65 (dd, *J* = 8.4, 1.0 Hz, 1 H), 7.42 (t, *J* = 8.1 Hz, 1 H), 7.35-7.28 (m, 5 H), 6.86 (dd, *J* = 7.5, 0.5 Hz, 1 H), 6.64 (s, 1 H), 4.50 (q, *J* = 10.2 Hz, 2 H), 3.97 (s, 3 H), 3.94 (s, 3 H), 3.86 (s, 3 H), 3.64 (t, *J* = 5.9 Hz, 2 H), 3.02 (ddd, *J* = 13.5, 9.2, 5.6 Hz, 1 H), 2.93-2.87 (m, 2 H), 2.02-1.91 (m, 4 H); ¹³C NMR (125 MHz, CDCl₃) δ 157.4, 153.5, 147.2, 137.9, 131.5, 128.8, 128.4, 127.7 (2 C), 126.7, 121.9, 117.6, 114.6, 108.0, 106.2, 73.3, 67.0, 61.8, 56.9, 56.4, 33.1, 32.5, 28.5, 28.1; HRMS (ESI) *m/z* calcd for C₂₆H₃₀NO₄ ([M+H]⁺) 420.2169, found 420.2167.



4.121

4-(Benzyloxy)-2-(2-(1,4,5-trimethoxynaphthalen-2-yl)ethyl)butanal (4.121). A solution of 4-(benzyloxy)-2-(2-(1,4,5-trimethoxynaphthalen-2-yl)ethyl)butanenitrile (**4.120**, 0.650 g, 1.55 mmol) in CH₂Cl₂ (7.8 mL) was cooled to -78 °C and treated with DIBAL (1.2 M in toluene, 1.4 mL, 1.70 mmol) over 5 min. The mixture was stirred at -78 °C for 30 min and

allowed to warm to rt over 2.5 h. The reaction was treated with satd. aqueous NH₄Cl solution (~ 1.5 mL) followed by Celite/florisil at 0 °C. The mixture was diluted with CH₂Cl₂ (20 mL), warmed slowly to room temperature, and stirred till all aluminum precipitated (20 min) and dried (MgSO₄). The solid was filtered through a pad of Celite/florisil and washed with CH₂Cl₂ (100 mL) and EtOAc (50 mL), and the combined filtrates were concentrated in vacuo. The crude residue was purified by chromatography on SiO₂ (CH₂Cl₂/EtOAc, 4:1) to give **4.121** (0.384 g, 0.909 mmol, 59%) as a red/brown oil: IR (CH₂Cl₂) 2934, 2841, 1720, 1600, 1583, 1454, 1381, 1263, 1071, 909, 729 cm⁻¹; ¹H NMR (400 MHz, CDCl₃) δ 7.64 (dd, *J* = 8.5, 0.9 Hz, 1 H), 7.40 (t, *J* = 8.1 Hz, 1 H), 7.34-7.27 (m, 5 H), 6.84 (d, *J* = 7.7 Hz, 1 H), 6.62 (s, 1 H), 4.46 (s, 2 H), 3.97 (s, 3 H), 3.93 (s, 3 H), 3.82 (s, 3 H), 3.56-3.48 (m, 2 H), 2.77 (ddd, *J* = 9.0, 6.9, 2.1 Hz, 2 H), 2.58-2.50 (m, 1 H), 2.07 (tt, *J* = 14.4, 7.1 Hz, 2 H), 1.94-1.76 (m, 2 H); ¹³C NMR (100 MHz, CDCl₃) δ 204.5, 157.4, 153.4, 147.0, 138.1, 131.4, 129.9, 128.4, 127.6 (2 C), 126.6, 117.4, 114.6, 108.1, 106.0, 73.1, 67.7, 61.7, 56.9 (2 C), 56.4, 49.0, 29.6, 27.6; HRMS (ESI) *m/z* calcd for C₂₆H₃₁O₅ ([M+H]⁺) 423.2166, found 423.2177.



4.126

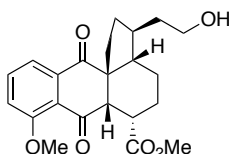
Methyl (3*S*,6*S*,6*aS*,12*aR*)-3-(2-(benzyloxy)ethyl)-8-methoxy-7,12-dioxo-1,2,3,3*a*,6,6*a*,7,12-octahydrocyclopenta[*d*]anthracene-6-carboxylate (4.126). A solution of 4-(benzyloxy)-2-(2-(1,4,5-trimethoxynaphthalen-2-yl)ethyl)butanal (**4.121**, 0.655 g, 1.55 mmol) in dry degassed CH₂Cl₂ (11 mL) at 0 °C was treated with (*E*)-methyl 4-(triphenylphosphoranylidene)but-2-enoate⁴⁷⁰ (**4.122**, 1.55 g, 3.87 mmol) and the reaction was warmed to 50 °C for 24 h. The reaction was concentrated in vacuo and the crude residue was

purified by chromatography on SiO₂ (hexanes/EtOAc, 2:1) to give **4.123** (0.437 g, 0.867 mmol) as a light brown oil that was taken on with no further purification.

A solution of (2*E*,4*E*)-methyl 8-(benzyloxy)-6-(2-(1,4,5-trimethoxynaphthalen-2-yl)ethyl)octa-2,4-dienoate (**4.123**, 0.437 g, 0.866 mmol) in CH₃CN (44 ml) was treated with a solution of CAN (1.14 g, 2.08 mmol) in H₂O (14 ml) at 0 °C and stirred for 10 min at 0 °C. The orange solution was diluted with CH₂Cl₂ (50 ml). The layers were separated and the aqueous layer was extracted with CH₂Cl₂ (1 x 50 ml). The organic layers were combined, dried (Na₂SO₄), and concentrated under reduced pressure. The crude residue was purified by chromatography on SiO₂ (hexanes/EtOAc, 1:1) to give **4.124** (0.387 g, 0.814 mmol) as a orange/brown oil.

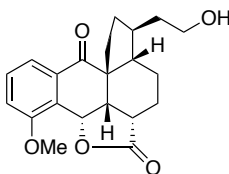
A solution of quinone (**4.124**, 0.387 g, 0.816 mmol) in dry CH₂Cl₂ (27 mL) was treated with BF₃•OEt₂ (0.60 mL, 4.89 mmol) at 0 °C and stirred at rt for 4 h. Analysis by TLC (hexanes/EtOAc, 1:1) the starting material had been consumed. The reaction was diluted with satd. aqueous NaHCO₃ solution and the reaction mixture was extracted with CH₂Cl₂ (3 x 20 mL). The organic layers were combined, dried (Na₂SO₄), and concentrated under reduced pressure. The crude residue was purified by chromatography on SiO₂ (hexanes/EtOAc, 1:2) to give **4.126** (0.181 g, 0.382 mmol, 25% (3 steps)) as a dark brown oil: IR (CH₂Cl₂) 2943, 1732, 1689, 1582, 1273, 1226, 1098, 995, 732, 697 cm⁻¹; ¹H NMR (400 MHz, CDCl₃) δ 7.63-7.56 (m, 2 H), 7.31-7.27 (m, 5 H), 7.21 (dd, *J* = 7.8, 1.7 Hz, 1 H), 6.26 (dt, *J* = 10.1, 2.3 Hz, 1 H), 5.58 (dt, *J* = 10.1, 3.0 Hz, 1 H), 4.51 (s, 2 H), 3.97 (s, 3 H), 3.79-3.74 (m, 1 H), 3.55 (t, *J* = 7.0 Hz, 2 H), 3.39 (d, *J* = 10.4 Hz, 1 H), 3.03 (s, 3 H), 2.78-2.68 (m, 1 H), 2.00-1.87 (m, 3 H), 1.78-1.66 (m, 3 H), 1.59-1.52 (m, 1 H), 1.50-1.42 (m, 1 H); ¹³C NMR (100 MHz, CDCl₃) δ 196.8, 195.4, 171.4, 158.6, 138.4, 136.5, 134.8, 131.1, 128.3, 127.6, 127.5, 122.7, 122.2, 119.1, 116.7, 77.3,

77.0, 76.7, 73.0, 69.4, 59.6, 59.4, 56.4, 52.3, 51.4, 43.5, 36.3, 33.8, 29.3; HRMS (ESI) m/z calcd for $C_{29}H_{31}O_6$ ($[M+H]^+$) 475.2115, found 475.2107.



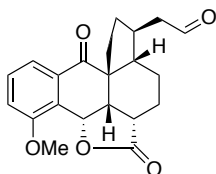
4.130

(3S,6S,6aS,12aR)-Methyl 3-(2-hydroxyethyl)-8-methoxy-7,12-dioxo-1,2,3,3a,4,5,6,6a,7,12-decahydrocyclopenta[d]anthracene-6-carboxylate (4.130). A solution of methyl (3S,6S,6aS,12aR)-3-(2-(benzyloxy)ethyl)-8-methoxy-7,12-dioxo-1,2,3,3a,6,6a,7,12-octahydrocyclopenta[d]anthracene-6-carboxylate (**4.126**, 0.311 g, 0.678 mmol) in THF (14 mL) was added 10% Pd/C (0.0722 g, 0.0678 mmol) and stirred at room temperature under hydrogen atmosphere for 2 d. The reaction mixture was filtered through Celite (eluting with EtOAc) and concentrated under reduced pressure. The crude residue was purified by chromatography on SiO_2 (4:1, EtOAc/hexanes to 100% EtOAc) to give **4.130** (0.217 g, 0.562 mmol, 83%) as a tan foam: IR (CH_2Cl_2) 3543, 2928, 2869, 1732, 1679, 1584, 1465, 1433, 1275, 1228, 1199, 999, 729 cm^{-1} ; 1H NMR (400 MHz, $CDCl_3$) δ 7.64-7.61 (m, 2 H), 7.23 (quint, $J = 4.6$ Hz, 1 H), 3.98 (s, 3 H), 3.73-3.68 (m, 2 H), 3.22-3.19 (m, 1 H), 2.92 (s, 3 H), 2.89 (d, $J = 6.6$ Hz, 1 H), 2.65-2.55 (m, 1 H), 2.23-2.12 (m, 2 H), 1.97-1.89 (m, 1 H), 1.84-1.71 (m, 3 H), 1.60-1.46 (m, 3 H), 1.38-1.27 (m, 2 H), 1.06-1.00 (m, 1 H); ^{13}C NMR (100 MHz, $CDCl_3$) δ 197.0, 196.4, 173.3, 159.2, 137.7, 134.9, 122.0, 119.0, 116.7, 62.3, 60.4, 56.9, 56.5, 55.0, 50.8, 42.2, 39.0, 36.7, 36.2, 28.9, 28.1, 21.1; HRMS (ESI) m/z calcd for $C_{22}H_{27}O_6$ ($[M+H]^+$) 387.1802, found 357.1802.



4.131

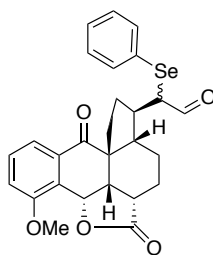
(2a*S*,2a¹*S*,5*S*,7a*R*,12b*S*)-5-(2-Hydroxyethyl)-12-methoxy-2a¹,3,4,4a,5,6,7,12b-octahydro-2*H*-cyclopenta[4,4a]anthra[9,1-*bc*]furan-2,8(2a*H*)-dione (4.131). A solution of ((3*S*,6*S*,6a*S*,12a*R*)-methyl 3-(2-hydroxyethyl)-8-methoxy-7,12-dioxo-1,2,3,3a,6,6a,7,12-octahydrocyclopenta[*d*]anthracene-6-carboxylate (4.130, 0.0630 g, 0.163 mmol) in CH₂Cl₂/MeOH (1:3, 9.3 mL) at -30 °C (cryocool) was treated with NaBH₄ (0.0154 g, 0.408 mmol) and warmed to rt over 3 h. Analysis by TLC (4:1, EtOAc/hexanes) and LCMS indicated that the starting material was consumed. The reaction was diluted with 1 M HCl at 0 °C, warmed to rt, and extracted with CH₂Cl₂ (3 x 20 mL). The combined organic layers were dried (MgSO₄), and concentrated under reduced pressure. The crude residue was purified by chromatography on SiO₂ (4:1, EtOAc/hexanes) to give **4.131** (0.0368 g, 0.103 mmol, 63%) as a colorless foam: IR (CHCl₃) 3536, 2934, 2865, 2252, 1754, 1679, 1588, 1471, 1273, 1182, 1061, 973, 731 cm⁻¹; ¹H NMR (400 MHz, CDCl₃) δ 7.52 (dd, *J* = 8.0, 1.1 Hz, 1 H), 7.46 (t, *J* = 8.0 Hz, 1 H), 7.14 (dd, *J* = 8.0, 1.1 Hz, 1 H), 6.16 (d, *J* = 10.0 Hz, 1 H), 3.92 (s, 3 H), 3.69 (t, *J* = 7.1 Hz, 2 H), 3.26 (t, *J* = 10.0 Hz, 1 H), 2.84 (ddd, *J* = 13.8, 11.3, 5.0 Hz, 1 H), 2.55 (qt, *J* = 10.0, 5.0 Hz, 1 H), 2.04-1.79 (m, 5 H), 1.71-1.66 (m, 1 H), 1.54-1.28 (m, 6 H); ¹³C NMR (100 MHz, CDCl₃) δ 198.9, 178.3, 158.3, 132.5, 130.8, 125.6, 118.9, 115.6, 72.1, 62.1, 56.1, 53.6, 52.2, 45.9, 39.4, 38.7, 37.0, 30.4, 23.7, 21.9; HRMS (ESI) *m/z* calcd for C₂₁H₂₅O₅ ([M+H]⁺) 357.1697, found 357.1693.



4.135

2-((2a*S*,2a¹*S*,5*S*,7a*R*,12b*S*)-12-Methoxy-2,8-dioxo-2a,2a¹,3,4,4a,5,6,7,8,12b-decahydro-2*H*-cyclopenta[4,4a]anthra[9,1-*bc*]furan-5-yl)acetaldehyde (4.135). A solution of

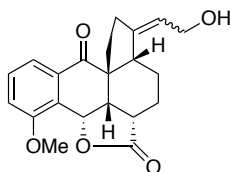
the (2a*S*,2a¹*S*,5*S*,7a*R*,12b*S*)-5-(2-hydroxyethyl)-12-methoxy-2a¹,3,4,4a,5,6,7,12b-octahydro-2*H*-cyclopenta[4,4a]anthra[9,1-*bc*]furan-2,8(2a*H*)-dione (**4.131**, 0.0667 g, 0.187 mmol) in CH₂Cl₂ (10.0 mL) at rt was treated with DMP (0.160 g, 0.374 mmol) and stirred at 0 °C for 2.5 h, diluted with CH₂Cl₂ (50 mL), 1 M Na₂S₂O₃ (25 mL) and satd. aqueous NaHCO₃ (25 mL). The organic layer was separated, and the aqueous layer was washed with CH₂Cl₂ (2 x 20 mL). The combined organic layers were washed with satd. aqueous NaHCO₃ (2 x 25 mL), 1 M Na₂S₂O₃ (25 mL), dried (Na₂SO₄) and concentrated under reduced pressure to give **4.135** (0.0632 g, 0.178 mmol, 95%) as a yellow-orange amorphous solid: IR (CH₂Cl₂) 3059, 2937, 2870, 1760, 1719, 1681, 1588, 1273, 1077, 736 cm⁻¹; ¹H NMR (400 MHz, CDCl₃) δ 9.79 (t, *J* = 2.3 Hz, 1 H), 7.55 (dd, *J* = 8.0, 1.1 Hz, 1 H), 7.48 (t, *J* = 8.0 Hz, 1 H), 7.16 (dd, *J* = 8.0, 1.1 Hz, 1 H), 6.18 (d, *J* = 9.9 Hz, 1 H), 3.93 (s, 3 H), 3.27 (t, *J* = 10.5 Hz, 1 H), 3.05 (dtd, *J* = 14.9, 9.9, 5.3 Hz, 1 H), 2.84 (ddd, *J* = 13.8, 11.3, 5.1 Hz, 1 H), 2.63 (ddd, *J* = 15.8, 5.3, 2.3 Hz, 1 H), 2.35 (ddd, *J* = 15.8, 8.8, 2.3 Hz, 1 H), 2.12-1.99 (m, 2 H), 1.93-1.81 (m, 2 H), 1.77-1.70 (m, 1 H), 1.51-1.33 (m, 4 H); ¹³C NMR (100 MHz, CDCl₃) δ 202.2, 198.7, 178.1, 158.4, 132.4, 131.0, 125.6, 119.0, 115.8, 72.0, 56.1, 53.5, 51.6, 50.1, 45.8, 39.3, 37.0, 36.5, 30.2, 23.6, 21.5; HRMS (ESI) *m/z* calcd for C₂₁H₂₃O₅ ([M+H]⁺) 355.1540, found 355.1539.



4.136

2-((2a*S*,2a¹*S*,5*R*,7a*R*,12b*S*)-12-Methoxy-2,8-dioxo-2a,2a¹,3,4,4a,5,6,7,8,12b-decahydro-2*H*-cyclopenta[4,4a]anthra[9,1-*bc*]furan-5-yl)-2-(phenylselanyl)acetaldehyde

(4.136). A solution of 2-((2a*S*,2a1*S*,4a*S*,5*S*,7a*R*,12b*S*)-12-methoxy-2,8-dioxo-2a,2a1,3,4,4a,5,6,7,8,12b-decahydro-2H-cyclopenta[4,4a]anthra[9,1-*bc*]furan-5-yl)acetaldehyde (**4.135**, 0.0632 g, 0.178 mmol) and *N*-(phenylseleno)phthalimide (0.0719 g, 0.214 mmol) in anhydrous CH₂Cl₂ (1.8 mL) at rt was treated with L-prolinamide (0.0010 g, 0.00892 mmol). After 2 h, analysis by TLC (2:1, EtOAc/hexanes) indicated the starting material was consumed. H₂O (5 mL) was added and the reaction was extracted with CH₂Cl₂ (3 × 10 mL). The combined organic layers were dried (Na₂SO₄), and concentrated under reduced pressure. The crude residue was purified by chromatography on SiO₂ (hexanes/EtOAc, 1:1) to give **4.136** (0.0650 g, 0.128 mmol, 72%) as a colorless foam as a 4:1 mixture of diastereomers (by ¹H NMR): IR (CH₂Cl₂) 3374, 3070, 2934, 2867, 1758, 1702, 1588, 1471, 1273, 1202, 1014, 979, 738 cm⁻¹; Characteristic ¹H NMR peaks for major diastereomer ¹H NMR (400 MHz, CDCl₃) δ 9.44 (d, *J* = 5.2 Hz, 1 H), 7.56-7.53 (m, 3 H), 7.49 (t, *J* = 8.0 Hz, 1 H), 7.34-7.29 (m, 4 H), 7.16 (dd, *J* = 8.0, 1.0 Hz, 1 H), 6.19 (d, *J* = 9.9 Hz, 1 H), 3.94 (s, 3 H), 3.62 (dd, *J* = 8.3, 5.2 Hz, 1 H), 3.30 (t, *J* = 10.6 Hz, 1 H), 3.11-3.03 (m, 1 H), 2.81 (ddd, *J* = 14.1, 11.4, 5.2 Hz, 1 H), 2.16-1.94 (m, 3 H), 1.87-1.69 (m, 6 H), 1.62-1.56 (m, 2 H), 1.36-1.24 (m, 2 H); Characteristic peaks for major diastereomer ¹³C NMR (100 MHz, CDCl₃) δ 198.4, 192.8, 178.0, 177.9, 158.4, 132.0, 131.0, 129.5, 129.4, 128.7, 127.2, 125.6, 119.0, 115.9, 72.0, 61.3, 54.6, 54.1, 45.6, 40.6, 39.1, 29.2, 23.5, 22.0; HRMS (ESI) *m/z* calcd for C₂₇H₂₇O₅Se ([M+H]⁺) 511.1018, found 511.1019.

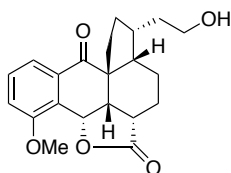


4.138

(2a*S*,2a¹*S*,7a*R*,12b*S*)-5-(2-Hydroxyethylidene)-12-methoxy-2a¹,3,4,4a,5,6,7,12b-octahydro-2*H*-cyclopenta[4,4a]anthra[9,1-*bc*]furan-2,8(2a*H*)-dione (4.138). A solution of 2-((2a*S*,2a¹*S*,4a*S*,5*R*,7a*R*,12b*S*)-12-methoxy-2,8-dioxo-2a,2a¹,3,4,4a,5,6,7,8,12b-decahydro-2*H*-cyclopenta[4,4a]anthra[9,1-*bc*]furan-5-yl)-2-(phenylselanyl)acetaldehyde (**4.136**, 0.0467 g, 0.0917 mmol) in THF (1.2 mL) at 0 °C was added a solution of NaIO₄ (0.0784 g, 0.367 mmol, 4 equiv.) in HPLC H₂O (1.2 mL) dropwise over 2 min and the mixture was stirred at 0 °C for 10 min and allowed to warm to rt over 3 h where by TLC the reaction looked complete. The reaction was cooled to 0 °C diluted with EtOAc (1 mL) and Satd. NaHCO₃ (1 mL) were added sequentially. The layers were separated; the aqueous layer was extracted with EtOAc (4 x 2 mL). The combined organic layers were dried (Na₂SO₄), filtered, and concentrated under reduced pressure. The crude enal **4.137** (0.0247 g) was carried on to the Luche reduction with no further purification.

A solution of crude 2-((2a*S*,2a¹*S*,7a*R*,12b*S*)-12-methoxy-2,8-dioxo-2a,3,4,4a,6,7-hexahydro-2*H*-cyclopenta[4,4a]anthra[9,1-*bc*]furan-5(2a¹*H*,8*H*,12b*H*)-ylidene)acetaldehyde (**4.137**, 0.0247 g, 0.0701 mmol) in THF (1.2 mL) and EtOH (0.2 mL) was cooled to 0 °C and treated with cerium (III) chloride heptahydrate (0.0522 g, 0.140 mmol) and NaBH₄ (0.0053 g, 0.140 mmol) and stirred at 0 °C for 2 h. The reaction was diluted with Satd. NH₄Cl (1 mL) and allowed to warm to rt for 10 min where the reaction was extracted with EtOAc (4 x 3 mL). The combined organic layers were dried (Na₂SO₄), filtered and concentrated in vacuo. The crude residue was dissolved in MeOH and concentrated onto C18-SiO₂ and purified by automated reverse phase chromatography on C18 (solid load, 10% ACN:H₂O to 95% ACN:H₂O) to give **4.138** (0.0070 g, 0.0198 mmol, 21% (2 steps)) as a 2:1 mixture of isomers as a pale yellow oil: Characteristic NMR for major isomer ¹H NMR (600 MHz, CDCl₃) δ 7.56 (d, *J* = 8.0 Hz, 1 H),

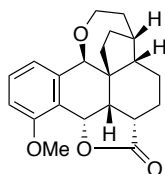
7.48 (t, $J = 8.0$ Hz, 1 H), 7.17 (d, $J = 8.0$ Hz, 1 H), 6.20 (d, $J = 10.0$ Hz, 1 H), 5.56 (dd, $J = 7.2$, 4.6 Hz, 1 H), 4.33 (dd, $J = 12.0$, 6.6 Hz, 1H), 4.22-4.19 (m, 1 H), 3.94 (s, 3 H), 3.36 (t, $J = 10.5$ Hz, 1 H), 2.89-2.83 (m, 1 H), 2.57-2.42 (m, 4 H), 2.29 (td, $J = 16.0$, 8.4 Hz, 1 H), 2.22-2.17 (m, 1 H), 2.07-2.03 (m, 2 H), 1.80 (ddd, $J = 13.1$, 6.0, 2.9 Hz, 2 H), 1.55 (dd, $J = 11.6$, 8.8 Hz, 1 H), 1.32-1.19 (m, 2 H); ^{13}C NMR (150 MHz, CDCl_3) δ 197.5, 178.1, 158.5, 145.7, 131.6, 131.0, 125.7, 119.6, 118.9, 116.0, 72.2, 59.7, 56.2, 54.4, 47.7, 45.1, 39.0, 35.9, 32.1, 23.7, 23.4; HRMS (ESI) m/z calcd for $\text{C}_{21}\text{H}_{23}\text{O}_5$ ($[\text{M}+\text{H}]^+$) 355.1540, found 355.1539.



4.140

(2a*S*,2a1*S*,4a*S*,5*R*,7a*R*,12b*S*)-5-(2-Hydroxyethyl)-12-methoxy-2a1,3,4,4a,5,6,7,12b-octahydro-2*H*-cyclopenta[4,4a]anthra[9,1-*bc*]furan-2,8(2a*H*)-dione (4.140). A solution of (2a*S*,2a1*S*,7a*R*,12b*S*,*Z*)-5-(2-hydroxyethylidene)-12-methoxy-2a1,3,4,4a,5,6,7,12b-octahydro-2*H*-cyclopenta[4,4a]anthra[9,1-*bc*]furan-2,8(2a*H*)-dione (**4.138**, 0.00400 g, 0.0113 mmol) in dry degassed CH_2Cl_2 (0.2 mL) in a 1 dram vial equipped with a magnetic stirbar was added Crabtree's catalyst (0.0010 g, 0.00113 mmol) under Ar. The vial was placed in a Parr bomb under Ar, sealed, purged with Ar, then purged with H_2 (3 x) and pressurized to 21 bar and stirred at rt for 4 h. Analysis by ^1H NMR and LCMS showed SM remaining. The reaction was treated with additional Crabtree's catalyst (0.0010 g, 0.00113 mmol) under Ar. The vial was placed in a Parr bomb under Ar, sealed, purged with Ar, then purged with H_2 (3 x), pressurized to 20 bar and stirred at rt for 16 h. The reaction was concentrated under reduced pressure. Crude ^1H NMR indicates consumption of the allylic alcohol SM and the product mass of **4.140** is present in the LCMS. Crude NMR peaks: ^1H NMR (400 MHz, CDCl_3) δ 7.55-7.44 (m, 2 H), 7.15 (d, $J = 7.0$

Hz, 1 H), 6.21-6.16 (m, 1 H), 3.99-3.91 (m, 3 H), 3.73-3.68 (m, 1 H), 3.36-3.22 (m, 1 H), 2.99-2.84 (m, 1 H), 2.33-2.17 (m, 2 H), 1.90-1.61 (m, 4 H), 1.51-1.16 (m, 4 H), 1.06-1.01 (m, 2 H), 0.89-0.85 (m, 2 H); HRMS (ESI) m/z calcd for $C_{21}H_{25}O_5$ ($[M+H]^+$) 357.1697, found 357.1695.



4.141

(2a*S*,2a1*S*,4a*S*,4a1*R*,5*R*,8a*S*,12b*S*)-12-methoxy-2a,2a1,3,4,4a,5,6,7,8a,12b-decahydro-2*H*-4a1,5-ethanofuro[4',3',2':4,10]anthra[9,1-*bc*]oxepin-2-one (4.141). A solution of crude (2a*S*,2a1*S*,4a*S*,5*R*,7a*R*,12b*S*)-5-(2-Hydroxyethyl)-12-methoxy-2a1,3,4,4a,5,6,7,12b-octahydro-2*H*-cyclopenta[4,4a]anthra[9,1-*bc*]furan-2,8(2a*H*)-dione (**4.140**, 0.0050 g, 0.0140 mmol) in dry CH_2Cl_2 (7.0 mL) cooled to 0 °C was treated with a freshly prepared solution of TMSOTf (1M in CH_2Cl_2) (28 μ L, 0.0281 mmol) followed by Et_3SiH (6.7 μ L, 0.0421 mmol) and stirred at 0 °C for 1 h. The reaction was warmed to rt for 4 h where analysis by TLC (EtOAc/hexanes, 4:1; CAM stain) indicated the formation of a new more non-polar spot. The reaction was cooled to 0 °C and diluted with Satd. $NaHCO_3$ (2 mL) and extracted with CH_2Cl_2 (3 x 2 mL). The combined organic layers were dried (Na_2SO_4), filtered, and concentrated under reduced pressure. The crude residue was purified by chromatography on SiO_2 (gradient, hexanes/EtOAc, 1:1 to EtOAc) to afford mostly recovered SM along with a mixed fraction of two non-polar spots (>0.5 mg): HRMS (ESI) m/z calcd for $C_{21}H_{25}O_4$ ($[M+H]^+$) 341.1747, found 341.1746.

APPENDIX A

X-RAY DATA

A.1 X-RAY STRUCTURE AND DATA FOR (1*R*,2*S*)-JJ450

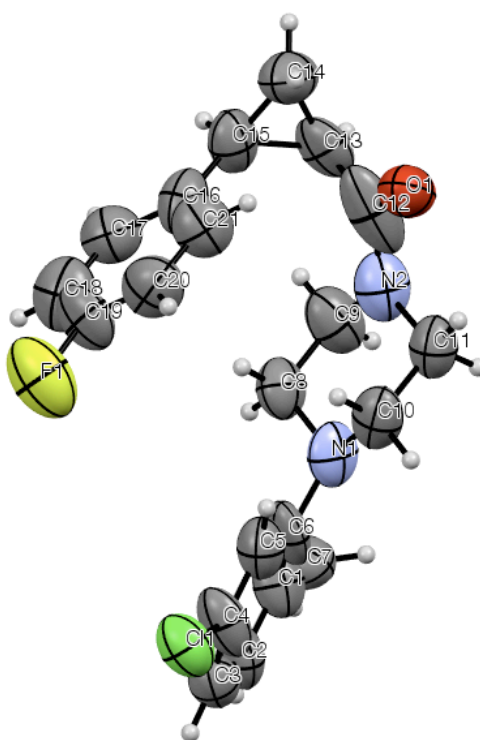


Figure A.1. X-ray crystal structure of (1*R*,2*S*)-JJ450.

Table A.1. Crystal data and structure refinement for (1*R*,2*S*)-**JJ450**.

Identification code	(1 <i>R</i> ,2 <i>S</i>)- JJ450	
Chemical formula	C ₂₁ H ₂₂ ClFN ₂ O	
Formula weight	372.85 g/mol	
Temperature	230(2) K	
Wavelength	1.54178 Å	
Crystal size	0.010 x 0.020 x 0.160 mm	
Crystal system	Monoclinic	
Space group	P 1 21 1	
Unit cell dimensions	a = 8.9297(6) Å	α = 90°
	b = 10.0143(7) Å	β = 93.382(5)°
	c = 10.7194(8) Å	γ = 90°
Volume	956.91(12) Å ³	
Z	2	
Density (calculated)	1.294 g/cm ³	
Absorption coefficient	1.942 mm ⁻¹	
F(000)	392	
Diffractometer	Bruker Apex II CCD	
Radiation source	IMuS micro-focus source, Cu	
Theta range for data collection	4.13 to 68.31°	
Index ranges	-10 ≤ h ≤ 10, -11 ≤ k ≤ 12, -12 ≤ l ≤ 12	
Reflections collected	13088	
Independent reflections	3491 [R(int) = 0.1250]	
Absorption correction	multi-scan	
Max. and min. transmission	0.9800 and 0.7500	
Structure solution technique	direct methods	
Structure solution program	SHELXS-97 (Sheldrick, 2008)	
Refinement method	Full-matrix least-squares on F ²	
Refinement program	SHELXL-97 (Sheldrick, 2008)	
Function minimized	Σ w(F _o ² - F _c ²) ²	
Data / restraints / parameters	3491 / 1 / 237	
Goodness-of-fit on F²	1.725	
Δ/σ_{max}	0.004	
Final R indices [I > 2σ(I)]	R1 = 0.1107, wR2 = 0.2229	
R indices (all data)	R1 = 0.2637, wR2 = 0.2932	
Weighting scheme	w = 1/[σ ² (F _o ²) + (0.0680P) ²] where P = (F _o ² + 2F _c ²)/3	
Absolute structure parameter	0.05(7)	
Extinction coefficient	0.0760(100)	
Largest diff. peak and hole	0.555 and -0.639 eÅ ⁻³	
R.M.S. deviation from mean	0.143 eÅ ⁻³	

Table A.2. Atomic coordinates and equivalent isotropic atomic displacement parameters (\AA^2) for (1*R*,2*S*)-**JJ450.**

	x/a	y/b	z/c	U(eq)
C11	0.8388(4)	0.4211(5)	0.6385(4)	0.0959(19)
F1	0.7333(11)	0.6332(12)	0.2209(12)	0.142(5)
O1	0.1000(13)	0.2703(13)	0.1361(11)	0.096(4)
N1	0.2734(15)	0.4723(13)	0.5135(14)	0.084(4)
N2	0.0834(15)	0.4113(18)	0.2985(18)	0.099(5)
C1	0.377(2)	0.5931(17)	0.692(2)	0.087(5)
C2	0.500(2)	0.6171(17)	0.7724(18)	0.088(5)
C3	0.6389(19)	0.5680(16)	0.7653(16)	0.080(5)
C4	0.6607(17)	0.4813(17)	0.660(2)	0.095(6)
C5	0.5424(19)	0.4540(14)	0.5773(16)	0.085(5)
C6	0.4026(18)	0.5086(19)	0.5993(19)	0.085(5)
C7	0.2290(17)	0.6514(18)	0.7079(14)	0.089(5)
C8	0.2331(17)	0.5738(15)	0.4151(16)	0.083(5)
C9	0.082(2)	0.5420(19)	0.3531(19)	0.104(6)
C10	0.2783(18)	0.3412(19)	0.4524(17)	0.090(6)
C11	0.1289(17)	0.3017(17)	0.3865(16)	0.084(5)
C12	0.074(2)	0.384(2)	0.173(3)	0.134(12)
C13	0.0245(17)	0.487(2)	0.0836(19)	0.094(6)
C14	0.071(2)	0.4722(19)	0.9512(17)	0.104(6)
C15	0.1354(19)	0.5830(16)	0.0329(17)	0.091(6)
C16	0.299(2)	0.588(2)	0.0775(16)	0.090(5)
C17	0.358(2)	0.717(2)	0.1101(15)	0.092(6)
C18	0.504(3)	0.731(2)	0.159(2)	0.117(7)
C19	0.591(2)	0.622(3)	0.1697(19)	0.100(6)
C20	0.536(2)	0.501(3)	0.1398(18)	0.108(7)
C21	0.388(2)	0.482(2)	0.0893(16)	0.097(6)

U(eq) is defined as one third of the trace of the orthogonalized U^j tensor.

Table A.3. Bond lengths (Å) for (1*R*,2*S*)-**JJ450**.

C11-C4	1.728(16)	F1-C19	1.36(2)
O1-C12	1.23(2)	N1-C10	1.47(2)
N1-C6	1.478(19)	N1-C8	1.494(17)
N2-C12	1.37(3)	N2-C9	1.43(2)
N2-C11	1.49(2)	C1-C6	1.33(2)
C1-C2	1.38(2)	C1-C7	1.46(2)
C2-C3	1.34(2)	C2-H2A	0.94
C3-C4	1.45(2)	C3-H3A	0.94
C4-C5	1.365(19)	C5-C6	1.40(2)
C5-H5A	0.94	C7-H7A	0.97
C7-H7B	0.97	C7-H7C	0.97
C8-C9	1.50(2)	C8-H8A	0.98
C8-H8B	0.98	C9-H9A	0.98
C9-H9B	0.98	C10-C11	1.525(19)
C10-H10A	0.98	C10-H10B	0.98
C11-H11A	0.98	C11-H11B	0.98
C12-C13	1.46(3)	C13-C15	1.51(2)
C13-C14	1.51(2)	C13-H13A	0.99
C14-C15	1.51(2)	C14-H14A	0.98
C14-H14B	0.98	C15-C16	1.51(2)
C15-H15A	0.99	C16-C21	1.33(2)
C16-C17	1.43(2)	C17-C18	1.39(2)
C17-H17A	0.94	C18-C19	1.34(3)
C18-H18A	0.94	C19-C20	1.34(3)
C20-C21	1.41(2)	C20-H20A	0.94
C21-H21A	0.94		

Table A.4. Bond angles (°) for (1*R*,2*S*)-**JJ450**.

C10-N1-C6	117.0(14)	C10-N1-C8	107.8(13)
C6-N1-C8	114.7(13)	C12-N2-C9	125.7(19)
C12-N2-C11	118.2(19)	C9-N2-C11	115.0(16)
C6-C1-C2	114.3(16)	C6-C1-C7	122.5(18)
C2-C1-C7	123.1(18)	C3-C2-C1	127.3(19)
C3-C2-H2A	116.4	C1-C2-H2A	116.4
C2-C3-C4	115.6(16)	C2-C3-H3A	122.2
C4-C3-H3A	122.2	C5-C4-C3	119.4(15)
C5-C4-C11	121.8(17)	C3-C4-C11	118.7(14)
C4-C5-C6	118.6(17)	C4-C5-H5A	120.7
C6-C5-H5A	120.7	C1-C6-C5	124.7(16)

C1-C6-N1	117.2(17)	C5-C6-N1	118.2(19)
C1-C7-H7A	109.5	C1-C7-H7B	109.5
H7A-C7-H7B	109.5	C1-C7-H7C	109.5
H7A-C7-H7C	109.5	H7B-C7-H7C	109.5
N1-C8-C9	109.9(13)	N1-C8-H8A	109.7
C9-C8-H8A	109.7	N1-C8-H8B	109.7
C9-C8-H8B	109.7	H8A-C8-H8B	108.2
N2-C9-C8	110.3(15)	N2-C9-H9A	109.6
C8-C9-H9A	109.6	N2-C9-H9B	109.6
C8-C9-H9B	109.6	H9A-C9-H9B	108.1
N1-C10-C11	113.0(14)	N1-C10-H10A	109.0
C11-C10-H10A	109.0	N1-C10-H10B	109.0
C11-C10-H10B	109.0	H10A-C10-H10B	107.8
N2-C11-C10	107.5(14)	N2-C11-H11A	110.2
C10-C11-H11A	110.2	N2-C11-H11B	110.2
C10-C11-H11B	110.2	H11A-C11-H11B	108.5
O1-C12-N2	120.(3)	O1-C12-C13	120.(3)
N2-C12-C13	120.(2)	C12-C13-C15	120.7(14)
C12-C13-C14	117.4(19)	C15-C13-C14	59.8(12)
C12-C13-H13A	115.8	C15-C13-H13A	115.8
C14-C13-H13A	115.8	C15-C14-C13	60.0(12)
C15-C14-H14A	117.8	C13-C14-H14A	117.8
C15-C14-H14B	117.8	C13-C14-H14B	117.8
H14A-C14-H14B	114.9	C14-C15-C16	122.3(16)
C14-C15-C13	60.2(10)	C16-C15-C13	123.4(15)
C14-C15-H15A	113.6	C16-C15-H15A	113.6
C13-C15-H15A	113.6	C21-C16-C17	119.2(18)
C21-C16-C15	124.7(18)	C17-C16-C15	116.1(17)
C18-C17-C16	120.4(19)	C18-C17-H17A	119.8
C16-C17-H17A	119.8	C19-C18-C17	119.(2)
C19-C18-H18A	120.7	C17-C18-H18A	120.7
C20-C19-C18	121.(2)	C20-C19-F1	120.(2)
C18-C19-F1	119.(2)	C19-C20-C21	122.6(19)
C19-C20-H20A	118.7	C21-C20-H20A	118.7
C16-C21-C20	118.2(18)	C16-C21-H21A	120.9
C20-C21-H21A	120.9		

Table A.5. Anisotropic atomic displacement parameters (\AA^2) for (1*R*,2*S*)-**JJ450**.

	U_{11}	U_{22}	U_{33}	U_{23}	U_{13}	U_{12}
C11	0.068(3)	0.090(3)	0.129(4)	-0.012(3)	-0.001(2)	0.004(2)
F1	0.073(8)	0.145(10)	0.209(13)	-0.035(9)	0.009(7)	0.001(6)
O1	0.102(10)	0.091(10)	0.092(8)	0.007(8)	-0.018(7)	-0.008(8)
N1	0.091(11)	0.040(8)	0.121(12)	0.009(9)	0.010(9)	0.012(7)
N2	0.081(10)	0.074(13)	0.142(15)	0.003(14)	0.014(10)	0.010(10)
C1	0.076(13)	0.056(11)	0.130(16)	-0.009(12)	0.020(12)	0.010(10)
C2	0.059(11)	0.082(12)	0.125(16)	0.013(11)	0.010(11)	-0.011(10)
C3	0.073(13)	0.074(12)	0.093(13)	0.010(11)	-0.008(10)	-0.001(9)
C4	0.043(10)	0.079(13)	0.161(18)	-0.013(12)	-0.003(11)	0.005(8)
C5	0.074(12)	0.069(12)	0.113(13)	0.013(10)	0.013(10)	-0.003(10)
C6	0.038(10)	0.071(12)	0.145(17)	0.017(12)	-0.012(10)	-0.013(9)
C7	0.082(12)	0.110(15)	0.076(12)	-0.003(10)	0.009(9)	-0.001(10)
C8	0.089(13)	0.059(12)	0.103(13)	-0.008(11)	0.015(10)	-0.004(10)
C9	0.092(15)	0.069(14)	0.149(19)	-0.006(13)	-0.017(12)	0.008(11)
C10	0.054(11)	0.092(16)	0.124(15)	0.033(13)	0.005(10)	0.010(10)
C11	0.073(13)	0.071(12)	0.111(14)	0.015(12)	0.015(10)	0.002(10)
C12	0.054(13)	0.061(15)	0.28(4)	-0.02(2)	-0.024(18)	0.017(10)
C13	0.040(10)	0.108(17)	0.132(18)	-0.008(13)	-0.015(10)	0.003(10)
C14	0.135(17)	0.096(15)	0.078(13)	0.002(11)	-0.008(12)	-0.012(11)
C15	0.078(13)	0.064(12)	0.129(16)	0.021(12)	-0.002(11)	0.003(10)
C16	0.102(15)	0.069(14)	0.103(13)	0.004(11)	0.036(11)	0.003(13)
C17	0.088(16)	0.099(17)	0.089(14)	-0.001(11)	0.010(12)	0.015(12)
C18	0.096(18)	0.115(17)	0.142(19)	0.004(14)	0.038(15)	0.019(15)
C19	0.039(11)	0.123(18)	0.139(17)	-0.014(14)	0.005(10)	-0.002(13)
C20	0.069(15)	0.13(2)	0.122(17)	0.019(15)	0.000(12)	0.012(13)
C21	0.088(14)	0.083(14)	0.119(16)	-0.005(11)	0.004(11)	0.016(11)

The anisotropic atomic displacement factor exponent takes the form: $-2\pi^2 [h^2 a^{*2} U_{11} + \dots + 2 h k a^* b^* U_{12}]$

Table A.6. Hydrogen atomic coordinates and isotropic atomic displacement parameters (\AA^2) for (1*R*,2*S*)-**JJ450**.

	x/a	y/b	z/c	$U(\text{eq})$
H2A	0.4847	0.6743	0.8400	0.106
H3A	0.7170	0.5885	0.8249	0.096
H5A	0.5548	0.3996	0.5072	0.102
H7A	0.2343	0.7099	0.7802	0.134
H7B	0.1974	0.7023	0.6340	0.134

	x/a	y/b	z/c	U(eq)
H7C	0.1572	0.5806	0.7204	0.134
H8A	0.3090	0.5741	0.3527	0.1
H8B	0.2308	0.6628	0.4530	0.1
H9A	0.0058	0.5460	0.4148	0.125
H9B	0.0569	0.6084	0.2881	0.125
H10A	0.3070	0.2735	0.5154	0.108
H10B	0.3556	0.3427	0.3913	0.108
H11A	0.1397	0.2179	0.3407	0.101
H11B	0.0528	0.2891	0.4477	0.101
H13A	-0.0778	0.5223	0.0925	0.113
H14A	0.1377	0.3976	-0.0671	0.124
H14B	-0.0017	0.4961	-0.1168	0.124
H15A	0.0921	0.6718	0.0119	0.109
H17A	0.2965	0.7933	0.0983	0.11
H18A	0.5417	0.8152	0.1841	0.14
H20A	0.5977	0.4259	0.1531	0.13
H21A	0.3538	0.3968	0.0647	0.116

APPENDIX B

CIRCULAR DICHROISM SPECTRA

All CD spectra were measured on a Jasco J-815 CD spectrometer using a quartz cuvette (0.1 cm) in length. All samples were dissolved in HPLC grade methanol using a 2 mL volumetric flask.

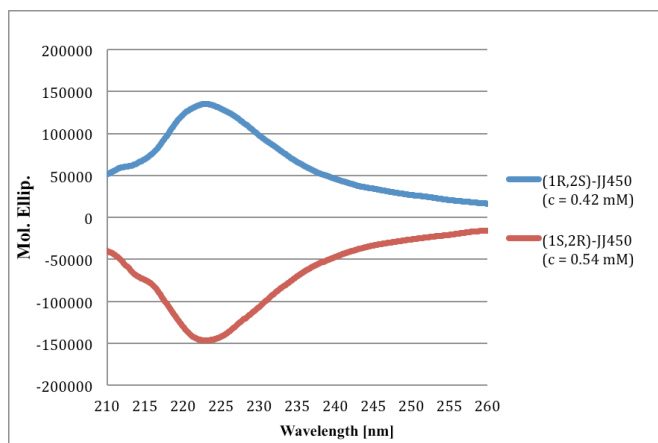


Figure B.1. CD spectra for enantiomers of JJ450.

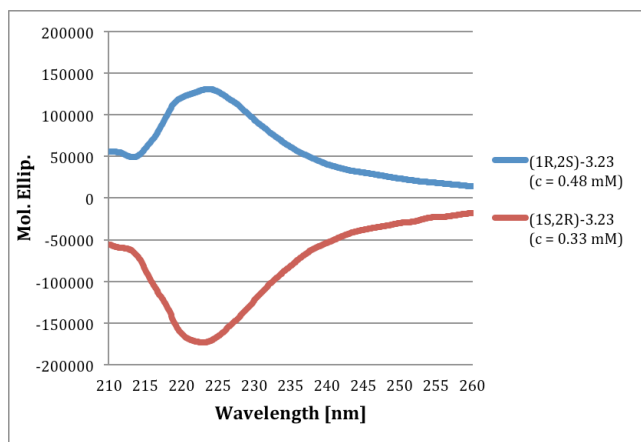


Figure B.2. CD spectra for enantiomers of 3.23.

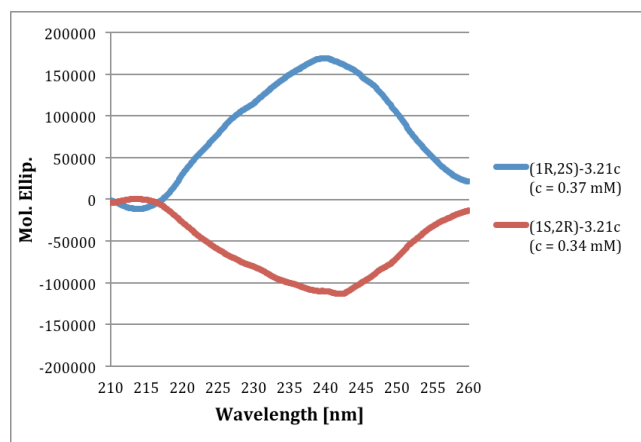


Figure B.3. CD spectra for enantiomers of 3.21c.

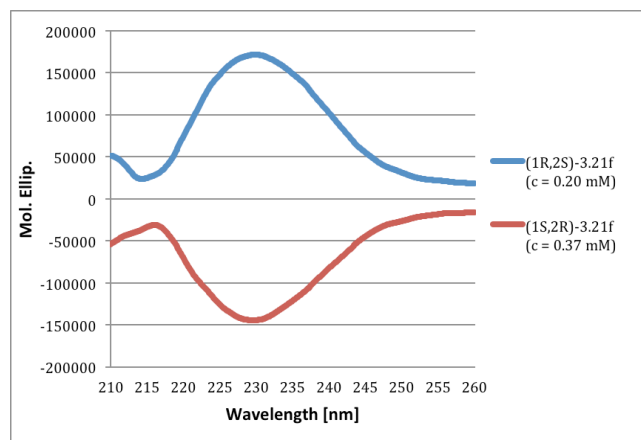


Figure B.4. CD spectra for enantiomers of 3.21f.

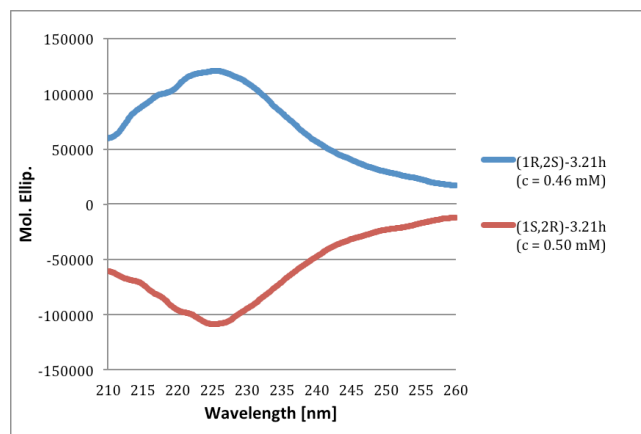


Figure B.5. CD spectra for enantiomers of **3.21h**.

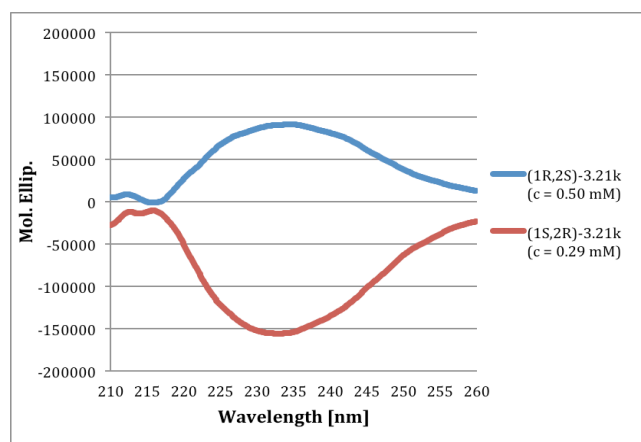


Figure B.6. CD spectra for enantiomers of **3.21k**.

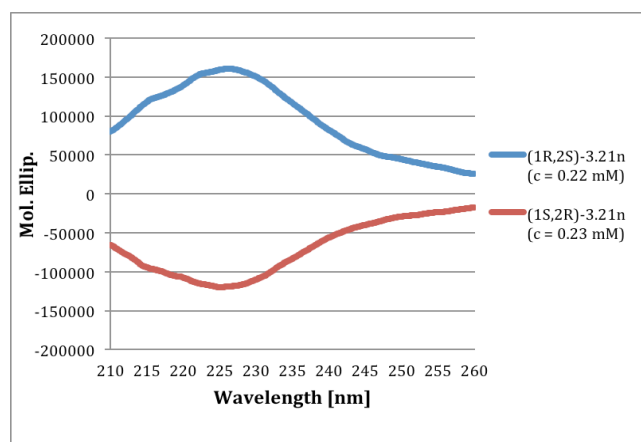


Figure B.7. CD spectra for enantiomers of **3.21n**.

APPENDIX C

EC50 CURVES

All EC₅₀'s are preliminary and were calculated using GraphPad prism using data obtained from the luciferase assay performed in the Wang lab. All data was normalized (0%, Y = 0; 100%, First value in data set). The normalized data was analyzed using a nonlinear regression (curve fit) (log(inhibitor) vs normalized response – Variable slope) with a least squares fit.

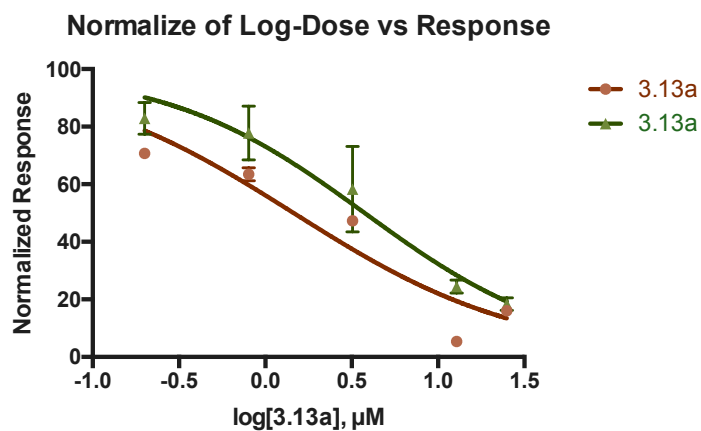


Figure C.1. EC₅₀ curves for 3.13a.

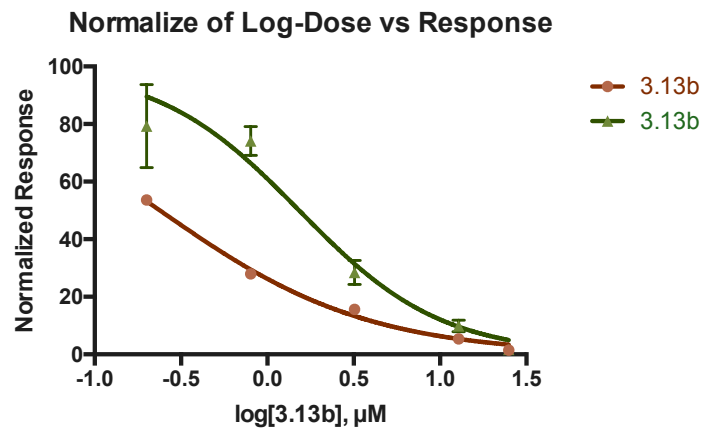


Figure C.2. EC_{50} curves for 3.13b.

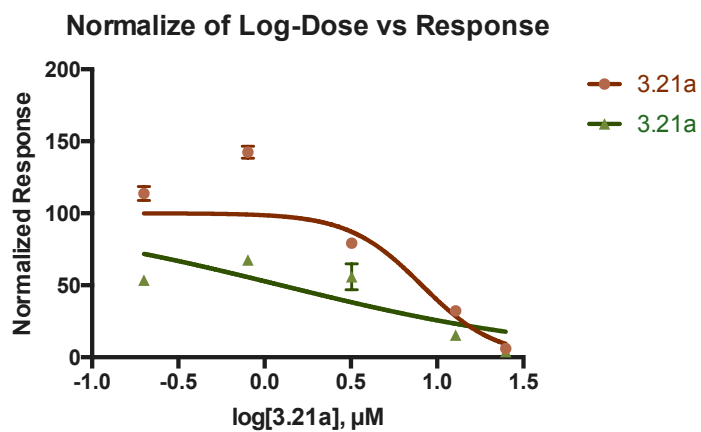


Figure C.3. EC_{50} curves for 3.21a.

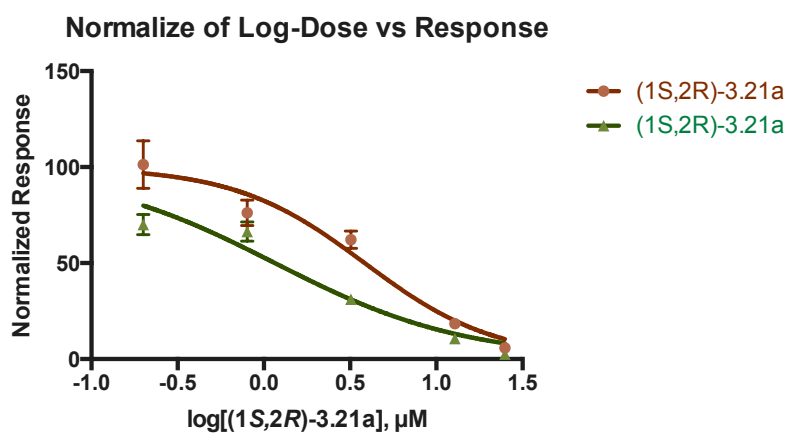


Figure C.4. EC_{50} curves for (1S,2R)-3.21a.

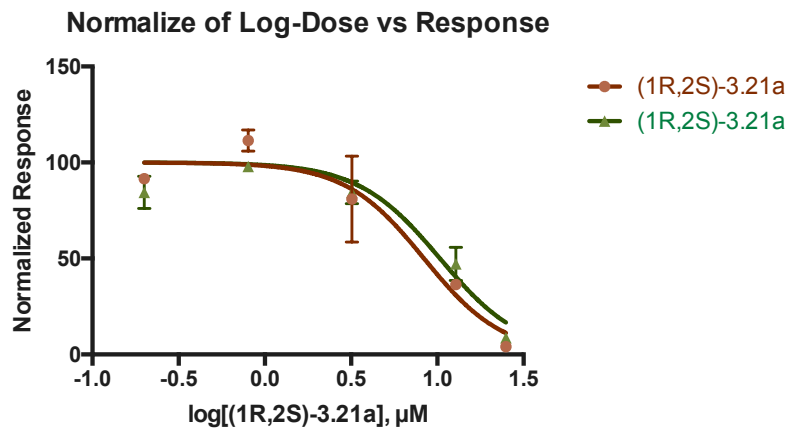


Figure C.5. EC₅₀ curves for (1R,2S)-3.21a.

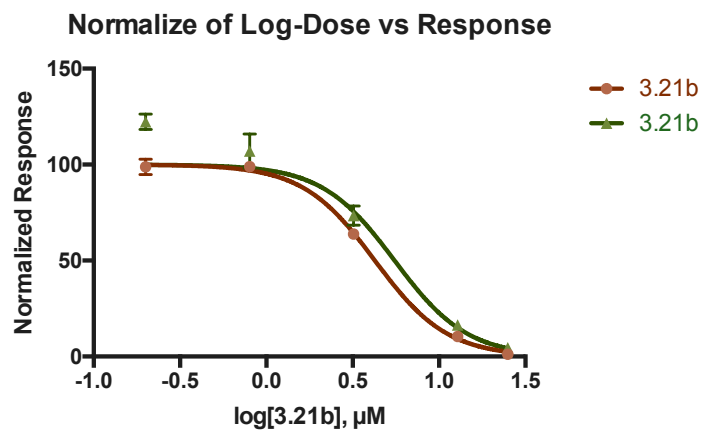


Figure C.6. EC₅₀ curves for 3.21b.

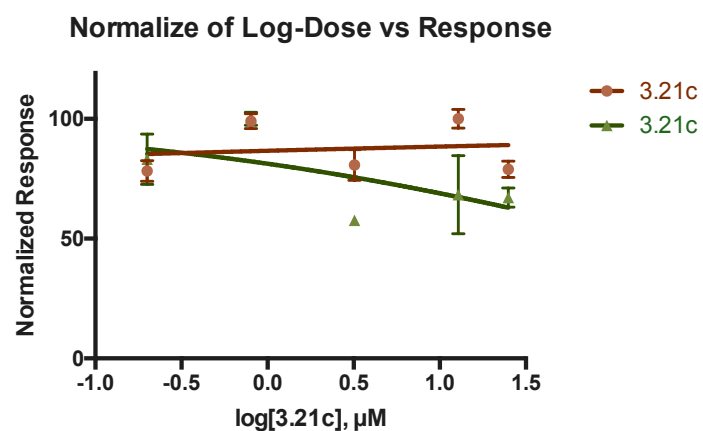


Figure C.7. EC₅₀ curves for 3.21c.

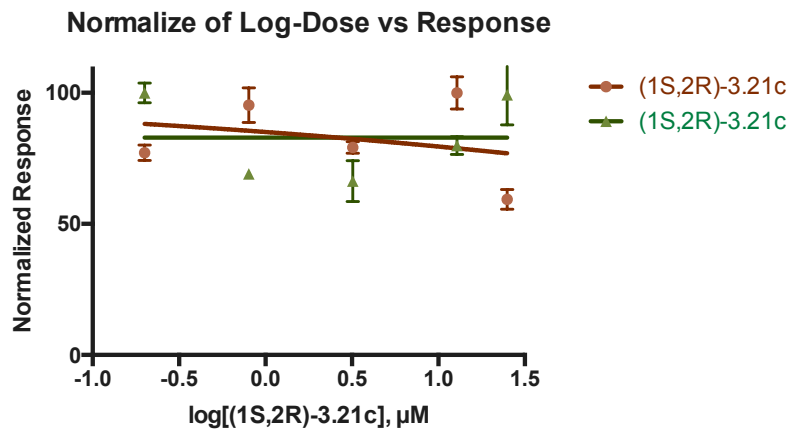


Figure C.8. EC_{50} curves for (1*S*,2*R*)-3.21c.

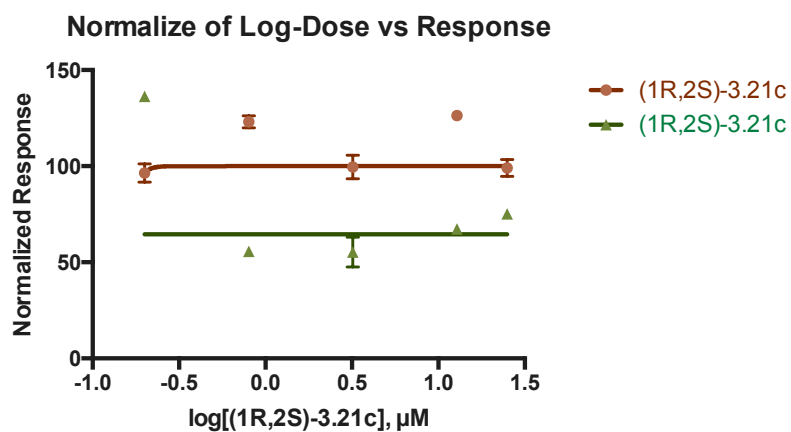


Figure C.9. EC_{50} curves for (1*R*,2*S*)-3.21c.

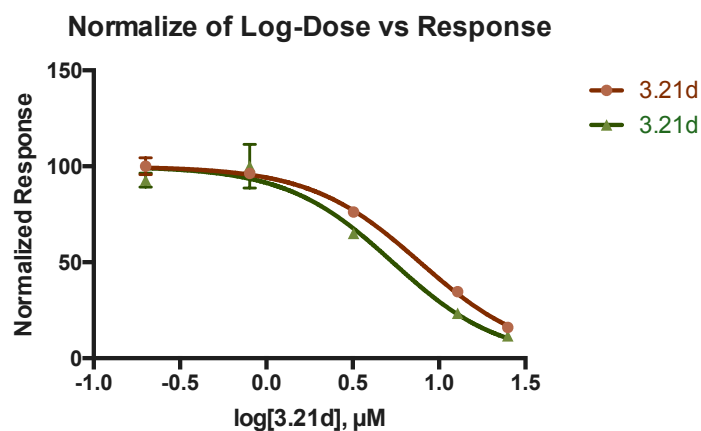


Figure C.10. EC_{50} curves for 3.21d.

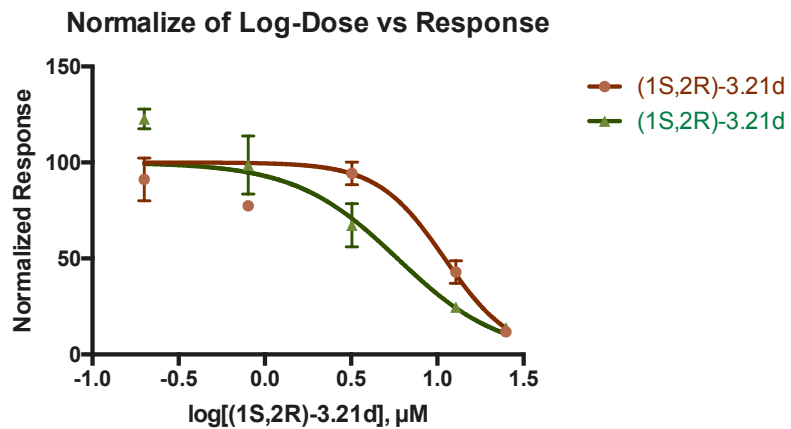


Figure C.11. EC₅₀ curves for (1*S*,2*R*)-3.21d.

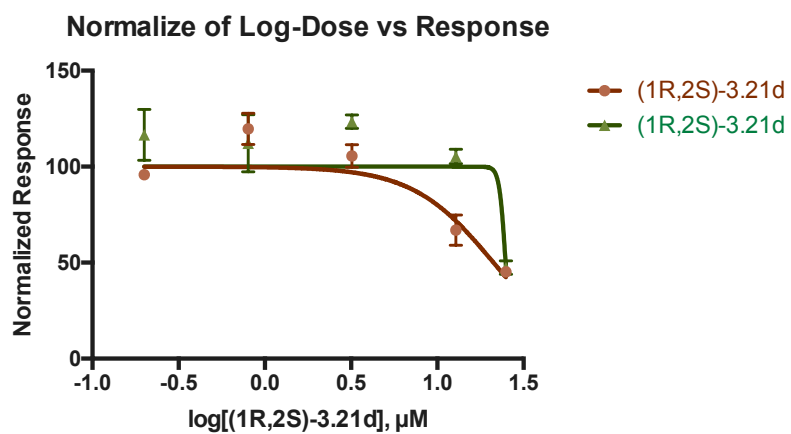


Figure C.12. EC₅₀ curves for (1*R*,2*S*)-3.21d.

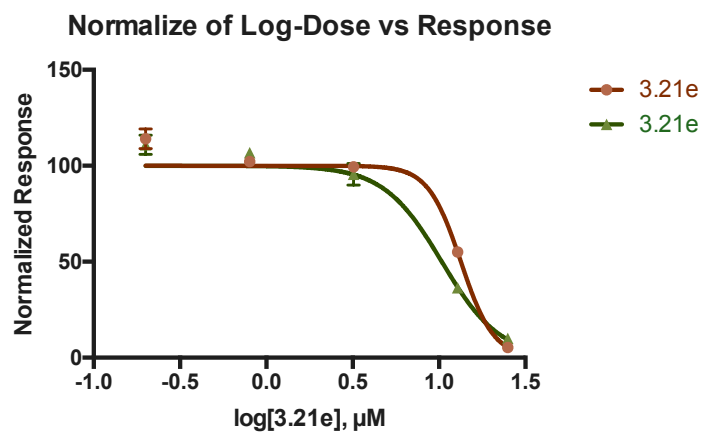


Figure C.13. EC₅₀ curves for 3.21e.

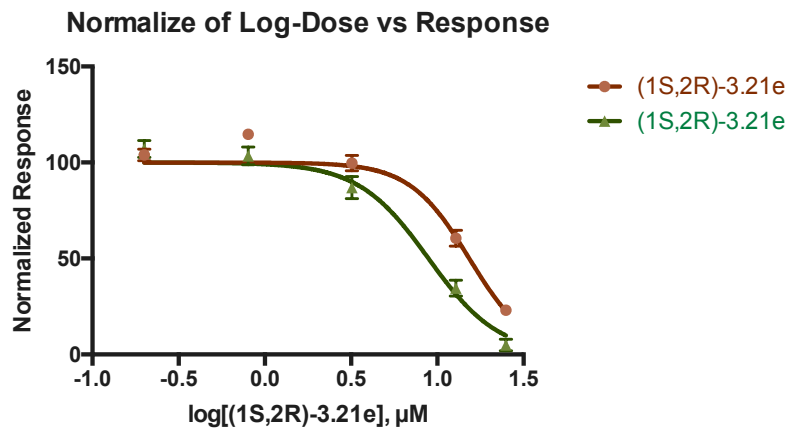


Figure C.14. EC_{50} curves for (1*S*,2*R*)-3.21e.

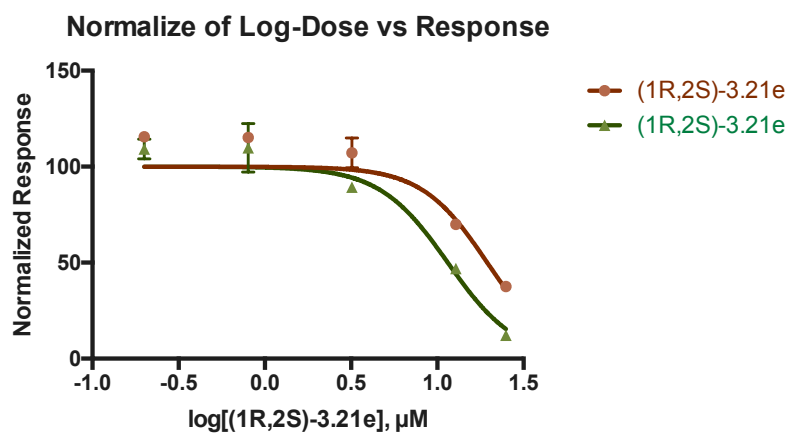


Figure C.15. EC_{50} curves for (1*R*,2*S*)-3.21e.

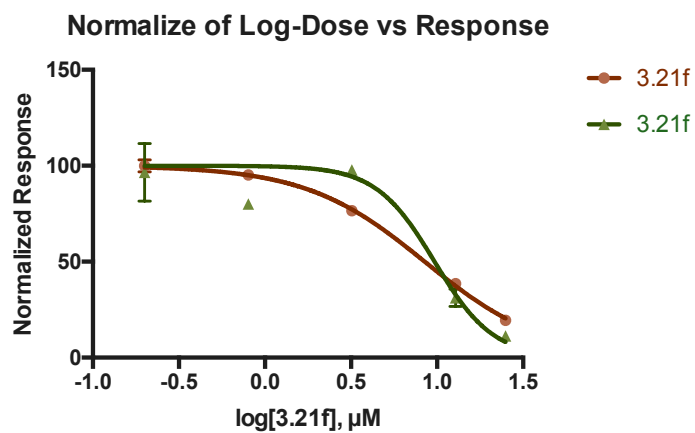


Figure C.16. EC_{50} curves for 3.21f.

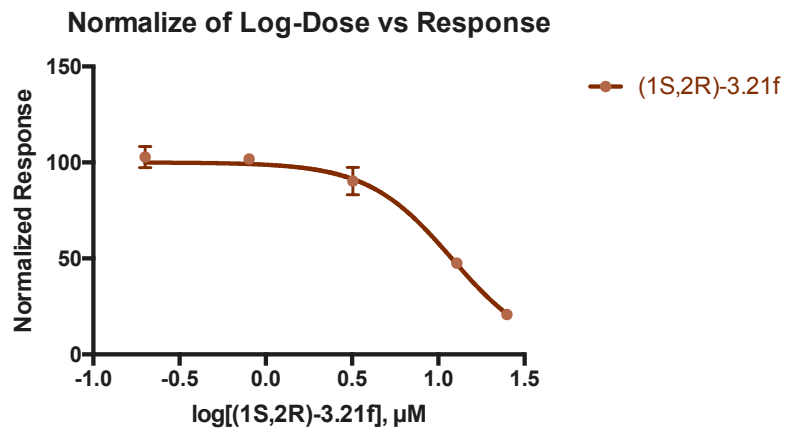


Figure C.17. EC_{50} curve for (1*S*,2*R*)-3.21f.

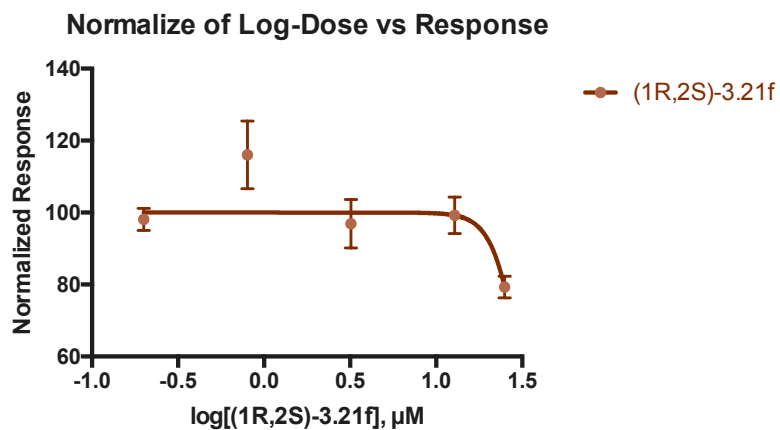


Figure C.18. EC_{50} curve for (1*R*,2*S*)-3.21f.

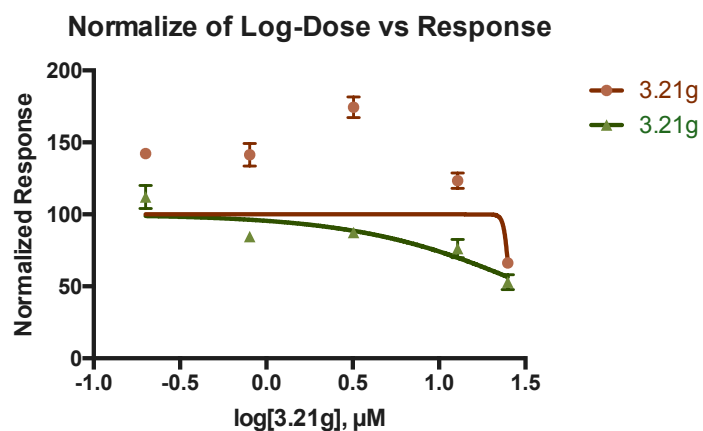


Figure C.19. EC_{50} curves for 3.21g.

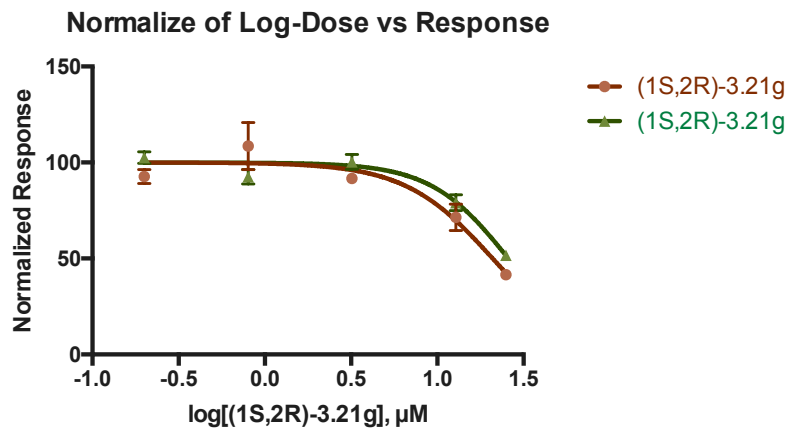


Figure C.20. EC₅₀ curves for (1*S*,2*R*)-3.21g.

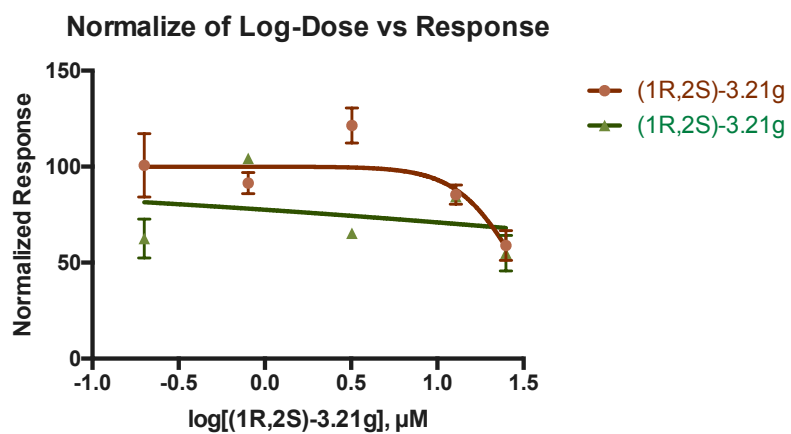


Figure C.21. EC₅₀ curves for (1*R*,2*S*)-3.21g.

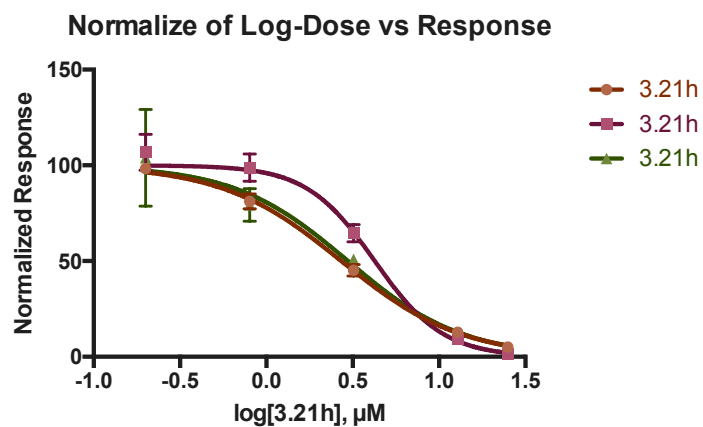


Figure C.22. EC₅₀ curves for 3.21h.

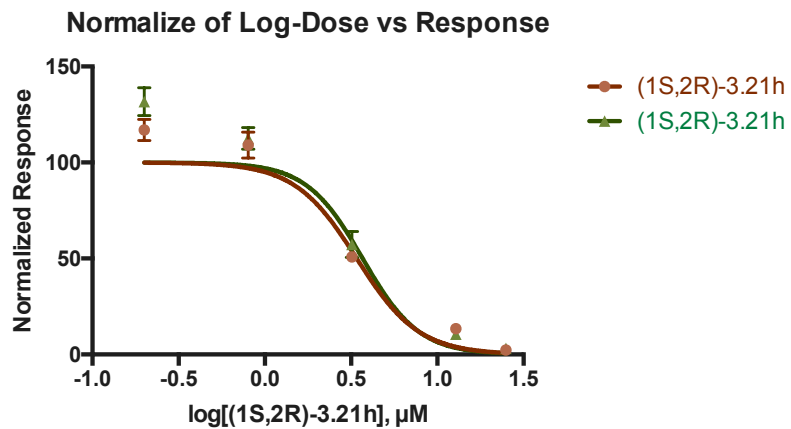


Figure C.23. EC_{50} curves for (1*S*,2*R*)-3.21h.

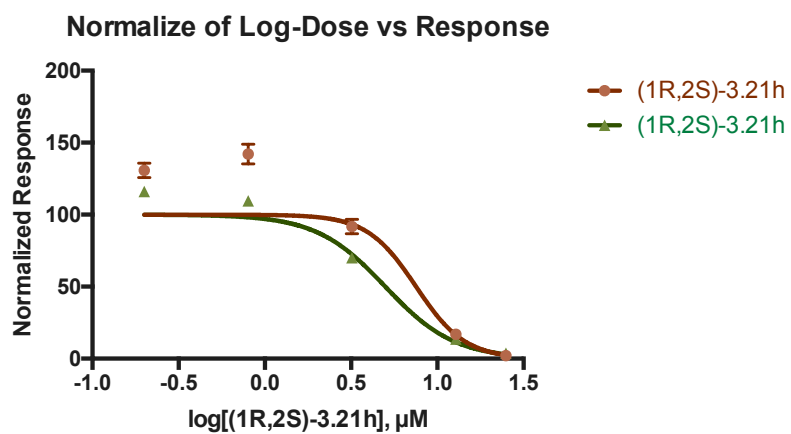


Figure C.24. EC_{50} curves for (1*R*,2*S*)-3.21h.

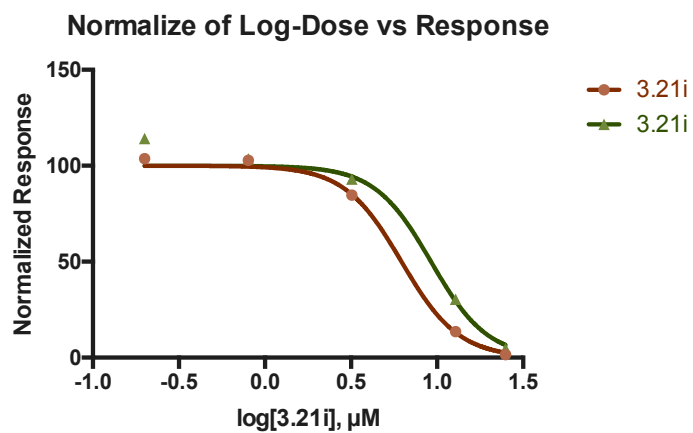


Figure C.25. EC_{50} curves for 3.21i.

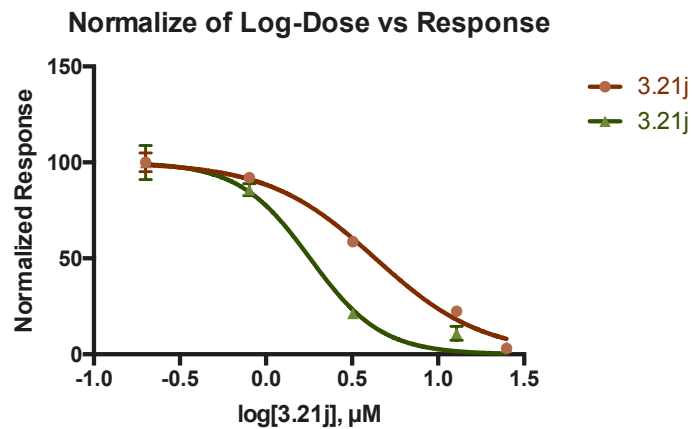


Figure C.26. EC₅₀ curves for 3.21j.

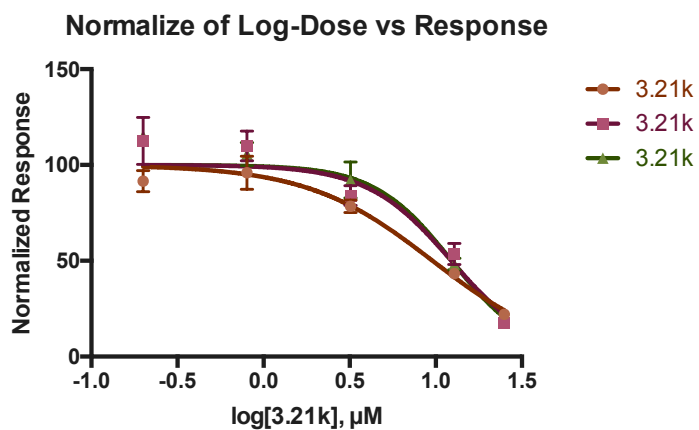


Figure C.27. EC₅₀ curves for 3.21k.

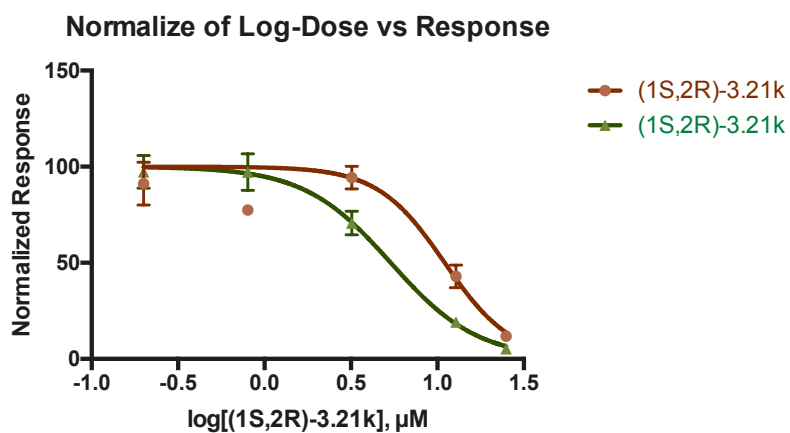


Figure C.28. EC₅₀ curves for (1*S*,2*R*)-3.21k.

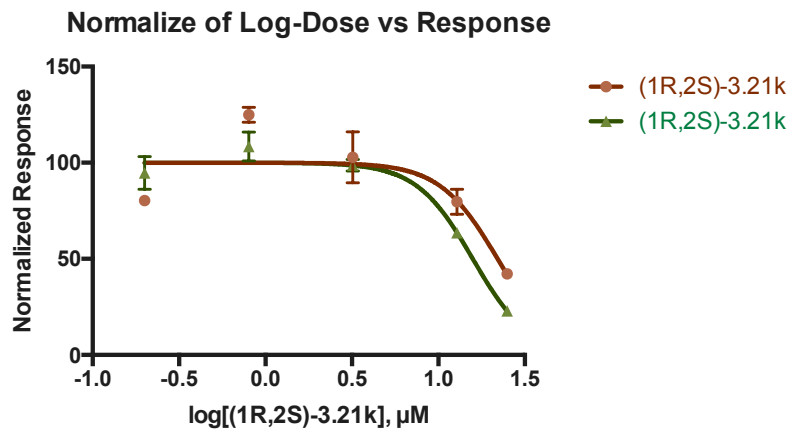


Figure C.29. EC_{50} curves for (1R,2S)-3.21k.

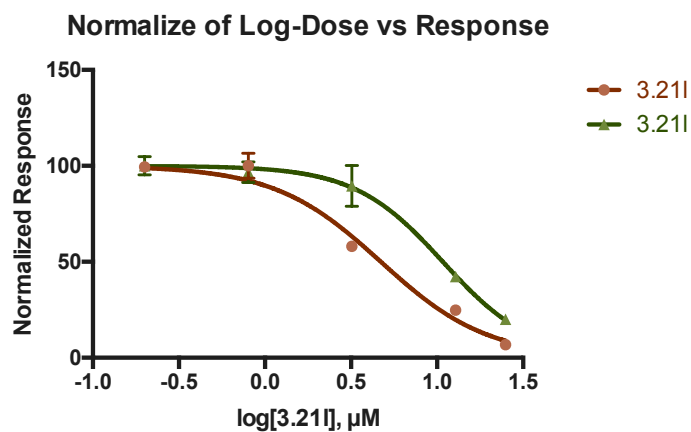


Figure C.30. EC_{50} curves for 3.21I.

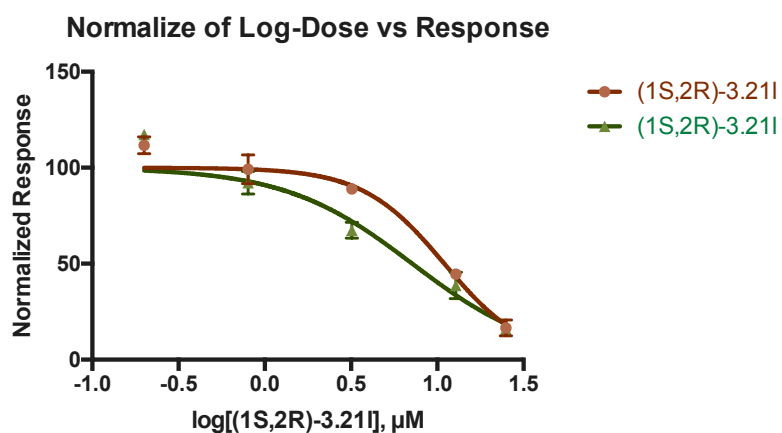


Figure C.31. EC_{50} curves for (1S,2R)-3.21I.

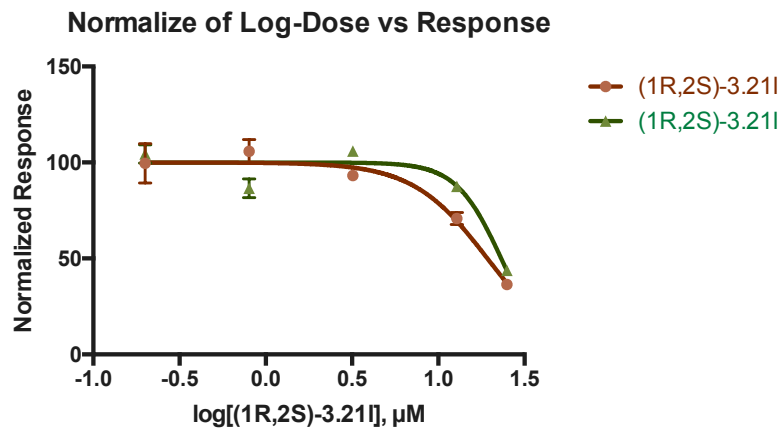


Figure C.32. EC_{50} curves for (1R,2S)-3.21I.

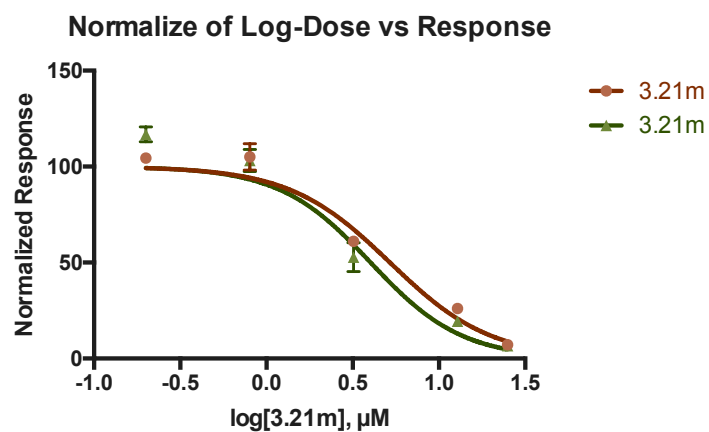


Figure C.33. EC_{50} curves for 3.21m.

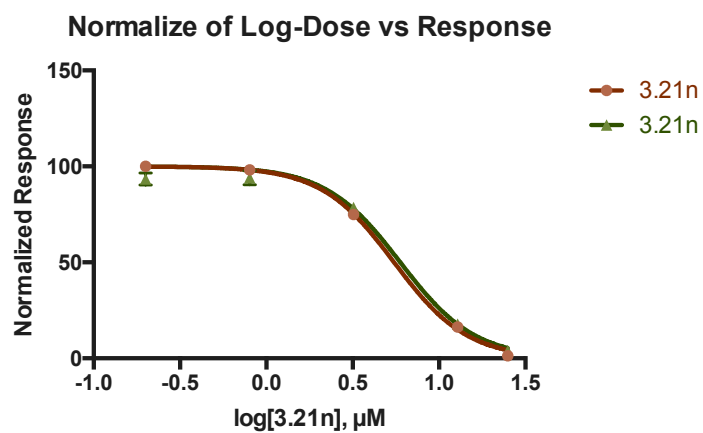


Figure C.34. EC_{50} curves for 3.21n.

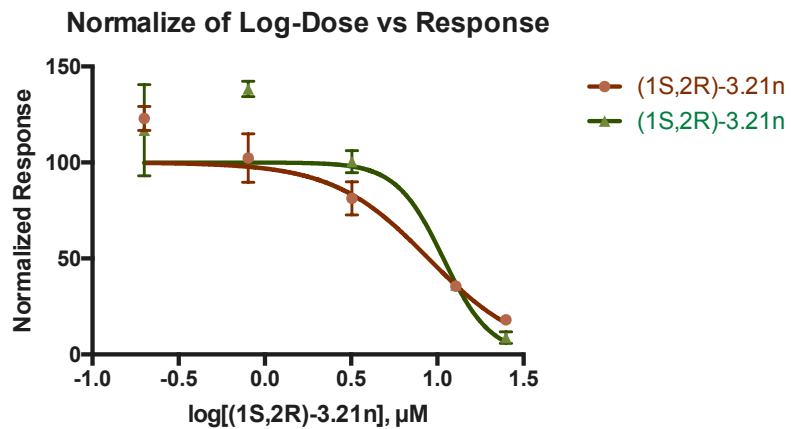


Figure C.35. EC_{50} curves for (1S,2R)-3.21n.

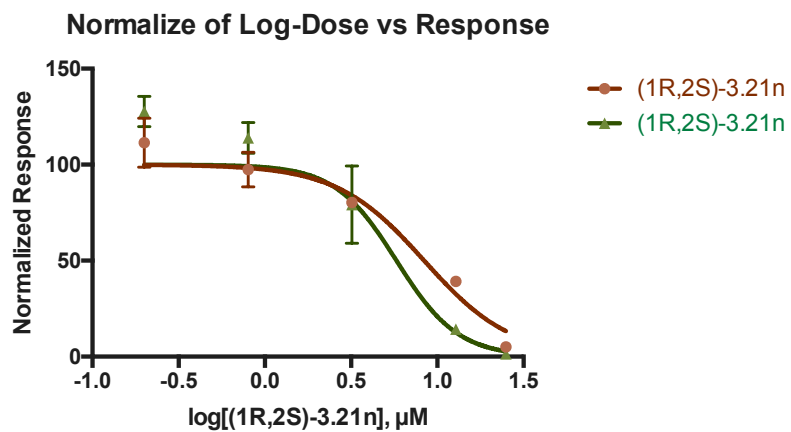


Figure C.36. EC_{50} curves for (1R,2S)-3.21n.

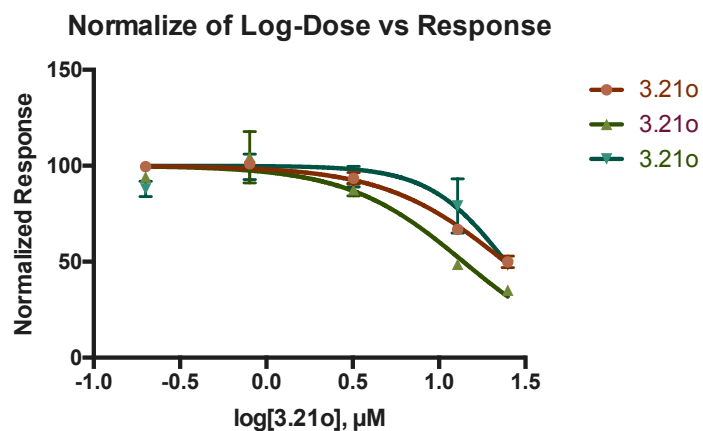


Figure C.37. EC_{50} curves for 3.21o.

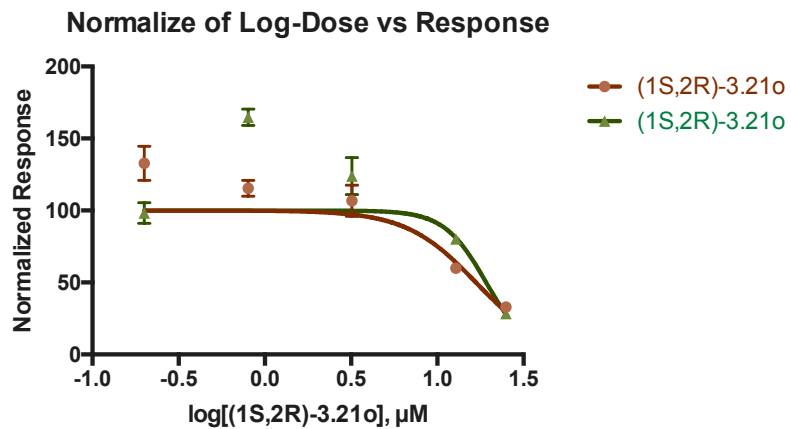


Figure C.38. EC₅₀ curves for (1*S*,2*R*)-3.21o.

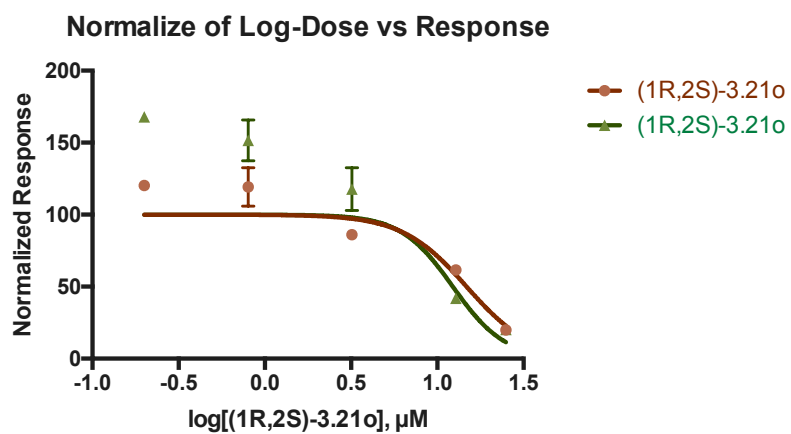


Figure C.39. EC₅₀ curves for (1*R*,2*S*)-3.21o.

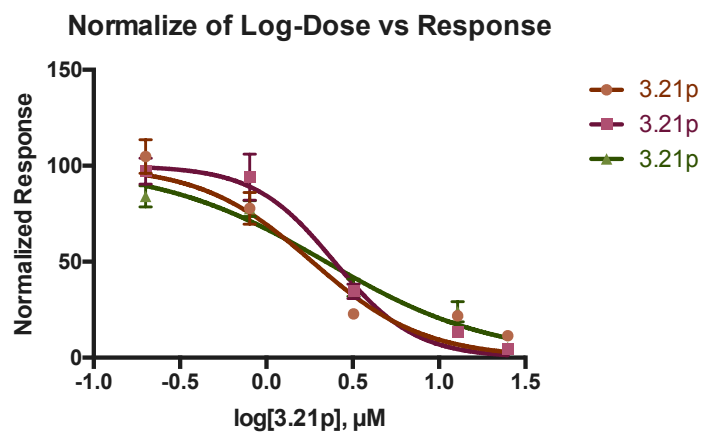


Figure C.40. EC₅₀ curves for 3.21p.

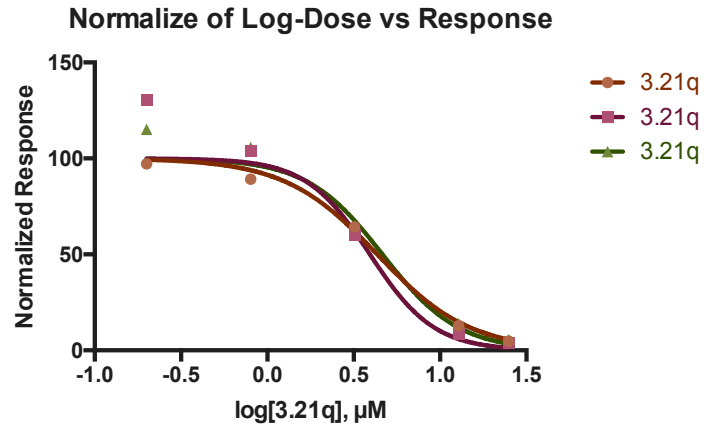


Figure C.41. EC₅₀ curves for 3.21q.

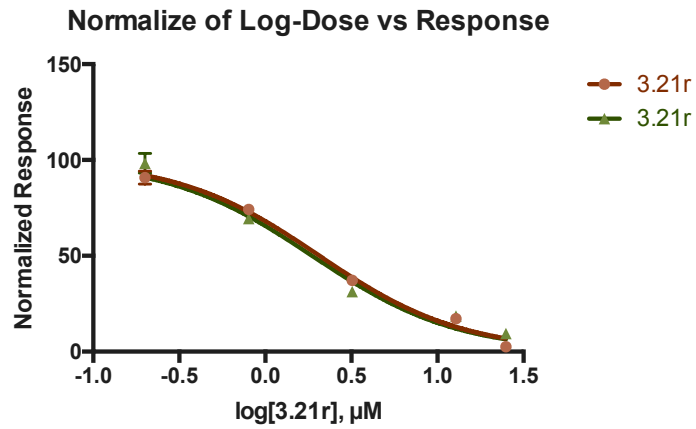


Figure C.42. EC₅₀ curves for 3.21r.

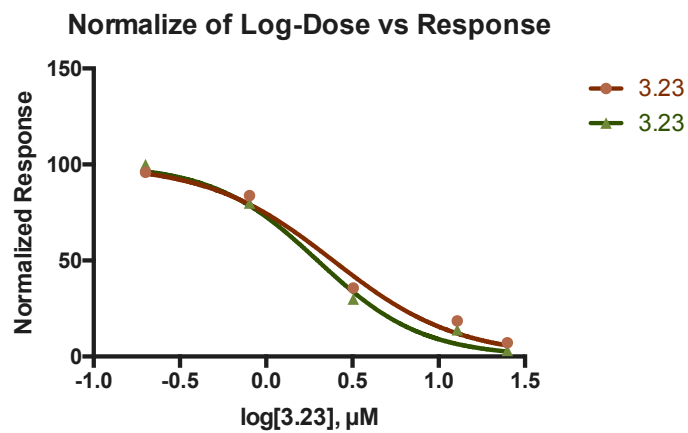


Figure C.43. EC₅₀ curves for 3.23.

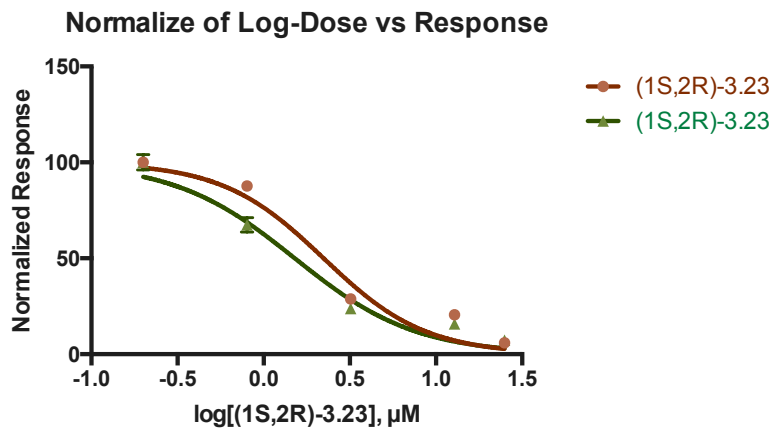


Figure C.44. EC₅₀ curves for (1*S*,2*R*)-3.23.

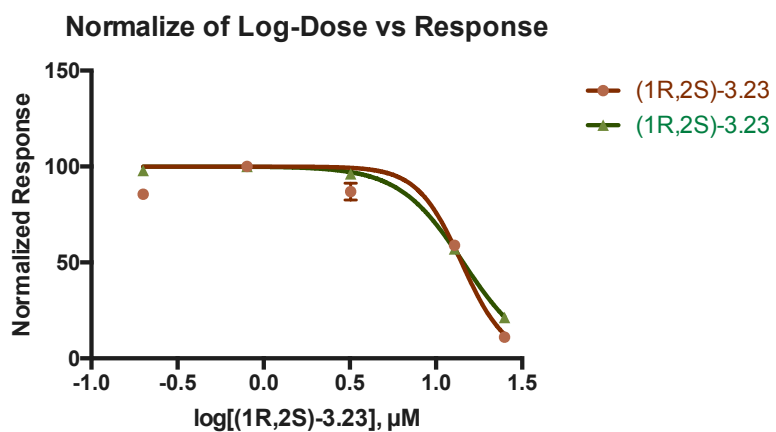


Figure C.45. EC₅₀ curves for (1*R*,2*S*)-3.23.

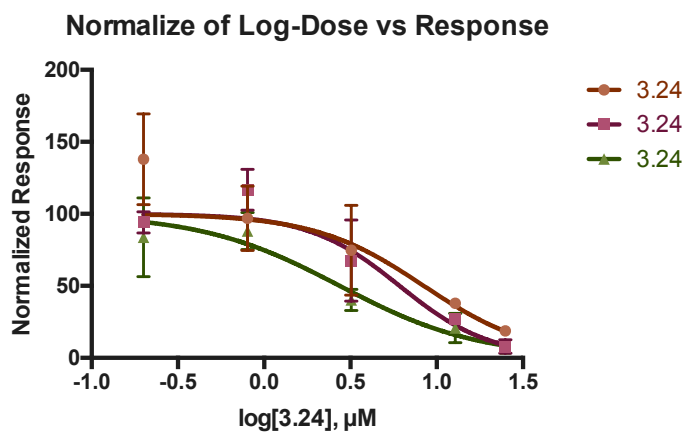


Figure C.46. EC₅₀ curves for 3.24.

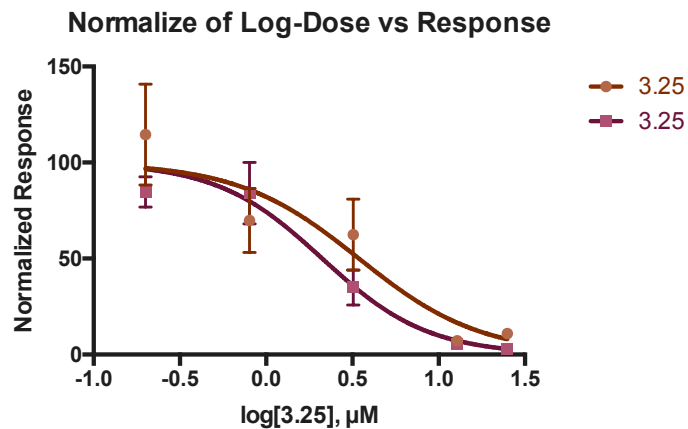


Figure C.47. EC₅₀ curves for 3.25.

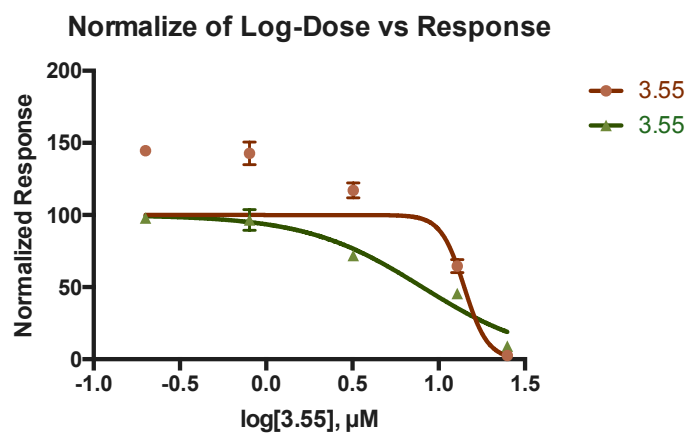


Figure C.48. EC₅₀ curves for 3.55.

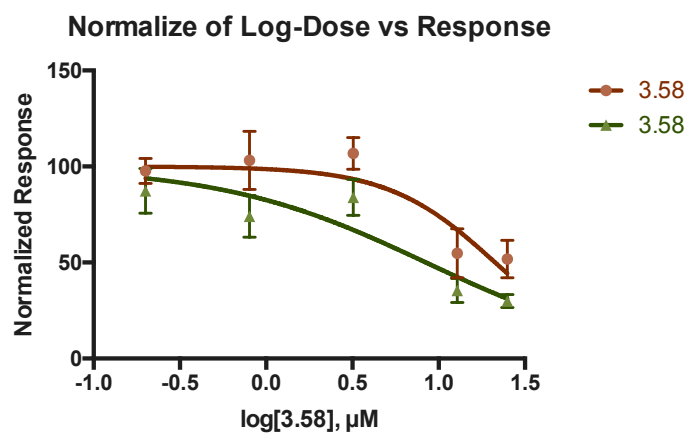
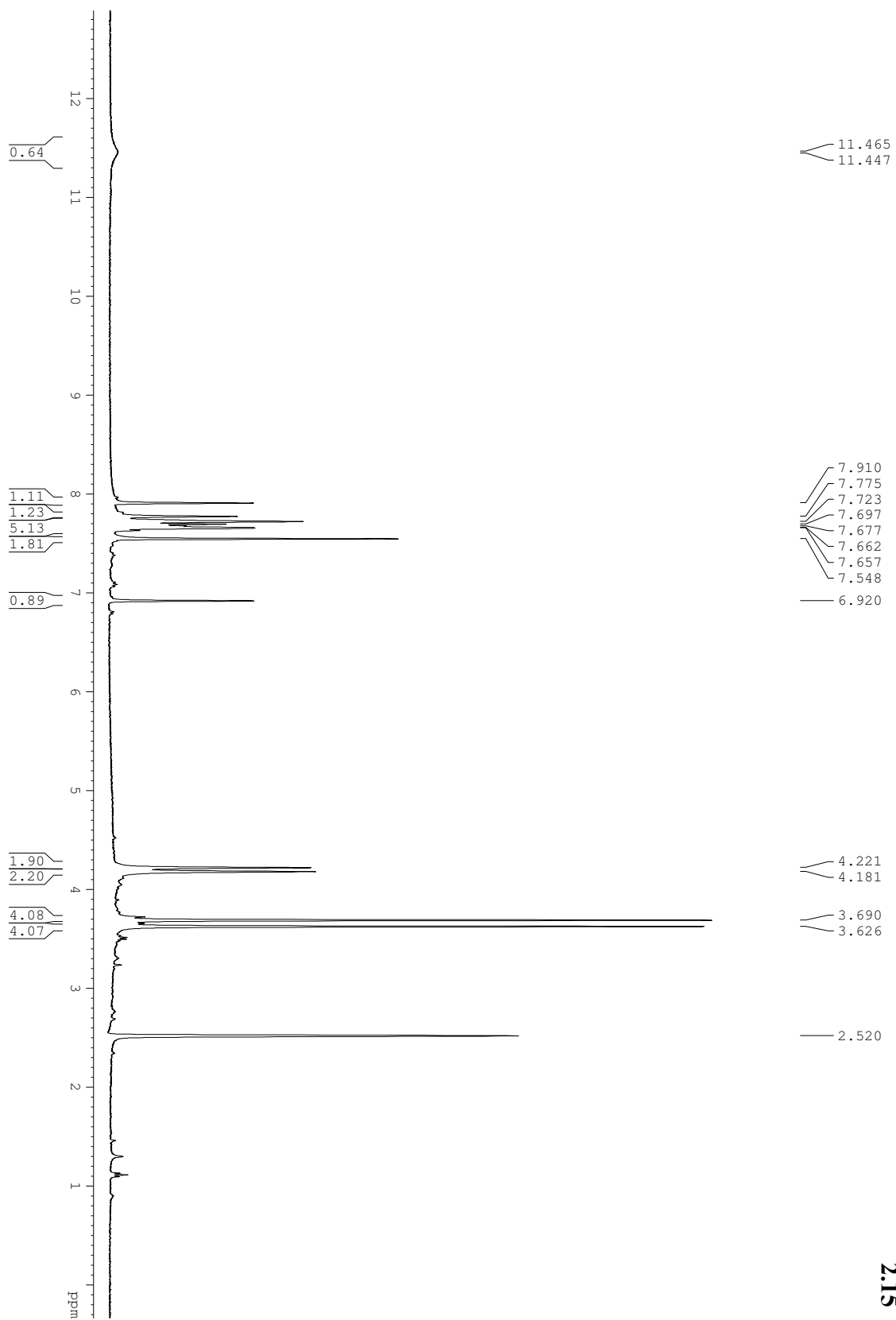


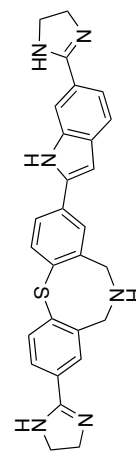
Figure C.49. EC₅₀ curves for 3.58.

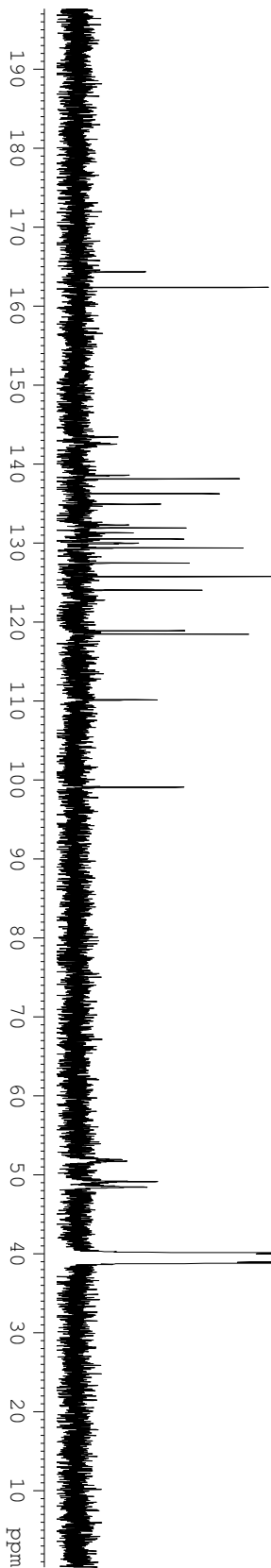
APPENDIX D

SELECTED NMR SPECTRA



2.15

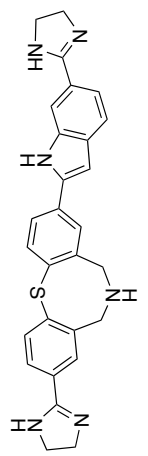


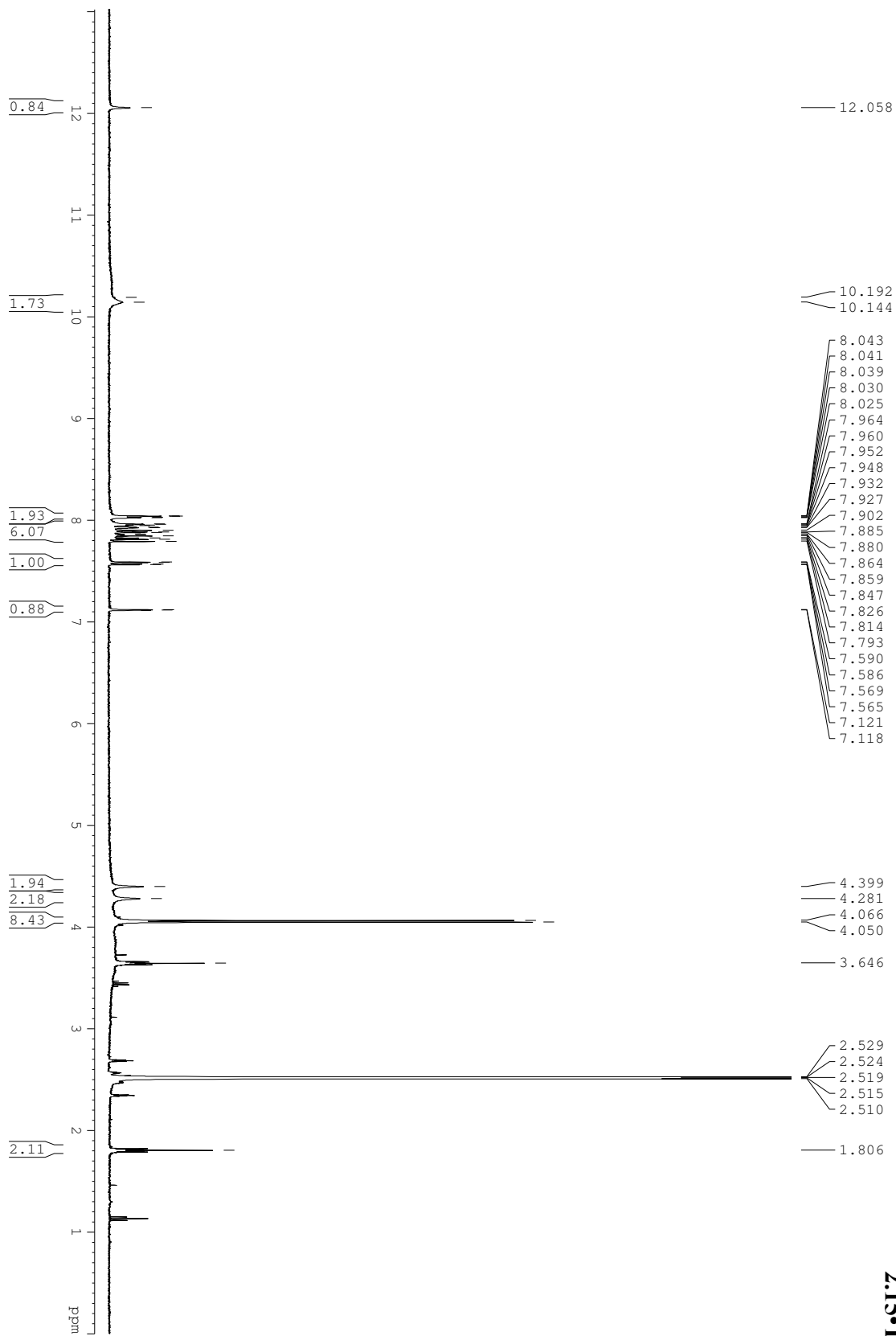


- 164.37
- 162.39
- 143.46
- 142.54
- 138.61
- 138.16
- 136.28
- 134.97
- 132.31
- 131.93
- 131.32
- 130.55
- 130.00
- 129.41
- 127.49
- 125.78
- 124.06
- 118.92
- 118.49
- 110.16
- 99.10

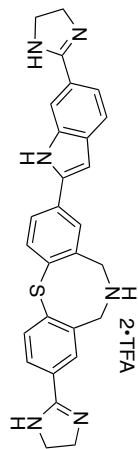
- 51.73
- 49.15
- 48.43
- 40.11
- 39.90
- 39.69
- 39.48
- 39.28
- 39.07
- 38.86

2.15





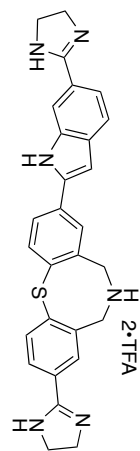
2.15-TFA



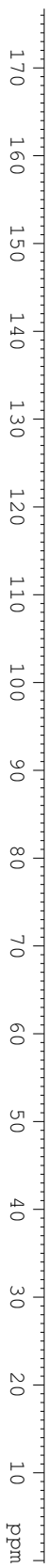
43-534-2-1-DMSO-400MHz-100C

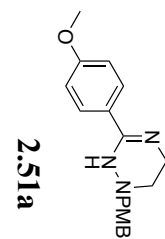
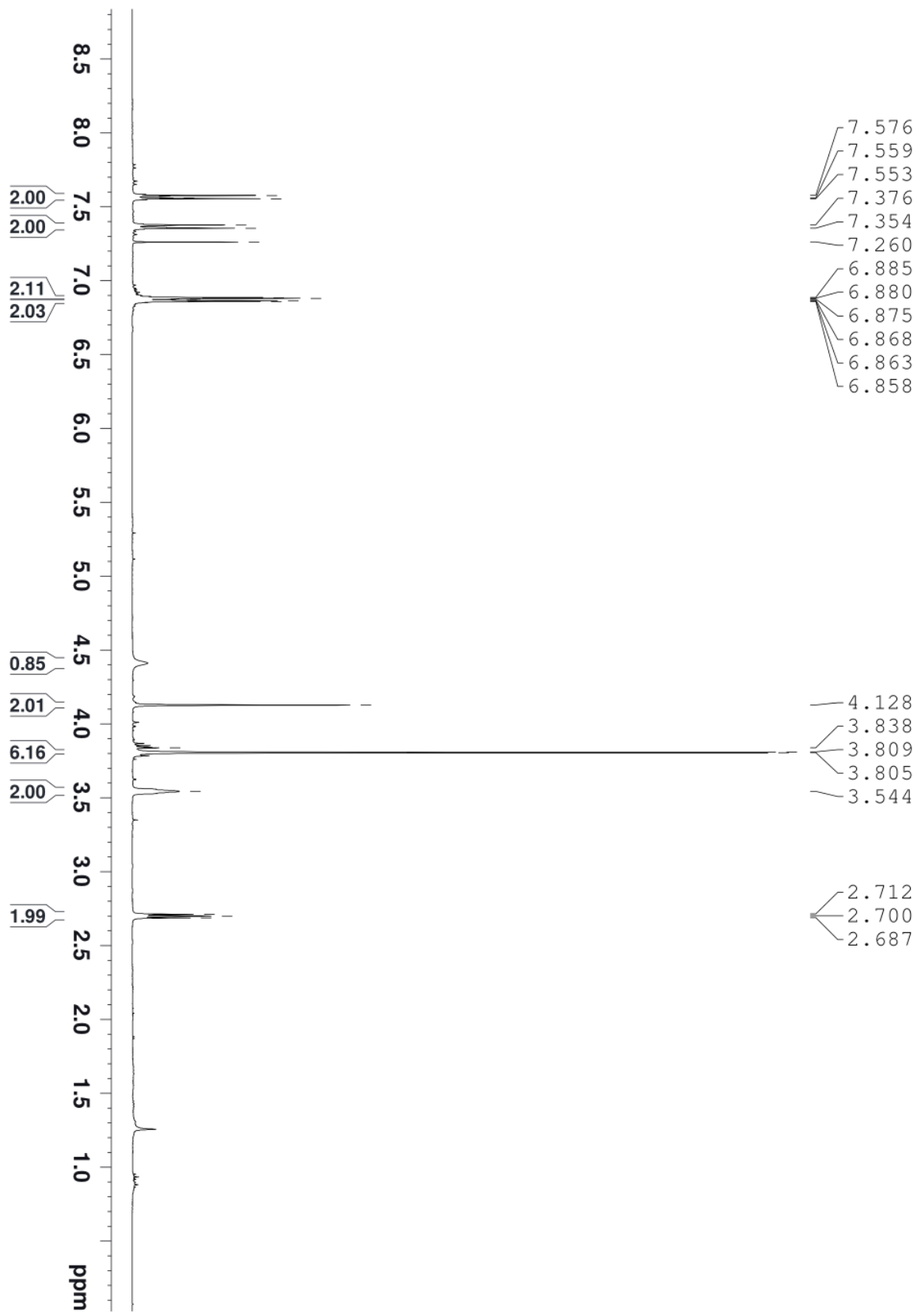
166.39
158.48
158.17
158.12
155.30
139.14
136.03
130.41
129.54
129.47
129.45
128.92
128.81
127.50
127.04
126.66
118.94
118.52
118.02
117.16
113.67
113.17
110.45
98.15

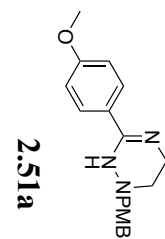
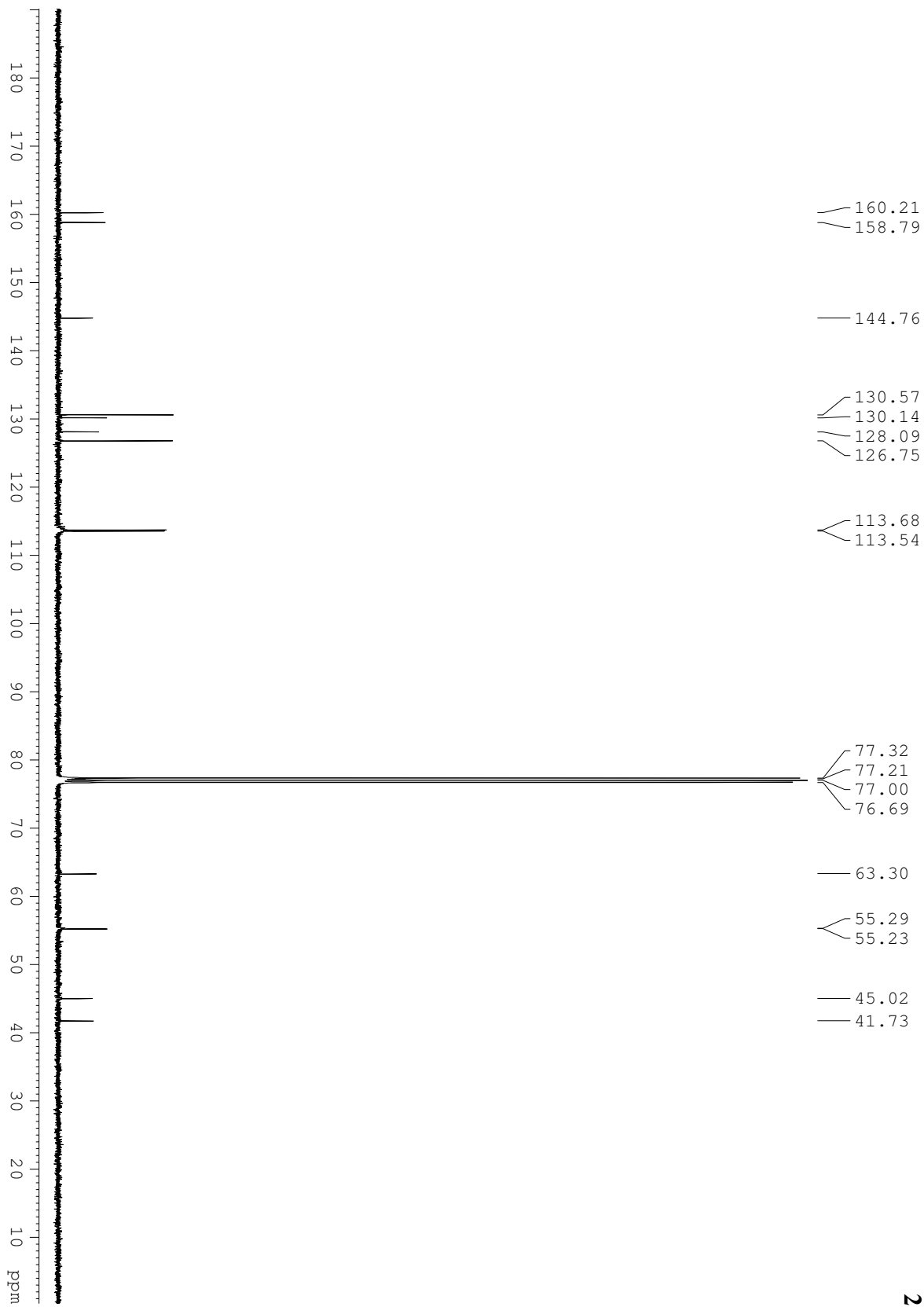
59.32
54.61
54.14
48.27
48.18
40.13
39.92
39.71
39.50
39.29
39.08
38.87

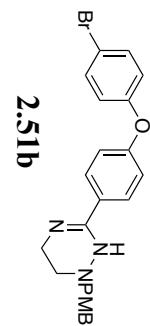
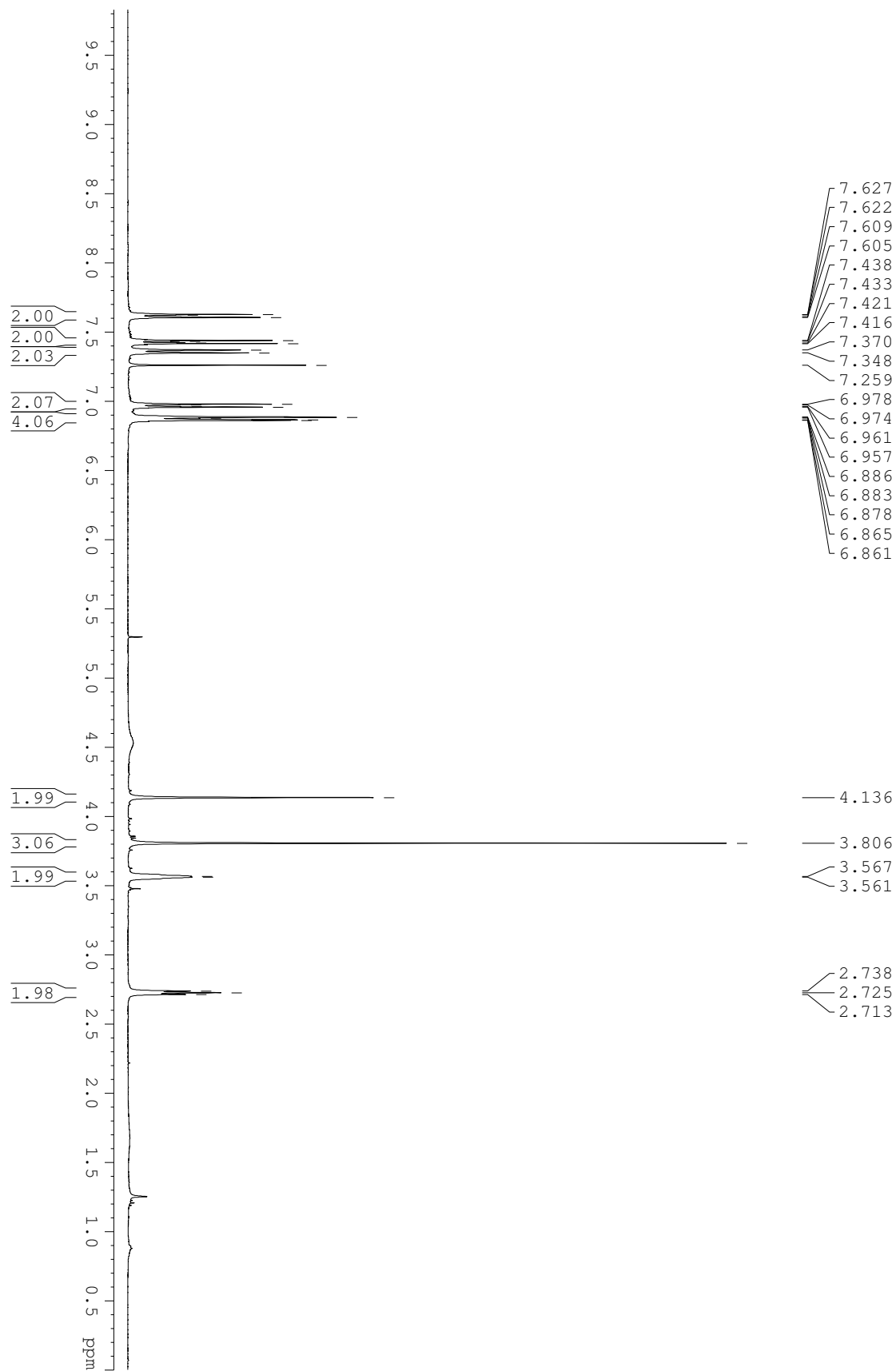


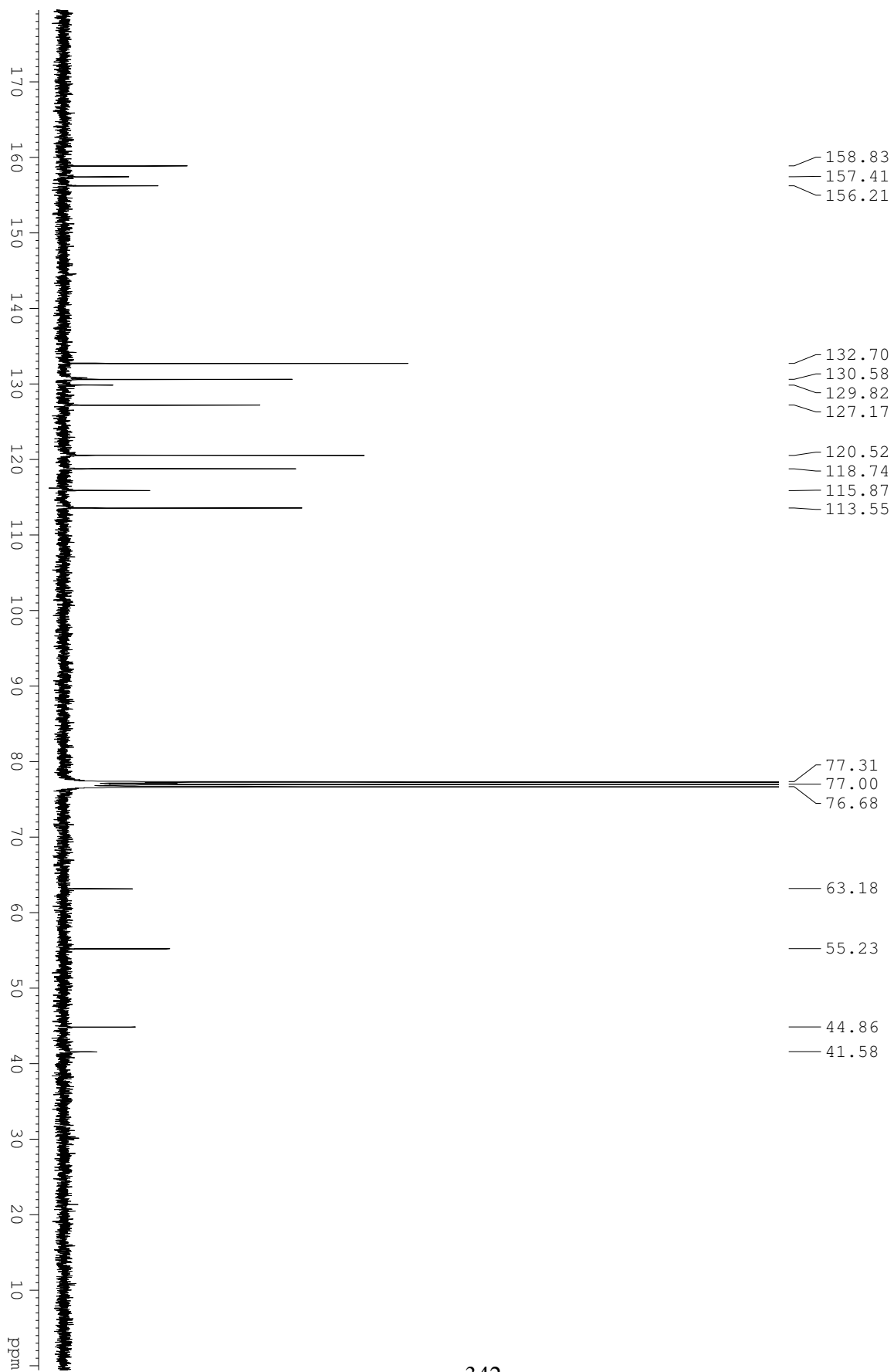
2.15•TFA

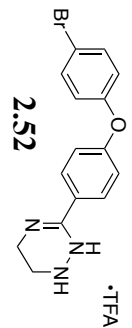
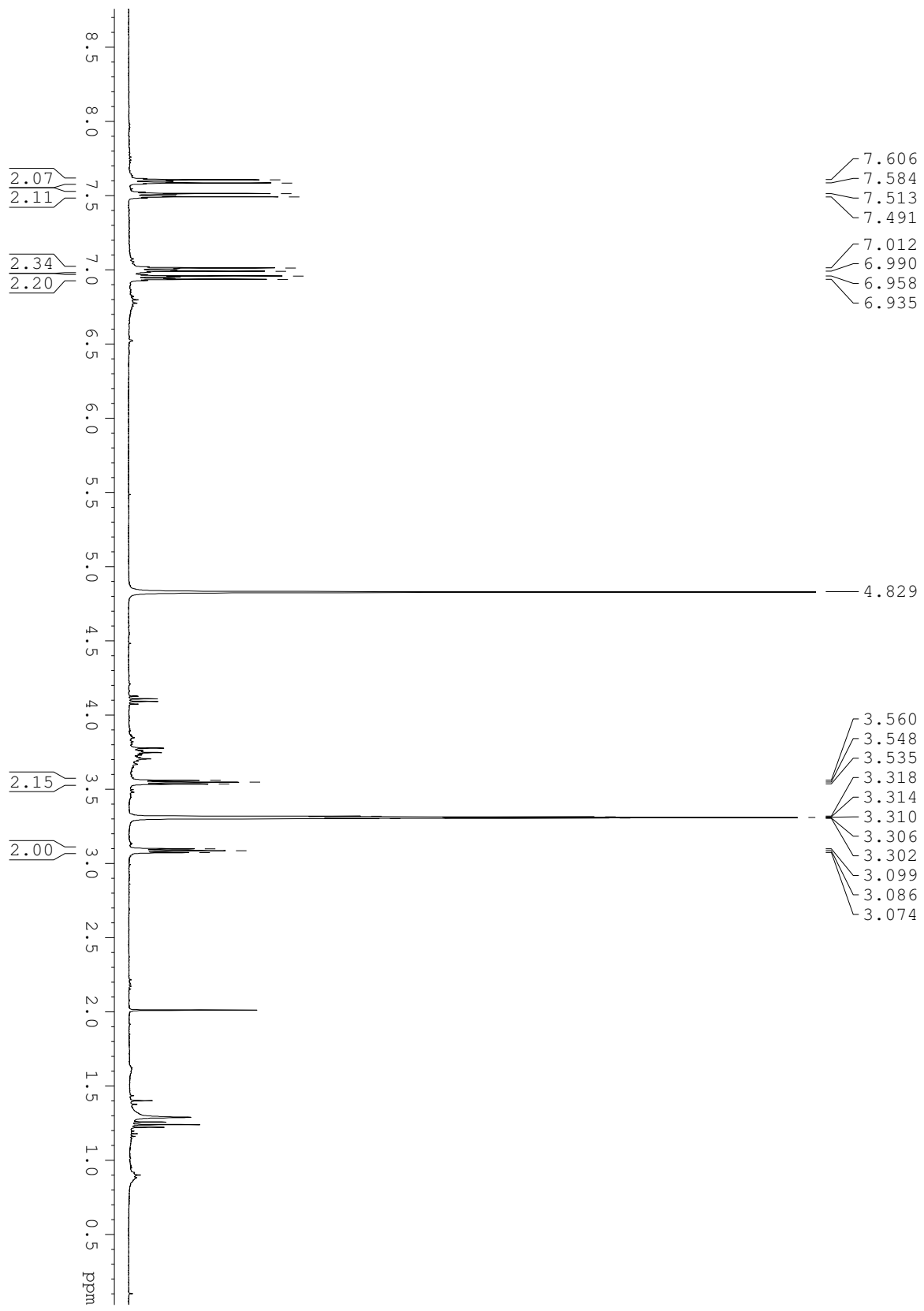


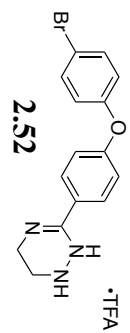
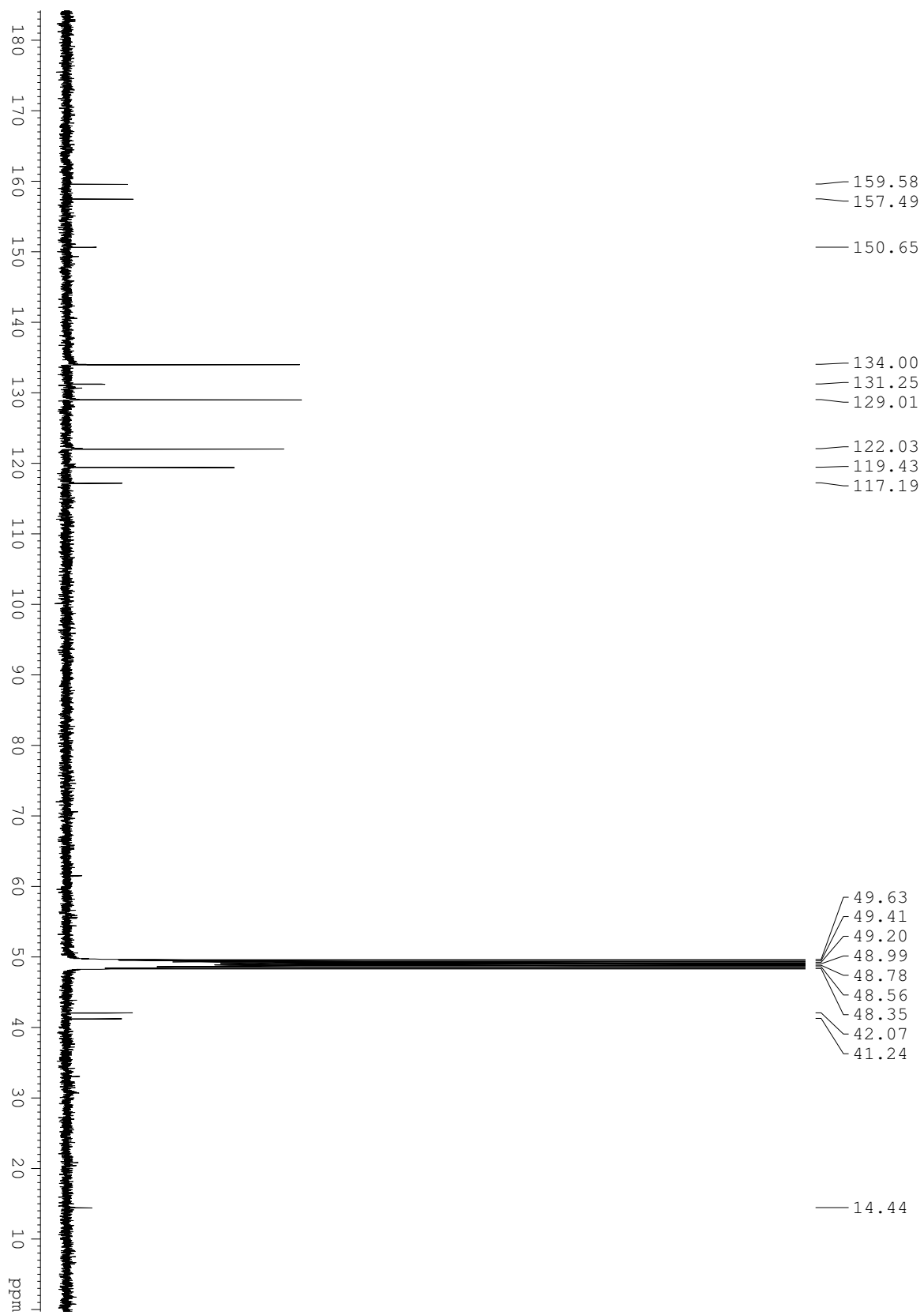


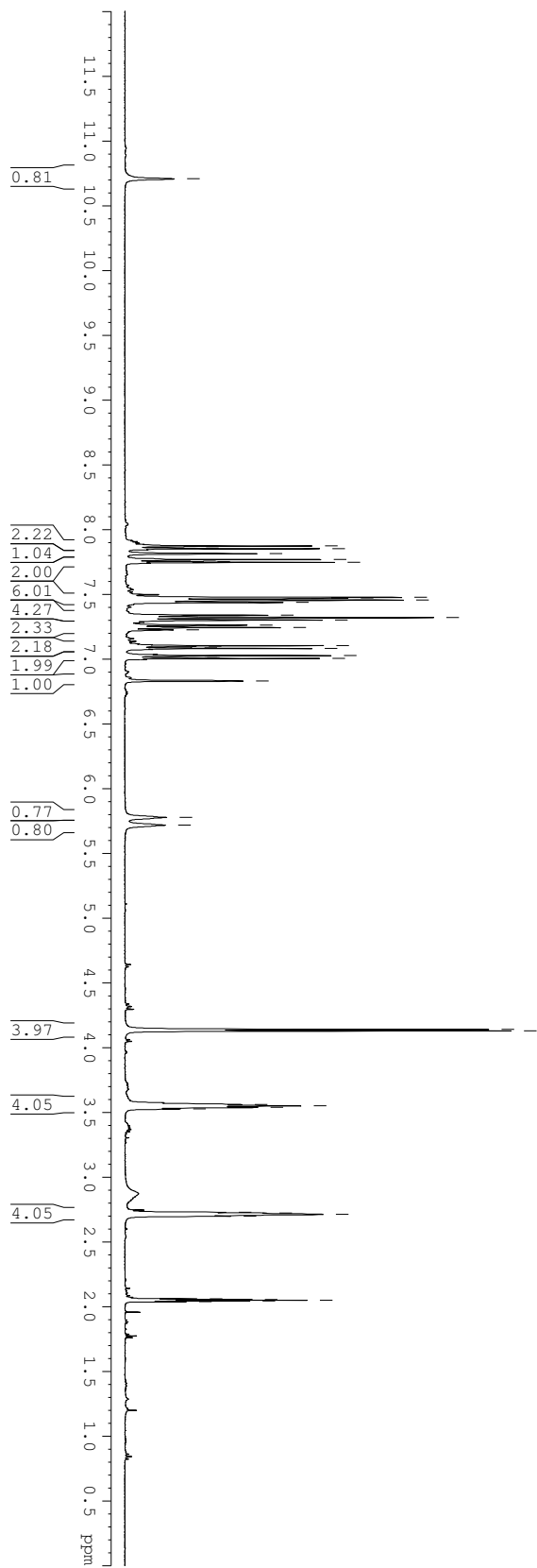












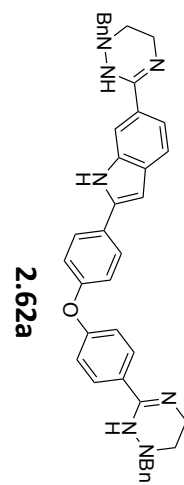
10.710

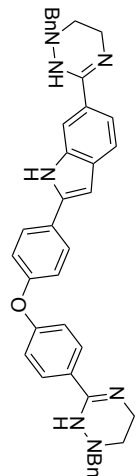
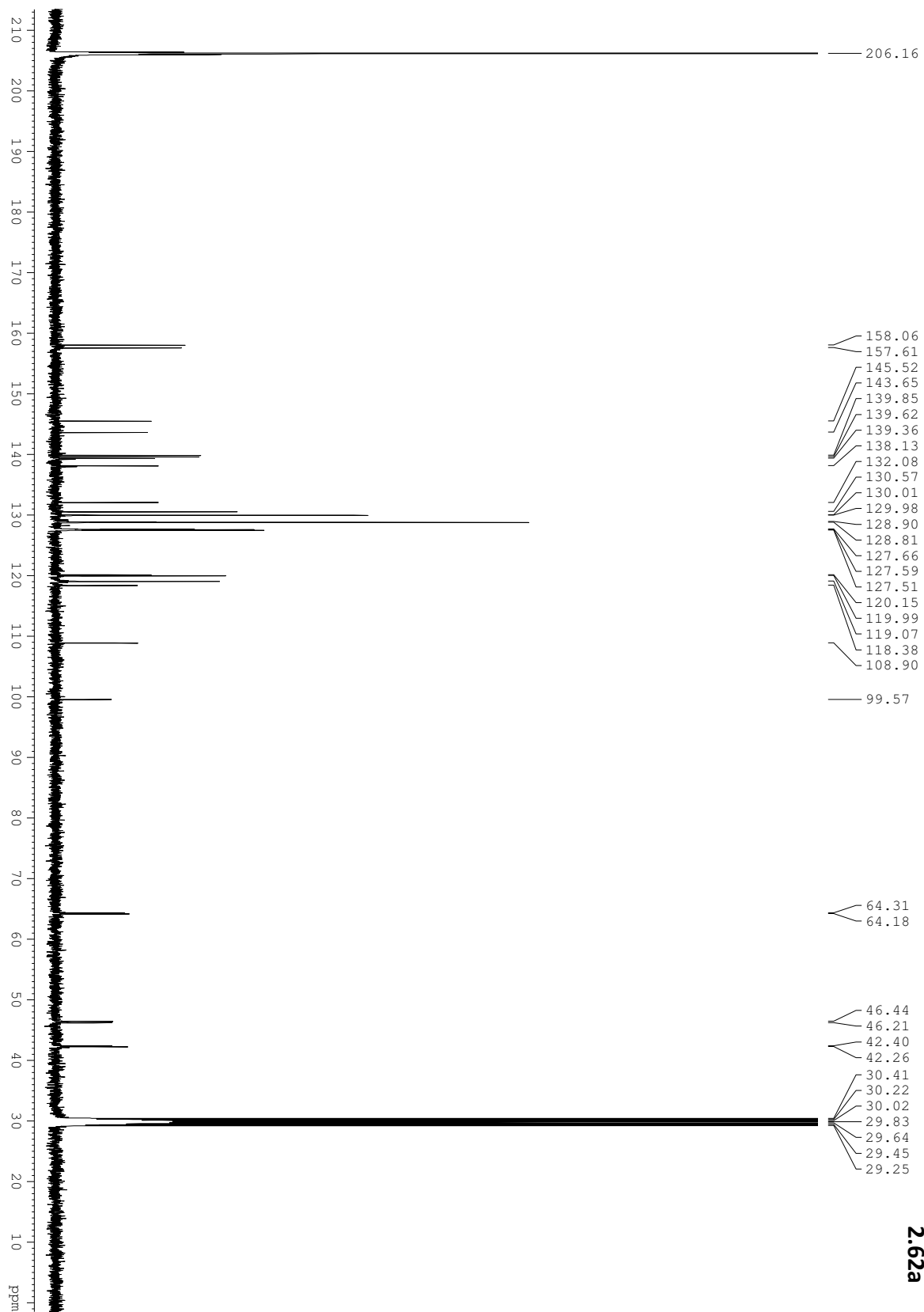
7.875
7.870
7.858
7.853
7.816
7.770
7.765
7.753
7.748
7.478
7.473
7.469
7.457
7.439
7.340
7.322
7.303
7.263
7.245
7.227
7.105
7.100
7.088
7.083
7.028
7.023
7.011
7.006
6.832
5.779
5.719

4.142
4.130

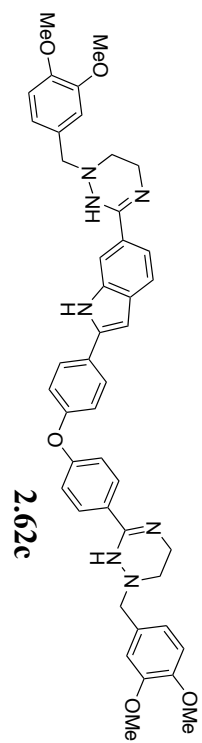
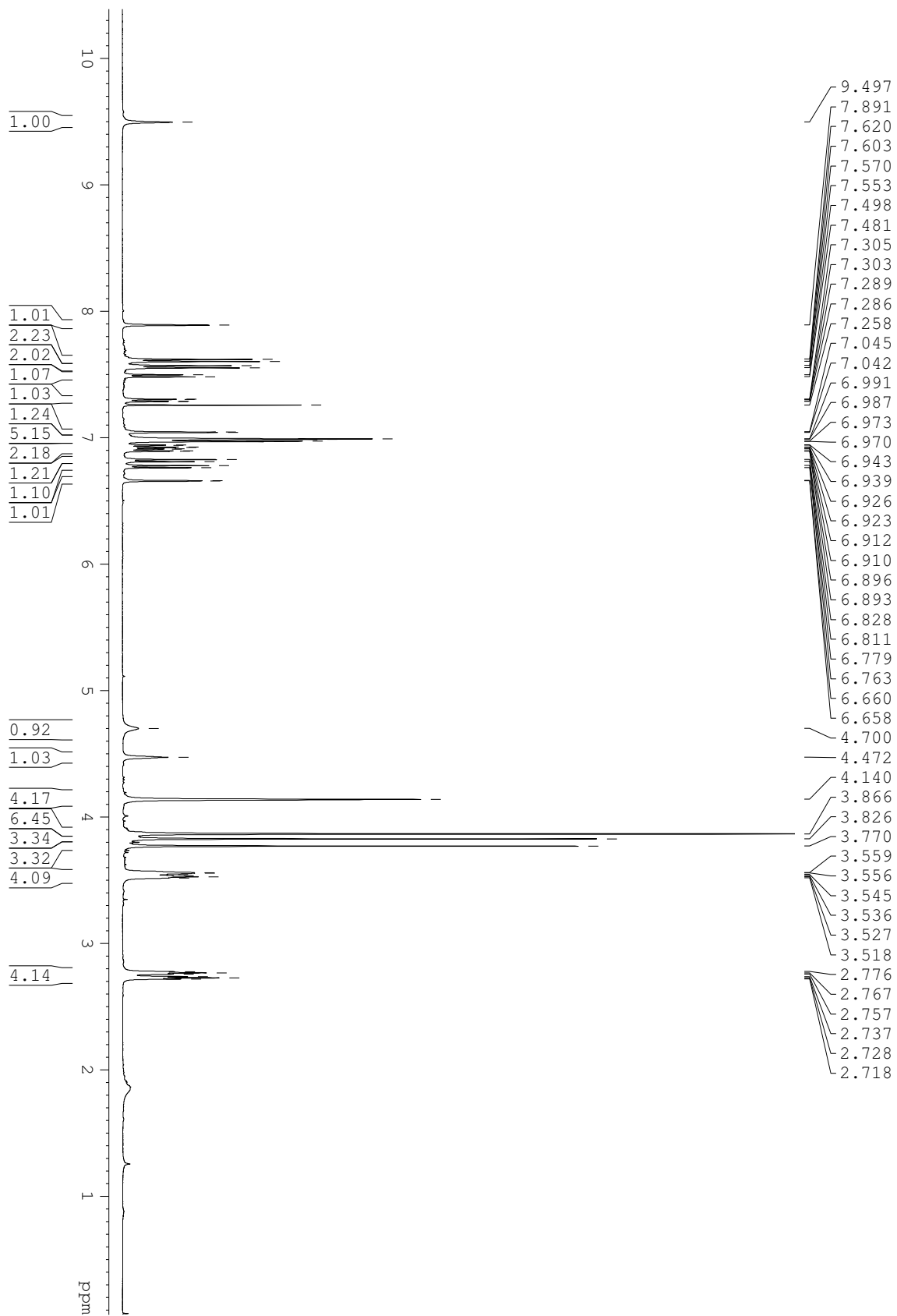
3.562
3.552
3.540
3.528

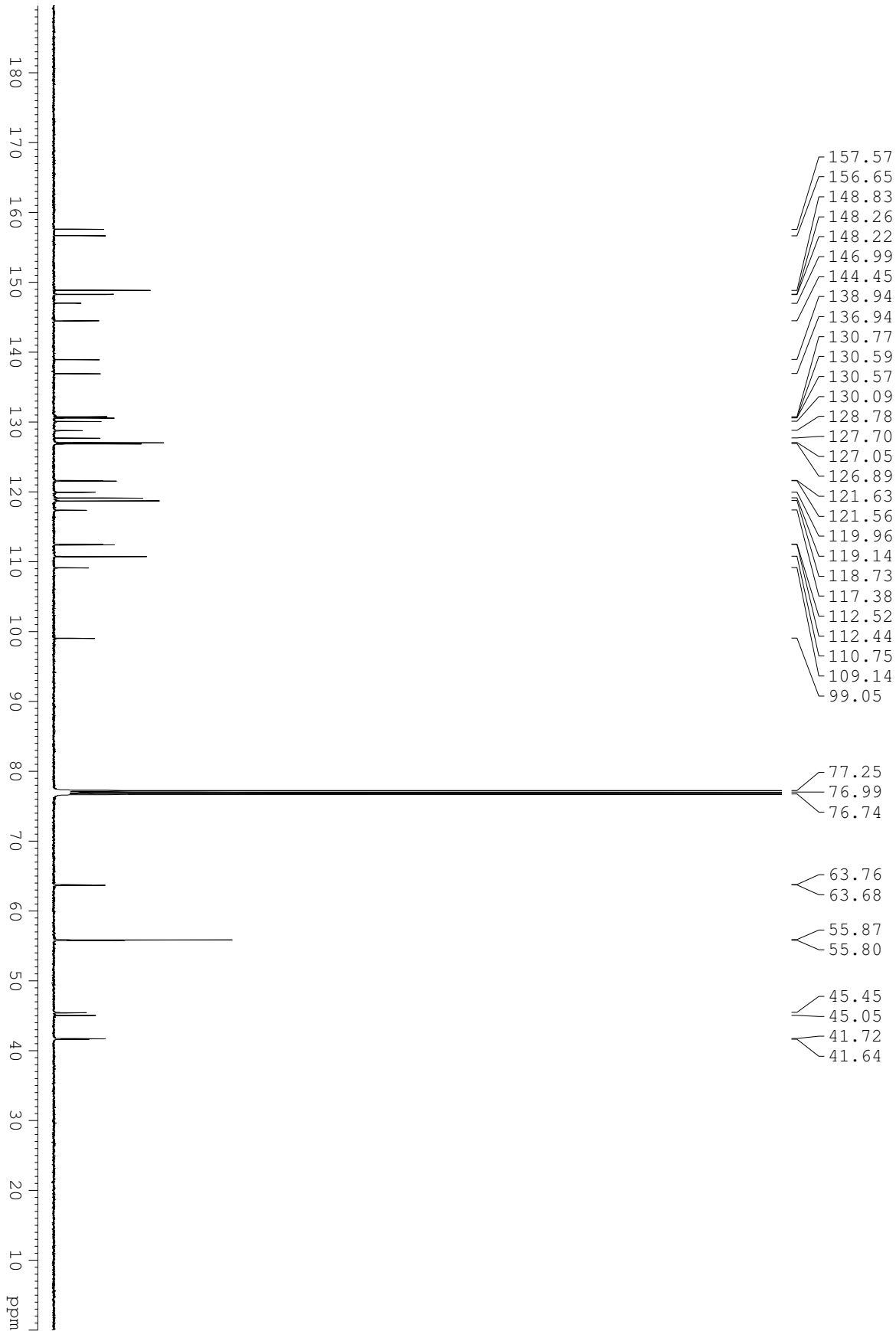
2.730
2.724
2.714
2.700
2.061
2.056
2.050
2.045
2.039

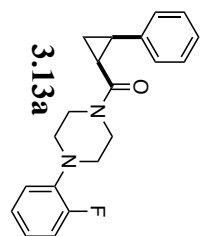
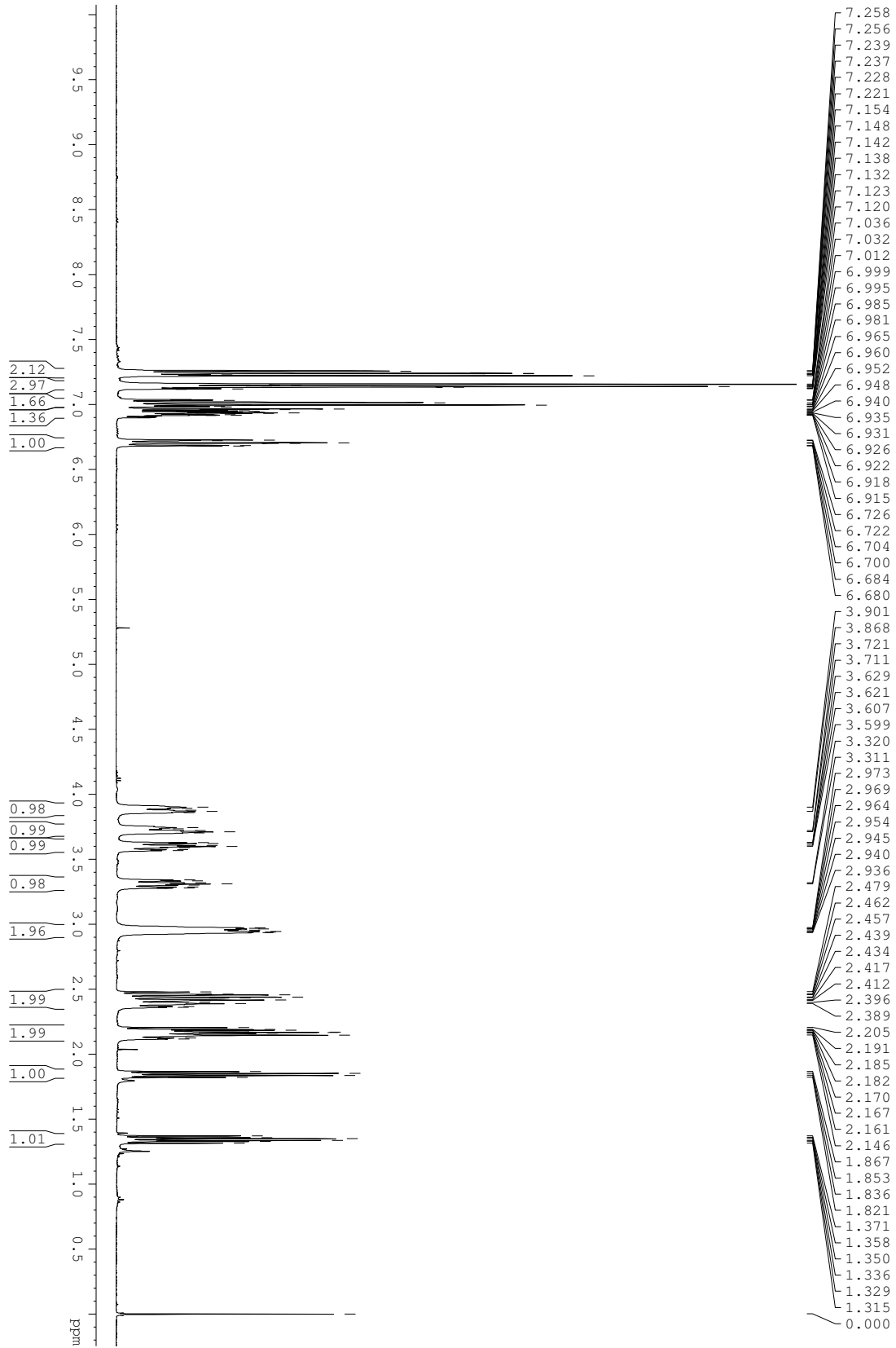


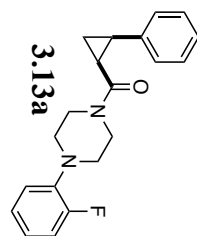
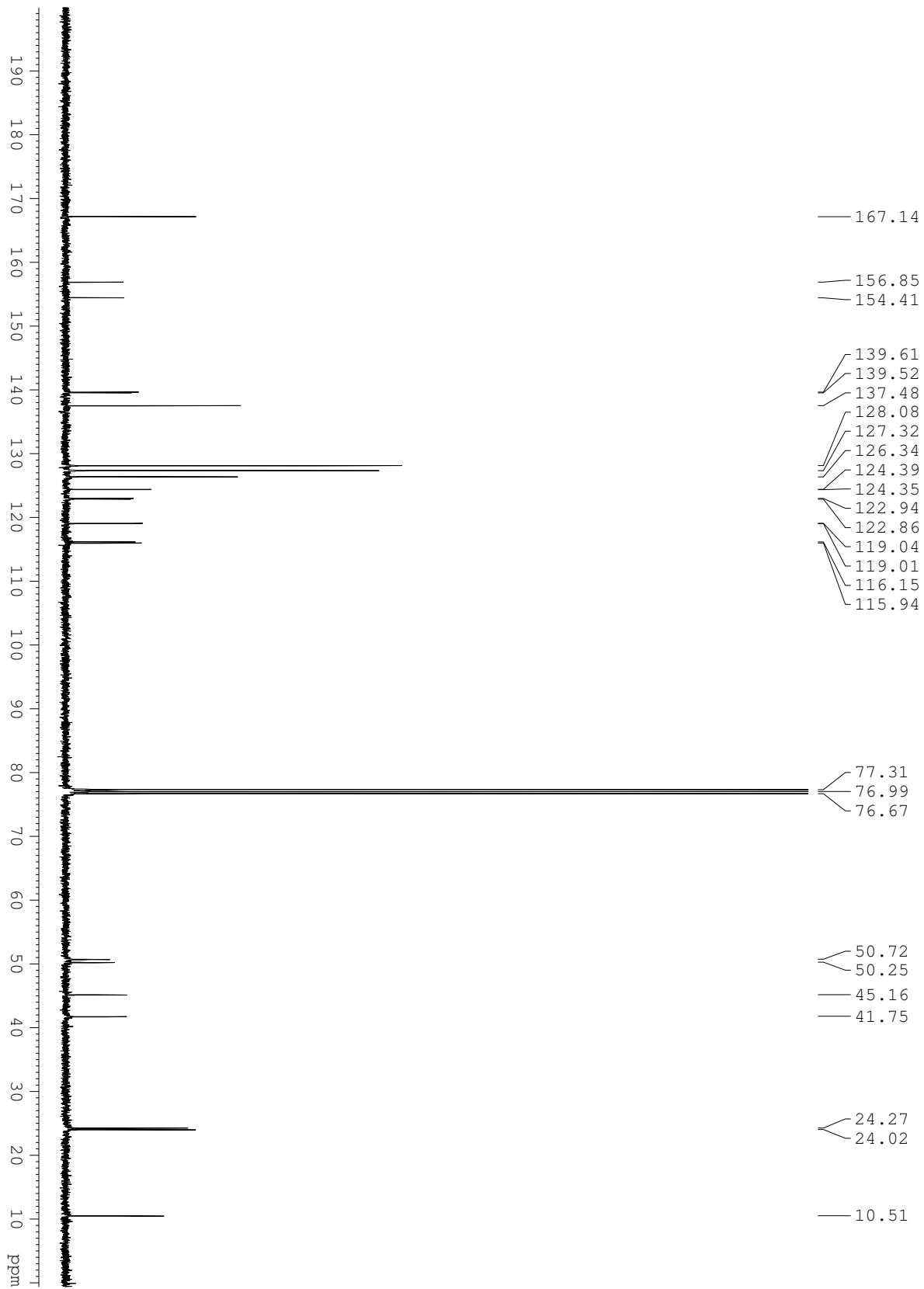


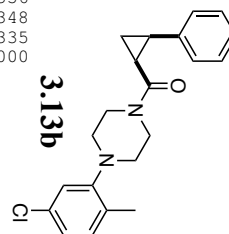
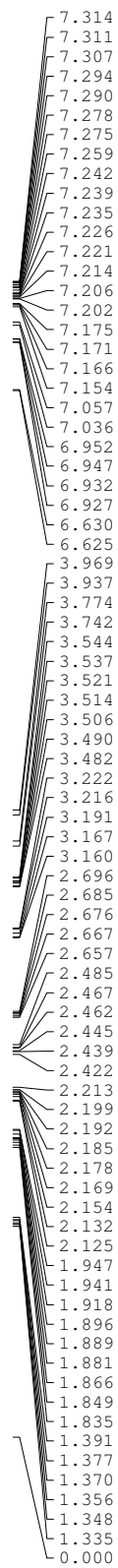
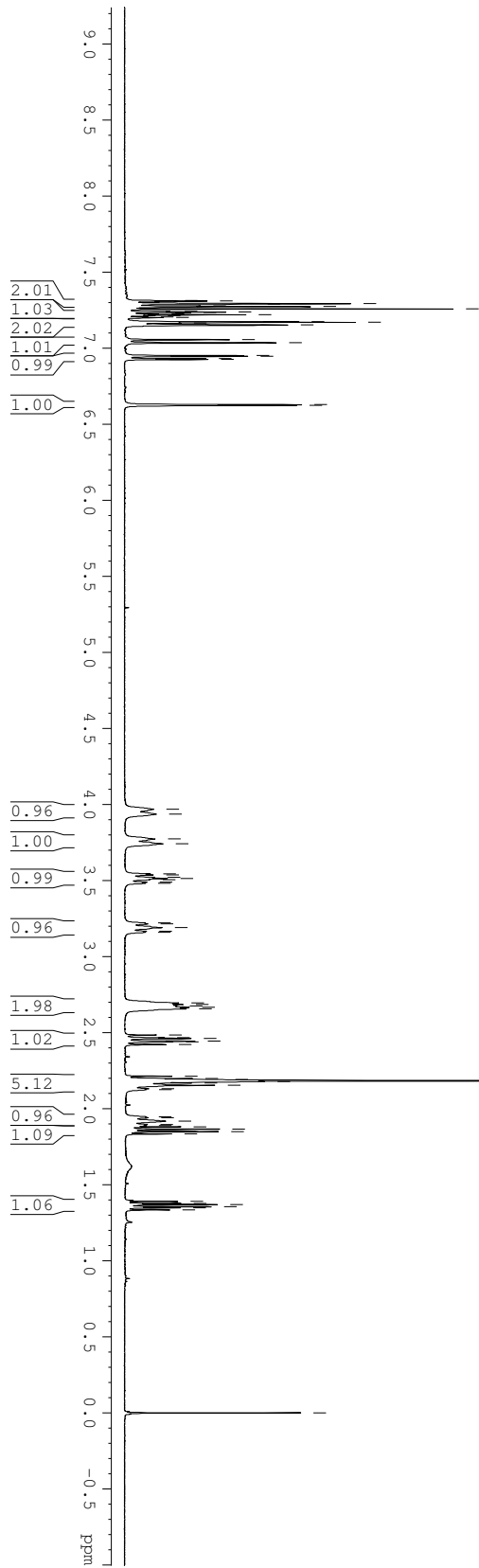
2.62a

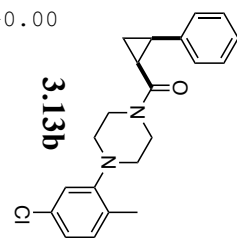
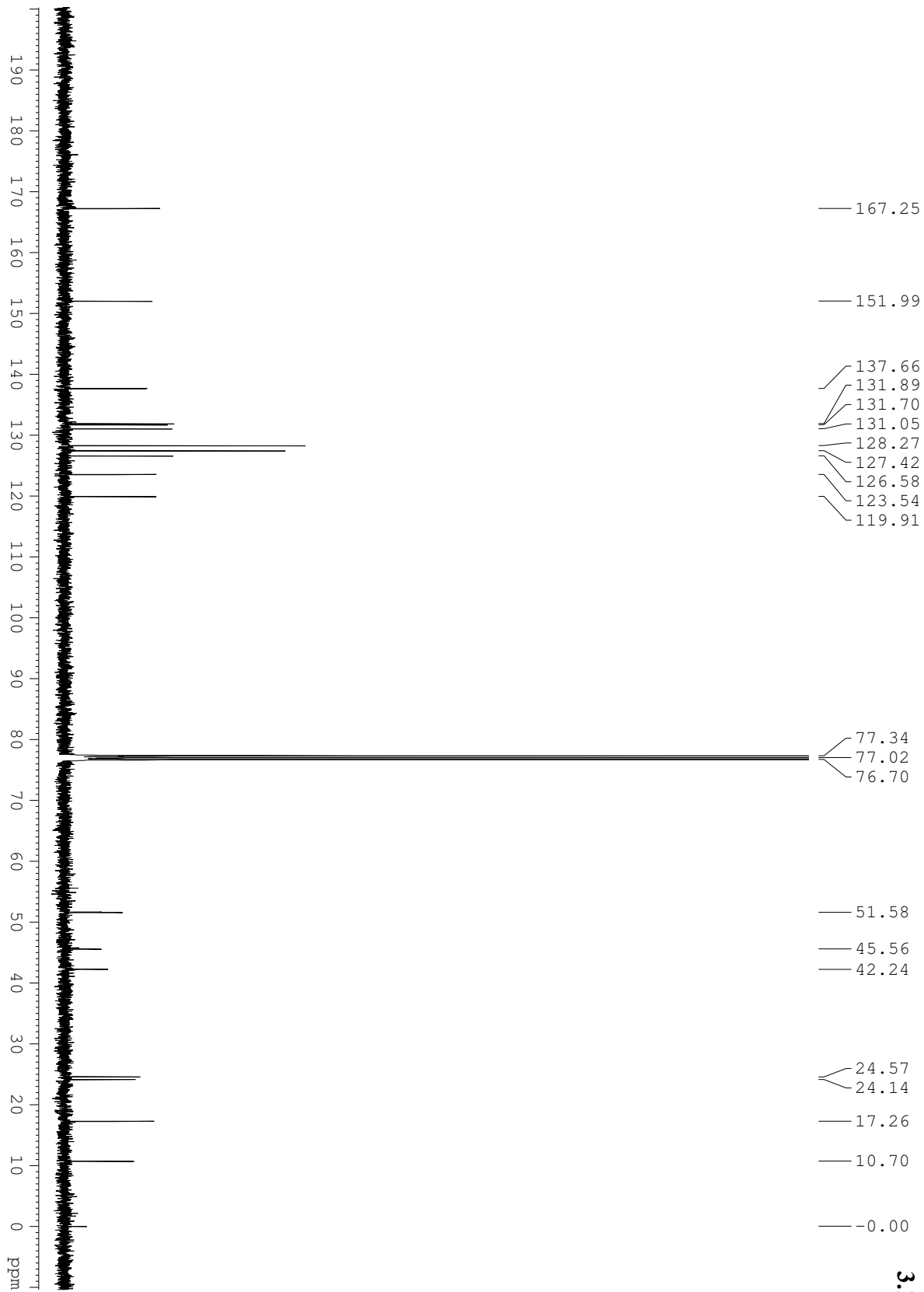


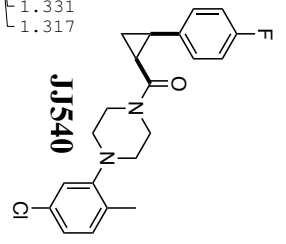
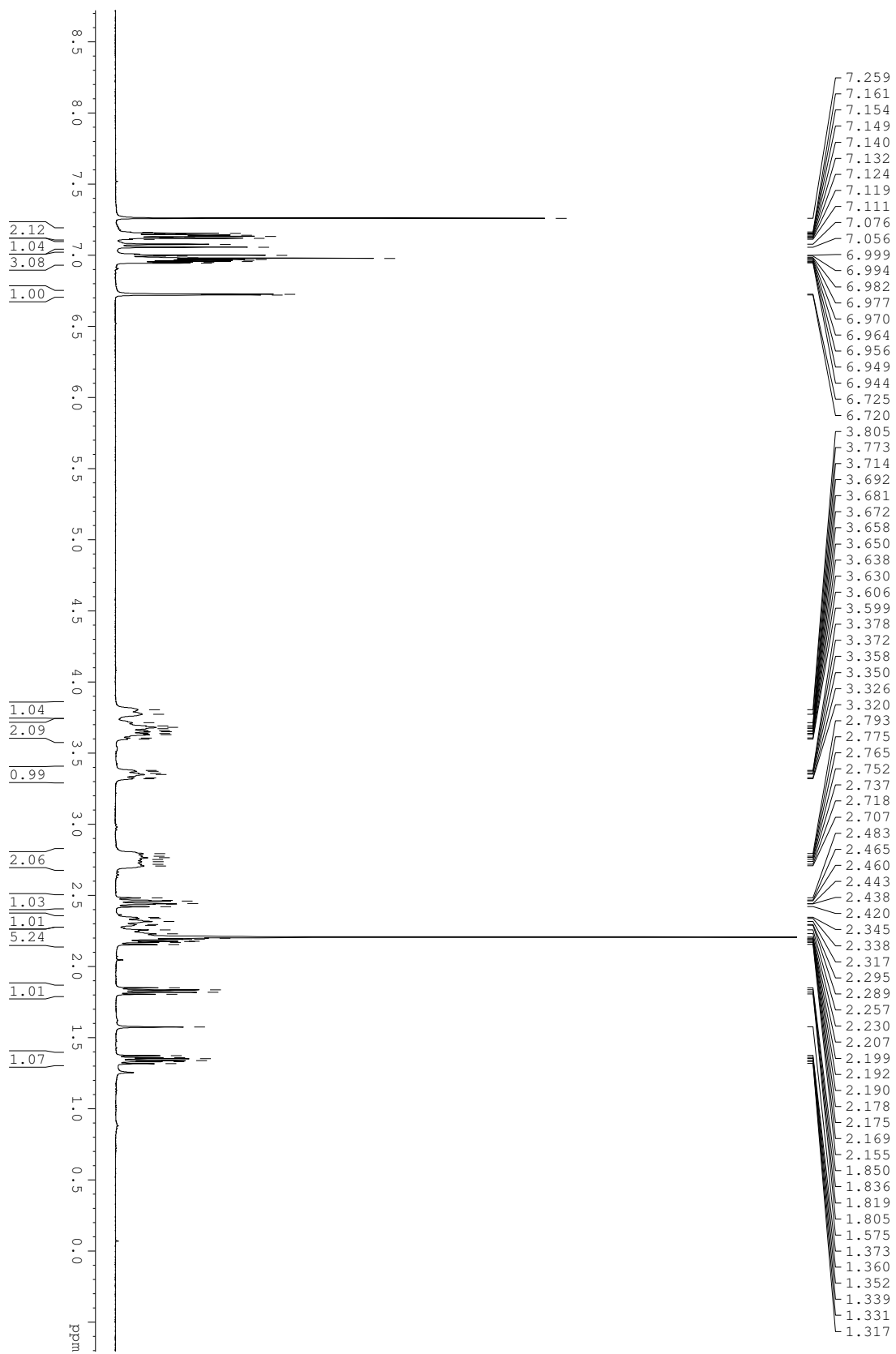


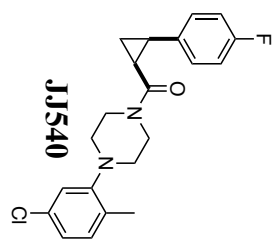
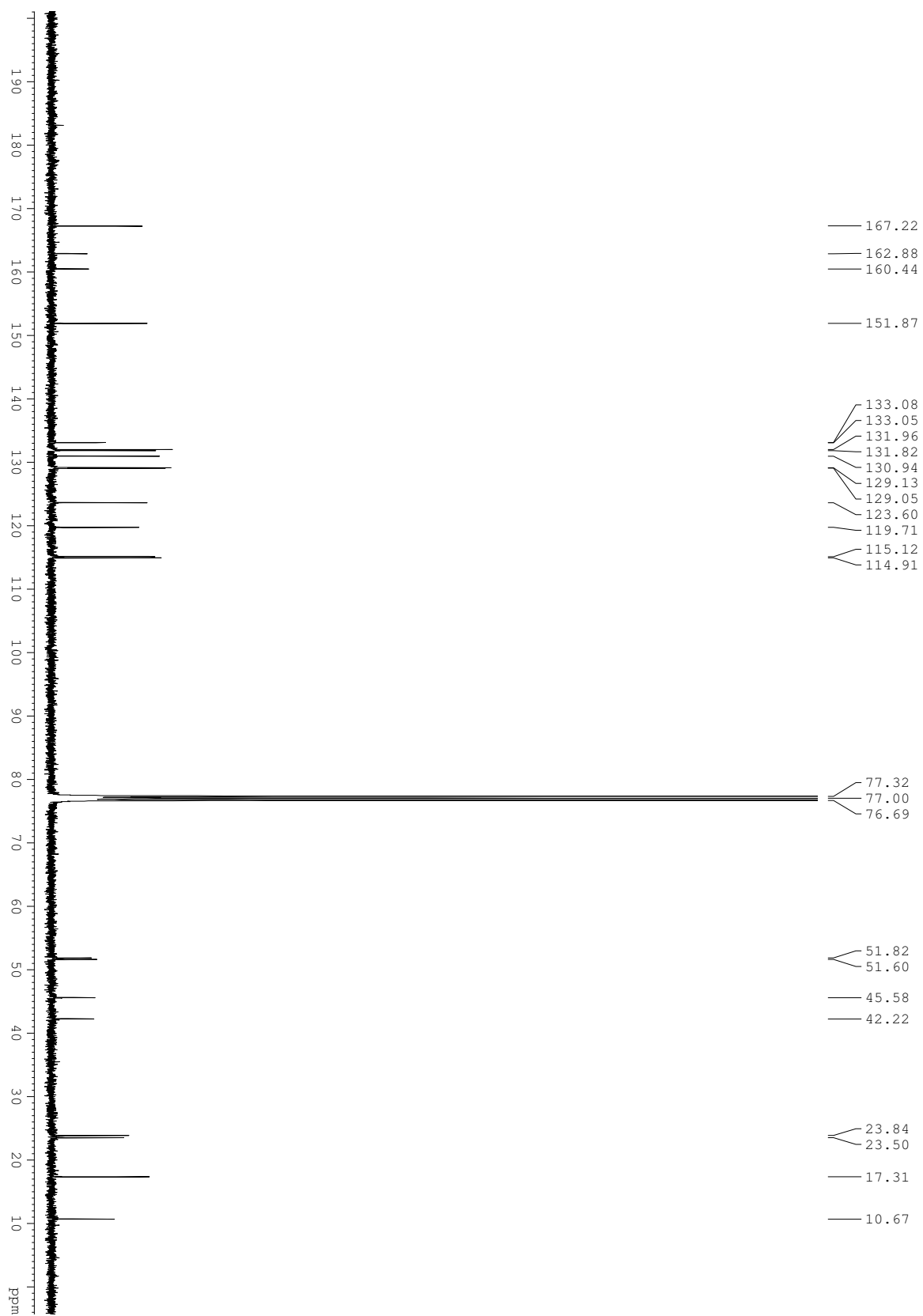


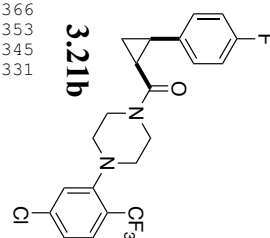
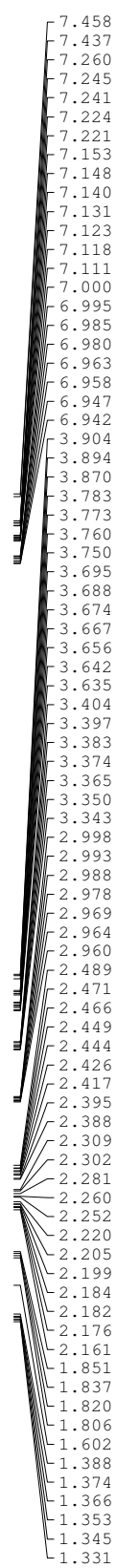
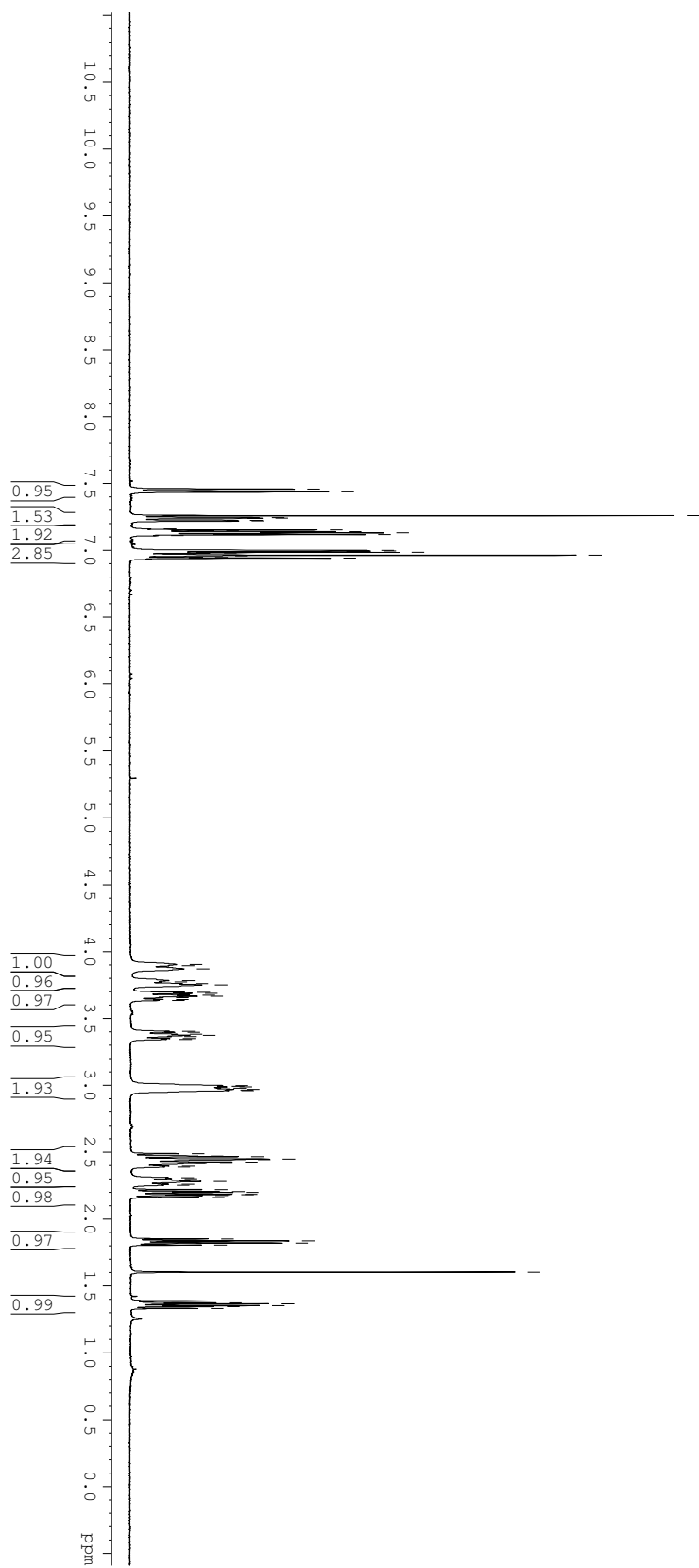


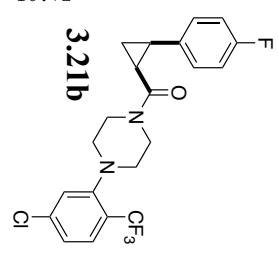
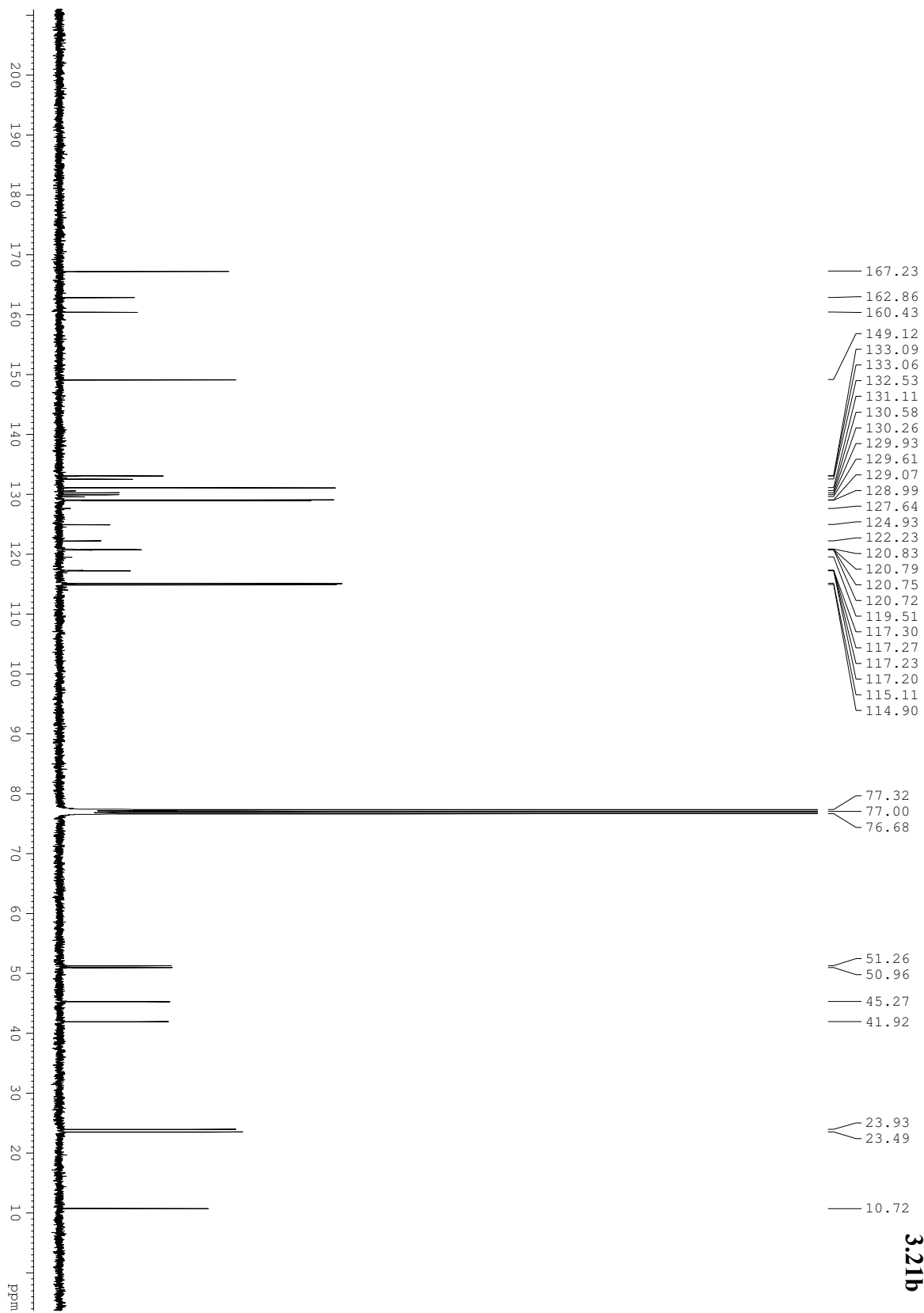


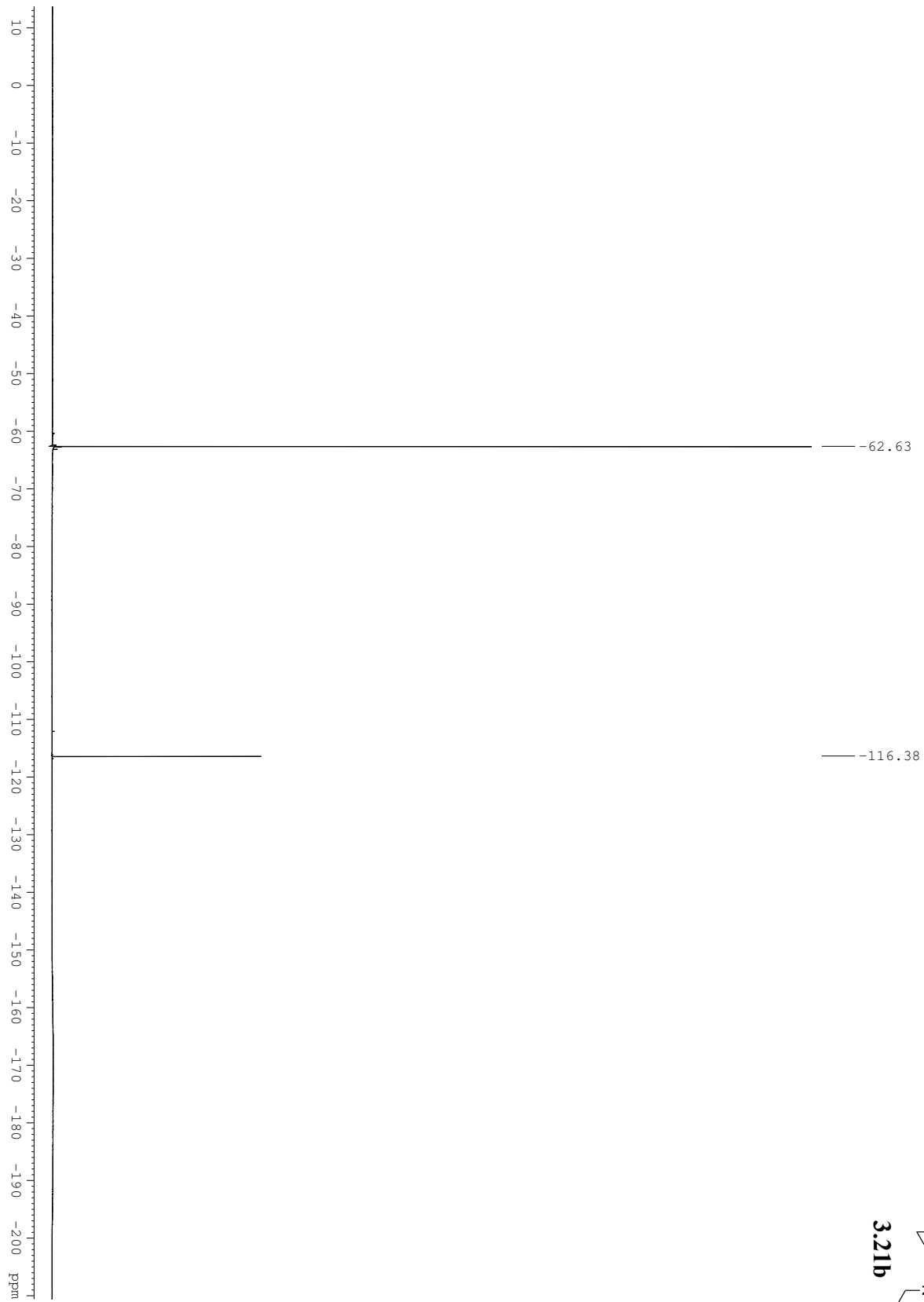
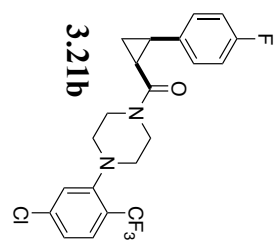


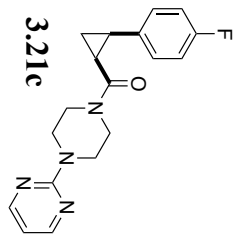
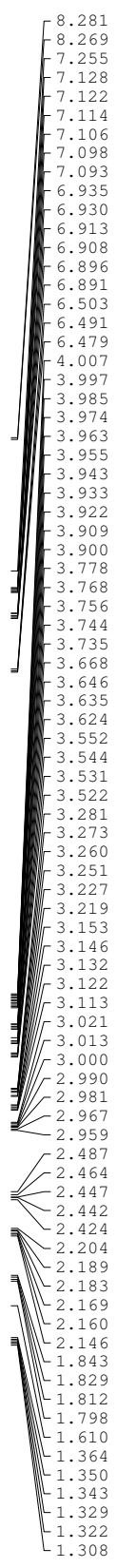
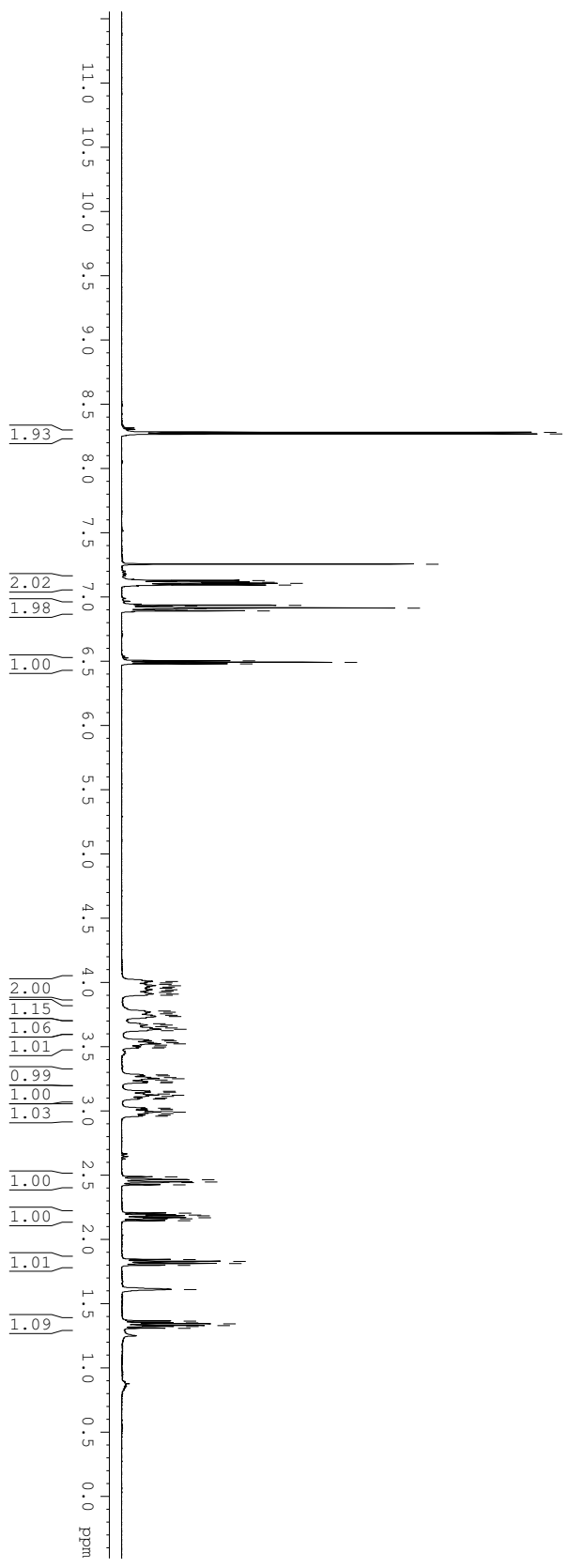


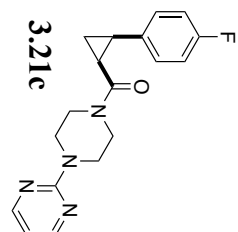
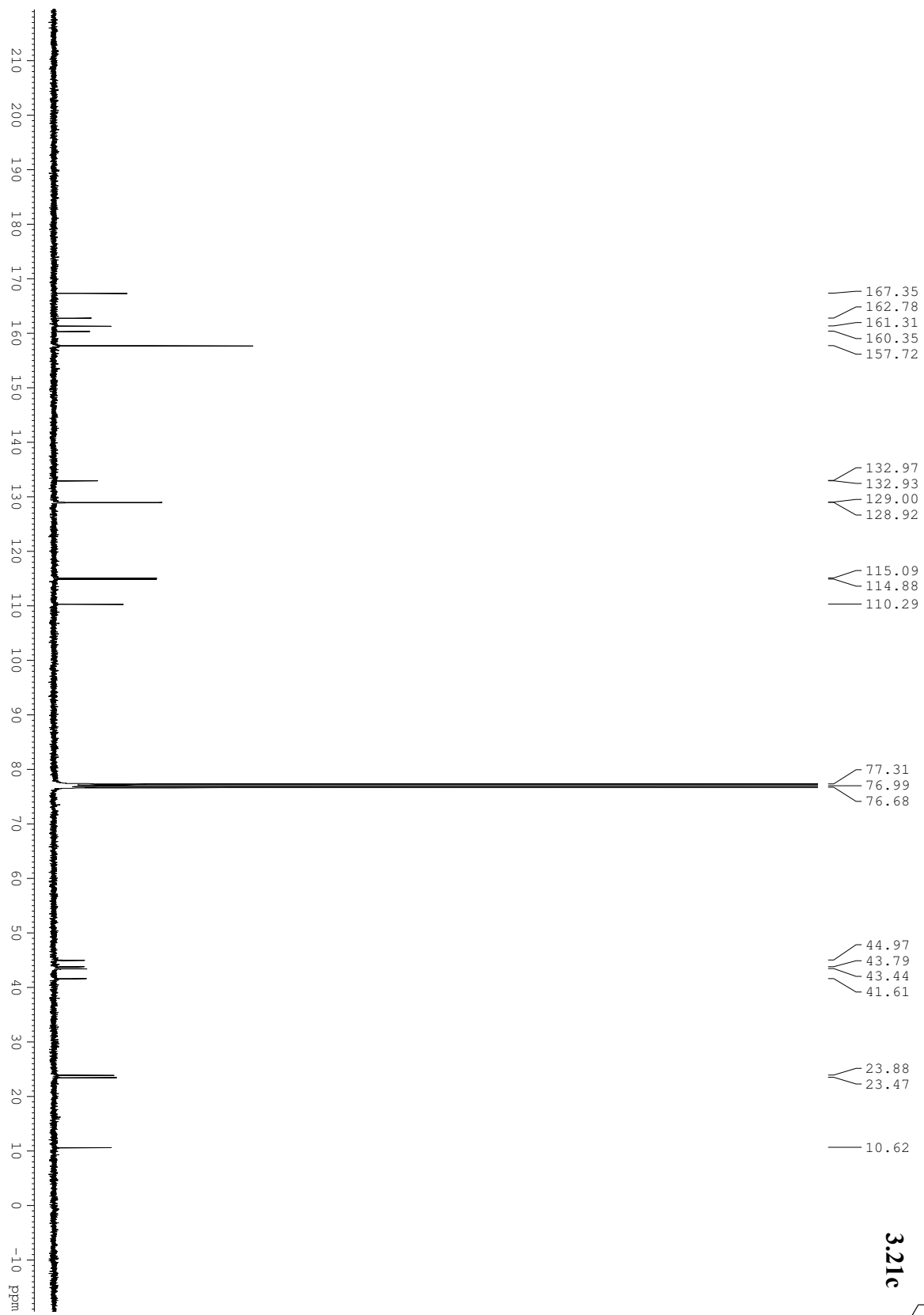


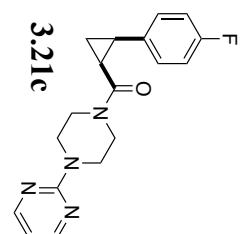




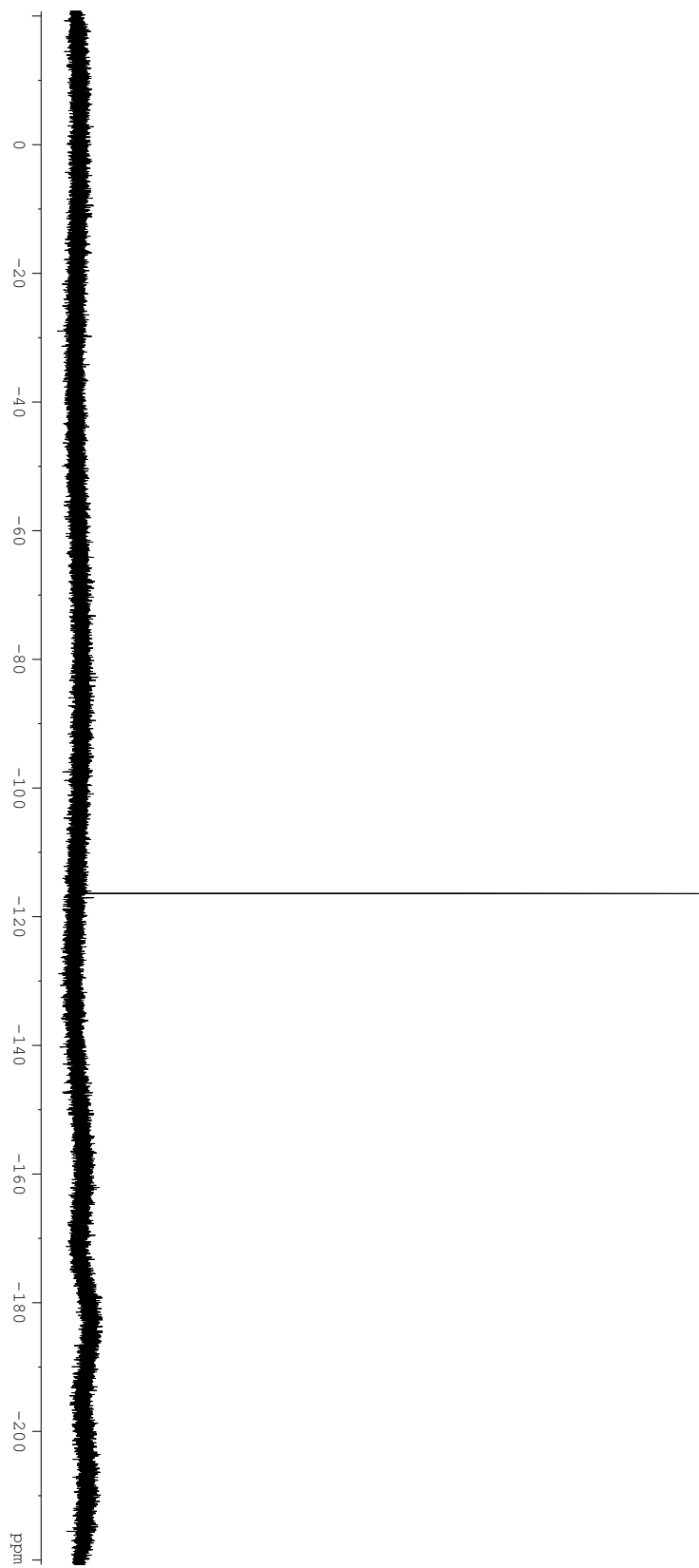


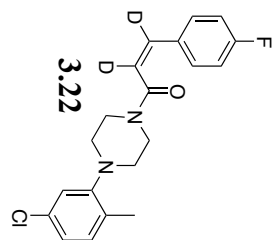
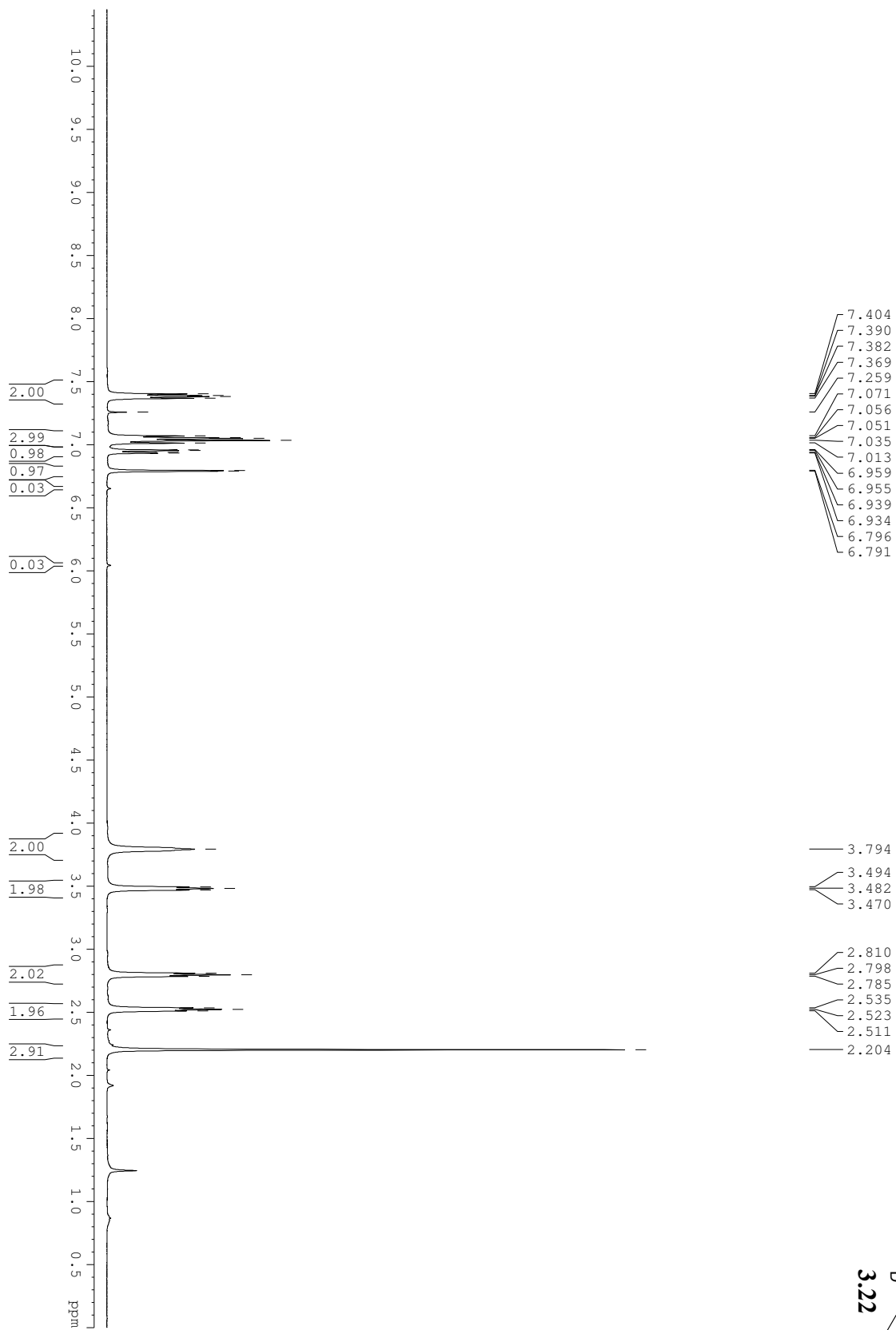


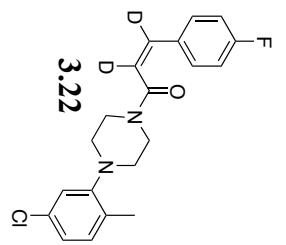
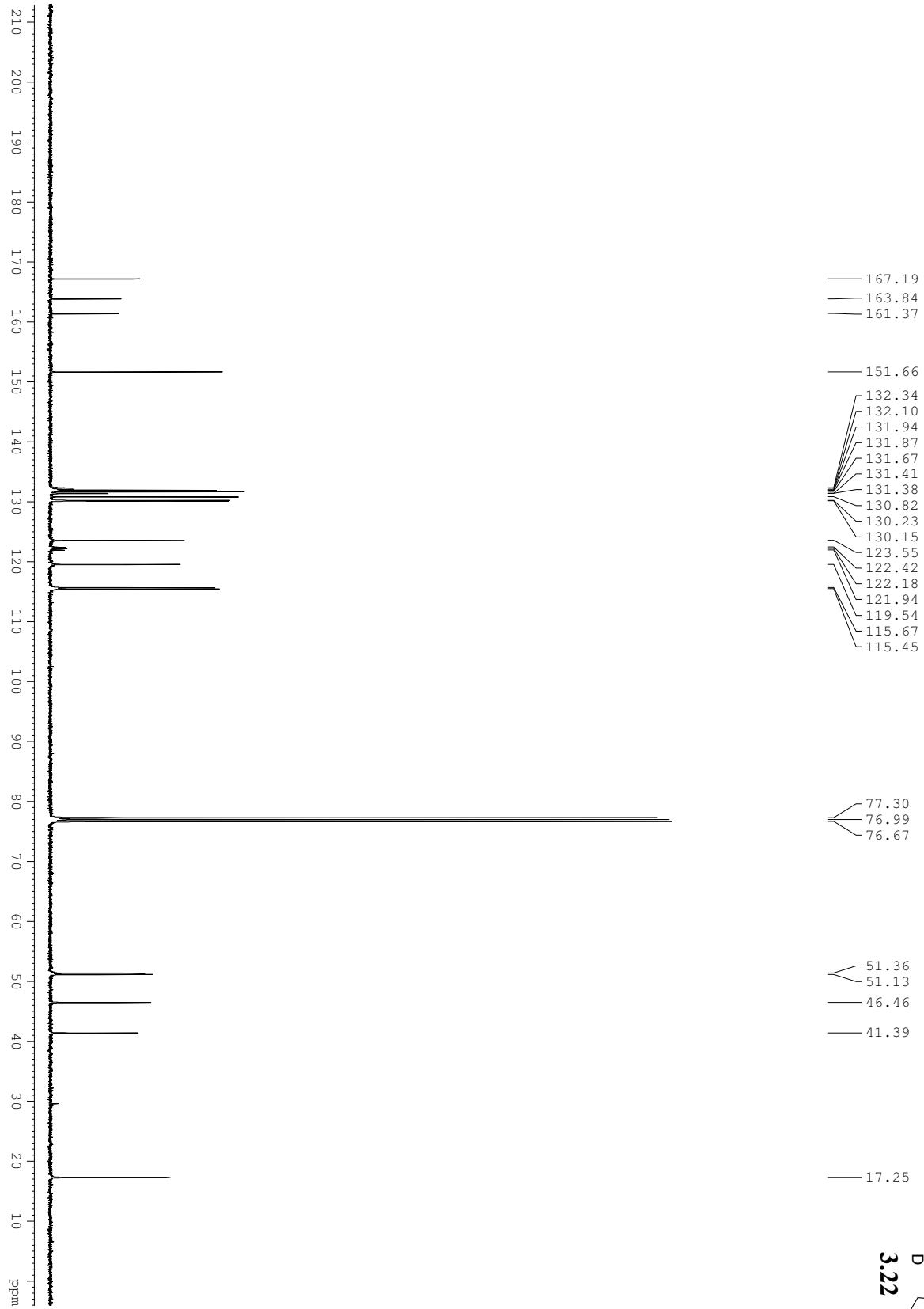


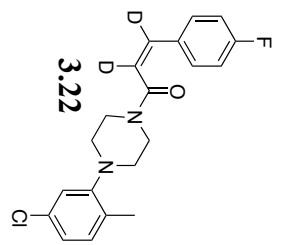


— -116.37



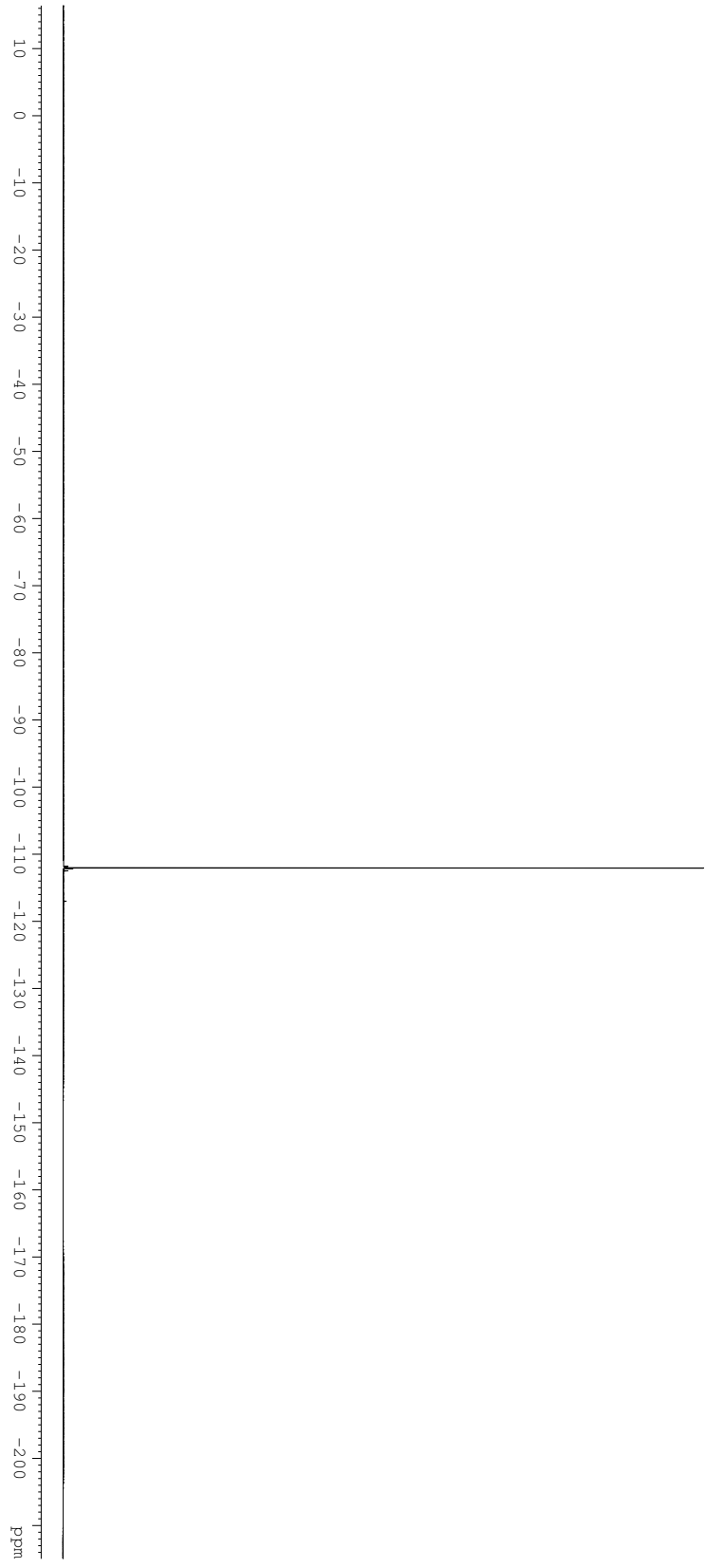


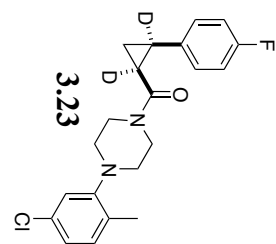
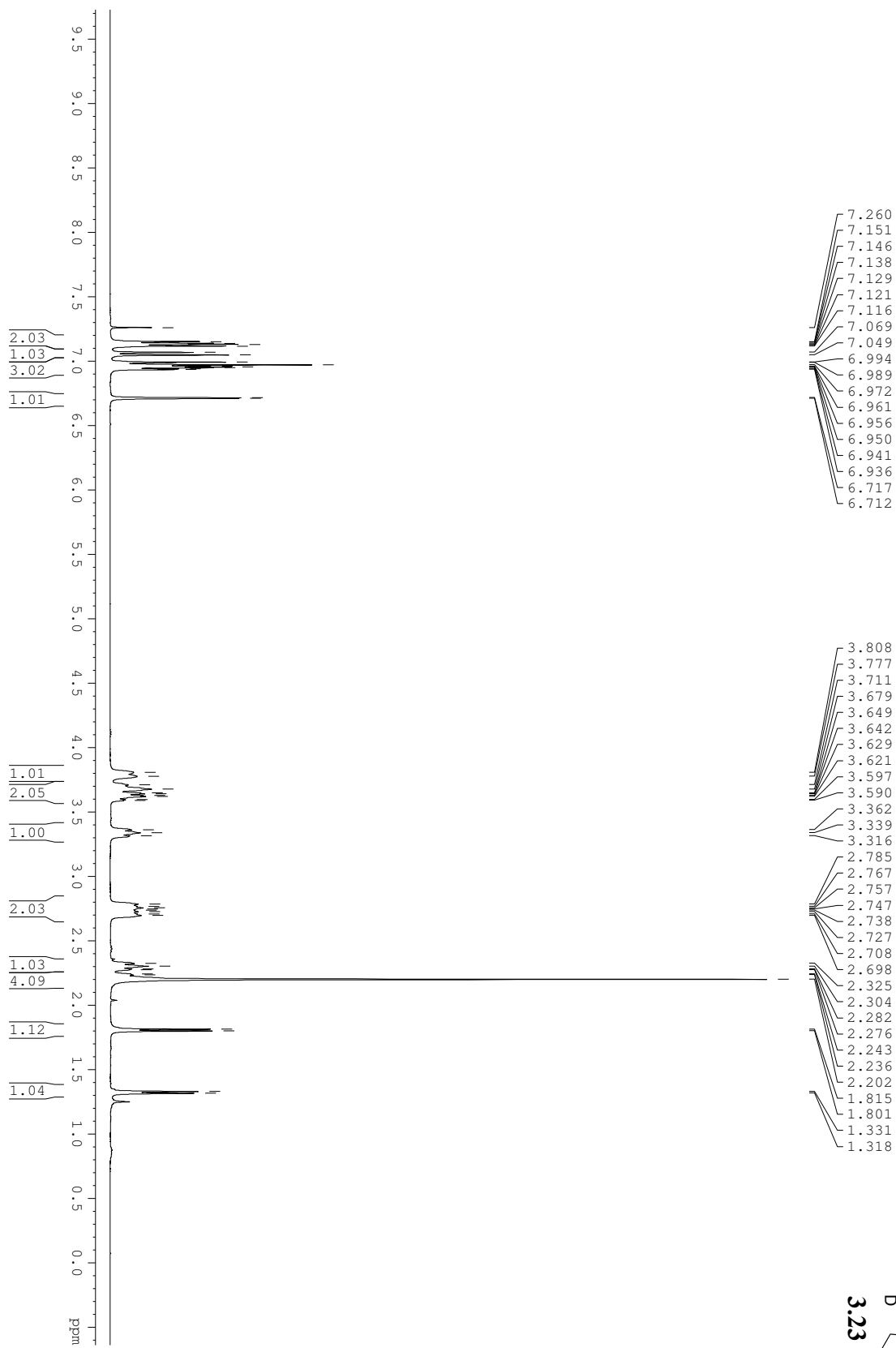


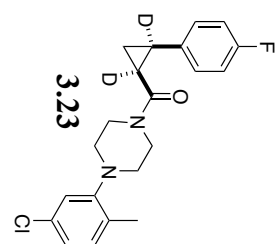
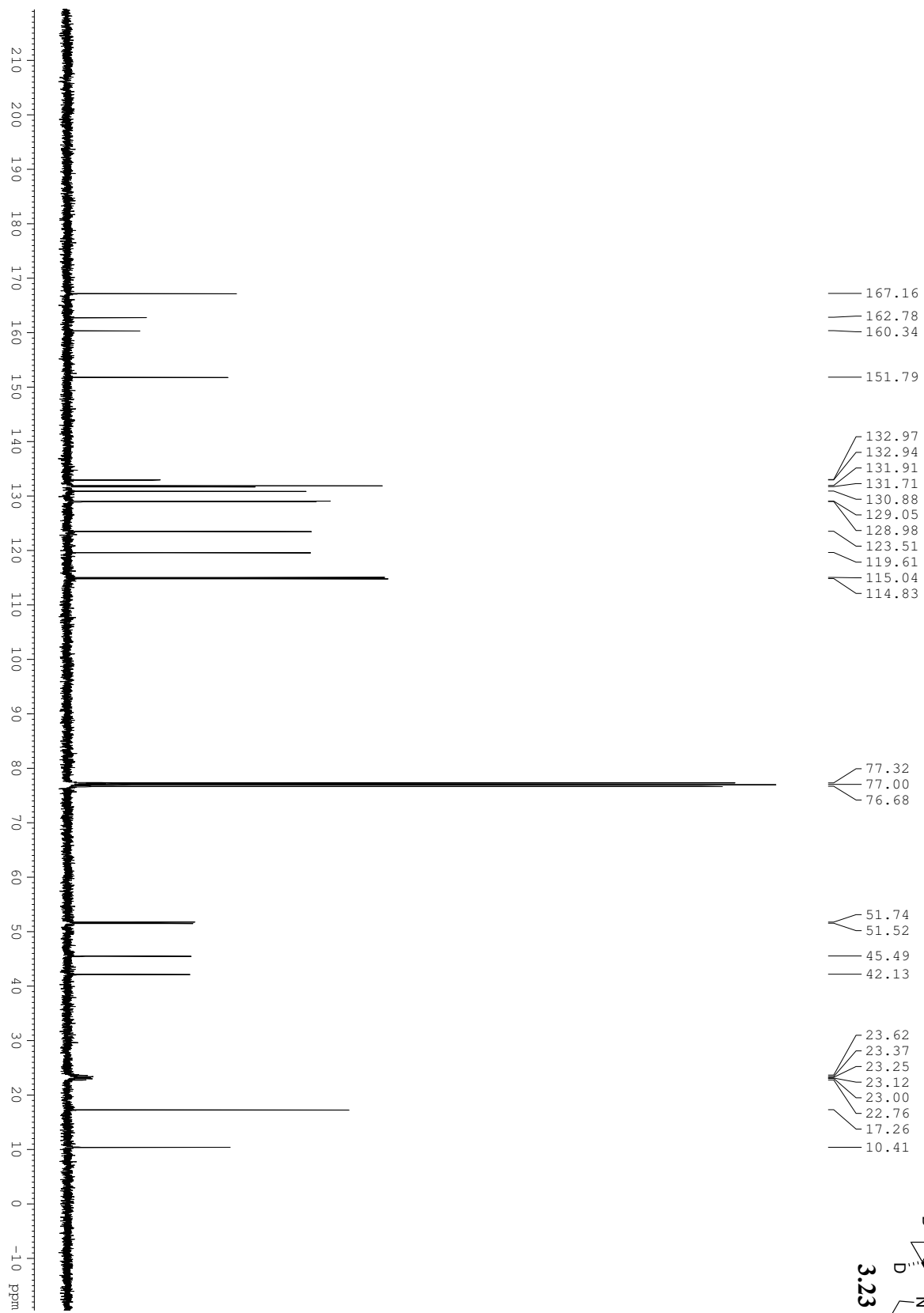


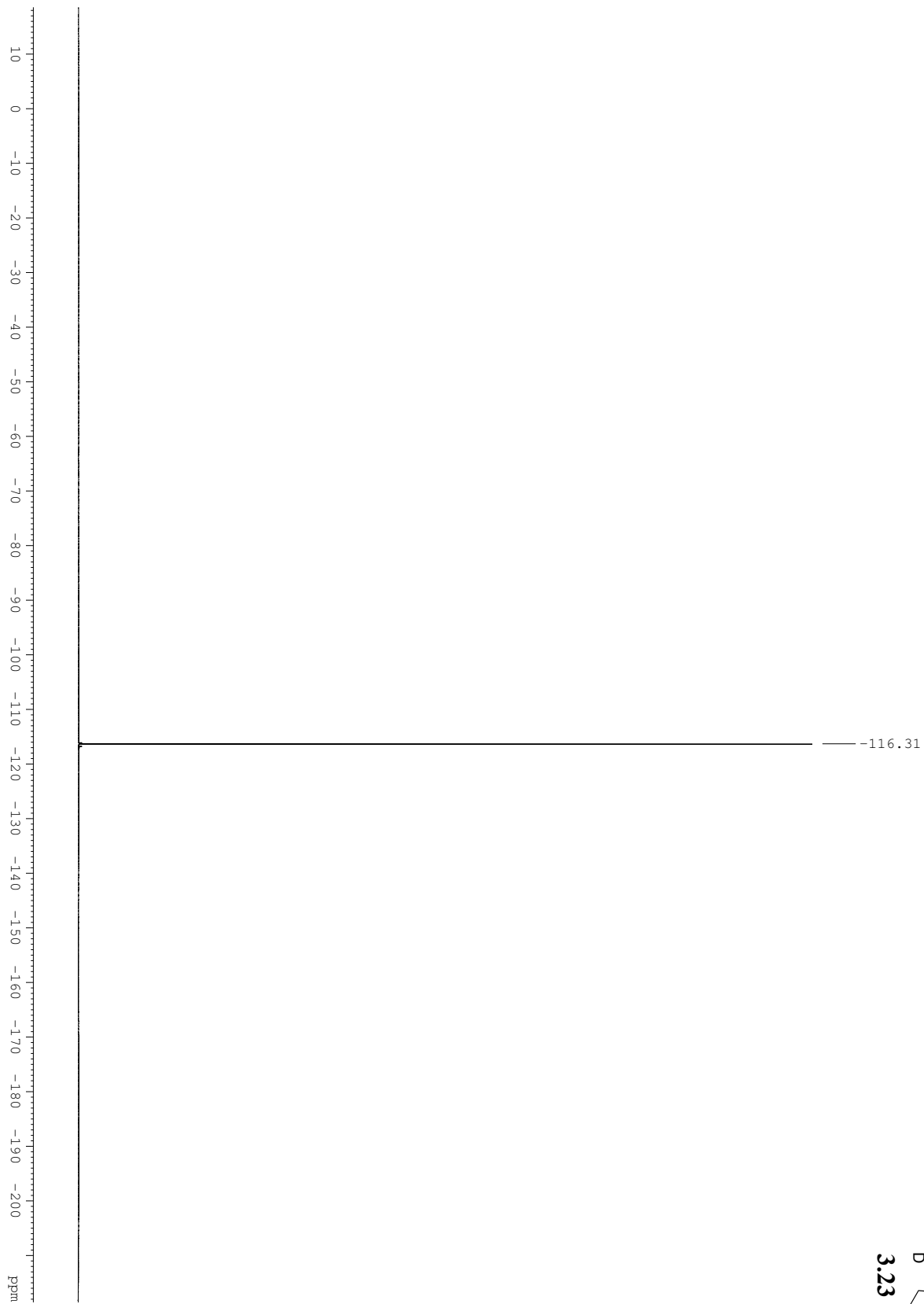
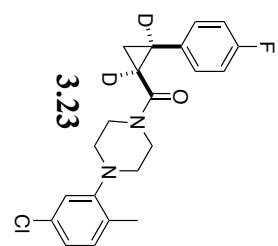
3.22

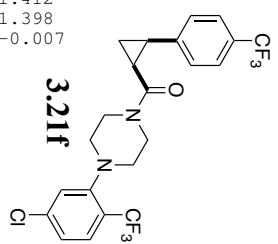
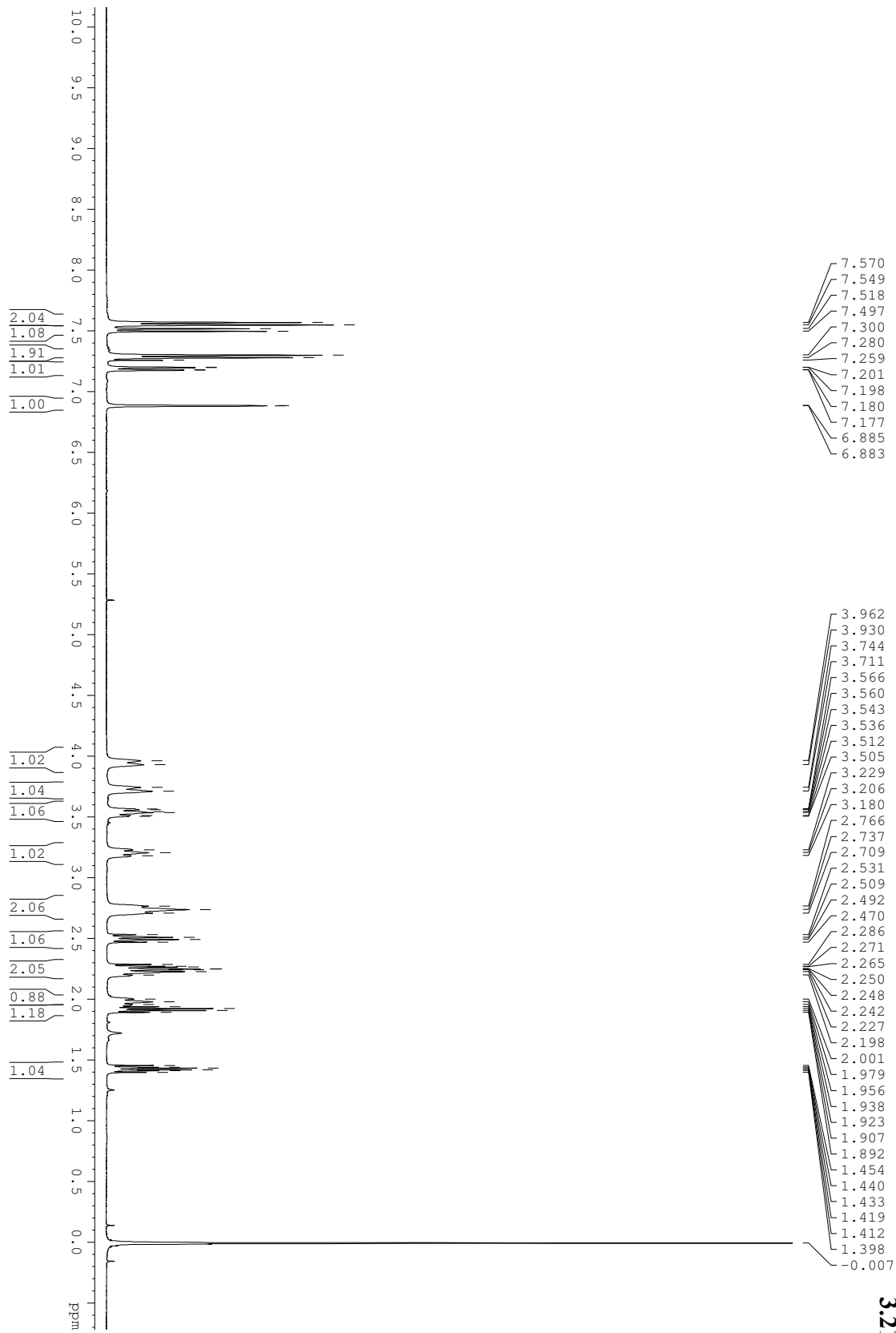
— -112.04

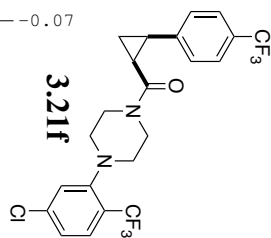
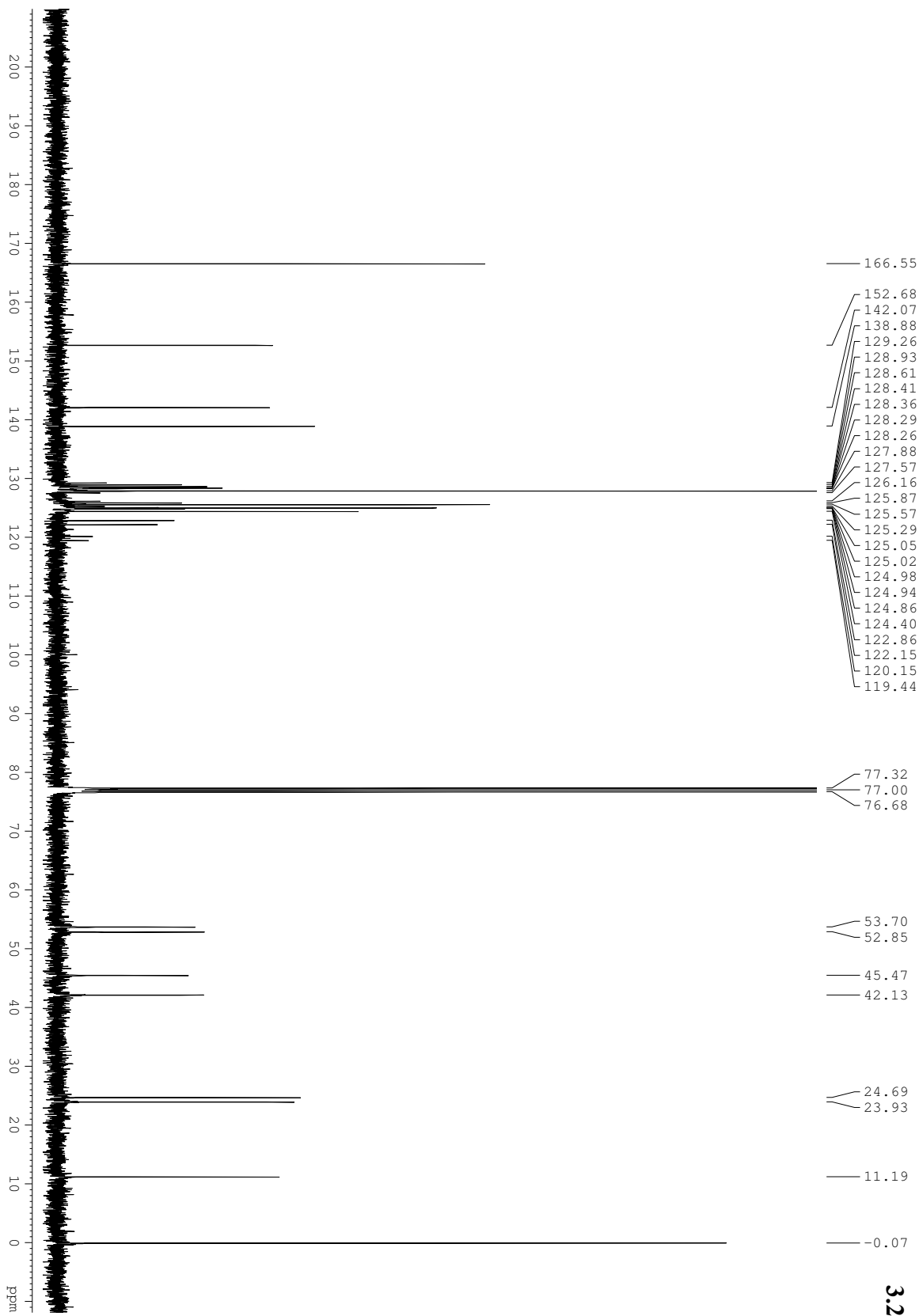


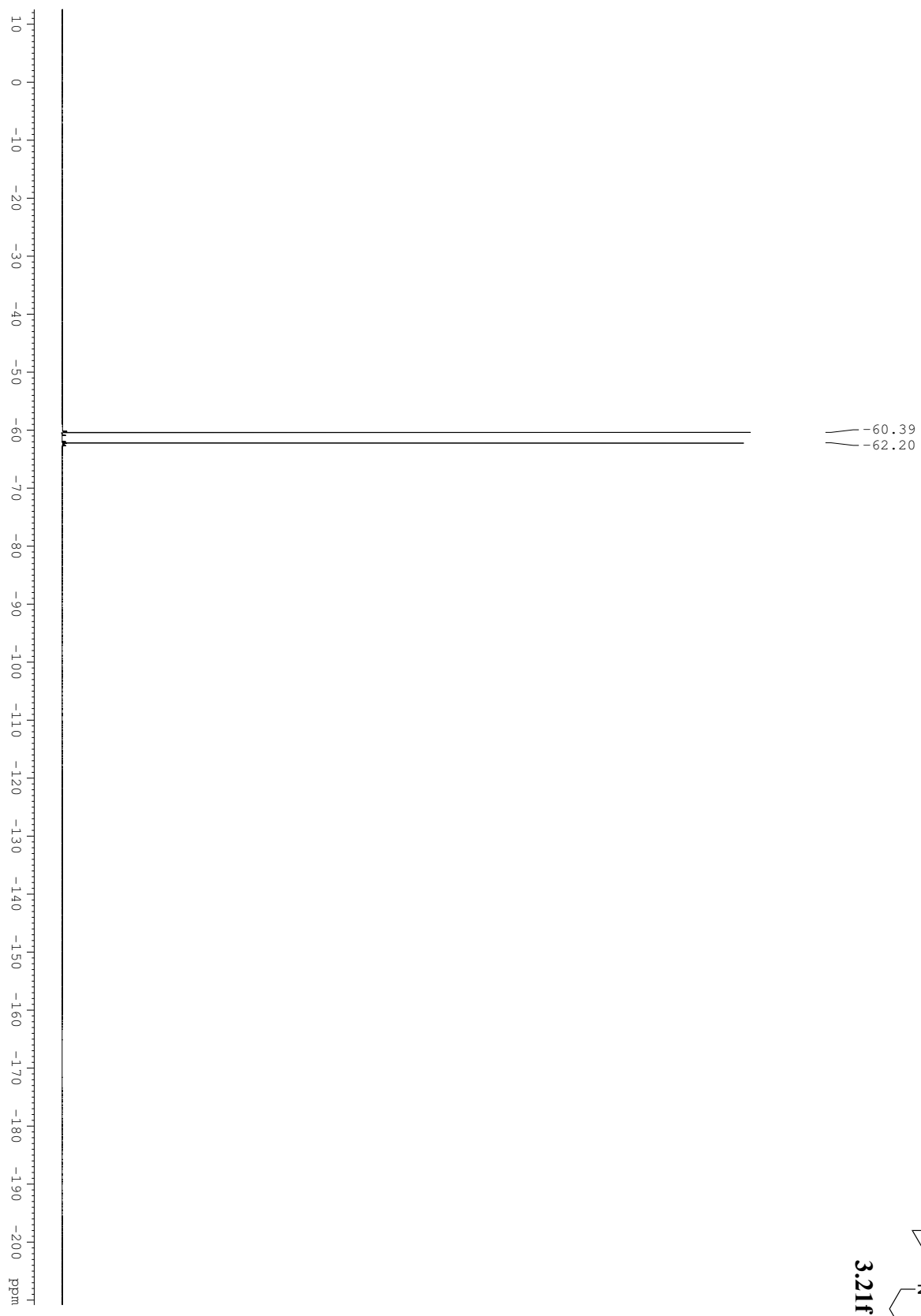
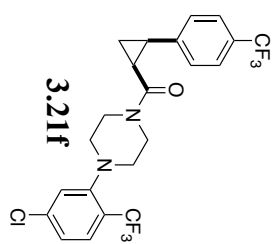


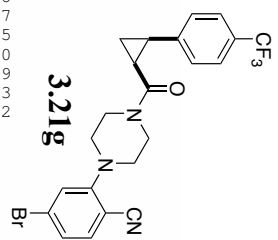
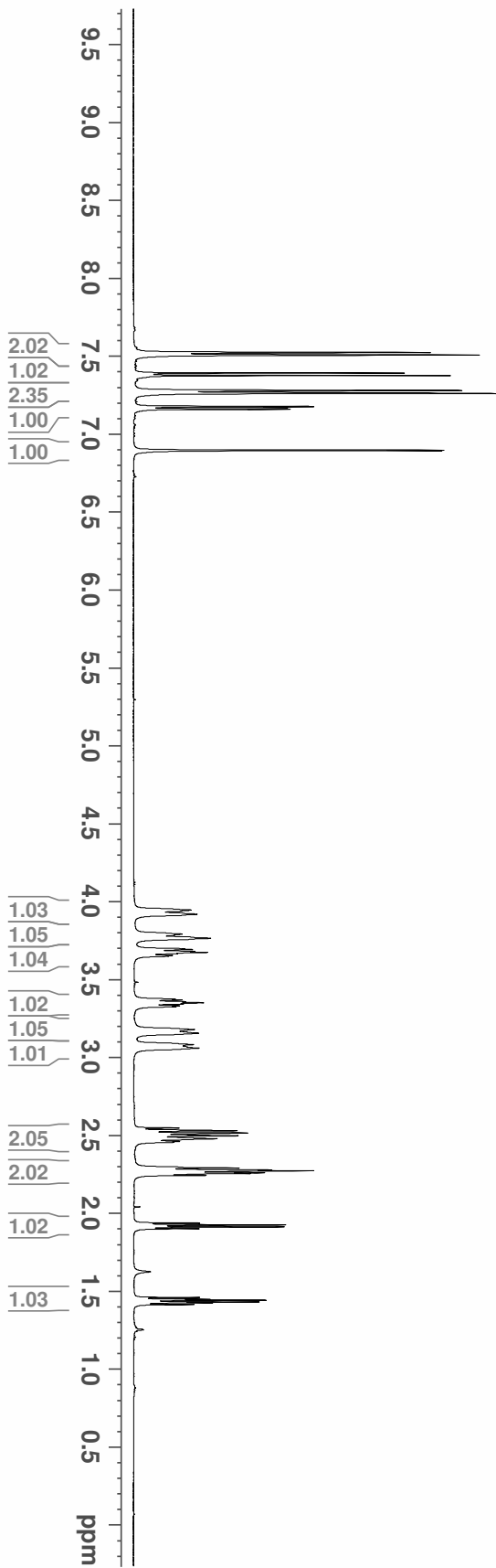


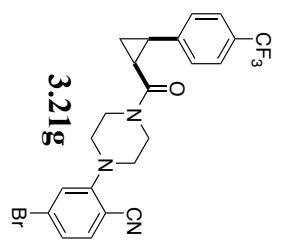
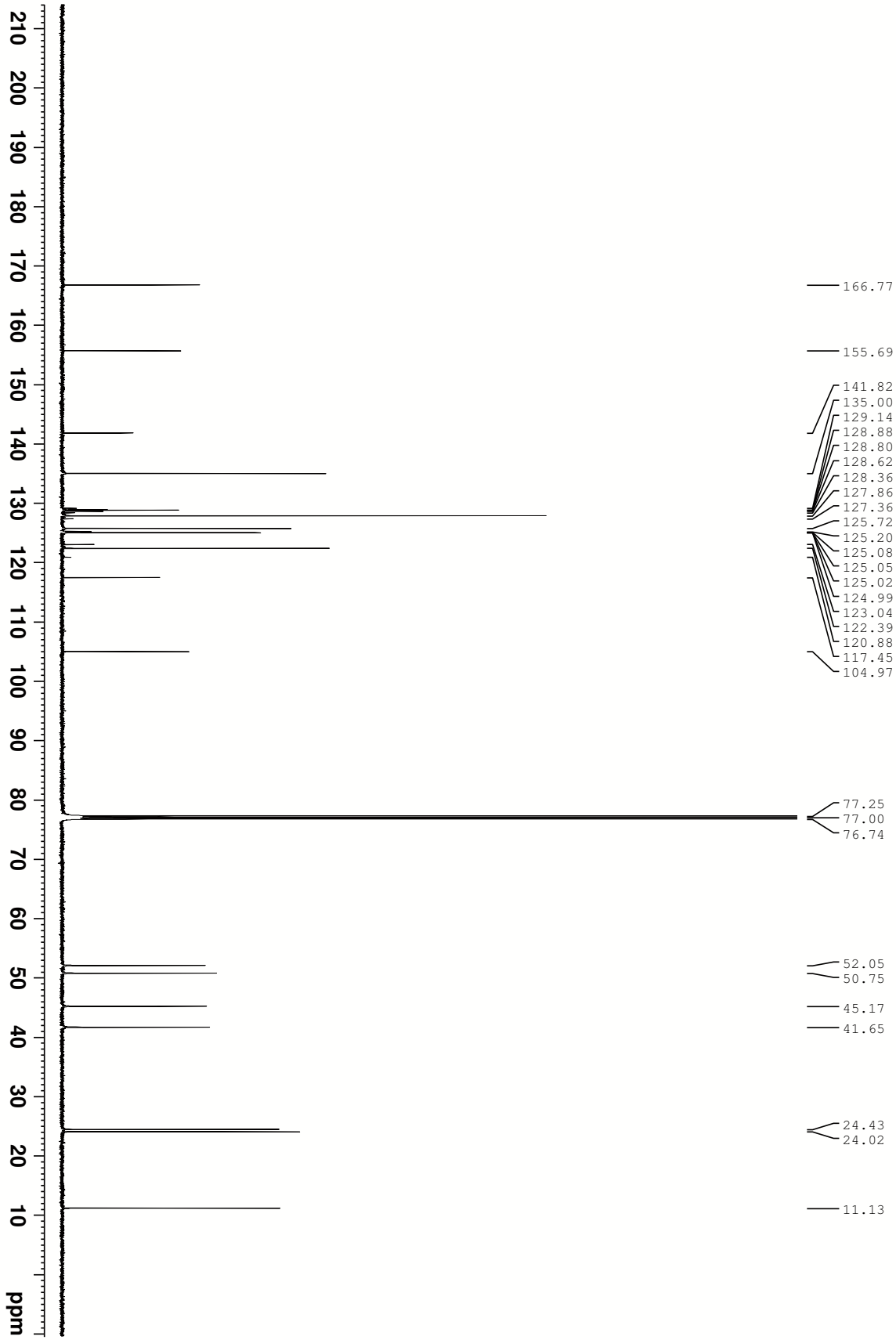


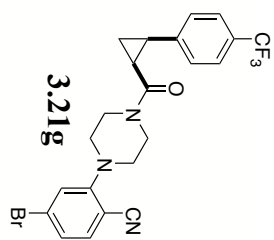
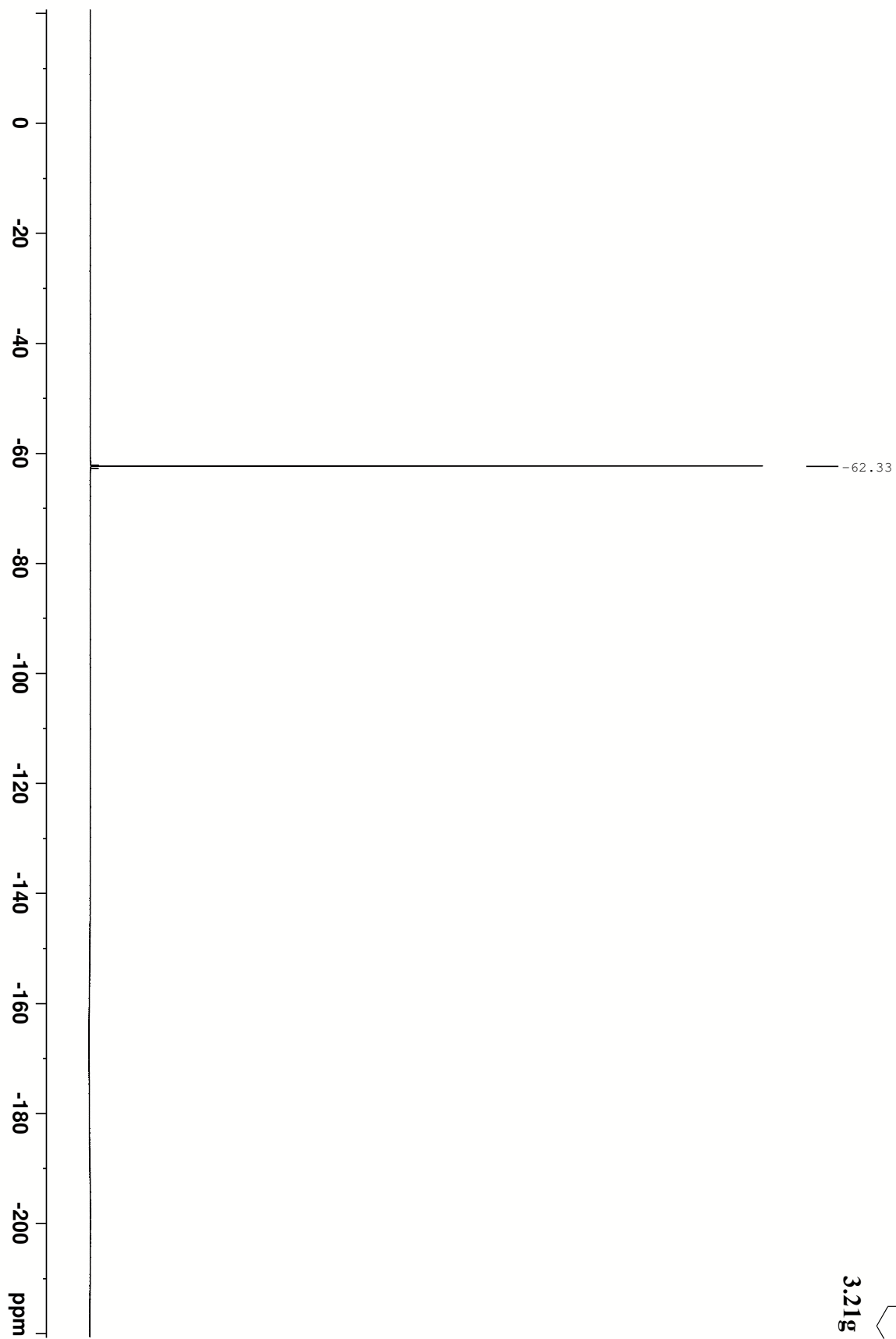


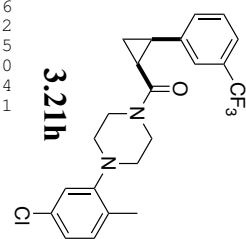
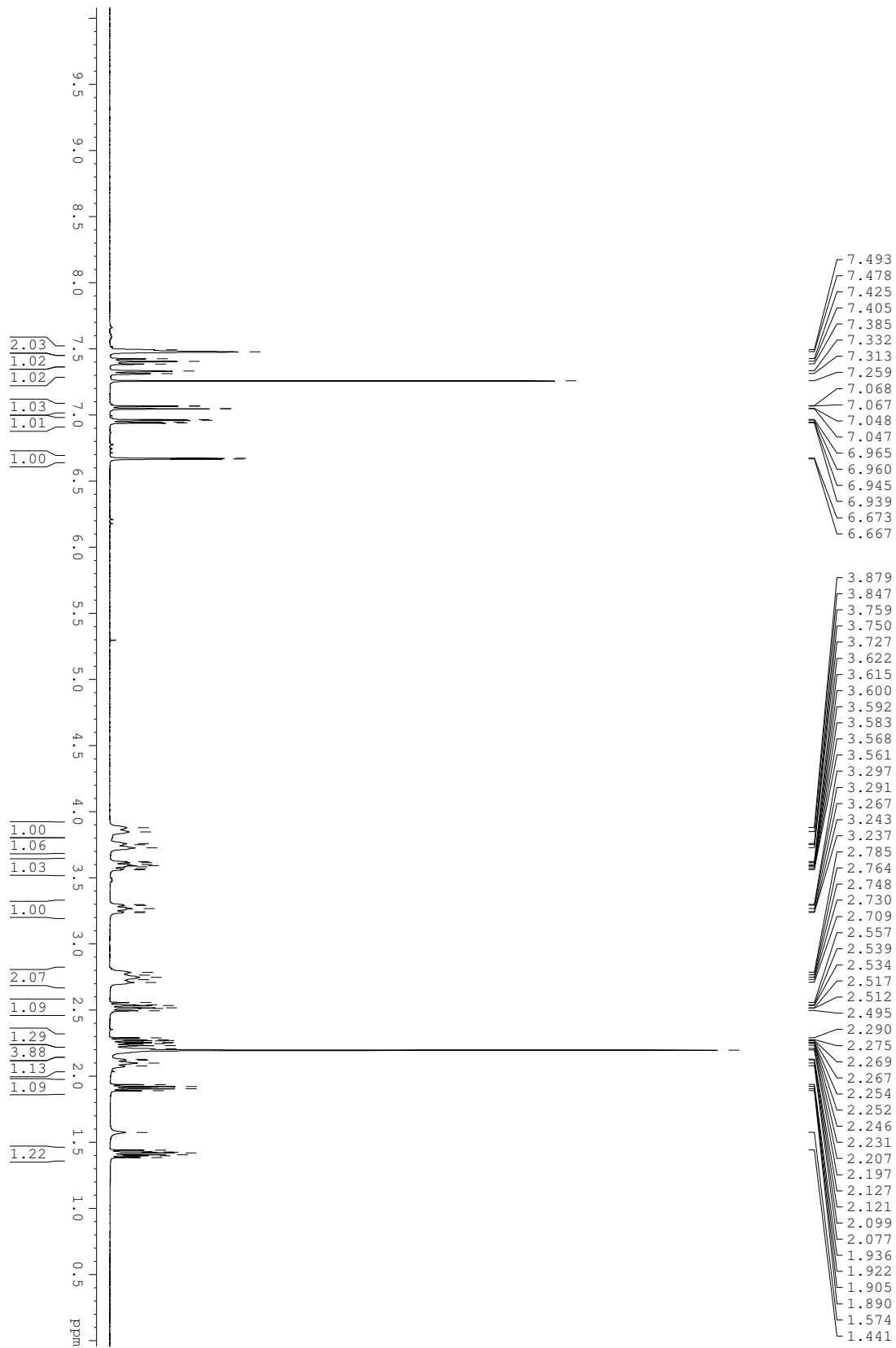


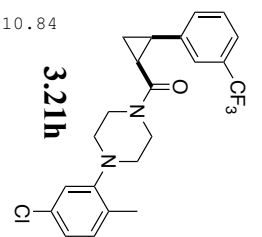
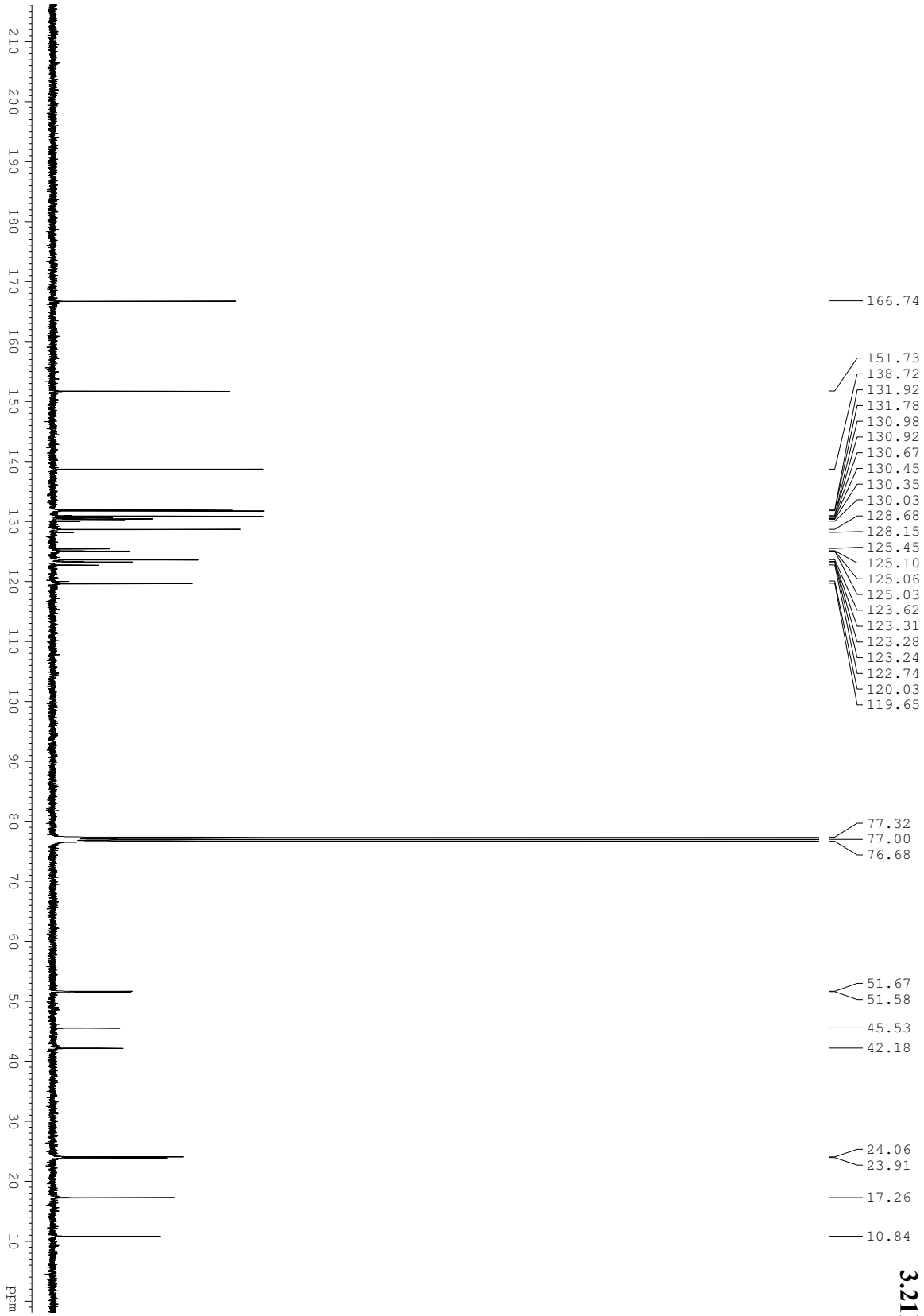


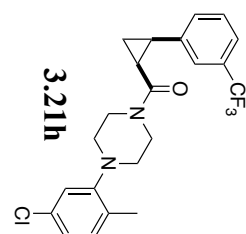




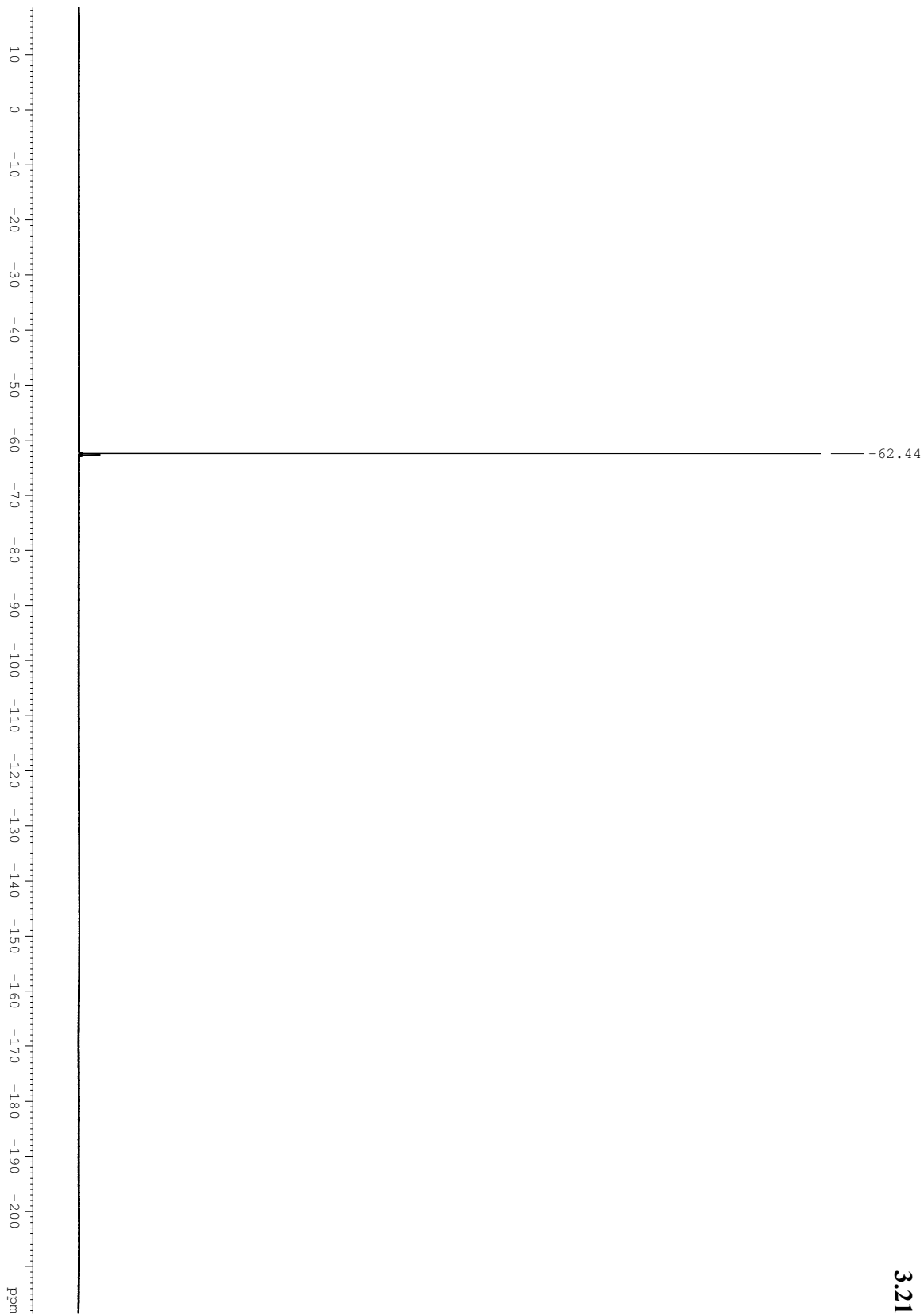


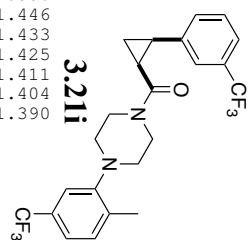
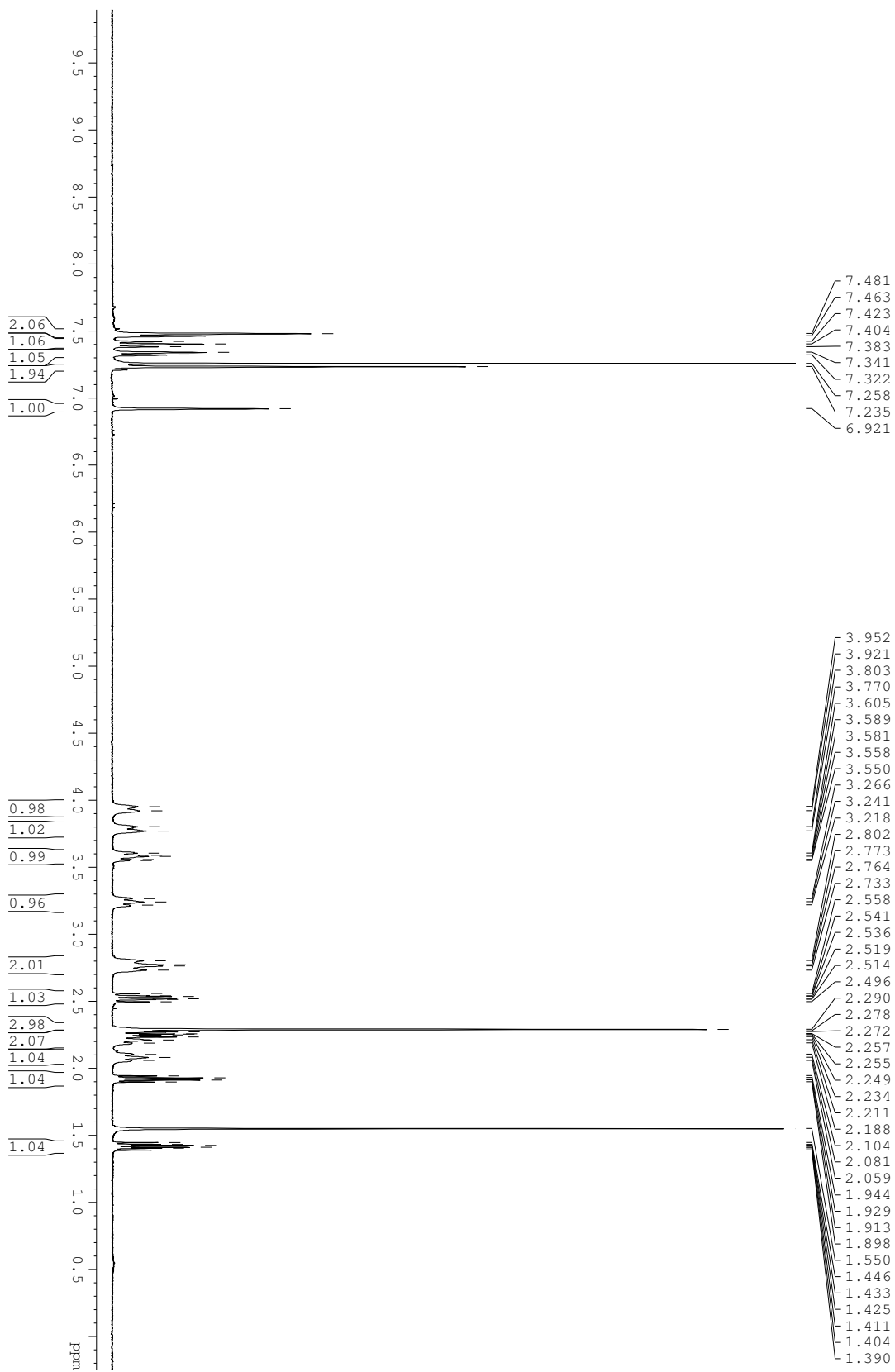


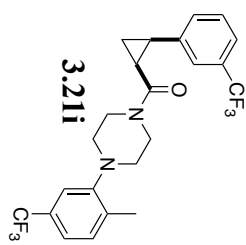
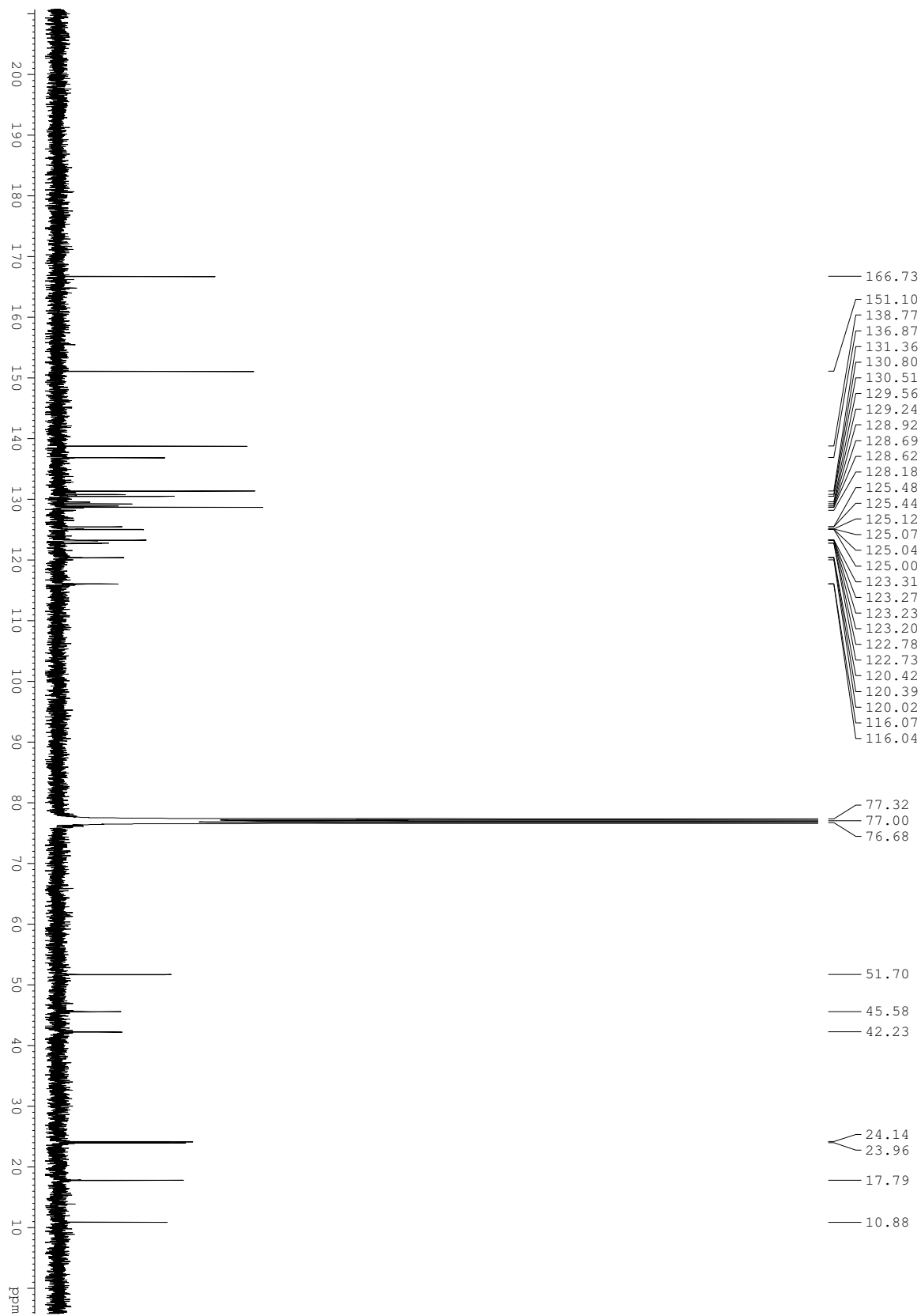


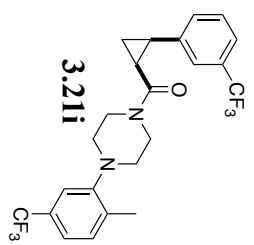
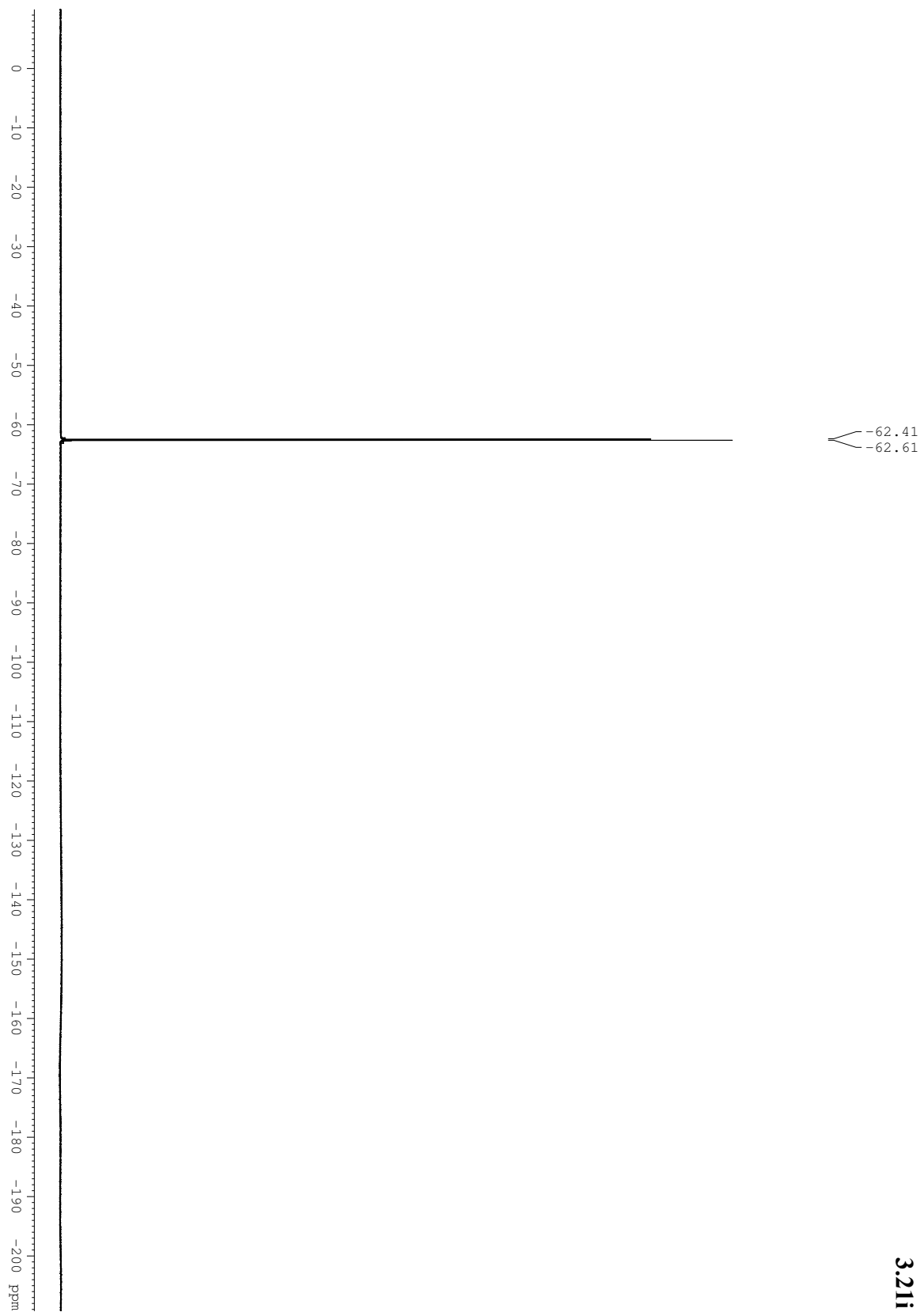


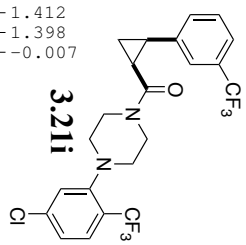
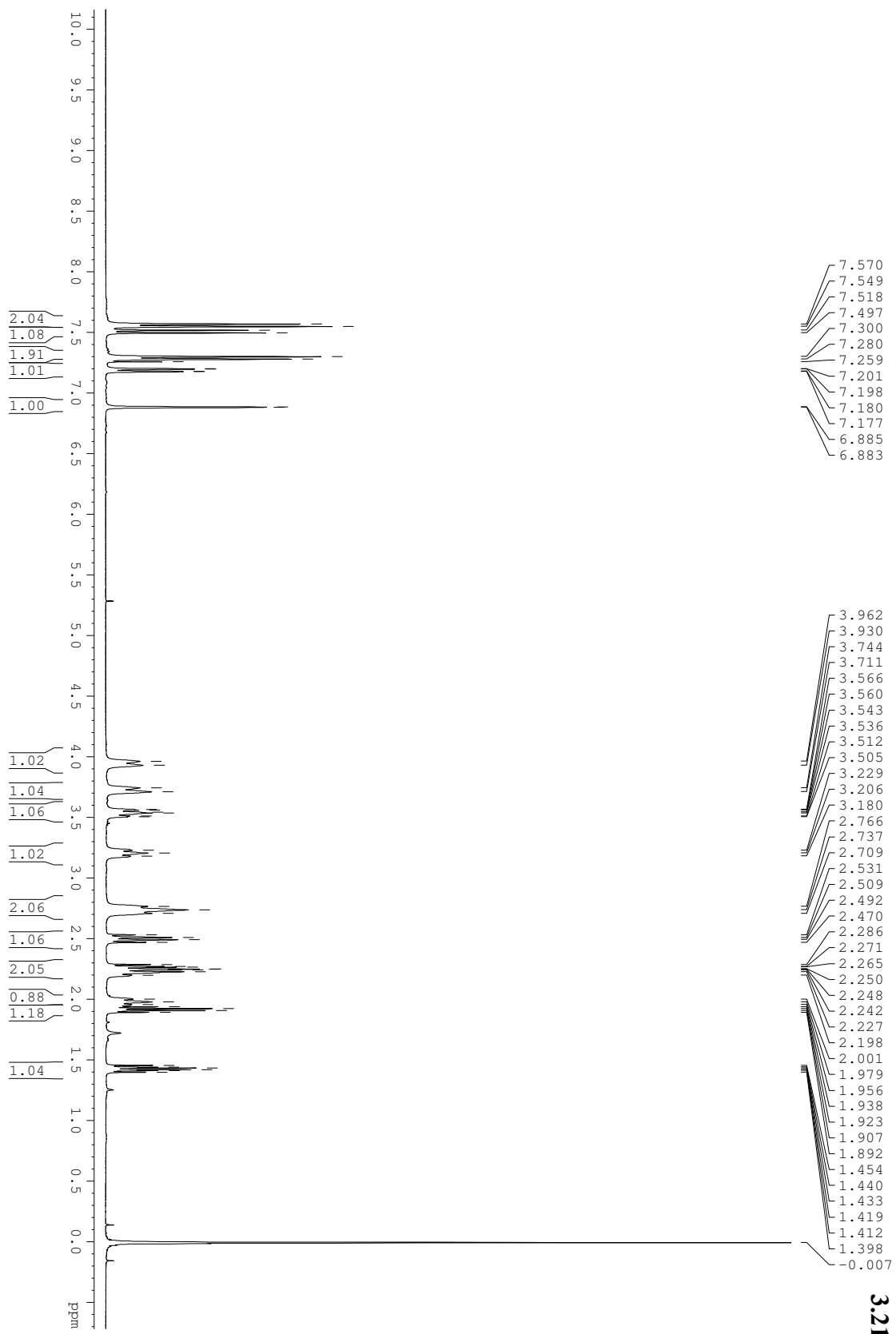
3.21h

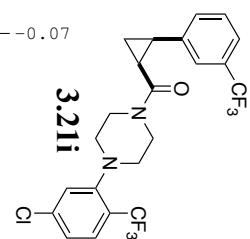
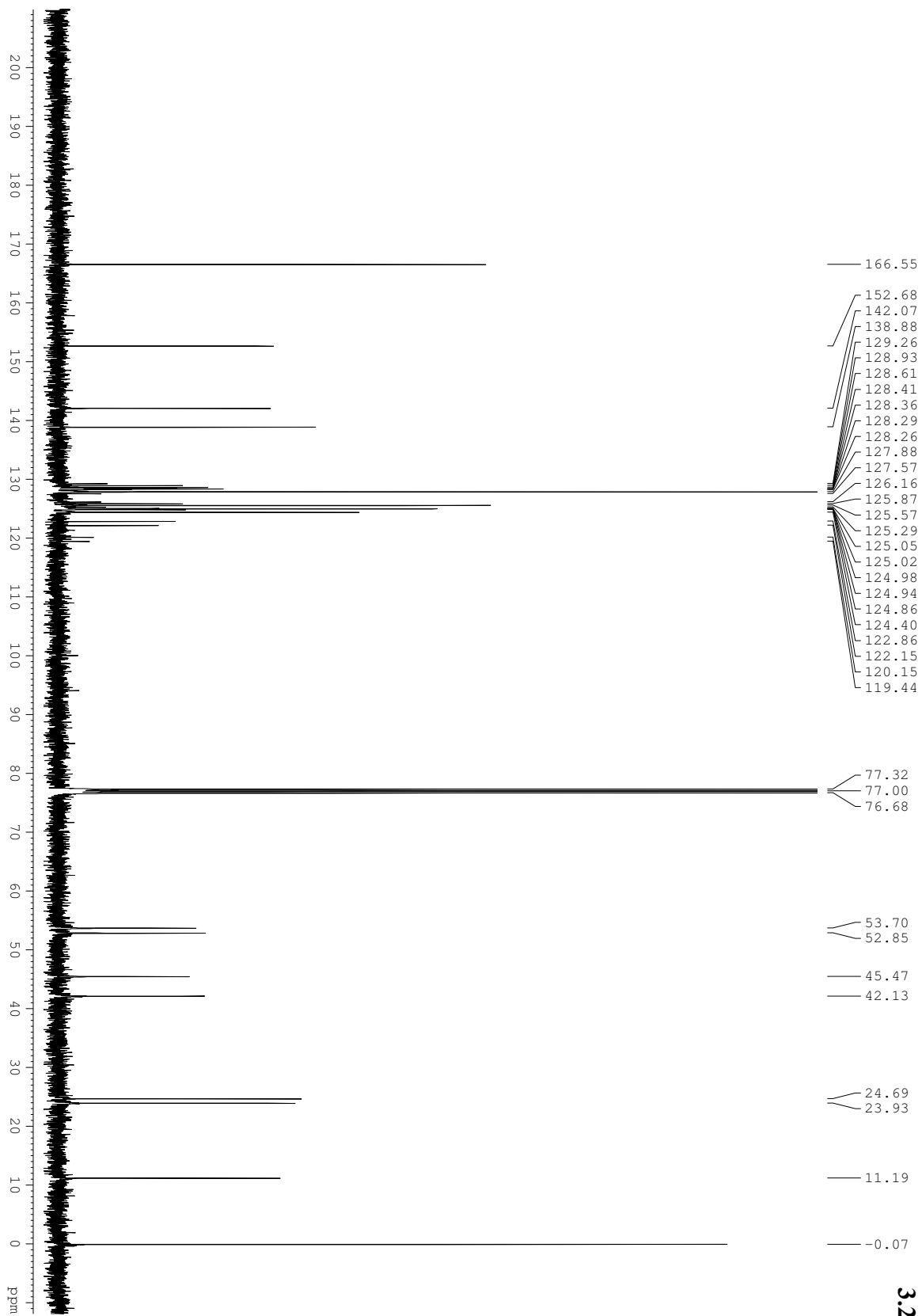






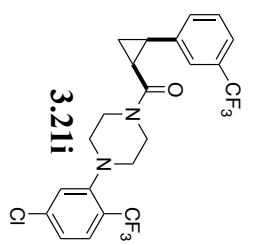


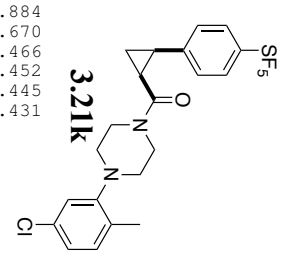
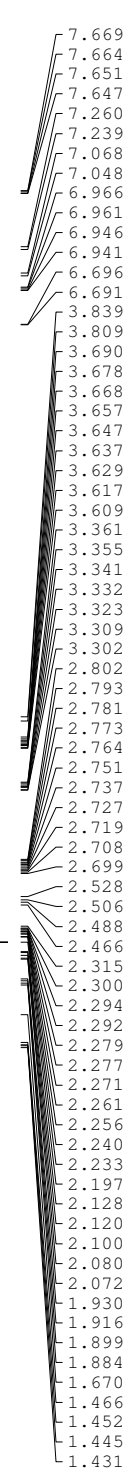
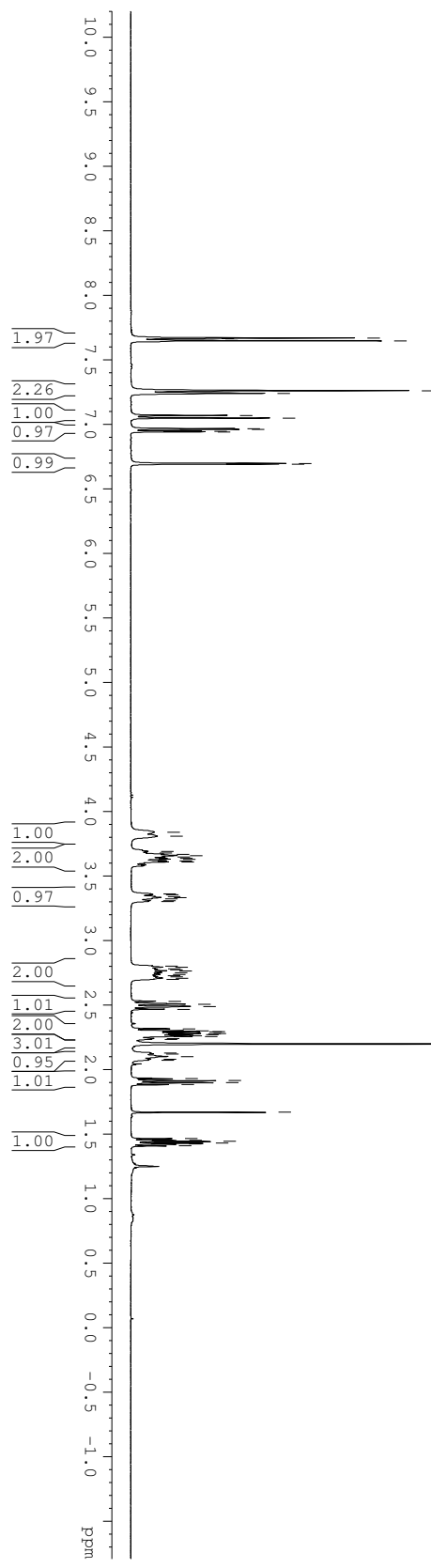


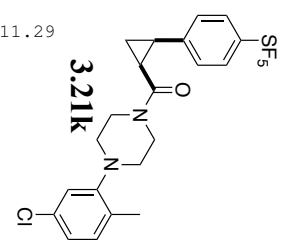
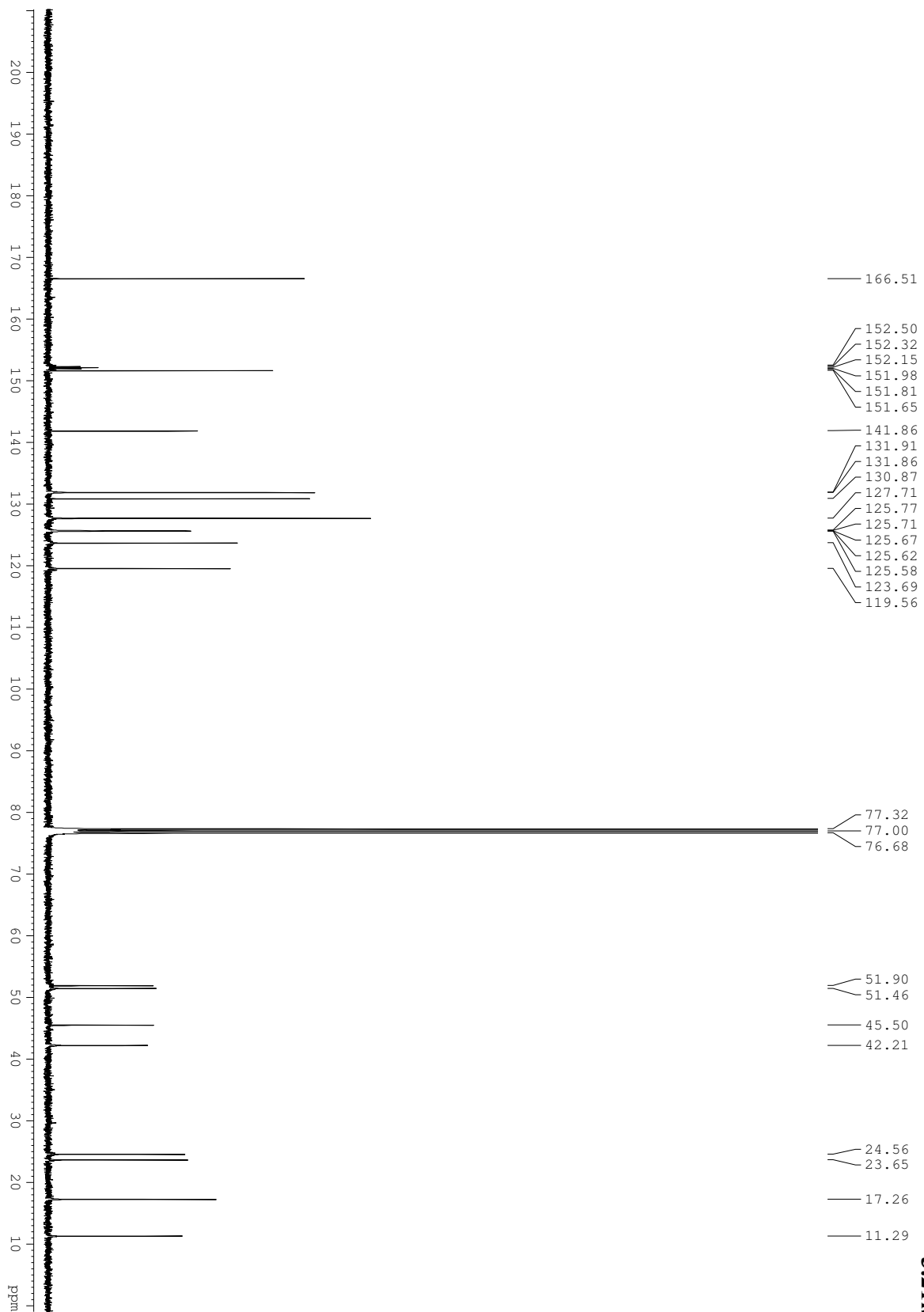


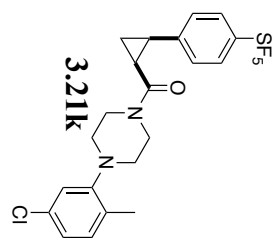
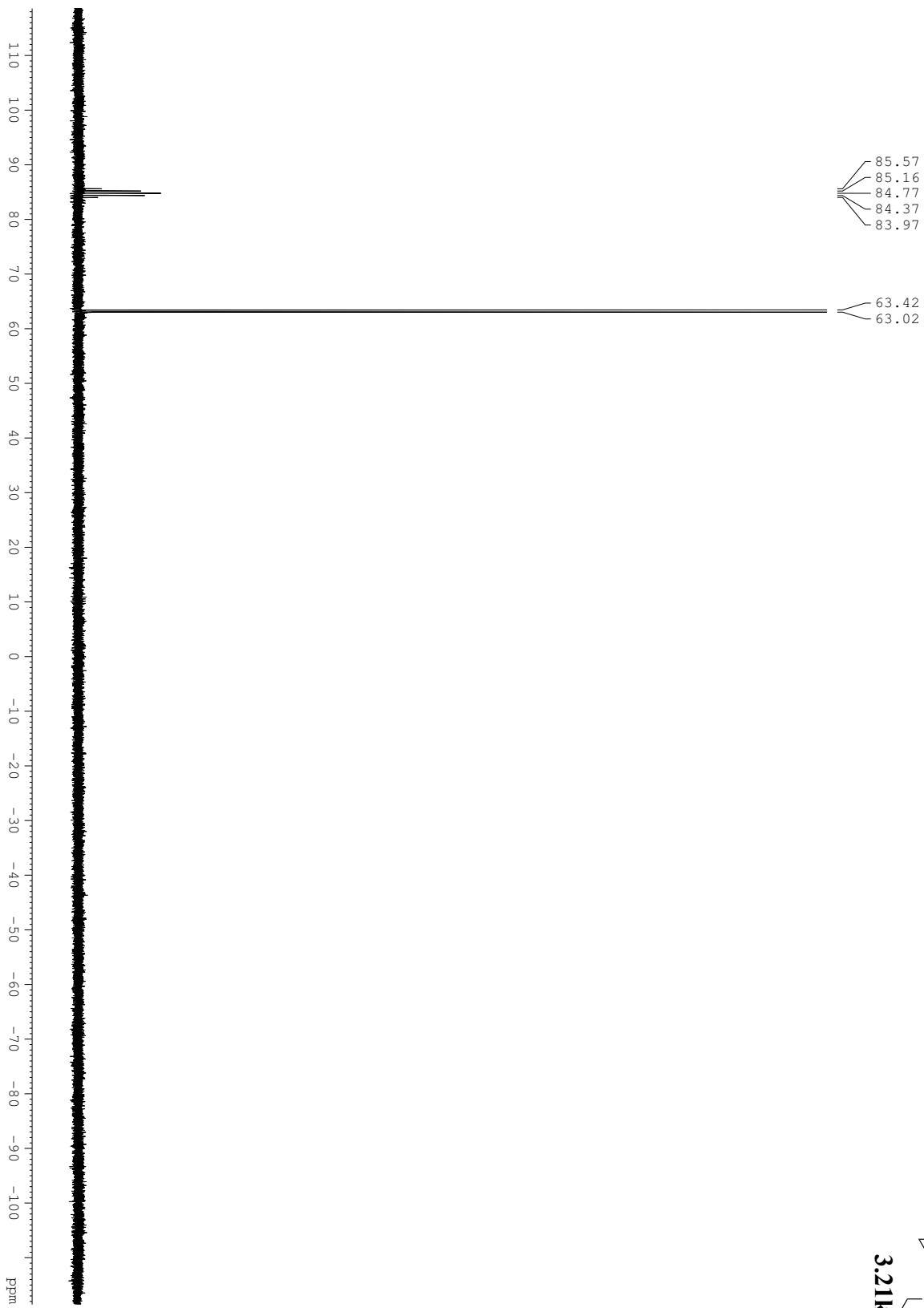
10
0
-10
-20
-30
-40
-50
-60
-70
-80
-90
-100
-110
-120
-130
-140
-150
-160
-170
-180
-190
-200 ppm

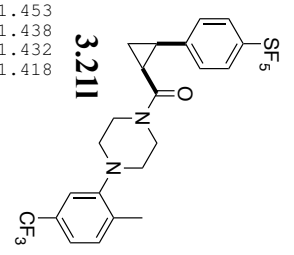
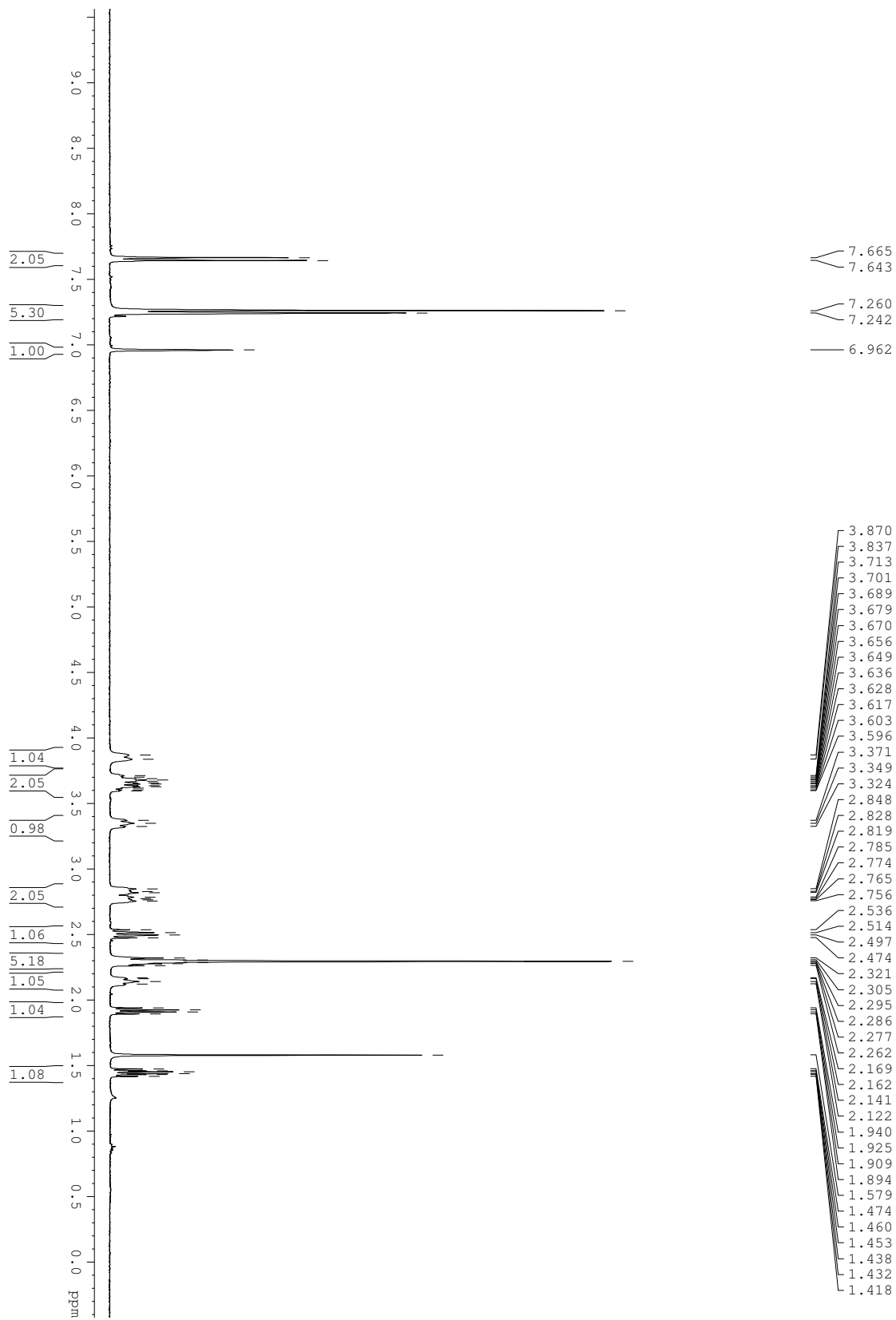
-60.39
-62.20

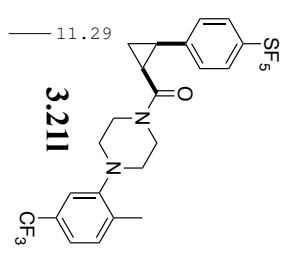
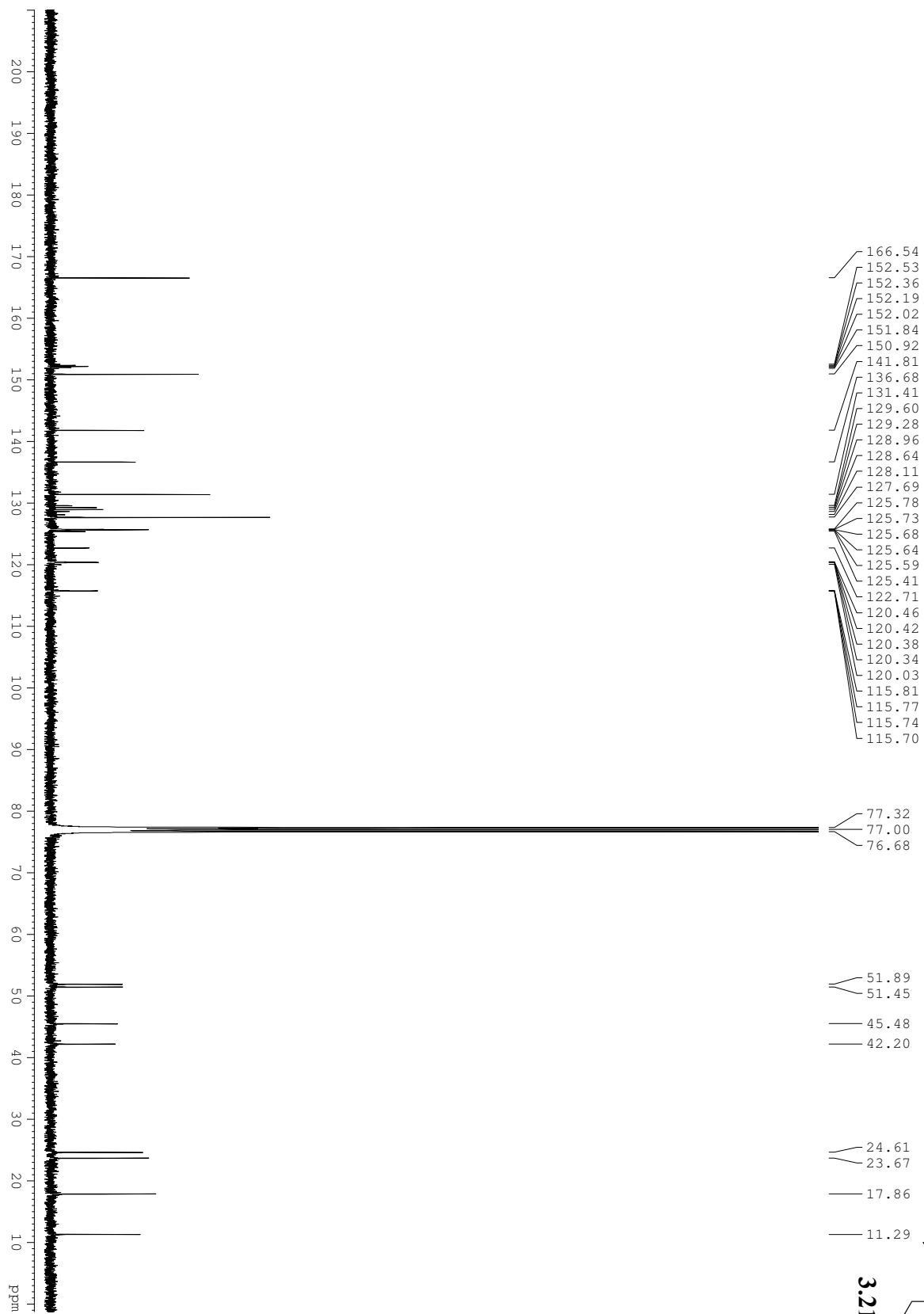


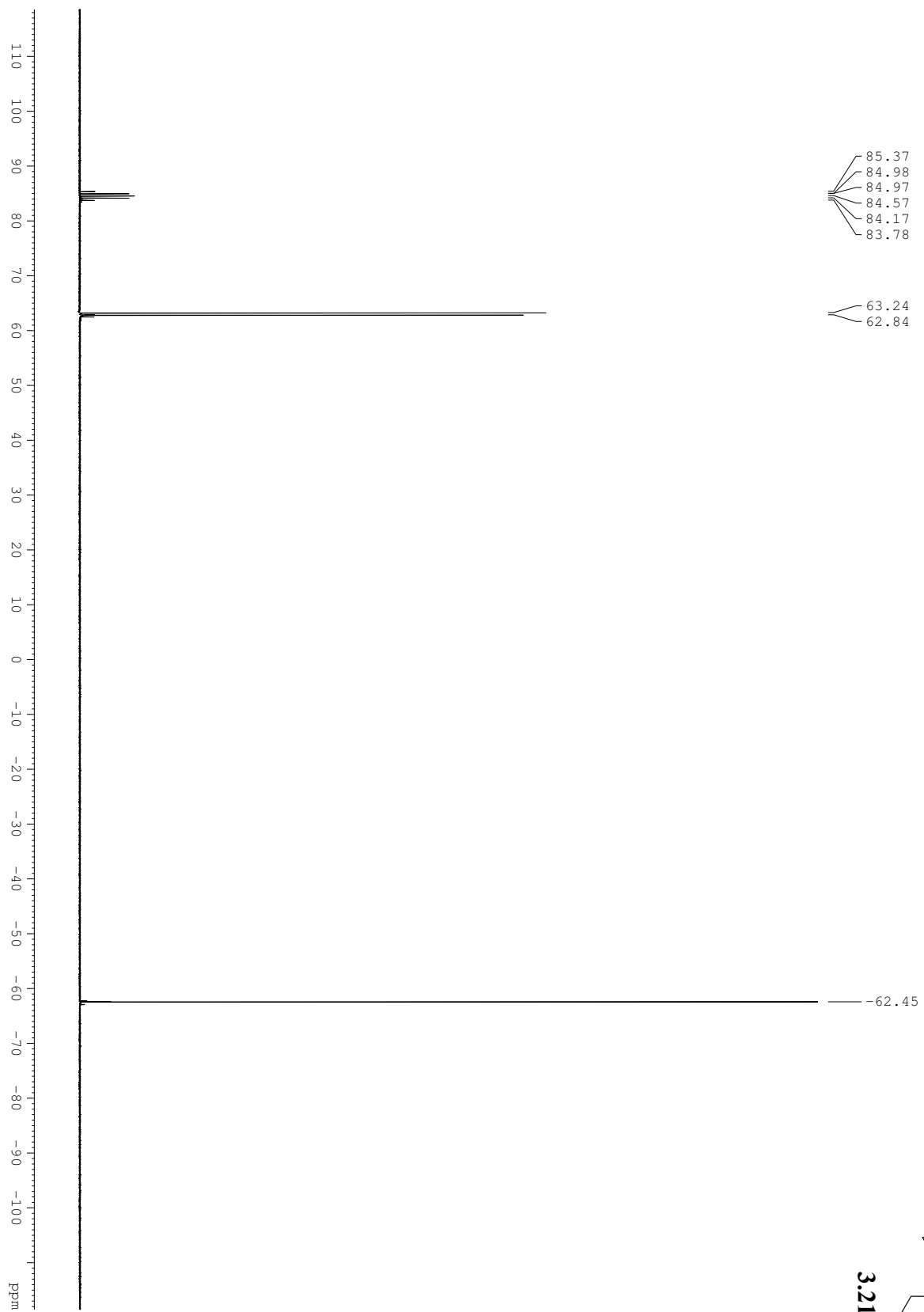


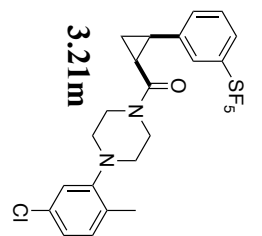
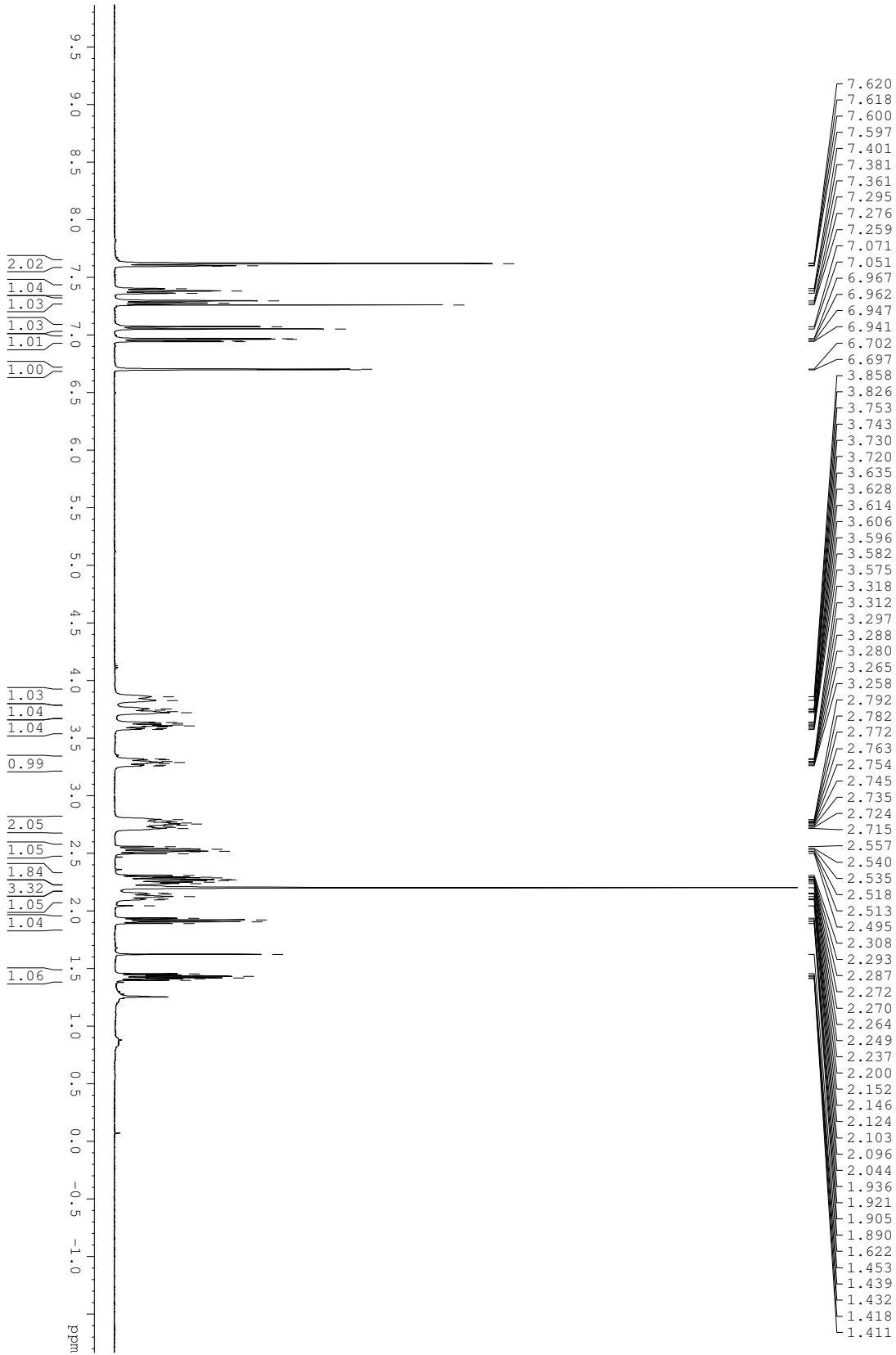


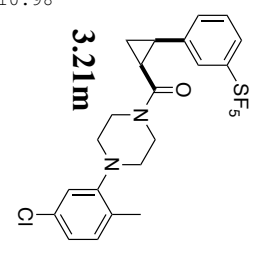
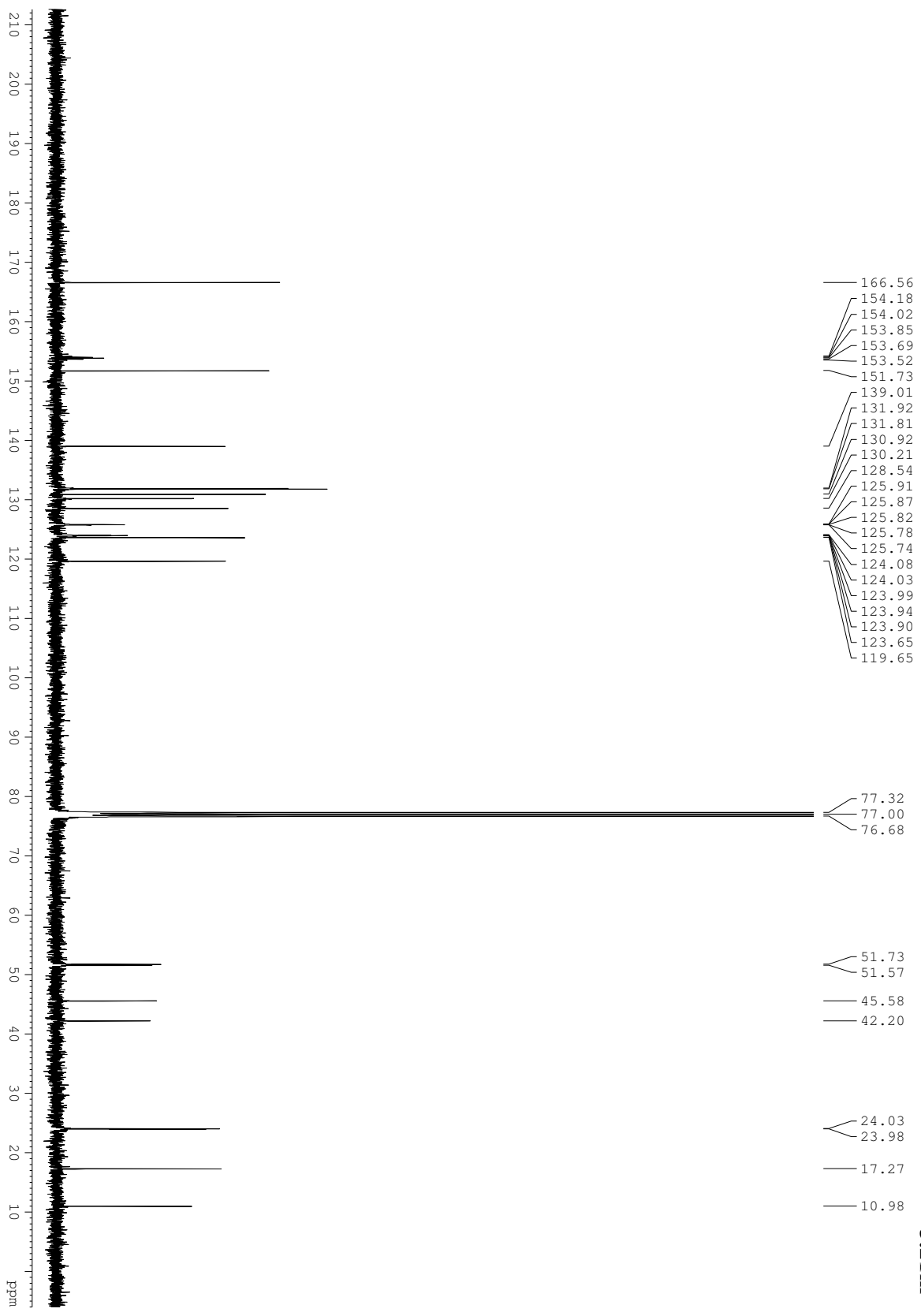


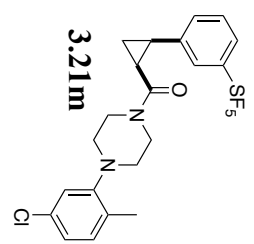
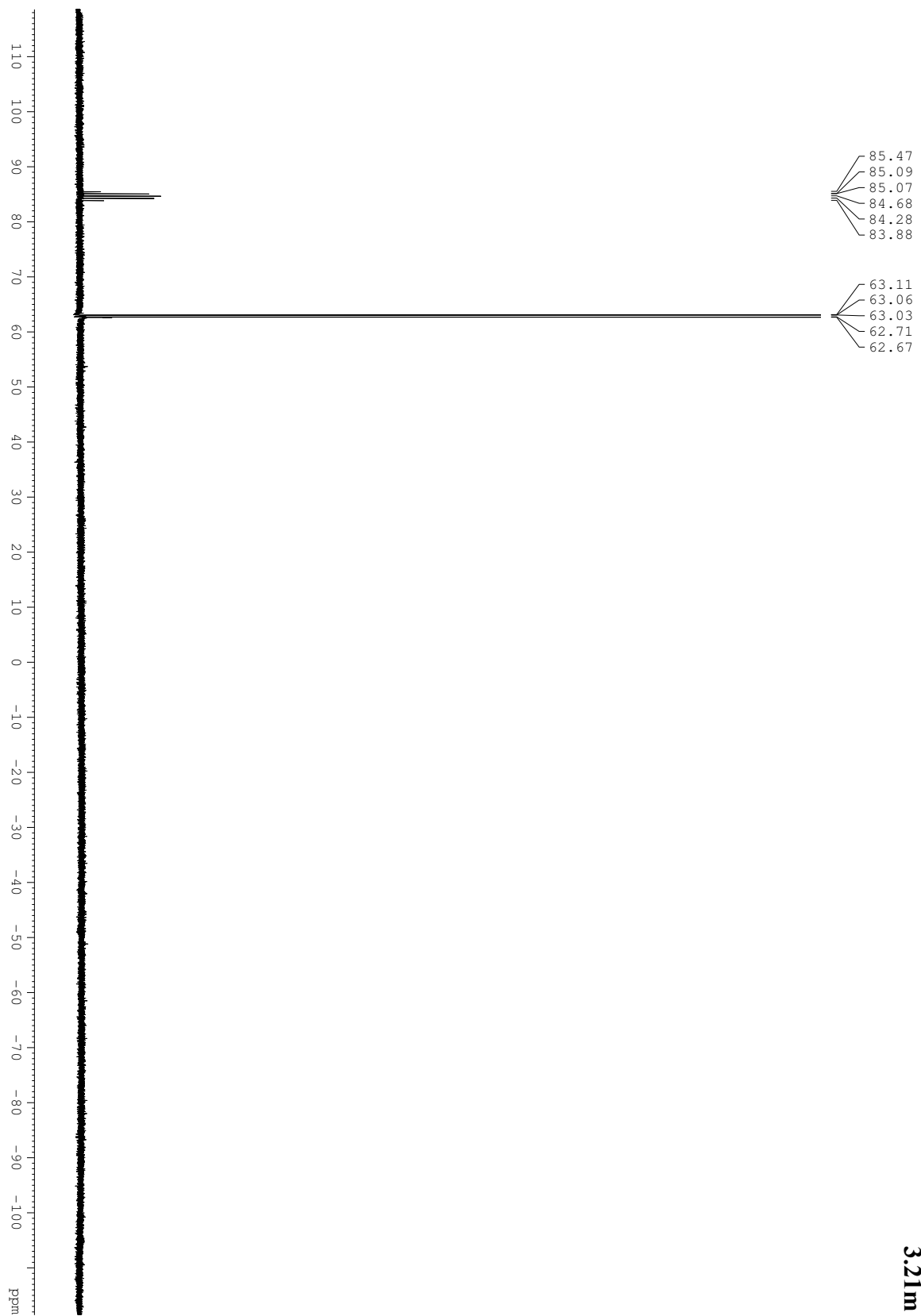


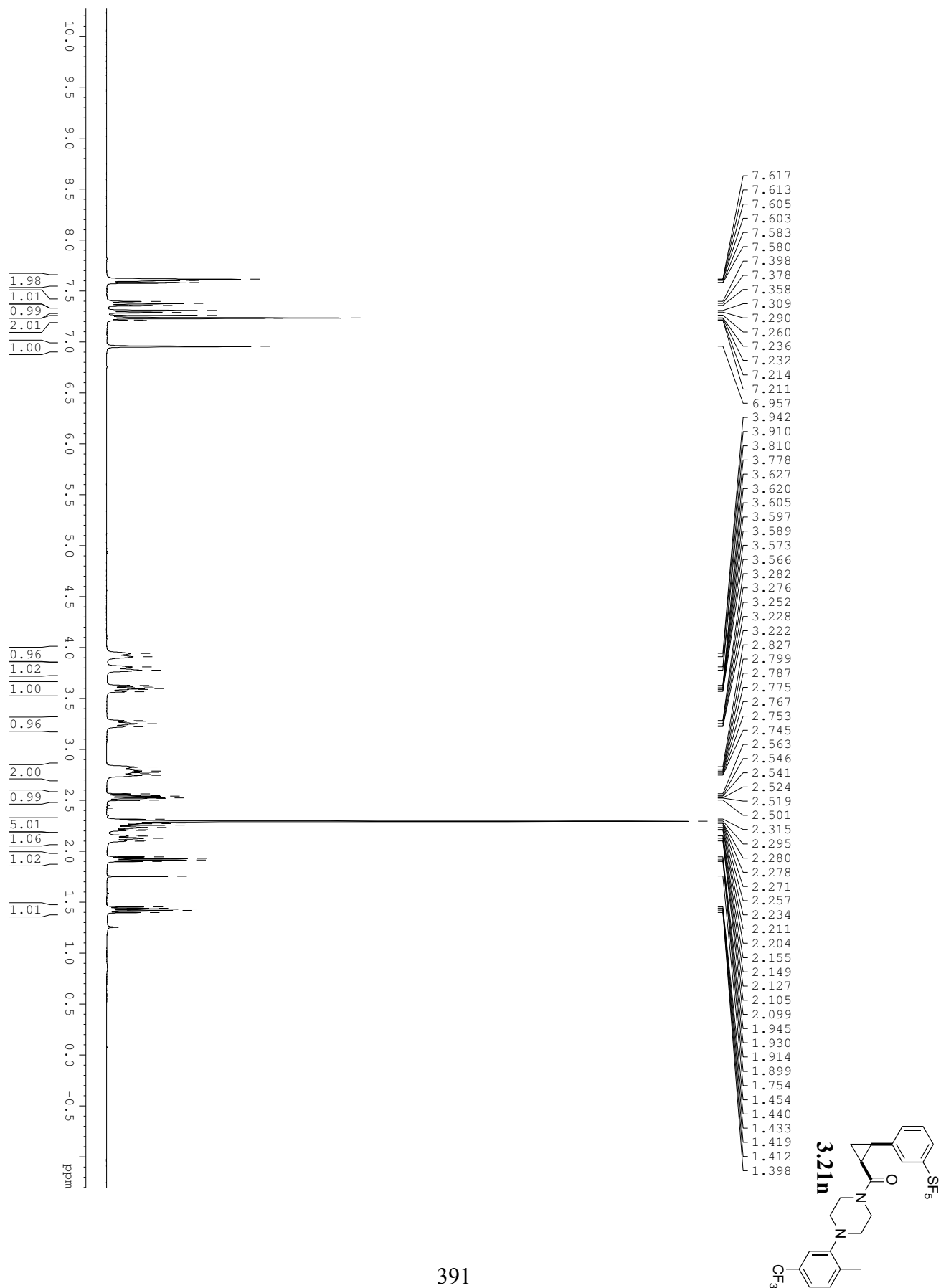


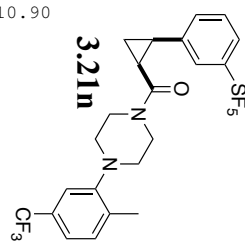
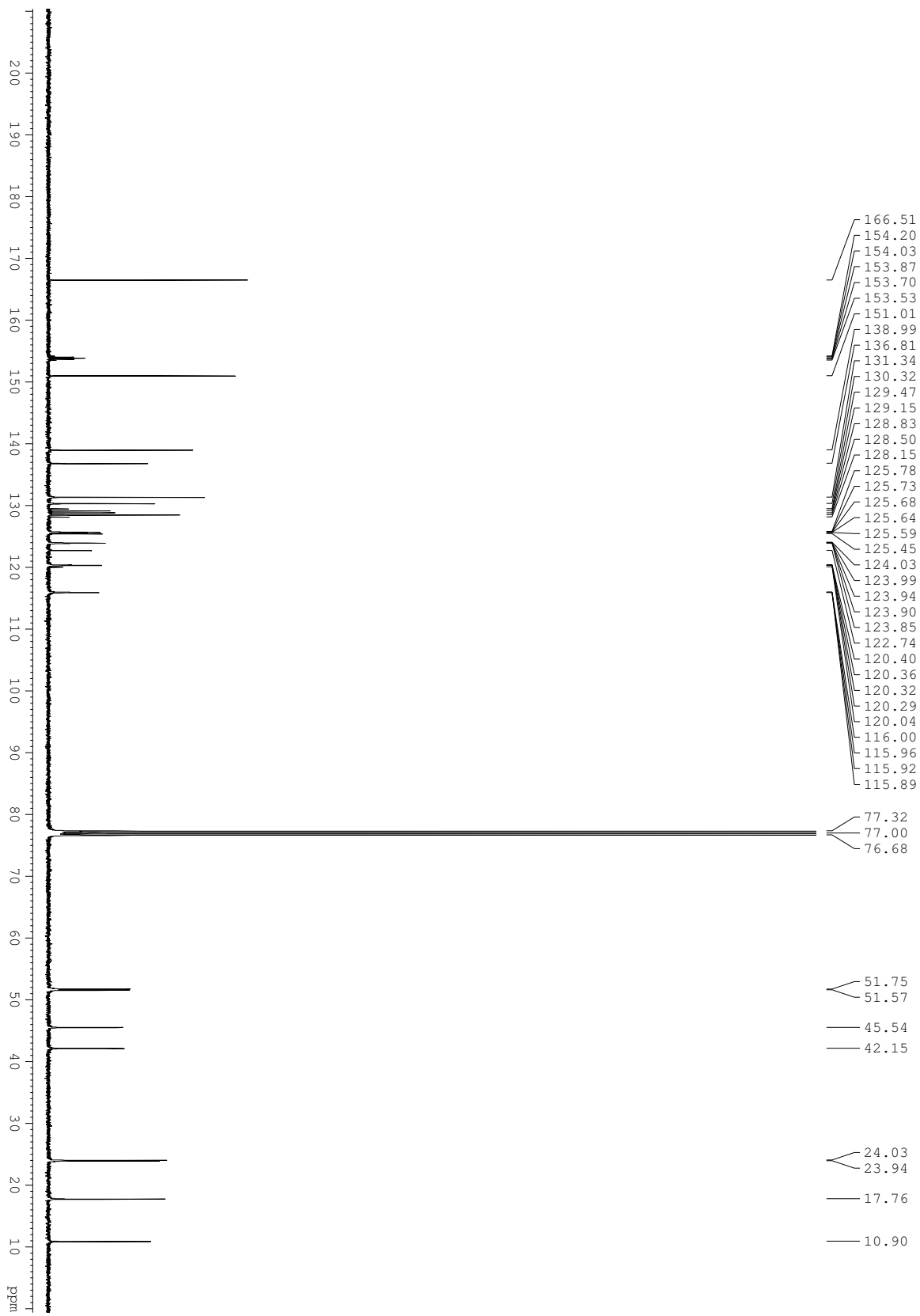


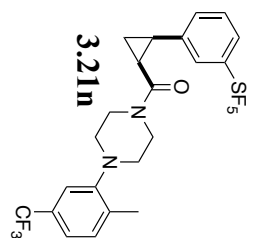
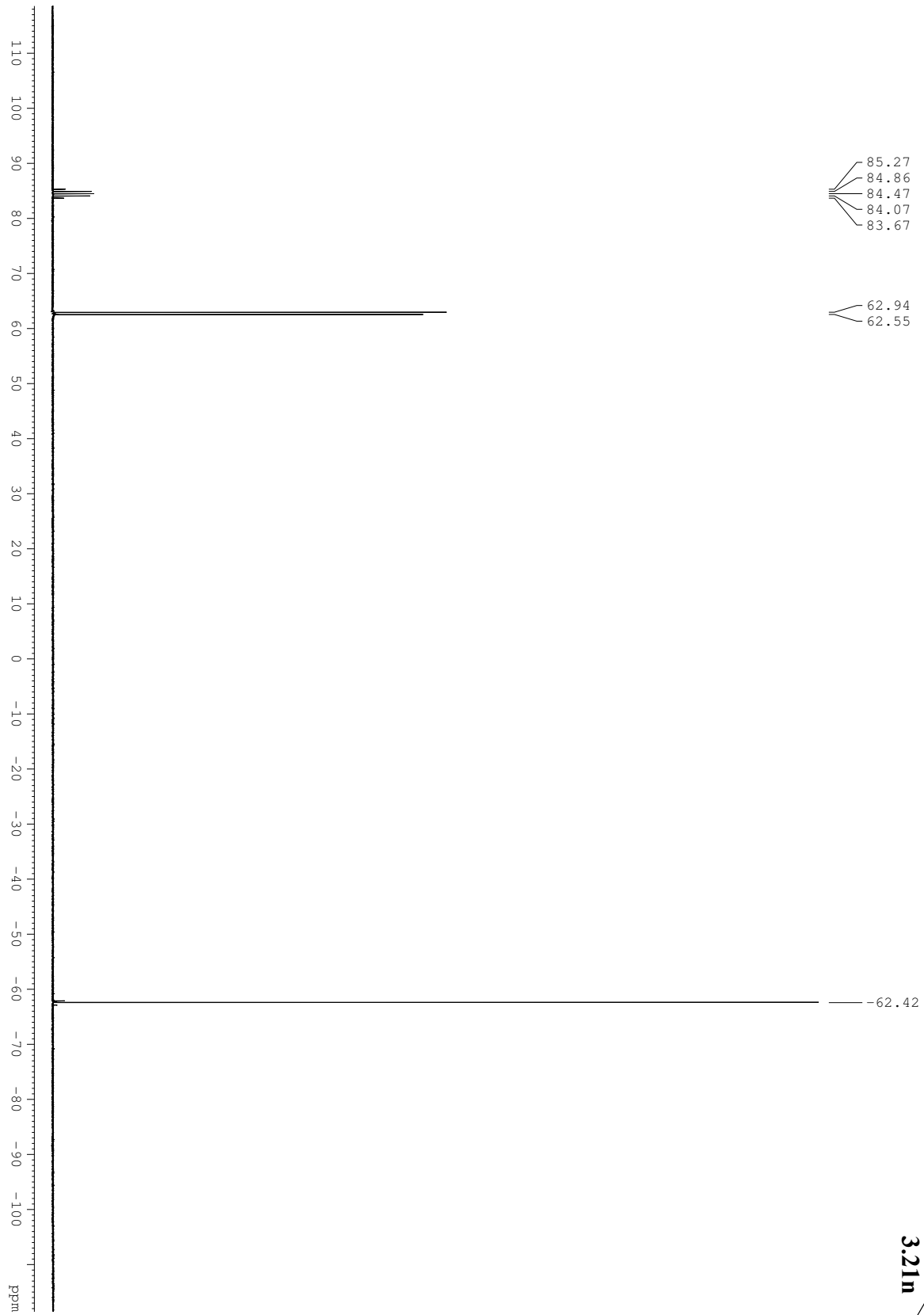


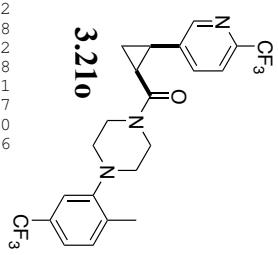
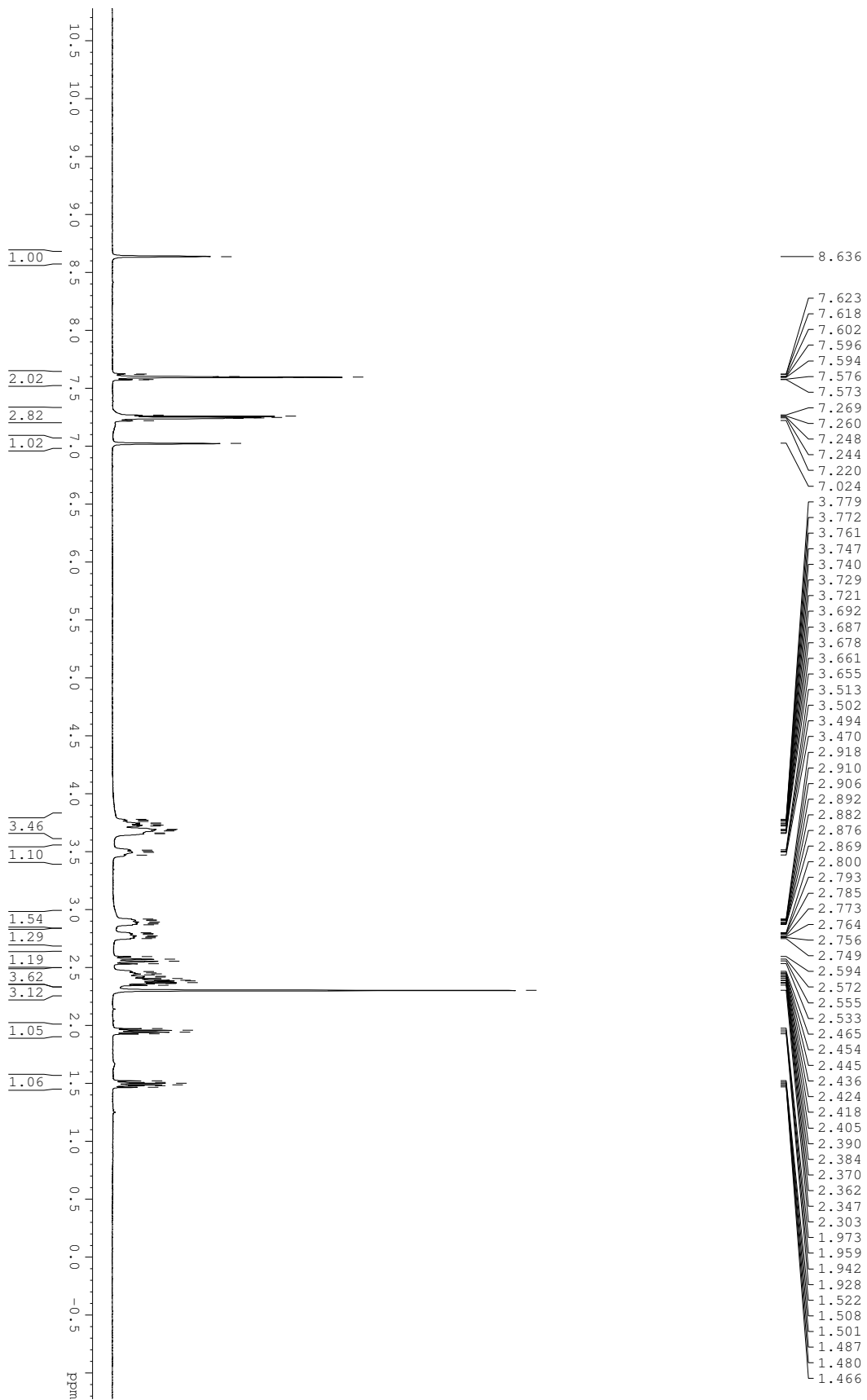


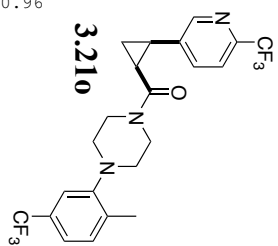
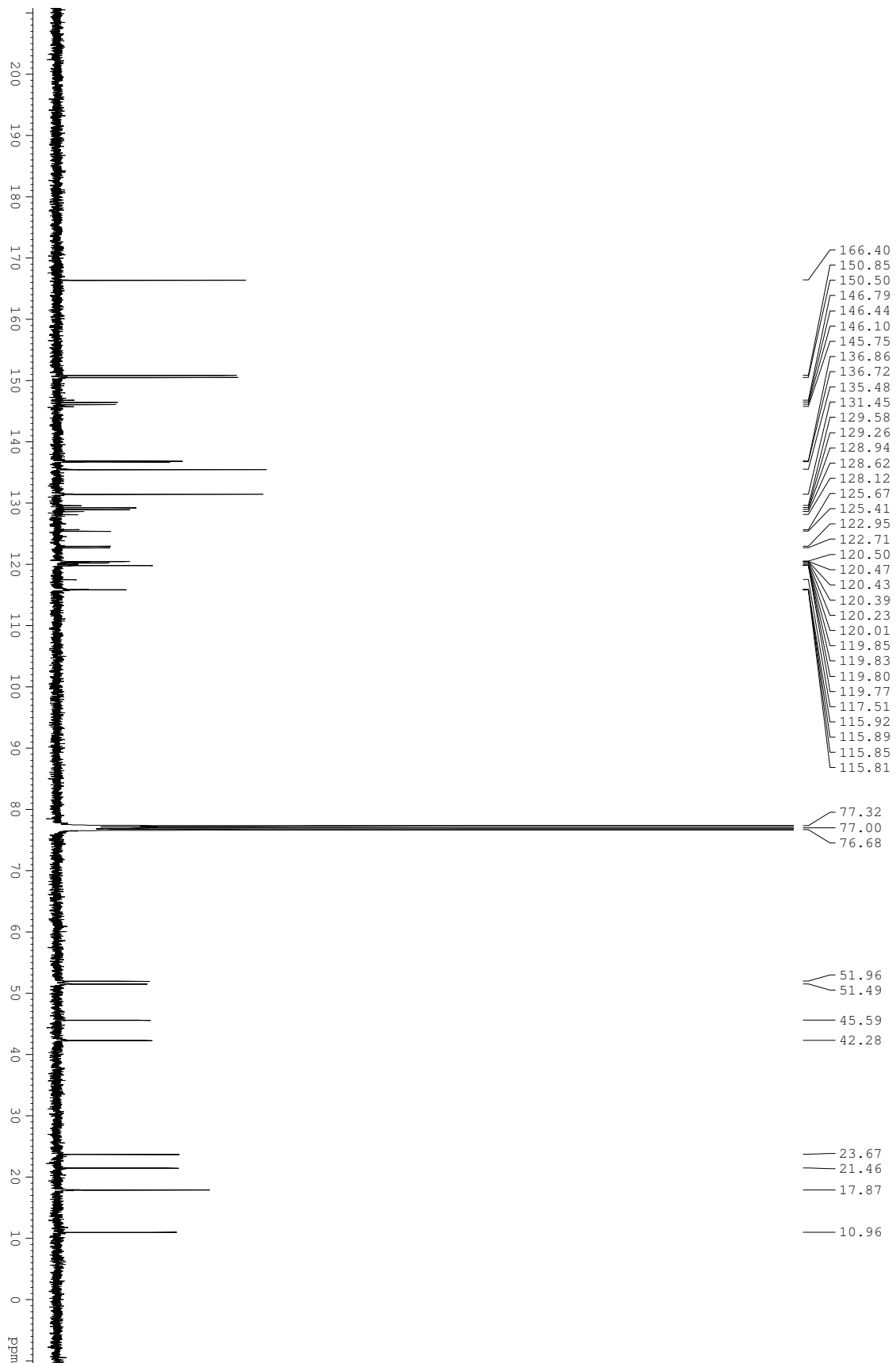


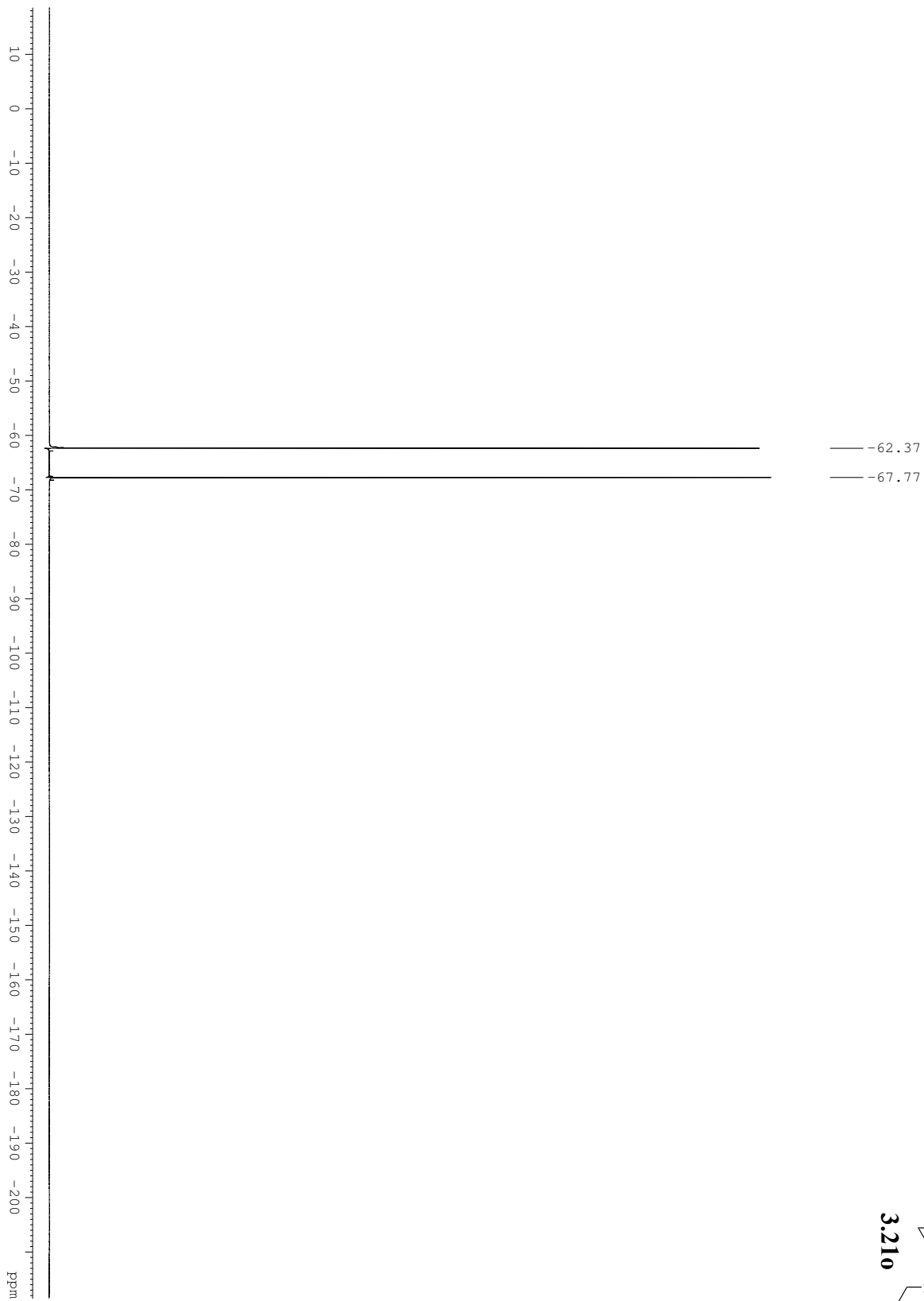
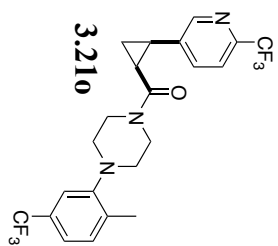


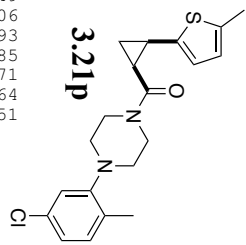
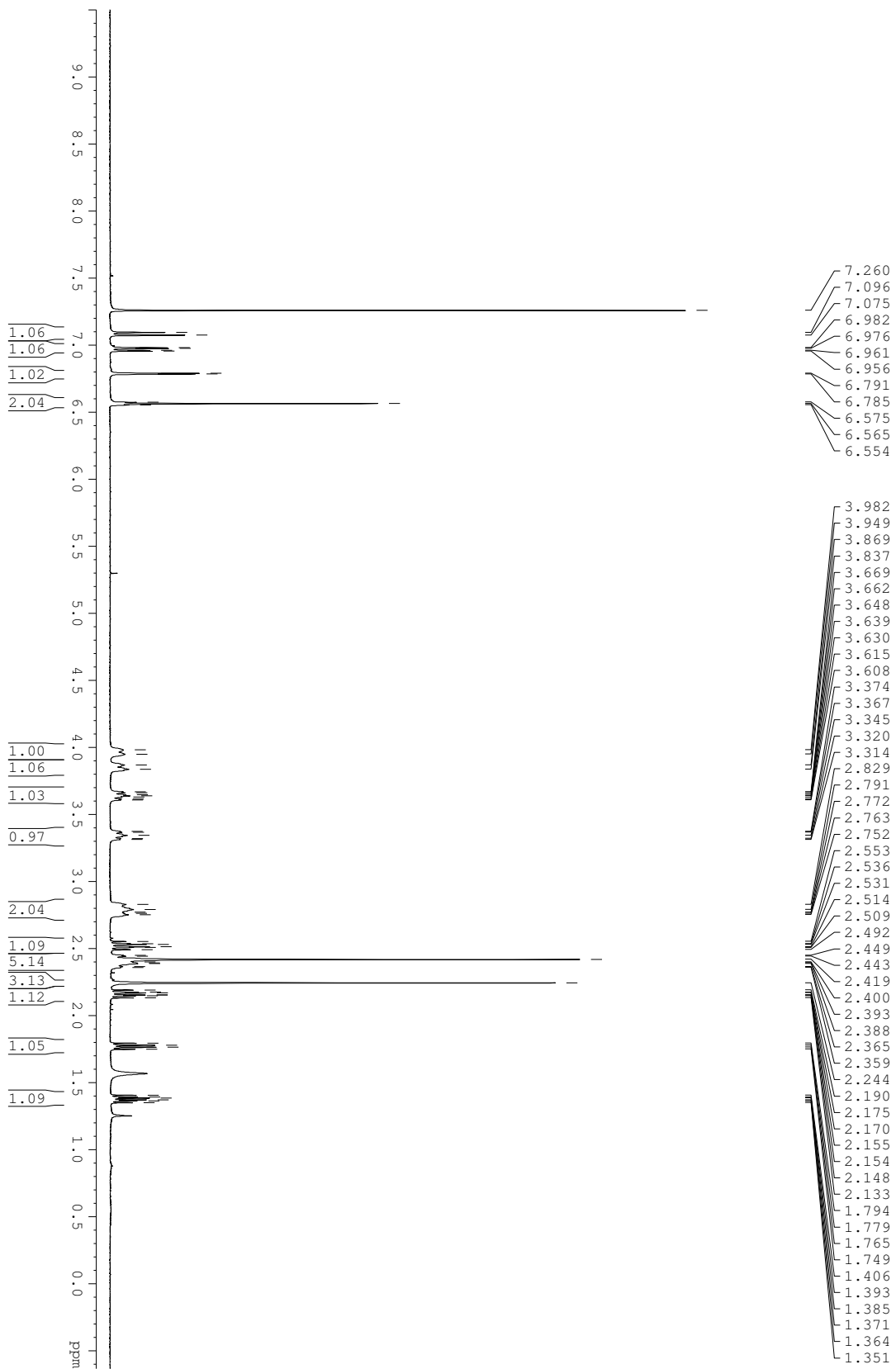


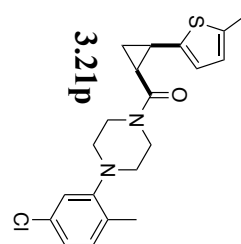
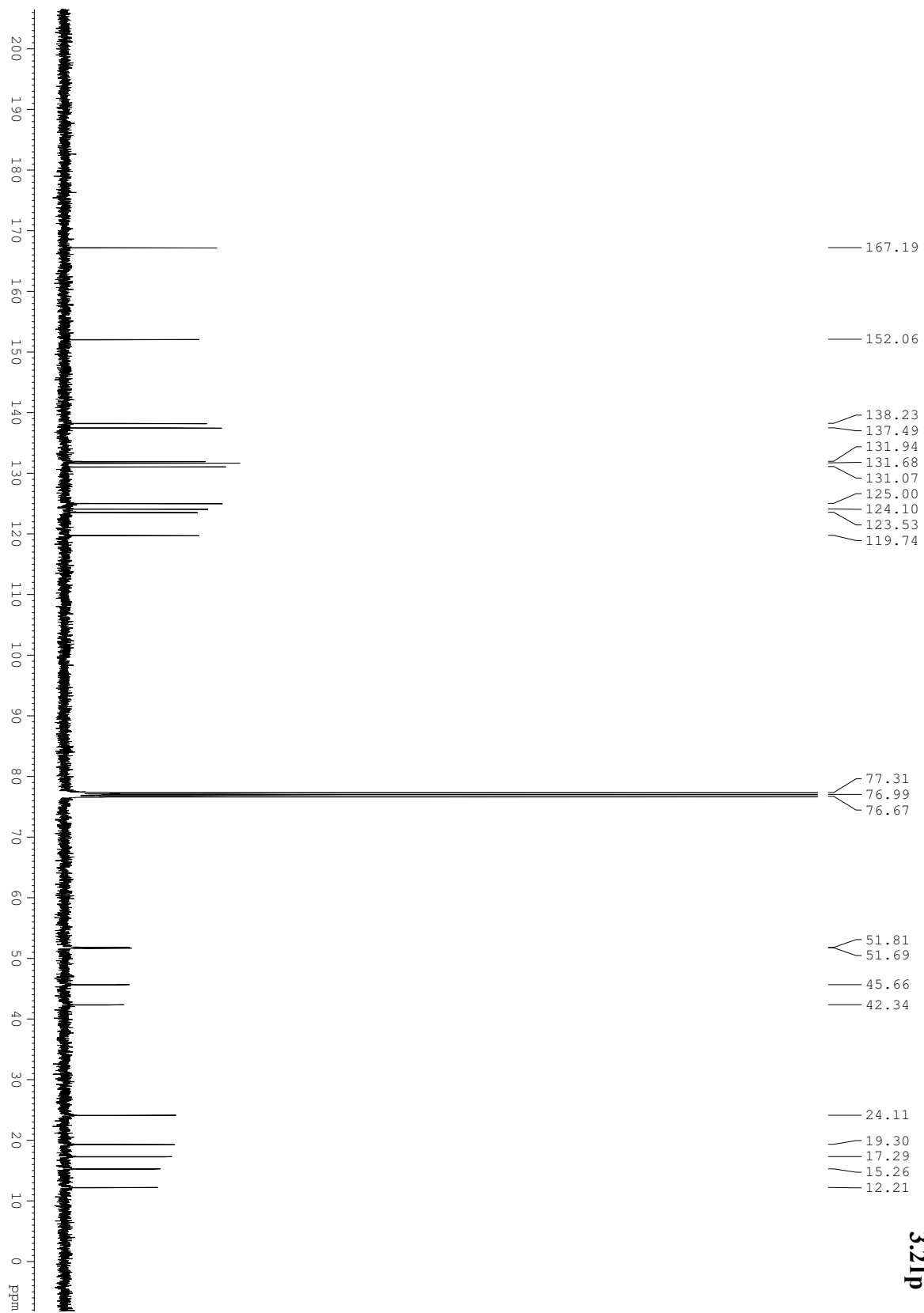


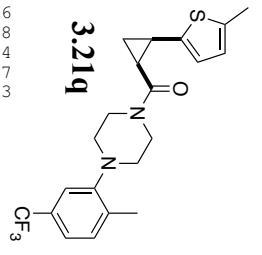
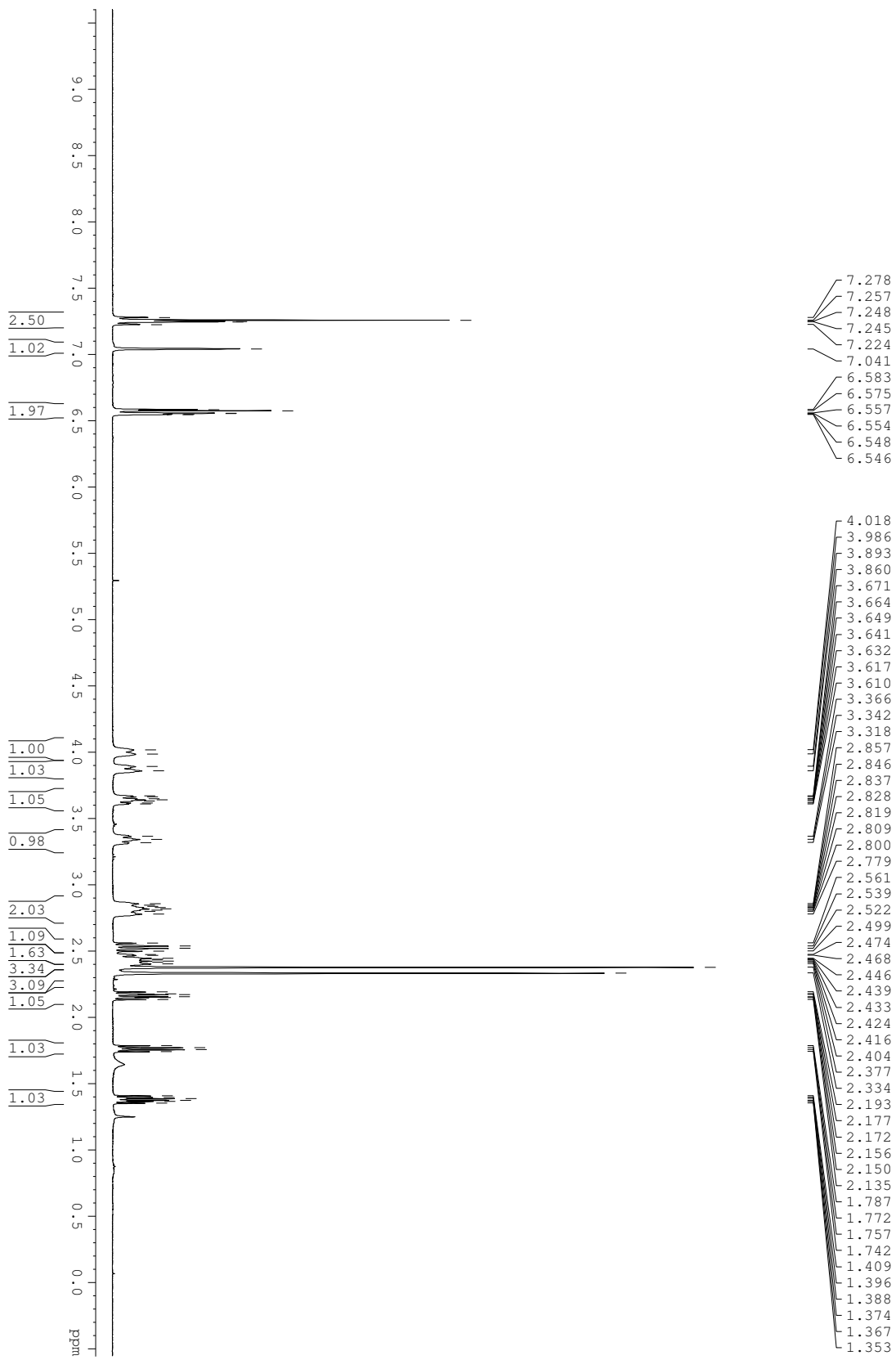


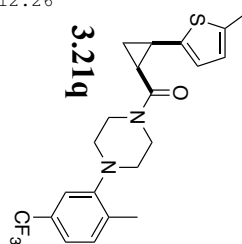
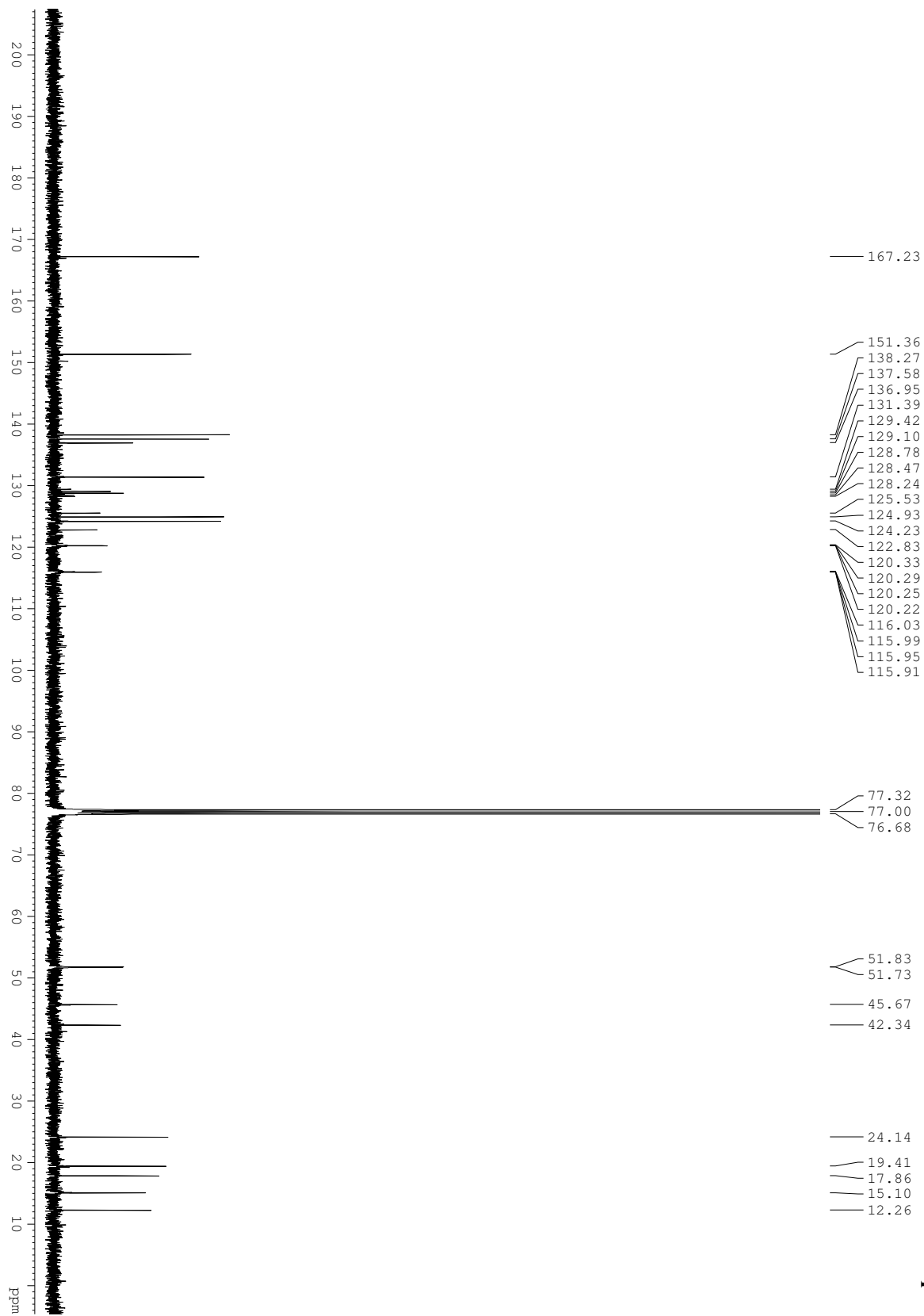


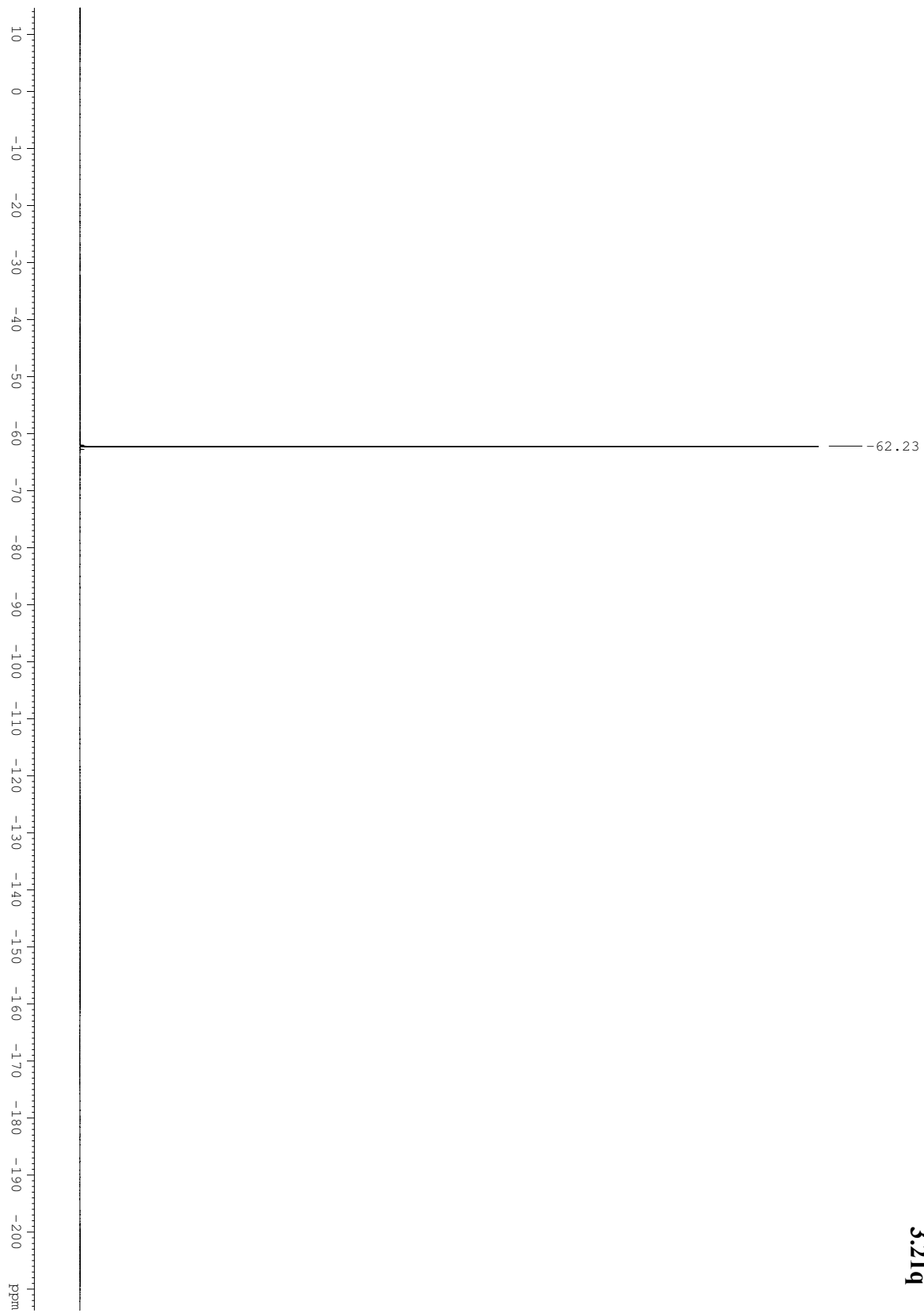
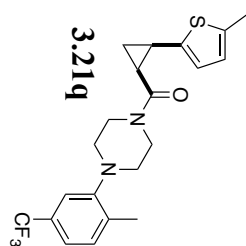


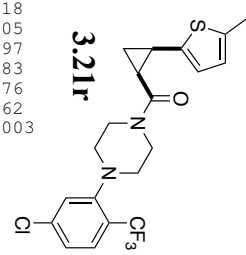
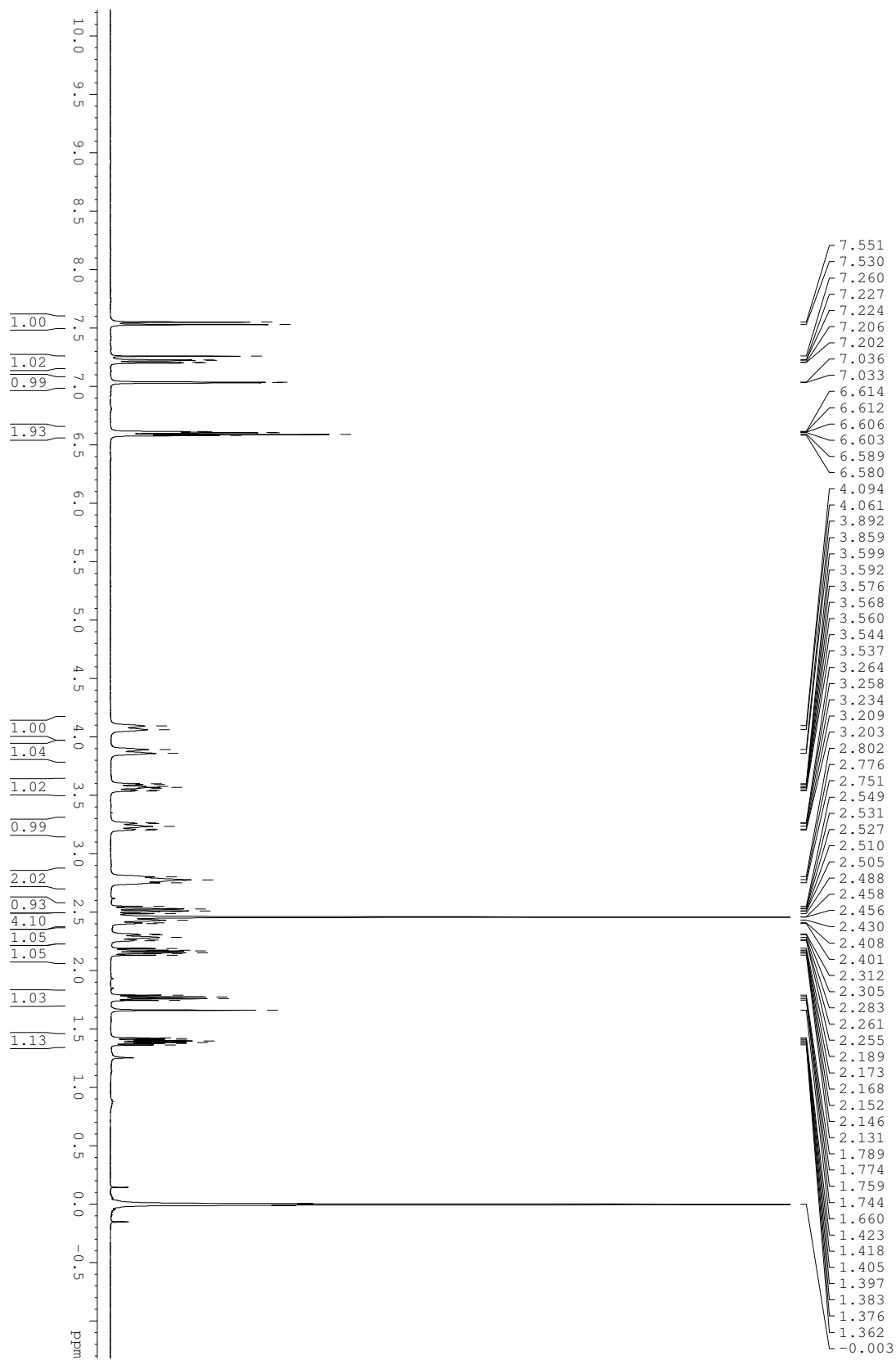


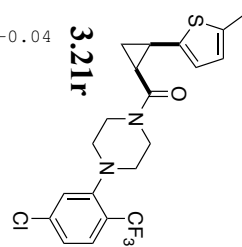
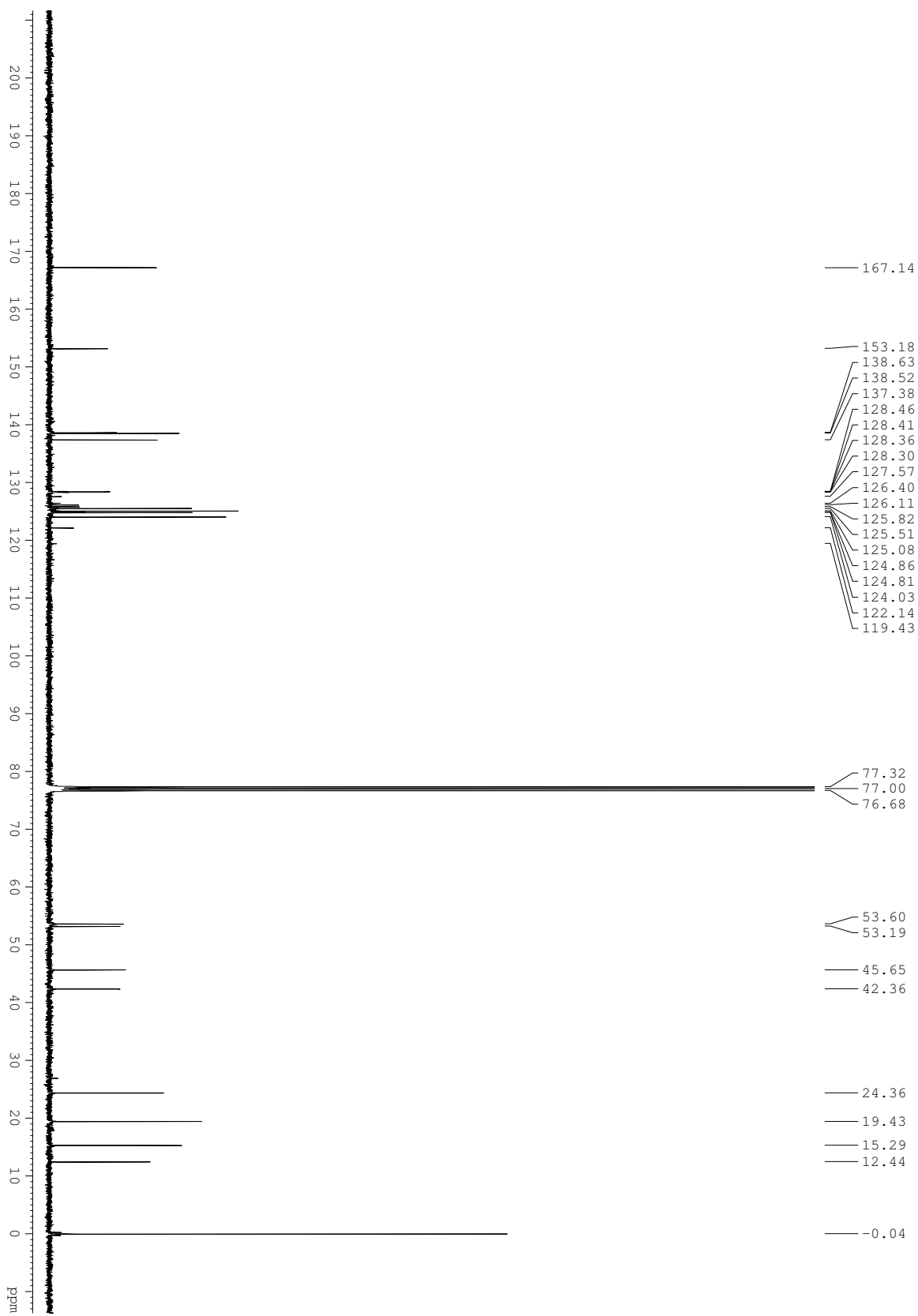


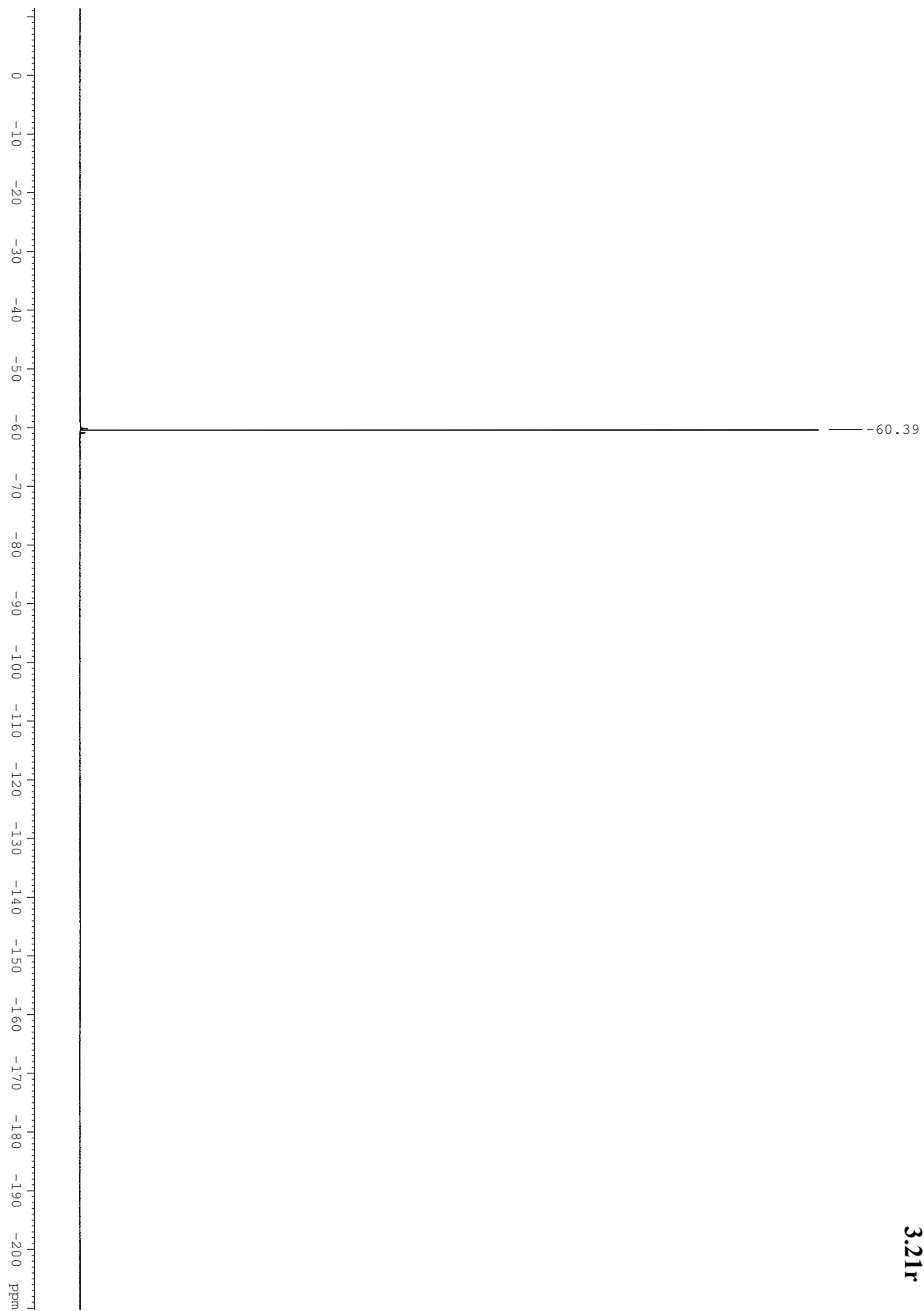
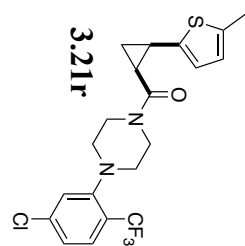


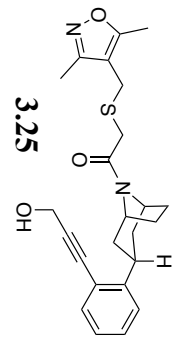
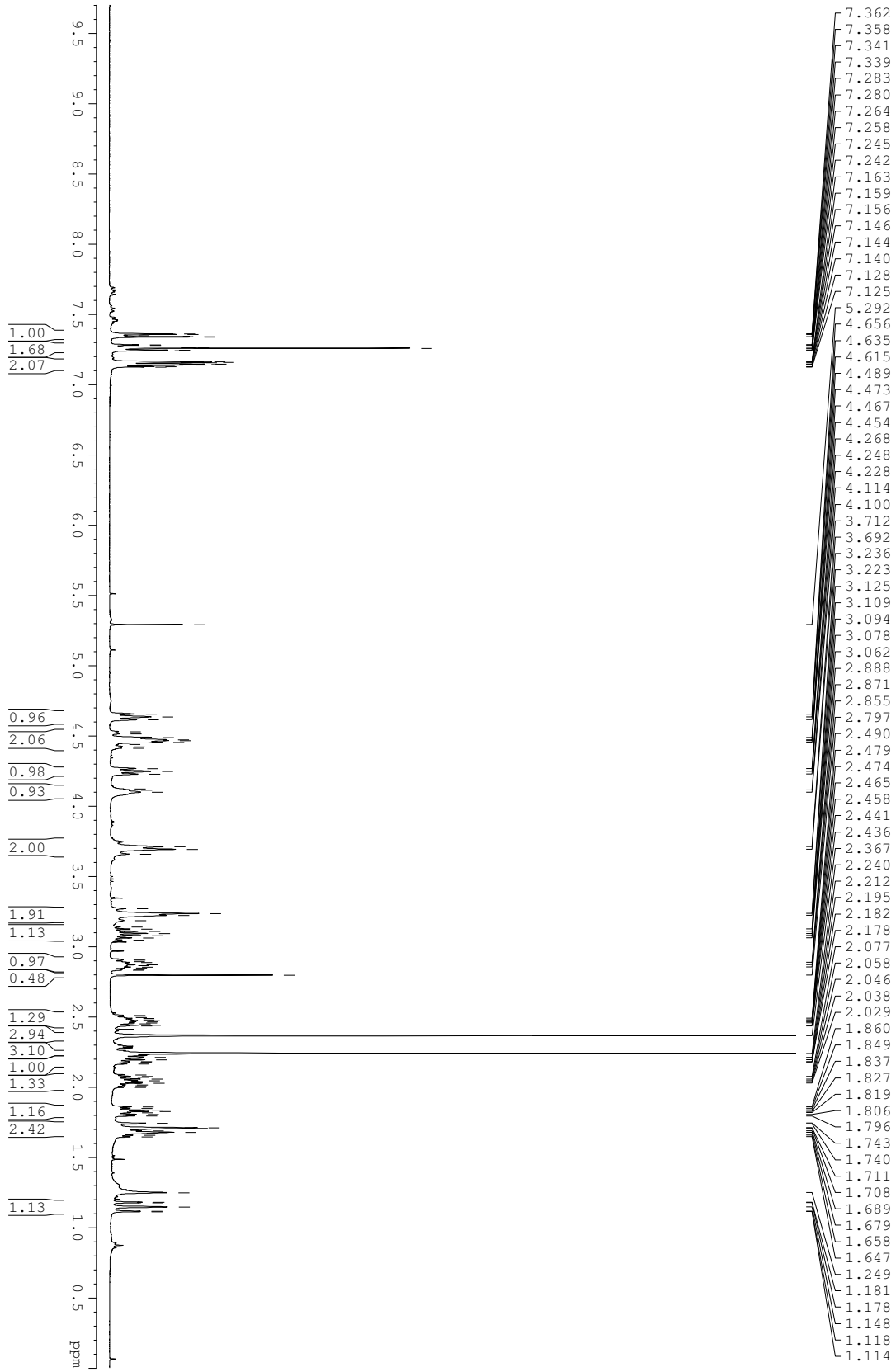


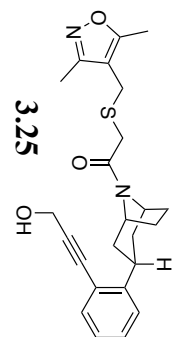
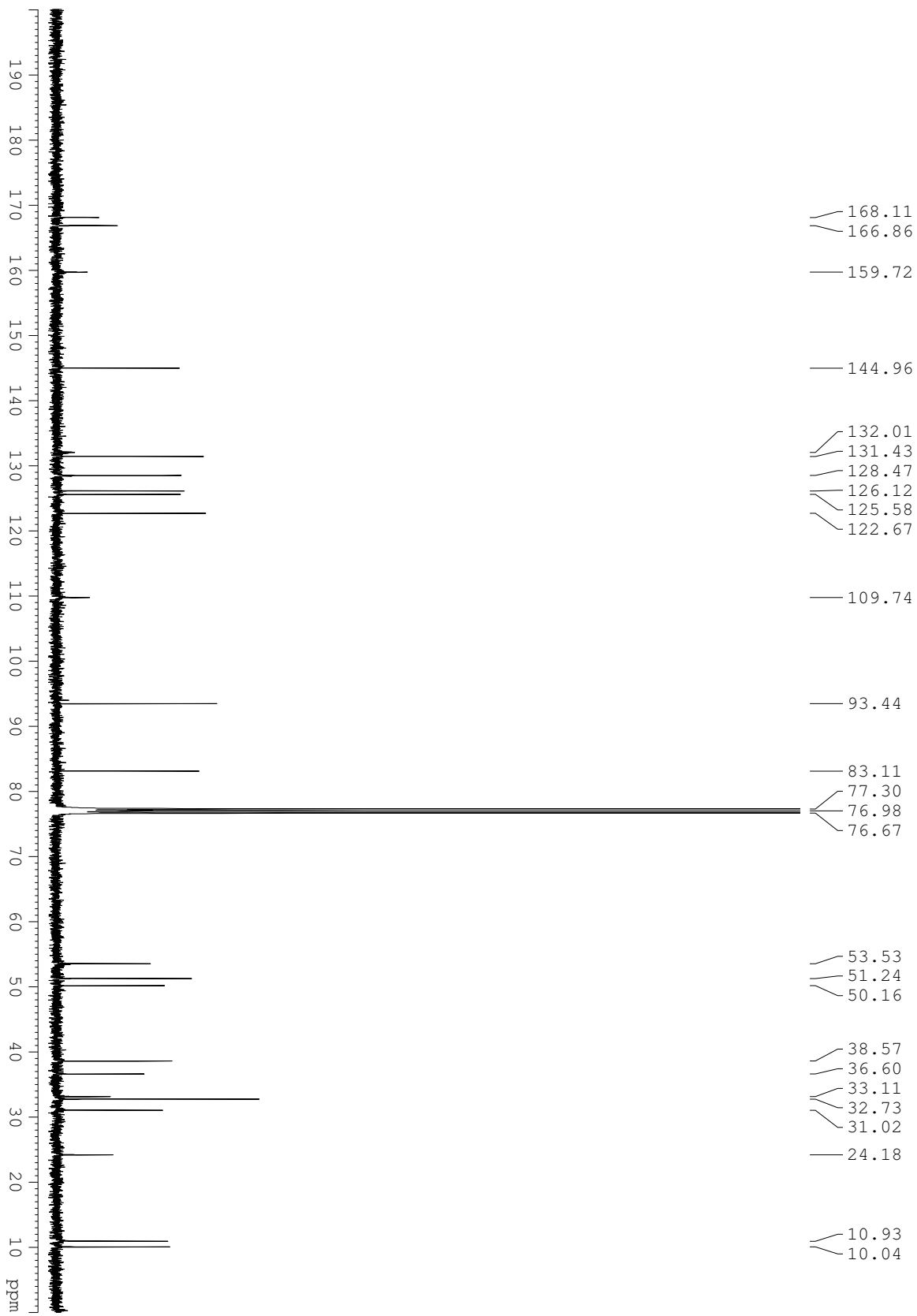


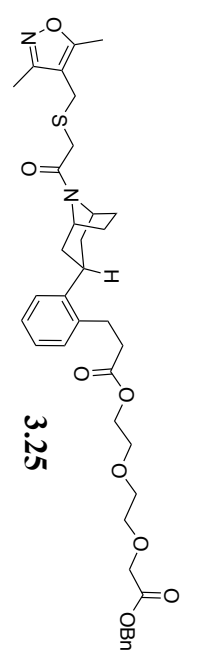
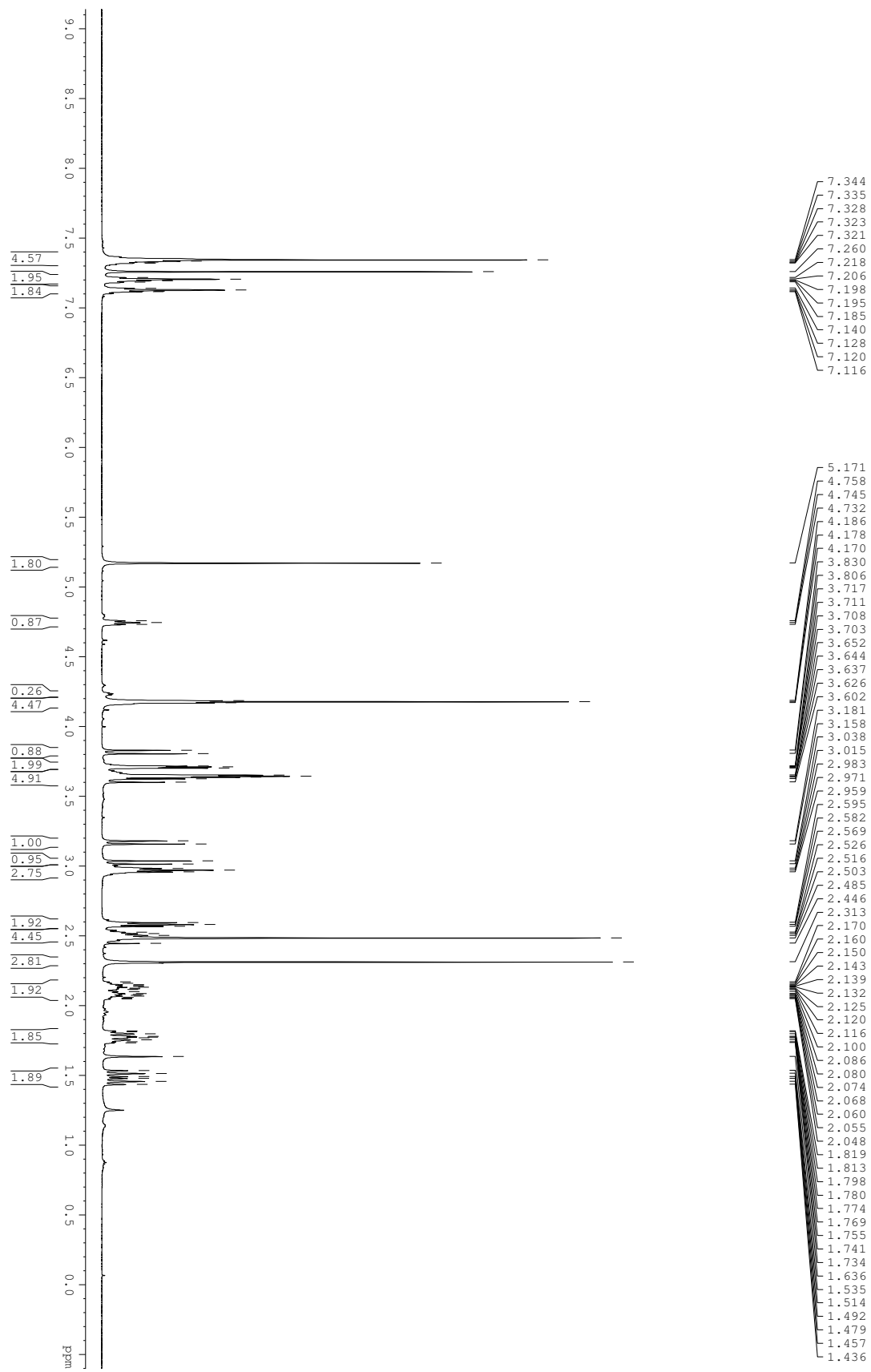


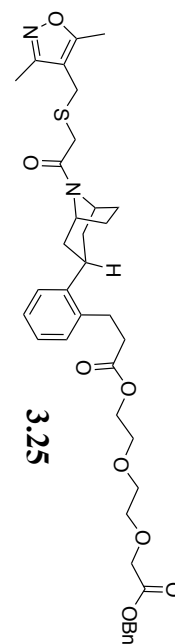
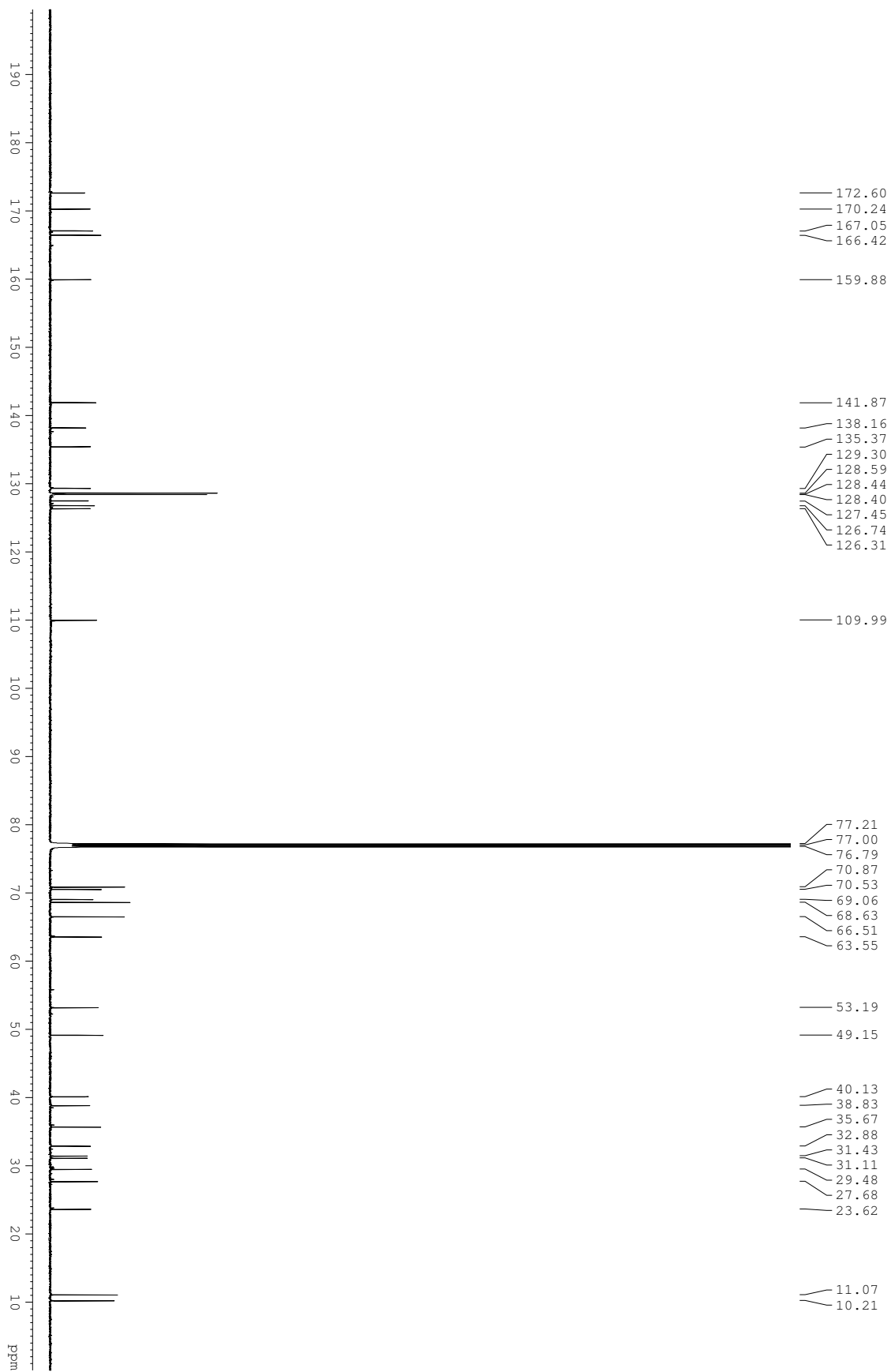


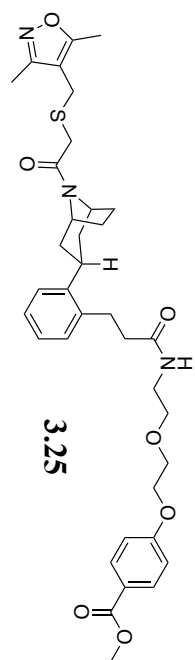
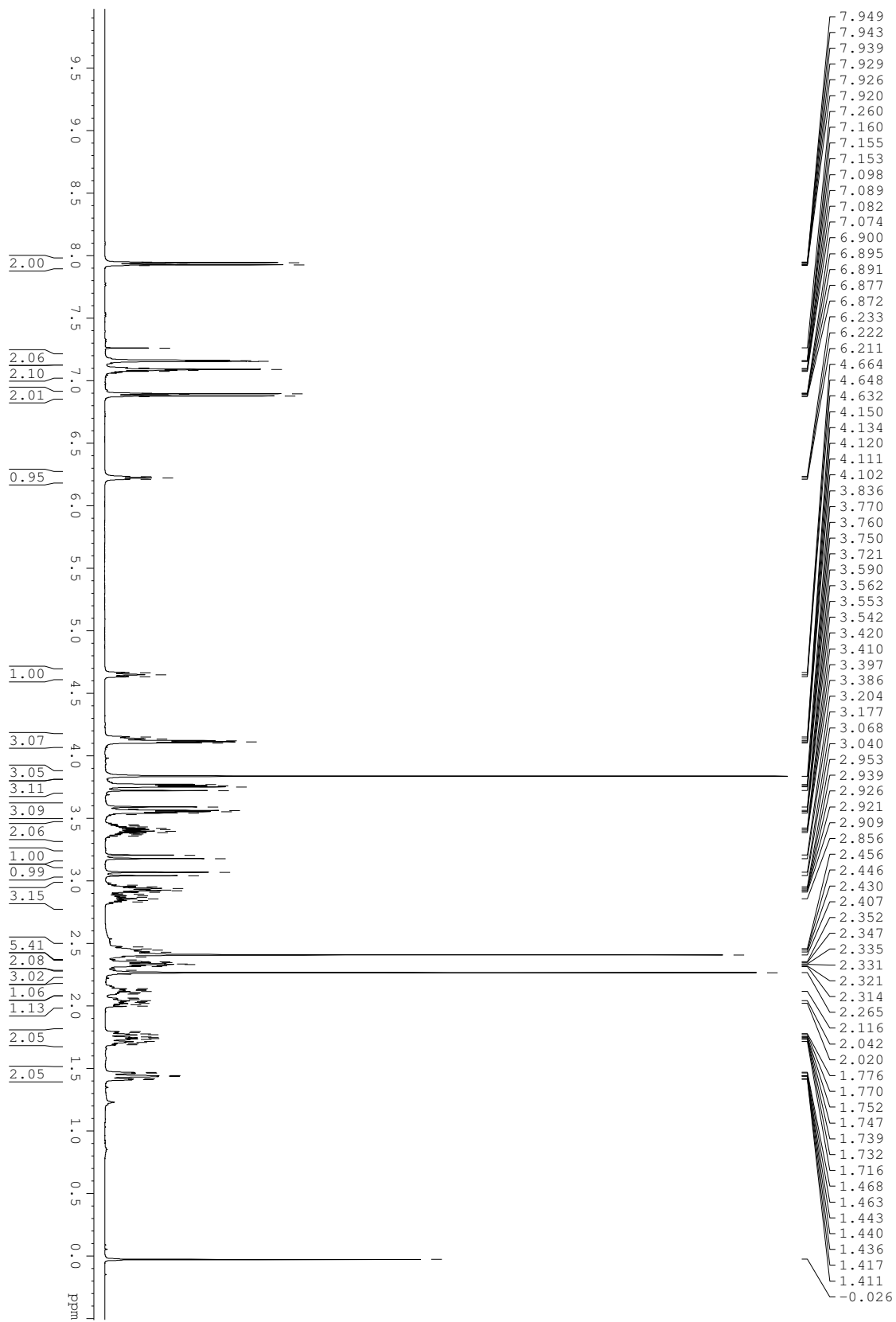


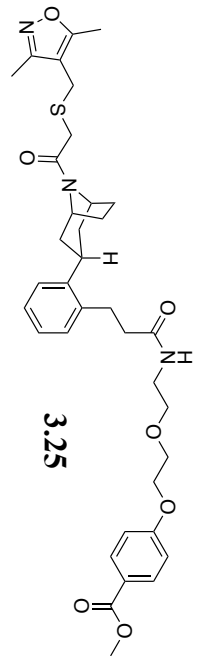
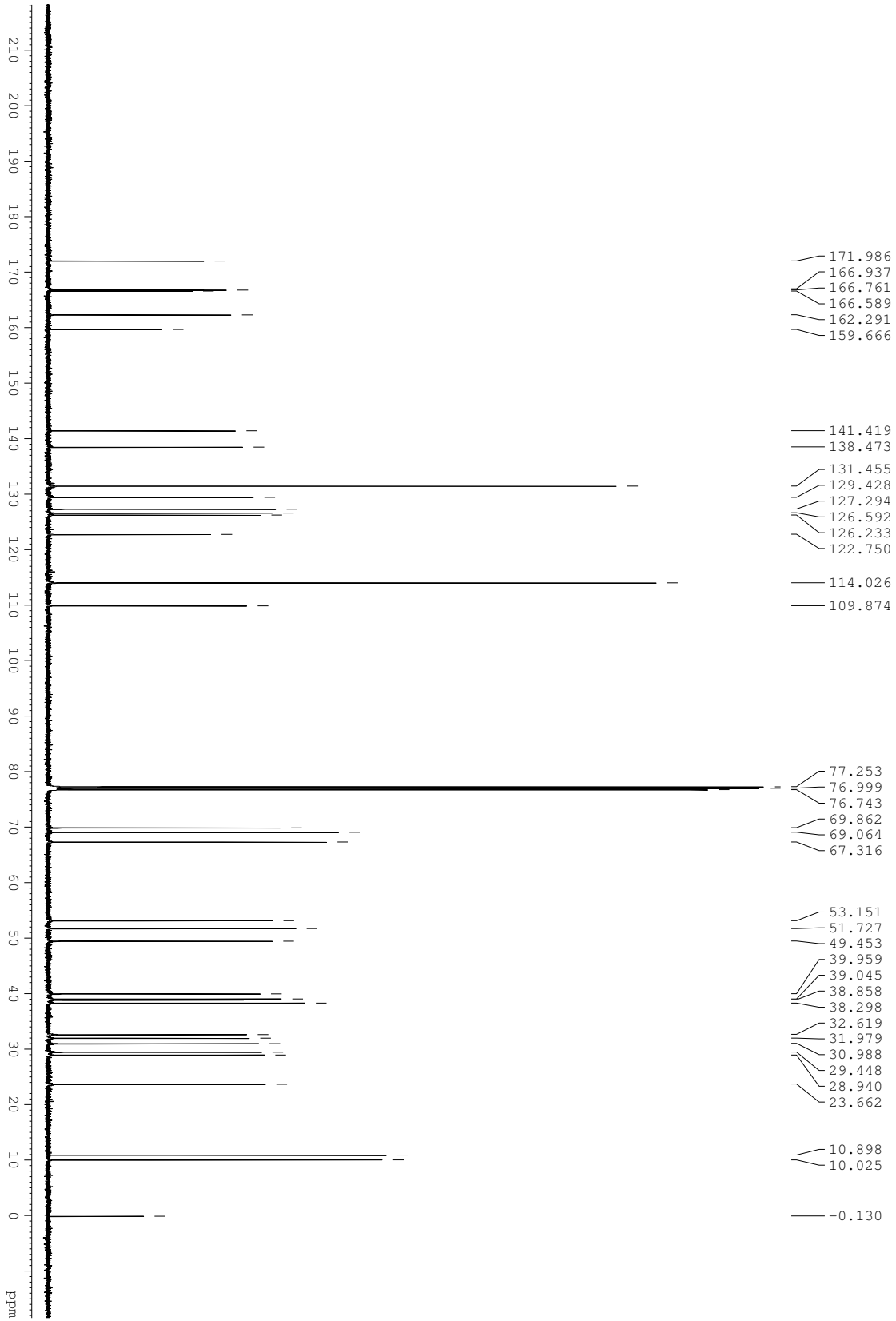


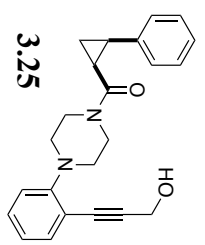
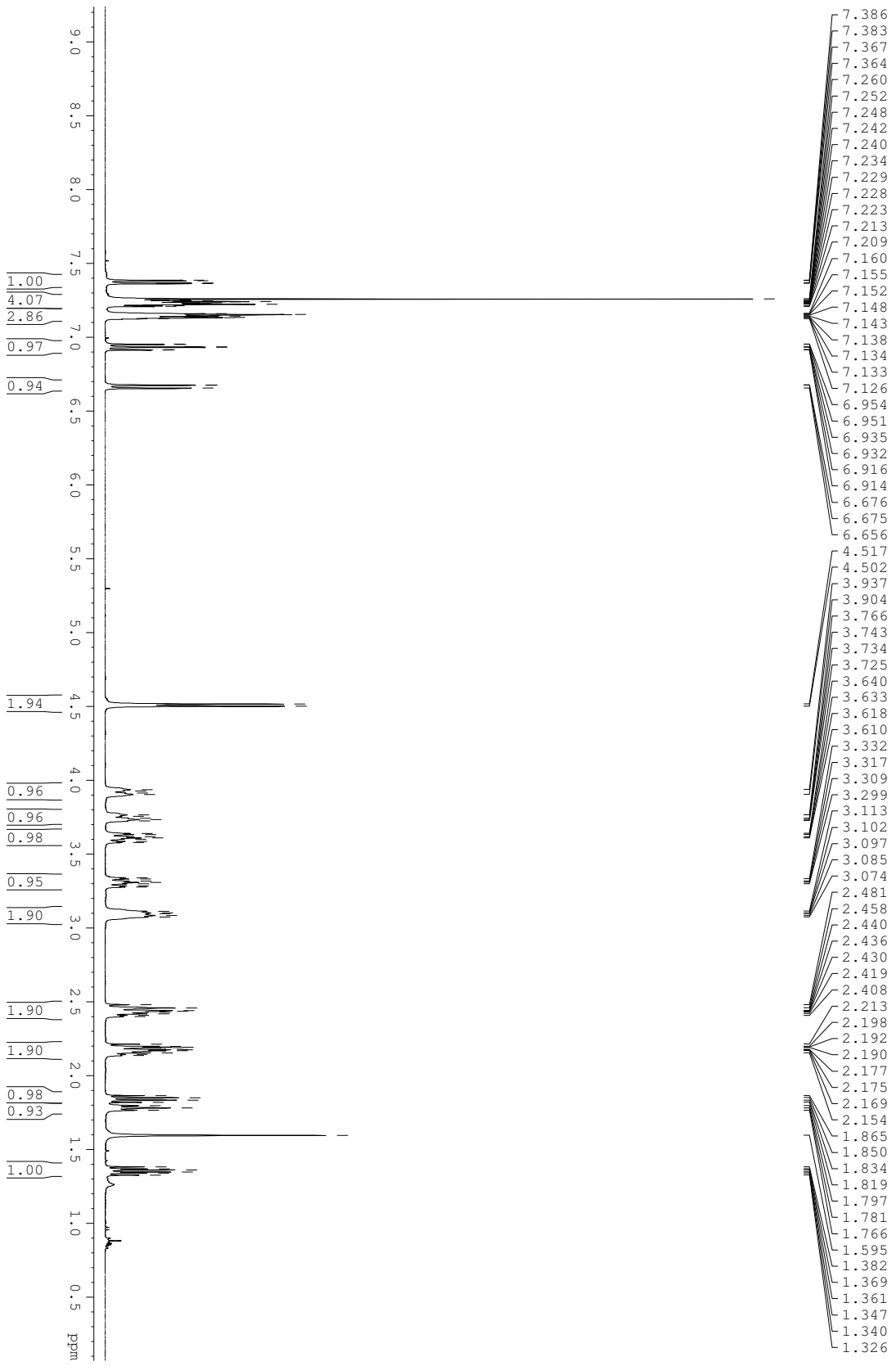


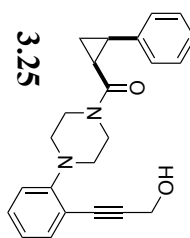
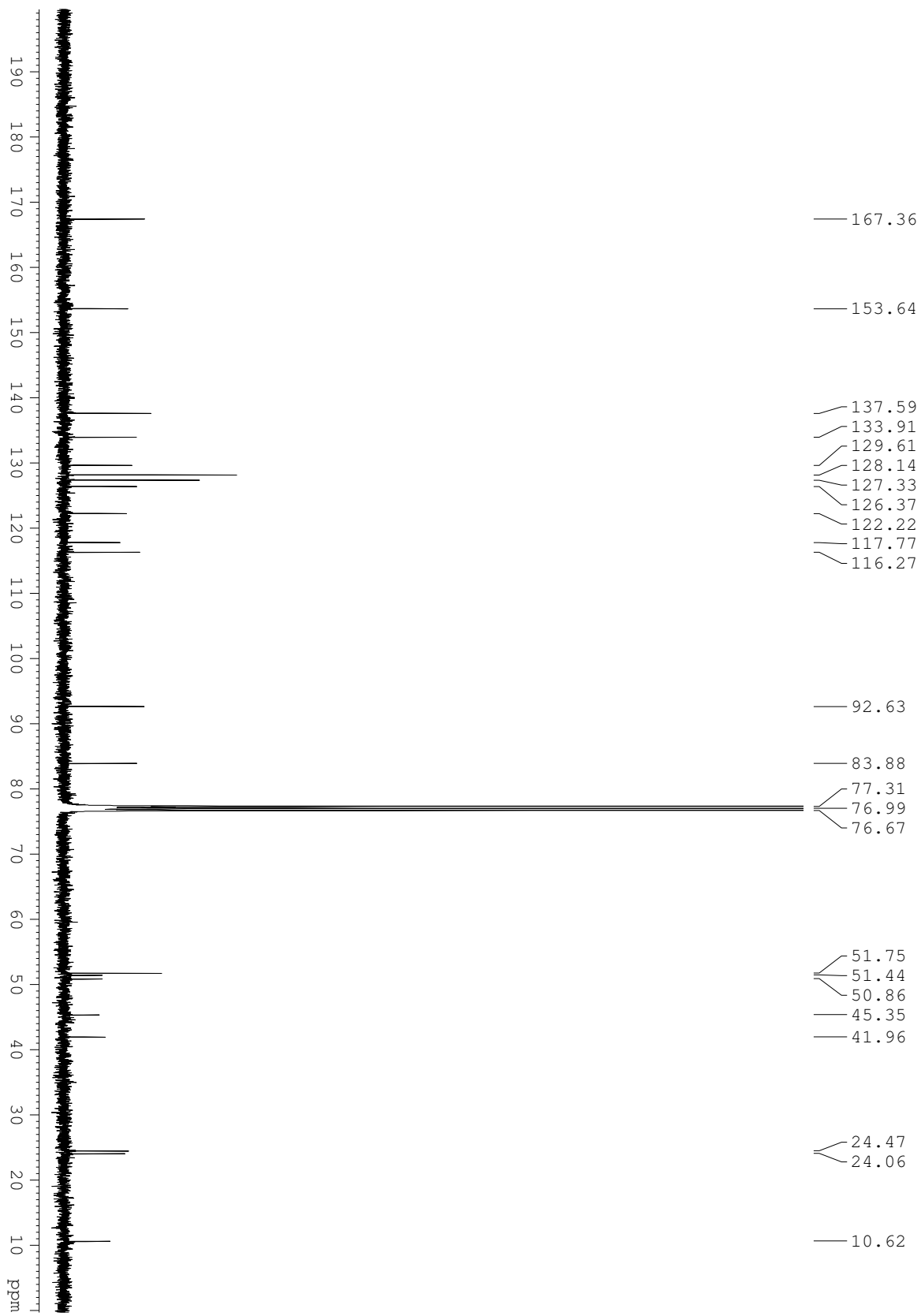


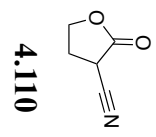
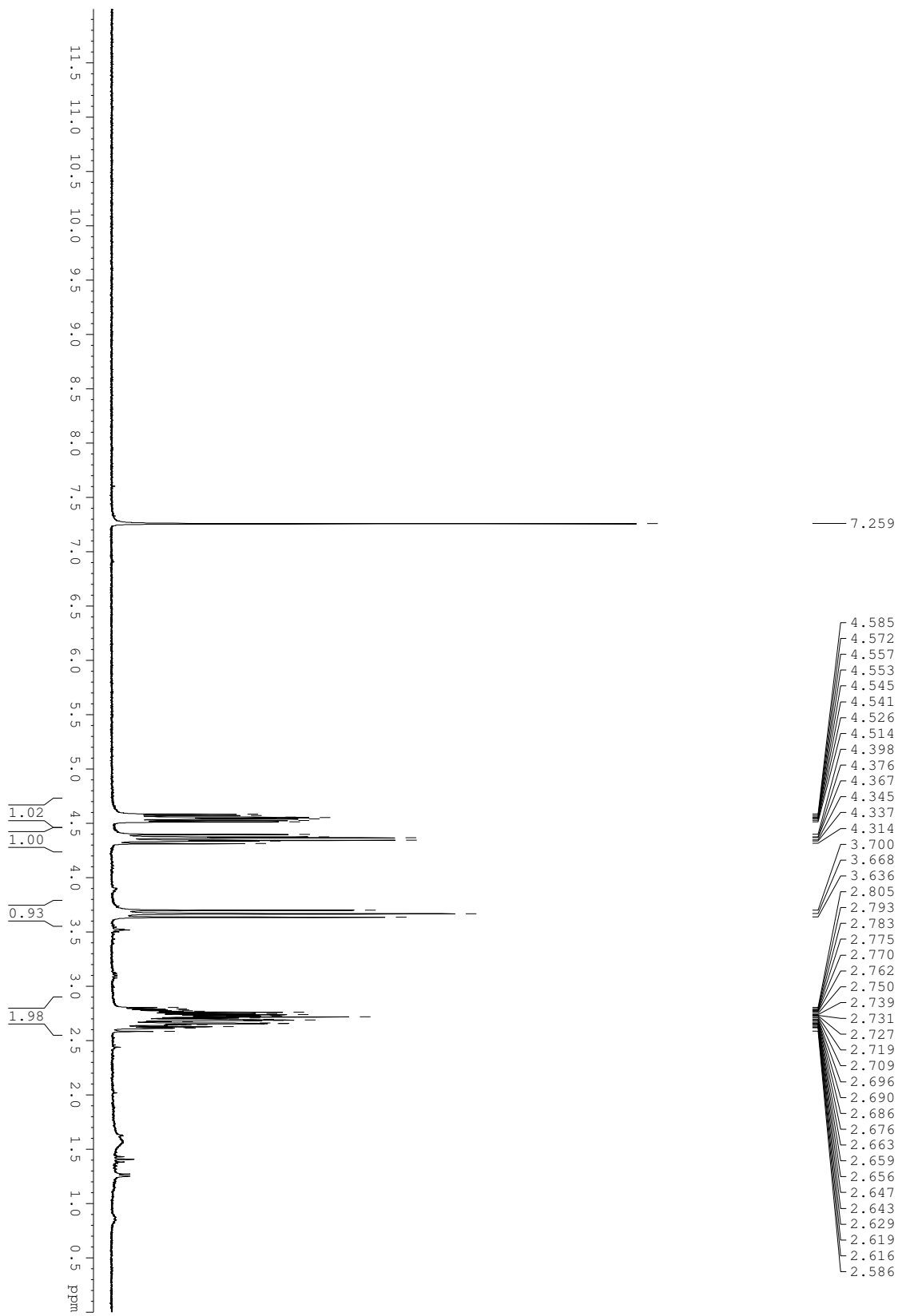


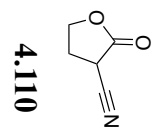
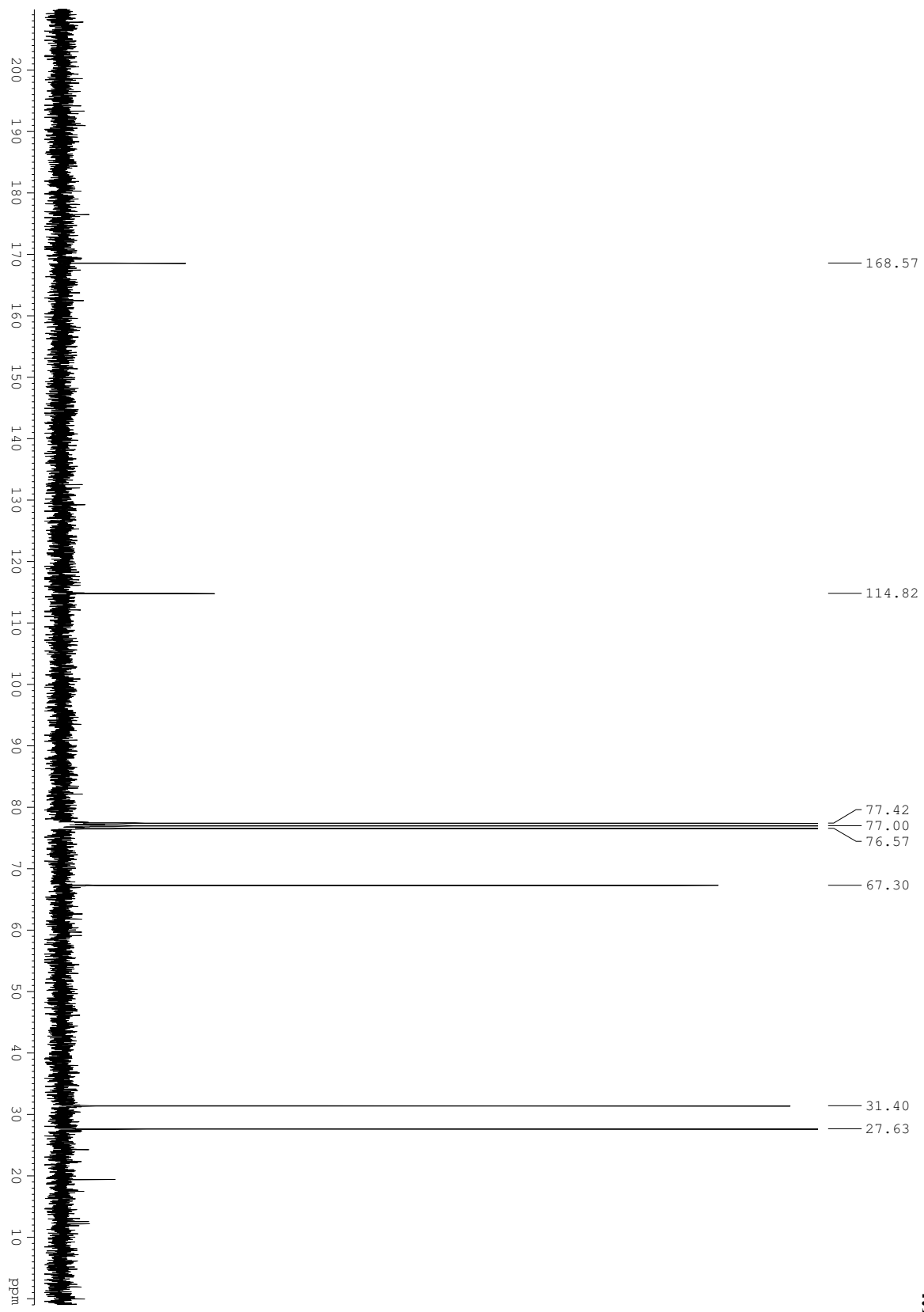


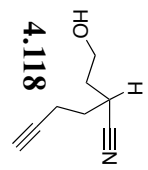
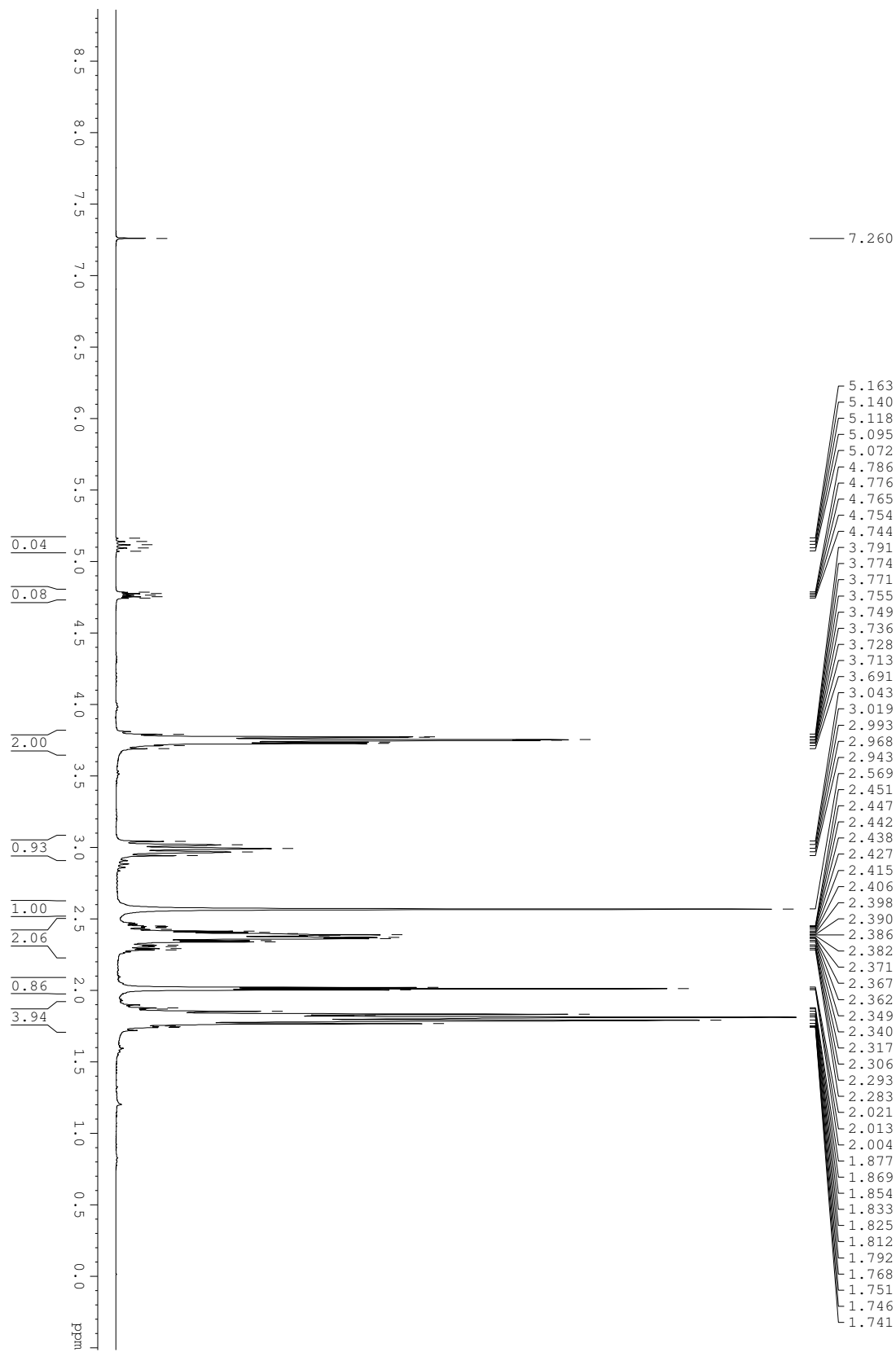


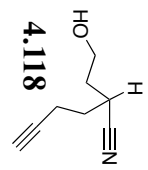
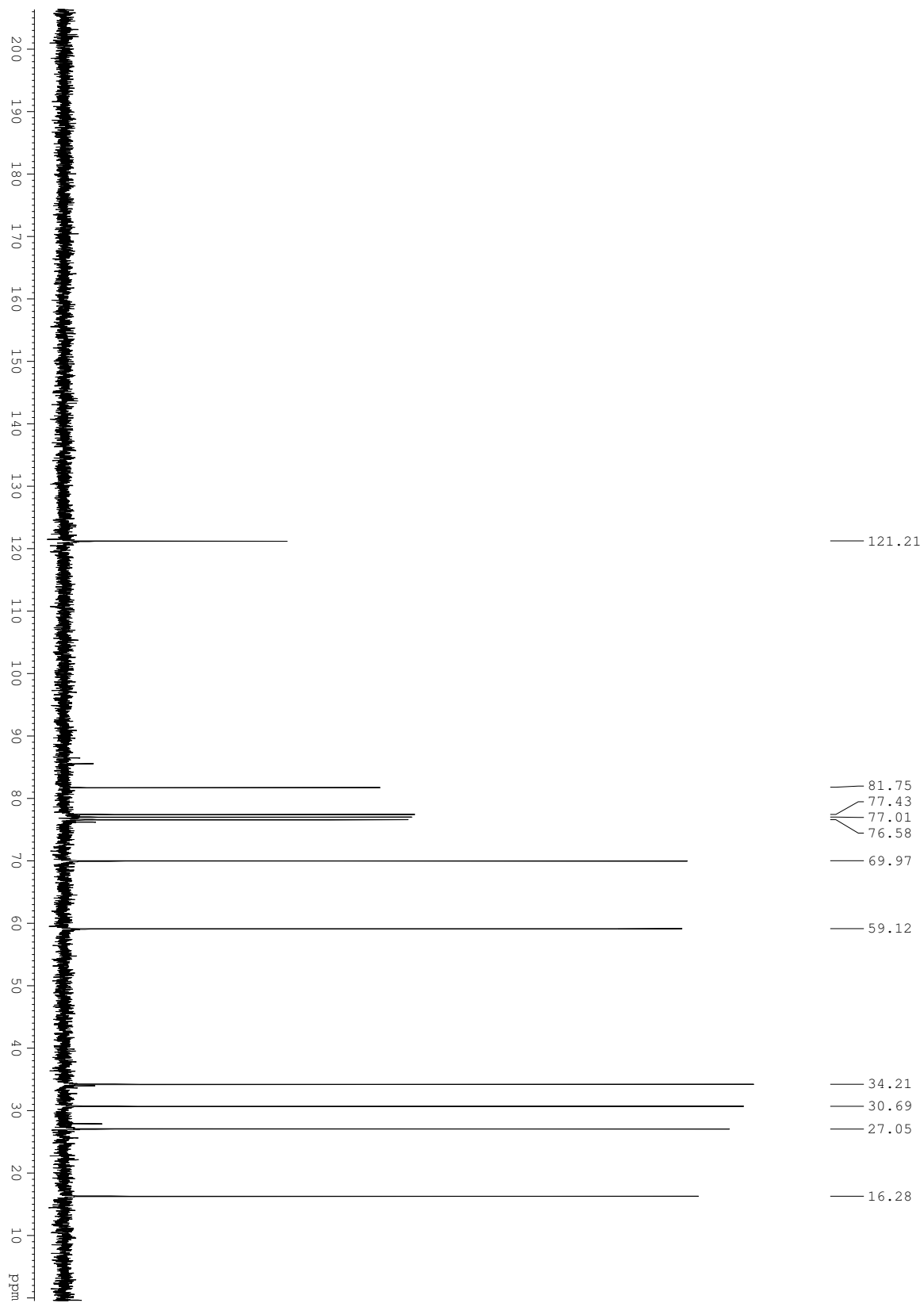


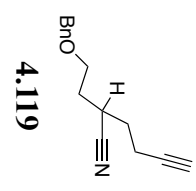
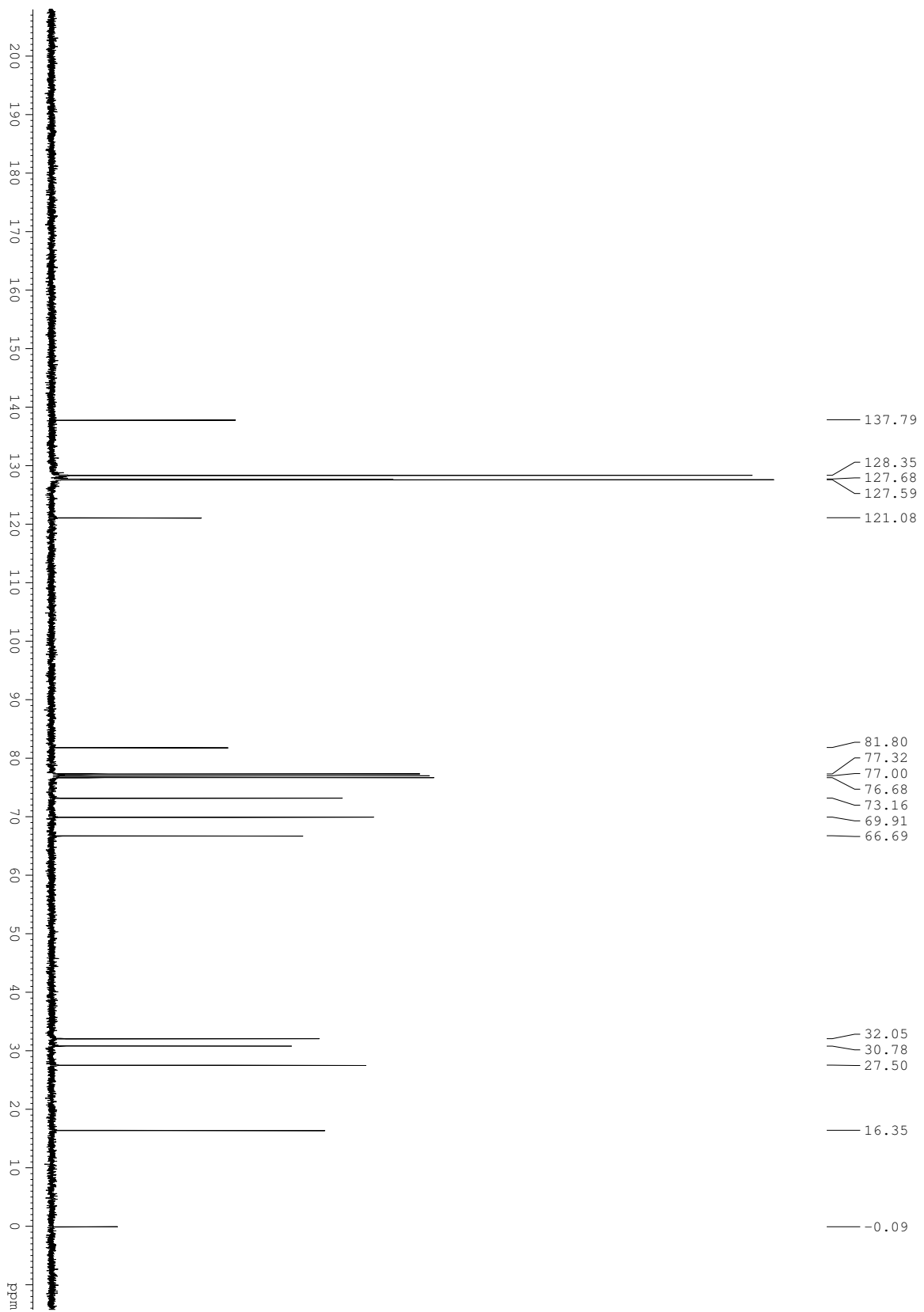


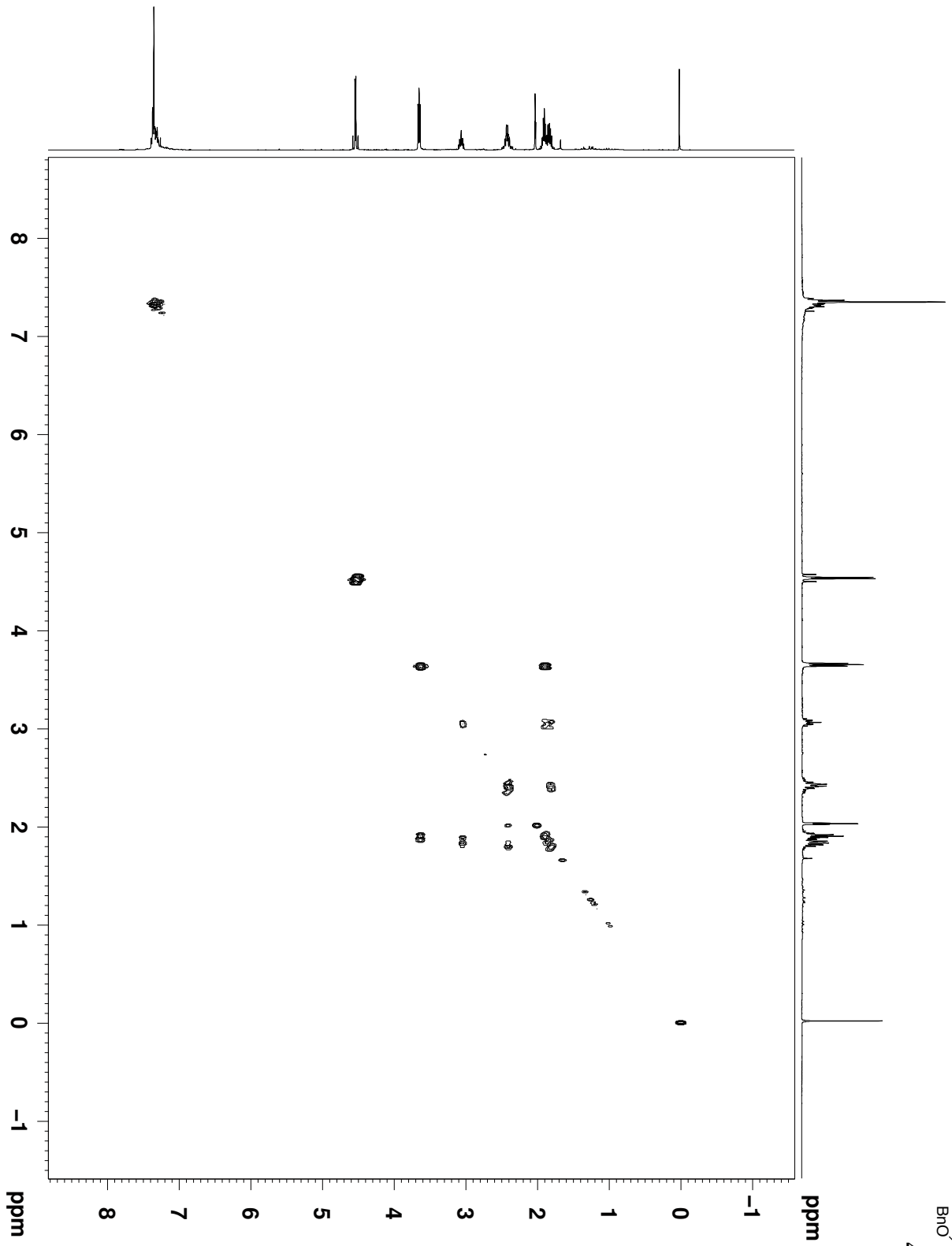
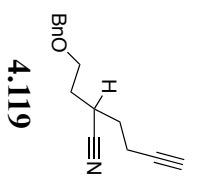


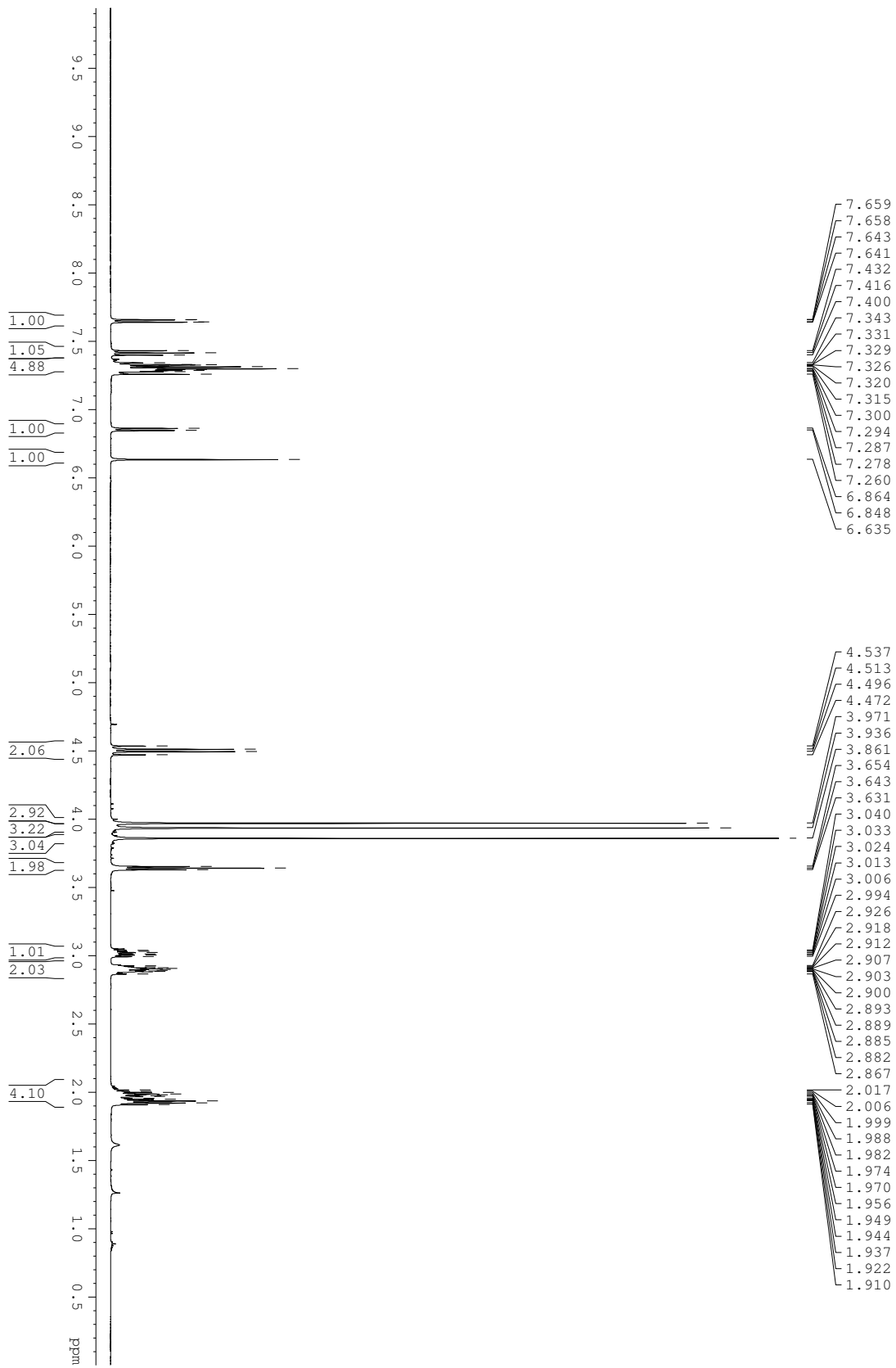
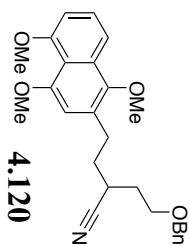


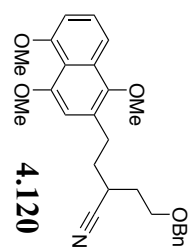
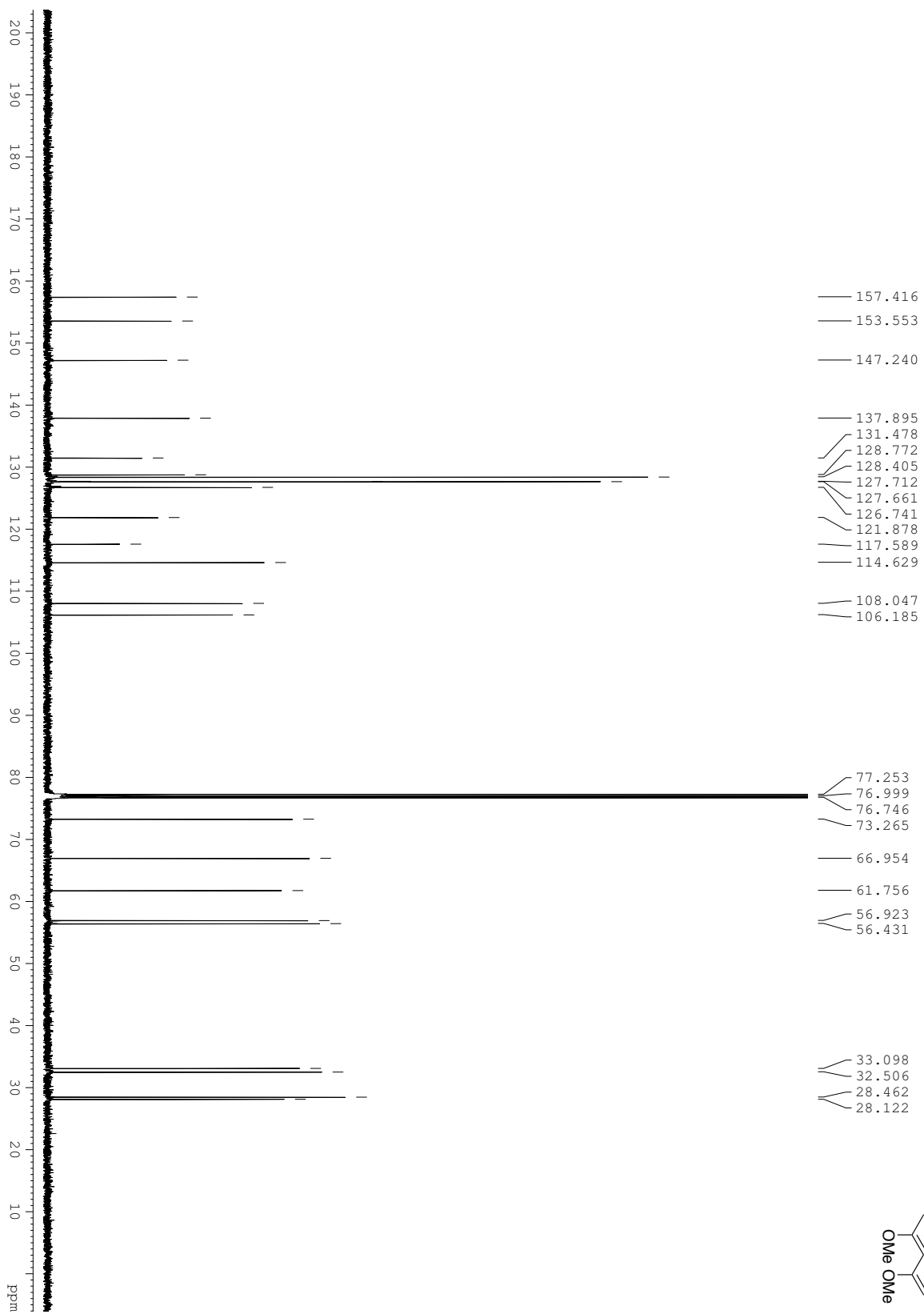


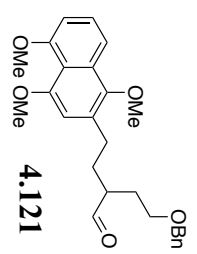
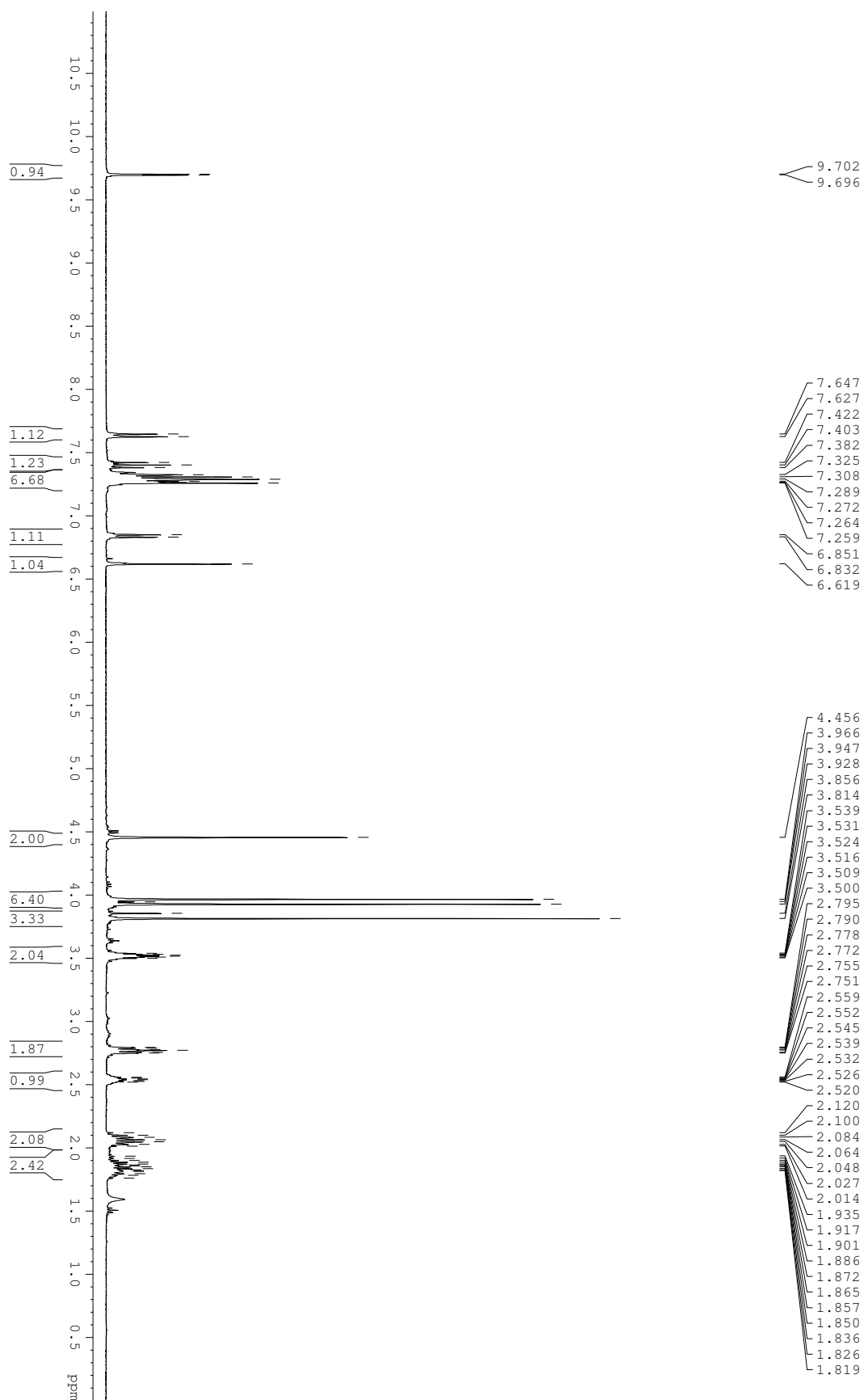


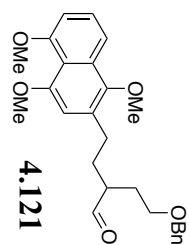
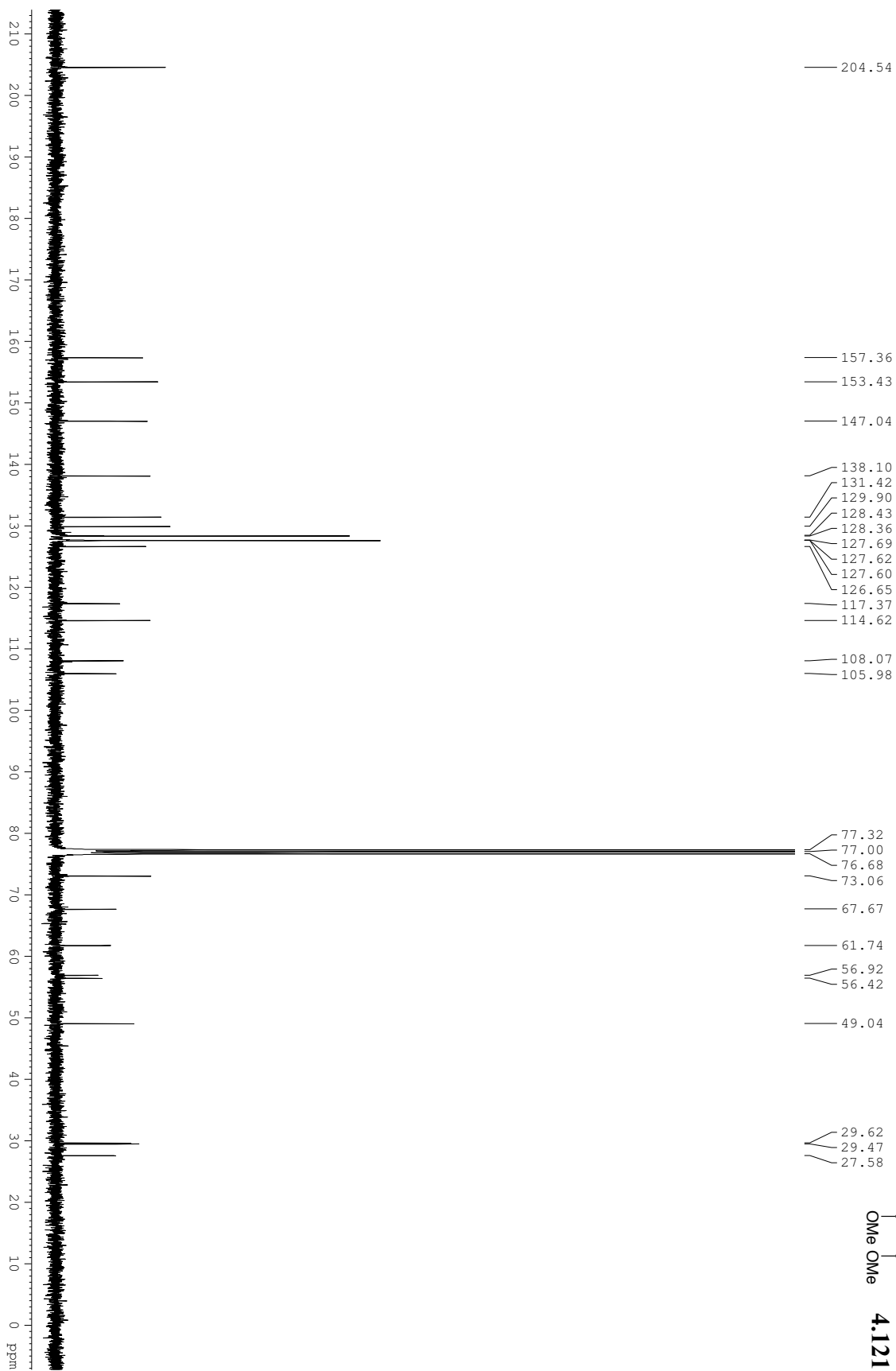


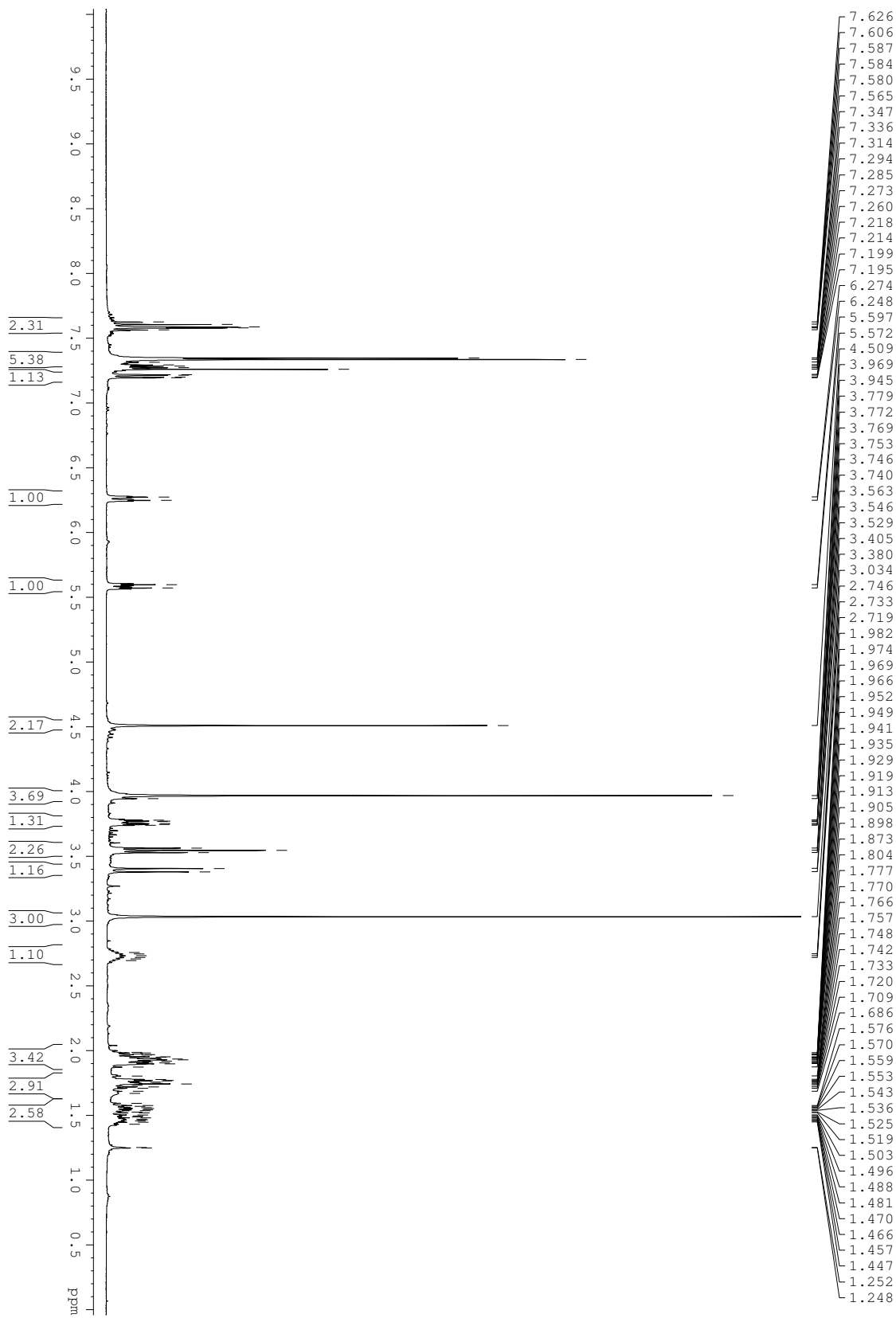




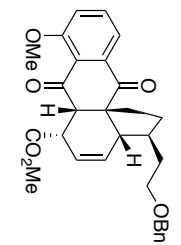


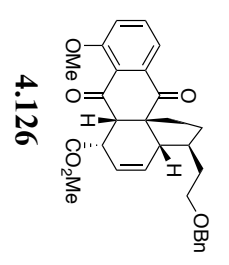
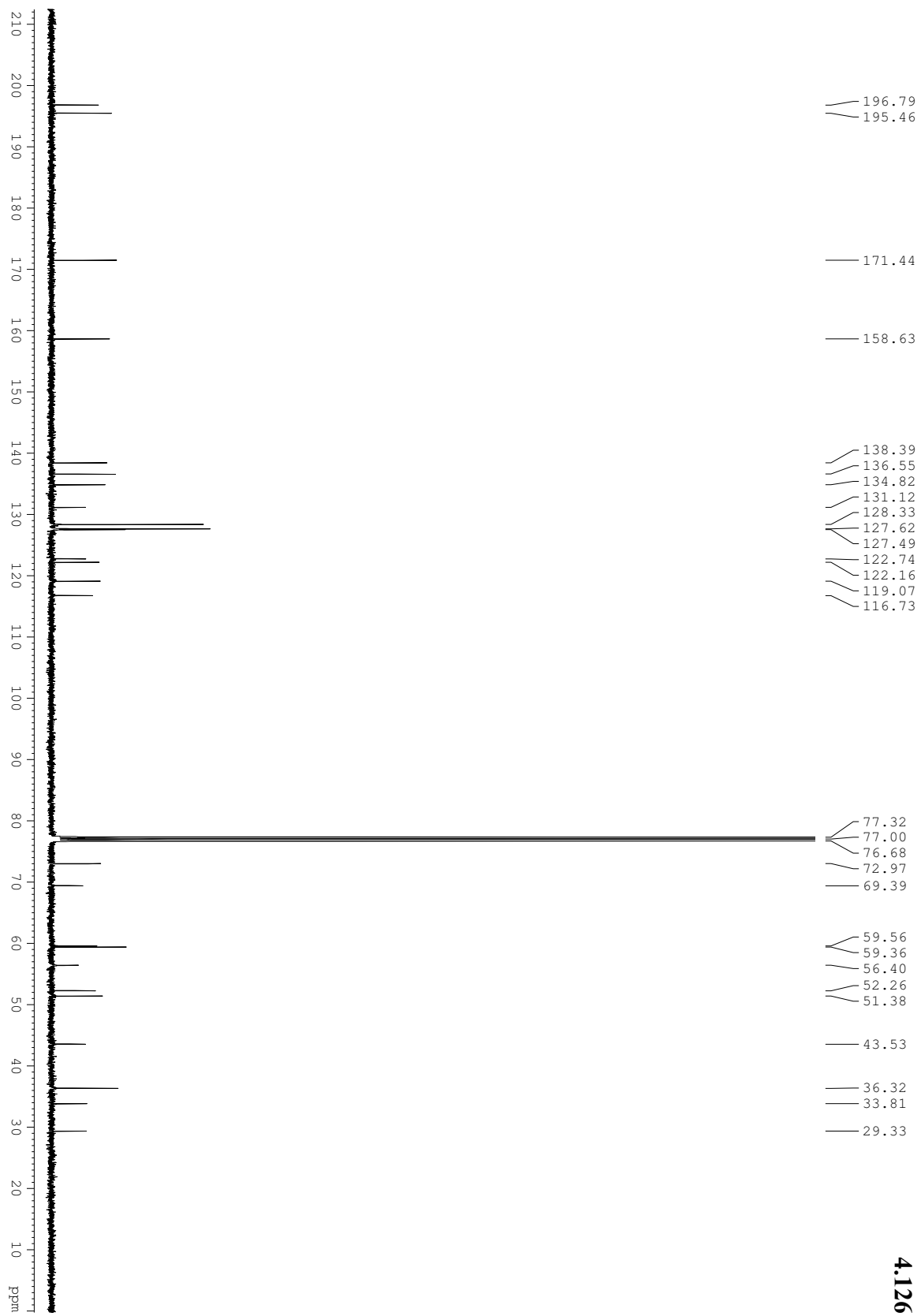


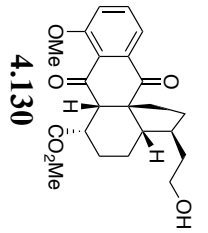
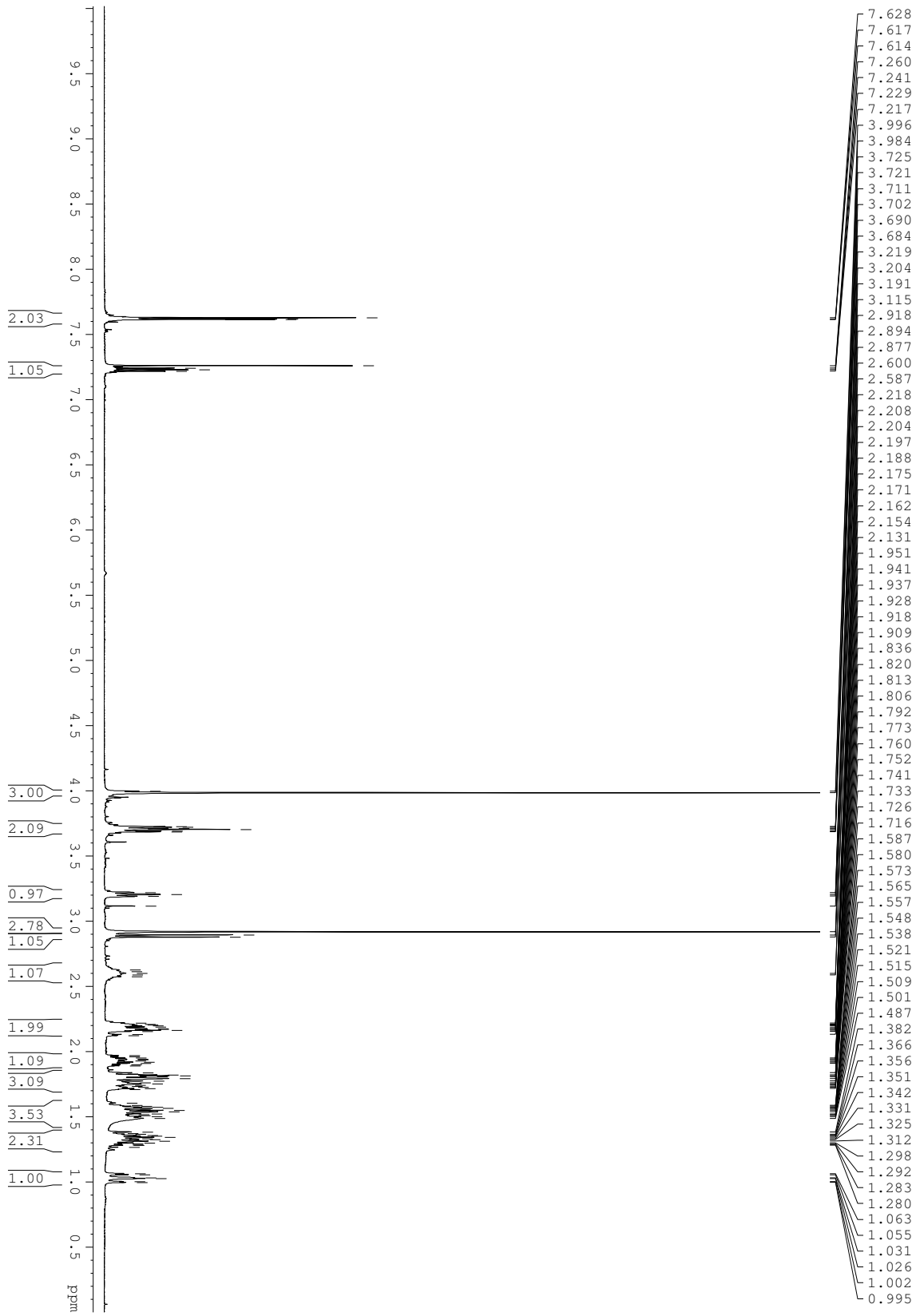


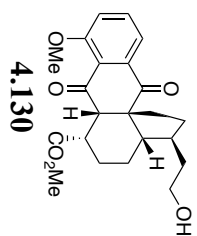
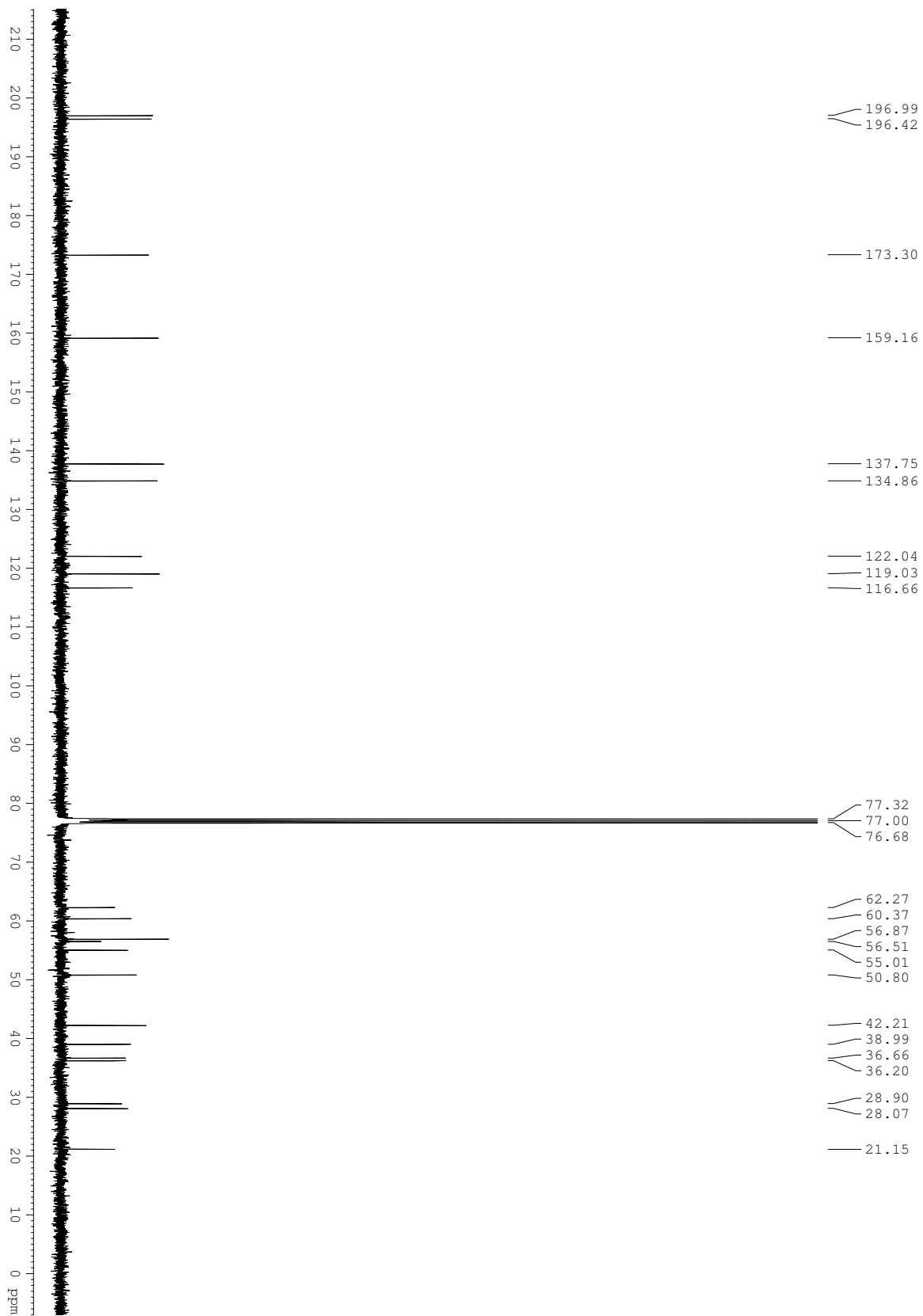


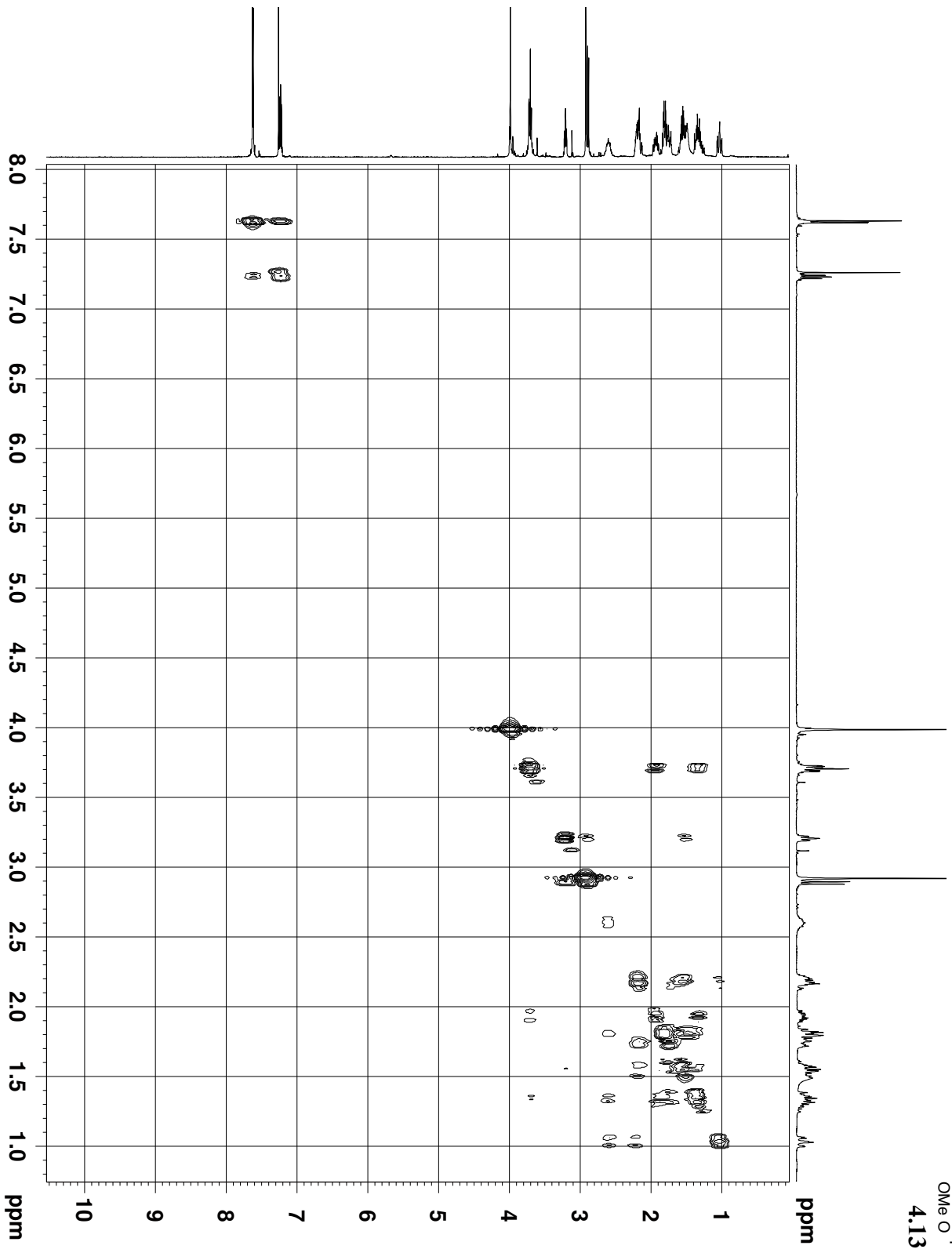
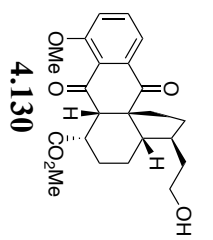
4.126

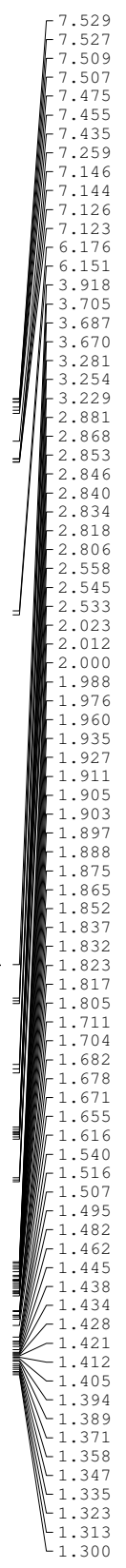
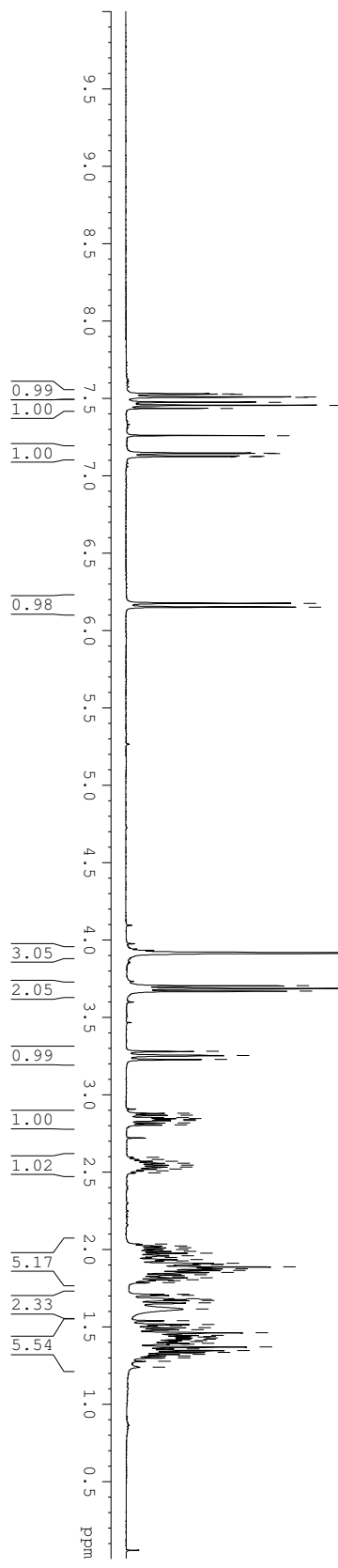




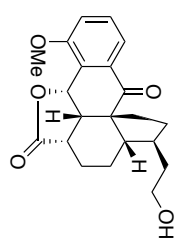


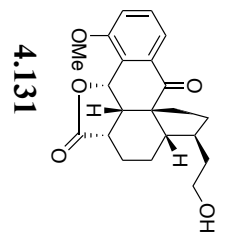
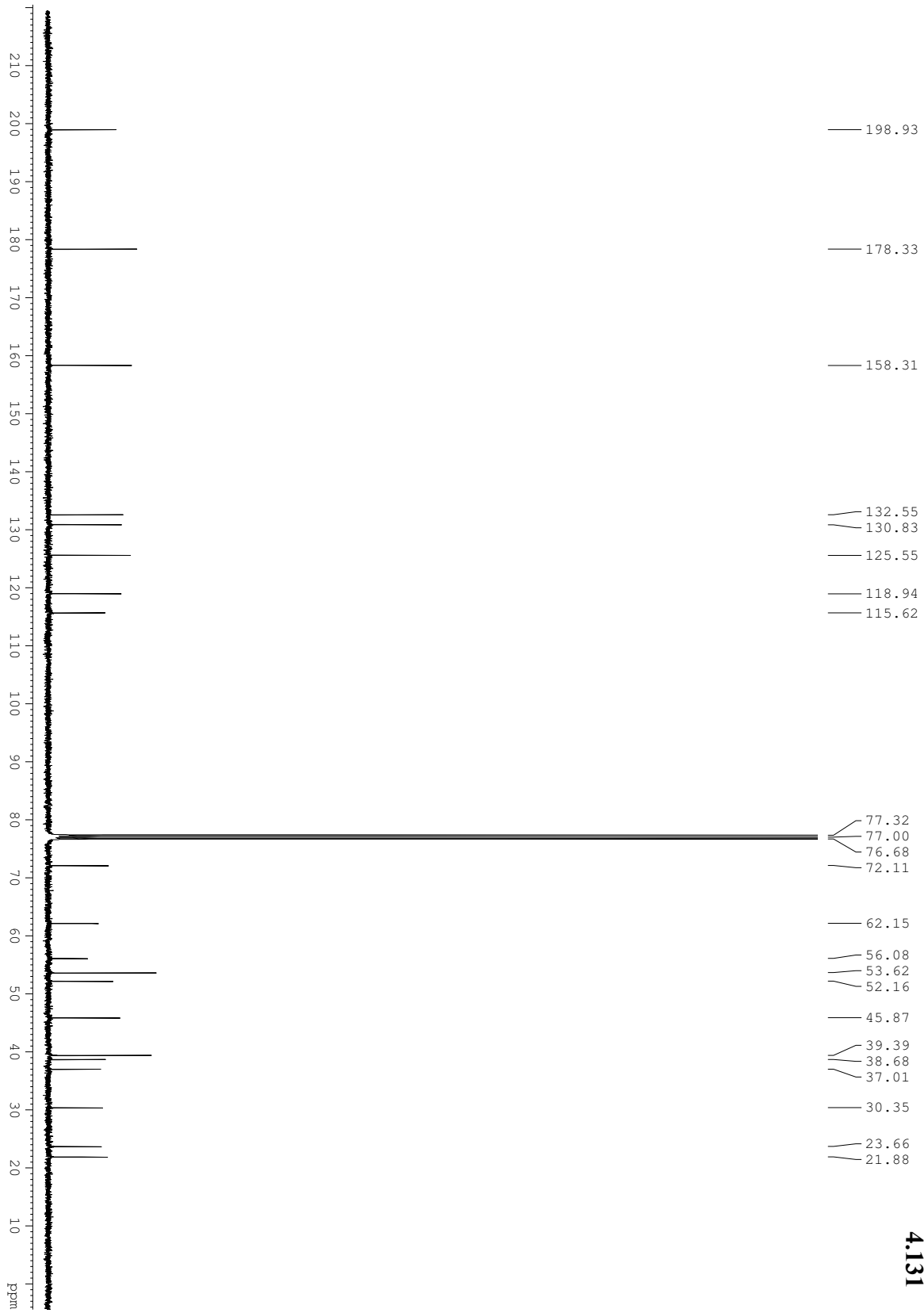


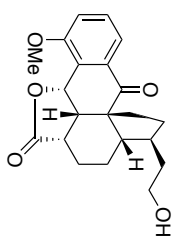




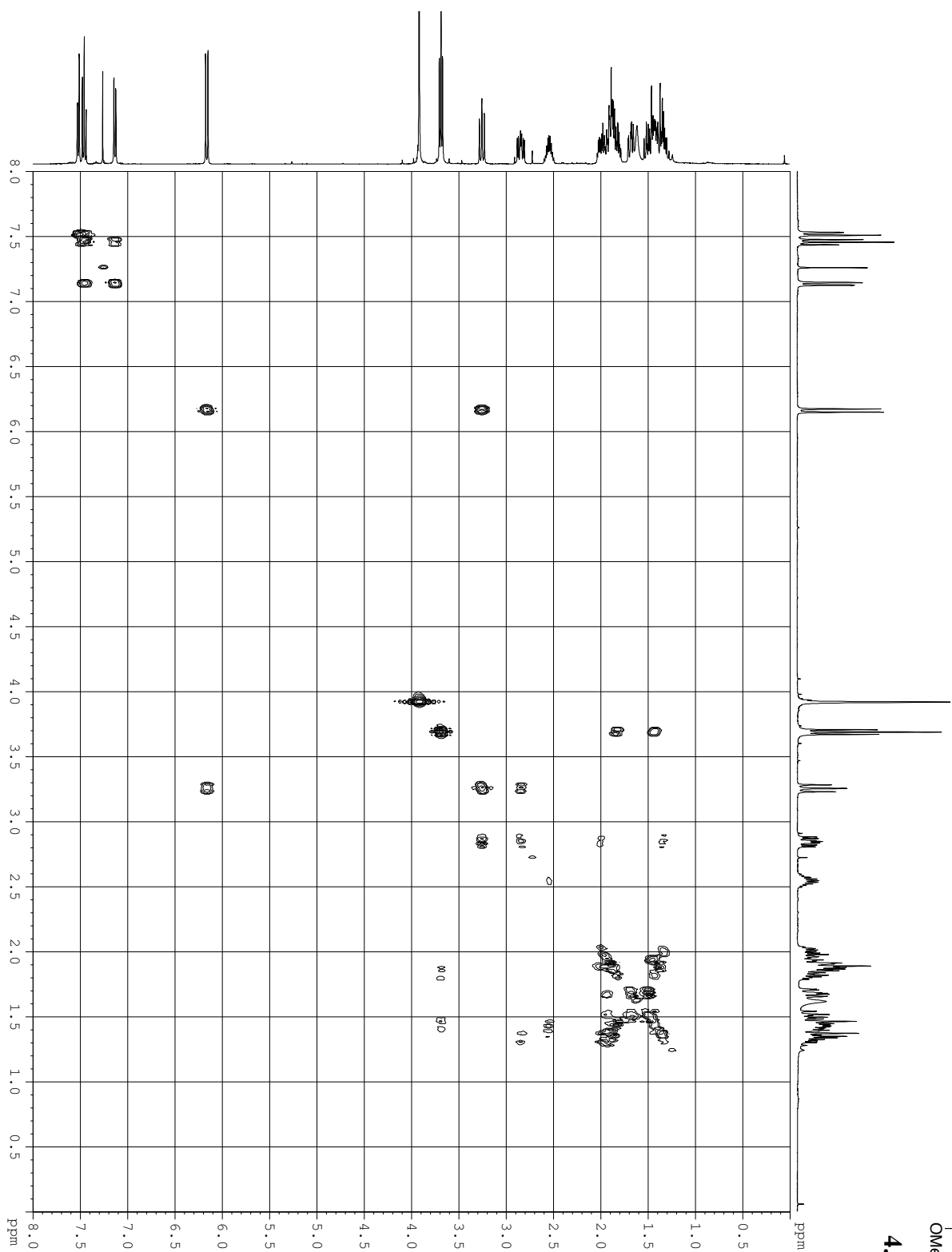
4.131

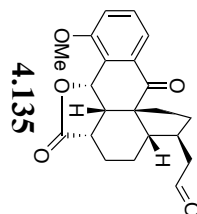
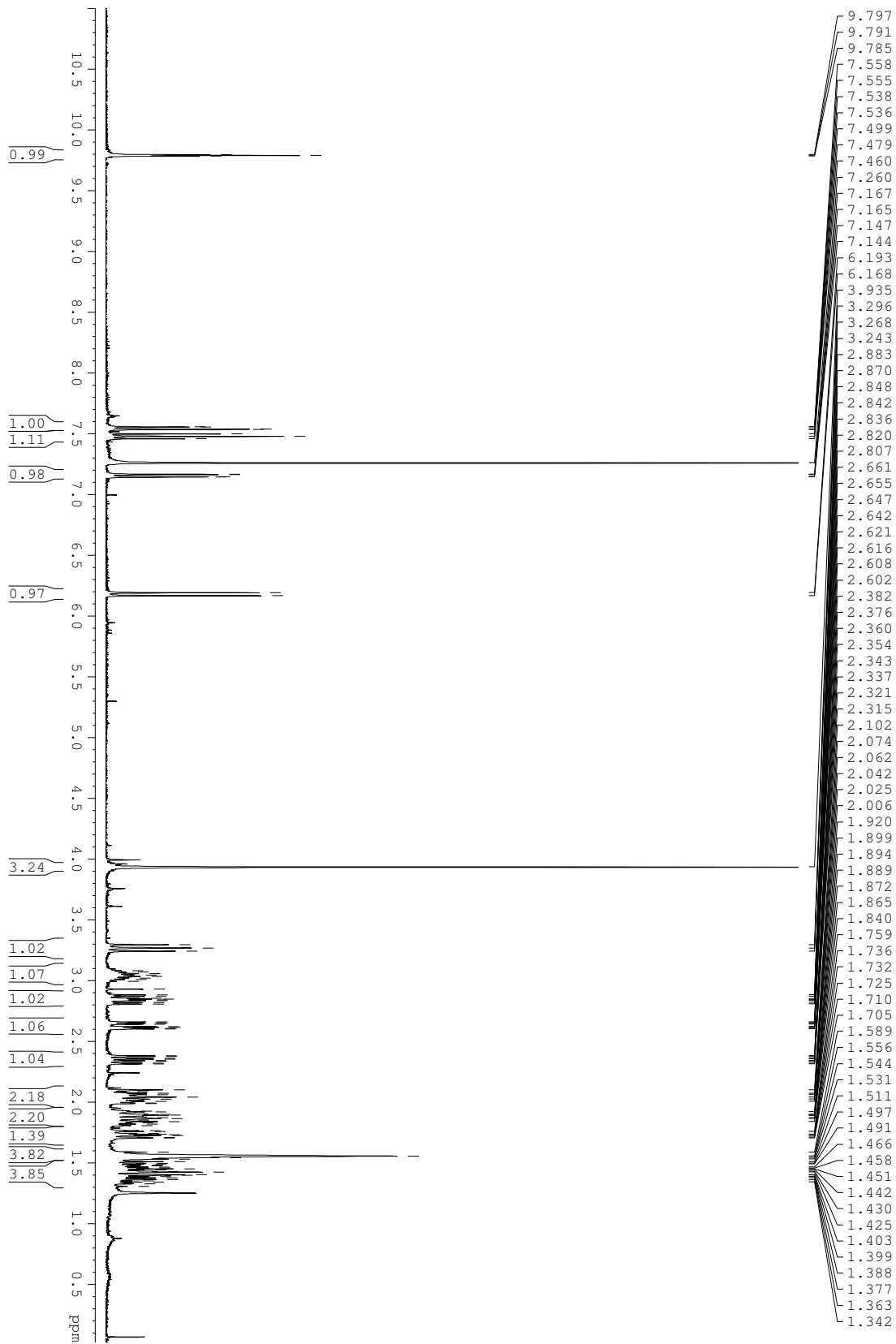


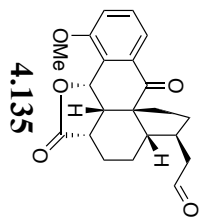
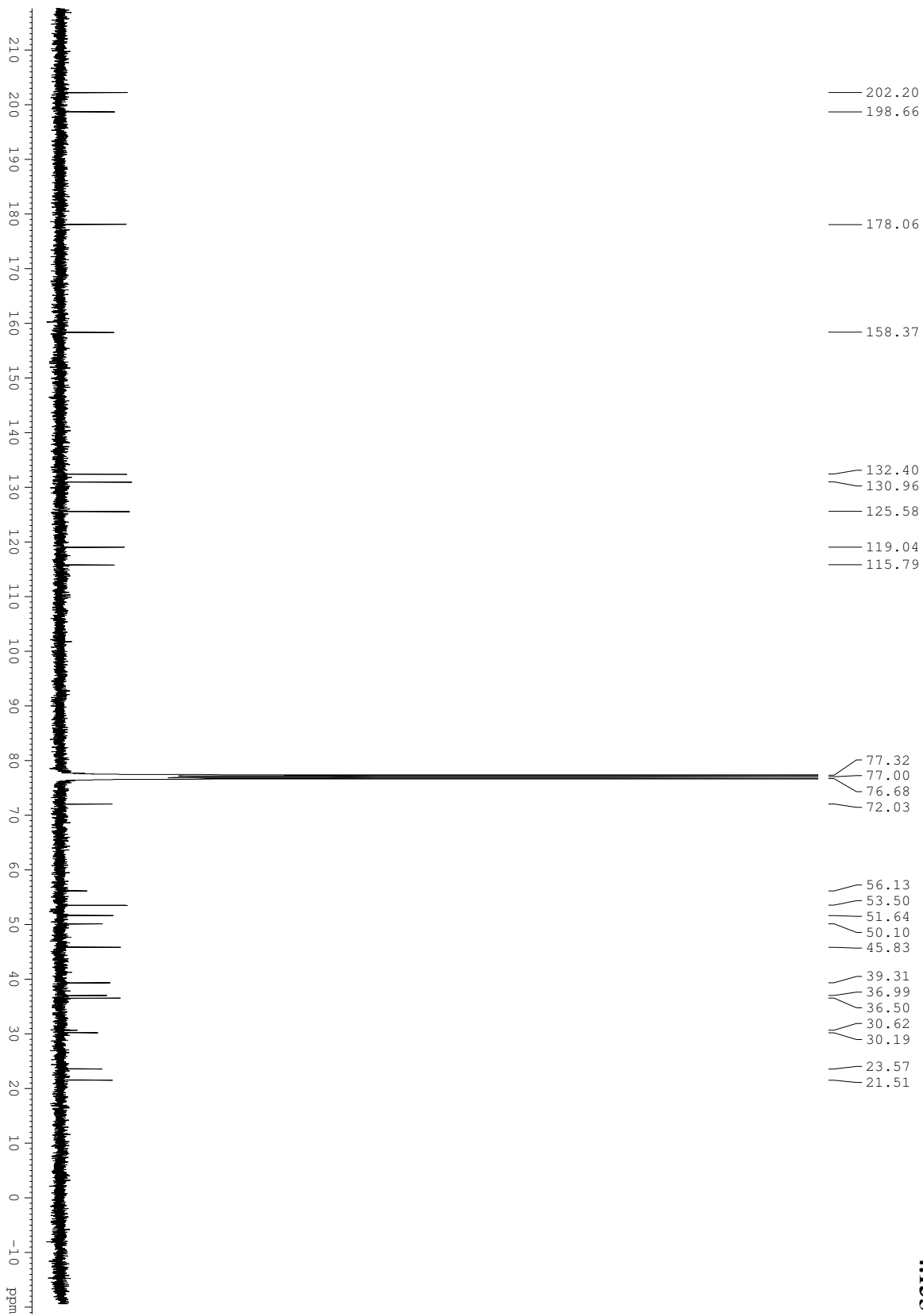


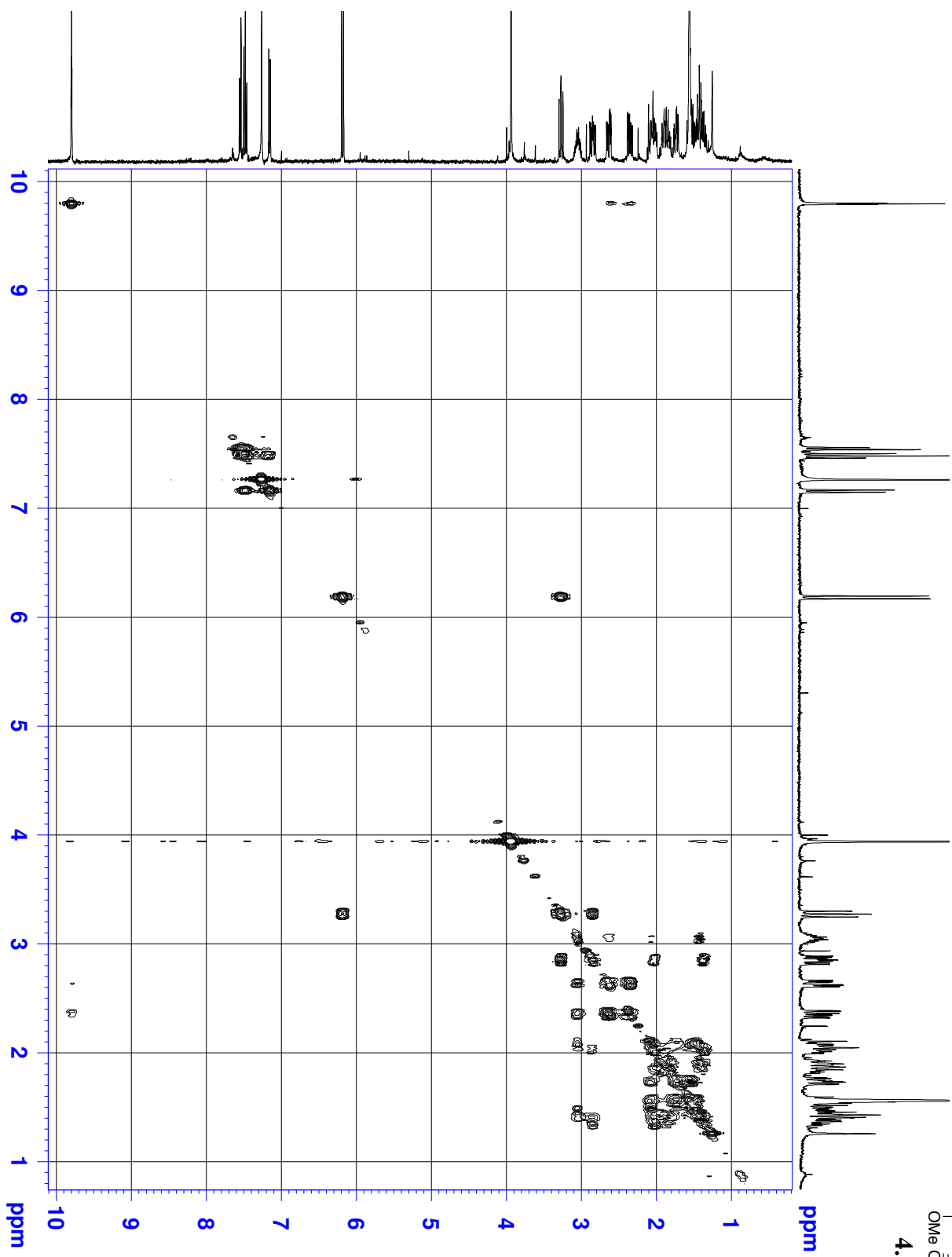
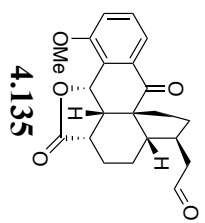


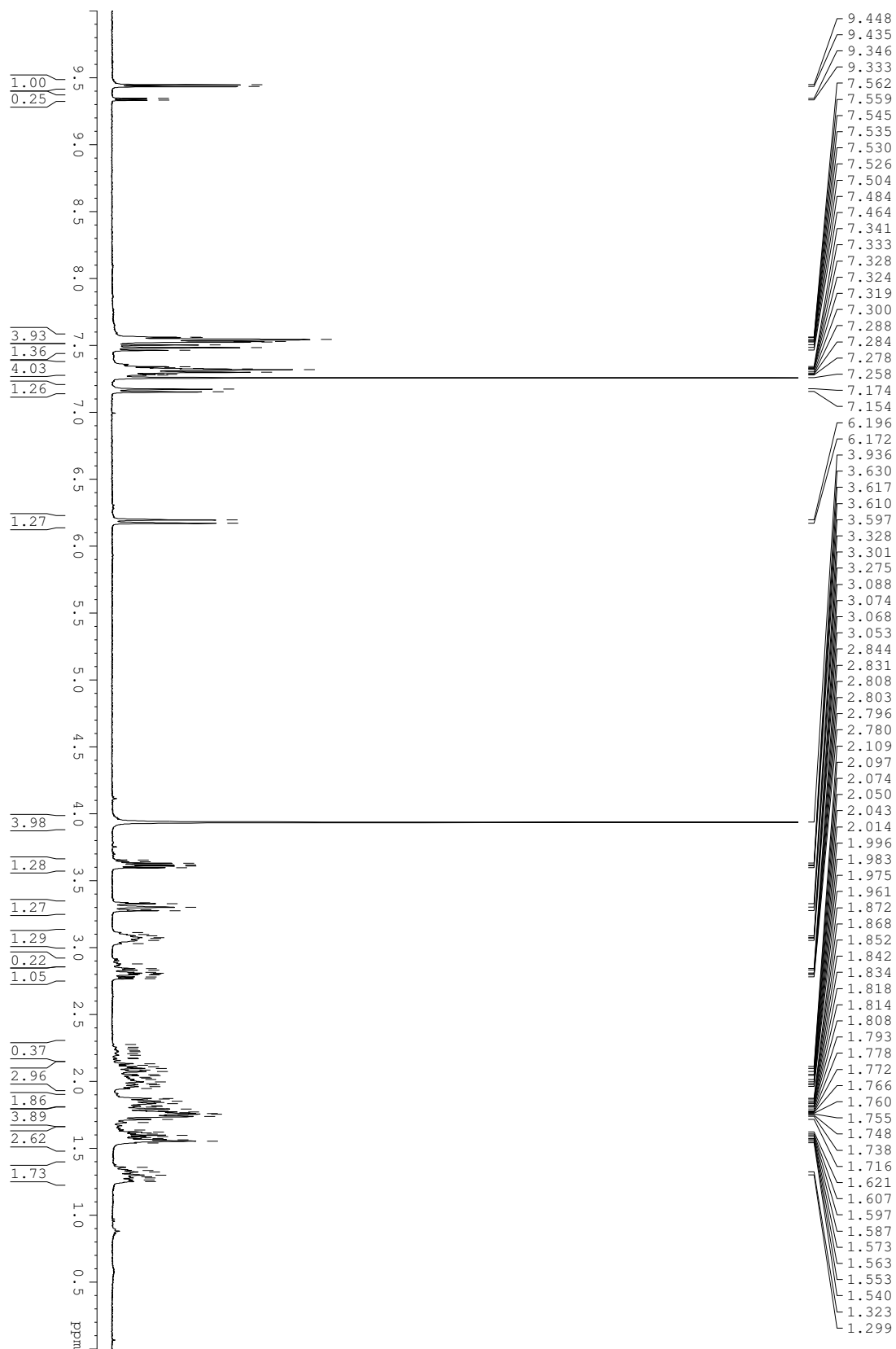
4.131



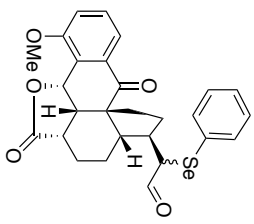


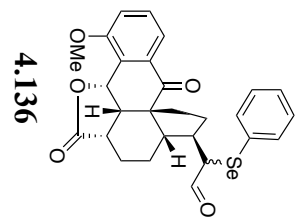
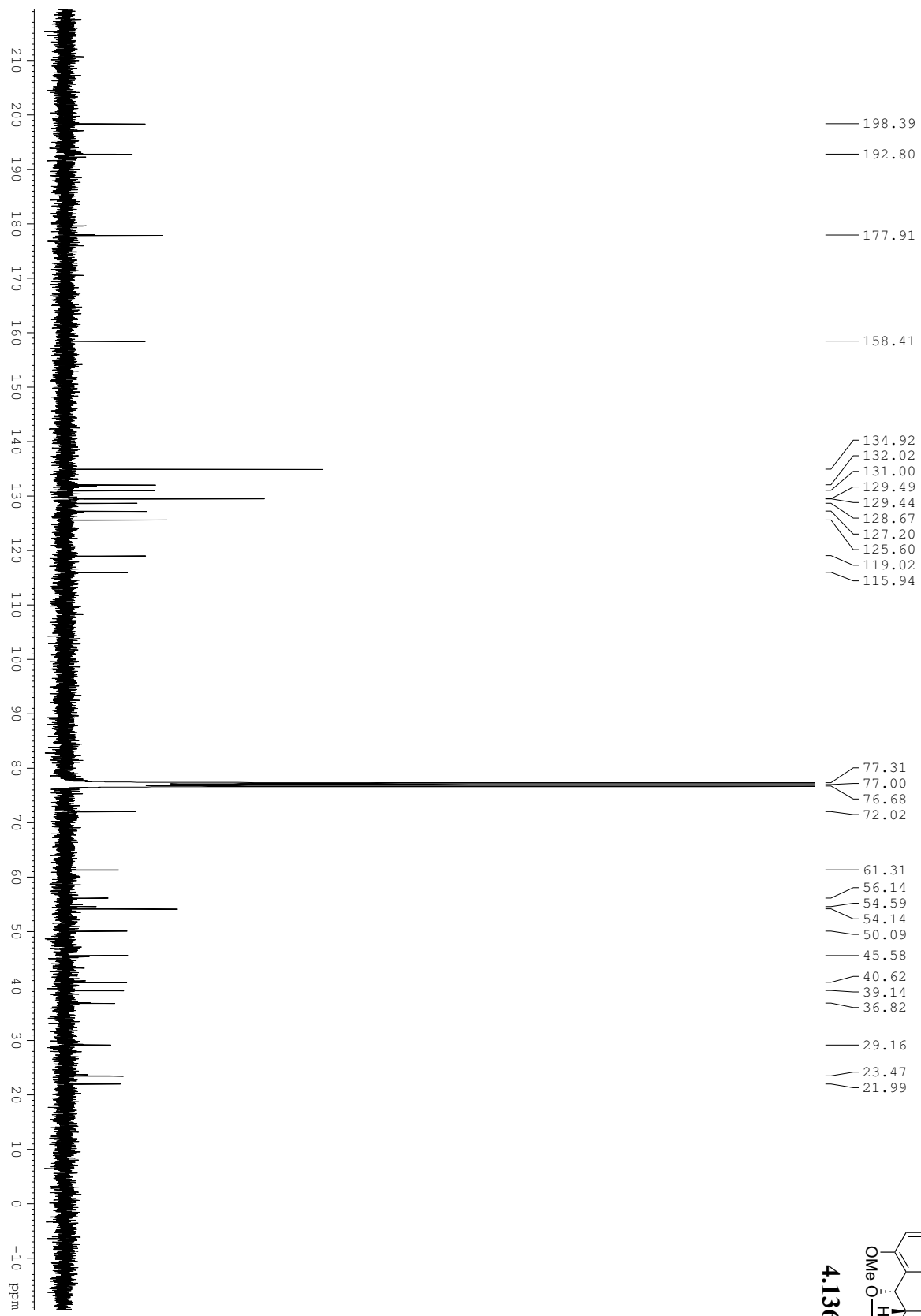


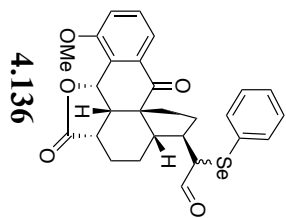
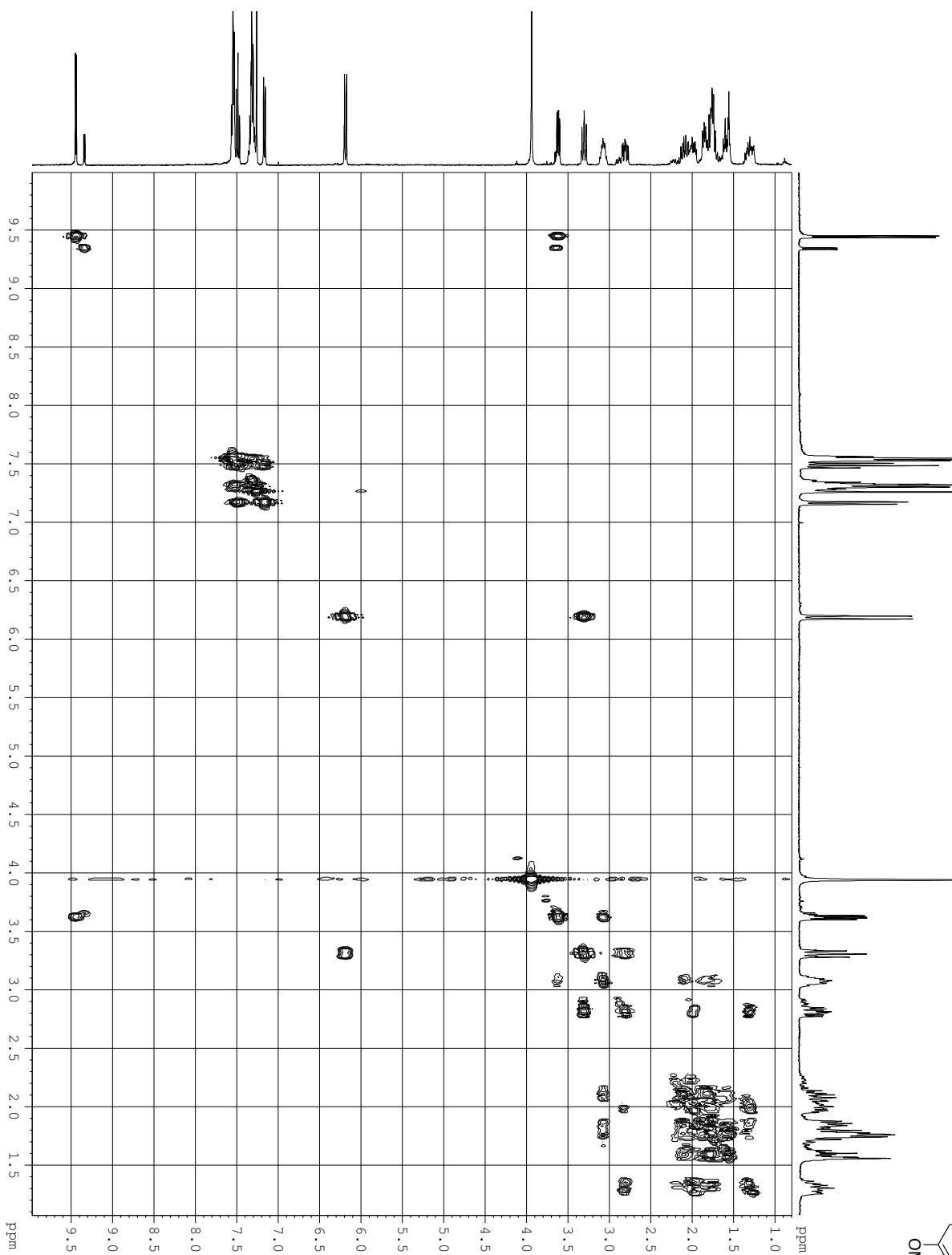


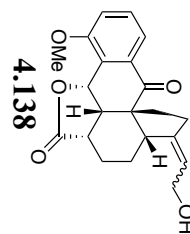
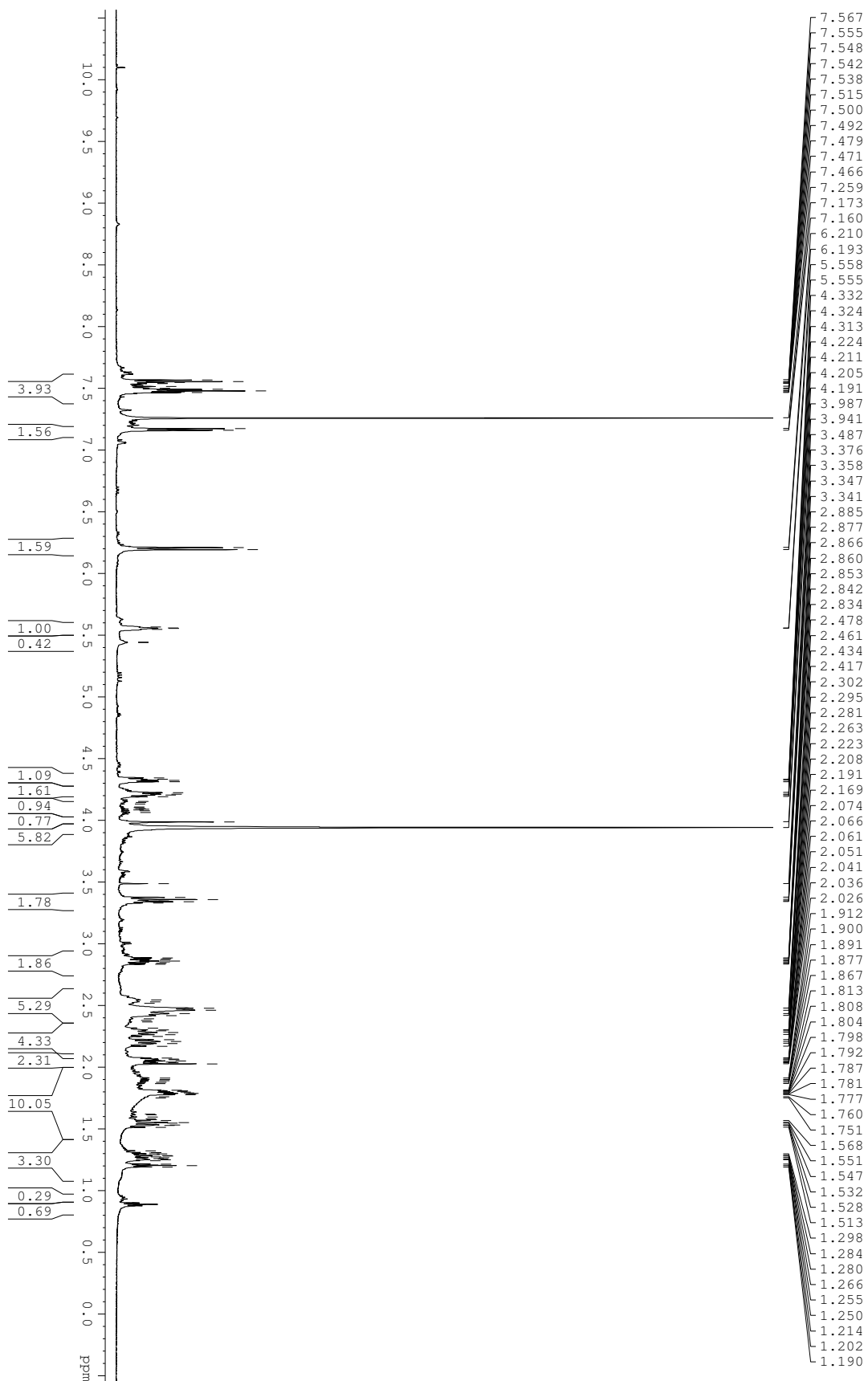


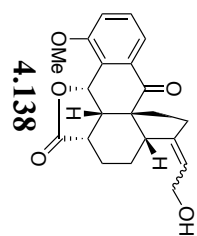
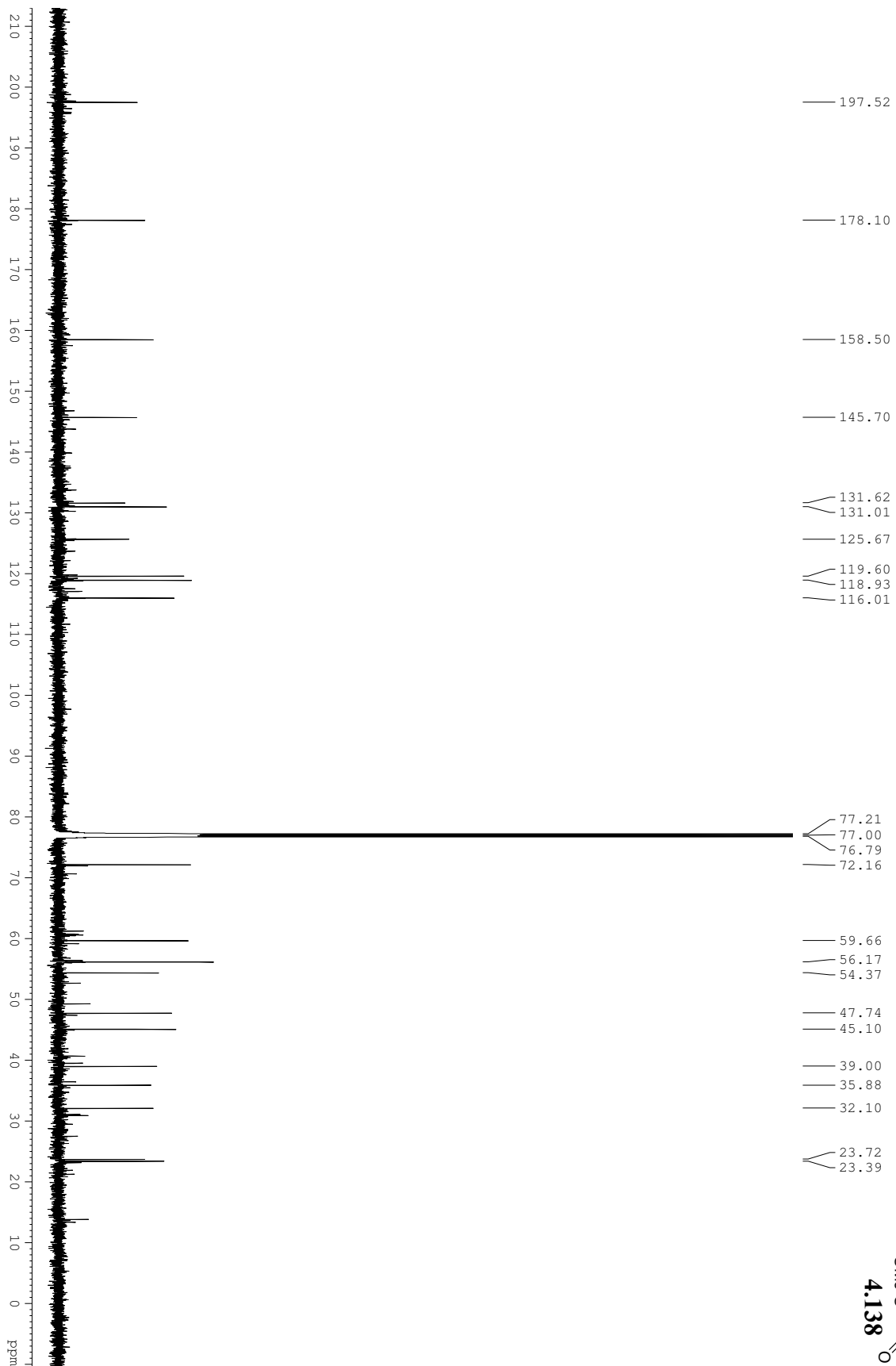
4.136

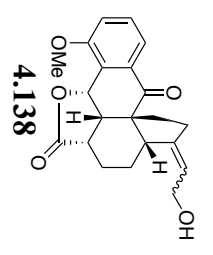
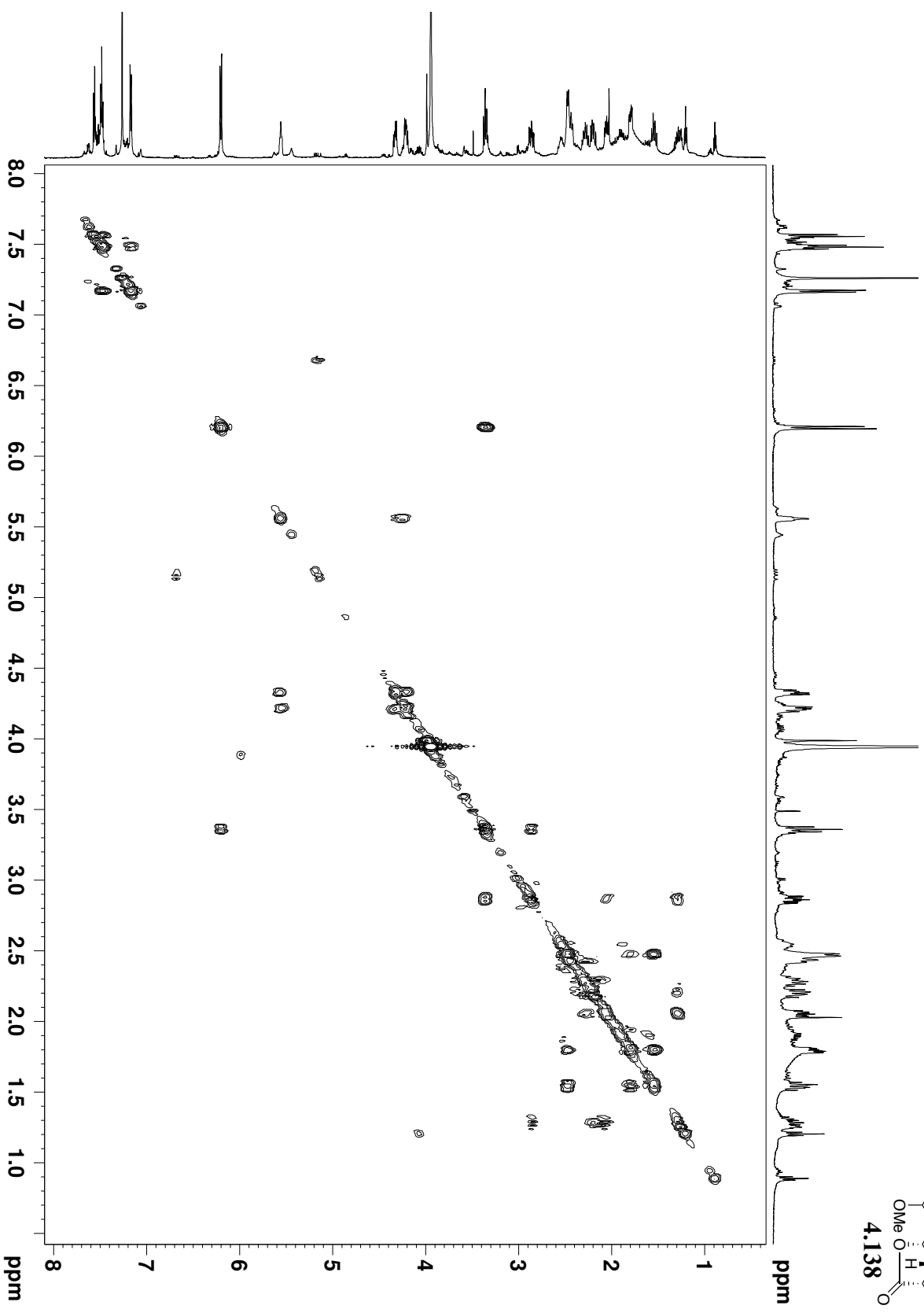


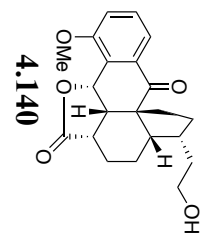
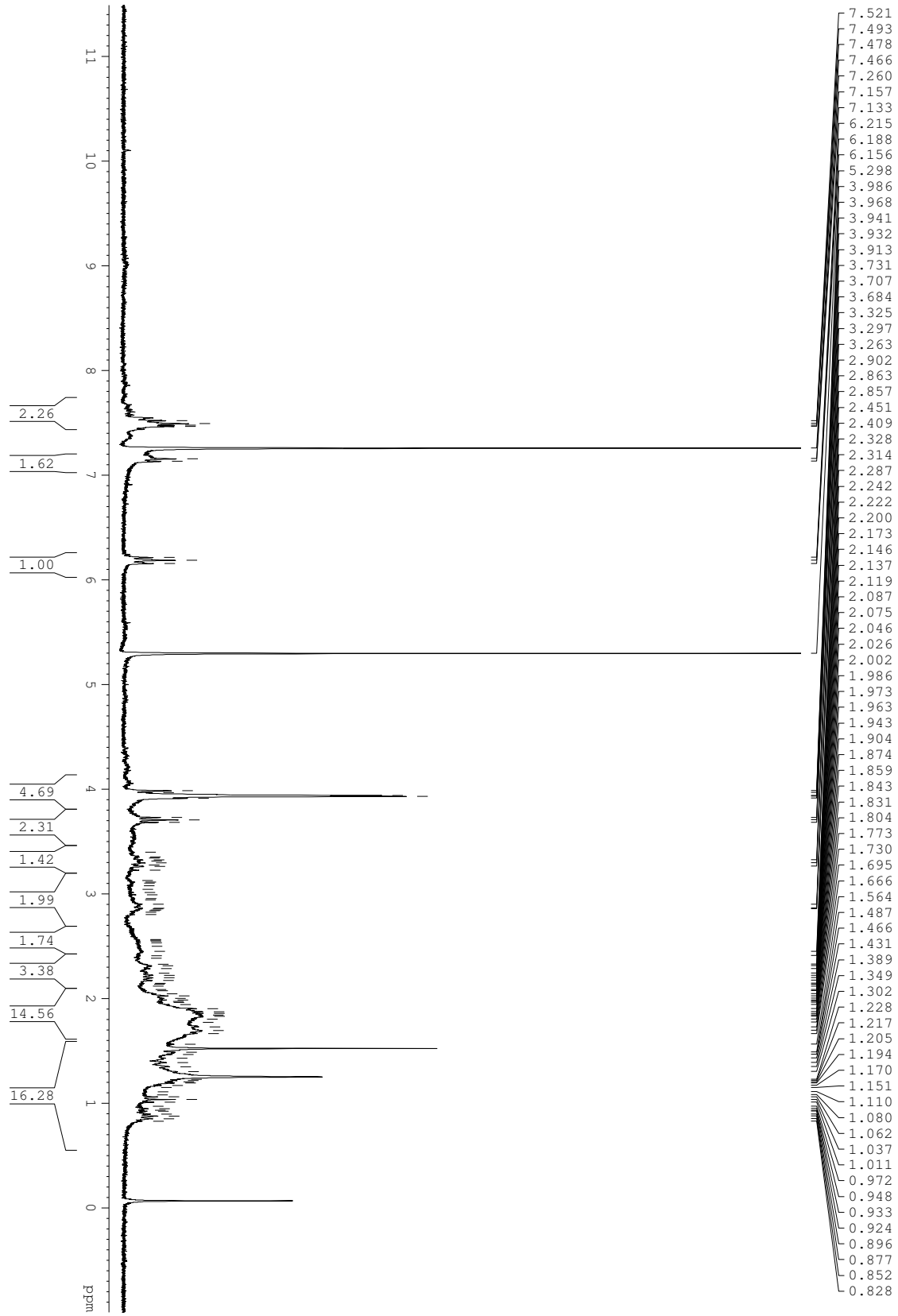












BIBLIOGRAPHY

- (1) Azoitei, N.; Kleger, A.; Schoo, N.; Thal, D. R.; Brunner, C.; Pusapati, G. V.; Filatova, A.; Genze, F.; Moller, P.; Acker, T.; Kuefer, R.; Van Lint, J.; Baust, H.; Adler, G.; Seufferlein, T. *Neuro-Oncol.* **2011**, *13*, 710-724.
- (2) Chen, J.; Giridhar, K. V.; Zhang, L.; Xu, S.; Wang, Q. J. *Carcinogenesis* **2011**, *32*, 1198-1206.
- (3) Hollenbach, M.; Stoll, S. J.; Jorgens, K.; Seufferlein, T.; Kroll, J. *PLoS ONE* **2013**, *8*, e68033.
- (4) Kleger, A.; Loebnitz, C.; Pusapati, G. V.; Armacki, M.; Muller, M.; Tumpel, S.; Illing, A.; Hartmann, D.; Brunner, C.; Liebau, S.; Rudolph, K. L.; Adler, G.; Seufferlein, T. *PLoS ONE* **2011**, *6*, e14599.
- (5) LaValle, C. R.; Zhang, L.; Xu, S.; Eiseman, J. L.; Wang, Q. J. *Mol. Cancer Ther.* **2012**, *11*, 1389-1399.
- (6) Manterola, L.; Hernando-Rodriguez, M.; Ruiz, A.; Apraiz, A.; Arrizabalaga, O.; Vellon, L.; Alberdi, E.; Cavaliere, F.; Lacerda, H. M.; Jimenez, S.; Parada, L. A.; Matute, C.; Zugaza, J. L. *Transl. Psychiatry* **2013**, *3*, e219.
- (7) Rodriguez Perez, C. E.; Nie, W.; Sinnett-Smith, J.; Rozengurt, E.; Yoo, J. *Am. J. Physiol. Gastrointest. Liver. Physiol.* **2011**, *300*, G637-G646.
- (8) Sinnett-Smith, J.; Rozengurt, N.; Kui, R.; Huang, C.; Rozengurt, E. *J. Biol. Chem.* **2011**, *286*, 511-520.
- (9) Guha, S.; Tanasanvimon, S.; Sinnett-Smith, J.; Rozengurt, E. *Biochem. Pharmacol.* **2010**, *80*, 1946-1954.
- (10) Lavalle, C. R.; Bravo-Altamirano, K.; Giridhar, K. V.; Chen, J.; Sharlow, E.; Lazo, J. S.; Wipf, P.; Wang, Q. J. *BMC Chem. Biol.* **2010**, *10*, 5.
- (11) Shirai, T. *Pathol. Int.* **2008**, *58*, 1-16.
- (12) Sarker, D.; Reid, A. H. M.; Yap, T. A.; de Bono, J. S. *Clin. Cancer Res.* **2009**, *15*, 4799-4805.

- (13) Chen, L.; Giorgianni, F.; Beranova-Giorgianni, S. *J. Proteome. Res.* **2010**, *9*, 174-178.
- (14) Guo, J.; Clausen, D.; Beumer, J.; Parise, R.; Egorin, M.; Bravo-Altamirano, K.; Wipf, P.; Sharlow, E.; Wang, Q.; Eiseman, J. *Cancer Chemoth. Pharm.* **2013**, *71*, 331-344.
- (15) Tandon, M.; Johnson, J.; Li, Z.; Xu, S.; Wipf, P.; Wang, Q. *J. PLoS ONE* **2013**, *8*, e75601.
- (16) Borges, S.; Storz, P. *Expert Rev. Anticancer Ther.* **2013**, *13*, 895-898.
- (17) Döppler, H.; Bastea, L. I.; Eiseler, T.; Storz, P. *J. Biol. Chem.* **2013**, *288*, 455-465.
- (18) Hao, Q.; McKenzie, R.; Gan, H.; Tang, H. *Anticancer Res.* **2013**, *33*, 393-399.
- (19) Borges, S.; Perez, E. A.; Thompson, E. A.; Radisky, D. C.; Geiger, X. J.; Storz, P. *Mol. Cancer Ther.* **2015**, *14*, 1306-1316.
- (20) Sumara, G.; Formentini, I.; Collins, S.; Sumara, I.; Windak, R.; Bodenmiller, B.; Ramracheya, R.; Caille, D.; Jiang, H.; Platt, K. A.; Meda, P.; Aebersold, R.; Rorsman, P.; Ricci, R. *Cell* **2009**, *136*, 235-248.
- (21) Harikumar, K. B.; Kunnumakkara, A. B.; Ochi, N.; Tong, Z.; Deorukhkar, A.; Sung, B.; Kelland, L.; Jamieson, S.; Sutherland, R.; Raynham, T.; Charles, M.; Bagherzadeh, A.; Foxton, C.; Boakes, A.; Farooq, M.; Maru, D.; Diagaradjane, P.; Matsuo, Y.; Sinnett-Smith, J.; Gelovani, J.; Krishnan, S.; Aggarwal, B. B.; Rozengurt, E.; Ireson, C. R.; Guha, S. *Mol. Cancer Ther.* **2010**, *9*, 1136-1146.
- (22) Ochi, N.; Tanasanvimon, S.; Matsuo, Y.; Tong, Z.; Sung, B.; Aggarwal, B. B.; Sinnett-Smith, J.; Rozengurt, E.; Guha, S. *J. Cell. Physiol.* **2011**, *226*, 1074-1085.
- (23) Thrower, E. C.; Yuan, J.; Usmani, A.; Liu, Y.; Jones, C.; Minervini, S. N.; Alexandre, M.; Pandol, S. J.; Guha, S. *Am. J. Physiol. Gastrointest. Liver. Physiol.* **2011**, *300*, G120-G129.
- (24) Shi, S.; Yao, W.; Xu, J.; Long, J.; Liu, C.; Yu, X. *Cancer Lett.* **2012**, *317*, 127-135.
- (25) Wille, C.; Seufferlein, T.; Eiseler, T. *Bioarchitecture* **2014**, *4*, 111-115.
- (26) Podar, K.; Raab, M. S.; Chauhan, D.; Anderson, K. C. *Expert Opin. Investig. Drugs* **2007**, *16*, 1693-1707.
- (27) Redig, A. J.; Plataniias, L. C. *Leuk. Lymphoma* **2008**, *49*, 1255-1262.
- (28) Klener, P.; Klener, P., Jr. *Klin. Onkol.* **2010**, *23*, 203-209.
- (29) Modak, C.; Chai, J. *World J. Gastrointest. Oncol.* **2009**, *1*, 26-33.
- (30) Azoitei, N.; Pusapati, G. V.; Kleger, A.; Moller, P.; Kufer, R.; Genze, F.; Wagner, M.; van Lint, J.; Carmeliet, P.; Adler, G.; Seufferlein, T. *Gut* **2010**, *59*, 1316-1330.

- (31) Valverde, A. M.; Sinnett-Smith, J.; Van Lint, J.; Rozengurt, E. *Proc. Natl. Acad. Sci. U. S. A.* **1994**, *91*, 8572-8576.
- (32) Hayashi, A.; Seki, N.; Hattori, A.; Kozuma, S.; Saito, T. *Biochim. Biophys. Acta.* **1999**, *1450*, 99-106.
- (33) LaValle, C. R.; George, K. M.; Sharlow, E. R.; Lazo, J. S.; Wipf, P.; Wang, Q. J. *Biochim. Biophys. Acta. Rev. Canc.* **2010**, *1806*, 183-192.
- (34) Rey, O.; Sinnett-Smith, J.; Zhukova, E.; Rozengurt, E. *J. Biol. Chem.* **2001**, *276*, 49228-49235.
- (35) Iglesias, T.; Rozengurt, E. *J. Biol. Chem.* **1998**, *273*, 410-416.
- (36) Waldron, R. T.; Rozengurt, E. *J. Biol. Chem.* **2003**, *278*, 154-163.
- (37) Rozengurt, E., Rey, O., Waldron, R.T. *J. Biol. Chem.* **2005**, *280*, 13205-13208.
- (38) Asaithambi, A.; Kanthasamy, A.; Saminathan, H.; Anantharam, V.; Kanthasamy, A. G. *Mol. Neurodegener.* **2011**, *6*, 43.
- (39) Nakajima, S.; Kitamura, M. *Free Radical Bio. Med.* **2013**, *65*, 162-174.
- (40) Hurd, C., Waldron, R.T., Rozengurt, E. *Oncogene* **2002**, *21*, 2154-2160.
- (41) Vega, R. B.; Harrison, B. C.; Meadows, E.; Roberts, C. R.; Papst, P. J.; Olson, E. N.; McKinsey, T. A. *Mol. Cell Biol.* **2004**, *24*, 8374-8385.
- (42) Wang, Q. J. *Trends Pharmacol. Sci.* **2006**, *27*, 317-323.
- (43) Rozengurt, E. *Physiology* **2011**, *26*, 23-33.
- (44) Fu, Y.; Rubin, C. S. *EMBO Rep.* **2011**, *12*, 785-796.
- (45) Azoitei, N.; Diepold, K.; Brunner, C.; Rouhi, A.; Genze, F.; Becher, A.; Kestler, H.; van Lint, J.; Chiosis, G.; Koren, J.; Fröhling, S.; Scholl, C.; Seufferlein, T. *Cancer Res.* **2014**, *74*, 7125-7136.
- (46) Azoitei, N.; Fröhling, S.; Scholl, C.; Seufferlein, T. *Mol. Cell. Oncol.* **2015**, *2*, e981444.
- (47) Chen, J.; Deng, F.; Li, J.; Wang, Q. J. *Biochem. J.* **2008**, *411*, 333-342.
- (48) Jacamo, R.; Sinnett-Smith, J.; Rey, O.; Waldron, R. T.; Rozengurt, E. *J. Biol. Chem.* **2008**, *283*, 12877-12887.
- (49) Wang, Y.; Waldron, R. T.; Dhaka, A.; Patel, A.; Riley, M. M.; Rozengurt, E.; Colicelli, J. *Mol. Cell Biol.* **2002**, *22*, 916-926.

- (50) Ziegler, S.; Eiseler, T.; Scholz, R.-P.; Beck, A.; Link, G.; Hausser, A. *Mol. Biol. Cell* **2011**, *22*, 570-580.
- (51) Chen, J.; Deng, F.; Singh, S. V.; Wang, Q. *J. Cancer Res.* **2008**, *68*, 3844-3853.
- (52) Sinnott-Smith, J.; Zhukova, E.; Hsieh, N.; Jiang, X.; Rozengurt, E. *J. Biol. Chem.* **2004**, *279*, 16883-16893.
- (53) Sinnott-Smith, J.; Zhukova, E.; Rey, O.; Rozengurt, E. *J. Cell. Physiol.* **2007**, *211*, 781-790.
- (54) Wong, C.; Jin, Z. G. *J. Biol. Chem.* **2005**, *280*, 33262-33269.
- (55) Lemonnier, J.; Ghayor, C.; Guicheux, J.; Caverzasio, J. *J. Biol. Chem.* **2004**, *279*, 259-264.
- (56) Waldron, R. T.; Whitelegge, J. P.; Faull, K. F.; Rozengurt, E. *Biochem. Biophys. Res. Commun.* **2007**, *356*, 361-367.
- (57) McEwen, D. G.; Peifer, M. *Curr. Biol.* **2000**, *10*, R562-R564.
- (58) Rincon, M.; Flavell, R. A.; Davis, R. J. *Oncogene* **2001**, *20*, 2490-2497.
- (59) Weston, C. R.; Davis, R. J. *Curr. Opin. Genet. Dev.* **2002**, *12*, 14-21.
- (60) Salamon, P.; Shefler, I.; Hershko, A. Y.; Mekori, Y. A. *Int. Arch. Allergy Immunol.* **2016**, *171*, 203-208.
- (61) Wagner, E. F.; Nebreda, A. R. *Nat. Rev. Cancer* **2009**, *9*, 537-549.
- (62) Harrison, B. C.; Kim, M. S.; van Rooij, E.; Plato, C. F.; Papst, P. J.; Vega, R. B.; McAnally, J. A.; Richardson, J. A.; Bassel-Duby, R.; Olson, E. N.; McKinsey, T. A. *Mol. Cell Biol.* **2006**, *26*, 3875-3888.
- (63) Liu, X.; Zheng, N.; Shi, Y. N.; Yuan, J. H.; Li, L. Y. *J. Mol. Endocrinol.* **2014**, *52*, 245-254.
- (64) Ha, C. H.; Jhun, B. S.; Kao, H. Y.; Jin, Z. G. *Arterioscler. Thromb. Vasc. Biol.* **2008**, *28*, 1782-1788.
- (65) Wang, S.; Li, X.; Parra, M.; Verdin, E.; Bassel-Duby, R.; Olson, E. N. *Proc. Natl. Acad. Sci. U. S. A.* **2008**, *105*, 7738-7743.
- (66) Ha, C. H.; Jin, Z. G. *Mol. Cells* **2009**, *28*, 1-5.
- (67) Monovich, L.; Vega, R. B.; Meredith, E.; Miranda, K.; Rao, C.; Capparelli, M.; Lemon, D. D.; Phan, D.; Koch, K. A.; Chappo, J. A.; Hood, D. B.; McKinsey, T. A. *FEBS Lett.* **2010**, *584*, 631-637.
- (68) Yang, X. J.; Gregoire, S. *Mol. Cell Biol.* **2005**, *25*, 2873-2884.

- (69) Trauzold, A.; Schmiedel, S.; Sipos, B.; Wermann, H.; Westphal, S.; Roder, C.; Klapper, W.; Arlt, A.; Lehnert, L.; Ungefroren, H.; Johannes, F. J.; Kalthoff, H. *Oncogene* **2003**, *22*, 8939-8947.
- (70) Kim, M.; Jang, H. R.; Kim, J. H.; Noh, S. M.; Song, K. S.; Cho, J. S.; Jeong, H. Y.; Norman, J. C.; Caswell, P. T.; Kang, G. H.; Kim, S. Y.; Yoo, H. S.; Kim, Y. S. *Carcinogenesis* **2008**, *29*, 629-637.
- (71) Fielitz, J.; Kim, M. S.; Shelton, J. M.; Qi, X.; Hill, J. A.; Richardson, J. A.; Bassel-Duby, R.; Olson, E. N. *Proc. Natl. Acad. Sci. U. S. A.* **2008**, *105*, 3059-3063.
- (72) Ha, C. H.; Wang, W.; Jhun, B. S.; Wong, C.; Hausser, A.; Pfizenmaier, K.; McKinsey, T. A.; Olson, E. N.; Jin, Z. G. *J. Biol. Chem.* **2008**, *283*, 14590-14599.
- (73) Bossuyt, J.; Chang, C. W.; Helmstadter, K.; Kunkel, M. T.; Newton, A. C.; Campbell, K. S.; Martin, J. L.; Bossuyt, S.; Robia, S. L.; Bers, D. M. *J. Biol. Chem.* **2011**, *286*, 33390-33400.
- (74) Phan, D.; Stratton, M. S.; Huynh, Q. K.; McKinsey, T. A. *Biochem. Biophys. Res. Commun.* **2011**, *411*, 335-341.
- (75) Yeaman, C.; Ayala, M. I.; Wright, J. R.; Bard, F.; Bossard, C.; Ang, A.; Maeda, Y.; Seufferlein, T.; Mellman, I.; Nelson, W. J.; Malhotra, V. *Nat. Cell Biol.* **2004**, *6*, 106-112.
- (76) Kienzle, C.; Eisler, S. A.; Villeneuve, J.; Brummer, T.; Olayioye, M. A.; Hausser, A. *Mol. Biol. Cell* **2013**, *24*, 222-233.
- (77) Jensen, D. D.; Zhao, P. S.; Jimenez-Vargas, N. N.; Lieu, T.; Gerges, M.; Yeatman, H. R.; Canals, M.; Vanner, S. J.; Poole, D. P.; Bunnett, N. W. *J. Biol. Chem.* **2016**, *291*, 11285-11299.
- (78) Bowden, E. T.; Barth, M.; Thomas, D.; Glazer, R. I.; Mueller, S. C. *Oncogene* **1999**, *18*, 4440-4449.
- (79) De Kimpe, L.; Janssens, K.; Derua, R.; Armacki, M.; Goicoechea, S.; Otey, C.; Waelkens, E.; Vandoninck, S.; Vandenheede, J. R.; Seufferlein, T.; Van Lint, J. *Cell. Signal.* **2009**, *21*, 253-263.
- (80) Eiseler, T.; Hausser, A.; De Kimpe, L.; Van Lint, J.; Pfizenmaier, K. *J. Biol. Chem.* **2010**, *285*, 18672-18683.
- (81) Sroka, R.; Van Lint, J.; Katz, S. F.; Schneider, M. R.; Kleger, A.; Paschke, S.; Seufferlein, T.; Eiseler, T. *J. Cell Sci.* **2016**, *129*, 2416-2429.
- (82) Watkins, J. L.; Lewandowski, K. T.; Meek, S. E.; Storz, P.; Toker, A.; Piwnicka-Worms, H. *Proc. Natl. Acad. Sci. U. S. A.* **2008**, *105*, 18378-18383.

- (83) Nishita, M.; Tomizawa, C.; Yamamoto, M.; Horita, Y.; Ohashi, K.; Mizuno, K. *J. Cell. Biol.* **2005**, *171*, 349-359.
- (84) Eiseler, T.; Doppler, H.; Yan, I. K.; Kitatani, K.; Mizuno, K.; Storz, P. *Nat. Cell Biol.* **2009**, *11*, 545-556.
- (85) Peterburs, P.; Heering, J.; Link, G.; Pfizenmaier, K.; Olayioye, M. A.; Hausser, A. *Cancer Res.* **2009**, *69*, 5634-5638.
- (86) Barisic, S.; Nagel, A. C.; Franz-Wachtel, M.; Macek, B.; Preiss, A.; Link, G.; Maier, D.; Hausser, A. *EMBO Rep.* **2011**, *12*, 527-533.
- (87) Spratley, S. J.; Bastea, L. I.; Doppler, H.; Mizuno, K.; Storz, P. *J. Biol. Chem.* **2011**, *286*, 34254-34261.
- (88) Bencsik, N.; Szíber, Z.; Liliom, H.; Tárnok, K.; Borbély, S.; Gulyás, M.; Rátkai, A.; Szűcs, A.; Hazai-Novák, D.; Ellwanger, K.; Rácz, B.; Pfizenmaier, K.; Hausser, A.; Schlett, K. *J. Cell Biol.* **2015**, *210*, 771-783.
- (89) Roy, R.; Yang, J.; Moses, M. A. *J. Clin. Oncol.* **2009**, *27*, 5287-5297.
- (90) Eiseler, T.; Wille, C.; Koehler, C.; Illing, A.; Seufferlein, T. *J. Biol. Chem.* **2016**, *291*, 462-477.
- (91) Poola, I.; DeWitty, R. L.; Marshalleck, J. J.; Bhatnagar, R.; Abraham, J.; Leffall, L. D. *Nat. Med.* **2005**, *11*, 481-483.
- (92) Cruz-Munoz, W.; Khokha, R. *Crit. Rev. Clin. Lab Sci.* **2008**, *45*, 291-338.
- (93) Eiseler, T.; Doppler, H.; Yan, I. K.; Goodison, S.; Storz, P. *Breast Cancer Res.* **2009**, *11*, R13.
- (94) Jezierska, A.; Motyl, T. *Med. Sci. Monit.* **2009**, *15*, RA32-RA40.
- (95) Kim, J. H.; Li, L.-H.; Cai, H.; Nguyen, V. H.; Min, J.-J.; Shin, B. A.; Choi, S.-Y.; Koh, Y. S. *Genes Genom.* **2016**, *38*, 217-223.
- (96) Durand, N.; Bastea, L. I.; Long, J.; Döppler, H.; Ling, K.; Storz, P. *Sci. Rep.* **2016**, *6*, 35963.
- (97) Zhang, T.; Braun, U.; Leitges, M. *Cell Cycle* **2016**, *15*, 1844-1854.
- (98) Storz, P. *Trends Cell. Biol.* **2007**, *17*, 13-18.
- (99) Steinberg, S. F. *Mol. Pharmacol.* **2012**, *81*, 284-291.
- (100) Storz, P.; Doppler, H.; Toker, A. *Mol. Cell Biol.* **2004**, *24*, 2614-2626.
- (101) Storz, P.; Doppler, H.; Johannes, F. J.; Toker, A. *J. Biol. Chem.* **2003**, *278*, 17969-17976.

- (102) Storz, P.; Toker, A. *EMBO J.* **2003**, *22*, 109-120.
- (103) Waldron, R. T.; Rey, O.; Zhukova, E.; Rozengurt, E. *J. Biol. Chem.* **2004**, *279*, 27482-27493.
- (104) Doppler, H.; Storz, P. *J. Biol. Chem.* **2007**, *282*, 31873-31881.
- (105) Storz, P.; Doppler, H.; Toker, A. *Mol. Cell Biol.* **2005**, *25*, 8520-8530.
- (106) Huang, D.; Zhou, T.; Lafleur, K.; Nevado, C.; Caflisch, A. *Bioinformatics* **2010**, *26*, 198-204.
- (107) Gschwendt, M.; Dieterich, S.; Rennecke, J.; Kittstein, W.; Mueller, H. J.; Johannes, F. J. *FEBS Lett.* **1996**, *392*, 77-80.
- (108) Disney, A. J. M.; Kellam, B.; Dekker, L. V. *ChemMedChem* **2016**, *11*, 972-979.
- (109) Martiny-Baron, G.; Kazanietz, M. G.; Mischak, H.; Blumberg, P. M.; Kochs, G.; Hug, H.; Marme, D.; Schachtele, C. *J. Biol. Chem.* **1993**, *268*, 9194-9197.
- (110) Rennecke, J.; Rehberger, P. A.; Furstenberger, G.; Johannes, F. J.; Stohr, M.; Marks, F.; Richter, K. H. *Int. J. Cancer.* **1999**, *80*, 98-103.
- (111) Lemon, D. D.; Harrison, B. C.; Horn, T. R.; Stratton, M. S.; Ferguson, B. S.; Wempe, M. F.; McKinsey, T. A. *FEBS Lett.* **2015**, *589*, 1080-1088.
- (112) Giacomini, E.; Rupiani, S.; Guidotti, L.; Recanatini, M.; Roberti, M. *Curr. Med. Chem.* **2016**, *23*, 2439-2489.
- (113) Filipa Brito, A.; Ribeiro, M.; Margarida Abrantes, A.; Salome Pires, A.; Jorge Teixo, R.; Guilherme Tralhao, J.; Filomena Botelho, M. *Curr. Med. Chem.* **2015**, *22*, 3025-3039.
- (114) Borges, S.; Doppler, H. R.; Storz, P. *Breast Cancer Res. Treat.* **2014**, *144*, 79-91.
- (115) Jaggi, M.; Chauhan, S. C.; Du, C.; Balaji, K. C. *Mol. Cancer Ther.* **2008**, *7*, 2703-2712.
- (116) Kollár, P.; Rajchard, J.; Balounov, Z.; Pazourek, J. *Pharm. Biol.* **2014**, *52*, 237-242.
- (117) Newman, D. J.; Cragg, G. M. *Planta Med* **2016**, *82*, 775-789.
- (118) Gamber, G. G.; Meredith, E.; Zhu, Q.; Yan, W.; Rao, C.; Capparelli, M.; Burgis, R.; Enyedy, I.; Zhang, J.-H.; Soldermann, N.; Beattie, K.; Rozhitskaya, O.; Koch, K. A.; Pagratis, N.; Hosagrahara, V.; Vega, R. B.; McKinsey, T. A.; Monovich, L. *Bioorg. Med. Chem. Lett.* **2011**, *21*, 1447-1451.
- (119) Meredith, E. L.; Ardayfio, O.; Beattie, K.; Dobler, M. R.; Enyedy, I.; Gaul, C.; Hosagrahara, V.; Jewell, C.; Koch, K.; Lee, W.; Lehmann, H.; McKinsey, T. A.; Miranda, K.; Pagratis, N.; Pancost, M.; Patnaik, A.; Phan, D.; Plato, C.; Qian, M.; Rajaraman, V.; Rao, C.; Rozhitskaya, O.; Ruppen, T.; Shi, J.; Siska, S. J.; Springer, C.;

- van Eis, M.; Vega, R. B.; von Matt, A.; Yang, L.; Yoon, T.; Zhang, J.-H.; Zhu, N.; Monovich, L. G. *J. Med. Chem.* **2010**, *53*, 5400-5421.
- (120) Meredith, E. L.; Beattie, K.; Burgis, R.; Capparelli, M.; Chapo, J.; DiPietro, L.; Gamber, G.; Enyedy, I.; Hood, D. B.; Hosagrahara, V.; Jewell, C.; Koch, K. A.; Lee, W.; Lemon, D. D.; McKinsey, T. A.; Miranda, K.; Pagratis, N.; Phan, D.; Plato, C.; Rao, C.; Rozhitskaya, O.; Soldermann, N.; Springer, C.; van Eis, M.; Vega, R. B.; Yan, W.; Zhu, Q.; Monovich, L. G. *J. Med. Chem.* **2010**, *53*, 5422-5438.
- (121) Huynh, Q. K.; McKinsey, T. A. *Arch. Biochem. Biophys.* **2006**, *450*, 141-148.
- (122) Bossuyt, J.; Helmstadter, K.; Wu, X.; Clements-Jewery, H.; Haworth, R. S.; Avkiran, M.; Martin, J. L.; Pogwizd, S. M.; Bers, D. M. *Circ. Res.* **2008**, *102*, 695-702.
- (123) Hardt, S. E.; Sadoshima, J. *Cardiovasc. Res.* **2004**, *63*, 500-509.
- (124) Yuan, J.; Liu, Y.; Tan, T.; Guha, S.; Gukovsky, I.; Gukovskaya, A.; Pandol, S. J. *Front. Physiol.* **2012**, *3*, 60.
- (125) Bernhart, E.; Damm, S.; Wintersperger, A.; DeVaney, T.; Zimmer, A.; Raynham, T.; Ireson, C.; Sattler, W. *Exp. Cell Res.* **2013**, *319*, 2037-2048.
- (126) Wei, N.; Chu, E.; Wipf, P.; Schmitz, J. C. *Mol. Cancer Ther.* **2014**, *13*, 1130-1141.
- (127) Wei, N.; Chu, E.; Wu, S.-y.; Schmitz, J. C.; Wei, N.; Chu, E.; Wu, S.-y.; Wipf, P.; Schmitz, J. C.; Wipf, P. *Oncotarget* **2015**, *6*, 4745-4756.
- (128) Evans, I. M.; Bagherzadeh, A.; Charles, M.; Raynham, T.; Ireson, C.; Boakes, A.; Kelland, L.; Zachary, I. C. *Biochem J* **2010**, *429*, 565-572.
- (129) Bishop, A. C.; Kung, C.-y.; Shah, K.; Witucki, L.; Shokat, K. M.; Liu, Y. *J. Am. Chem. Soc.* **1999**, *121*, 627-631.
- (130) Murphy, R. C.; Ojo, K. K.; Larson, E. T.; Castellanos-Gonzalez, A.; Perera, B. G. K.; Keyloun, K. R.; Kim, J. E.; Bhandari, J. G.; Muller, N. R.; Verlinde, C. L. M. J.; White, A. C.; Merritt, E. A.; Van Voorhis, W. C.; Maly, D. J. *ACS Med. Chem. Lett.* **2010**, *1*, 331-335.
- (131) Verschueren, K.; Cobbaut, M.; Demaerel, J.; Saadah, L.; Voet, A. R. D.; Van Lint, J.; De Borggraeve, W. M. *MedChemComm* **2017**, *8*, 640-646.
- (132) Golkowski, M.; Vidadala, R. S. R.; Lombard, C. K.; Suh, H. W.; Maly, D. J.; Ong, S.-E. *J. Proteome Res.* **2017**, *16*, 1216-1217.
- (133) Médard, G.; Pachel, F.; Ruprecht, B.; Klaeger, S.; Heinzlmeir, S.; Helm, D.; Qiao, H.; Ku, X.; Wilhelm, M.; Kuehne, T.; Wu, Z.; Dittmann, A.; Hopf, C.; Kramer, K.; Kuster, B. *J. Proteome Res.* **2015**, *14*, 1574-1586.

- (134) Bantscheff, M.; Eberhard, D.; Abraham, Y.; Bastuck, S.; Boesche, M.; Hobson, S.; Mathieson, T.; Perrin, J.; Raida, M.; Rau, C.; Reader, V.; Sweetman, G.; Bauer, A.; Bouwmeester, T.; Hopf, C.; Kruse, U.; Neubauer, G.; Ramsden, N.; Rick, J.; Kuster, B.; Drewes, G. *Nat Biotech* **2007**, *25*, 1035-1044.
- (135) Sharlow, E. R.; Giridhar, K. V.; LaValle, C. R.; Chen, J.; Leimgruber, S.; Barrett, R.; Bravo-Altamirano, K.; Wipf, P.; Lazo, J. S.; Wang, Q. J. *J. Biol. Chem.* **2008**, *283*, 33516-33526.
- (136) Torres-Marquez, E.; Sinnott-Smith, J.; Guha, S.; Kui, R.; Waldron, R. T.; Rey, O.; Rozengurt, E. *Biochem. Biophys. Res. Commun.* **2010**, *391*, 63-68.
- (137) George, K. M.; Frantz, M.-C.; Bravo-Altamirano, K.; LaValle, C. R.; Tandon, M.; Leimgruber, S.; Sharlow, E. R.; Lazo, J. S.; Wang, Q. J.; Wipf, P. *Pharmaceutics* **2011**, *3*, 186-228.
- (138) Guo, J.; Clausen, D. M.; Beumer, J. H.; Parise, R. A.; Egorin, M. J.; Bravo-Altamirano, K.; Wipf, P.; Sharlow, E. R.; Wang, Q. J.; Eiseman, J. L. *Cancer Chemoth. Pharm.* **2013**, *71*, 331-344.
- (139) Tandon, M.; Salamoun, J. M.; Carder, E. J.; Farber, E.; Xu, S.; Deng, F.; Tang, H.; Wipf, P.; Wang, Q. J. *PLOS ONE* **2015**, *10*, e0119346.
- (140) Tandon, M.; Wang, L.; Xu, Q.; Xie, X.; Wipf, P.; Wang, Q. J. *PLoS ONE* **2012**, *7*, e44653.
- (141) Guo, X.; Schmitz, J. C.; Kenney, B. C.; Uchio, E. M.; Kulkarni, S.; Cha, C. H. *Cancer Sci.* **2012**, *103*, 1474-1480.
- (142) Bishop, A. C.; Ubersax, J. A.; Petsch, D. T.; Matheos, D. P.; Gray, N. S.; Blethrow, J.; Shimizu, E.; Tsien, J. Z.; Schultz, P. G.; Rose, M. D.; Wood, J. L.; Morgan, D. O.; Shokat, K. M. *Nature* **2000**, *407*, 395-401.
- (143) Endo, S.; Satoh, Y.; Shah, K.; Takishima, K. *Biochem. Biophys. Res. Commun.* **2006**, *341*, 261-265.
- (144) Verheijen, J. C.; Richard, D. J.; Curran, K.; Kaplan, J.; Lefever, M.; Nowak, P.; Malwitz, D. J.; Brooijmans, N.; Toral-Barza, L.; Zhang, W.-G.; Lucas, J.; Hollander, I.; Ayrál-Kaloustian, S.; Mansour, T. S.; Yu, K.; Zask, A. *J. Med. Chem.* **2009**, *52*, 8010-8024.
- (145) Montecucco, C.; Schiavo, G. *Mol. Microbiol.* **1994**, *13*, 1-8.
- (146) Pellizzari, R.; Rossetto, O.; Schiavo, G.; Montecucco, C. *Phil. Trans. R. Soc. Lond. B Biol. Sci.* **1999**, *354*, 259-268.
- (147) Turton, K.; Chaddock, J. A.; Acharya, K. R. *Trends Biochem. Sci.* **2002**, *27*, 552-558.
- (148) Sakurai, J.; Nagahama, M.; Oda, M. *J. Biochem.* **2004**, *136*, 569-574.

- (149) Oda, M. *Nihon Rinsho* **2012**, *70*, 1313-1317.
- (150) Burke, G. S. *J. Bacteriol.* **1919**, *4*, 555-570.
- (151) Meyer, K. F.; Gunnison, J. B. *J. Infect. Dis.* **1929**, *45*, 106-118.
- (152) Hazen, E. L. *J. Infect. Dis.* **1937**, *60*, 260-264.
- (153) L. L. Simpson; *Botulinum Neurotoxin and Tetanus Toxin*. Academic Press: New York, 1989.
- (154) Dover, N.; Barash, J. R.; Hill, K. K.; Xie, G.; Arnon, S. S. *J. Infect. Dis.* **2014**, *209*, 192-202.
- (155) Kessler, K. R.; Benecke, R. *Neurotoxicology* **1997**, *18*, 761-770.
- (156) Franciosa, G.; Floridi, F.; Maugliani, A.; Aureli, P. *Appl. Environ. Microbiol.* **2004**, *70*, 7192-7199.
- (157) Whitmarsh, R. C. M.; Tepp, W. H.; Bradshaw, M.; Lin, G.; Pier, C. L.; Scherf, J. M.; Johnson, E. A.; Pellett, S. *Infect. Immun.* **2013**, *81*, 3894-3902.
- (158) Arnon, S. S.; Schechter, R.; Inglesby, T. V.; Henderson, D. A.; Bartlett, J. G.; Ascher, M. S.; Eitzen, E.; Fine, A. D.; Hauer, J.; Layton, M.; Lillibridge, S.; Osterholm, M. T.; O'Toole, T.; Parker, G.; Perl, T. M.; Russell, P. K.; Swerdlow, D. L.; Tonat, K. *JAMA* **2001**, *285*, 1059-1070.
- (159) Caya, J. G.; Agni, R.; Miller, J. E. *Arch. Pathol. Lab. Med.* **2004**, *128*, 653-662.
- (160) Wein, L. M.; Liu, Y. *Proc. Natl. Acad. Sci. U. S. A.* **2005**, *102*, 9984-9989.
- (161) Bossi, P.; Garin, D.; Guihot, A.; Gay, F.; Crance, J. M.; Debord, T.; Autran, B.; Bricaire, F. *Cell Mol. Life Sci.* **2006**, *63*, 2196-2212.
- (162) Villar, R. G.; Elliott, S. P.; Davenport, K. M. *Infect. Dis. Clin. North Am.* **2006**, *20*, 313-327.
- (163) Opsenica, I.; Filipovic, V.; Nuss, J. E.; Gomba, L. M.; Opsenica, D.; Burnett, J. C.; Gussio, R.; Solaja, B. A.; Bavari, S. *Eur. J. Med. Chem.* **2012**, *53*, 374-379.
- (164) Singh, P.; Singh, M. K.; Chaudhary, D.; Chauhan, V.; Bharadwaj, P.; Pandey, A.; Upadhyay, N.; Dhaked, R. K. *PLoS ONE* **2012**, *7*, e47110.
- (165) <https://emergency.cdc.gov/agent/agentlist.asp>.
- (166) Hambleton, P. *J. Neurol.* **1992**, *239*, 16-20.
- (167) Albanese, A.; Bentivoglio, A. R.; Cassetta, E.; Viggiano, A.; Maria, G.; Gui, D. *Aliment Pharmacol. Ther.* **1995**, *9*, 599-604.

- (168) Glogau, R. G. *Dermatol. Surg.* **1998**, *24*, 817-819.
- (169) Shapiro, R. L.; Hatheway, C.; Swerdlow, D. L. *Ann. Intern. Med.* **1998**, *129*, 221-228.
- (170) Rossetto, O.; Seveso, M.; Caccin, P.; Schiavo, G.; Montecucco, C. *Toxicon* **2001**, *39*, 27-41.
- (171) Rowland, L. P. *New Engl. J. Med.* **2002**, *347*, 382-383.
- (172) Sposito, M. M. *Plast. Reconstr. Surg.* **2002**, *110*, 601-613.
- (173) Sposito, M. M. *Aesthetic. Plast. Surg.* **2002**, *26*, 89-98.
- (174) Gui, D.; Rossi, S.; Runfola, M.; Magalini, S. C. *Aliment Pharmacol. Ther.* **2003**, *18*, 1-16.
- (175) Foster, K. A. *Expert Opin. Investig. Drugs.* **2004**, *13*, 1437-1443.
- (176) Bhidayasiri, R.; Truong, D. D. *J. Neurol. Sci.* **2005**, *235*, 1-9.
- (177) Foster, K. A. *Drug Disc. Today* **2005**, *10*, 563-569.
- (178) Shukla, H. D.; Sharma, S. K. *Crit. Rev. Microbiol.* **2005**, *31*, 11-18.
- (179) Chen, S. *Toxins* **2012**, *4*, 913-939.
- (180) Alter, K. E.; Hallett, M.; Karp, B.; Lungu, C. *Toxicon* **2013**, *68*, 68-69.
- (181) Auguet, M.; Favre-Guilmond, C.; Cornet, S.; Carre, D.; Rocher, M. N.; Pignol, B.; Pham, B.; Chabrier, P. E. *Toxicon* **2013**, *68*, 82.
- (182) Coelho, M. *Toxicon* **2013**, *68*, 72.
- (183) Colasante, C.; Morbiato, L.; Paoli, M.; Shone, C. C.; Muraro, L.; Sheikh, K.; Rossetto, O.; Montecucco, C.; Molgó, J. *Toxicon* **2013**, *68*, 70-71.
- (184) Comella, C. L. *Toxicon* **2013**, *68*, 68.
- (185) Marchand-Pauvert, V.; Aymard, C.; Giboin, L.-S.; Dominici, F.; Rossi, A.; Mazzocchio, R. *J. Physiol.* **2013**, *591*, 1017-1029.
- (186) Naumann, M. *Toxicon* **2013**, *68*, 71.
- (187) Silberstein, S. *Toxicon* **2013**, *68*, 64.
- (188) Voller, B. *Toxicon* **2013**, *68*, 64-65.
- (189) Wollmer, M. A.; Krüger, T. H. C. *Toxicon* **2013**, *68*, 72.
- (190) Yaksh, T. L. *Toxicon* **2013**, *68*, 63-64.

- (191) Allen, J. D.; Christopher, D. K.; Sina, B. *Curr. Top. Med. Chem.* **2016**, *16*, 2330-2349.
- (192) Pellett, S.; Yaksh, L. T.; Ramachandran, R. *Toxins* **2015**, *7*, 4519-4563.
- (193) Moore, C. D.; Cohn, A. J.; Dmochowski, R. R. *Toxins* **2016**, *8*, 88.
- (194) Luvisetto, S.; Gazerani, P.; Cianchetti, C.; Pavone, F. *Toxins* **2015**, *7*, 3818-3844.
- (195) Noland, M. E.; Lalonde, D. H.; Yee, G. J.; Rohrich, R. J. *Plast. Reconstr. Surg.* **2016**, *138*, 519e-530e.
- (196) Schiavo, G.; Rossetto, O.; Santucci, A.; DasGupta, B. R.; Montecucco, C. *J. Biol. Chem.* **1992**, *267*, 23479-23483.
- (197) Schiavo, G.; Malizio, C.; Trimble, W. S.; De Laureto, P. P.; Milan, G.; Sugiyama, H.; Johnson, E. A.; Montecucco, C. *J. Biol. Chem.* **1994**, *269*, 20213-20216.
- (198) Anne, C.; Blommaert, A.; Turcaud, S.; Martin, A. S.; Meudal, H.; Roques, B. P. *Bioorg. Med. Chem.* **2003**, *11*, 4655-4660.
- (199) Wey, J.-j.; Tang, S.-s.; Wu, T.-y. *Acta. Pharmacol. Sin.* **2006**, *27*, 1238-1246.
- (200) Mizanur, R. M.; Frasca, V.; Swaminathan, S.; Bavari, S.; Webb, R.; Smith, L. A.; Ahmed, S. A. *J. Biol. Chem.* **2013**, *288*, 24223-24233.
- (201) Montecucco, C.; Papini, E.; Schiavo, G. *FEBS Lett.* **1994**, *346*, 92-98.
- (202) Dickerson, T. J.; Janda, K. D. *ACS Chem. Biol.* **2006**, *1*, 359-369.
- (203) Simpson, L. *Toxicon* **2013**, *68*, 40-59.
- (204) Sugil, S.; Sakaguchi, G. *Infect. Immun.* **1975**, *12*, 1262-1270.
- (205) Singh, B. R.; Li, B.; Read, D. *Toxicon* **1995**, *33*, 1541-1547.
- (206) Arndt, J. W.; Gu, J.; Jaroszewski, L.; Schwarzenbacher, R.; Hanson, M. A.; Lebeda, F. J.; Stevens, R. C. *J. Mol. Biol.* **2005**, *346*, 1083-1093.
- (207) Benefield, D. A.; Dessain, S. K.; Shine, N.; Ohi, M. D.; Lacy, D. B. *Proc. Natl. Acad. Sci. U. S. A.* **2013**, *110*, 5630-5635.
- (208) Miyashita, S.-I.; Sagane, Y.; Suzuki, T.; Matsumoto, T.; Niwa, K.; Watanabe, T. *Sci. Rep.* **2016**, *6*, 31043.
- (209) Montecucco, C. *Trends Biochem. Sci.* **1986**, *11*, 314-317.
- (210) Lacy, D. B.; Stevens, R. C. *J. Mol. Biol.* **1999**, *291*, 1091-1104.
- (211) Baldwin, M. R.; Kim, J. J.; Barbieri, J. T. *Nat. Struct. Mol. Biol.* **2007**, *14*, 9-10.

- (212) Dong, M.; Yeh, F.; Tepp, W. H.; Dean, C.; Johnson, E. A.; Janz, R.; Chapman, E. R. *Science* **2006**, *312*, 592-596.
- (213) Koriazova, L. K.; Montal, M. *Nat. Struct. Biol.* **2003**, *10*, 13-18.
- (214) Fischer, A.; Mushrush, D. J.; Lacy, D. B.; Montal, M. *PLoS Pathog.* **2008**, *4*, e1000245.
- (215) Araye, A.; Goudet, A.; Barbier, J.; Pichard, S.; Baron, B.; England, P.; Pérez, J.; Zinn-Justin, S.; Chenal, A.; Gillet, D. *PLoS ONE* **2016**, *11*, e0153401.
- (216) Schiavo, G.; Benfenati, F.; Poulain, B.; Rossetto, O.; Polverino De Laureto, P.; DasGupta, B. R.; Montecucco, C. *Nature* **1992**, *359*, 832-835.
- (217) Schiavo, G.; Rossetto, O.; Catsicas, S.; De Laureto, P. P.; DasGupta, B. R.; Benfenati, F.; Montecucco, C. *J. Biol. Chem.* **1993**, *268*, 23784-23787.
- (218) Schiavo, G.; Shone, C. C.; Rossetto, O.; Alexander, F. C. G.; Montecucco, C. *J. Biol. Chem.* **1993**, *268*, 11516-11519.
- (219) Binz, T.; Blasi, J.; Yamasaki, S.; Baumeister, A.; Link, E.; Sudhof, T. C.; Jahn, R.; Niemann, H. *J. Biol. Chem.* **1994**, *269*, 1617-1620.
- (220) Keller, J. E.; Neale, E. A. *J. Biol. Chem.* **2001**, *276*, 13476-13482.
- (221) Blasi, J.; Chapman, E. R.; Yamasaki, S.; Binz, T.; Niemann, H.; Jahn, R. *EMBO J.* **1993**, *12*, 4821-4828.
- (222) Zuniga, J. E.; Schmidt, J. J.; Fenn, T.; Burnett, J. C.; Arac, D.; Gussio, R.; Stafford, R. G.; Badie, S. S.; Bavari, S.; Brunger, A. T. *Structure* **2008**, *16*, 1588-1597.
- (223) Kumaran, D.; Rawat, R.; Ludivico, M. L.; Ahmed, S. A.; Swaminathan, S. *J. Biol. Chem.* **2008**, *283*, 18883-18891.
- (224) Arnon, S. S.; Schechter, R.; Inglesby, T. V.; et al. *J. Amer. Med. Assoc.* **2001**, *285*, 1059-1070.
- (225) Willis, B.; Eubanks, L. M.; Dickerson, T. J.; Janda, K. D. *Angew. Chem. Int. Ed.* **2008**, *47*, 8360-8379.
- (226) Al-Saleem, F. H.; Nasser, Z.; Olson, R. M.; Cao, L.; Simpson, L. L. *J. Pharmacol. Exp. Ther.* **2011**, *338*, 503-517.
- (227) Schmidt, J. J.; Bostian, K. A. *J. Protein Chem.* **1997**, *16*, 19-26.
- (228) Schmidt, J. J.; Stafford, R. G.; Bostian, K. A. *FEBS Lett.* **1998**, *435*, 61-64.
- (229) Schmidt, J. J.; Stafford, R. G. *FEBS Lett.* **2002**, *532*, 423-426.

- (230) Anne, C.; Turcaud, S.; Quancard, J.; Teffo, F.; Meudal, H.; Fournie-Zaluski, M. C.; Roques, B. P. *J. Med. Chem.* **2003**, *46*, 4648-4656.
- (231) Sukonpan, C.; Oost, T.; Goodnough, M.; Tepp, W.; Johnson, E. A.; Rich, D. H. *J. Pept. Res.* **2004**, *63*, 181-193.
- (232) Yiadom, K. P. A. B.; Muhie, S.; Yang, D. C. H. *Biochem. Biophys. Res. Commun.* **2005**, *335*, 1247-1253.
- (233) Zuniga, J. E.; Hammill, J. T.; Drory, O.; Nuss, J. E.; Burnett, J. C.; Gussio, R.; Wipf, P.; Bavari, S.; Brunger, A. T. *PLoS ONE* **2010**, *5*, e11378.
- (234) Kumar, G.; Kumaran, D.; Ahmed, S. A.; Swaminathan, S. *Acta. Crystallogr. D* **2012**, *68*, 511-520.
- (235) Schmidt, J. J.; Bostian, K. A. *J. Protein Chem.* **1995**, *14*, 703-708.
- (236) Schmidt, J. J.; Stafford, R. G. *Appl. Environ. Microbiol.* **2003**, *69*, 297-303.
- (237) Schmidt, J. J.; Stafford, R. G.; Millard, C. B. *Anal. Biochem.* **2001**, *296*, 130-137.
- (238) Burnett, J. C.; Schmidt, J. J.; Stafford, R. G.; Panchal, R. G.; Nguyen, T. L.; Hermone, A. R.; Vennerstrom, J. L.; McGrath, C. F.; Lane, D. J.; Sausville, E. A.; Zaharevitz, D. W.; Gussio, R.; Bavari, S. *Biochem. Biophys. Res. Commun.* **2003**, *310*, 84-93.
- (239) Boldt, G. E.; Kennedy, J. P.; Hixon, M. S.; McAllister, L. A.; Barbieri, J. T.; Tzipori, S.; Janda, K. D. *J. Comb. Chem.* **2006**, *8*, 513-521.
- (240) Capkova, K.; Hixon, M. S.; McAllister, L. A.; Janda, K. D. *Chem. Commun.* **2008**, 3525-3527.
- (241) Čapková, K.; Salzameda, N. T.; Janda, K. D. *Toxicol.* **2009**, *54*, 575-582.
- (242) Šilhár, P.; Alakurtti, S.; Čapková, K.; Xiaochuan, F.; Shoemaker, C. B.; Yli-Kauhaluoma, J.; Janda, K. D. *Bioorg. Med. Chem. Lett.* **2011**, *21*, 2229-2231.
- (243) Feltrup, T. M.; Singh, B. R. *Anal. Chem.* **2012**, *84*, 10549-10553.
- (244) Burnett, J. C.; Ruthel, G.; Stegmann, C. M.; Panchal, R. G.; Nguyen, T. L.; Hermone, A. R.; Stafford, R. G.; Lane, D. J.; Kenny, T. A.; McGrath, C. F.; Wipf, P.; Stahl, A. M.; Schmidt, J. J.; Gussio, R.; Brunger, A. T.; Bavari, S. *J. Biol. Chem.* **2007**, *282*, 5004-5014.
- (245) Burnett, J. C.; Schmidt, J. J.; McGrath, C. F.; Nguyen, T. L.; Hermone, A. R.; Panchal, R. G.; Vennerstrom, J. L.; Kodukula, K.; Zaharevitz, D. W.; Gussio, R.; Bavari, S. *Bioorg. Med. Chem.* **2005**, *13*, 333-341.
- (246) Merino, I.; Thompson, J. D.; Millard, C. B.; Schmidt, J. J.; Pang, Y.-P. *Bioorg. Med. Chem.* **2006**, *14*, 3583-3591.

- (247) Burnett, J. C.; Opsenica, D.; Sriraghavan, K.; Panchal, R. G.; Ruthel, G.; Hermone, A. R.; Nguyen, T. L.; Kenny, T. A.; Lane, D. J.; McGrath, C. F.; Schmidt, J. J.; Vennerstrom, J. L.; Gussio, R.; Solaja, B. A.; Bavari, S. *J. Med. Chem.* **2007**, *50*, 2127-2136.
- (248) Hale, M.; Oyler, G.; Swaminathan, S.; Ahmed, S. A. *J. Biol. Chem.* **2011**, *286*, 1802-1811.
- (249) Kumaran, D.; Adler, M.; Levit, M.; Krebs, M.; Sweeney, R.; Swaminathan, S. *Bioorg. Med. Chem.* **2015**, *23*, 7264-7273.
- (250) Fu, Z.; Chen, S.; Baldwin, M. R.; Boldt, G. E.; Crawford, A.; Janda, K. D.; Barbieri, J. T.; Kim, J. J. *Biochemistry* **2006**, *45*, 8903-8911.
- (251) Park, J. G.; Sill, P. C.; Makiyi, E. F.; Garcia-Sosa, A. T.; Millard, C. B.; Schmidt, J. J.; Pang, Y.-P. *Bioorg. Med. Chem.* **2006**, *14*, 395-408.
- (252) Smith, G. R.; Caglič, D.; Čapek, P.; Zhang, Y.; Godbole, S.; Reitz, A. B.; Dickerson, T. J. *Bioorg. Med. Chem. Lett.* **2012**, *22*, 3754-3757.
- (253) Boldt, G. E.; Kennedy, J. P.; Janda, K. D. *Org. Lett.* **2006**, *8*, 1729-1732.
- (254) Eubanks, L. M.; Hixon, M. S.; Jin, W.; Hong, S.; Clancy, C. M.; Tepp, W. H.; Baldwin, M. R.; Malizio, C. J.; Goodnough, M. C.; Barbieri, J. T.; Johnson, E. A.; Boger, D. L.; Dickerson, T. J.; Janda, K. D. *Proc. Natl. Acad. Sci. U. S. A.* **2007**, *104*, 2602-2607.
- (255) Čapek, P.; Zhang, Y.; Barlow, D. J.; Houseknecht, K. L.; Smith, G. R.; Dickerson, T. J. *ACS Chem. Neurosci.* **2011**, *2*, 288-293.
- (256) Thyagarajan, B.; Potian, J. G.; Garcia, C. C.; Hognason, K.; Čapková, K.; Moe, S. T.; Jacobson, A. R.; Janda, K. D.; McArdle, J. J. *Neuropharmacol.* **2010**, *58*, 1189-1198.
- (257) Tang, J.; Park, J. G.; Millard, C. B.; Schmidt, J. J.; Pang, Y.-P. *PLoS ONE* **2007**, *2*, e761.
- (258) Pang, Y.-P.; Davis, J.; Wang, S.; Park, J. G.; Nambiar, M. P.; Schmidt, J. J.; Millard, C. B. *PLoS ONE* **2010**, *5*, e10129.
- (259) O'Brien, E. C.; Farkas, E.; Gil, M. J.; Fitzgerald, D.; Castineras, A.; Nolan, K. B. *J. Inorg. Biochem.* **2000**, *79*, 47-51.
- (260) Grant, S.; Easley, C.; Kirkpatrick, P. *Nat. Rev. Drug Discov.* **2007**, *6*, 21-22.
- (261) Saban, N.; Bujak, M. *Cancer Chemoth. Pharm.* **2009**, *64*, 213-221.
- (262) Cardinale, S. C.; Butler, M. M.; Ruthel, G.; Nuss, J.; Wanner, L. M.; Li, B.; Pai, R. P.; Peet, N. P.; Bavari, S.; Bowlin, T. L. *Botulinum J.* **2011**, *2*, 16-29.
- (263) Li, B.; Cardinale, S. C.; Butler, M. M.; Pai, R.; Nuss, J. E.; Peet, N. P.; Bavari, S.; Bowlin, T. L. *Bioorg. Med. Chem.* **2011**, *19*, 7338-7348.

- (264) Johnson, D. S.; Weerapana E Fau - Cravatt, B. F.; Cravatt, B. F. *Future Med. Chem.* **2010**, *2*, 949-964.
- (265) Roxas-Duncan, V.; Enyedy, I.; Montgomery, V. A.; Eccard, V. S.; Carrington, M. A.; Lai, H.; Gul, N.; Yang, D. C.; Smith, L. A. *Antimicrob. Agents Chemother.* **2009**, *53*, 3478-3486.
- (266) Harrell Jr, W. A.; Vieira, R. C.; Ensel, S. M.; Montgomery, V.; Guernieri, R.; Eccard, V. S.; Campbell, Y.; Roxas-Duncan, V.; Cardellina Ii, J. H.; Webb, R. P.; Smith, L. A. *Bioorg. Med. Chem. Lett.* **2017**, *27*, 675-678.
- (267) Bremer, P. T.; Adler, M.; Phung, C. H.; Singh, A. K.; Janda, K. D. *J. Med. Chem.* **2017**, *60*, 338-348.
- (268) Wang, C.; Widom, J.; Petronijevic, F.; Burnett, J. C.; Nuss, J. E.; Bavari, S.; Gussio, R.; Wipf, P. *Heterocycles* **2009**, *79*, 487-520.
- (269) Burnett, J. C.; Li, B.; Pai, R.; Cardinale, S. C.; Butler, M. M.; Peet, N. P.; Moir, D.; Bavari, S.; Bowlin, T. *OA Bioinformatics* **2010**, *2010*, 11-18.
- (270) Lovering, F.; Bikker, J.; Humblet, C. *J. Med. Chem.* **2009**, *52*, 6752-6756.
- (271) Feinberg, A. P.; Snyder, S. H. *Proc. Natl. Acad. Sci. U. S. A.* **1975**, *72*, 1899-1903.
- (272) Bond angles obtained from Spartan (Wavefunction Inc.) for the lowest energy conformer. Using molecular mechanics MMFF minimization
- (273) Campiani, G.; Butini, S.; Gemma, S.; Nacci, V.; Fattorusso, C.; Catalanotti, B.; Giorgi, G.; Cagnotto, A.; Goegan, M.; Mennini, T.; Minetti, P.; Di Cesare, M. A.; Mastroianni, D.; Scafetta, N.; Galletti, B.; Stasi, M. A.; Castorina, M.; Pacifici, L.; Ghirardi, O.; Tinti, O.; Carminati, P. *J. Med. Chem.* **2001**, *45*, 344-359.
- (274) Sugiyama, H.; Yoshida, M.; Mori, K.; Kawamoto, T.; Sogabe, S.; Takagi, T.; Oki, H.; Tanaka, T.; Kimura, H.; Ikeura, Y. *Chem. Pharm. Bull.* **2007**, *55*, 613-624.
- (275) Igarashi, M.; Fuchikami, T. *Tetrahedron Lett.* **2001**, *42*, 1945-1947.
- (276) Bannister, R. M.; Brookes, M. H.; Evans, G. R.; Katz, R. B.; Tyrrell, N. D. *Org. Process Res. Dev.* **2000**, *4*, 467-472.
- (277) Bonini, C.; Chiummiento, L.; Bonis, M. D.; Funicello, M.; Lupattelli, P.; Suanno, G.; Berti, F.; Campaner, P. *Tetrahedron* **2005**, *61*, 6580-6589.
- (278) Das, S.; Addis, D.; Junge, K.; Beller, M. *Chem. Eur. J.* **2011**, *17*, 12186-12192.
- (279) Choi, Y.; Ishikawa, H.; Velcicky, J.; Elliott, G. I.; Miller, M. M.; Boger, D. L. *Org. Lett.* **2005**, *7*, 4539-4542.
- (280) Sundberg, R. J.; Walters, C. P.; Bloom, J. D. *J. Org. Chem.* **1981**, *46*, 3730-3732.

- (281) Charette, A. B.; Grenon, M. *J. Org. Chem.* **2003**, *68*, 5792-5794.
- (282) Bergman, J.; Pettersson, B.; Hasimbegovic, V.; Svensson, P. H. *J. Org. Chem.* **2011**, *76*, 1546-1553.
- (283) King, F. D.; Aliev, A. E.; Caddick, S.; Tocher, D. A.; Courtier-Murias, D. *Org. Biomol. Chem.* **2009**, *7*, 167-177.
- (284) Confalone, P. N.; Huie, E. M. *J. Org. Chem.* **1987**, *52*, 79-83.
- (285) Pala, G.; Mantegani, A.; Zugna, E. *Tetrahedron* **1970**, *26*, 1275-1279.
- (286) Ohkata, K.; Takee, K.; Akiba, K. *Bull. Chem. Soc. Jpn.* **1985**, *58*, 1946-1952.
- (287) Brieady, L. E.; Hurlbert, B. S.; Mehta, N. B. *J. Org. Chem.* **1981**, *46*, 1630-1634.
- (288) Kan, T.; Fujiwara, A.; Kobayashi, H.; Fukuyama, T. *Tetrahedron* **2002**, *58*, 6267-6276.
- (289) Abdel-Magid, A. F.; Carson, K. G.; Harris, B. D.; Maryanoff, C. A.; Shah, R. D. *J. Org. Chem.* **1996**, *61*, 3849-3862.
- (290) Zhu, X.; Wei, Y. *J. Cell. Physiol.* **2012**, *36*, 363-364.
- (291) Huang, W.; Shen, Q.; Wang, J.; Zhou, X. *J. Org. Chem.* **2008**, *73*, 1586-1589.
- (292) Boyle, R. G.; Travers, S. US Patent 270416 A1 2009.
- (293) Hintermann, L. *Beilstein J. Org. Chem.* **2007**, *3*, 22.
- (294) Boy, K. M.; Guernon, J. M.; Shi, J.; Toyn, J. H.; Meredith, J. E.; Barten, D. M.; Burton, C. R.; Albright, C. F.; Marcinkeviciene, J.; Good, A. C.; Tebben, A. J.; Muckelbauer, J. K.; Camac, D. M.; Lentz, K. A.; Bronson, J. J.; Olson, R. E.; Macor, J. E.; Thompson Iii, L. A. *Bioorg. Med. Chem. Lett.* **2011**, *21*, 6916-6924.
- (295) Olah, G. A.; Narang, S. C.; Gupta, B. G. B.; Malhotra, R. *J. Org. Chem.* **1979**, *44*, 1247-1251.
- (296) Yang, B. V.; O'Rourke, D.; Li, J. *Synlett.* **1993**, *1993*, 195-196.
- (297) de la Hoz, A.; Díaz-Ortiz, Á.; del Carmen Mateo, M.; Moral, M.; Moreno, A.; Elguero, J.; Foces-Foces, C.; Rodríguez, M. L.; Sánchez-Migallón, A. *Tetrahedron* **2006**, *62*, 5868-5874.
- (298) Li, B.; Pai, R.; Cardinale, S. C.; Butler, M. M.; Peet, N. P.; Moir, D. T.; Bavari, S.; Bowlin, T. L. *J. Med. Chem.* **2010**, *53*, 2264-2276.
- (299) Cereda, E.; Ezhaya, A.; Gil Quintero, M.; Bellora, E.; Dubini, E.; Micheletti, R.; Schiavone, A.; Brambilla, A.; Schiavi, G. B.; Donetti, A. *J. Med. Chem.* **1990**, *33*, 2108-2113.

- (300) Iley, J.; Norberto, F.; Rosa, E. *J. Chem. Soc., Perkin Trans. 2* **1989**, 1471-1475.
- (301) Zhu, Y. Y., W. Y.; Kelly-Borges, M.; Scheuer, P. J. *Heterocycles* **1998**, *49*, 355-360.
- (302) Wipf, P.; Halter, R. J. *Org. Biomol. Chem.* **2005**, *3*, 2053-2061.
- (303) Cao, L.; Maciejewski, J. P.; Elzner, S.; Amantini, D.; Wipf, P. *Org. Biomol. Chem.* **2012**, *10*, 5811-5814.
- (304) Bräse, S.; Gil, C.; Knepper, K.; Zimmermann, V. *Angew. Chem. Int. Ed.* **2005**, *44*, 5188-5240.
- (305) Iula, D. M. In *Staudinger reaction*, John Wiley & Sons, Inc.: 2007; pp 129-151.
- (306) Van, d. G. J. C. *Organophosphorus Chem.* **2007**, *36*, 313-351.
- (307) Hajos, G.; Nagy, I. *Curr. Org. Chem.* **2008**, *12*, 39-58.
- (308) Fresneda, P. M.; Molina, P. *Synlett.* **2004**, *2004*, 1-17.
- (309) Liao, H.-Y. *J. Chin. Chem. Soc.* **2011**, *58*, 645-652.
- (310) González-Bobes, F.; Kopp, N.; Li, L.; Deerberg, J.; Sharma, P.; Leung, S.; Davies, M.; Bush, J.; Hamm, J.; Hrytsak, M. *Org. Process Res. Dev.* **2012**, *16*, 2051-2057.
- (311) Liebeschuetz, J. W.; Wylie, W. A.; Waszkowycz, B.; Murray, C. W.; Rimmer, A. D.; Welsh, P. M.; Jones, S. D.; Roscoe, J. M. E.; Young, S. C.; Morgan, P. J. US Patent, 7928137B2, 2011.
- (312) Lipshutz, B. H.; Miller, T. A. *Tetrahedron Lett.* **1989**, *30*, 7149-7152.
- (313) Lipshutz, B. H.; Vaccaro, W.; Huff, B. *Tetrahedron Lett.* **1986**, *27*, 4095-4098.
- (314) Whitten, J. P.; Matthews, D. P.; McCarthy, J. R. *J. Org. Chem.* **1986**, *51*, 1891-1894.
- (315) Muchowski, J. M.; Solas, D. R. *J. Org. Chem.* **1984**, *49*, 203-205.
- (316) Kolb, H. C.; Martin, H.; Hoffmann, R. *Tetrahedron: Asymmetry* **1990**, *1*, 237-250.
- (317) Kim, S.; Park, Y. H.; Kee, I. S. *Tetrahedron Lett.* **1991**, *32*, 3099-3100.
- (318) Zeng, Z.; C. Zimmerman, S. *Tetrahedron Lett.* **1988**, *29*, 5123-5124.
- (319) Saito, K.; Higashijima, T.; Miyazawa, T.; Wakimasu, M.; Fujino, M. *Chem. Pharm. Bull.* **1984**, *32*, 2187-2193.
- (320) Akaji, K.; Yoshida, M.; Tatsumi, T.; Kimura, T.; Fujiwara, Y.; Kiso, Y. *Chem. Commun.* **1990**, 288-290.

- (321) Fujino, M.; Wakimasu, M.; Kitada, C. *Chem. Commun.* **1982**, 445-446.
- (322) Mesch, S.; Lemme, K.; Wittwer, M.; Koliwer-Brandl, H.; Schwardt, O.; Kelm, S.; Ernst, B. *ChemMedChem* **2012**, *7*, 134-143.
- (323) Zuo, M.; Xu, X.; Li, T.; Ge, R.; Li, Z. *Future Med. Chem.* **2016**, *8*, 765-788.
- (324) Lubahn, D. B.; Joseph, D. R.; Sullivan, P. M.; Willard, H. F.; French, F. S.; Wilson, E. M. *Science* **1988**, *240*, 327-330.
- (325) Shukla, G. C.; Plaga, A. R.; Shankar, E.; Gupta, S. *Andrology* **2016**, *4*, 366-381.
- (326) Siegel, R. L.; Miller, K. D.; Jemal, A. *CA Cancer J. Clin.* **2017**, *67*, 7-30.
- (327) Romero Otero, J.; Garcia Gomez, B.; Campos Juanatey, F.; Touijer, K. A. *Urol. Oncol.* **2014**, *32*, 252-260.
- (328) Gilgunn, S.; Conroy, P. J.; Saldova, R.; Rudd, P. M.; O'Kennedy, R. J. *Nat Rev Urol* **2013**, *10*, 99-107.
- (329) Hessels, D.; Klein Gunnewiek, J. M. T.; van Oort, I.; Karthaus, H. F. M.; van Leenders, G. J. L.; van Balken, B.; Kiemeny, L. A.; Witjes, J. A.; Schalken, J. A. *Eur. Urol.* **2003**, *44*, 8-16.
- (330) Attard, G.; Clark, J.; Ambrosine, L.; Fisher, G.; Kovacs, G.; Flohr, P.; Berney, D.; Foster, C. S.; Fletcher, A.; Gerald, W. L.; Moller, H.; Reuter, V.; De Bono, J. S.; Scardino, P.; Cuzick, J.; Cooper, C. S. *Oncogene* **2007**, *27*, 253-263.
- (331) Hamid, A. R.; Pfeiffer, M. J.; Verhaegh, G. W.; Schaafsma, E.; Brandt, A.; Sweep, F. C.; Sedelaar, J. P.; Schalken, J. A. *Mol Med* **2013**, *18*, 1449-1455.
- (332) Mangelsdorf, D. J.; Thummel, C.; Beato, M.; Herrlich, P.; Schütz, G.; Umesono, K.; Blumberg, B.; Kastner, P.; Mark, M.; Chambon, P.; Evans, R. M. *Cell* **1995**, *83*, 835-839.
- (333) Gelmann, E. P. *J. Clin. Oncol.* **2002**, *20*, 3001-3015.
- (334) Evans, R. M. *Science* **1988**, *240*, 889-895.
- (335) Myung, J.-K.; Banuelos, C. A.; Fernandez, J. G.; Mawji, N. R.; Wang, J.; Tien, A. H.; Yang, Y. C.; Tavakoli, I.; Haile, S.; Watt, K.; McEwan, I. J.; Plymate, S.; Andersen, R. J.; Sadar, M. D. *J. Clin. Invest.* **2013**, *123*, 2948-2960.
- (336) Verrijdt, G.; Haelens, A.; Claessens, F. *Mol. Gen. Metab.* **2003**, *78*, 175-185.
- (337) Jenster, G.; Trapman, J.; Brinkmann, A. O. *Biochem. J.* **1993**, *293*, 761-768.
- (338) Zhou, Z. X.; Kempainen, J. A.; Wilson, E. M. *Mol. Endocrinol.* **1995**, *9*, 605-615.

- (339) Jenster, G.; van der Korput, H. A. G. M.; van Vroonhoven, C.; van der Kwast, T. H.; Trapman, J.; Brinkmann, A. O. *Mol. Endocrinol.* **1991**, *5*, 1396-1404.
- (340) Livermore, K. E.; Munkley, J.; Elliott, D. J. *AIMS Mol. Sci.* **2016**, *3*, 280-299.
- (341) Kumar, R. *Asian J. Androl.* **2016**, *18*, 682-686.
- (342) Querol Cano, L.; Lavery, D. N.; Bevan, C. L. *Mol. Cell Endocrinol.* **2013**, *369*, 52-62.
- (343) Zarif, J. C.; Miranti, C. K. *Cell. Signal.* **2016**, *28*, 348-356.
- (344) Dehm, S. M.; Tindall, D. J. *Mol. Endocrinol.* **2007**, *21*, 2855-2863.
- (345) Reid, K. J.; Hendy, S. C.; Saito, J.; Sorensen, P.; Nelson, C. C. *J. Biol. Chem.* **2001**, *276*, 2943-2952.
- (346) Heemers, H. V.; Tindall, D. J. *Endocr. Rev.* **2006**, *28*, 778-808.
- (347) Huggins, C.; Hodges, C. V. *Arch Surg.* **1941**, *43*, 209-223.
- (348) Perlmutter, M. A.; Lepor, H. *Rev. Urol.* **2007**, *9*, S3-S8.
- (349) Johnson, J. K.; Skoda, E. M.; Zhou, J.; Parrinello, E.; Wang, D.; O'Malley, K.; Eyer, B. R.; Kazancioglu, M.; Eisermann, K.; Johnston, P. A.; Nelson, J. B.; Wang, Z.; Wipf, P. *ACS Med. Chem. Lett.* **2016**, *7*, 785-790.
- (350) Yuan, X.; Balk, S. P. *Urol. Oncol.* **2009**, *27*, 36-41.
- (351) Liu, W.; Xie, C. C.; Zhu, Y.; Li, T.; Sun, J.; Cheng, Y.; Ewing, C. M.; Dalrymple, S.; Turner, A. R.; Sun, J.; Isaacs, J. T.; Chang, B.-L.; Zheng, S. L.; Isaacs, W. B.; Xu, J. *Neoplasia* **2008**, *10*, 897-907.
- (352) Donovan, M. J.; Osman, I.; Khan, F. M.; Vengrenyuk, Y.; Capodiecici, P.; Koscuizska, M.; Anand, A.; Cordon-Cardo, C.; Costa, J.; Scher, H. I. *BJU Int.* **2010**, *105*, 462-467.
- (353) Mohler, J. L.; Gregory, C. W.; Ford, O. H.; Kim, D.; Weaver, C. M.; Petrusz, P.; Wilson, E. M.; French, F. S. *Clin. Cancer Res.* **2004**, *10*, 440-448.
- (354) Steinkamp, M. P.; Mahony, O. A.; Brogley, M.; Rehman, H.; LaPensee, E. W.; Dhanasekaran, S.; Hofer, M. D.; Kuefer, R.; Chinnaiyan, A.; Rubin, M. A.; Pienta, K. J.; Robins, D. M. *Cancer Res.* **2009**, *69*, 4434-4442.
- (355) Gregory, C. W.; He, B.; Johnson, R. T.; Ford, O. H.; Mohler, J. L.; French, F. S.; Wilson, E. M. *Cancer Res.* **2001**, *61*, 4315-4319.
- (356) Locke, J. A.; Guns, E. S.; Lubik, A. A.; Adomat, H. H.; Hendy, S. C.; Wood, C. A.; Ettinger, S. L.; Gleave, M. E.; Nelson, C. C. *Cancer Res.* **2008**, *68*, 6407-6415.

- (357) Locke, J. A.; Nelson, C. C.; Adomat, H. H.; Hendy, S. C.; Gleave, M. E.; Guns, E. S. T. *J. Steroid Biochem. Mol. Biol.* **2009**, *115*, 126-136.
- (358) Chang, K.-H.; Li, R.; Papari-Zareei, M.; Watumull, L.; Zhao, Y. D.; Auchus, R. J.; Sharifi, N. *Proc. Natl. Acad. Sci. U. S. A.* **2011**, *108*, 13728-13733.
- (359) Mostaghel, E. A.; Solomon, K. R.; Pelton, K.; Freeman, M. R.; Montgomery, R. B. *PLOS ONE* **2012**, *7*, e30062.
- (360) Stuchbery, R.; McCoy, P. J.; Hovens, C. M.; Corcoran, N. M. *Nat Rev Urol* **2017**, *14*, 49-58.
- (361) Li, Y.; Alsagabi, M.; Fan, D.; Bova, G. S.; Tewfik, A. H.; Dehm, S. M. *Cancer Res.* **2011**, *71*, 2108-2117.
- (362) Dehm, S. M.; Schmidt, L. J.; Heemers, H. V.; Vessella, R. L.; Tindall, D. J. *Cancer Res.* **2008**, *68*, 5469-5477.
- (363) Sun, S.; Sprenger, C. C.; Vessella, R. L.; Haugk, K.; Soriano, K.; Mostaghel, E. A.; Page, S. T.; Coleman, I. M.; Nguyen, H. M.; Sun, H.; Nelson, P. S.; Plymate, S. R. *J. Clin. Invest.* **2010**, *120*, 2715-2730.
- (364) De Laere, B.; van Dam, P.-J.; Whittington, T.; Mayrhofer, M.; Diaz, E. H.; Van den Eynden, G.; Vandebroek, J.; Del-Favero, J.; Van Laere, S.; Dirix, L.; Grönberg, H.; Lindberg, J. *Eur. Urol.* **2017**, <http://dx.doi.org/10.1016/j.eururo.2017.01.011>.
- (365) Guo, Z.; Yang, X.; Sun, F.; Jiang, R.; Linn, D. E.; Chen, H.; Chen, H.; Kong, X.; Melamed, J.; Tepper, C. G.; Kung, H.-J.; Brodie, A. M. H.; Edwards, J.; Qiu, Y. *Cancer Res.* **2009**, *69*, 2305-2313.
- (366) Antonarakis, E. S.; Lu, C.; Wang, H.; Lubner, B.; Nakazawa, M.; Roeser, J. C.; Chen, Y.; Mohammad, T. A.; Chen, Y.; Fedor, H. L.; Lotan, T. L.; Zheng, Q.; De Marzo, A. M.; Isaacs, J. T.; Isaacs, W. B.; Nadal, R.; Paller, C. J.; Denmeade, S. R.; Carducci, M. A.; Eisenberger, M. A.; Luo, J. *New Engl. J. Med.* **2014**, *371*, 1028-1038.
- (367) Xu, D.; Zhan, Y.; Qi, Y.; Cao, B.; Bai, S.; Xu, W.; Gambhir, S. S.; Peng, L.; Sartor, O.; Flemington, E. K.; Zhang, H.; Hu, C.-D.; Dong, Y. *Cancer Res.* **2015**, *75*, 3663-3671.
- (368) Qu, F.; Xie, W.; Nakabayashi, M.; Zhang, H.; Jeong, S. H.; Wang, X.; Komura, K.; Sweeney, C. J.; Sartor, O.; Lee, G.-S. M.; Kantoff, P. W. *Clin. Cancer Res.* **2017**, *23*, 726-734.
- (369) Welti, J.; Rodrigues, D. N.; Sharp, A.; Sun, S.; Lorente, D.; Riisnaes, R.; Figueiredo, I.; Zafeiriou, Z.; Rescigno, P.; de Bono, J. S.; Plymate, S. R. *Eur. Urol.* **2016**, *70*, 599-608.
- (370) Culig, Z.; Hobisch, A.; Cronauer, M. V.; Radmayr, C.; Trapman, J.; Hittmair, A.; Bartsch, G.; Klocker, H. *Cancer Res.* **1994**, *54*, 5474-5478.

- (371) Djakiew, D. *Prostate* **2000**, *42*, 150-160.
- (372) Manin, M.; Baron, S.; Goossens, K.; Beaudoin, C.; Jean, C.; Veyssiere, G.; Verhoeven, G.; Morel, L. *Biochem. J.* **2002**, *366*, 729-736.
- (373) Wen, Y.; Hu, M. C. T.; Makino, K.; Spohn, B.; Bartholomeusz, G.; Yan, D.-H.; Hung, M.-C. *Cancer Res.* **2000**, *60*, 6841-6845.
- (374) Signoretti, S.; Montironi, R.; Manola, J.; Altimari, A.; Tam, C.; Bubley, G.; Balk, S.; Thomas, G.; Kaplan, I.; Hlatky, L.; Hahnfeldt, P.; Kantoff, P.; Loda, M. *J. Natl. Cancer Inst.* **2000**, *92*, 1918-1925.
- (375) Craft, N.; Shostak, Y.; Carey, M.; Sawyers, C. L. *Nat. Med.* **1999**, *5*, 280-285.
- (376) Suh, J.; Payvandi, F.; Edelstein, L. C.; Amenta, P. S.; Zong, W.-X.; Gélinas, C.; Rabson, A. B. *Prostate* **2002**, *52*, 183-200.
- (377) Zhang, L.; Altuwaijri, S.; Deng, F.; Chen, L.; Lal, P.; Bhanot, U. K.; Korets, R.; Wenske, S.; Lilja, H. G.; Chang, C.; Scher, H. I.; Gerald, W. L. *Am. J. Pathol.* **2009**, *175*, 489-499.
- (378) Barradell, L. B.; Faulds, D. *Drug & Aging* **1994**, *5*, 59-80.
- (379) Neri, R. O.; Monahan, M. D.; Meyer, J. G.; Afonso, B. A.; Tabachnick, I. A. *Eur. J. Pharmacol.* **1967**, *1*, 438-444.
- (380) Schröder, F. H.; Whelan, P.; de Reijke, T. M.; Kurth, K. H.; Pavone-Macaluso, M.; Mattelaer, J.; van Velthoven, R. F.; Debois, M.; Collette, L. *Eur. Urol.* **2004**, *45*, 457-464.
- (381) de Voogt, H. J. *Prostate Suppl.* **1992**, *4*, 91-95.
- (382) Mahler, C.; Verhelst, J.; denis, L. *Clin. Pharmacokinet.* **1998**, *34*, 405-417.
- (383) McLeod, D. G. *Oncologist* **1997**, *2*, 18-27.
- (384) O'Connor, K. M.; Fitzpatrick, J. M. *BJU Int.* **2006**, *97*, 22-28.
- (385) Tran, C.; Ouk, S.; Clegg, N. J.; Chen, Y.; Watson, P. A.; Arora, V.; Wongvipat, J.; Smith-Jones, P. M.; Yoo, D.; Kwon, A.; Wasielewska, T.; Welsbie, D.; Chen, C. D.; Higano, C. S.; Beer, T. M.; Hung, D. T.; Scher, H. I.; Jung, M. E.; Sawyers, C. L. *Science* **2009**, *324*, 787-790.
- (386) Penson, D. F.; Armstrong, A. J.; Concepcion, R.; Agarwal, N.; Olsson, C.; Karsh, L.; Dunshee, C.; Wang, F.; Wu, K.; Krivoshik, A.; Phung, D.; Higano, C. S. *J. Clin. Oncol.* **2016**, *34*, 2098-2106.
- (387) Scher, H. I.; Beer, T. M.; Higano, C. S.; Anand, A.; Taplin, M.-E.; Efstathiou, E.; Rathkopf, D.; Shelkey, J.; Yu, E. Y.; Alumkal, J.; Hung, D.; Hirmand, M.; Seely, L.;

- Morris, M. J.; Danila, D. C.; Humm, J.; Larson, S.; Fleisher, M.; Sawyers, C. L. *Lancet* **2010**, *375*, 1437-1446.
- (388) Scher, H. I.; Fizazi, K.; Saad, F.; Taplin, M.-E.; Sternberg, C. N.; Miller, K.; de Wit, R.; Mulders, P.; Chi, K. N.; Shore, N. D.; Armstrong, A. J.; Flaig, T. W.; Fléchon, A.; Mainwaring, P.; Fleming, M.; Hainsworth, J. D.; Hirmand, M.; Selby, B.; Seely, L.; de Bono, J. S. *N. Engl. J. Med.* **2012**, *367*, 1187-1197.
- (389) Foster, W. R.; Car, B. D.; Shi, H.; Levesque, P. C.; Obermeier, M. T.; Gan, J.; Arezzo, J. C.; Powlin, S. S.; Dinchuk, J. E.; Balog, A.; Salvati, M. E.; Attar, R. M.; Gottardis, M. M. *Prostate* **2011**, *71*, 480-488.
- (390) Kregel, S.; Chen, J. L.; Tom, W.; Krishnan, V.; Kach, J.; Brechka, H.; Fessenden, T. B.; Isikbay, M.; Paner, G. P.; Szmulewitz, R. Z.; Vander Griend, D. J. *Oncotarget* **2016**, *7*, 26259-26274.
- (391) Clegg, N. J.; Wongvipat, J.; Joseph, J. D.; Tran, C.; Ouk, S.; Dilhas, A.; Chen, Y.; Grillot, K.; Bischoff, E. D.; Cai, L.; Aparicio, A.; Dorow, S.; Arora, V.; Shao, G.; Qian, J.; Zhao, H.; Yang, G.; Cao, C.; Sensintaffar, J.; Wasielewska, T.; Herbert, M. R.; Bonnefous, C.; Darimont, B.; Scher, H. I.; Smith-Jones, P.; Klang, M.; Smith, N. D.; De Stanchina, E.; Wu, N.; Ouerfelli, O.; Rix, P. J.; Heyman, R. A.; Jung, M. E.; Sawyers, C. L.; Hager, J. H. *Cancer Res.* **2012**, *72*, 1494-1503.
- (392) Barrie, S. E.; Potter, G. A.; Goddard, P. M.; Haynes, B. P.; Dowsett, M.; Jarman, M. J. *Steroid Biochem. Mol. Biol.* **1994**, *50*, 267-273.
- (393) Fizazi, K.; Scher, H. I.; Molina, A.; Logothetis, C. J.; Chi, K. N.; Jones, R. J.; Staffurth, J. N.; North, S.; Vogelzang, N. J.; Saad, F.; Mainwaring, P.; Harland, S.; Goodman Jr, O. B.; Sternberg, C. N.; Li, J. H.; Kheoh, T.; Haqq, C. M.; de Bono, J. S. *Lancet Oncol.* **2012**, *13*, 983-992.
- (394) Ryan, C. J.; Smith, M. R.; Fong, L.; Rosenberg, J. E.; Kantoff, P.; Raynaud, F.; Martins, V.; Lee, G.; Kheoh, T.; Kim, J.; Molina, A.; Small, E. J. *J. Clin. Oncol.* **2010**, *28*, 1481-1488.
- (395) Ryan, C. J.; Smith, M. R.; de Bono, J. S.; Molina, A.; Logothetis, C. J.; de Souza, P.; Fizazi, K.; Mainwaring, P.; Piulats, J. M.; Ng, S.; Carles, J.; Mulders, P. F. A.; Basch, E.; Small, E. J.; Saad, F.; Schrijvers, D.; Van Poppel, H.; Mukherjee, S. D.; Suttman, H.; Gerritsen, W. R.; Flaig, T. W.; George, D. J.; Yu, E. Y.; Efstathiou, E.; Pantuck, A.; Winquist, E.; Higano, C. S.; Taplin, M.-E.; Park, Y.; Kheoh, T.; Griffin, T.; Scher, H. I.; Rathkopf, D. E. *New Eng. J. Med.* **2012**, *368*, 138-148.
- (396) Cicero, G.; De Luca, R.; Dorangricchia, P.; Galvano, A.; Lo Re, G.; Serretta, V.; Dispensa, N.; Dieli, F. *Oncology* **2017**, *92*, 94-100.
- (397) Paller, C. J.; Antonarakis, E. S. *Drug Des. Dev. Ther.* **2011**, *5*, 117-124.

- (398) Antonarakis, E. S.; Lu, C.; Lubber, B.; Wang, H.; Chen, Y.; Nakazawa, M.; Nadal, R.; Paller, C. J.; Denmeade, S. R.; Carducci, M. A.; Eisenberger, M. A.; Luo, J. *JAMA Oncol.* **2015**, *1*, 582-591.
- (399) Shirley, M.; McCormack, P. *Drugs* **2014**, *74*, 579-586.
- (400) Hague, C.; Logue, J. P. *Ther. Adv. Urol.* **2016**, *8*, 175-180.
- (401) Yilmaz, H.; Aksu, G.; Dillioglugil, O. *Asian J. Androl.* **2015**, *17*, 892-898.
- (402) Sundén, H.; Holland, M. C.; Poutiainen, P. K.; Jääskeläinen, T.; Pulkkinen, J. T.; Palvimo, J. J.; Olsson, R. *J. Med. Chem.* **2015**, *58*, 1569-1574.
- (403) Balog, A.; Rampulla, R.; Martin, G. S.; Krystek, S. R.; Attar, R.; Dell-John, J.; DiMarco, J. D.; Fairfax, D.; Gougoutas, J.; Holst, C. L.; Nation, A.; Rizzo, C.; Rossiter, L. M.; Schweizer, L.; Shan, W.; Spengel, S.; Spires, T.; Cornelius, G.; Gottardis, M.; Trainor, G.; Vite, G. D.; Salvati, M. E. *ACS Med. Chem. Lett.* **2015**, *6*, 908-912.
- (404) Shan, W.; Balog, A.; Nation, A.; Zhu, X.; Chen, J.; Cvijic, M. E.; Geng, J.; Rizzo, C. A.; Spires Jr, T.; Attar, R. M.; Obermeier, M.; Traeger, S.; Dai, J.; Zhang, Y.; Galella, M.; Trainor, G.; Vite, G. D.; Gavai, A. V. *Bioorg. Med. Chem. Lett.* **2016**, *26*, 5707-5711.
- (405) Xu, Y.-M.; Liu, M. X.; Grunow, N.; Wijeratne, E. M. K.; Paine-Murrieta, G.; Felder, S.; Kris, R. M.; Gunatilaka, A. A. L. *J. Med. Chem.* **2015**, *58*, 6984-6993.
- (406) Andersen, R. J.; Mawji, N. R.; Wang, J.; Wang, G.; Haile, S.; Myung, J.-K.; Watt, K.; Tam, T.; Yang, Y. C.; Bañuelos, C. A.; Williams, D. E.; McEwan, I. J.; Wang, Y.; Sadar, M. D. *Cancer Cell* **2010**, *17*, 535-546.
- (407) De Mol, E.; Fenwick, R. B.; Phang, C. T. W.; Buzón, V.; Szulc, E.; de la Fuente, A.; Escobedo, A.; García, J.; Bertoncini, C. W.; Estébanez-Perpiñá, E.; McEwan, I. J.; Riera, A.; Salvatella, X. *ACS Chem. Biol.* **2016**, *11*, 2499-2505.
- (408) Imamura, Y.; Sadar, M. D. *Int J Urol* **2016**, *23*, 654-665.
- (409) Sadar, M. D.; Williams, D. E.; Mawji, N. R.; Patrick, B. O.; Wikanta, T.; Chasanah, E.; Irianto, H. E.; Soest, R. V.; Andersen, R. J. *Org. Lett.* **2008**, *10*, 4947-4950.
- (410) Banuelos, C. A.; Tavakoli, I.; Tien, A. H.; Caley, D. P.; Mawji, N. R.; Li, Z.; Wang, J.; Yang, Y. C.; Imamura, Y.; Yan, L.; Wen, J. G.; Andersen, R. J.; Sadar, M. D. *J. Biol. Chem.* **2016**, *291*, 22231-22243.
- (411) Johnston, P. A.; Nguyen, M. M.; Dar, J. A.; Ai, J.; Wang, Y.; Masoodi, K. Z.; Shun, T.; Shinde, S.; Camarco, D. P.; Hua, Y.; Huryn, D. M.; Wilson, G. M.; Lazo, J. S.; Nelson, J. B.; Wipf, P.; Wang, Z. *Assay Drug Dev. Technol.* **2016**, *14*, 226-239.
- (412) Demchenko, A. M.; Sinchenko, V. G.; Prodanchuk, N. G.; Kovtunencko, V. A.; Patrati, V. K.; Tytilin, A. K.; Babichev, F. S. *Pharm. Chem. J.* **1987**, *21*, 789-791.

- (413) Abe, M.; Nishikawa, K.; Fukuda, H.; Nakanishi, K.; Tazawa, Y.; Taniguchi, T.; Park, S.-y.; Hiradate, S.; Fujii, Y.; Okuda, K.; Shindo, M. *Phytochemistry* **2012**, *84*, 56-67.
- (414) Boehm, H.-J.; Banner, D.; Bendels, S.; Kansy, M.; Kuhn, B.; Mueller, K.; Obst-Sander, U.; Stahl, M. *ChemBioChem* **2004**, *5*, 637-643.
- (415) Yonemoto-Kobayashi, M.; Inamoto, K.; Tanaka, Y.; Kondo, Y. *Org. Biomol. Chem.* **2013**, *11*, 3773-3775.
- (416) Scheffer, J. R.; Wostradowski, R. A. *J. Org. Chem.* **1972**, *37*, 4317-4324.
- (417) Concellón, J. M.; Rodríguez-Solla, H.; Gómez, C. *Angew. Chem. Int. Ed.* **2002**, *41*, 1917-1919.
- (418) <https://www.epa.gov/dwstandardsregulations/chromium-drinking-water>.
- (419) Yamaguchi, K.; Kazuta, Y.; Abe, H.; Matsuda, A.; Shuto, S. *J. Org. Chem.* **2003**, *68*, 9255-9262.
- (420) Kim, T. H.; Jeong, J. W.; Song, J. H.; Lee, K. R.; Ahn, S.; Ahn, S. H.; Kim, S.; Koo, T. S. *Arch Pharm Res* **2015**, *38*, 2076-2082.
- (421) Xenograft studies were performed using racemic JJ450 in the Wang Lab.
- (422) St. Jean, D. J.; Fotsch, C. *J. Med. Chem.* **2012**, *55*, 6002-6020.
- (423) Li, S.-S.; Liu, X.; Liu, Y.-M.; He, H.-Y.; Fan, K.-N.; Cao, Y. *Chem. Commun.* **2014**, *50*, 5626-5628.
- (424) Kawatani, M.; Osada, H. *MedChemComm* **2014**, *5*, 277-287.
- (425) Lee, H.; Lee, J. W. *Arch. Pharmacol Res.* **2016**, *39*, 1193-1201.
- (426) Wang, X.; Imber, B. S.; Schreiber, S. L. *Bioconjugate Chem.* **2008**, *19*, 585-587.
- (427) Wullschleger, C. W.; Gertsch, J.; Altmann, K.-H. *Org. Lett.* **2010**, *12*, 1120-1123.
- (428) Mascitti, V.; Corey, E. J. *J. Am. Chem. Soc.* **2004**, *126*, 15664-15665.
- (429) Heathcock, C. H.; Brown, R. C. D.; Norman, T. C. *J. Org. Chem.* **1998**, *63*, 5013-5030.
- (430) Lu, Z.; Tata, J. R.; Cheng, K.; Wei, L.; Chan, W. W. S.; Butler, B.; Schleim, K. D.; Jacks, T. M.; Hickey, G.; Patchett, A. A. *Bioorg. Med. Chem. Lett.* **2003**, *13*, 1817-1820.
- (431) Iwasaki, K.; Wan, K. K.; Oppedisano, A.; Crossley, S. W. M.; Shenvi, R. A. *J. Am. Chem. Soc.* **2014**, *136*, 1300-1303.
- (432) Robbins, W. J.; Kavanagh, F.; Hervey, A. *Proc. Natl. Acad. Sci. U. S. A.* **1947**, *33*, 171-176.

- (433) Grandjean, J.; Huls, R. *Tetrahedron Lett.* **1974**, 1893-1895.
- (434) Cohen-Addad, C.; Riondel, J. *Acta Crystallogr., Sect. B* **1981**, B37, 1309-1311.
- (435) Carraz, G. French Patent, 2407718A2, 1979.
- (436) Riondel, J.; Beriel, H.; Dardas, A.; Carraz, G.; Oddoux, L. *Arzneim.-Forsch.* **1981**, 31, 293-299.
- (437) Murakami, R.; Muramatsu, Y.; Minami, E.; Masuda, K.; Sakaida, Y.; Endo, S.; Suzuki, T.; Ishida, O.; Takatsu, T.; Miyakoshi, S.; Inukai, M.; Isono, F. *J. Antibiot.* **2009**, 62, 153-158.
- (438) Biological data for pleurotin (NSC 401005); <https://pubchem.ncbi.nlm.nih.gov>.
- (439) Welsh, S. J.; Williams, R. R.; Birmingham, A.; Newman, D. J.; Kirkpatrick, D. L.; Powis, G. *Mol. Cancer Ther.* **2003**, 2, 235-243.
- (440) Shipley, S. M.; Barr, A. L.; Graf, S. J.; Collins, R. P.; McCloud, T. G.; Newman, D. J. *J. Ind. Microbiol. Biotechnol.* **2006**, 33, 463-468.
- (441) Gromer, S.; Urig, S.; Becker, K. *Med. Res. Rev.* **2004**, 24, 40-89.
- (442) Semenza, G. L. *Crit. Rev. Biochem. Mol. Biol.* **2000**, 35, 71-103.
- (443) Muz, B.; de la Puente, P.; Azab, F.; Azab, A. K. *Hypoxia* **2015**, 3, 83-92.
- (444) Moore, H. W. *Science* **1977**, 197, 527-532.
- (445) Bradner, W. T. *Cancer Treat. Rev.* **2001**, 27, 35-50.
- (446) Chuang, C. P.; Hart, D. J. *J. Org. Chem.* **1983**, 48, 1782-1784.
- (447) Hart, D. J.; Huang, H. C. *Tetrahedron Lett.* **1985**, 26, 3749-3752.
- (448) Hart, D. J.; Huang, H. C. *J. Am. Chem. Soc.* **1988**, 110, 1634-1635.
- (449) Hart, D. J.; Huang, H. C.; Krishnamurthy, R.; Schwartz, T. *J. Am. Chem. Soc.* **1989**, 111, 7507-7519.
- (450) Kraus, G.; Chen, L. *Synlett.* **1991**, 89-90.
- (451) Kraus, G. A.; Chen, L.; Jacobson, R. A. *Synth. Commun.* **1993**, 23, 2041-2049.
- (452) Kraus, G. A.; Chen, L. *J. Am. Chem. Soc.* **1990**, 112, 3464-3466.
- (453) Wipf, P.; Hopkins, T. D.; Jung, J. K.; Rodriguez, S.; Birmingham, A.; Southwick, E. C.; Lazo, J. S.; Powis, G. *Bioorg. Med. Chem. Lett.* **2001**, 11, 2637-2641.

- (454) Wipf, P.; Lynch, S. M.; Birmingham, A.; Tamayo, G.; Jimenez, A.; Campos, N.; Powis, G. *Org. Biomol. Chem.* **2004**, *2*, 1651-1658.
- (455) Wipf, P.; Lynch, S. M.; Powis, G.; Birmingham, A.; Englund, E. E. *Org. Biomol. Chem.* **2005**, *3*, 3880-3882.
- (456) Balachandran, R.; Hopkins, T. D.; Thomas, C. A.; Wipf, P.; Day, B. W. *Chem. Biol. Drug Des.* **2008**, *71*, 117-124.
- (457) Powis, G.; Wipf, P.; Lynch, S. M.; Birmingham, A.; Kirkpatrick, D. L. *Mol. Cancer Ther.* **2006**, *5*, 630-636.
- (458) Jung, M. E.; Hagenah, J. A. *J. Org. Chem.* **1987**, *52*, 1889-1902.
- (459) Palais, L.; Alexakis, A. *Chem. Eur. J.* **2009**, *15*, 10473-10485.
- (460) Negishi, E.; Boardman, L. D.; Sawada, H.; Bagheri, V.; Stoll, A. T.; Tour, J. M.; Rand, C. *L. J. Am. Chem. Soc.* **1988**, *110*, 5383-5396.
- (461) Dieter, R. K.; Chen, N. *J. Org. Chem.* **2006**, *71*, 5674-5678.
- (462) Kawada, H.; Ebiike, H.; Tsukazaki, M.; Nakamura, M.; Morikami, K.; Yoshinari, K.; Yoshida, M.; Ogawa, K.; Shimma, N.; Tsukuda, T.; Ohwada, J. *Bioorg. Med. Chem. Lett.* **2013**, *23*, 673-678.
- (463) Fernandes, R. A.; Chavan, V. P. *Tetrahedron Lett.* **2008**, *49*, 3899-3901.
- (464) Schuppan, J.; Wehlan, H.; Keiper, S.; Koert, U. *Angew. Chem. Int. Ed.* **2001**, *40*, 2063-2066.
- (465) Carrillo, J.; Costa, A. M.; Sidera, M.; Vilarrasa, J. *Tetrahedron Lett.* **2011**, *52*, 5153-5156.
- (466) Fristad, W. E.; Peterson, J. R.; Ernst, A. B. *J. Org. Chem.* **1985**, *50*, 3143-3147.
- (467) Mazal, C.; Jonas, J.; Zak, Z. *Tetrahedron* **2002**, *58*, 2729-2733.
- (468) Glickman, S. A.; Cope, A. C. *J. Am. Chem. Soc.* **1945**, *67*, 1012-1016.
- (469) Rao, V. S. *Synth. Commun.* **1989**, *19*, 1389-1393.
- (470) Mathieson, J. E.; Crawford, J. J.; Schmidtman, M.; Marquez, R. *Org. Biomol. Chem.* **2009**, *7*, 2170-2175.
- (471) Fernandes, R. A.; Chavan, V. P.; Ingle, A. B. *Tetrahedron Lett.* **2008**, *49*, 6341-6343.
- (472) Hoffmann, R. W. *Chem. Rev.* **1989**, *89*, 1841-1860.
- (473) Pham, H. V.; Paton, R. S.; Ross, A. G.; Danishefsky, S. J.; Houk, K. N. *J. Am. Chem. Soc.* **2014**, *136*, 2397-2403.

- (474) Wang, W.; Wang, J.; Li, H. *Org. Lett.* **2004**, *6*, 2817-2820.
- (475) Roush, W. R.; Barda, D. A.; Limberakis, C.; Kunz, R. K. *Tetrahedron* **2002**, *58*, 6433-6454.
- (476) Hassan, N. P. S.; Naysmith, B. J.; Sperry, J.; Brimble, M. A. *Tetrahedron* **2015**, *71*, 7137-7143.
- (477) Halley, F.; Sava, X. *Synth. Commun.* **1997**, *27*, 1199-1207.
- (478) Kumar, A.; Say, M.; Boykin, D. W. *Synthesis* **2008**, *2008*, 707-710.
- (479) Fotsch, C.; Sonnenberg, J. D.; Chen, N.; Hale, C.; Karbon, W.; Norman, M. H. *J. Med. Chem.* **2001**, *44*, 2344-2356.
- (480) Kantaro, U.; Nakamura, K.; Natsutani, I. World Patent 111675, 2011.
- (481) Everett, R. K.; Wolfe, J. P. *Org. Lett.* **2013**, *15*, 2926-2929.
- (482) Solomon, I. J.; Filler, R. *J. Am. Chem. Soc.* **1963**, *85*, 3492-3496.
- (483) Austin, W. B.; Bilow, N.; Kelleghan, W. J.; Lau, K. S. Y. *J. Org. Chem.* **1981**, *46*, 2280-2286.
- (484) He, Z.; Zhang, R.; Hu, M.; Li, L.; Ni, C.; Hu, J. *Chem. Sci.* **2013**, *4*, 3478-3483.
- (485) Paegle, E.; Belyakov, S.; Petrova, M.; Liepinsh, E.; Arsenyan, P. *Eur. J. Org. Chem.* **2015**, *2015*, 4389-4399.
- (486) Kub, C.; Tolosa, J.; Zuccherro, A. J.; McGrier, P. L.; Subramani, C.; Khorasani, A.; Rotello, V. M.; Bunz, U. H. F. *Macromolecules* **2010**, *43*, 2124-2129.
- (487) Westerlind, U.; Westman, J.; Toernquist, E.; Smith, C. I. E.; Oscarson, S.; Lahmann, M.; Norberg, T. *Glycoconjugate J.* **2004**, *21*, 227-241.
- (488) Butini, S.; Brindisi, M.; Gemma, S.; Minetti, P.; Cabri, W.; Gallo, G.; Vincenti, S.; Talamonti, E.; Borsini, F.; Caprioli, A.; Stasi, M. A.; Di Serio, S.; Ros, S.; Borrelli, G.; Maramai, S.; Fezza, F.; Campiani, G.; Maccarrone, M. *J. Med. Chem.* **2012**, *55*, 6898-6915.
- (489) Evans, A. R.; Miriyala, S.; St. Clair, D. K.; Butterfield, D. A.; Robinson, R. A. S. *J. Proteome Res.* **2012**, *11*, 1054-1064.
- (490) Doepner, A. M.; Aboagye, E. O.; Barrett, A. G. M. *Tetrahedron Lett.* **2015**, *56*, 3293-3297.
- (491) Bos, M. E.; Wulff, W. D.; Miller, R. A.; Chamberlin, S.; Brandvold, T. A. *J. Am. Chem. Soc.* **1991**, *113*, 9293-9319.

(492) Salikov, R. F.; Platonov, D. N.; Frumkin, A. E.; Lipilin, D. L.; Tomilov, Y. V.
Tetrahedron **2013**, *69*, 3495-3505.

(493) Jermaine, T.; Xiaogao, L. World Patent 017561 A1, 2011.